Imperial College London
Department of Chemical Engineering

Control and operation of centrifugal gas compressors, with an emphasis on CO_2 compression

by Sara Budinis

September 2015

Supervised by Professor Nina F. Thornhill

Submitted in part fulfilment of the requirements for the degree of Doctor of Philosophy in Chemical Engineering of Imperial College London

Declaration of originality

The author declares that the present thesis reports the results of her own research and that all else is appropriately referenced. In addition, the presented materials are not submitted elsewhere for another degree.

The copyright of this thesis rests with the author and is made available under a Creative Commons Attribution Non-Commercial No Derivatives licence. Researchers are free to copy, distribute or transmit the thesis on the condition that they attribute it, that they do not use it for commercial purposes and that they do not alter, transform or build upon it. For any reuse or redistribution, researchers must make clear to others the licence terms of this work.

Abstract

The PhD project focuses on operation and control of centrifugal gas compressors for carbon dioxide application. The analysis of the industrial background and the review of the academic literature have highlighted some research needs consisting in:

- Improvement of the performance of the pressure controller of the compressor
- Integration of pressure and surge control
- Analysis of the effect of the recycle configuration on the operation of the compressor.

Control configurations have been proposed in order to:

- Reduce the interaction between control loops
- Guarantee the stable and safe operation of the control system
- Deal with partial and full recycle operation in supercritical carbon dioxide applications.

Dynamic modelling and simulations have been employed in order to analyse the effect of boundary disturbances on the operation of the open and closed loop compression system. The performance of the system has been evaluated by means of graphical representation of controlled and manipulated variables and also by means of proposed performance indicators. These indicators focus on specific aspects of the operation of a compressor such as control performance, power consumption and amount of gas recycled.

The results of the thesis demonstrate that better pressure control reduces the risk of surge. Moreover the interaction between pressure controller and surge controller can be avoided by employing a linear model predictive controller. The controller has been tuned according to various control purposes such as energy saving, surge avoidance or pressure control performance.

The results also demonstrate that the recycle configuration influences surge occurrence, control stability and power consumption of the compression station. This phenomenon is emphasised when dealing with supercritical carbon dioxide because of the high density of the fluid.

Acknowledgement

My first, deepest and most grateful acknowledgement goes to my supervisor, Professor Nina Thornhill. During the past four years she has always been present, patient, engaged and professional. She taught me how to organise my thinking and my doing and she has been an example of kindness and integrity.

I would also like to thank my mentor, Professor Geoffrey Maitland, who has been very helpful especially in the first year of PhD, when I most needed guidance, advice and reassurance.

Bob Hodder and Mark Dixon have had a pivotal role in the development of the content of my research. They enthusiastically followed my progresses and facilitated my secondments. I must also thank Craig MacKay and Stefano Belloni, who supported me during the time I spent respectively at Xodus Group, Aberdeen and CCC, Milan.

The Energy SmartOps team has really been a happy cohort of researchers and supervisors and I will always remember the time we spent together while abroad or in London. Special thanks go to John Pretlove, Esperanza and Dennis.

Cristina Romano, Selassie Senait and Angela Lonergan facilitated my work while supporting and guiding me in various activities. Everyday life would have been much harder without them.

I cannot forget the role Davide Fabozzi and Trond Haugen had in my life as a PhD student. They both gave me a hand when I mostly needed it.

I also want to thank the Sustainable Gas Institute team, Professor Nigel Brandon, Dr Adam Hawkes and Victoria Harding Platt, who did not rush me when time was the only thing I really needed.

New and old friends have been supporting me throughout this long journey, and so did my family. I want to specially thank my parents, my sister and my nephew. For them it must have been hard to see me going abroad and leave everything I had and knew for this new adventure. However they accepted my decision and they have been supportive ever since.

Finally, I would like to thank Marco, because he makes me laugh, he cooks the best meals and he still stands me.

Content list

Declaration of originality 1
Abstract 2
Acknowledgement 3
Content list 4
List of figures 11
List of tables 18
Notation for compressor modelling and simulation 22
1. Introduction 24
1.1 Introduction to the project 25
1.1.1 Energy SmartOps Project 25
1.1.2 PhD project 26
1.1.3 Project outcomes 27
1.1.4 Consortium activities 29
1.1.5 Milestones of the PhD project 31
1.1.6 Summary 31
1.2 Introduction to the technology 32
1.2.1 Generation and utilisation of carbon dioxide 32
1.2.2 Carbon capture and storage 33
1.2.3 Transportation of carbon dioxide 34
1.2.4 Selection of gas compressors 34
1.2.5 Control of gas compressors 36
1.2.6 Summary 36
1.3 Introduction to the thesis 38
1.3.1 Structure of the thesis 38
1.3.2 Novel contribution of the thesis 40
1.3.3 Research outcomes 42
1.3.4 Summary 44
1.4 Summary of the chapter 45
2 Review of Relevant Background 46
2.1 Centrifugal compressor and their operation 48
2.1.1 Centrifugal compressors selection and geometry 48

2.1.2 Performance characteristics and operating range 50
2.1.3 Summary 53
2.2 Centrifugal compressor and surge modelling 54
2.2.1 Modelling of compressors and surge 54
2.2.2 Summary 62
2.3 Control systems for centrifugal compressors 63
2.3.1 Traditional PID control 63
2.3.2 Active and passive control 66
2.3.3 MPC control 70
2.3.4 Summary 77
2.4 Compression of carbon dioxide 78
2.4.1 Carbon dioxide properties 78
2.4.2 Carbon dioxide transportation 80
2.4.3 Modelling and simulation of compression to supercritical state 83
2.4.4 Control systems for supercritical CO_2 applications 85
2.4.5 Summary 87
2.5 Summary of the chapter 88
3 Theory and methods 90
3.1 Task description 91
3.2 Compressor modelling 92
3.2.1 Single stage compressor 92
3.2.2 Recycle line 96
3.2.3 Recycle volume 98
3.2.4 Summary 100
3.3 Feedback control system modelling 101
3.3.1 Generic form of a feedback control algorithm 101
3.3.2 Capacity controller 102
3.3.3 Antisurge controller 104
3.3.4 Overall control system 108
3.3.5 Summary 110
3.4 Model implementation 111
3.4.1 Selection of the numerical tool 111
3.4.2 Implementation of the open loop model 112
3.4.3 Implementation of the closed loop model 117

3.4.4 Summary 118
3.5 Case study 120
3.5.1 Description of the case study 120
3.5.2 Methodology of validation of ESD simulator 123
3.5.3 Data collection 124
3.5.4 Summary 124
3.6 Estimation of parameters and model validation 125
3.6.1 Estimation of model parameters 125
3.6.2 Model validation 139
3.6.3 Control system tuning 146
3.6.4 Summary 147
3.7 Summary of the chapter 149
4 Analysis of capacity control solutions 151
4.1 Task description 152
4.2 Analysis of disturbance scenarios 153
4.2.1 Disturbance scenarios for compression stations 153
4.2.2 Disturbance scenarios for the specific case study 154
4.2.3 Summary 156
4.3 Analysis of the interaction between controllers 157
4.3.1 Case study 157
4.3.2 Beneficial interaction 158
4.3.3 Problematical interaction 159
4.3.4 Summary 162
4.4 Proposed modification to the control system 163
4.4.1 Definition of model-based feedforward controller 163
4.4.2 Generation of an empirical compressor map 164
4.4.3 Implementation of model-based feedforward controller 166
4.4.4 Tuning of model-based feedforward controller 168
4.4.5 Summary 170
4.5 Simulation results and performance evaluation 171
4.5.1 Simulation of boundary disturbances 171
4.5.2 Analysis of responses to the inlet pressure disturbance 180
4.5.3 Reduction of interaction between control loops 185
4.5.4 Summary 187

4.6 Summary of the chapter 188
5 Analysis of antisurge control solutions 189
5.1 Task description 190
5.2 Analysis of disturbance scenarios 191
5.2.1 Case study 191
5.2.2 Design point and off-load operation 192
5.2.3 Disturbance analysis and selection 192
5.2.4 Evaluation of performance for a controller 193
5.2.5 Summary 194
5.3 Control variables 195
5.3.1 Controlled variables 195
5.3.2 Manipulated variables 195
5.3.3 Disturbance variables 195
5.3.4 Summary 196
5.4 Model predictive controller 197
5.4.1 Linearized model of the process 197
5.4.2 Overview of the optimization problem 197
5.4.3 Cost function 198
5.4.4 Controller state estimation 200
5.4.5 Optimization constraints 201
5.4.6 Controller implementation 202
5.4.7 Controller tuning 203
5.4.8 Summary 205
5.5 Simulation results and performance evaluation 206
5.5.1 Analysis of the response of the open loop system 206
5.5.2 Analysis of the model predictive controller response 212
5.5.3 Comparison between PI and MPC responses 230
5.5.4 Second set of tuning parameters 237
5.5.5 Third set of tuning parameters 252
5.5.6 Discussion 265
5.6 Summary of the chapter 267
6 Investigation of supercritical fluid recycle for surge control 268
6.1 Task description 269
6.2 Analysis of disturbance scenarios 270

6.2.1 Case study 270
6.2.2 Disturbances analysis and selection 272
6.2.3 Evaluation of performance for a controller 273
6.2.4 Control system implementation 274
6.2.5 Summary 274
6.3 Preliminary analysis 275
6.3.1 Steady-state operation 275
6.3.2 Inlet valve of the system 275
6.3.3 Outlet valve of the system 280
6.3.4 Inlet pressure of the system 284
6.3.5 Outlet pressure of the system 289
6.3.6 Summary 292
6.4 Further analysis 293
6.4.1 Further analysis on boundary valve disturbances 293
6.4.2 Further analysis on boundary pressure disturbances 296
6.5 Analysis of full recycle operation 301
6.6 Discussion 304
6.6.1 Selection of gas recycle configuration 304
6.6.2 Subcritical and supercritical compression 306
6.7 Summary of the chapter 308
7 Critical discussion and future work 309
7.1 Summary of the methodology 310
7.1.1 Research tasks 311
7.1.2 Contribution of the project 311
7.2 Critical evaluation of the adopted methodology 312
7.2.1 Mathematical modelling of compressors 312
7.2.2 Parameter estimation and model validation 315
7.2.3 Model-based control 316
7.2.4 Hierarchy and timescales of process control 318
7.3 Critical evaluation of reported findings 320
7.3.1 Analysis of boundary disturbances 320
7.3.2 Industrial approaches to compressor control 323
7.3.3 Gas recycle configuration 324
7.4 Future research development 325

7.4.1 Compressor modelling 325
7.4.2 Compressor control 327
7.4.3 Supercritical compression 328
8 Conclusions 330
8.1 Conclusion of the project 330
8.2 Conclusion of the thesis 331
8.3 Conclusion of the research 332
8.3.1 Aims of the research activity 332
8.3.2 Tasks and contributions 332
8.3.3 Modelling of compression systems 333
8.3.4 Interaction between control loops 334
8.3.5 Performance parameters and surge margin representation 335
8.3.6 Control of pressure 336
8.3.7 Control of surge 336
8.3.8 Reduction of recycle flow rate 337
8.3.9 Effect of recycle configuration on control stability 337
8.3.10 Final comment 338
9 Appendix 339
9.1 Appendix 1: Implementation of the open loop model of the compression system 339
9.1.1 Main block 339
9.1.2 Inlet block 342
9.1.3 Outlet block 343
9.1.4 Recycle block 345
9.1.5 Compressor block 347
9.1.6 Inlet temperature and power block 350
9.1.7 Surge margin block 353
9.2 Appendix 2: methodology of validation of ESD Simulation Tool 355
9.2.1 Software interface 355
9.2.2 Steady state validation 357
9.2.3 Analysis of performance maps 358
9.2.4 Off-peak point analysis 358
9.2.5 Controller and alarm analysis 358
9.2.6 Cause-effect analysis on trips 359
9.2.7 Shut down procedure 360

9.2.8 Start-up procedure 361
9.2.9 Summary 363
References 364

List of figures

Figure 1-1. Compressors classification, modified from Totten et al. (2003) 35
Figure 2-1. Compressors classification, modified from Totten et al. (2003) 48
Figure 2-2. CAD image of a STC-SH single-shaft centrifugal compressor with horizontally split casing (Siemens, 2007) 49
Figure 2-3. Performance characteristic of a centrifugal compressor 51
Figure 2-4. Simplified representation of the compression system, modified from Greitzer (1976b) .. 56
Figure 2-5. Academic contributions to the research field of compressor modelling 59
Figure 2-6. Schematic representation of the compression system, modified from Morini et al. (2009) 61
Figure 2-7. Modular codes for compressor modelling 61
Figure 2-8. Avoidance and dynamic control of compressors..... 70
Figure 2-9. Block diagram for model predictive control, modified from Seborg et al. (2004b) 71
Figure 2-10. Model predictive control for compressor applications 77
Figure 2-11. Density of supercritical CO_2 as a function of temperature..... 80
Figure 2-12. Transportation of supercritical carbon dioxide 83
Figure 2-13. Modelling and simulation of CO_2 compressors 85
Figure 2-14. Control applications for supercritical CO_2 industry 86
Figure 3-1. Schematic representation of the compression system including a hot gas recycle..... 92
Figure 3-2. Model of the main compression line..... 93
Figure 3-3.Model of the main compression line including inlet and outlet throttling elements 96
Figure 3-4. Model of the compression system including main line and hot gas recycle line 97
Figure 3-5. Model of the compression system including main line and cold gas recycle line..... 98
Figure 3-6. Model of the compression system including main line and hot (left, a) or cold (right, b) gas recycle line..... 99
Figure 3-7. Cause-effect block diagram of a single-input single-output feedback controller 102
Figure 3-8. Cause-effect block diagram of a single-input single-output feedback controller in the Laplace domain..... 102
Figure 3-9. Capacity control system showing pressure transmitter PT and pressure controller PC .. 103
Figure 3-10. Cause-effect block diagram of a single feedback controller..... 104
Figure 3-11. Cause-effect block diagram of a cascade feedback controller..... 104
Figure 3-12. Antisurge control system showing mass flow transmitter MT and mass flow controller MC..... 105
Figure 3-13. Cause-effect block diagram of the antisurge feedback controller 105
Figure 3-14. Performance map for a single speed compressor..... 106
Figure 3-15. Performance map for a multiple speed compressor..... 106
Figure 3-16. Representation of the surge margin over time 108
Figure 3-17. Overall control system for a hot gas recycle compressor station 109
Figure 3-18. Cause-effect block diagram of multiple-input multiple-output control system for compression application..... 109
Figure 3-19. Open loop compression system 113
Figure 3-20. Simulink block for the open loop compression system..... 114

Figure 3-21. Parallel form of a generic PID controller (MathWorks, 2015f) 118
Figure 3-22. Schematic representation of the multistage compressor system (open loop) 121
Figure 3-23. Schematic representation of the multistage compressor system (closed loop) 122
Figure 3-24. Cause-effect block diagram 128
Figure 3-25. Compressor outlet pressure response to inlet pressure disturbance (stage 1) 129
Figure 3-26. Mass flow rate response to inlet pressure disturbance (stage 1) 130
Figure 3-27. Evaluation of the total inertia of the system 131
Figure 3-28. Compressor outlet pressure response to inlet pressure disturbance (stage 2) 132
Figure 3-29. Mass flow rate response to inlet pressure disturbance (stage 2) 132
Figure 3-30. Compressor outlet pressure response to inlet pressure disturbance (stage 3) 133
Figure 3-31. Mass flow rate response to inlet pressure disturbance (stage 3) 134
Figure 3-32. Compressor outlet pressure response to inlet pressure disturbance (stage 4) 135
Figure 3-33. Mass flow rate response to inlet pressure disturbance (stage 4) 136
Figure 3-34. Outlet pressure response to inlet pressure step change (stage 1) 139
Figure 3-35. Mass flow rate response to inlet pressure step change (stage 1) 140
Figure 3-36. Outlet pressure response to inlet pressure step change (stage 2) 141
Figure 3-37. Mass flow rate response to inlet pressure step change (stage 2) 141
Figure 3-38. Outlet pressure response to inlet pressure step change (stage 3) 142
Figure 3-39. Mass flow rate response to inlet pressure step change (stage 3) 143
Figure 3-40. Outlet pressure response to inlet pressure step change (stage 4) 144
Figure 3-41. Mass flow rate response to inlet pressure step change (stage 4) 144
Figure 4-1. Overall control system for a hot gas recycle compression system 153
Figure 4-2. Controlled variables during a negative step change of the system outlet pressure starting at t=10s 159
Figure 4-3. Manipulated variables during a negative step change of the system outlet pressure starting at t=10s 159
Figure 4-4. Controlled variables during a negative step change of the system outlet pressure starting at t=10s 160
Figure 4-5. Controlled variables during a negative step change of the system outlet pressure starting at t=10s (zoomed view) 161
Figure 4-6. Manipulated variables during a negative step change of the system outlet pressure starting at t=10s 161
Figure 4-7. Manipulated variables during a negative step change of the system outlet pressure starting at t=10s (zoomed view) 162
Figure 4-8. Cause-effect block diagram of the model-based feedforward controller (MBFC) 164
Figure 4-9. Generic representation of a performance map 165
Figure 4-10. Cause-effect block diagram of the closed loop model-based feedforward controller (MBFC) 167
Figure 4-11. Cause-effect block diagram of the overall control system for compression application including model-based feedforward controller and antisurge controller 167
Figure 4-12. Response of the pressure control system to a set point change for PI controller (master loop) 168
Figure 4-13. Response of the pressure control system to a set point change for PI controller (slave loop) 169

Figure 4-14. Response of the pressure control system to a set point change for MBF controller (master loop)..... 169
Figure 4-15. Response of the pressure control system to a set point change for MBF controller (slave loop)..... 170
Figure 4-16. Compressor outlet pressure following a positive step change of the system inlet pressure (scenario 2)..... 172
Figure 4-17. Compressor outlet pressure following a positive ramp change of the system inlet pressure (scenario 4)..... 173
Figure 4-18. Compressor outlet pressure following a negative step change (-20%) of the opening position of the inlet valve (scenario 7)..... 174
Figure 4-19. Compressor outlet pressure following a negative step change (-40%) of the opening position of the inlet valve (scenario 8)..... 174
Figure 4-20. Driver torque and rotational shaft speed (scenario 8)..... 175
Figure 4-21. Compressor outlet pressure following a positive ramp change of the system outlet pressure (scenario 12)..... 176
Figure 4-22. Compressor outlet pressure following a sinusoidal change of the system outlet pressure (scenario 14)..... 176
Figure 4-23. Compressor outlet pressure following a negative step change (-5%) of the opening position of the outlet valve (scenario 15)..... 177
Figure 4-24. Compressor outlet pressure following a negative step change (-10%) of the opening position of the outlet valve (scenario 16)..... 177
Figure 4-25. Compressor outlet pressure following a negative (-2%, above) and positive (2%, below) of the pressure set point (scenarios 17 above, scenario 18 below)..... 178
Figure 4-26. Compressor outlet pressure following negative ramp changes (slope -0.01, scenario 23) of the system inlet pressure..... 181
Figure 4-27. Compressor outlet pressure following positive ramp changes (slope 0.01, scenario 24) of the system inlet pressure..... 181
Figure 4-28. Compressor outlet pressure following negative ramp changes (slope -0.001, scenario 25) of the system inlet pressure..... 182
Figure 4-29. Driver torque and rotational shaft speed following negative ramp changes (slope -0.001, scenario 25) of the system inlet pressure..... 182
Figure 4-30. Compressor outlet pressure following positive ramp changes (slope 0.001, scenario 26) of the system inlet pressure..... 183
Figure 4-31. Driver torque and rotational shaft speed following positive ramp changes (slope 0.001, scenario 26) of the system inlet pressure..... 183
Figure 4-32. Compressor outlet pressure following sinusoidal changes (radial frequency 0.01 $rads^{-1}$, scenario 31) of the system inlet pressure..... 184
Figure 4-33. Driver torque and rotational shaft speed following sinusoidal changes (radial frequency 0.01 $rads^{-1}$, scenario 31) of the system inlet pressure..... 185
Figure 4-34. Compressor mass flow rates following sinusoidal changes (radial frequency 0.105 $rads^{-1}$, scenario 29) of the system inlet pressure..... 186
Figure 4-35. Compressor mass flow rates following sinusoidal changes (radial frequency 0.01 $rads^{-1}$, scenario 31) of the system inlet pressure..... 186
Figure 4-36. Oscillation of the operating point of the compressor following a sinusoidal disturbance (radial frequency 0.105 $rads^{-1}$, scenario 29) of the system inlet pressure..... 187

Figure 4-37. Oscillation of the operating point of the compressor following a sinusoidal disturbance (radial frequency 0.01 rads^{-1}, scenario 31) of the system inlet pressure 187
Figure 5-1. Controller state variables, modified from MathWorks (2015b) 201
Figure 5-2. Open loop system response following inlet valve opening 208
Figure 5-3. Open loop system response following outlet valve opening 208
Figure 5-4. Open loop system response following system inlet pressure decreasing 209
Figure 5-5. Open loop system response following system inlet pressure increasing 210
Figure 5-6. Open loop system response following system outlet pressure decreasing 211
Figure 5-7. Open loop system response following system outlet pressure increasing 211
Figure 5-8. Manipulated variables during disturbance scenario 3 213
Figure 5-9. Compressor outlet pressure during disturbance scenario 3 214
Figure 5-10. Compressor mass flow rates during disturbance scenario 3 214
Figure 5-11. Manipulated variables during disturbance scenario 6 215
Figure 5-12. Compressor outlet pressure during disturbance scenario 6 216
Figure 5-13. Compressor mass flow rates during disturbance scenario 6 216
Figure 5-14. Manipulated variables during disturbance scenario 9 217
Figure 5-15. Compressor outlet pressure during disturbance scenario 9 218
Figure 5-16. Compressor mass flow rates during disturbance scenario 9 218
Figure 5-17. Manipulated variables during disturbance scenario 13 219
Figure 5-18. Compressor outlet pressure during disturbance scenario 13 220
Figure 5-19. Compressor mass flow rates during disturbance scenario 13 220
Figure 5-20. Manipulated variables during disturbance scenario 17 221
Figure 5-21. Compressor outlet pressure during disturbance scenario 17 222
Figure 5-22. Compressor mass flow rates during disturbance scenario 17 222
Figure 5-23. Manipulated variables during disturbance scenario 20 224
Figure 5-24. Manipulated variables during disturbance scenario 20 (zoomed view) 224
Figure 5-25. Rotational shaft speed and opening of antisurge valve during disturbance scenario 20 225
Figure 5-26. Compressor outlet pressure during disturbance scenario 20 225
Figure 5-27. Compressor mass flow rates during disturbance scenario 20 226
Figure 5-28. Compressor power consumption and outlet temperature during disturbance scenario 7 227
Figure 5-29. Compressor power consumption and outlet temperature during disturbance scenario 11 228
Figure 5-30. Compressor power consumption and outlet temperature during disturbance scenario 15 228
Figure 5-31. Compressor power consumption and outlet temperature during disturbance scenario 16 229
Figure 5-32. Response of the pressure control system to a set point change for PI control 231
Figure 5-33. Compressor outlet pressure during disturbance scenario 24 232
Figure 5-34. Compressor mass flow rates during disturbance scenario 24 233
Figure 5-35. Manipulated variables during disturbance scenario 24 233
Figure 5-36. Manipulated variables during disturbance scenario 24 (zoomed view) 234
Figure 5-37. Compressor outlet pressure during disturbance scenario 29 235
Figure 5-38. Compressor mass flow rates during disturbance scenario 29 235

Figure 5-39. Manipulated variables during disturbance scenario 29 236
Figure 5-40. Manipulated variables during disturbance scenario 29 (zoomed view) 236
Figure 5-41. Manipulated variables during disturbance scenario 3 239
Figure 5-42. Compressor outlet pressure during disturbance scenario 3 240
Figure 5-43. Compressor mass flow rates during disturbance scenario 3 240
Figure 5-44. Manipulated variables during disturbance scenario 6 241
Figure 5-45. Compressor outlet pressure during disturbance scenario 6 242
Figure 5-46. Compressor inlet mas flow rate during disturbance scenario 6 242
Figure 5-47. Manipulated variables during disturbance scenario 9 243
Figure 5-48. Compressor outlet pressure during disturbance scenario 9 244
Figure 5-49. Compressor mass flow rates during disturbance scenario 9 244
Figure 5-50. Manipulated variables during disturbance scenario 13 245
Figure 5-51. Compressor outlet pressure during disturbance scenario 13 246
Figure 5-52. Compressor mass flow rates during disturbance scenario 13 246
Figure 5-53. Manipulated variables during disturbance scenario 17 247
Figure 5-54. Compressor outlet pressure during disturbance scenario 17 248
Figure 5-55. Compressor mass flow rates during disturbance scenario 17 248
Figure 5-56. Manipulated variables during disturbance scenario 20 249
Figure 5-57. Rotational shaft speed and opening of antisurge valve during disturbance scenario 20 250
Figure 5-58. Compressor outlet pressure during disturbance scenario 20 250
Figure 5-59. Compressor mass flow rates during disturbance scenario 20 251
Figure 5-60. Manipulated variables during disturbance scenario 6 254
Figure 5-61. Compressor outlet pressure during disturbance scenario 6 254
Figure 5-62. Compressor mass flow rates during disturbance scenario 6 255
Figure 5-63. Manipulated variables during disturbance scenario 10 256
Figure 5-64. Compressor outlet pressure during disturbance scenario 10 256
Figure 5-65. Compressor mass flow rates during disturbance scenario 10 257
Figure 5-66. Manipulated variables during disturbance scenario 14 258
Figure 5-67. Compressor outlet pressure during disturbance scenario 14 258
Figure 5-68. Compressor mass flow rates during disturbance scenario 14 259
Figure 5-69. Manipulated variables during disturbance scenario 17 260
Figure 5-70. Compressor outlet pressure during disturbance scenario 17 260
Figure 5-71. Compressor mass flow rates during disturbance scenario 17 261
Figure 5-72. Manipulated variables during disturbance scenario 20 262
Figure 5-73. Rotational shaft speed and opening of antisurge valve during disturbance scenario 20 262
Figure 5-74. Compressor outlet pressure during disturbance scenario 20 263
Figure 5-75. Compressor mass flow rates during disturbance scenario 20 263
Figure 6-1. Enthalpy of vaporization of carbon dioxide as a function of the temperature of the gas (modified from Knovel (2015)) 271
Figure 6-2. Mass flow rates for hot gas recycle configuration (disturbance scenario 3) 278
Figure 6-3. Mass flow rates for cold gas recycle configuration (disturbance scenario 3) 279
Figure 6-4. Compressor outlet pressure (disturbance scenario 3) 279
Figure 6-5. Manipulated variables (disturbance scenario 3) 280

Figure 6-6. Mass flow rates for hot gas recycle configuration (disturbance scenario 6)..... 282
Figure 6-7. Mass flow rates for cold gas recycle configuration (disturbance scenario 6) 283
Figure 6-8. Compressor outlet pressure (disturbance scenario 6) 283
Figure 6-9. Manipulated variables (disturbance scenario 6) 284
Figure 6-10. Mass flow rates for hot gas recycle configuration (disturbance scenario 11)..... 286
Figure 6-11. Mass flow rates for hot gas recycle configuration (disturbance scenario 11, zoomed view)..... 286
Figure 6-12. Mass flow rates for cold gas recycle configuration (disturbance scenario 11, zoomed view)..... 287
Figure 6-13. Compressor outlet pressure (disturbance scenario 11) 287
Figure 6-14. Manipulated variables (disturbance scenario 11, zoomed view)..... 288
Figure 6-15. Manipulated variables (disturbance scenario 11, zoomed view)..... 288
Figure 6-16. Mass flow rates for hot gas recycle configuration (disturbance scenario 15)..... 290
Figure 6-17. Mass flow rates for hot gas recycle configuration (disturbance scenario 15, zoomed view)..... 290
Figure 6-18. Mass flow rates for cold gas recycle configuration (disturbance scenario 15) 291
Figure 6-19. Compressor outlet pressure (disturbance scenario 15) 291
Figure 6-20. Manipulated variables (disturbance scenario 15) 292
Figure 6-21. Mass flow rates for hot gas recycle configuration (disturbance scenario 26, zoomed view)..... 297
Figure 6-22. Mass flow rates for cold gas recycle configuration (disturbance scenario 26, zoomed view)..... 298
Figure 6-23. Compressor outlet pressure (disturbance scenario 26) 298
Figure 6-24. Manipulated variables (disturbance scenario 26, zoomed view)..... 299
Figure 6-25. Schematic representation of the multistage compressor system (open loop) 303
Figure 7-1. Schematic representation of the multistage compressor system (open loop) – modified from Figure 3-24 314
Figure 7-2. Qualitative representation of pressure change along the points A, B and C 315
Figure 7-3. Antisurge piping configurations – modified from CCC (2013)..... 326
Figure 9-1. Inlet and outlet variables of the Simulink main block 340
Figure 9-2. Structure of the Simulink main block (tree diagram) 340
Figure 9-3. Structure of the Simulink main block 341
Figure 9-4. Inlet and outlet variables of the Simulink inlet block 342
Figure 9-5. Structure of the Simulink inlet block 343
Figure 9-6. Inlet and outlet variables of the Simulink outlet block..... 344
Figure 9-7. Structure of the Simulink outlet block..... 345
Figure 9-8. Inlet and outlet variables of the Simulink recycle block..... 346
Figure 9-9. Structure of the Simulink recycle block..... 347
Figure 9-10. Inlet and outlet variables of the Simulink compressor block 348
Figure 9-11. Structure of the Simulink compressor block 349
Figure 9-12. Structure of the Simulink compressor characteristic block..... 350
Figure 9-13. Inlet and outlet variables of the Simulink temperature-power block..... 351
Figure 9-14. Structure of the Simulink block for estimating compressor inlet temperature and power consumption 352
Figure 9-15. Inlet and outlet variables of the Simulink surge margin block 353

Figure 9-16. Structure of the Simulink surge limit block 354
Figure 9-17. Main window of the ESD simulation tool 356
Figure 9-18. Second compressor of the multistage configuration 356
Figure 9-19. Speed controller 357
Figure 9-20. Inlet valve of the system 361
Figure 9-21. Inter-stage isolation valve 362

List of tables

Table 2-1. Main properties of carbon dioxide 79
Table 3-1. Degrees of freedom analysis for the open loop model of the compression system 112
Table 3-2. Input and output variables for the open loop compression system 113
Table 3-3. Input and output variables for the compressor block 114
Table 3-4. Input and output variables for the inlet section 115
Table 3-5. Input and output variables for the outlet section 115
Table 3-6. Input and output variables for the recycle section 116
Table 3-7. Input and output variables for outlet temperature and power estimation 116
Table 3-8. Input and output variables for the surge estimation block 117
Table 3-9. Units of the process gains and time constants employed for evaluating the model optimisation 128
Table 3-10. Estimated parameters for the first stage of compression 129
Table 3-11. Comparison of time constants between reference data and optimised model (stage 1) 130
Table 3-12. Comparison of process gains between reference data and optimised model (stage 1) . 130
Table 3-13. Estimation of moment of inertia for two compressor geometries 131
Table 3-14. Estimated parameters for the second stage of compression 131
Table 3-15. Comparison of time constants between reference data and optimised model (stage 2) 133
Table 3-16. Comparison of process gains between reference data and optimised model (stage 2) . 133
Table 3-17. Estimated parameters for the third stage of compression 133
Table 3-18. Comparison of time constants between reference data and optimised model (stage 3) 134
Table 3-19. Comparison of process gains between reference data and optimised model (stage 3) . 134
Table 3-20. Estimated parameters for the fourth stage of compression 135
Table 3-21. Comparison of time constants between reference data and optimised model (stage 4) 136
Table 3-22. Comparison of process gains between reference data and optimised model (stage 4) . 136
Table 3-23. Preliminary estimation of the geometrical dimensions of the compressor station 137
Table 3-24. Comparison of time constants between reference data and optimised model (stage 1, set data 2) 140
Table 3-25. Comparison of process gains between reference data and optimised model (stage 1, set data 2) 140
Table 3-26. Comparison of time constants between reference data and optimised model (stage 2, set data 2) 142
Table 3-27. Comparison of process gains between reference data and optimised model (stage 2, set data 2) 142
Table 3-28. Comparison of time constants between reference data and optimised model (stage 3, set data 2) 143

Table 3-29. Comparison of process gains between reference data and optimised model (stage 3, set data 2) 143
Table 3-30. Comparison of time constants between reference data and optimised model (stage 4, set data 2) 145
Table 3-31. Comparison of process gains between reference data and optimised model (stage 4, set data 2) 145
Table 3-32. Initial tuning of the capacity controller (assuming single loop controller) 146
Table 3-33. Tuning of the master loop of the cascade capacity controller 147
Table 3-34. Tuning of the slave loop of the cascade capacity controller 147
Table 3-35. Tuning of the antisurge controller of the first stage of compression 147
Table 4-1. Maximum variation for the boundary variables during off-load operation 155
Table 4-2. Maximum variation for the boundary disturbances during boundary disturbances 155
Table 4-3. Tuning parameters for slave and master controllers 168
Table 4-4. Disturbance scenarios for the inlet pressure of the system 172
Table 4-5. Disturbance scenarios for the inlet valve of the system 173
Table 4-6. Disturbance scenarios for the outlet pressure of the system 175
Table 4-7. Disturbance scenarios for the outlet valve of the system 177
Table 4-8. Disturbance scenarios for the pressure set point of the system 178
Table 4-9. Ramp disturbance scenarios for the inlet pressure of the system 180
Table 4-10. Sinusoidal disturbance scenarios for the inlet pressure of the system 184
Table 5-1. Maximum variation for the boundary variables during off load operation 192
Table 5-2. Maximum variation for the boundary disturbances during boundary disturbances 193
Table 5-3. Scaled measured and manipulated variables at the design point 201
Table 5-4. Constraints for measured and manipulated variables 202
Table 5-5. Sampling period and control horizons 203
Table 5-6. Initial tuning parameters for model predictive controller (tuning set 1) 205
Table 5-7. Final tuning parameters for model predictive controller (tuning set 1) 205
Table 5-8. Maximum variation for the boundary disturbances during boundary disturbances 207
Table 5-9. Steady state operation at the design point 212
Table 5-10. Disturbance scenarios for the inlet valve of the system 213
Table 5-11. Disturbance scenarios for the outlet valve of the system 215
Table 5-12. Disturbance scenarios for the inlet pressure of the system 217
Table 5-13. Disturbance scenarios for the outlet pressure of the system 219
Table 5-14. Disturbance scenarios for the pressure set point of the system 221
Table 5-15. Disturbance scenario 20: saturation of the rotational shaft speed 223
Table 5-16. Disturbance scenarios with highest recycle flow rate 226
Table 5-17. Tuning parameters for slave and master controllers 230
Table 5-18. Comparison between PI and MPC response during inlet valve disturbance scenarios 232
Table 5-19. Comparison between PI and MPC response during out valve disturbances 235
Table 5-20. Tuning parameters for model predictive controller (tuning set 2) 238
Table 5-21. Steady state operation at the design point 238
Table 5-22. Disturbance scenarios for the inlet valve of the system 239
Table 5-23. Disturbance scenarios for the outlet valve of the system 241
Table 5-24. Disturbance scenarios for the inlet pressure of the system 243
Table 5-25. Disturbance scenarios for the outlet pressure of the system 245

Table 5-26. Disturbance scenarios for the pressure set point of the system 247
Table 5-27. Disturbance scenario 20: saturation of the rotational shaft speed 249
Table 5-28. Tuning parameters for model predictive controller (tuning set 3) 252
Table 5-29. Steady state operation at the design point 252
Table 5-30. Disturbance scenarios for the inlet valve of the system 253
Table 5-31. Disturbance scenarios for the outlet valve of the system 253
Table 5-32. Disturbance scenarios for the inlet pressure of the system 256
Table 5-33. Disturbance scenarios for the outlet pressure of the system 257
Table 5-34. Disturbance scenarios for the pressure set point of the system 260
Table 5-35. Disturbance scenario 20: saturation of the rotational shaft speed 261
Table 6-1. Maximum variation for the disturbance variables during boundary disturbances 273
Table 6-2. Steady state operation at the design point 275
Table 6-3. Disturbance scenarios for the inlet valve of the system for hot gas recycle configuration 278
Table 6-4. Disturbance scenarios for the inlet valve of the system for cold gas recycle configuration 278
Table 6-5. Disturbance scenarios for the outlet valve of the system for hot gas recycle configuration 282
Table 6-6. Disturbance scenarios for the outlet valve of the system for cold gas recycle configuration 282
Table 6-7. Disturbance scenarios for the inlet pressure of the system for hot gas recycle configuration 285
Table 6-8. Disturbance scenarios for the inlet pressure of the system for cold gas recycle configuration 285
Table 6-9. Disturbance scenarios for the outlet pressure of the system for hot gas recycle configuration 289
Table 6-10. Disturbance scenarios for the outlet pressure of the system for cold gas recycle configuration 290
Table 6-11. Disturbance scenarios for the inlet valve of the system for hot gas recycle configuration 294
Table 6-12. Disturbance scenarios for the inlet valve of the system for cold gas recycle configuration 294
Table 6-13. Disturbance scenarios for the outlet valve of the system for hot gas recycle configuration 295
Table 6-14. Disturbance scenarios for the outlet valve of the system for cold gas recycle configuration 295
Table 6-15. Disturbance scenarios for the inlet pressure of the system for hot gas recycle configuration 297
Table 6-16. Disturbance scenarios for the inlet pressure of the system for cold gas recycle configuration 297
Table 6-17. Disturbance scenarios for the outlet pressure of the system for hot gas recycle configuration 300
Table 6-18. Disturbance scenarios for the outlet pressure of the system for cold gas recycle configuration 300
Table 6-19. Recycle variables for subcritical compression (third stage of compression) 302

Table 6-20. Recycle variables for supercritical compression (fourth stage of compression) 302
Table 7-1. Summary of the effect of the disturbance on controlled variables 320

Notation for compressor modelling and simulation

Symbol	Name	Unit
a_{01}	Sonic velocity at ambient conditions	ms^{-1}
A_1	Duct throughflow area	m^2
c_p	Specific heat at constant pressure	-
c_v	Specific heat at constant volume	-
CH	Control horizon	s
h_{01}	Specific gas enthalpy at compressor inlet	Jkg^{-1}
h_{02}	Specific gas enthalpy at compressor outlet	Jkg^{-1}
J	Moment of inertia	kgm^2
k_{ASV}	Antisurge valve constant	-
k_{in}	Inlet valve constant	-
k_{out}	Outlet valve constant	-
K_c	Controller proportional gain	-
K_d	Controller derivative gain	-
K_i	Controller integral gain	-
K_m	Process gain for mass flow rate	$kgs^{-2}m^{-1}$
K_p	Process gain for pressure	-
L_c	Duct length	m
m	Inlet mass flow rate of the compressor	kgs^{-1}
m_c	Corrected mass flow rate	kgs^{-1}
m_{ctrl}	Control mass flow rate	kgs^{-1}
m_{in}	Inlet mass flow rate of the system	kgs^{-1}
m_{out}	Outlet mass flow rate of the system	kgs^{-1}
m_{pout}	Outlet mass flow rate of the plenum	kgs^{-1}
m_r	Recycle mass flow rate	kgs^{-1}
m_{RV}	Mass flow rate of the recycle volume	kgs^{-1}
m_{surge}	Surge mass flow rate	kgs^{-1}
MH	Model horizon	s
n	Polytropic coefficient	-
N	Rotational shaft speed	rpm
N_c	Corrected rotational shaft speed	rpm
N_f	Derivative filter constant	-
op_{ASV}	Opening position of the antisurge valve	-
op_{in}	Opening position of the inlet valve	-
op_{out}	Opening position of the outlet valve	-
p	Pressure	bar
p_{01}	Inlet pressure of the compressor	bar
p_{02}	Outlet pressure of the compressor	bar
p_{in}	Inlet pressure of the system	bar
p_{out}	Outlet pressure of the system	bar
p_{ref}	Reference pressure	bar
p_{RV}	Pressure of the recycle volume	bar
PH	Prediction horizon	s
P_m	Power consumption of the compressor	kW
Q	Heat flow rate	J

Symbol	Name	Unit
r_2	Impeller radius	m
t	Time	s
t_s	Settling time	s
T	Temperature	K
T_{01}	Inlet temperature of the compressor	K
T_{02}	Outlet temperature of the compressor	K
T_{in}	Inlet temperature of the system	K
T_{out}	Outlet temperature of the system	K
T_r	Recycle temperature	K
T_{ref}	Reference temperature	K
v	Specific volume	m^3kg^{-1}
V	Plenum volume	m^3
x_i	Mass fraction of component i	-
z	Compressibility factor	-
β_d	Derivative time	-
β_f	First order derivative filter time constant	-
β_i	Integrator time	-
β_m	Process time constant for flow rate	s
β_p	Process time constant for pressure	s
B	Time constant	s^{-1}
$\mathrm{B_d}$	Time delay	-
γ	Specific heat ratio	-
η_p	Polytropic efficiency of the compressor	-
η_is	Isentropic efficiency of the compressor	-
μ	Sip factor	-
ρ	Density	kgm^{-3}
τ_d	Torque of the driver	Nm
τ_c	Torque of the compressor	Nm
ψ_c	Pressure ratio of the compressor	-
ω	Angular velocity	$rads^{-1}$

1. Introduction

This chapter is the introduction of the thesis. It introduces three main aspects:

- The Energy SmartOps Project
- The technology analysed and developed in the PhD project and therefore in the thesis
- The thesis itself.

The PhD project is part of the Energy SmartOps ("Energy savings from smart operation of electrical, process and mechanical equipment") Project, funded by the scheme Marie Curie Initial Training Networks (ITN), thankfully acknowledged. The principal aim of Energy SmartOps is to realise energy saving from integrated operation.

The structure of the chapter is the following. Section 1 is the introduction to the Energy SmartOps project and includes its general aim, the project consortium, the research objectives and the work packages.

Section 2 is the introduction to the technology and it covers in general terms the compression and transportation of carbon dioxide and the selection and control of gas compressors.

Finally Section 3 is the introduction of the thesis. It gives an overview on its content and structure and also introduces the novelty presented in the thesis and the research outcomes of the PhD project.

1.1 Introduction to the project

1.1.1 Energy SmartOps Project

1.1.1.1 General aim of Energy SmartOps Project

The PhD project focuses on control systems for centrifugal compressors, with an emphasis on carbon dioxide application. The project is part of the Energy SmartOps ("Energy savings from smart operation of electrical, process and mechanical equipment") Project, funded by the scheme Marie Curie Initial Training Networks (ITN). The main technical objective of the Energy SmartOps Project is to realise energy saving from integrated operation. Therefore this PhD project is about compressor control because good control saves energy and makes the process operation more efficient.

Energy SmartOps was a four-year project funded by the European Commission and it has been completed in January 2015. Its general aims are the integrated control and automation of systems processes, rotating machinery and electrical equipment and the optimization of equipment operation and workflows. The research objectives of the project have been divided into three main categories: equipment monitoring systems, performance monitoring and control and integrated energy saving. This PhD project falls within the second research objective, dealing with industrial centrifugal compressors and with their operation and control.

1.1.1.2 Energy SmartOps Consortium

Energy SmartOps is part of the FP7 Marie Curie ITN (initial training network) initiatives of the European Commission. It includes fifteen young researchers, at the early stage of their career, and also senior experts in drives, motors and rotating machinery, condition monitoring and signal analysis, automation, control and process operation, modelling and optimization. The applications include various industrial sectors such as chemicals, steel, oil and gas, power electronics and automation. Marie Curie ITN initiatives are based on mobility and training and therefore they are an opportunity for young and also experienced researchers to experience academic research as well as industrial research work.

The Energy SmartOps Consortium includes a network of academic and industrial partners. They are Imperial College London, ABB Germany, ABB Norway, ABB Poland, BASF, Cranfield University, ETH Zurich, ThyssenKrupp and Polytechnic University of Krakow. The associated partners of the project are ESD Simulation Training, Carnegie Mellon University and Statoil.

The partners of the interdisciplinary consortium have been working together towards the common goal of energy saving. The industrial partners provide researchers with practical experience and hands-on training and also industrial case studies. On the other side the partner universities look at the more theoretical side of the engineering problems and they also provide short and long-term training, both technical and non-technical.

1.1.1.3 Research objectives and work packages

The general aim of Energy SmartOps has been divided in three research objectives:

- Research objective 1: To develop scalable and complete equipment monitoring system
- Research objective 2: To devise new algorithms for overall performance monitoring and control
- Research objective 3: To study ways that energy savings can be achieved.

The research objectives have been divided in the following work packages:

- Work package 1: electromachinery
- Work package 2: turbomachinery
- Work package 3: maintenance and diagnosis
- Work package 4: energy optimization
- Work package 5: electricity optimization.

The work package 2 has been divided into the following subtasks:

- Adaptive monitoring of condition and performance of centrifugal compressors
- Optimization of centrifugal compressor operation and maintenance
- Aerodynamic impact of fouling in centrifugal compressors
- Control systems for centrifugal CO_2 compressors.

1.1.2 PhD project

The PhD project focuses on operation and control systems for centrifugal compressors, with an emphasis on compression of carbon dioxide.

In the gas compression industry the control of the compressor has a key role in affecting the performance of the machine and its operating cost. There are two main control objectives: the operation of the machine according to the plant request, and its protection against damage i.e. surge. The antisurge controller is the part of the control system that protects the compressor against surge.

The purpose of antisurge control is to keep the flow through a compressor high enough to avoid the surge condition, achieved by opening a recycle valve which circulates gas back round and through the compressor. It is necessary to challenge cautious but wasteful operation with antisurge valves open. The energy to compress the gas is wasted when it is recycled.

However the surge phenomenon is not well understood yet and therefore a wide safety margin is usually adopted. This conservative approach results in the overprotection of the compressor. This lack of confidence of the design engineer is due to difficulty in fully understanding the dynamic behaviour of the machine, especially when it is inserted in the broad and unsteady context of a process plant. Moreover the integration between the capacity controller and the antisurge controller is small and generally limited to detuning or decoupling.

Therefore the necessity of further analysis in this area is evident. The industrial interest in this research field is also high due to the high operative costs related with gas compression.

The project focuses in particular on carbon dioxide compression. In fact there is a growing need for CO_2 compression for the development of new Carbon Capture and Sequestration (CCS) technology solutions. These solutions involve the separation of carbon dioxide from a main process stream, its compression to transport it to a storage site and then its storage. In this way it is possible to avoid the release of carbon dioxide into the atmosphere. The reason why CCS is needed is because of climate change. There are several potential remedies for dealing with climate change. CCS will be an important technology in future and it requires carbon dioxide compression.

Saving energy is beneficial in its own right because reducing energy consumption leads to reduced CO_2 emissions if the energy source is fossil fuel. Therefore the project makes contributions to the problems of handling carbon dioxide emissions in two ways.

Therefore the three main topics of research are:

- Analysis and improvement of the capacity controller
- Analysis and improvement of antisurge controller and its integration with the performance controller
- Investigation of supercritical transition in the compression of carbon dioxide.

1.1.3 Project outcomes

The main outcomes of the PhD project include publications and presentations at international conferences, collaboration with the partners of the Energy SmartOps consortium and outreach activities. They have been briefly summarised in the following sub-sections.

1.1.3.1 Publications and presentations

Publications include:

- Budinis, S. & Thornhill, N. F. (2014) An integrated control technique for compressor operation. *10th International Conference on Control*, 9th-11th July 2014 Loughborough University (Budinis and Thornhill, 2014)
- Budinis, S. & Thornhill, N. F. (2015). Control of centrifugal compressors via model predictive control for enhanced oil recovery applications. *2nd IFAC Workshop on Automatic Control in Offshore Oil and Gas Production*, May 2015a Florianópolis, Brazil (Budinis and Thornhill, 2015a)
- Budinis, S. & Thornhill, N. F. (2015). Supercritical gas recycle analysis for surge control of centrifugal compressors. *PSE2015/ESCAPE25*, May 2015b Copenhagen, Denmark (Budinis and Thornhill, 2015b)
- Budinis, S. & Thornhill, N. F. (2015). Supercritical gas recycle analysis for surge control of centrifugal compressors. *Computer Aided Chemical Engineering: Special Issue* (invited paper) (Budinis and Thornhill, 2015c).

Conference presentations include:

- 2013 AIChE Budinis, S., Thornhill, N. F. & Fabozzi, D. (2013). A control technique based on compressor characteristics with applications to carbon capture and storage systems. *2013 AIChE Annual Meeting*, 7th November 2013 San Francisco CA (Budinis et al., 2013)
- Budinis, S. & Thornhill, N. F. (2014) An integrated control technique for compressor operation. *10th International Conference on Control*, 9th-11th July 2014 Loughborough University (Budinis and Thornhill, 2014)
- Budinis, S. & Thornhill, N. F. (2015). Control of centrifugal compressors via model predictive control for enhanced oil recovery applications. *2nd IFAC Workshop on Automatic Control in Offshore Oil and Gas Production*, May 2015a Florianópolis, Brazil (Budinis and Thornhill, 2015a)
- Budinis, S. & Thornhill, N. F. (2015). Supercritical gas recycle analysis for surge control of centrifugal compressors. *PSE2015/ESCAPE25*, May 2015b Copenhagen, Denmark (Budinis and Thornhill, 2015b).

Internal presentations and posters include:

- Centre for Process System Engineering (CPSE) Annual Industrial Consortium Meeting 2012 (December 2012, Imperial College London)
- CPSE Annual Industrial Consortium Meeting 2013 (December 2013, Imperial College London)
- Energy Future Lab Annual Lecture 2014- Poster presentation (June 2014, Imperial College London)
- Chemical Engineering PhD Symposium (June 2014, Imperial College London)
- CPSE Annual Industrial Consortium Meeting 2014 (December 2014, Imperial College London)
- Energy Future Lab Annual Lecture 2015- Poster presentation (January 2015, Imperial College London).

1.1.3.2 Collaboration with partners

Within this PhD project the main collaboration took place with the company ESD Simulation Training. This company is an associated partner of the Energy SmartOps project. They provided technical training and also simulation tools for compressor applications. They also provided the case study presented later on in the thesis. The case study included data sheets for steady state operation and transient data for dynamic operation. Transient data were available through a fully validated industrial standard state-of-the-art simulation tool. The simulation tool was further tested and validated in the preliminary part of the PhD project. This activity will be described more in details in Chapter 3.

1.1.3.3 Outreach activities

Within Energy SmartOps, outreach activities took place in order to communicate the outcomes of the project to the public and inspire new generations towards science and engineering. The main outreach activities included:

- Participation in Imperial Festival 2014

- Publication of Energy SmartOps Blog
- Recording of a commercial video in collaboration with the associated partner ESD Simulation Training.

During Imperial Festival 2014 some of the early stage researchers had a stand with interactive games showing practical applications of mathematical modelling, simulation, control and optimisation. It was also an opportunity to speak with young people who were interested in a future as scientists or engineers.

A synoptic website (http://www.energy-smartops.eu/) has been created in order to inform the public about Energy SmartOps project, the project consortium and the scientific results. This website contains information about energy saving, links to resources, results from energy saving projects and finally summaries and short papers. A section of the website is called "Blog" and it aims at communicating science in simpler terms to a more general audience. The posts of the blog have been presented in the form of white papers.

Finally a commercial video was recorded in order to advertise the collaboration between Imperial College London and ESD Simulation Training within Energy SmartOps. The video is now publicly available on the media platform Vimeo (https://vimeo.com/116281783) and it has also been shared on the Facebook page 'ChemEng Discovery Space and Summer School' of Imperial College London (https://www.facebook.com/Chemengdiscoveryspace).

1.1.4 Consortium activities

The activities of the Energy SmartOps consortium included regular network meetings, secondments and training courses.

1.1.4.1 Network meetings and workshops

During the full duration of the project regular networking meetings took place each three to six months. The main aim of the meetings was to update the consortium regarding the research progresses. They were also an opportunity for group training such as workshops and industrial site visits.

1.1.4.2 Industrial secondment

A secondment has been undertaken in April 2012 at Xodus Group in Aberdeen, UK. Xodus Group is an independent energy consultancy operating worldwide in two energy markets: oil and gas and low carbon market.

The secondment took place within the Process Dynamics Group of Xodus Group. The team leader was Mr Craig MacKay and he was also the reference person for the duration of the secondment. Planned activities for the secondment covered both training and research into a specific case study.

The Process Dynamics Group offered the input data of a project they completed few months earlier. In this project a client has commissioned Xodus Group to carry out a dynamic simulation study of the proposed new Long Term Compression (LTC) facilities on an offshore platform. The LTC project involved installing a new booster compressor and associated equipment downstream of the high pressure (HP) separator. The pressure of the HP separator could then be reduced, thereby increasing the flow from the platform and subsea wells. Hydrocarbon gas was going to be returned to the existing process upstream of the inlet gas coolers.

The two main parts to this study were:

- Surge analysis of the compressor
- Start-up analysis.

The work of the secondment focussed on the surge analysis, specifically looking at:

- The operation of the proposed Cold Gas Bypass Loop
- Alternative surge protection methods.

In order to complete this activity the main technical challenges consisted of:

- Modelling a compression system starting from the client documentation and input data
- Using Aspen HYSYS for both steady state and dynamic modelling
- Modelling the control system of the compressor.

This secondment was an opportunity to:

- Train with Aspen HYSYS in the simulation of compressor applications
- Take a different work approach, focused on the requests of the client of Xodus
- Get insights on the state-of-the-art industrial practice for compressor control.

At the same time it involved theoretical aspects of modelling, simulation and control analysis of centrifugal compressors.

1.1.4.3 Training and education

Training has been undertaken by research on the job and within the PhD programme, both in the home institution and via secondment. Educational objectives included the attendance at technical courses covering the following areas:

- Control and operation of centrifugal gas compressors
- Practical aspects of process control and instrumentation
- Carbon dioxide compression
- Practical aspects of compressor control using the CCC system
- Process simulation and design
- Dynamic behaviour of process systems
- Advanced process operation.

The training program also included non-technical courses to improve personal skills (some examples include personal effectiveness, presentation skills, research effectiveness, writing skills, business and commercialisation skills and information skills) and language skills (including English and French).

1.1.5 Milestones of the PhD project

The main milestones of the PhD project consisted of:

- Research plan review (November 2011)
- English language assessment (December 2011)
- Early stage review (June-December 2012)
- Late stage review (December 2013).

All the previous reviews have been successfully completed within the official deadlines of the Chemical Engineering Department.

1.1.6 Summary

This section of the chapter has given an introduction on the PhD project presented in the thesis.

The PhD project focuses on operation and control systems for centrifugal compressors, with an emphasis on carbon dioxide application. It is part of the Energy SmartOps ("Energy savings from smart operation of electrical, process and mechanical equipment") Project, funded by the scheme Marie Curie Initial Training Networks (ITN).

The Energy SmartOps consortium is constituted by academic and industrial partners working together with the common goal of energy saving. Activities organised within the consortium included regular network meetings, industrial secondments, technical and non-technical training.

The outcomes of the project include conference presentations and publications, collaboration with industrial partners and outreach activities.

1.2 Introduction to the technology

1.2.1 Generation and utilisation of carbon dioxide

The interest towards carbon dioxide and its separation, compression, transportation, storage and utilization has progressively increased in recent years. This is due to the increasing awareness of climate change and its connection with atmospheric emission of greenhouse gases. These gases include carbon dioxide, methane, nitrous oxide and fluorinated gases. Anthropogenic activity has increased the concentration of CO_2 into the atmosphere from 280 ppm to 384 ppm (Plasynski et al., 2009). For this reason recent studies and international directives and guidelines (IPCC, 2007) are suggesting to reduce carbon dioxide emission in order to stabilize its concentrations in the atmosphere at 450–550 ppm by 2050 (Page et al., 2009). In order to do so, carbon dioxide generated by the industrial sector should be either used as a chemical feedstock or stored rather than being emitted (Song, 2006).

1.2.1.1 Generation of carbon dioxide

Carbon dioxide is generated via different chemical reactions but especially via fuel combustion. The main industrial sources of CO_2 emissions are the following industrial sectors:

- Power generation
- Cement production
- Fertilizer production
- Ammonia production
- Fermentation
- Natural gas separation (Hunt et al., 2010).

1.2.1.2 Utilisation of carbon dioxide

On the other hand carbon dioxide can be directly used in a wide variety of processes. Some examples include:

- Small volume applications such as fire suppression, carbonation of beverages, food preservation and refrigeration
- Supercritical extraction processes involving edible materials such as hops, coffee and oils
- Synthesis of esters, lactones, carbonates, urea, salicylic acid and polycarbonate (Centi and Perathoner, 2009)
- Reactions of hydrogenation, hydroformylation, oxidation, polymerization, biocatalysis and CO_2 reforming
- Biological fixation (Hunt et al., 2010)
- Conversion into fuels such as alcohol, methanol and syngas (Centi and Perathoner, 2009, Jiang et al., 2010, Omae, 2006).

Nevertheless there are market size limitations as the need for carbon dioxide is much lower than its industrial production. For example it has been estimated that about 5 to 10% of the total CO_2

emissions could be suited for fuels and chemicals production (Centi and Perathoner, 2009). Other barriers for the utilization of carbon dioxide are the cost of capture, separation, purification and transport, the energy requirement for chemical conversion and also the lack of socio-economical driving forces (Song, 2006). In the past this surplus of carbon dioxide was released into the atmosphere. The main reason was that CO_2 is a colourless and odourless gas, chemically unreactive and does not support combustion (Daintith, 2008). At ambient concentration it is not toxic (Pohanish, 2012) and therefore its release into the atmosphere was widely accepted. However its concentration has increased by 12% in the last 100 years and this has been postulated as the main cause of the average increase of 0.5°C in global temperatures over the same period (Daintith, 2008).

1.2.2 Carbon capture and storage

In order to reduce the carbon dioxide emission and compensate for the market surplus, carbon capture and storage technology (CCS) has been proposed as a technology aiming at capturing and storing CO_2 in long term geological reservoirs. This technology can be applied where there is a static continuous source of carbon dioxide, for example a power generation plant.

1.2.2.1 Separation processes

Carbon capture and storage offers at the moment three different types of separation processes:

- Post combustion separation, where CO_2 is separated after fuel combustion from the flue stream via absorption, adsorption or membrane separation
- Precombustion, where the fuel is gasified in order to obtain a hydrogen-rich fuel and CO_2 is typically separated via solid solvent
- Oxycombustion, where the fuel is burnt with pure oxygen and CO_2 can be easily separated from water via water condensation (Gibbins and Chalmers, 2008)

Carbon capture and storage is currently feasible based on existing technology. The separation, compression and injection of carbon dioxide have already been practised for many years in the oil and gas sector in order to enhance oil recovery. However CCS is facing many barriers to its development. Many of these barriers are non-technical and include lack of funding and legal and regulatory framework. The main technical challenges include operating costs of CCS plant and identification and monitoring of suitable storage sites.

1.2.2.2 Energy penalty of CCS

The capture of CO_2 is the most expensive step within CCS technology (Gibbins and Chalmers, 2008). Although separation via liquid absorption using monoethanolamine (MEA) and ceramic and metallic membrane represent promising capture options (Aaron and Tsouris, 2005), the cost of the separation step remains around 75% of the total cost (Plasynski et al., 2009). This cost also includes gas conditioning processes such as dehumidification, removal of impurities and compression. The cost of these processes depends on many factors such as gas composition, pressure and

transportation mode and they can be estimated to be around 90-120 kWh per tonne of CO_2 (Pires et al., 2011). For a power generation plant based on sub-critical pulverized coal combustion, the overall energy penalty of CCS technology is around 43.5%. Within this penalty, 9.3% is due to compression alone (Page et al., 2009). Also General Electric (GE) quantified the reduction in efficiency of a CCS plant due to compression and transport to 6-10% (GE, 2011). Therefore there is clearly a need to reduce the cost of the gas conditioning processes and especially the cost of the compression of CO_2 in order to enhance the development of CCS and reduce its energy penalty.

1.2.3 Transportation of carbon dioxide

Compression of carbon dioxide is necessary in order to transport it as it reduces its specific volume. Pipelines are employed when a high volume of fluid must be transported (Plasynski et al., 2009). The cost of transportation varies depending on the regions of construction of the pipeline, its length and design capacity (McCoy and Rubin, 2008) and it is also affected by the concentrations of impurities and water. Various equations of state such as Peng and Robinson (1976) and Soave (1972) have been used to represent the behaviour of carbon dioxide in the subcritical and supercritical states (Chaczykowski and Osiadacz, 2012) however Span and Wagner (Span and Wagner, 1996) is considered nowadays the reference for pure carbon dioxide (Aursand et al., 2013). Technically CO_2 can be transported as gas, subcooled liquid or in the supercritical state. Operationally most of the pipelines transport gas in supercritical state. This is due to the thermodynamic properties of supercritical carbon dioxide, especially its high density and low pressure drop along the pipeline. Moreover temperature fluctuation would not cause two phase flow (Pires et al., 2011): with pipeline a stable condition is more desirable and therefore supercritical state is suggested (Svensson et al., 2004).

1.2.4 Selection of gas compressors

Gas compressors are employed in order to compress carbon dioxide to supercritical state. A classification of gas compressors according to Totten et al. (2003) includes the two following categories, also represented in Figure 1-1:

- Reciprocating compressors: single acting and double acting
- Rotating compressors: positive displacement (lobe, screw and vane) and dynamic (radial and axial).

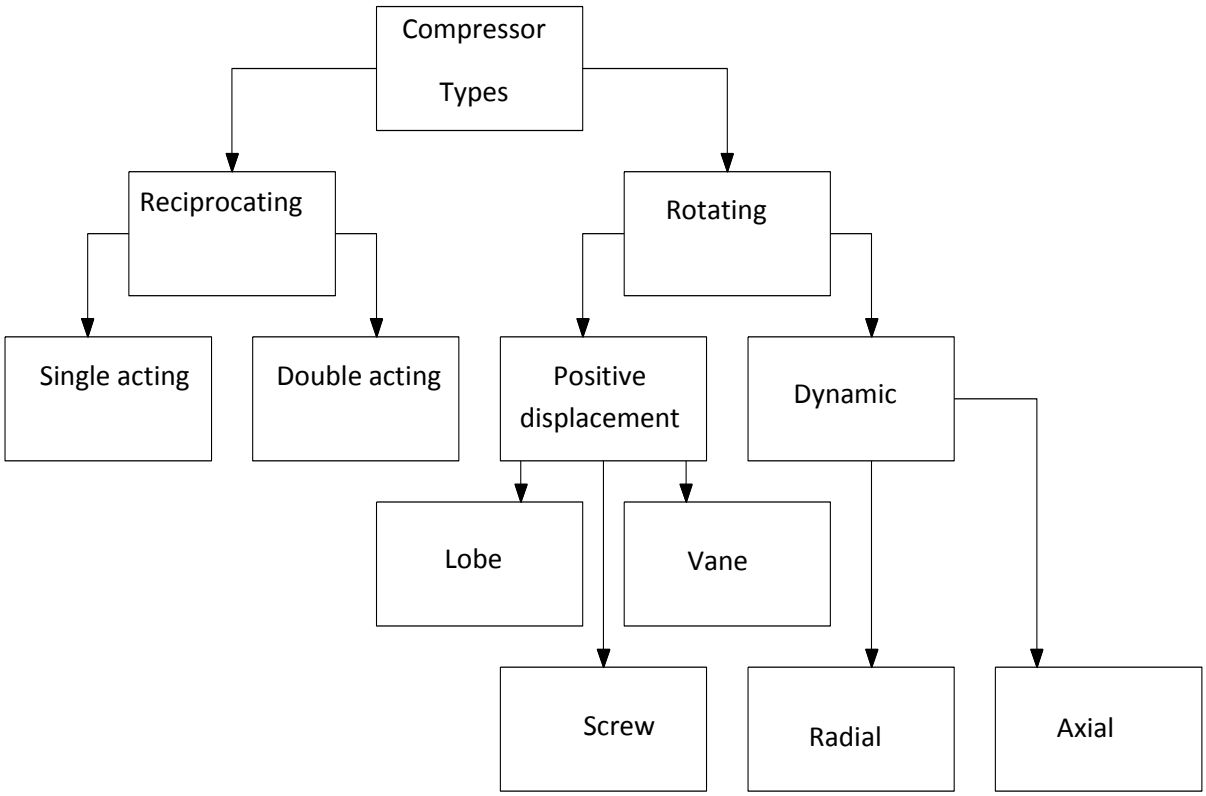


Figure 1-1. Compressors classification, modified from Totten et al. (2003)

The selection of the compressor depends on its operating range, expressed by flow rate and the pressure ratio. For medium-high flow rate ($0.47 m^3 s^{-1}$ to $4.72 m^3 s^{-1}$) and low-medium pressure ratio (2 to 20) rotating dynamic radial compressors are the most suitable machines (Brown, 2005). In order to compensate for the low pressure ratio of a single stage compressor, more compressors are placed in a multistage configuration in order to achieve the wanted discharge pressure. Pumps can also be used to boost compression along a pipeline when subcooled liquid is used (Zhang et al., 2006). Different options have been proposed by compressors suppliers and contractors working in the field of carbon capture and storage. Some examples include the following:

- General Electric suggests the use of reciprocating and centrifugal compressors, centrifugal pumps and integrally geared centrifugal compressors, proposing an overall compressor–pump train for discharge pressures above 200 bar (GE, 2011)
- Alstom also suggests the use of combined compressors and pumps (ALSTOM, 2014)
- Sulzer proposes the uses of pump for the compression of carbon dioxide before injection into the well (SULZER, 2010)
- Siemens employs integrally geared multistage centrifugal compressors (Siemens, 2014)
- Dresser Rand proposes multistage centrifugal compressors with interstage cooling and supersonic compressors derived from aerospace technology (Kidd and Miller, 2010).

1.2.5 Control of gas compressors

Compression stations need to be operated and controlled according to two main control objectives: compressor operation and compressor protection. These control objectives are usually handled by different process controllers. The interaction of these controllers is a known issue that has not yet been addressed and until now it has only been limited to decoupling or detuning.

The operation of the compressors needs to guarantee that the machine delivers the right amount of flow rate at the desired pressure. The compressor must meet the process demands and ideally its operating point should fall into the central part of its performance map, where the efficiency of the machine is higher. From a control point of view the controlled variable may be either pressure or flow rate of the compressor. On the other hand the protection of the machine needs to guarantee its integrity during operation and its protection against damage. The most dangerous condition for a centrifugal compressor is surge. Surge is a dynamic instability of the flow that takes place when the compressor does not meet anymore the load of the process. The flow reverses inside the machine causing strong vibrations that can damage blades, bearings and shaft (Boyce, 2012). In order to avoid surge, part of the gas is recycled back into the inlet of the machine, in order to increase the flow rate and push the compressor out of the surge region. Although many control architectures and algorithms have been proposed and sometimes tested in order to prevent surge, industrial practice for full size compressors still relies on gas recycle. Among the reasons for that are cost and reliability of the additional devices they require (Uddin and Gravdahl, 2012). On the other hand gas recycling increases the operating cost of a compression station as the recycled gas is compressed but it is not delivered as a final product of this plant section. Moreover when recycling supercritical carbon dioxide the thermodynamic properties of the gas change dramatically depending on the recycle configuration. This affects the amount of gas recycled and therefore the protection of the machine.

1.2.6 Summary

As a summary of what has been stated above, these are the challenges that have been identified and need to be addressed in the compression industry dealing with carbon dioxide:

- The cost of gas conditioning and especially the cost of compression
- The control and stability of the compression station
- The identification of the key issues in the compression and recycling of supercritical carbon dioxide

Therefore the general aims of this thesis are the following:

- The reduction of the cost of gas compression
- The reduction of the interactions between controllers in order to achieve process controllability and stability
- The identification of the key issues in the compression and recycling of supercritical carbon dioxide.

These aims will be presented in more detail at the end of the following chapter, after the review of the academic literature.

1.3 Introduction to the thesis

This section of the chapter is the introduction to the thesis. It includes the structure of the thesis with a short summary of each chapter. It summaries the novel contributions and also the research outcomes, presented in the form of abstracts of published papers.

1.3.1 Structure of the thesis

The thesis contains ten chapters including Chapter 1 and is structured in the following way.

Chapter 2 covers the literature review regarding the following research areas:

- Centrifugal compressor modelling and simulation
- Compressor and surge control
- Compression of carbon dioxide.

Regarding modelling and simulation of centrifugal compressors, steady state or quasi-steady approaches are not appropriate as they do not capture the dynamic behaviour of the compression system. Therefore a dynamic model must be used.

Regarding compressor and surge control, the main research focus of the academic community has been on surge control rather than on joint capacity and surge control. Different control strategies will be presented and they fall within three main categories: avoidance control, dynamic control, and model predictive control. All these control strategies were mainly focussing on surge control. Capacity control was almost neglected in the academic literature. However in a compression system, capacity and surge control have a strong interaction and the operation of the machine must be guaranteed together with its protection. Therefore an overall control approach is appropriate.

Regarding the compression of carbon dioxide, different equations of state have been investigated and the Span and Wagner equation of state is the most accurate. Few compressor configurations were specifically designed for the compression of carbon dioxide. In most cases natural gas facilities are employed. Control systems for carbon dioxide compression systems usually neglect the compressor itself.

Chapter 3 covers the following tasks:

- Modelling of the compression system
- Modelling of the reference control system
- Implementation of the model
- Description of the reference case study
- Validation of the model.

The model of the compression system includes a main forward process line and a secondary recycle line. Various configurations will be considered and they mainly differ because of the thermodynamic condition of the gas and the hold-up volume along the recycle line.

The modelling of the reference control system represents the state of the art control system for gas compressors. It includes two separate control loops. The interaction between the control loops should be reduced in order to guarantee smooth and stable operation and protection of the compressor from surge. The limitation of the current state of the art will be presented via analysis of the current practice and literature.

The implementation of the closed loop model includes the selection of modelling and simulation tool, of the method for the resolution of the algebraic and differential equations, of the input and output variables. The validation of the closed loop model is fundamental in order to guarantee the accuracy and reliability of the model. The estimation of the model parameters will be followed by the validation of the model. The validation of the model also includes the tuning of the feedback control system according to the desired performance.

The fourth chapter of the thesis has three main tasks to fulfil:

- Demonstration of control loops interactions
- Improvement of the response of the capacity controller
- Reduction of the interaction between control loops.

The improvement of the performance of the capacity controller will be achieved by proposing a model-based feedforward controller. It will be defined, implemented, tuned and tested. The controller will be compared with the traditional cascade PI controller during various disturbances.

Chapter 5 has three main tasks to fulfil:

- Analysis of the open loop response of the compression system
- Integration of pressure and surge control action
- Reduction of the recycle flow rate.

A linear model predictive controller will be proposed in order to control the compressor outlet pressure while avoiding surge. Different disturbance scenarios will be tested and three tuning sets will be proposed.

Chapter 6 has five tasks to fulfil. The first task involves the analysis of the disturbance scenarios able to cause the recycle of the gas from the outlet of the compressor to the inlet of the compressor. The second task requires the analysis of the recycle configurations in order to identify their tendency towards surge. The third task is the estimation of pressure control and stability of the compression system. The fourth task is the identification of the energy consumption of the systems. Finally subcritical and supercritical full recycle operation will be analysed and compared.

Chapters 7 is the critical evaluation of the results coming from the previous chapters and also includes suggestions for future development of the work here presented. Chapter 8 contains the conclusion of the thesis. Finally the thesis includes references and appendices.

1.3.2 Novel contribution of the thesis

The novel contributions of the thesis can be here summarised as follow:

- Identification of research needs for compressor control
- Analysis of the effect of boundary disturbances on open and closed loop system
- Improvement of the response of the capacity controller
- Integration of pressure and surge control
- Definition of performance parameters for performance monitoring tools
- Representation of the margin between the operating point and the surge point over time
- Analysis of the effect of the recycle configuration on the response of the control system during supercritical compression of carbon dioxide.

1.3.2.1 Identification of research needs

This contribution is the results of the background analysis and literature review presented in Chapter 2. Some specific needs in the research areas of centrifugal compressor operation and control and carbon dioxide compression have been identified and they include:

- Improvement of the response of the capacity controller
- Reduction of control loop interaction by integrated control approach
- Investigation of supercritical CO_2 compression, operation and control.

More details will be given in Chapter 2.

1.3.2.2 Analysis of the effect of boundary disturbances on the system

Boundary disturbances have been employed in order to demonstrate their effect on the open loop compression system. In particular disturbance scenarios causing the recycle of the gas flow rate for surge protection are particularly interesting for the purpose of this thesis.

Various examples of interactions between control loops within the compressor control system will also be reported. These examples are employed in order to analyse and compare beneficial and problematic interactions between control loops. They demonstrate the importance of reducing the interaction between control loops.

1.3.2.3 Improvement of the response of the capacity controller

A model-based controller will be proposed in the thesis. It employs the compressor map in order to estimate the set point for the rotational shaft speed of the machine. In all the tested cases the controller will demonstrate better performance than the reference traditional PI controller. Simulation results will demonstrate that the rate of change of the disturbance does not affect the operation of the controller. Finally the simulation results will also demonstrate that better pressure

control reduces the oscillation of compressor mass flow rate and surge flow rate over time and therefore reduces the risk of gas recycle and potentially surge.

1.3.2.4 Integration of pressure and surge control

A model predictive controller will be proposed in order to provide integrated pressure and surge control. The results will demonstrate that the MPC controller is able to control the outlet pressure of the compressor while avoiding surge. Therefore pressure and surge control action has been integrated in a single controller. The results also demonstrate that the MPC controller is more suitable than a PI controller for a multiple-input multiple-output process system such as a centrifugal compressor. The tuning of the MPC controller has been performed in order to give priority to respectively energy saving, surge avoidance or pressure control performance. In all the tested cases the MPC controller performed as requested. Therefore the MPC controller can be tuned accordingly to the desired control purpose.

1.3.2.5 Definition of performance parameters

Performance parameters will be proposed in order to evaluate the performance of the control system for compression applications. These parameters will be focussing on various aspects of compressor operation and control such as:

- The distance of the controlled variable from their set points over time
- The amount of gas recycled for surge prevention
- The energy consumption of the compression system.

1.3.2.6 Representation of the surge margin

A novel method for representing the distance between the operating point of the compressor and the surge region will be presented. Traditional representation includes the employment of steady-state or corrected compressor maps. However this representation is not suitable when the system is affected by boundary disturbances and it is not in steady state.

1.3.2.7 Analysis of gas recycle for supercritical compression

The results presented in the thesis will demonstrate the effect of the recycle configuration on:

- Surge occurrence
- Overall control performance
- System stability
- Amount of gas recycled
- Energy consumption
- Amount of gas recycled during full recycle operation.

In the selection between hot and cold gas recycle the process parameters that are usually considered include time delay in the process response and machine integrity. In particular recycling of hot gas should be limited over time in order to guarantee the integrity of the machine. The results presented in the thesis will demonstrated that other aspects should be taken into account as well, especially when the process fluid is supercritical carbon dioxide. These aspects include:

- Surge occurrence
- Energy consumption
- Maximum recycle flow rate during full recycle operation.

1.3.3 Research outcomes

In the following part of the chapter, the abstracts of the papers listed in section 1.1.3.1 have been reported as evidence of novel outcomes of the work.

1.3.3.1 Abstract of the paper Budinis and Thornhill (2014)

"In the gas industry the control of the compression system has two primary objectives: the operation of the machine and also its protection against damage such as that following a surge cycle. The interaction between these two control actions can be strong, causing instability and oscillations. Moreover whenever the gas is recycled for surge protection, it is not delivered as final product and energy is wasted during its compression. These observations provide the incentive for better integrated control.

While many researchers have been working on the control of surge, not much has been done to improve the control of the performance or the integration between the two control objectives, even though this need has already been highlighted in the past.

The paper proposes a control scheme based on the characteristic map of the compressor, taking into account inlet disturbances. The proposed control solution is comparable to the state-of-the-art control solution under slow disturbance dynamics and allows a tighter pressure control during fast changing dynamics, reducing at the same time the proximity to the surge region. For this reason it represents a step forward in the direction of process control integration for compressor applications."

1.3.3.2 Abstract of the paper Budinis and Thornhill (2015a)

"The paper proposes a control system for integrated pressure and surge control of centrifugal compressors for enhanced oil recovery application. The proposed control system is based on linear model predictive control. A fully validated non-linear dynamic model was developed in order to simulate the operation of the compressor at full and partial load. The model of the compression system includes a main process line with the compressor and a recycle line with the antisurge recycle valve. Different disturbance and control tuning scenarios were tested and the response of

the model predictive controller was analysed, evaluated and also compared with a traditional control system. Temperature effects have been taken into account in the model of the process and in the constraint formulation of the MPC optimization problem. The results show that the proposed control technique is able to meet the process demand while preventing surge and also minimizing the amount of gas recycle."

1.3.3.3 Extended abstract of the paper Budinis and Thornhill (2015b)

"The compression of carbon dioxide for transportation and storage has progressively increased in recent years. This is due to its importance within carbon capture and storage technology, where large-scale transportation via pipeline network is suggested.

In order to increase the gas density while reducing the pressure drop along the pipeline, the gas is compressed to supercritical state. In order to do so, centrifugal compressors are the most suitable machines due to their operating range. Usually a series of compressors is necessary in order to achieve the needed pressure ratio. The supercritical transition takes place in the last compressor. However, practical problems can arise in the operation of such a compressor, especially when dealing with gas recycle for antisurge protection.

There is a gap in the literature on the effect of dealing with supercritical fluid while controlling a centrifugal compressor. Some studies have been conducted regarding the performance of compressors in the supercritical region, however there has been little work regarding the control system and the effect of dealing with high density fluid. Of particular interest is the antisurge recycle system because the transition from supercritical to subcritical state takes place along the recycle line when the antisurge valve opens. The amount of gas recycled is crucial for surge protection and it depends on the temperature and pressure of the gas.

Prior work on transcritical CO_2 compression operation is found from other research areas such as refrigeration plants and power generation based on a supercritical CO_2 Brayton cycle. However in the refrigeration industry the research goal is the thermal optimization of the cycle, reciprocating and positive displacement machines are used and therefore surge is not a problem. On the other hand, technology involving rotating dynamic compressors, such as power generation based on a supercritical CO_2 gas turbine, is still in the early stage of development. Therefore in the future it will need a suitable control system able to deal with the recycle of supercritical CO_2.

The paper reports on the analysis and design of control systems for centrifugal compressors when the operating fluid is supercritical CO_2. It demonstrates that the design of the control system of the compressor must take into account the state of the fluid. It also evaluates if the plant configuration allows compressor operation within a given surge margin.

In order to do so, a fully validated non-linear dynamic model was developed in order to simulate the operation of the compressor at full and partial load. The model includes a main process line with the compressor and also a recycle line with gas cooler and antisurge valve. A control system is implemented in order to control the outlet pressure of the machine while protecting it from surge by means of gas recycle.

Boundary disturbances were run in order to show their effect on the compression system and especially on the recycle line. Transient operations are simulated at various recycle temperatures in order to show the effect of this variable on the energy requirement of the process under multiple scenarios. The results show the impact of the operating conditions of the compression station on surge prevention and also their effect on the energy consumption, suggesting better ways of dealing with supercritical fluid while controlling a compressor."

1.3.4 Summary

This section of the chapter is the introduction to the thesis. It summarises the structure and the content of each chapter. It also summarises the novel contributions of the thesis and they consist of:

- Identification of research needs for compressor control
- Analysis of the effect of boundary disturbances on open and closed loop system
- Improvement of the response of the capacity controller
- Integration of pressure and surge control
- Definition of performance parameters for performance monitoring tools
- Representation of the operating point from surge over time
- Analysis of the effect of the recycle configuration on the response of the control system during supercritical compression of carbon dioxide.

The research outcomes have been presented in the form of abstract of published papers.

1.4 Summary of the chapter

This chapter is the introduction of the thesis. It introduces three topics: the PhD project, the research work and the thesis itself.

The PhD project focuses on operation and control systems for centrifugal compressors, with an emphasis on carbon dioxide application. It is part of the Energy SmartOps ("Energy savings from smart operation of electrical, process and mechanical equipment") Project, funded by the scheme Marie Curie Initial Training Networks (ITN). The outcomes of the project include conference presentations and publications, collaboration with industrial partners and outreach activities.

The challenges of the research work that have been identified and need to be addressed in the compression industry dealing with carbon dioxide are:

- The cost of gas conditioning and especially the cost of compression
- The control and stability of the compression station
- The identification of the key issues in the compression and recycling of supercritical carbon dioxide.

These challenges have been employed in order to define the general aims of the thesis:

- The reduction of the cost of gas compression
- The reduction of the interactions between controllers in order to achieve process controllability and stability
- The identification of the key issues in the compression and recycling of supercritical carbon dioxide.

The general aims have been divided in more specific tasks and therefore research contributions, here summarised:

- Identification of research needs for compressor control
- Analysis of the effect of boundary disturbances on open and closed loop system
- Improvement of the response of the capacity controller
- Integration of pressure and surge control
- Definition of performance parameters for performance monitoring tools
- Representation of the operating point from surge over time
- Analysis of the effect of the recycle configuration on the response of the control system during supercritical compression of carbon dioxide.

2 Review of Relevant Background

The previous chapter has given an introduction on the topic of carbon dioxide compression, centrifugal gas compressors and compressor control. Some challenges have already been identified and they include:

- Cost of gas compression
- Control and stability of the compression stations
- Compression and recycling of supercritical carbon dioxide.

This chapter covers the relevant background regarding the following research areas:

- Centrifugal compressor modelling and simulation
- Compressor and surge control
- Compression of carbon dioxide.

The main findings from the chapter can be summarised as follows.

Regarding centrifugal compressor modelling, the model proposed by Greitzer (1976b) is a strong reference that has been employed and further developed by other researchers. Main contributions include Hansen et al. (1981) who demonstrated that the model from Greitzer, originally developed for axial compressors, was also applicable to centrifugal compressors and Fink et al. (1992) who included the conservation of angular momentum in the turbocharger spool.

On compressor and surge control, White (1972) was the first scientist to propose gas recycling as a method to control surge. Dynamic control was firstly proposed in 1989 as a method to stabilise the compression system by feeding back additional disturbances. Dynamic control was introduced in its active form by Epstein et al. (1989) and in its passive form by Gysling et al. (1991). However dynamic control has not been successful in industrial application, mainly because of safety, reliability and also cost of such a system (Uddin and Gravdahl, 2012). Model predictive control was also proposed to control compression system. However, the temperature effects and minimisation of the recycle have not been included (Cortinovis et al., 2012) and this has been identified as a gap of knowledge in the field.

Finally regarding the compression of carbon dioxide, some studies have reported on compression and transportation of supercritical CO_2. In fact this gas has been employed for refrigeration and also for power generation via closed loop Brayton cycle. However the focus of research has mainly been the optimisation of the thermal cycle rather than the effect on compressor operation. Therefore there is a gap in the literature on the effect of supercritical fluid on compressor operation and control.

The structure of the Chapter is the following. Section 2.1 gives a general description of centrifugal compressors, covering their application, selection and geometry. It also presents their operating range and performances estimation and representation. Section 2.2 covers the topic of compressor and surge modelling. The need for understanding surge has pushed the scientific community to model its behaviour in order to predict its occurrence. Section 2.3 presents the development of

control systems for centrifugal compressors, starting from traditional avoidance controllers, to dynamic control theory and finally model predictive control. Section 2.4 discusses the main properties of carbon dioxide with a focus on compression and transportation. Design, modelling and simulations of centrifugal compressors for supercritical carbon dioxide are also included, together with their control systems. Finally Section 2.5 summaries the conclusions of the chapter, highlighting the main findings and the need for further research in the field.

2.1 Centrifugal compressor and their operation

2.1.1 Centrifugal compressors selection and geometry

A compressor is a device that increases the pressure of a fluid. The main reasons to increase the pressure of a fluid are storage and transportation.

Different types of compressors exist and they can be classified according to the following sketch.

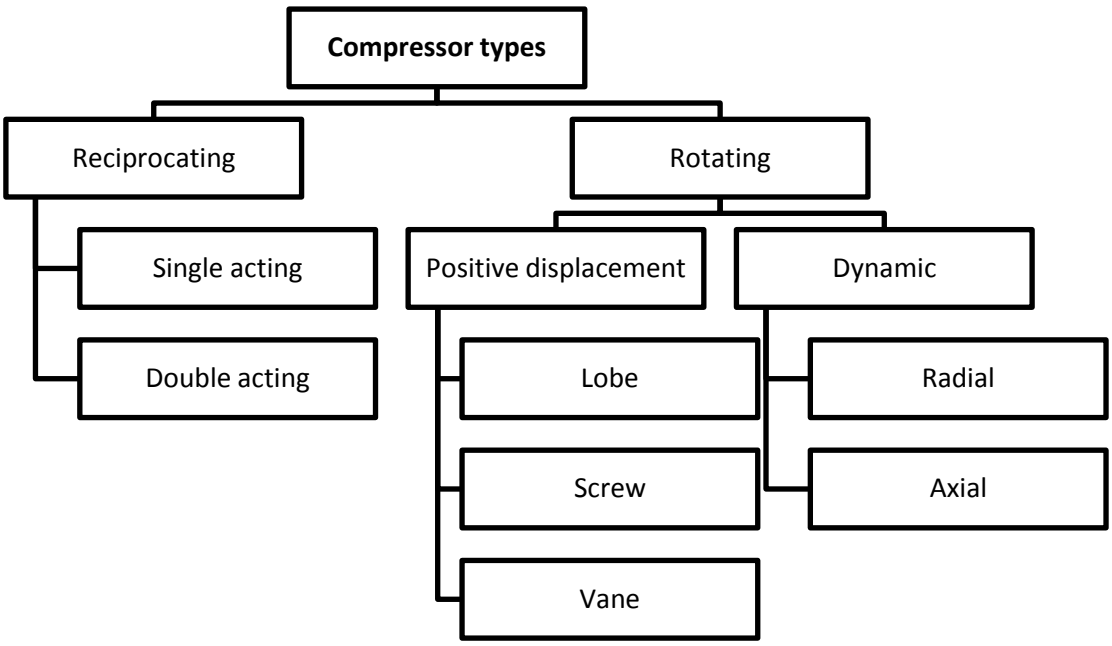


Figure 2-1. Compressors classification, modified from Totten et al. (2003)

Reciprocating compressors are used for high pressure and low flow rate applications. They compress the gas by reducing its volume by means of piston action. As the gas volume is decreased, its pressure increases. Reciprocating compressors may be single acting or double acting. Single acting compressors make use of a one-sided piston while double acting compressors make use of a double-sided piston.

Rotating compressors are classified as positive displacement compressors or dynamic compressors. A positive displacement compressor reduces the volume of the gas in order to increase its pressure. They can be lobe, screw or vane compressors. Dynamic compressors are either radial or axial compressors. They increase the speed of the gas by means of rotating blades. The gas is then discharged into a diffuser where the gas velocity is reduced and its kinetic energy converted to static pressure (Totten et al., 2003).

The selection of the most appropriate type of compressor depends on the specific application. The most important parameters for the selection are the process fluid, the flow rate and the pressure ratio. Axial compressors are usually employed for very high flows and low pressure ratios. Centrifugal compressors operate most efficiently at medium flow rates and high pressure ratios. Positive-displacement and reciprocating compressors are best employed for low flow rates and high pressure ratios.

This thesis concerns centrifugal compressors which are typically used in the process industries for large scale conveying of industrial gases such as natural gas, carbon dioxide, and air. The use of centrifugal compressors has been growing since the 1960s because of their efficiency, smooth operation, large tolerance to process fluctuations, lower maintenance costs and higher reliability than other types of compressors. Today they are the most employed machines in the process and pipeline industries. Within their operating range, centrifugal compressors have many applications. Centrifugal compressors operating in the process industry need large operating range while operating at a small pressure ratio. Some important applications of centrifugal compressors include (Boyce, 2003):

- Gas turbines
- Iron and steel industry
- Mining and metallurgy
- Natural gas
- Refrigeration
- Utilities.

In a typical centrifugal compressor, the main components include casing, bearings, seals, rotor assembly and stationary components. The case is the shell of the compressor and also its pressure-containing component. It houses the stationary internal components and the compressor rotor and can be horizontally or vertically split.

Centrifugal compressors are equipped with two radial bearings to support the rotor weight and one thrust bearing to ensure the desired axial position. Shaft seals are required to seal the gas inside the compressor while internal seals minimize internal recirculation losses.

The rotor assembly is fundamentally an assembly of impellers mounted on a steel shaft, as represented in Figure 2-2.

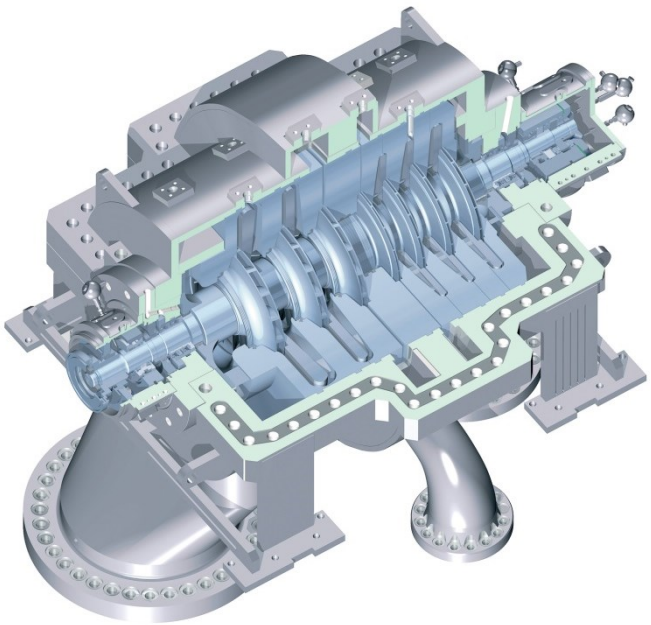


Figure 2-2. CAD image of a STC-SH single-shaft centrifugal compressor with horizontally split casing (Siemens, 2007)

The fluid impeller consists of inducer, usually an integral part of the impeller, and of blades that impart energy to a fluid. The velocity of the fluid is converted to pressure, partially in the impeller and partially in the following stationary diffuser. The diffuser consists of vane passages that diverge to convert the velocity head into pressure energy. In the centrifugal or mixed-flow compressor, the air enters the compressor in an axial direction and exits in a radial direction into a diffuser. From the exit of the diffuser, the air enters a scroll or collector.

2.1.2 Performance characteristics and operating range

In order to estimate the performance of a centrifugal compressor for both full and partial load operation the operational losses must be estimated. This evaluation is usually a combination of experimental and theoretical analysis. Centrifugal compressor losses can be divided into:

- Rotor losses: shock, incidence, disc friction, diffusion blading, clearance and skin friction losses
- Stator losses: recirculating, wake mixing, diffuser and exit losses (Boyce, 2012).

A loss in the compressor performance is usually expressed as a loss of enthalpy. The work in a compressor under ideal conditions occurs at constant entropy. Therefore isentropic efficiency can be estimated as the ratio between isentropic work and actual work. It can also be expressed in terms of enthalpy changes according to the following equation:

$$\eta_{is} = \frac{\Delta H_{isentropic}}{\Delta H_{actual}} \quad \textbf{(2-1)}$$

where η_{is} is the isentropic efficiency of the compressor while ΔH is the enthalpy variation.

Polytropic efficiency η_p is another type of efficiency, also called small stage or infinitesimal stage efficiency. It can be expressed as a function of the specific heat ratio γ and of the polytropic coefficient n according to the following equation:

$$\eta_p = \frac{\frac{\gamma - 1}{\gamma}}{\frac{n - 1}{n}} \quad \textbf{(2-2)}$$

The polytropic coefficient n defines the polytropic process via the equation $pv = constant$, where p is the pressure and v is the specific volume of the fluid.

The polytropic efficiency of a multistage compressor is equal to the single stage efficiency if each stage has the same efficiency. The polytropic coefficient is employed in order to estimate the polytropic head H_p according to Boyce (2003):

$$H_p = \frac{nRT_{01}}{n - 1}\left(\left(\frac{P_{02}}{P_{01}}\right)^{\frac{n-1}{n}} - 1\right) \quad \textbf{(2-3)}$$

where T_{01} and P_{01} are respectively the compressor inlet temperature and pressure, P_{02} is the compressor outlet pressure and R is the gas constant.

In the head equation, the ratio between the outlet pressure P_{02} and the inlet pressure P_{01} is called pressure ratio. The pressure ratio of the machine can be used instead of the head in order to express the performance of the compressor.

Compressor performance can be represented in various ways. In the following graph, the performance characteristic is represented as a function of the mass flow rate entering the compressor. Four speed lines are represented, where N_1 is the lower speed line while N_4 is the higher speed line.

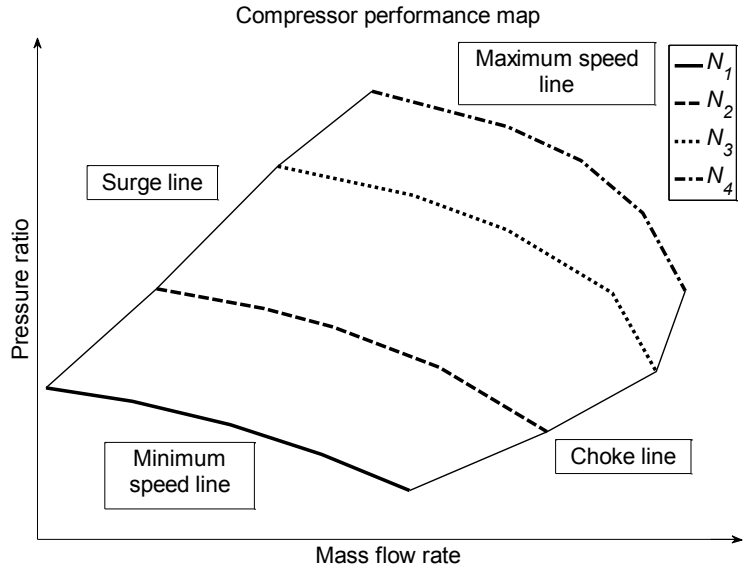


Figure 2-3. Performance characteristic of a centrifugal compressor

The area defined by the minimum speed line, the maximum speed line, the surge line and the choke line is the operating region of the compressor, also called compressor envelop. Minimum and maximum speed generally depend on the driver of the compressor, while surge and choke line depend on the compressor itself. For each constant speed curve, the operating margin of a machine is defined by the flow margin between the surge line and the choke.

2.1.2.1 Surge and choke lines

The surge line connects the surge points of each constant speed line. A compressor is in surge when the flow of the process fluid reverses direction inside the machine for short time intervals. When the flow reverts, the exit pressure drops below the inlet pressure and therefore this involves forward flow. This process is then followed by a rise in backpressure that causes the main flow to reverse again. This is called surge cycle and it persists if the operating condition of the machine does not change. If the cycle persists, it may result in irreparable damage to the machine, due mainly to

mechanical and thermal stress. Mechanical stress is caused by vibration of the machine connected with flow reversal, while thermal stress is due to local overheating of the flow.

The choke line indicates the maximum flow rate that can flow though a compressor at variable shaft speed. On the choke line Mach number is equal to one while on its right a phenomenon known as stone walling occurs, causing a rapid drop in efficiency and pressure ratio.

Other variables can limit the operating envelop, such as power or process limit, therefore the actual operating envelop may be smaller (Mirsky et al., 2012).

2.1.2.2 Corrected compressor map

The performance characteristic of a compressor is usually provided by the compressor supplier. It is determined via steady state experiments where the compressor runs at constant inlet conditions and various rotational shaft speeds and the operating point of the machine is recorded and plotted. However during normal operation of the compressor, when it is installed within a process plant, it operates in conditions that are not constant and that influences the compressor characteristic. The most important factors are:

- Molecular weight and compressibility of the process fluid
- Inlet pressure
- Inlet temperature
- Modification of the geometry of the compressor for example due to erosion or fouling.

If the composition of the gas remains constant and appropriate maintenance is in place in order to guarantee constant performance of the machine, then only inlet pressure and inlet temperature of the gas can influence the performance characteristic. In order to take into account this effect, it is possible to make use of corrected performance characteristics, such as corrected mass flow rate m_c and corrected rotational shaft speed N_c, defined as:

$$m_c = \frac{m\sqrt{T_{01}/T_{ref}}}{p_{01}/p_{ref}} \quad \textbf{(2-4)}$$

$$N_c = \frac{N}{\sqrt{T_{01}/T_{ref}}} \quad \textbf{(2-5)}$$

where T_{ref} and p_{ref} are respectively the reference temperature and reference pressure.

In 1996 Batson (1996), who was part of Compressor Control Corporation (CCC), presented a system of invariant coordinates in order to represent the interface between stable compressor operation and surge region. These coordinates were invariant to compressor suction conditions. He demonstrated that this system satisfied the requirement of dynamic similarity by applying the

Buckingham Pi Theorem on a compression system. He demonstrated that the use of an invariant coordinate system allows clear identification of the location of the surge line.

2.1.3 Summary

In this section of the thesis centrifugal compressor have been presented together with their application and operation. The operation of a centrifugal compressor can be represented on a map called compressor characteristic. This map includes the operating envelop of the machine, which is limited by four lines:

- Minimum rotational shaft speed line
- Maximum rotational shaft speed line
- Surge line
- Choke line.

The location of the surge line depends on the inlet condition of the gas and especially on its pressure and temperature. Corrected compressor maps can be employed in order to estimate the location of the surge region even with variant gas condition. Surge can seriously damage the compressor and for this reason a deeper investigation on this phenomenon and its modelling within compressor operation is presented in the next section.

2.2 Centrifugal compressor and surge modelling

2.2.1 Modelling of compressors and surge

Rotating stall and surge are two instabilities of the flow that take place inside the compressor under certain flow conditions. Surge was recognised for the first time by Stodola in 1924 (Stodola, 1924) while in 1953 Whittle (Whittle, 1953) identified it as a serious problem for the design of the first jet engines.

The work from Emmons et al. (1955) was the first one to report on surge and stall propagation. The existence of violent instabilities occurring in flow regimes characterised by high angle of incidence on the blades and low flow regime were already know at that time. However the generic term surge was used to indicate any flow instabilities. Typical symptoms were “audible thumping and honking” at the inlet or the outlet of the machine. Emmons emphasised the importance of being able to predict and control surge. Until that time experimental testing was vague and conflicting, however he assumed there were several modes of instabilities resulting in an overall flow instability. He was able to demonstrate the existence of two different instabilities, rotating stall and surge, through experimental investigation on both axial and centrifugal test rigs.

2.2.1.1 Dynamic non-linear model of compression system

In 1976 Greitzer (1976b) made a first distinction between rotating stall and surge while theoretically modelling an axial compression system. According to Greitzer, rotating stall involves only one sector of the cross sectional area of the compressor. In this sector the flow recirculates instead of moving forward and therefore the flow is circumferentially non uniform and the passage area is reduced. Instead during surge the flow oscillates axially and this perturbation involves the full cross sectional area of passage. Both phenomena were associated with oscillation of the flow, however the oscillation frequency of rotating stall was recognised to be one order of magnitude higher than the frequency of oscillation of surge. Greitzer highlighted the importance of distinguishing between rotating stall and surge as they have different consequences. If rotating stall takes place, the efficiency of the machine can go as low as 20% causing the overheating of the flow. This can locally damage the machine, especially the blades. If surge happens, the most likely consequence is vibration that can damage blades, casing and bearings. Before this publication, there were only qualitative analyses regarding the speed at which surge takes place and the effect of the plenum on the compressor operation. Other analyses covered operational areas close to the stable operating point and therefore they were not able to explain and model wide oscillations of the flow as those caused by surge. For these reasons Greitzer aimed at modelling rotating stall and surge and especially at providing a criterion that would have helped to distinguish them. In order to do so, he proposed the development of a dynamic nonlinear mathematical model of compression system that was able to simulate transient behaviour. He also compared the numerical results with the experimental results (Greitzer, 1976a).

In Figure 2-4 the simplified compressor sketch proposed by Greitzer is shown. The next page summarises the model of the compression system.

Equations of the model from Greitzer (1976b):

The model proposed by Greitzer included the following equations:

$$-\Delta P + C = \frac{L_c}{A_c}\frac{d\dot{m}_c}{dt} \quad \textbf{(2-6)}$$

$$\Delta P - F = \frac{L_T}{A_T}\frac{d\dot{m}_T}{dt} \quad \textbf{(2-7)}$$

$$\dot{m}_c - \dot{m}_T = \frac{\rho V_p}{\gamma P}\frac{dP_p}{dt} \quad \textbf{(2-8)}$$

Equation (2-6) is the first integral of the one-dimensional momentum equation expressed in terms of compressor mass flow. ΔP is the pressure difference across the duct while C is the pressure rise across the compressor. L_c and A_c are respectively the length and cross sectional area of the duct and $\dot{m}_c$ is the mass flow rate through the duct.

Equation (2-7) represents the flow rate through the throttle duct. F is the pressure drop across the throttle while L_T and A_T are respectively the length and the cross sectional area of the exit duct. $\dot{m}_T$ is the mass flow rate across the throttle valve.

Equation (2-8) is the continuity equation for the plenum, where ρ is the density of the fluid, V_p is the volume of the plenum, γ is the specific heat ratio and P_p is the pressure inside the plenum.

The equations he developed in order to predict the transient behaviour of the compression systems are the following, where the symbol ($\tilde{}$) indicate the nondimensionalised variables:

$$\frac{d\tilde{\dot{m}}_c}{d\tilde{l}} = B(\tilde{C} - \Delta\tilde{P}) \quad \textbf{(2-9)}$$

$$\frac{d\tilde{\dot{m}}_T}{d\tilde{l}} = \left(\frac{B}{G}\right)(\Delta\tilde{P} - \tilde{F}) \quad \textbf{(2-10)}$$

$$\frac{d\Delta\tilde{P}}{dt} = \left(\frac{1}{B}\right)(\dot{m}_c - \dot{m}_T) \quad \textbf{(2-11)}$$

$$\frac{d\tilde{C}}{d\tilde{t}} = \left(\frac{1}{\tilde{\tau}}\right)(\widetilde{C_{ss}} - \tilde{C}) \quad \textbf{(2-12)}$$

where $\tilde{l}$ is the effective flow passage and B and G are defined according to the following equations:

$$B = \frac{U}{2\omega L_c} \quad \textbf{(2-13)}$$

$$G = \frac{L_T A_C}{L_C A_T} \quad \textbf{(2-14)}$$

U is the impeller blade tip velocity while ω is the Helmholtz frequency.
The relaxation time parameter $\tilde{\tau}$ (also called nondimensionalised compressor time constant) was defined according to the following equation:

$$\tilde{\tau} = \left(\frac{\pi R}{L_C}\right)\left(\frac{N}{B}\right) \quad \textbf{(2-15)}$$

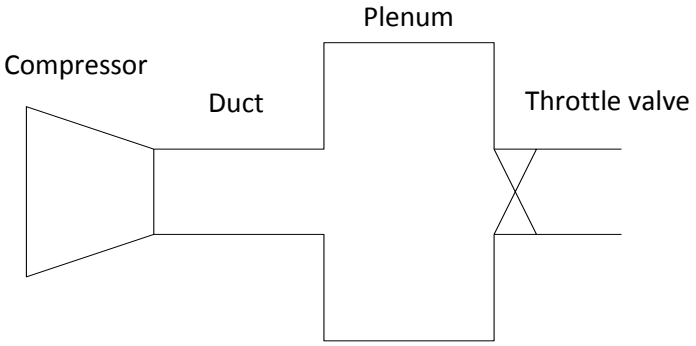


Figure 2-4. Simplified representation of the compression system, modified from Greitzer (1976b)

The main assumptions of the model from Greitzer were the following:

- The flow in the duct is incompressible
- Fluid velocities in the plenum are negligible
- Static pressure is uniform throughout the plenum at any instant of time
- $n = \gamma = c_p/c_v$ where n is the polytropic exponent.

The last assumption is a good approximation for ideal or quasi-ideal gas. Therefore it can be applied to low pressure gases.

Greitzer also analysed the shape of the curve representing the pressure rise as a function of flow rate. He recognised it as a non-linear function and he stated that it had to be obtained by experiments at steady state operation (as he described in Greitzer (1976a)). At that time it was not possible to predict the pressure rise function from a theoretical point of view. According to Greitzer, in previous analyses it was assumed that the compressor responded quasi-steadily to changes in mass flow. However he affirmed that a quasi-steady state modelling was not adequate as there was a definite time lag (around two stall cell revolutions or seven rotor revolution) between the onset of a fluid instability and its full development. Therefore he proposed a first order transient response model in order to simulate this lag, where he also included a relaxation time parameter.

The model highlighted in the panel on the previous page permitted the understanding that the transient response of an axial compressor system subsequent to a perturbation in operating conditions strongly depends on the nondimensionalised parameter B and on the shape of the characteristic curve. For B there was a critical value: above this value surge takes place, while below rotating stall takes place.

In 1981 Hansen (Hansen et al., 1981) demonstrated that the model from Greitzer was also applicable to centrifugal compressors. The transient compressor response to departures from steady state operation involves complex mechanisms that are different between axial and centrifugal compressors. However Hansen found a good agreement between the numerical results and the experimental results when the relaxation time employed was smaller than in the model from Greitzer.

Moore and Greitzer extended the previous work in order to describe the growth and also the possible decay of a rotating stall cell. They described pure rotating stall as steady but not

axisymmetric and pure surge as axisymmetric but unsteady. These two phenomena were described in Moore and Greitzer (1986) from a mathematical point of view, while the applications of the equations was described in Greitzer and Moore (1986). The final equations of the model presented in these two papers represented the circumferentially averaged flow coefficient, the total-to-static pressure rise and the squared amplitude of angular variations. The authors concluded that the ultimate mode of system response did not depend only on the parameter B presented in Greitzer (1976b) but also on the ratio between the length and the radius of the compressor l_c:

$$l_c = \frac{L_c}{R} \tag{2-16}$$

Compressors characterised by small values of l_c would more likely go into surge rather than rotating stall. The compressor characteristic ψ_c was defined as a cubic axisymmetric function depending on the flow coefficient ϕ. This notation has been used by many other authors afterwards.

2.2.1.2 Introduction of the turbocharger spool dynamic

Fink et al. (1992) attributed the occurrence of either surge or rotating stall to the compressor itself but also on the system in which the machine was installed. Fink stated that it was not clear if centrifugal compressors stalled before going into full surge. He also classified surge according to the amplitude of the mass flow fluctuation. Mild surge was characterised by oscillating forward flow while in deep surge the flow reversed. The work was divided into two parts, where the first part presented the experimental analysis of two compression systems. The first system had a large plenum volume and therefore a large value of the parameter B while the second system had a small plenum volume and therefore small B, thanks to a throttle valve placed immediately downstream the compressor. In the second part of the paper the model of the compression system was presented and included the effect of the variation of speed during the surge cycle on the operation of the compressor. The following assumptions were taken into account in this formulation:

- One-dimensional incompressible flow in the compressor duct
- Isentropic plenum expansion and compression
- Density and pressure discontinuity due to the compressor response simulated by a first order time lag
- Chocked throttle nozzle
- Short throttle duct length
- Negligible velocity in the plenum
- Negligible gas angular momentum in the compressor passages.

The major contribution of the model presented by Fink was the inclusion of the conservation of angular momentum in the turbocharger spool:

$$J\frac{d\omega}{dt} = \tau_d - \tau_c \tag{2-17}$$

where τ_d and τ_c are respectively the driver torque and the compressor torque while J is the moment of inertia of the overall driver-compressor system.

2.2.1.3 Further developments of the compressor model

In 1991 Botros (Botros et al., 1991) proposed a compressor model including the continuity equation, the polytropic pressure ratio, the polytropic head and the polytropic efficiency. The work was then extended in Botros (1994) in order to include the shaft inertia. In this way it was possible to accurately simulate fast transient operations such as surge protection and unit shut down. Therefore he confirmed that the equation of the shaft dynamic that Fink firstly introduced was an important feature of a compressor system model.

The effect of having a gas cooler in the recycle path was also analysed. Botros found that it might prevent the compressor backward spinning, depending mainly on the inertia of the unit and on the volume of the cooler. If the cooler was placed along the antisurge recycle path this could cause compressor surge under severe disturbances. Also the closure of the recycle valve during emergency shutdown could cause flow reversal within the compressor however it also resulted in decreasing the rate of deceleration of the machine. The dynamics of the recycle system were investigated further in Botros et al. (1996b) where transient phenomena following the emergency shutdown of the machine were studied both experimentally and numerically. Various process configurations were tested and the results demonstrated the importance of recycle valve prestroke time and overall inertia on surge occurrence. The recycle valve prestroke time is the time between valve open solenoid drop out and the start of stem movement. According to Botros the recycle valve prestroke time should be as small as possible. He also noticed that for higher shaft inertia the operating point of the compressor moved more slowly as the compressor decelerated during emergency shutdown. Therefore the risk of surge increased with smaller inertia values. Botros also concluded that the recycle valve should be placed as close as possible to the compressor, either upstream or downstream, in order to reduce the gas hold up volume along the recycle line.

In 1999 Arnulfi performed a surge analysis via experimental investigation (Arnulfi et al., 1999a) and numerical simulation (Arnulfi et al., 1999b) of a low-pressure multistage centrifugal compressor. This compression system was suitable for operation during fully developed deep surge and was tested with and without discharge plenum. The mathematical model of the compressor was derived from the model proposed by Greitzer (1976b) and then validated against experimental data. The model included a nondimensionalised time constant in order to take into account the delay in the compressor response. Surge was observed at low flow rates and at all the tested speeds when the compressor was connected to a large plenum. Therefore this demonstrated the influence of the hold-up volume on surge occurrence.

In 1999 Gravdahl and Egeland (1999) proposed a model for centrifugal compressor. The process configuration under analysis included the compressor itself, the compressor duct, the plenum volume and a throttle valve at the exit of the compression system. This model was based on the models of Greitzer (1976b) and Fink et al. (1992) and included the equation for the mass balance, momentum balance, moment of momentum balance and mass flow through the throttle valve. The model was later validated (Gravdahl et al., 2004) via experiments. The energy balance was used to develop the equation of the pressure rise of the fluid during forward flow. The compressor characteristic of the compressor was developed mathematically instead of being measured during

steady state experiments. For backward flow it was assumed that the pressure rise was proportional to the square of the mass flow.

Figure 2-5 summarises the main academic contributions to the research field of compressor and surge modelling.

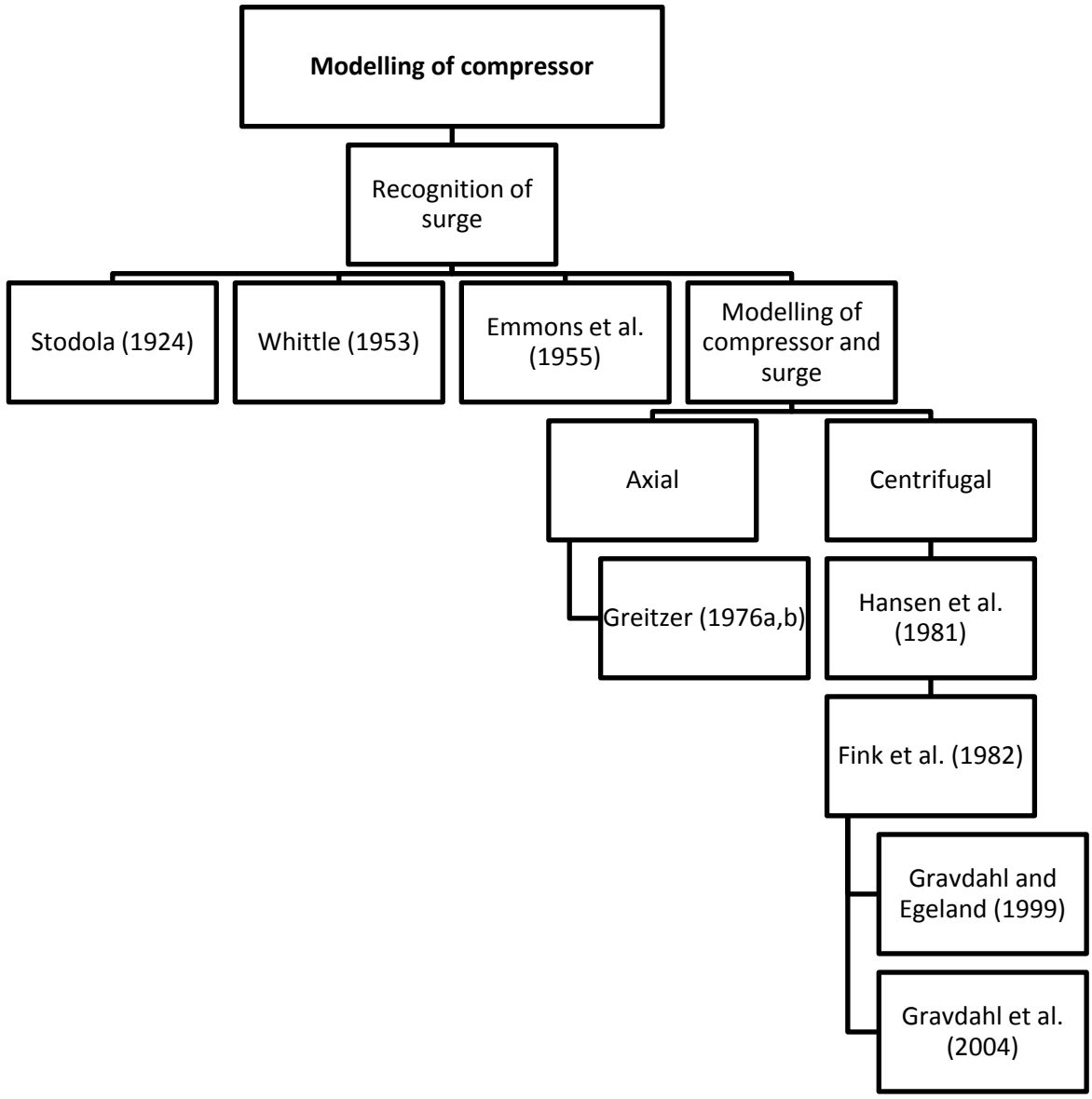


Figure 2-5. Academic contributions to the research field of compressor modelling

2.2.1.4 Modular codes for compressor modelling

In 2005 Venturini (2005) proposed a nonlinear modular dynamic model for the simulation of compression systems. The mathematical model was developed via a physics-based approach and included mass, momentum and energy balance, moment of momentum balance and thermal balance. The sensitivity analysis on the model parameters showed the influence of the friction factors on both inlet and outlet compressor pressures. The model was calibrated and validated against an axial-centrifugal compressor driven by an asynchronous reversible electric motor. The performance maps of the compressor were determined experimentally and then interpolated by

means of a second degree polynomial curve. The operating region of the compressor was identified between the surge line and the line of maximum flow rate for the given compression system.

A similar work was carried out by Camporeale et al. (2006) who proposed a modular code for the dynamic simulation of gas turbines. They emphasised the importance of dynamic modelling when simulating the operation of a machine over a wide operating range. Linearization of model equations had sometimes being adopted in order to reduce the computational effort. However it did not guarantee a good approximation. Therefore the paper described the mathematical model of the system and the solving procedure. The mathematical model proposed was a set of algebraic and ordinary differential equations describing the dynamic behaviour of the system. The model took into account the actual gas composition and the variation of the specific heats with the temperature. Both compressor and turbine were modelled as volume-less elements and a plenum was introduced in order to represent the hold-up volume of these two elements. The compressor was assumed to behave as a quasi-steady element during transient operation and therefore a steady state compressor map was adopted.

The model presented in Venturini (2005) was extended in Morini et al. (2007) in order to take into account reverse flow during compressor surge. In the paper four different types of surge were presented (mild, classic, modified and deep surge). Morini highlighted that surge and stall were recognised as coupled oscillation modes of the compression system and therefore should be considered together. The authors reviewed some models for stall and surge and grouped them according to their dimension:

- One-dimensional model, able to simulate surge but not stall
- Bi-dimensional models, able to simulate both stall and surge
- Three-dimensional models, based on computational fluid dynamics.

The model proposed in the paper was a one-dimensional non-linear dynamic model based on the equations of continuity and momentum balance for fluids and the momentum balance for rotating masses. Energy balances were also presented for both fluid and pipe however they were not implemented into the model. The system analysed included inlet and outlet ducts and the compressor. The main difference between this model and the model presented by Venturini (2005) was the definition of the characteristic curve of the compressor for both direct and inverse flow. For direct flow (normal operation) the characteristic curve of the compressor was defined by experiments on a test facility. The points were then interpolated using a second degree polynomial curve. For inverse flow (deep surge mode) the compressor characteristic was represented by pressure ratio and corrected mass flow rate via a third order polynomial function.

In 2009 Morini et al. (2009) proposed the analysis of the dynamic of a biogas compression system. The model developed and adopted was a non-linear one-dimensional modular dynamic model based on Morini et al. (2007). In this case the arrangement of the compression station consisted of both main line and recycle line and it is represented in Figure 2-6.

The recycle line included a fast acting recycle valve activated by the control system when the operating point of the compressor crossed the antisurge control line. The model included six continuity equations, five momentum balance equations, one equation for the spool dynamic and

three equations for the flow through the process valves. The flow through the valve depends on upstream and downstream pressure and on upstream density, according to:

$$m_v = k_v\sqrt{\rho_{in}(p_{in} - p_{out})} \quad \textbf{(2-18)}$$

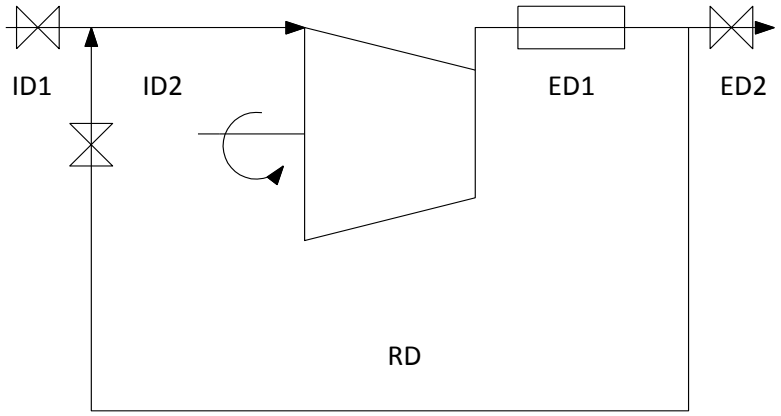


Figure 2-6. Schematic representation of the compression system, modified from Morini et al. (2009)

Starting from the model presented in Camporeale et al. (2006), Chacartegui et al. (2011) proposed a non-linear model for gas turbine incorporating a PI control system with serial lookup table. The authors tested three different control systems however they selected this one because of its stability, reliability and robustness.

Figure 2-7 summarises the references to the main modular codes for compression applications.

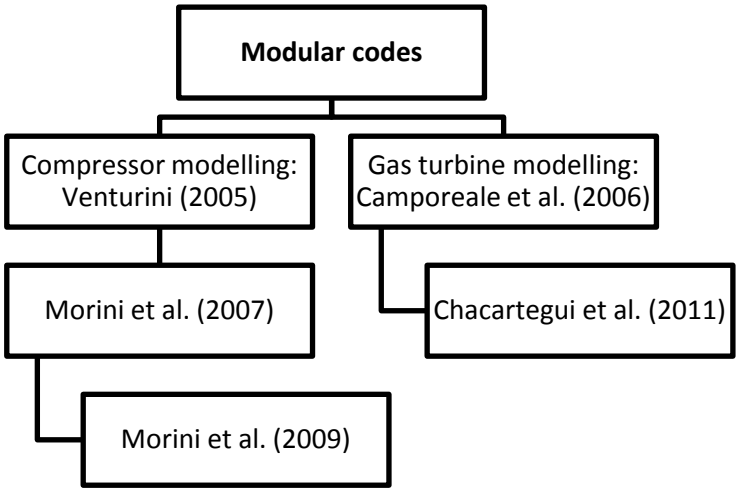


Figure 2-7. Modular codes for compressor modelling

2.2.2 Summary

In this section of the thesis the main contributions to the academic literature in the field of compressor and surge modelling have been presented and discussed. Some general conclusion can be here summarised.

Surge is a dangerous phenomenon for the operation of centrifugal compressors and it must be avoided. In its most intense form it causes flow reversal (deep surge) however it can happen in milder forms where an oscillation of the flow is already present. Rotating stall happens before surge however it can also happens on its own.

Regarding the compressor modelling:

- A complete model of a compression system must include the following equations: mass balance for the plenum element, momentum balance for the duct element, moment of momentum balance for the rotating shaft, the flow through the throttle valves, the equation of the torque of the compressor and the equation of the compressor characteristic
- Steady state or quasi-steady approach to compressor modelling and compressor characteristic modelling is not appropriate as it does not capture the dynamic behaviour of the compression system
- The compressor characteristic is usually fitted with second degree polynomial in the positive flow area and a third degree polynomial in the negative flow area.

The parameters influencing surge occurrence are:

- Hold up volume in the recycle line, expressed by different authors as: the position of the antisurge valve along the recycle line, plenum volume, gas cooler volume, B coefficient (equation (2-13)), l_c ratio (equation (2-16))
- Prestroke time of the antisurge valve
- Inertia of the overall compressor-driver system.

The importance of controlling surge is now clear. At the same time it is clear that process variables and parameters not strictly related with the compressor itself but rather linked with the recycle line are affecting surge. Therefore an overall control approach seems appropriate.

The next section covers the literature review on compressor and surge control in order to see how these problems have been handled until nowadays.

2.3 Control systems for centrifugal compressors

2.3.1 Traditional PID control

The previous section has presented the consequence of rotating stall and surge and how compressor operation and surge have been modelled in the academic literature. However the control system of a centrifugal compressor has two main control objectives, not only one. The first control objective is to operate the machine in order to meet the load of the plant. The second control objective is to protect the compressor from damage such as that caused by surge. Each control objective is addressed in industrial practice by separate controllers.

The *capacity controller* operates the machine in order to match either the pressure or the flow rate request from the plant. According to the controlled variable it can therefore be called pressure or flow controller. Some methods to control pressure or flow include (King, 2010):

- Throttling discharge
- Throttling suction
- Adjusting speed
- Inlet guide vane manipulation
- Recycle manipulation.

The *antisurge controller* maintains the operating point of the machine inside the operating envelop and specifically maintains the inlet flow rate of the compressor above the surge limit. In order to do that, it usually acts on a recycle valve, also called antisurge valve. This valve allows part of the compressed gas to be recycled back to the inlet of the compressor and therefore to increase the total inlet flow rate.

Some methods to measure and control surge include:

- Minimum flow upstream or maximum pressure downstream (King, 2010)
- Compressor pressure rise vs differential across suction flow meter
- Pressure ratio vs actual volumetric flow
- Break horsepower vs mass flow
- Pressure ratio vs Mach number squared
- Incipient surge
- Surge spike detection (Horowitz et al., 2006).

Recycling gas is not the only solution. Some other actuators are considered for this purpose, for example:

- Blow off valve
- Venting valve
- Flaring valve.

The selection of the actuator depends on the specific application. Two important parameters in order to evaluate the most appropriate actuator are the economic value and the toxicity of the

process fluid. For air compressor blow off valves are often employed as air cost is limited to the pre-treatment cost and the gas is non-toxic so it can be directly released into the atmosphere. Gas recycling is the most common practice in the oil and gas industry mainly because of the value of the product. In carbon dioxide applications there are two main reasons to recycle gas for surge protection and avoid its release:

- Carbon dioxide is not toxic however it can cause suffocation in confined environment due to the lack of oxygen
- CO_2 release into the atmosphere should be avoided when the purpose of the process plant is to reduce atmospheric emissions, such as in carbon capture and storage applications.

The interaction between capacity controller and antisurge controller is a known issue in industry and is usually prevented by:

- Detuning via relative gain
- Decoupling (Horowitz et al., 2006).

Detuning requires slowing down one of the controllers in order to reduce its response to disturbances. As the antisurge controller must always be able to respond quickly in order to prevent surge, the capacity controller is usually slowed down.

Decoupling aims at decomposing a multivariable process into a series of independent single-loop sub-systems. If such a situation can be achieved, the multivariable process can be controlled using independent loop controllers. However the interactions within a compressor station are strong and decoupling may not be feasible.

Therefore detuning and decoupling do not represent a robust, reliable control solution able to avoid control system interactions.

2.3.1.1 Surge avoidance via gas recycling

In 1972 White (White, 1972) was the first scientist to propose a surge control system based on gas recycle for surge avoidance and to present it in an academic publication. In his formulation he included the effect of temperature and molecular weight changes on the performance of the control system. The control configuration he proposed was very similar to the configuration that is still employed nowadays. The system included two differential-pressure transmitters. The first transmitter measured the differential pressure across the flow device in order to estimate the flow rate. The second transmitter measured the differential pressure across the compressor. White proposed a control margin between 20 and 25% and also gave some suggestions regarding complex compressor stations including machines in series or in parallel.

In 1994 Botros and Henderson (1994) wrote a review on industrial patents and academic publications on the previous 20 years regarding surge control for centrifugal compressors. They initially distinguished between surge control, surge detection and control and surge suppression. They found sixty-seven patents considered comprehensive and relevant. Among them, the trends indicated that most of the research activity was related with surge control rather than surge

detection or surge detection and control. The main reasons for the wide development of surge control technique was their wider scope, wider acceptance in industry, while a promising breakthrough was still missing in the surge detection research field. Two third of the patents were related to the development of surge prevention via either bleeding, venting or blowing off, with recycling preferred to bleeding. The authors noticed a shift from overall general control techniques to more specific detailed techniques that included:

- Conventional flow-ΔP control
- Flow rotational speed control
- Microprocessor and PLC based control
- Control without flow measurements.

The limited control techniques based on the detection of surge were based on:

- Temperature measurements
- Pressure measurements and pressure derivatives analyses
- A combination of pressure, speed and velocity measurements.

The authors noticed that in this latter field a major breakthrough was missing and mechanical components were not fast enough to act on time and prevent incipient surge. The most pressing need was the availability of fast acting recycle antisurge valves. Moreover process signals were not reliable and detection techniques were very specific to certain machines rather than being more general. Therefore these techniques were not well accepted in industry and especially in the gas transmission system, where system reliability and safety are mandatory.

For surge suppression there were mainly two types of publications. The first category regarded modification to the internal design of the compressor, where publications included:

- Modification of the impeller such as backward leaned angle at its exit
- Modification of the diffuser, for example to reduce its exit width
- Casing treatments such as inclined axial grooves or circumferential grooves.

The second category included modification of the compression system outside the compressor itself. This category required additional devices and component attached to the compressor either at its entrance or exit.

One suggested technique was to impose a pre-rotation to the fluid before the entrance of the compressor, for example by the use of inlet guide vanes. Another technique that was investigated later on was the use of a resistance element placed very close to the compressor discharge. This element was able to change the shape of the compressor characteristic and to separate the compressor from the system capacitance (or plenum) that was a basic component for surging. This study resulted very useful later as it helped the development of dynamic control techniques.

2.3.2 Active and passive control

Dynamic suppression of surge made use of active or passive control devices and was first initiated by the analyses of Greitzer (1976b) and Moore and Greitzer (1986) and then fully developed by Epstein et al. (1989) and Gysling et al. (1991). This control theory was based on suppressing flow perturbations when their amplitude was still low in order to prevent them from developing into surge. Dynamic control of compressor surge can therefore be divided in:

- Active control, aiming at actively suppressing surge by action of an actuator
- Passive control, aiming at passively suppressing surge by absorbing and then dissipating flow oscillations generated by surge.

2.3.2.1 Active control

In 1989 Epstein et al. (1989) proposed a control system for compressor surge based on what has been later called dynamic control. He was the first scientist talking about active control for compressor surge. He developed a control strategy in which additional disturbances were fed back into the compression system, by means of a moving plenum wall, in order to stabilise the operation of the machine. He analysed rotating stall and surge and in both cases the operating range of the machine was enlarged by up to 20%.

2.3.2.2 Passive control

In 1991 Gysling et al. (1991) proposed a dynamic passive control system for supressing surge and enlarging the operating region of the compressor. The theoretical analysis was developed for a generic compressor while the experimental validation was based on a centrifugal machine. Gysling was inspired by Epstein and thought that the key for dynamic suppression of surge was the dissipation of the disturbance energy. However he proposed a passive system constituted by a tailored structure able to stabilise the system via structural feedback. The structure he proposed was a movable plenum able to act as a mass-spring-damper system and absorb surge oscillations. The system he proposed was able to move the surge line to the left by 25% and also to suppress existing surge cycles. The effectiveness of the system was due to a set of nondimensional parameters governing the aeroelastic coupling between the wall of the plenum and the compression system dynamics.

2.3.2.3 Further developments of dynamic control

On these bases several experimental and theoretical studied were proposed in order to stabilise compression systems on the left of their surge line. The most relevant contributions were analysed by Gu (Gu et al., 1999), who wrote an overview on surge and stall for axial compressors. He distinguished between:

- Rotating stall, a severely non-axisymmetric distribution of the axial flow velocity around the annulus of the compressor
- Pure surge, axisymmetric oscillation of the mass flow along the compressor length
- Deep surge, mostly axisymmetric oscillation also involving reverse flow
- Classic surge, where rotating stall and surge are coupled.

He specified that the frequency of the surge oscillation was recognised to be about one order of magnitude smaller than the frequency of oscillation of stall.

Gu identified three important modelling developments in stall and surge control for axial compressors:

- The non-linear low order state-space model developed by Moore and Greitzer in 1986
- Simplified approaches based on bifurcation theory
- Linear control methods base on the use of inlet guide vanes as actuators and pursued by the MIT research group including Epstein (Epstein et al., 1989) and Paduano (Feulner et al., 1996, Paduano et al., 1993).

According to Gu three types of actuators were implemented and tested: inlet guide vanes, air injection and throttle valves. He suggested that a combination of these actuators should have been investigated.

Willems and de Jager (Willems and de Jager, 1998, Willems and de Jager, 1999) presented an overview on active control systems applied in experimental studies in order to stabilise rotating stall and surge in both axial and centrifugal compressors. According to them the main limitation regarding what was available in the literature was the lack of an accurate model able to describe all forms of instabilities. Moreover only feedback controllers were used, therefore they suggested the development of advanced model based controllers as a beneficial solution for stall and surge.

The authors distinguished between rotating stall and surge. Rotating stall was described as a two dimensional local instability phenomenon. According to their analysis, cells of stalled flow were rotating at a speed between 20 and 70% of the rotor speed. The annulus averaged compressor mass flow was steady in time however it was not circumferentially uniform. They also classified rotating stall as part span or full span stall and short length or long length scale cells. Rotating stalls caused a drop in compressor performance and efficiency and could also lead to thermal load of the machine.

Surge was described as a one dimensional instability that involved fluctuation of the pressure rise and of the mass flow. Willems and de Jager distinguished between mild surge, classic surge, modified surge and deep surge. The frequency of oscillations of mild surge was estimated to be around the Helmholtz frequency of the compression system, while deep surge had a much lower frequency. Surge caused loss of performance and efficiency and also blade and casing stress due to vibration and fluid overheating.

Although axial and centrifugal compressors generally present similar instabilities, the understanding of axial compressors was much deeper at that time. The reason was that in centrifugal compressors there was a very wide range of speed and geometries, and flow instabilities were affected by the matching between the different elements. The most important elements were diffuser geometry

and plenum volume. Rotating stall and surge were recognised to be related phenomena as the first one can trigger the second one and this was also demonstrated by experimental results.

As rotating stall and surge were caused by small amplitude disturbance, active control theory aimed at preventing the growth of these disturbances by feedback perturbation. Sensors and actuators were considered critical elements in active control. For surge prevention the use of a single sensor and a single actuator was demonstrated to be sufficient, while for rotating stall control an array of sensor was used. The reason was that the flow was not uniform and had to be monitored along the circumference of the compressors.

Willems and de Jager concluded recognising an improvement in the active control area however they also recognised that it was not implemented yet in industrial applications. Among the possible reasons they included weight, cost and reliability of additional sensors and actuators.

The work reported by these authors established the relation between rotating stall and surge and permitted a better understanding of both phenomena.

2.3.2.4 Control via close coupled valve and driver actuation

In 1999 Gravdahl and Egeland (1999) proposed an active control system that used a close coupled valve in order to stabilise the compressor operation. For the first time they included the angular velocity of the compressor in the controller formulation. This work was later extended (Gravdahl et al., 2002) in order to use the driver itself as actuator for surge prevention. The driver was already part of the compression system and therefore no additional actuation device was required. The model employed was the same presented in Gravdahl and Egeland (1999). It was based on the model from Fink et al. (1992) however it also included a speed dependent compressor characteristic. The open loop unstable operating points of the compressor map located on the left of the surge line were made stable. The work was further extended in Bohagen and Gravdahl (2008).

In 2011 Uddin and Gravdahl (2011) proposed an active control system based on a piston actuation. However it is interesting that this work was further extended (Uddin and Gravdahl, 2012) in order to include a back-up system in case of failure of the active control system. In this second publication the authors admitted that the active surge control system was mainly implemented in university laboratory and, although successful, they were not yet implemented in any industrial application. Among the reasons they highlight the safety and therefore reliability of such a system. The reason is that an active control system pushed the controller in an area of the compressor map that is open loop unstable i.e. on the left of the surge line. In case of failure of the active control system, the compressor would go immediately into surge.

In 2002 Blanchini and Giannattasio (Blanchini and Giannattasio, 2002) proposed an adaptive controller for the surge stabilisation of compression system. The controlled variable was the inlet pressure of the compressor while the manipulated variable was the position of the throttle valve located at the exit of the compressor plenum. The proposed controller was validated by both numerical and experimental testing.

In 2006 Arnulfi et al. (2006) wrote a review on dynamic control and proposed both an active and a passive control strategy for a compression application. They modelled the system using a lumped parameter approach, as Greitzer did. They proposed the concept of surge unsteady energy E as an index to measure surge intensity. E represented the difference between the area of the surge cycle and the area of the pressure cycle at the exit of the compressor. If the transient response τ is neglected then E is equal to the area of the surge cycle.

The active controller they proposed was a closed loop control system where the actuator was represented by a throttle valve placed at the exit of the compressor plenum.

The passive controller they proposed was a system with low natural frequency. It was represented by a hydraulic oscillator i.e. a water column. One surface of the water column was facing the atmosphere while the other surface was facing the gas contained in the plenum.

These two systems were both able to stabilise the system however they had different features. The passive control system did not require sensors or actuators or electronic devices that would need maintenance. It also showed better steady state performance. On the other hand the active controller was more versatile and could theoretically handle any type of control laws. It could also be tuned online and act on a wide range of disturbances.

In 2006 Boinov (Boinov et al., 2006) proposed an active controller of surge for centrifugal compressor via actuation of the driver speed. The controller was applied and tested on a fuel cell system and the aim was to improve the system efficiency during the reduced fuel cell load.

The work with a close coupled valve was driven by growing academic interest in dynamic surge avoidance. It reflects the latest academic state of the art.

2.3.2.5 Discussion

The main academic contributions to the field of avoidance and dynamic control of gas compressors are summarised in Figure 2-8.

The figure shows that many solutions for the dynamic control of surge have been proposed. They all aimed at stabilising the operation of the compressor on the left of the surge line by either feeding back disturbances into the control system or by absorbing and dissipating surge flow oscillation. It is interesting to notice that the lack of implementation of these control system in real industrial full size applications was mainly due to the nature of the dynamic control theory. A failure in a dynamic control system would mean surge, as all these system are open loop unstable. Other reasons did not help the development of the dynamic control theory, such as cost and reliability of sensors and actuators able to capture surge oscillations.
Moreover it is interesting to notice that surge control has received so much attention in the academic literature, while the same cannot be stated regarding capacity control. However it is important to remember that both controllers act on the same system and therefore, once more, the integration of the two control objectives must be taken into account while dealing with compressor control.

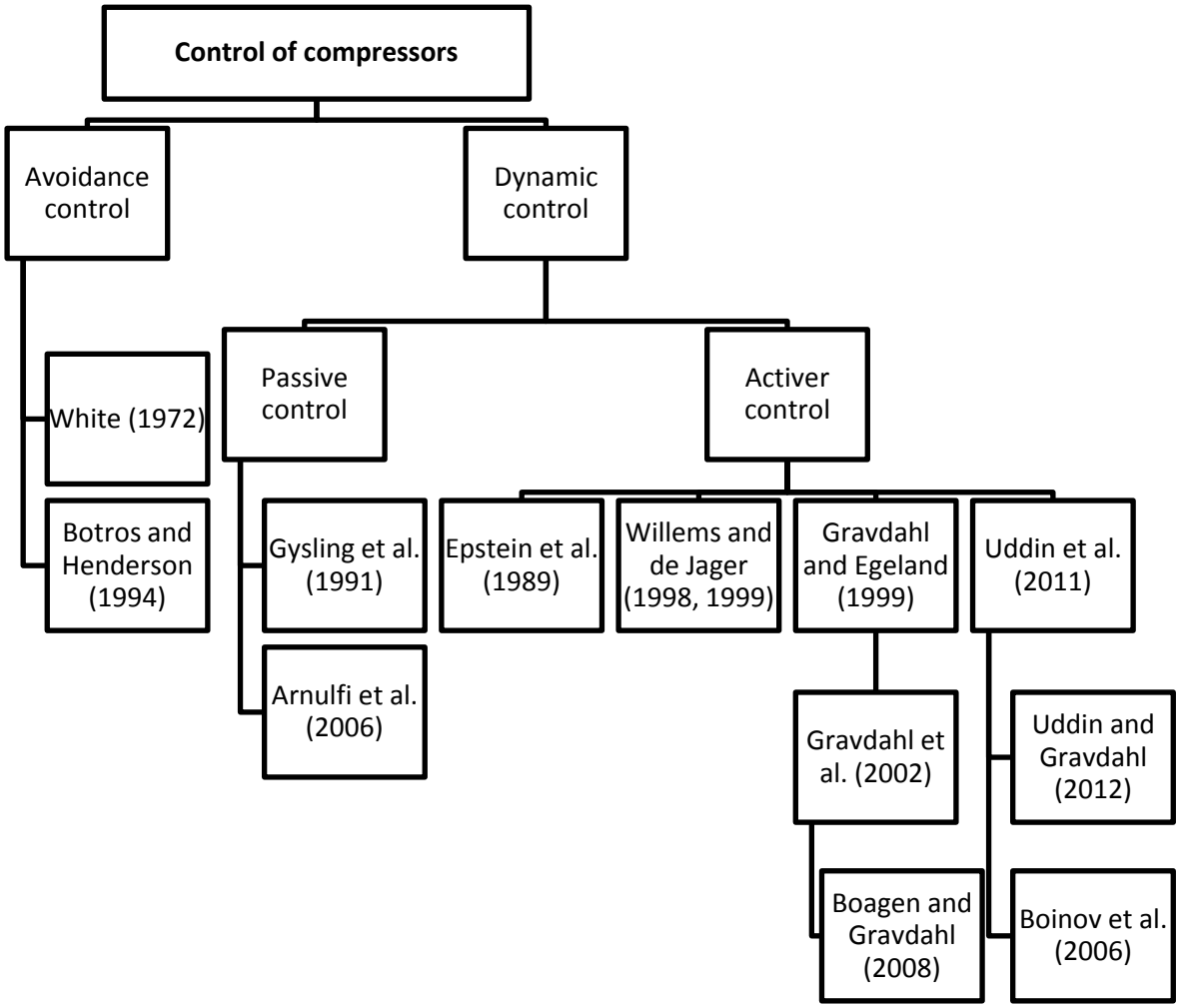


Figure 2-8. Avoidance and dynamic control of compressors

2.3.3 MPC control

Model predictive control (MPC) is an appropriate type of control technique for difficult multivariable control problems. It is especially suited for multiple-input multiple-output (MIMO) constrained problems (Seborg et al., 2004b). The constraints are defined by inequalities on inputs and outputs of the controller. MPC was born around 1970 and was generally very successful, especially in the oil and gas industry who counted 4500 applications by the end of the 20th century (Qin and Badgwell, 2003).

2.3.3.1 Introduction on MPC control

MPC is a model-based control technique that estimates the control action using optimization techniques. In order to control a MIMO process while satisfying inequality constraints on input and output variables, a dynamic model of the process is used. Current measurements are used to estimate future values of the outputs in order to calculate appropriate changes in the input variables.

When dealing with model predictive control technology the main controller variables are:

- The state variables, estimated by resolution of differential equations
- The output variables, controlled by the MPC
- The input variables that the model predictive controller manipulates
- The disturbance variables that affects the controlled system and that can be measured or unmeasured.

The overall objectives of an MPC controller include preventing violations of input and output constraints, driving some output variables to their set points while keeping the other variables within their range and also preventing excessive movement of the input variables (Seborg et al., 2004b).

A block diagram of a model predictive control system is represented in the following figure. A model of the process is employed in order to estimate the current process outputs. The real current outputs are compared with the estimated outputs and the errors between them (called residuals) are fed to the prediction block. The prediction block is employed for both set point calculations and control calculations.

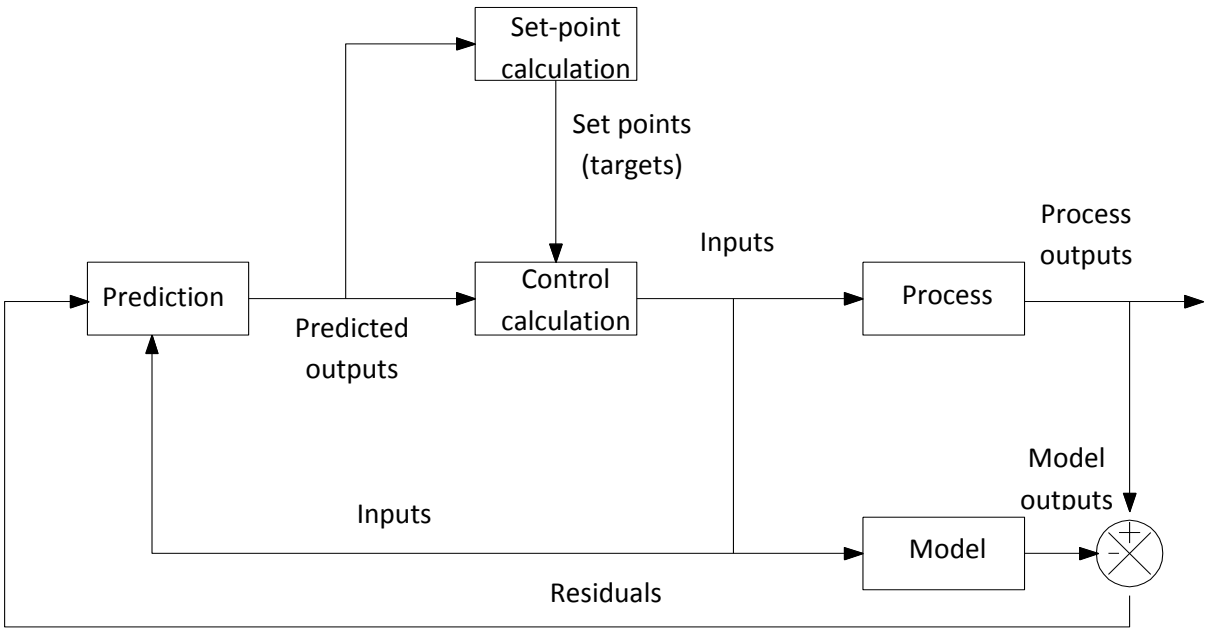


Figure 2-9. Block diagram for model predictive control, modified from Seborg et al. (2004b)

The set points calculations are estimated from an economical optimization based usually on a linear model of the process. Typical optimization objectives include:

- Maximization of the operating profit
- Minimization of the deviation from reference values
- Maximization of the production rate.

The best decision in the control action depends on the selected criterion. Therefore the criterion is defined via a cost function J.

The control calculations are based on current measurements and predictions of the future values of the outputs. The objective of the control calculations is to determine a sequence of control moves. The predictions are made thanks to a simplified dynamic model of the process.

The success of MPC strongly depends on the accuracy of the process model. Three general approaches to model design for MPC are:

- Finite impulse response models
- Transfer function models
- State space models (Wang, 2009).

Most of the current MPC research is based on state space models as they provide a unified framework for both linear and nonlinear control problems. MPC can be linear or nonlinear depending on the linearity of the process model. However nonlinear MPC is usually applied only to very nonlinear systems because it is computationally heavy.

MPC is based on time horizons approach. The prediction horizon is the number of predictions P while the control horizon is the number of control moves M. The prediction horizon is based on the value of the process states and it represents the length of the optimization window, while control horizon represents a control trajectory. The receding horizon approach means that only the first control action over a full control trajectory is actually implemented.

2.3.3.2 MPC model

MPC can be employed for simple systems such as single-input single-output (SISO) systems. For a SISO system the process model is described by the two following equations (Wang, 2009):

$$\underline{\mathbf{x_m}}(k+1) = A_m \underline{\mathbf{x_m}}(k) + B_m \underline{\mathbf{u}}(k) \quad \textbf{(2-19)}$$

$$\underline{\mathbf{y}}(k) = C_m \underline{\mathbf{x_m}}(k) \quad \textbf{(2-20)}$$

where u is the manipulated or input variable, y is the controlled or output variable and $\underline{\mathbf{x_m}}$ is the state variable vector with assumed dimension n_1. Equation (2-19) defines the state vector at time $k+1$ as a function of the previous state vector $\underline{\mathbf{x_m}}(k)$ and of the previous manipulated vector $\underline{\mathbf{u}}(k)$. Equation (2-20) is the state-space model of the plant.

The state-space model can be modified in order to introduce the difference of the state variable $\Delta\underline{\mathbf{x_m}}$ and the difference of the control variable $\Delta\underline{\mathbf{u}}$:

$$\begin{bmatrix} \Delta\underline{\mathbf{x_m}}(k+1) \\ \underline{\mathbf{y}}(k+1) \end{bmatrix} = \begin{bmatrix} A_m & o_m^T \\ C_m A_m & 1 \end{bmatrix} \begin{bmatrix} \Delta\underline{\mathbf{x_m}}(k) \\ \underline{\mathbf{y}}(k) \end{bmatrix} + \begin{bmatrix} B_m \\ C_m B_m \end{bmatrix} \Delta\underline{\mathbf{u}}(k) \quad \textbf{(2-21)}$$

$$\underline{\mathbf{y}}(k) = [o_m \quad 1] \begin{bmatrix} \Delta\underline{\mathbf{x_m}}(k) \\ \underline{\mathbf{y}}(k) \end{bmatrix} \quad \textbf{(2-22)}$$

where:

$$A = \begin{bmatrix} A_m & o_m^T \\ C_m A_m & 1 \end{bmatrix} \quad \textbf{(2-23)}$$

$$B = \begin{bmatrix} B_m \\ C_m B_m \end{bmatrix} \quad \textbf{(2-24)}$$

$$C = [o_m \quad 1] \quad \textbf{(2-25)}$$

The triplet (A, B, C) is called the augmented model and is used in the design of the predictive controller.

SISO MPC theory can also be applied to MIMO systems thanks to the principle of superposition. If the plant is a multiple-input multiple-output system with m inputs, q outputs and n_1 states, with $q \leq m$, the same principle applies:

$$\underline{\mathbf{x_m}}(k+1) = A_m \underline{\mathbf{x_m}}(k) + B_m \underline{\mathbf{u}}(k) + B_d \underline{\boldsymbol{\omega}}(k) \quad \textbf{(2-26)}$$

$$\underline{\mathbf{y}}(k) = C_m \underline{\mathbf{x_m}}(k) \quad \textbf{(2-27)}$$

where $\underline{\boldsymbol{\omega}}(k)$ is the input disturbance. Therefore:

$$\begin{bmatrix} \Delta\underline{x_m}(k+1) \\ \underline{\mathbf{y}}(k+1) \end{bmatrix} = \begin{bmatrix} A_m & o_m^T \\ C_m A_m & I_{qxq} \end{bmatrix} \begin{bmatrix} \Delta\underline{\mathbf{x_m}}(k) \\ \underline{\mathbf{y}}(k) \end{bmatrix} + \begin{bmatrix} B_m \\ C_m B_m \end{bmatrix} \Delta\underline{\mathbf{u}}(k) + \begin{bmatrix} B_d \\ C_m B_d \end{bmatrix} \underline{\boldsymbol{\varepsilon}}(k) \quad \textbf{(2-28)}$$

$$\underline{\mathbf{y}}(k) = [o_m \quad I_{qxq}] \begin{bmatrix} \Delta\underline{\mathbf{x_m}}(k) \\ \underline{\mathbf{y}}(k) \end{bmatrix} \quad \textbf{(2-29)}$$

where I_{qxq} is the identity matrix with dimension qxq, and o_m is a qxn_1 zero matrix. A_m, B_m and C_m have dimensions $n_1 x n_1$, $n_1 x m$ and qxn_1 respectively. For simplicity the previous model can be written as:

$$\underline{\mathbf{x}}(k+1) = A\underline{\mathbf{x}}(k) + B\Delta\underline{\mathbf{u}}(k) + B_\varepsilon \underline{\boldsymbol{\varepsilon}}(k) \quad \textbf{(2-30)}$$

$$\underline{\mathbf{y}}(k) = C\underline{\mathbf{x}}(k) \quad \textbf{(2-31)}$$

where A, B and C are matrices representing again the augmented model while $\boldsymbol{\varepsilon}$ is the white noise sequence defined according to the following equation (Wang, 2009):

$$\underline{\boldsymbol{\omega}}(k) - \underline{\boldsymbol{\omega}}(k-1) = \underline{\boldsymbol{\varepsilon}}(k) \quad \textbf{(2-32)}$$

In the MPC formulation many outputs do not have a set point and they are controlled via range control. This means that these variables have to be within their constraints, but not at a specific set

point. Set points are specified only for the most relevant variables depending on the specific application and control objectives. Constrained problems involve inequality constraints that can be hard or soft. Hard constraints cannot be violated at any time while soft constrains can be violated. It is common to have hard constraints on input variables (representing for example the saturation limits of the actuators) and soft constraint on output variables (as hard constraint could bring the optimisation problem toward infeasible solutions). When soft constraints are violated the action of the controller is penalised by a modification of the cost function. Therefore small violations can be tolerated for short periods of time. When inequality constraints are present the constrained optimisation problem can be solved numerically via linear or quadratic programming techniques.

In order to tune a model predictive controller, the first design parameter to consider is the sampling period Δt, defined as:

$$\Delta t = \frac{t_s}{MH} \tag{2-33}$$

where:

- t_s is the settling time
- MH is the model horizon (usually between 30 and 120).

Then control and prediction horizons must be defined. Some general rules are:

- Control horizon: typically $5 < CH < 20$ or $MH/3 < CH < MH/2$
- Prediction horizon typically $PH = MH + CH$

Finally weighting matrices must be defined:

- $\boldsymbol{Q}$ is the output weighting matrix
- $\boldsymbol{R}$ is the input weighting matrix.

Variables that need tighter control have larger weight in the output matrix $\boldsymbol{Q}$. $\boldsymbol{R}$ is also called move suppression matrix as increasing its values means being more conservative towards changing the corresponding input variable.

The formulation presented here is applied to compressor control later in the thesis in Chapter 5.

2.3.3.3 MPC for compression applications

Even if dynamic control theory did not find a widespread development in industrial application for the reason stated in the previous section, very few papers covering MPC applications for compressors are available in the open literature. Some of them demonstrated that model predictive control is applicable for the control of complex compression systems (Øvervåg, 2013, Smeulers et al., 1999) and for surge prevention via close coupled valve (Johansen, 2002) and drive torque actuation (Cortinovis et al., 2012). However the research development in this area is still limited.

In 1999 Smeulers et al. (1999) demonstrated that MPC was applicable for the control of complex compression systems. They implemented MPC on a compressor systems composed of two compressors in parallel driven by a variable speed gas turbine. For each compressor there are three manipulated variables: the opening position of the inlet throttle valve, the opening position of the recycle valve and the power supply. General control objectives were the integration of surge avoidance and capacity control. They considered two control cases. The first case was called flow pattern while the second case regarded the control of the delivery pressure within specified margins. Constraints included:

- Surge flow rate
- Minimum and maximum speed
- Maximum temperature in the outlet plenum
- Minimum and maximum pressure in the discharge header
- Minimum, maximum and move constraints on supply power.

The control strategy was based on the compression station control. This means that the main focus was on load sharing based on either maximum distance or same distance from surge of the two machines.

In 2002 Johansen (2002) proposed an approximate multi-parametric nonlinear programming (mp-NLP) algorithm for the solution of local sub-problems and he tested it for the surge control of a compressor via close coupled valve. Therefore only one control objective was included in the formulation and it was the stabilisation of the compressor. Nonlinear model predictive control was also analysed by Grancharova et al. (2007), who presented a paper focussing on the implementation and computation of a NMPC for general nonlinear systems with state and input constraints. The proposed controller was tested for surge control. They employed the same model and the same control objective presented by Johansen (2002). Comparing this analysis with the previous work, they suggested some additional mechanisms in order to handle the non-convexity in mp-NLP problems.

In 2007 Molenaar (2007) tested a model predictive controller in order to increase the stable operating region of the machine and compared its response with a Positive Feedback Stabilisation (PFS) controller. Positive stabilisation controllers are dynamic active controllers. The manipulated variable was a throttle valve placed at the exit of the compressor plenum. The work demonstrated that the MPC controller was not able to stabilise the compressor operation as the positive feedback stabilisation controller did.

In 2012 Cortinovis et al. (2012) proposed a compressor antisurge control system based on model predictive control acting on the driver torque (Torque Assisted Antisurge Control, TASC). This linear controller was implemented on an embedded system for the control of compressor stations. The manipulated variables were the torque of the driver and the opening of the antisurge valve, while measured variables were the pressure ratio and gas flow rate. Surge line was considered a constraint in the MPC formulation. The model predictive controller was compared with conventional antisurge controller and demonstrated better performance. However the control system did not include flow minimisation through the recycle valve and temperature effects.

In 2013 Camacho and Alba (2013) presented an application of constrained model predictive control. The case study consisted of an air compressor. In the original control system the compressor outlet pressure was controlled via inlet guide vane manipulation and surge was controlled by blow off valve manipulation. They propose the use of MPC for pressure and surge control. Therefore the manipulated variables were the position of the inlet guide vanes and the position of the recycle valve while the controlled variables were the air pressure and flow rate.

In 2013 Øvervåg (2013) proposed the use of MPC control for load sharing of two compressors in parallel. Manipulated variables were the rotational shaft speed and the flow though the throttle valve while measured variables were pressure and mass flow for both machines. However he did not take surge into account.

In 2013 Quartarone et al. (2013) proposed a model predictive controller for adjustable speed drive compressors however they did not take surge into account.

Therefore linear and nonlinear model predictive controllers were developed and implemented for the control of compressors. However they mainly focused on surge control while neglecting capacity control. Moreover some important control aspects such as temperature profile within the machine and flow profile through the antisurge valve were not included in these analyses.

Figure 2-10 summarises the main contributions to the field of MPC control for compressor applications. They have been divided depending on the control purpose:

- Load sharing of parallel compressors
- Capacity only control
- Surge only control
- Capacity and surge control.

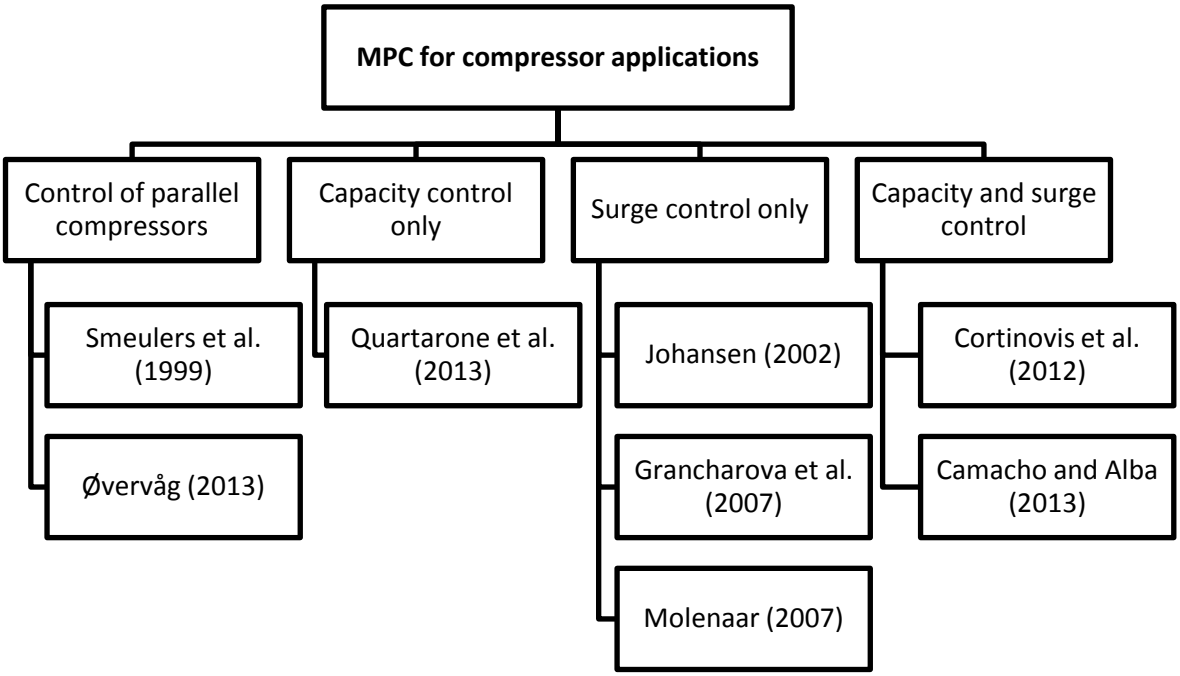


Figure 2-10. Model predictive control for compressor applications

2.3.4 Summary

This section of the thesis has covered the literature review on the research topic of compressor control. Different control strategies were presented and they can be summarised as following:

- Avoidance control, based on the increase of the inlet flow rate by gas recycling or on the reduction of the backpressure by blow off or flaring
- Dynamic control, based on the stabilisation of the compression system on the left of the surge line by means of active or passive control devices
- Model predictive control, based on dynamic modelling of the process plant and optimisation of an objective function in order to estimate the control action.

All these control strategies were mainly focussing on surge control. Capacity control was almost neglected in the academic literature. However in a compression system capacity and surge control have a strong interaction and the operation of the machine must be guaranteed as well as its protection.

Traditional control based on surge avoidance does not represent a robust control solution. Interaction between control loops is a known issues not yet solved. Dynamic control has not yet found a widespread industrial implementation mainly due to safety reasons. Model predictive control has been tested in compressor application but some important control variables have been neglected such as the temperature and flow rate profile long the recycle line.

2.4 Compression of carbon dioxide

2.4.1 Carbon dioxide properties

Carbon dioxide is a colourless, odourless and non-combustible gas. It is chemically unreactive and does not support combustion. Its concentration in the atmosphere is 0.04% v/v however its residence time is quite short. In fact in this phase it is consumed by plants during the photosynthetic cycle and produced by respiration and by combustion. Carbon dioxide is also a by-product of manufacture of lime and of fermentation processes.

In the last century human activity has increased the concentration of CO_2 in the atmosphere by 12%. Scientific studies on the greenhouse effect have attributed to these emissions the average increase of the global temperatures of 0.5°C (Daintith, 2008).

Some applications of gaseous carbon dioxide include:

- Carbonated beverages
- Textile, leather, and chemical industries
- Water treatment
- Manufacture of aspirin and white lead
- Molds hardening in foundries
- Food preservation
- Fire extinguishing
- Welding.

It is also utilized as a pressure medium:

- As a propellant in aerosols
- To promote plant growth in green houses
- As a respiratory stimulant
- In the manufacture of carbonates
- To produce an inert atmosphere when an explosive or flammable hazard exists.

It is used in liquid phase in:

- Fire extinguishing equipment
- Cylinders for inflating life rafts
- Manufacturing of dry ice
- As a refrigerant (Pohanish, 2012).

Table 2-1 summarises the main properties of carbon dioxide (DIPPR, 2012, Wypych, 2014). Carbon dioxide has a low critical point (73.83 bar and 304.21K) compared to other gases. It is also non-toxic, non-flammable, and chemically inert, therefore it has been preferred to other potential gases for use in large-scale extraction processes under pressure (Grandison and Lewis, 1996). Some examples include removal of excess fats from food and coffee decaffeination process. Supercritical CO_2 is also

employed in large scale applications for the oil and gas industry. It is used for the enhancement of oil recovery from nearly depleted reservoirs (Swaddle, 1990).

Supercritical fluids exhibit some physiochemical properties that are characteristic of the liquid phase and other properties that are characteristic of the gas phase. For example their density range goes from gas-density values at low pressure to liquid-density values at elevated pressure, as represented in Figure 2-6.

Table 2-1. Main properties of carbon dioxide

Name	Carbon dioxide
Chemical category	miscellaneous
CAS Registry no.	124-38-9
EC number	204-696-9
RTECS number	FF6400000
Empirical formula	CO_2
Molecular weight	44.01
Critical temperature	304.21 K
Critical pressure	73.83 bar
Critical volume	0.094 m^3kmol^{-1}
Critical compressibility	0.274
Mixture	N
Freezing temperature	-78.5 °C
Colour	colourless
Dielectric constant	1.6
Molar volume	37.2 cm^3mol^{-1}
Specific gravity	1.03 gcm^{-3}
Vapour density, air = 1	1.53
Odour	odourless
State	G
Surface tension	16.2 mNm^{-1}
Viscosity	0.064 mPas
Viscosity temperature	25 °C
Carcinogenicity IARC	N
Carcinogenicity NTP	N
Carcinogenicity OSHA	N
LC50, inhalation, rat	90000/5M ppm
NFPA health	0
Enthalpy of vaporization	22.5 $kJmol^{-1}$
Enthalpy of vaporization temperature	255.35 K
NFPA flammability	0
NFPA reactivity	0
Maximum concentration, 30 min exposure, NIOSH-IDLH	40000 ppm
Threshold limiting value, ACGIH	5000 ppm

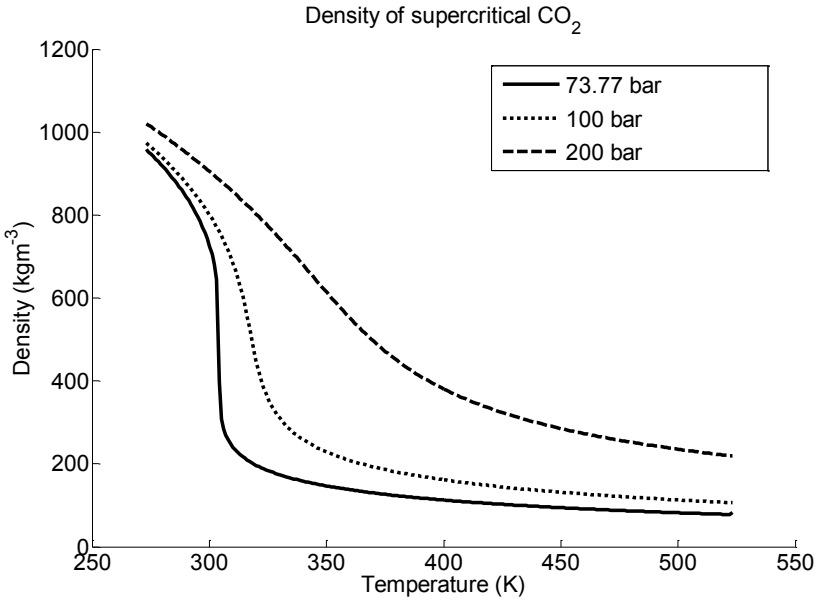


Figure 2-11. Density of supercritical CO_2 as a function of temperature

The supercritical state is not delineated by phase boundaries and therefore there are not sharp changes of the physical properties of the fluid around its critical point (Grandison and Lewis, 1996).

Supercritical fluids comprise weakly interacting molecules. This characteristic gives rise to a high degree of molecular mobility that involves lower viscosity and higher diffusivity than liquid solvents. The state of a supercritical fluid approaches that of a gas at low pressure and that of a low-viscosity liquid at elevated pressure (Grandison and Lewis, 1996). In the proximity to the critical point, CO_2 viscosity is 0.02 cP while it increases with pressure to about 0.1 cP at 700 bar (Fink, 2012).

Because of its high density and low viscosity, supercritical state is employed for pipeline transportation. More details are given in the following subheading about pipeline transportation of CO_2.

2.4.2 Carbon dioxide transportation

For transportation of carbon dioxide via pipelines, supercritical state is preferred because of the high density and low viscosity of the fluid in this condition. Most of the existing pipelines are high pressure lines, with operating pressure between 86 and 200 bar and operating temperature between 4°C and 38°C. Mixed phase flow should be avoided as it causes liquid slugs along the pipeline and therefore operational problems, especially regarding pumping compression (Maroto-Valer, 2010).

Before being transported via pipeline, carbon dioxide must be compressed above its critical point. The critical point depends on the impurities in the gas. The pipeline may need to be operated at higher pressure because of the impurities.

The minimum pressure for transportation must be fixed in order to have single phase supercritical fluid. It must also be high enough to overcome the frictional and static pressure drops along the pipeline between recompression stations. However in some cases, such as subsea application, intermediate booster stations are not feasible. Therefore the pressure at the beginning of the pipe must be high enough to remain in supercritical state along the full length of the pipeline, from the compressor to the delivery location. The maximum pressure for transportation usually depends on pipeline integrity limits (Maroto-Valer, 2010).

2.4.2.1 Modelling and simulation in the literature

Transportation of carbon dioxide in the supercritical state has received much attention in the academic literature. Optimization of pipeline operation mainly aims at cost reduction for CO_2 transportation (Svensson et al., 2004, Zhang et al., 2006). Many studies focus on carbon capture and storage (CCS) applications. Other studies focus on the utilization of supercritical carbon dioxide for enhanced oil recovery. Various models have been developed for the simulation of transportation of CO_2 in supercritical state (Aursand et al., 2013, Chaczykowski and Osiadacz, 2012, McCoy and Rubin, 2008). These models employ equations of state in order to estimate the thermodynamic properties of the process fluid (Peng and Robinson, 1976, Soave, 1972, Span and Wagner, 1996).

Svensson et al. (2004) analysed different transportation scenarios in order to evaluate their cost. In order to maximize the throughput and facilitate loading and unloading for pipeline transportation they considered both liquid phase and supercritical state transportation. However they suggested the use of supercritical state in order to avoid multiphase flow. In this analysis they also compared different transportation module combinations including pipeline on shore and off shore; pipelines and water carriers; railway transport and water carriers; pipeline networks. The results suggested the use of pipeline, water carriers or a combination of both of them in order to reduce the costs for CO_2 transportation.

Zhang et al. (2006) compared different transport methods in order to optimize the operation of a CO_2 pipeline. They identified a lack in the academic literature regarding the optimization of carbon dioxide compression and transportation. Therefore they proposed to maximise the efficiency and minimise the costs of CO_2 compression and transport. However most of this analysis focussed on the optimization of the pipeline operation while the operation of the compressor had a marginal role. Rather than optimizing the operation of the compressor they limited their analysis to its power consumption in two different fluid regimes.

In 2008 McCoy and Rubin (2008) proposed an engineering-economic model for the transportation of carbon dioxide via pipeline in supercritical state. According to previous work, they stated that pipeline transportation of CO_2 in supercritical state was the most economical method and wanted to estimate the total cost of transportation and the cost per tonne of CO_2 transported. They considered various transport scenarios and employed the Peng Robinson (Peng and Robinson, 1976) equation of state (EOS). They concluded that the cost for the transportation of carbon dioxide was mainly influenced by the region of construction and the length and capacity of the pipeline.

Chaczykowski and Osiadacz (2012) confirmed that pipeline transportation was the most suitable transportation method when large quantity of CO_2 must be transported. They identified three equations of state used in the academic literature to estimate the thermodynamic properties of carbon dioxide:

- Peng-Robinson equation of state (Peng and Robinson, 1976)
- Soave-Redlich-Kwong equation of state (Soave, 1972)
- Span and Wagner equation of state (Span and Wagner, 1996).

They selected the last equation of state and included it in a dynamic simulation of transport of a dense phase CO_2 rich mixture. The compressor model employed in the simulation included required work and isentropic efficiency. In their work they highlighted the influence of the impurities on the dynamic behaviour of the fluid during pipeline transport.

Transient simulation was considered in the review by Aursand et al. (2013). They highlighted the difference between natural gas compression and carbon dioxide compression. Carbon dioxide facilities are often employed for compression of carbon dioxide. However the two gases differ for critical point, triple point, phase of transport and quality. They highlighted that the Span and Wagner equation of state gives good prediction for pure or almost pure carbon dioxide. For higher amount of impurities new equations of state are still under development.

The studies presented above are summarised in Figure 2-12.

In conclusion the literature review on carbon dioxide transportation highlighted some important findings:

- Pipeline transportation is the most economical method to move high quantity of CO_2
- Different equations of state have been proposed for the simulation of the thermodynamic properties of carbon dioxide
- The Span and Wagner EOS is the most accurate and therefore appropriate
- The role of compression for transportation is relevant however the knowledge in this field seems limited
- Facilities for natural gas compression have often been employed for carbon dioxide, however CO_2 has different thermodynamical and therefore transportation properties.

Therefore the next section investigates the research development regarding modelling and simulation of compression of carbon dioxide into supercritical state.

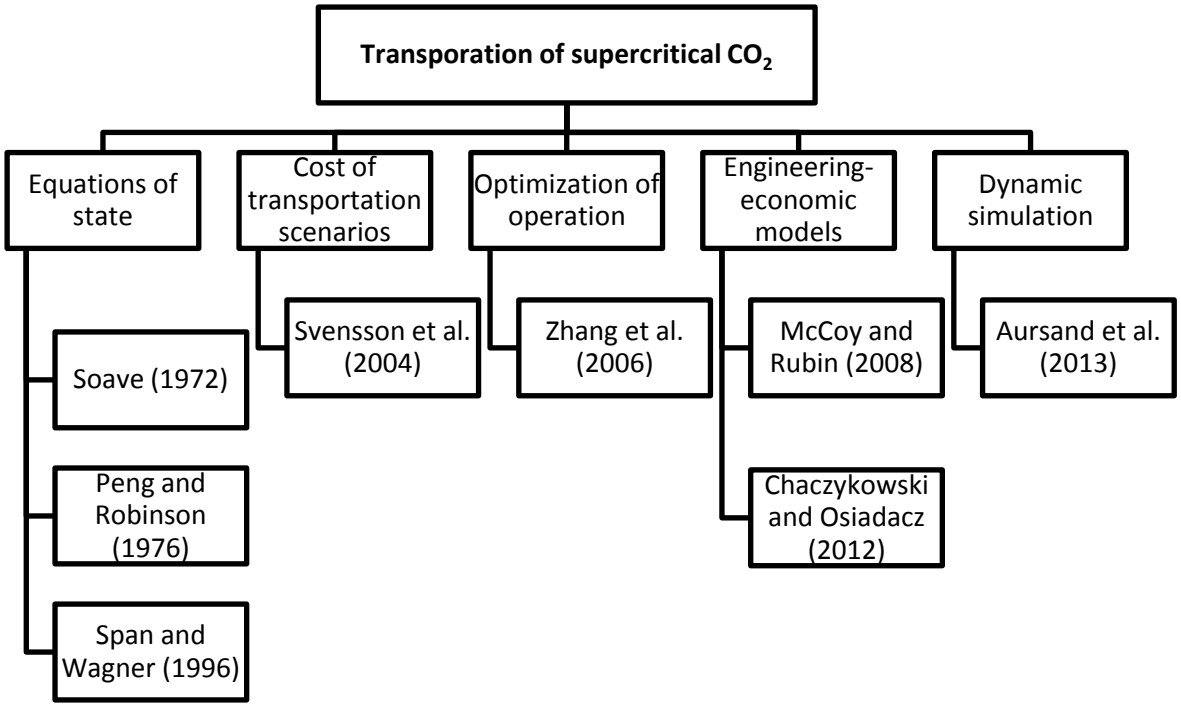


Figure 2-12. Transportation of supercritical carbon dioxide

2.4.3 Modelling and simulation of compression to supercritical state

As highlighted by Aursand et al. (2013) natural gas compressors were usually employed for supercritical CO_2 applications. However some analyses are available in the literature regarding carbon dioxide compressors dealing with supercritical conditions. While some papers focus on reciprocating and positive displacement machines (Kim et al., 2004), other papers report two dimensional (Utamura et al., 2012) and three dimensional (Kim et al., 2014, Lettieri et al., 2014, Moore et al., 2012, Pecnik et al., 2012) CFD analysis of the supercritical fluid.

In 2004 Kim et al. (2004) analysed the state of the art for the utilisation of transcritical carbon dioxide in industry. They focussed specifically on three main industrial sectors: refrigeration, air-condition and heat pump applications. Most of the compressor technology was based on reciprocating and positive displacement machine. These machines are not affected by surge and therefore this phenomenon was not considered.

Pecnik et al. (2012) performed a three-dimensional computational fluid dynamic analysis of a high speed centrifugal compressor operating with supercritical carbon dioxide. The simulation code was coupled with a library of the thermodynamic properties of the fluid. Pecnik proposed this analysis after finding a lack of studies regarding fluid behaving as non-ideal. He adopted the Span and Wagner equation of state (Span and Wagner, 1996) in order to compute the thermodynamic properties of the gas mixture. The calculation was very accurate due to the number of parameters,

however it was also computationally expensive. Therefore all the properties were precomputed and stored in two look-up tables, one for the vapour liquid phase and one for the single supercritical state. He highlighted the need for improved models able to take into account appropriate turbulence models and density fluctuation close to the pseudocritical line.

Real gas effects were taken into account in the work of Utamura et al. (2012). In this paper he described the performance characteristic of a centrifugal compressor that was part of a demonstration test for power generation. He compared the numerical results coming from a meanline model with the experimental results obtained from the test rig. Meanline model prediction were accurate in the supercritical state region while discrepancies between numerical and experimental results started to appear when the compressor was moving towards subcritical state.

Moore et al. (2012) proposed an internally cooled centrifugal compressor for the compression of carbon dioxide. Tests were performed in the operating range between 2.1 and 6.2 bar and experimental results were compared with the numerical results coming from a 3-dimensional computation fluid dynamics analysis. The internal cooling system was able to remove more than 50% of the heat generated by compression. Deviation between experimental results and simulation results were found also by Kim et al. (2014). He performed a CFD numerical investigation of a centrifugal compressor dealing with supercritical carbon dioxide. In order to simulate the nonlinear behaviour of carbon dioxide around the critical point, he employed a table including real gas properties, focussing especially on specific heat ratio and density. The tabulated region included pressure between 73.8 bar and 500 bar and temperature between 304 K and 400 K. Around the critical region the numerical results returned errors around 20% for the compressor efficiency and around 4% for the pressure ratio. This suggested that further investigations were needed.

Lettieri et al. (2014) proposed the redesign of a centrifugal compressor in order to account for a low flow coefficient when dealing with supercritical carbon dioxide. The flow coefficient is a non-dimensional unit which takes the volumetric flow into consideration for a given tip speed and impeller diameter (Khan, 1984). Lettieri suggested the use of impellers with wide flow channels and of vaned diffuser. The redesign was supported by computational fluid dynamic analysis, which proved an efficiency increase of 1%.

The previous analyses proved the difficulty in properly defining the operation of a compressor around the fluid critical point and also confirmed the utilisation of the Span and Wagner EOS as the most accurate equation available at the moment.

The following figure highlights the academic contributions to the field of CO_2 compressor development.

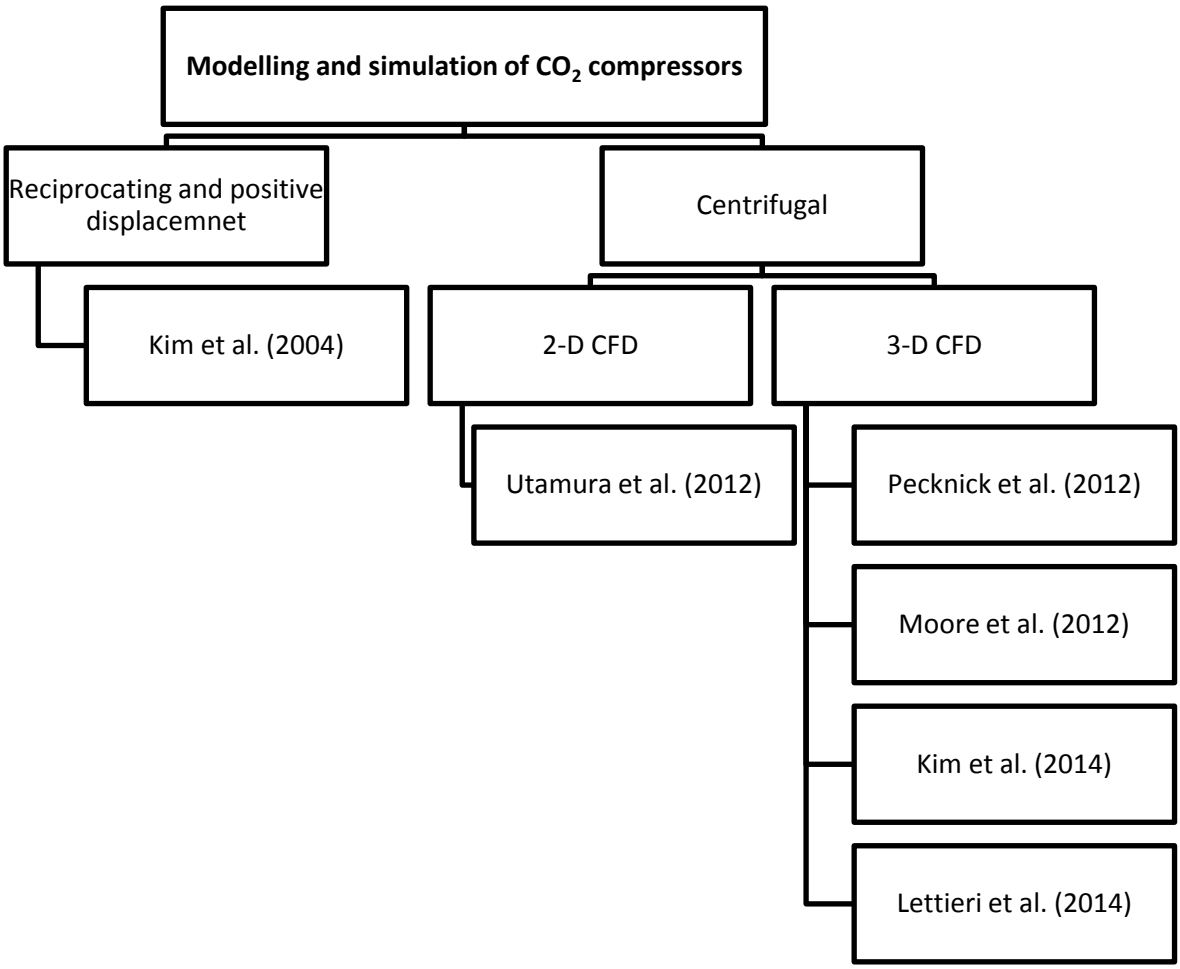


Figure 2-13. Modelling and simulation of CO_2 compressors

The next section covers the control of compression systems dealing with supercritical carbon dioxide.

2.4.4 Control systems for supercritical CO_2 applications

In the academic literature some papers deal with control of systems involving the compression of carbon dioxide. However the control objective is often the thermal optimization of the compression station rather than the control of the compressor itself. Others involve compression technology where rotating compressors are not employed and therefore surge is not a problem. Some of these papers are presented below and they show that there is clearly a need for control of centrifugal compressors dealing with supercritical carbon dioxide. A summary of the main contributions is presented in Figure 2-14.

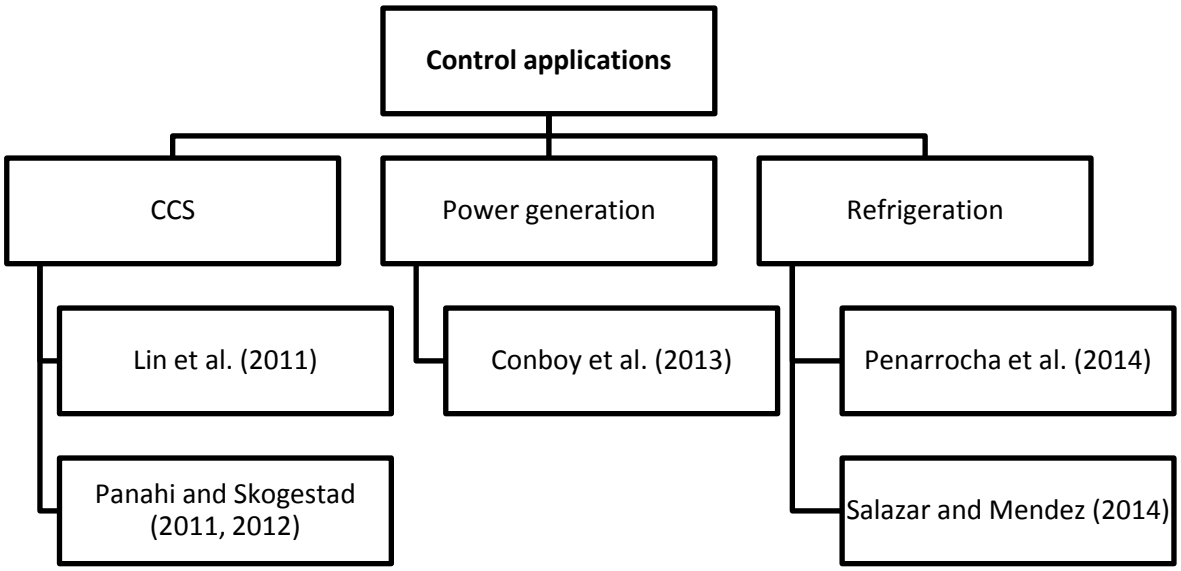


Figure 2-14. Control applications for supercritical CO_2 industry

In 2011 Lin et al. (2011) proposed a plantwide control system for absorption and stripping of carbon dioxide using monoethanolamine solution. They adopted a plant wide approach however they did not include the compressor in the simulation of the separation step.

In 2012 Panahi and Skogestad (Panahi and Skogestad, 2011, Panahi and Skogestad, 2012) proposed a control system for a CCS application. Controlled variables were CO_2 recovery in the absorber and temperature distribution in the stripper.

In 2013 Conboy et al. (2013) proposed a control scheme for a supercritical CO_2 recompression Brayton cycle. The paper reported on the strategies employed by the operators in order to bring the demonstration loop from cold start up condition to steady state power production.

In 2014 Penarrocha et al. (2014) proposed a new approach to optimize the energy efficiency of CO_2 transcritical refrigeration plants. His strategy aimed at minimising the power consumption of the compressor. He included a centrifugal compressor in the refrigeration plant he proposed however he did not include surge in his control strategy.

Salazar and Mendez (2014) proposed a PID control system for a single stage transcritical refrigeration cycle. They modelled the compressor and the throttle elements via simplified relationship. Their main concern was the improvement of the efficiency of the overall system rather than surge control. Therefore they conducted a thermal control analysis that did not include surge modelling or simulation.

The review presented in this section demonstrated lack in the control of sCO_2 compressors. Main findings are summarised in the following list:

- Generally speaking there are few publications dealing with control of supercritical compression systems
- Depending on the applications, the compressor is rarely the most important element and it is modelled via simplified equations
- Control objectives generally include thermal or economical optimisations.

2.4.5 Summary

This section of the thesis has presented the literature review on the compression of carbon dioxide, together with compressor modelling for machines specifically designed for this purpose and their control system. The review has highlighted some major points, here summarised.

The mismatch between numerical and experimental results for the compression of carbon dioxide to supercritical conditions is still high. However different equations of state have been investigated and the Span and Wagner EOS is the most accurate.

Few compressor configurations were specifically designed for the compression of carbon dioxide. In most cases natural gas facilities are employed.

Control systems for carbon dioxide compression systems usually neglect the control of the compressor itself. The reason is that technology based on supercritical CO_2 is still in its early stage and therefore still aims at optimising the process operation.

2.5 Summary of the chapter

This chapter has covered the literature review regarding the following research areas:

- Centrifugal compressor modelling and simulation
- Compressor and surge control
- Compression of carbon dioxide.

Regarding modelling and simulation of centrifugal compressors, steady state or quasi-steady approaches are not appropriate as they do not capture the dynamic behaviour of the compression system. Therefore a dynamic model must be used. Some process parameters influence surge occurrence and they include the recycle hold-up volume, the prestroke time of the antisurge valve and the inertia of the overall compressor-driver system.

Regarding compressor and surge control, the main research focus has been on surge control rather than on joint capacity and surge control. Different control strategies were presented and they fall within three main categories: avoidance control, dynamic control, and model predictive control.

Traditional control based on surge avoidance does not represent a robust control solution as it incurs an interaction between control loops. Dynamic control has not yet found a widespread industrial implementation mainly due to safety reasons. Model predictive control has been tested in compressor applications but some important control variables have been neglected such as the temperature and flow rate profile along the recycle line.

All these control strategies were mainly focussing on surge control. Capacity control was almost neglected in the academic literature. However in a compression system, capacity and surge control have a strong interaction and the operation of the machine must be guaranteed together with its protection. Therefore an overall control approach is appropriate.

Regarding the compression of carbon dioxide, the mismatch between numerical and experimental results for the compression of carbon dioxide to supercritical conditions is still present. However different equations of state have been investigated and the Span and Wagner EOS is the most accurate. Few compressor configurations were specifically designed for the compression of carbon dioxide. In most cases natural gas facilities are employed. Control systems for carbon dioxide compression systems usually neglect the control of the compressor itself. The reason is that technology based on supercritical CO_2 is still in its early stage and therefore still aims at optimising the process operation.

Therefore at this point more specific research objectives can be defined and they include:

- Modelling and simulation of a compression station
- Reduction of control loop interaction by integrated control approach
- Investigation of supercritical CO_2 compression, operation and control.

The next Chapter include the design, development, implementation and validation of a compression system together with a traditional control system. This control system will be used later in the thesis as a reference in order to estimate the performance of the proposed control solutions.

3 Theory and methods

The previous chapter has highlighted the importance of modelling and simulating a compression station in order to understand its behaviour during steady state and transient operation. A steady state or quasi-steady state approach has been demonstrated as unsuitable to represent the behaviour of the compressor therefore a dynamic model must be employed. The second chapter has also highlighted what is the current practice in the industrial control of gas compressors. This practice consists of the utilisation of two separated control loops, one loop for capacity control and the other loop for surge control. Academic research has focussed on surge control, proposing different configurations based on avoidance control, dynamic control and model predictive control. However avoidance control is still the most diffused control strategy for surge prevention in compressor configurations.

Therefore, the avoidance control configuration has been selected as a reference for the present work and it is presented in this chapter. In order to evaluate advanced control configurations it is important to have a realistic reference benchmark. The benchmark gives an indication of a reference response of the control system and can also highlight specific issues that can be targeted by academic research. The control configuration here adopted as benchmark has a simple and clear structure without losing the main properties of a fully specified control system. At the same time it does not include any feature that would need the operator intervention. The human factor has been limited to the decision of the control set point. In fact the intention of the author has been to have a fully automated system. The reason is the possibility to evaluate the response of the control system through quantitative parameters.

The chapter is organised in the following way. Section 3.1 presents and describes the tasks of the chapter. Section 3.2 describes the mathematical models that have been developed and employed with the purpose of improving the control system. This section includes the modelling of single stage compressor, recycle line and hold-up volumes. In Section 3.3 the model of the reference control system is presented. Section 3.4 covers the implementation of the model in the selected tool while Section 3.5 summarises the estimation of the model parameters and the tuning of the control system. Finally in Section 3.6 the main findings are highlighted and the conclusions are summarised.

3.1 Task description

This chapter includes various tasks that can be summarised as follows:

- Task 1: modelling of the compression system
- Task 2: modelling of the reference control system
- Task 3: implementation of the model
- Task 4: description of the reference case study
- Task 5: validation of the model.

The first task is the modelling of the compression system. The compression system includes a main forward process line and a secondary recycle line. Various configurations have been considered (closed or open recycle, hot or cold recycle). These configurations mainly differ because of the thermodynamic condition of the gas and the hold-up volume along the recycle line.

The second task is the modelling of the reference control system. The reference control system represents the state of the art control system for gas compressors. This reference system has been modelled taking into account its popularity and widespread use in industrial applications and also the reasons why other control architectures have not been selected by the practitioners. This control system represents the benchmark and reference for comparison of control performance and is also called 'feedback control system'.

The third task of this chapter is the implementation of the process model in the selected numerical tool. This task included the selection of modelling and simulation tool, the method for the resolution of the algebraic and differential equations, the selection of input and output variables. The model of the compression system and of its control system has been implemented in MATLAB Simulink. The implementation of a mathematical model into the modelling software is crucial for the correct resolution of the model equations. Decisions were made according to the purpose of the model i.e. the evaluation of the control system and its improvement.

The fourth task is the description of the reference case study. This case study has been provided by the research partner ESD Simulation Training. The chapter will cover the main feature of the case study and also the outcomes of the collaboration with ESD. More details on this collaboration will be given in the Appendix.

The fifth task is the validation of the model. This task is fundamental in order to guarantee the accuracy and reliability of the model. The model must be able to predict the performance of the machine in both steady state and dynamic operation and at the design point as well as during off-load operation. The completion of this task guarantees the availability of a model that represents a good reference for the control configurations that will be proposed later on in the thesis. Moreover this task guarantees the understanding of the main issues regarding the reference feedback control system.

3.2 Compressor modelling

This section presents the modelling of the compression system. The model has been developed starting from what is available in the literature, in order to estimate the realistic dynamic operation of a centrifugal compressor.

The compression system includes a main forward process line and a secondary recycle line and it is represented in Figure 3-1. The main forward line includes boundary valves and a single stage compressor. A single stage compressor is a single shaft, single casing, multi-impeller machine while a multistage compressor has a multiple single-stage compressors configuration. The model of the compressor includes its characteristic and the evaluation of its outlet temperature and power consumption.

The recycle line is also included in the compression system in order to model the gas recycle. Various configurations that have already been presented in Chapter 2 have been considered and they include closed or open recycle, hot or cold recycle. These configurations differ because of the thermodynamic condition of the gas and the hold-up volume along the recycle line. The configuration represented in the figure is the hot gas recycle configuration.

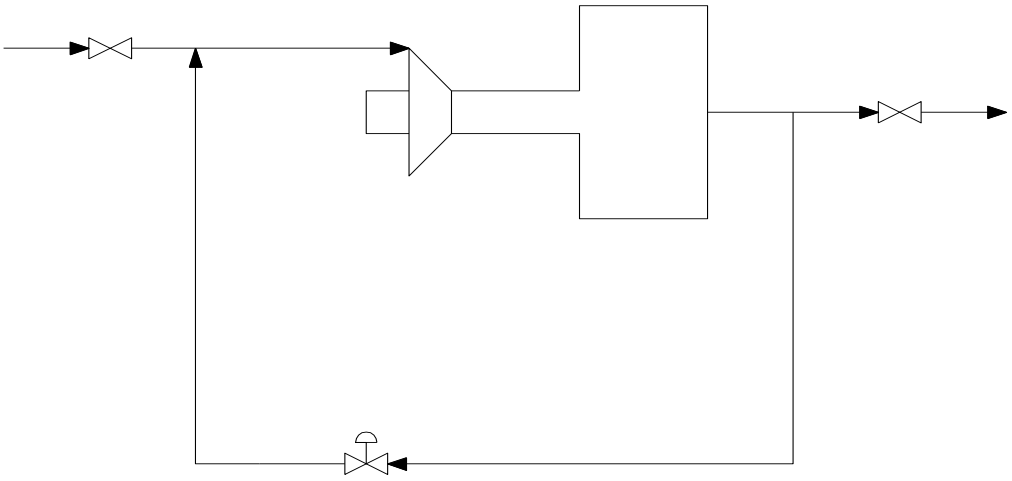


Figure 3-1. Schematic representation of the compression system including a hot gas recycle

3.2.1 Single stage compressor

3.2.1.1 Forward compression line

The model of the main compression line developed during the research work and here presented is inspired by the models of Greitzer (1976b), Fink et al. (1992) and Gravdahl and Egeland (1999).

The layout of the main compression line is represented in Figure 3-2 and includes the single stage compressor with its variable speed driver, the duct connecting the compressor with the downstream plenum and the outlet throttle valve.

In this schematic representation of the compression line, p_{01} and T_{01} are respectively the pressure and the temperature of the gas upstream the compressor while p_{02} and T_{02} are respectively the pressure and the temperature of the gas downstream the compressor. The condition of the gas inside the plenum is defined by its pressure p, temperature T and density ρ. p_{out} is the pressure downstream the outlet valve, and in an open loop configuration $p_{01} = p_{out}$ and $T_{01} = T_{out}$.

The model of this compression system is represented by the equations collected in the next page. The equations were developed starting from first principles. They include the mass and the momentum balance of the compressor (Greitzer, 1976b), the moment of momentum balance of the rotating shaft (Fink et al., 1992), the compressor torque (Gravdahl and Egeland, 1999) and characteristic and the equation of the flow through the outlet valve (Morini et al., 2007).

The variables include the mass flow rate through the duct m and through the outlet valve m_{out}, the radial velocity of the shaft ω, the opening position of the outlet throttle valve op_{out}, the driver torque τ_d and the compressor torque τ_c. Parameters include the sonic velocity at ambient conditions a_{01}, the volume of the plenum V, the cross section area of the duct A_1 and its length L, the inertia of the overall driver-compressor system J, the slip factor μ, the radius of the impeller r_2 and the constant of the outlet throttle valve k_{out}.

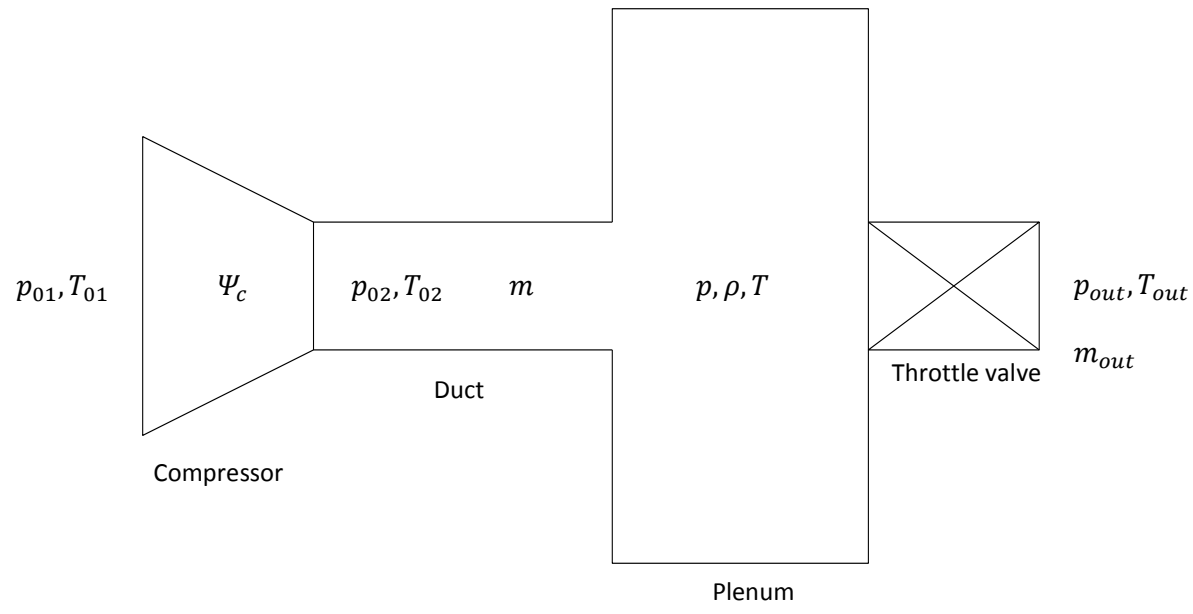


Figure 3-2. Model of the main compression line

Equations of the model of the compressor

The model includes the following main equations:

Mass balance of the plenum:

$$\frac{dp}{dt} = \frac{a^2{}_{01}}{V}(m - m_{out}) \quad \textbf{(3-1)}$$

Momentum balance of the duct:

$$\frac{dm}{dt} = \frac{A_1}{L}(\Psi_c p_{01} - p) \quad \textbf{(3-2)}$$

Moment of momentum balance of the rotating shaft:

$$\frac{d\omega}{dt} = \frac{1}{J}(\tau_d - \tau_c) \quad \textbf{(3-3)}$$

Equation of angular velocity:

$$\omega = \frac{2\pi N}{60} \quad \textbf{(3-4)}$$

Equation of the torque of the compressor:

$$\tau_c = \mu r_2^2 \omega m \quad \textbf{(3-5)}$$

Equation of the pressure ratio as a function of ω and m:

$$\Psi_c = \Psi_c(\omega, m) \quad \textbf{(3-6)}$$

Equation of the pressure ratio as ratio between outlet and inlet pressure:

$$\Psi_c = \frac{p_{02}}{p_{01}} \quad \textbf{(3-7)}$$

Polytropic efficiency of the compressor:

$$\eta_p = \eta_p(\omega, m) \quad \textbf{(3-8)}$$

Mass flow rate through the outlet throttle valve:

$$m_{out} = op_{out} k_{out} \sqrt{\rho(p - p_{out})} \quad \textbf{(3-9)}$$

Equation of the density as a function of pressure and temperature of the gas:

$$\rho = \rho(p, T) \quad \textbf{(3-10)}$$

3.2.1.2 Compressor characteristic

The compressor characteristic Ψ_c represents the pressure ratio between the compressor outlet pressure p_{02} and the compressor inlet pressure p_{01} and is a function of ω and m.

The compressor characteristic is usually provided by the compressor supplier. It is evaluated through steady-state tests in which the compressor runs at various rotational shaft speeds and its performance is recorded. As discussed in Chapter 2, these steady-state performance maps are only valid at the inlet reference conditions, i.e. at the same constant pressure, temperature and gas composition in which the performance tests were performed.

When the inlet conditions of the gas change over time, the use of corrected performance maps is more appropriate, as discussed in Chapter 2. These maps take into account the influence of transient inlet conditions on the performance of the machine, according to the following equations:

$$m_c = \frac{m\sqrt{T_{01}/T_{ref}}}{p_{01}/p_{ref}} \tag{3-11}$$

$$N_c = \frac{N}{\sqrt{T_{01}/T_{ref}}} \tag{3-12}$$

where p_{ref} and T_{ref} are respectively the reference pressure and temperature. These reference values must be constant and can be arbitrary selected. Equation (3-11) is the equation of the corrected mass flow rate while equation (3-12) is the equation of the corrected rotational shaft speed.

Corrected compressor maps have been employed in the present work in order to include into the model the influence of p_{01} and T_{01} on the performance of the compressor and they have been employed in order to estimate the location of the surge line. More details on this procedure are included in section 3.3.

3.2.1.3 Power consumption and outlet temperature

The thermodynamic power P_m consumed by the compressor during the compression of the gas from the pressure p_{01} to the pressure p_{02} depends on the mass flow rate and on its inlet and outlet thermodynamic state, according to Camporeale et al. (2006):

$$P_m = m(h_{02} - h_{01}) \tag{3-13}$$

$$h_{02} - h_{01} = \Delta h = m\int_{T01}^{T02} c_p(T)dT \tag{3-14}$$

where h_{01} and h_{02} are respectively the inlet and outlet enthalpy of the gas. The value of h_{02} has been estimated as a function of the heat capacity of the gas mixture c_p and of the temperature of the gas at the outlet of the compressor T_{02}:

$$c_p(T) = \sum_{i=1}^{2} x_i c_{p,i}(T) \quad \textbf{(3-15)}$$

$$c_{p,1} = c_{p,1}(T) \quad \textbf{(3-16)}$$

$$c_{p,2} = c_{p,2}(T) \quad \textbf{(3-17)}$$

$$T_{02} = T_{01}\left[1 + \frac{1}{\eta_p}\left(\Psi_c^{(\gamma-1)/\gamma} - 1\right)\right] \quad \textbf{(3-18)}$$

where i represents the number of component in the gas mixture, η_p is the polytropic efficiency of the compressor, $\gamma = {c_p}/{c_v}$ is the heat ratio and $T_m = {T_{01} + T_{02}}/{2}$.

3.2.1.4 Inlet and outlet throttling elements

The configuration presented in Figure 3-2 has been modified in order to include also an inlet valve. Both inlet and outlet valves are not proper control valves but they rather represent throttle elements in the plant layout. The updated layout is represented in Figure 3-3:

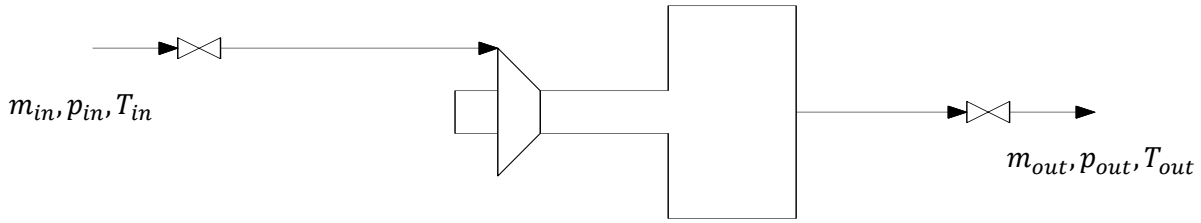


Figure 3-3.Model of the main compression line including inlet and outlet throttling elements

The flow thought the inlet valve has been estimated according to:

$$m_{in} = op_{in} k_{in} \sqrt{\rho_{in}(p_{in} - p_{01})} \quad \textbf{(3-19)}$$

$$\rho_{in} = \rho_{in}(p_{in}, T_{in}) \quad \textbf{(3-20)}$$

where p_{in}, T_{in} and ρ_{in} define the thermodynamic state (pressure, temperature and density) of the gas upstream the inlet throttling element while op_{in} represents the opening position of the inlet valve.

3.2.2 Recycle line

A recycle line has been also included in the model of the system. The recycle line is necessary in order to model the gas recycle from the outlet of the compressor to the inlet of the compressor.

The two most common recycle configurations for gas recycle are the hot gas recycle configuration and the cold gas recycle configuration.

3.2.2.1 Hot gas recycle configuration

In the hot gas recycle configuration, part of the compressed gas is recycled back to the inlet of the compressor without any treatment or modification. Therefore hot gas is recycled and this gives the name to this type of configuration.

This configuration includes two nodes. In the first node the freshly fed gas m_{in} mixes with the recycled gas $m_{r,HR}$ while in the second node the compressed gas m_{pout} splits between recycled gas $m_{r,HR}$ and delivered gas m_{out}.

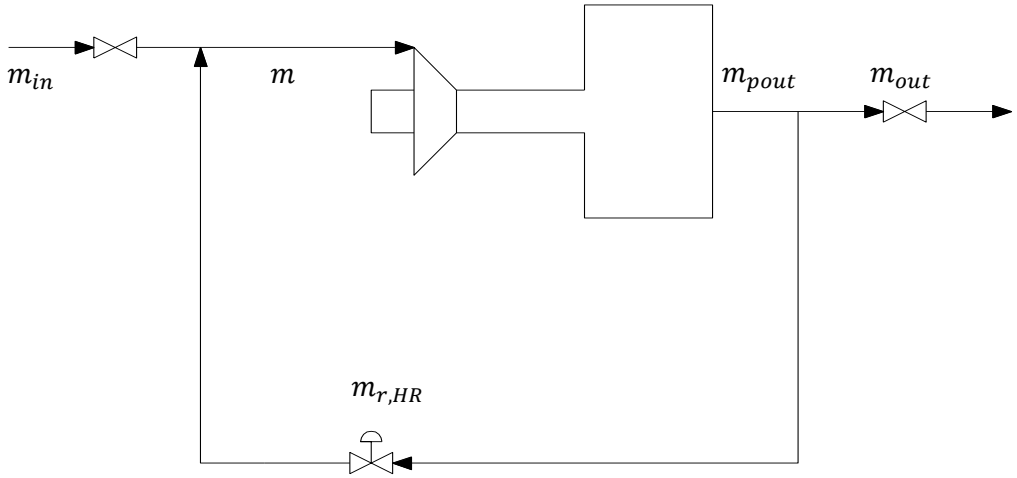


Figure 3-4. Model of the compression system including main line and hot gas recycle line

Equations (3-2), (3-3), (3-5), (3-6), (3-9) and (3-19) are still valid, however Equation (3-1) has been substituted by equation (3-23). Equations (3-21) and (3-22) represent the mass balances for respectively the first and second node while Equation (3-24) represents the mass flow rate through the recycle valve characterised by the constant parameter k_{ASV} and opening position op_{ASV}:

$$m_{in} + m_{r,HR} = m \tag{3-21}$$

$$m_{pout} = m_{out} + m_{r,HR} \tag{3-22}$$

$$\frac{dp}{dt} = \frac{a^2{}_{01}}{V}\left(m - m_{pout}\right) \tag{3-23}$$

$$m_{r,HR} = op_{ASV} k_{ASV} \sqrt{\rho(p - p_{01})} \tag{3-24}$$

The temperature of the outlet gas can still be estimated using equation (3-18). However the compressor inlet temperature T_{01} is not constant but depends on the system inlet temperature T_{in}, inlet flow rate m_{in}, recycle flow rate $m_{r,HR}$ and recycle temperature T_r. As the gas is recycled as it is when it exits the compressor this means $T_r = T_{02}$. The temperature of the gas at the inlet of the compressor, T_{01}, has been estimated by means of the following equation, which takes into account the possibility that c_p varies with temperature:

$$m_{in}\int_{Tref}^{Tin} c_p(T)dT + m_{r,HR}\int_{Tref}^{T02} c_p(T)dT = m\int_{Tref}^{T01} c_p(T)dT \quad \textbf{(3-25)}$$

3.2.2.2 Cold gas recycle configuration

In the cold gas recycle configuration, the recycled gas is cooled to the same temperature as the freshly fed gas. In order to do that, a gas cooler is placed along the recycle line, as shown in Figure 3-5:

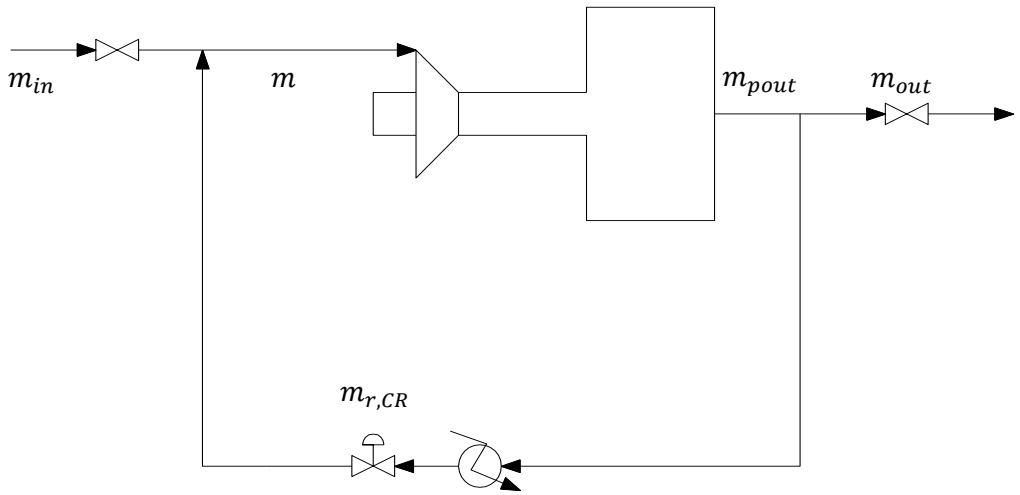


Figure 3-5. Model of the compression system including main line and cold gas recycle line

Therefore the mass flow of gas recycle depends on the condition of the gas at the outlet of the gas cooler, according to:

$$m_{r,CR} = k_{ASV}\sqrt{\rho_{HE}(p_{HE} - p_{01})} \quad \textbf{(3-26)}$$

where the condition of the gas downstream the heat exchanger is defined by its pressure p_{HE} and density ρ_{HE}. It has been assumed that the pressure drop along the heat exchanger is negligible and therefore equation (3-26) gives the mass flow rate through the recycle valve.

In this case T_{01} is constant as ideal cooling is assumed. The heat removed from the recycled flow rate $m_{r,CR}$ in order to cool it from T_{02} to T_{01} is defined by the following equation:

$$-Q = m_{r,CR}(h_{02} - h_{r,CR}) \quad \textbf{(3-27)}$$

The heat removed from the recycled gas has a negative sign as it is removed from the system. $h_{r,CR}$ is the enthalpy of the gas at the outlet of the gas cooler, and by assumption $h_{r,CR} = h_{01}$.

3.2.3 Recycle volume

The review of the relevant background has highlighted the importance of the process configuration on the dynamic of the compression system. In particular the hold-up volume along the recycle line

has been highlighted as a critical parameter for the tendency of a compression system towards surge. This hold up volume has been expressed in various ways by different scientists, depending on:

- The position of the antisurge valve along the recycle line
- The volume of the plenum downstream from the compressor
- The volume of the gas cooler (Botros, 1994)
- The length of the duct connecting compressor and plenum (Greitzer, 1976b)
- The ratio between the length and the radius of the compressor itself (Moore and Greitzer, 1986).

In this thesis the effect of the hold-up volume along the recycle line has been analysed by including a recycle duct and a recycle volume along the recycle line, between the second node and the recycle valve. In the following figure this configuration has been represented for both hot (left) and cold (right) gas recycle configurations:

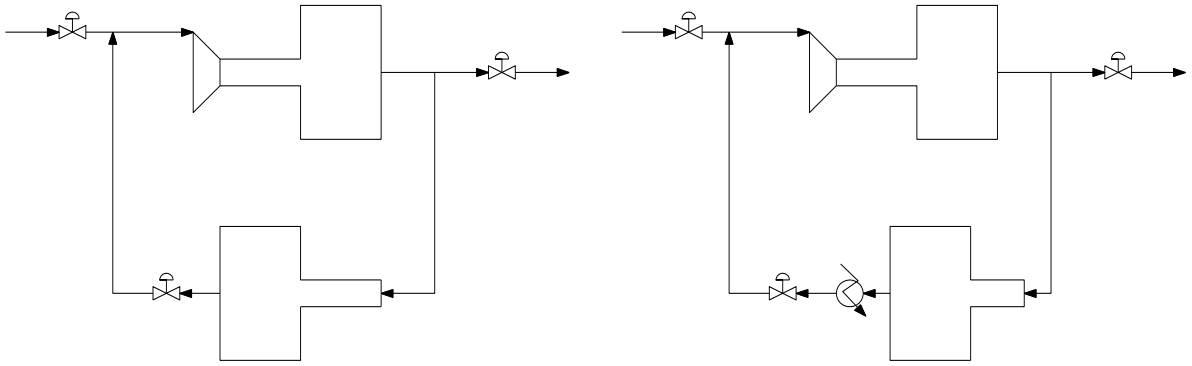


Figure 3-6. Model of the compression system including main line and hot (left, a) or cold (right, b) gas recycle line

For these two new elements (recycle duct and recycle plenum) mass and momentum balance equations must be included. The mass balance of the plenum (Equation (3-27)) depends on the mass flow rate through the recycle duct m_{RV} and through the recycle valve m_r while the momentum balance depends on the pressure p_{RV} inside the plenum, according to:

$$\frac{dp_{RV}}{dt} = \left(\frac{a^2{}_{01}}{V}\right)_{RV} (m_{RV} - m_r) \quad \textbf{(3-28)}$$

$$\frac{dm_{RV}}{dt} = \left(\frac{A_1}{L}\right)_{RV} (p - p_{RV}) \quad \textbf{(3-29)}$$

where $\left(\frac{a^2{}_{01}}{V}\right)_{RV}$ and $\left(\frac{A_1}{L}\right)_{RV}$ represent the geometry of the recycle volume RV including both duct and plenum.

The mass flow rate through the recycle valve is a function of the condition on the gas inside the recycle plenum, according to the following two equations:

$$m_{r,HR} = op_{ASV} k_{ASV} \sqrt{\rho_{RV}(p_{RV} - p_{01})} \quad \textbf{(3-30)}$$

$$m_{r,CR} = k_{ASV}\sqrt{\rho_{HE}(p_{HE} - p_{01})} \quad \textbf{(3-31)}$$

where $m_{r,HR}$ is the recycled mass flow rate for the hot gas recycle configuration while $m_{r,CR}$ is the recycled mass flow rate for the cold gas recycle configuration. Also in this case, the pressure drop along the heat exchanger has been neglected.

3.2.4 Summary

This section of the thesis has presented the model of the compression system including boundary and recycle valves, centrifugal compressor, hold-up volumes and gas cooler along the recycle line.

It is important to analyse not only the compressor itself, but the overall compression system. The literature review, presented in the previous chapter, has highlighted the strong interaction existing among the different elements and especially between the compressor and the downstream volume.

The types of recycle configurations are numerous however they can be mainly characterised by the temperature and the volume of the recycle. There are two reasons for this. The first reason is that the temperature of the recycle influences the power consumption of the system during off-loads and also the amount of gas recycled. The second reason is that the volume of the recycle influences the time constant of the system and therefore the risk of undergoing surge. Therefore these two parameters will be taken into special account in the following analyses.

Now that the basic model has been presented it is appropriate to present the feedback control system.

3.3 Feedback control system modelling

Section 3.2 has presented the model of the compression system, including main process line and recycle line according to various configurations.

This section presents the second task of the chapter, which is the modelling of the reference control system. As stated before, the reference control system is also called feedback control system. This is because of its feedback structure.

This section of the chapter presents the design of the reference control system for a single stage compression station. The reference control system has been identified after the literature review has highlighted the tendency of the gas compression industry to rely on surge avoidance control and feedback control configurations.

The reference control system represents the state of the art control system for gas compressors. This reference system has been selected and modelled taking into account its widespread industrial application and also the motivations behind its popularity. It represents the benchmark and reference for comparison of control performance.

Therefore the purpose of this section is to model a control system able to:

- Represent in a realistic way the state of the art in this field
- Be a reference benchmark for future development of the control system of the compressor.

The first part of this section is a recall of the compressor control structure and it also gives a brief introduction on the generic structure of a feedback control algorithm. The section then presents in details the two control loops implemented in the system: capacity control loop and antisurge control loop. Finally it combines them in the overall control system. This represents the system actually employed when controlling a compression system. The main issues are also highlighted and they give the motivation for the development presented in this thesis later on.

3.3.1 Generic form of a feedback control algorithm

The generic form of a feedback control algorithm is shown in Figure 3-7. It represents the cause-effect block diagram of a closed loop system controlled by a feedback controller. In the summing point the set point (sp) of the controlled variable is compared with the measured variable (pv). The difference between them is called error (e) and it is the input of the feedback controller. The control action is defined by the output of the controller (op) that is the input of the actuator. The actuator changes the manipulated variable (mv) in order to reject the disturbance that is affecting the controlled system. The controlled variable (cv) is measured by the sensor and then transmitted to the summing point.

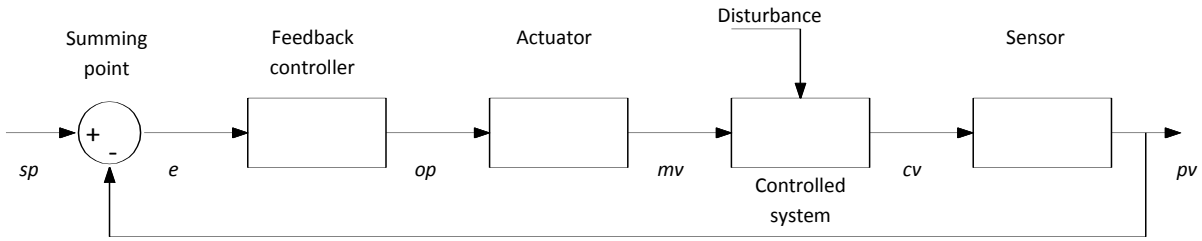


Figure 3-7. Cause-effect block diagram of a single-input single-output feedback controller

The same block diagram can be represented in the Laplace domain, as represented in Figure 3-8.

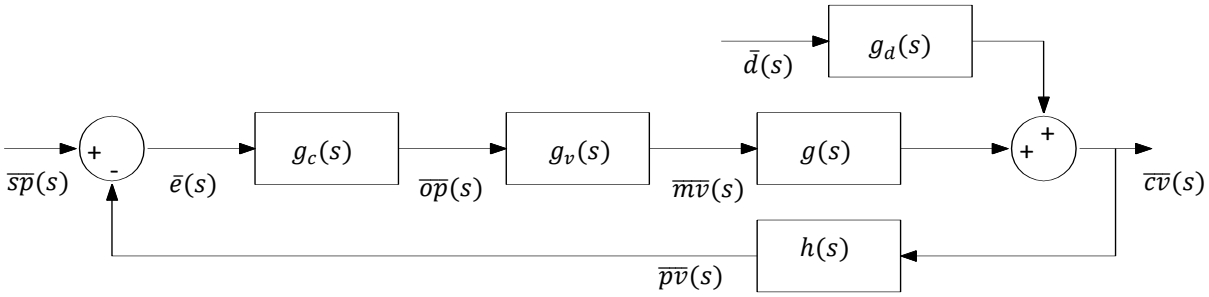


Figure 3-8. Cause-effect block diagram of a single-input single-output feedback controller in the Laplace domain

In this representation $g_c(s)$ represents the feedback controller. It is a continuous-time Proportional-Integral-Derivative (PID) controller with proportional, integral, and derivative gains K_c, K_i, and K_d and first-order derivative filter time constant β_f, according to:

$$g_c(s) = K_c + \frac{K_i}{s} + \frac{K_d s}{\beta_f s + 1} \tag{3-32}$$

Equation (3-32) is the parallel form of the continuous-time PID controller. The continuous-time PID controller can also be represented in standard form, as in the following equation:

$$g_c(s) = K_c \left(1 + \frac{1}{\beta_i s} + \frac{T_d s}{\frac{\beta_d}{N_f} s + 1} \right) \tag{3-33}$$

The two forms differ in the parameters used to express the proportional, integral, and derivative actions and the filter on the derivative term. In fact in this second form K_c is the proportional gain, β_i is the integrator time, β_d is the derivative time and N_f is the derivative filter constant.

3.3.2 Capacity controller

The capacity controller of a generic compressor has the task to guarantee its operation in terms of either pressure or flow rate.

The plenum pressure p has been selected as controlled variable. The reason is that this variable represents the pressure delivered by the compressor.

The torque of the driver has been selected as manipulated variable, according to Gravdahl et al. (2002). The speed depends on the balance between the torque provided by the driver and the torque requested by the compressor during the compression process.

The sensor is assumed to be ideal and therefore the measured variable and the controlled variable have the same value over time.

Figure 3-9 represents the capacity control system. PT is the pressure transmitter while PC is the pressure controller.

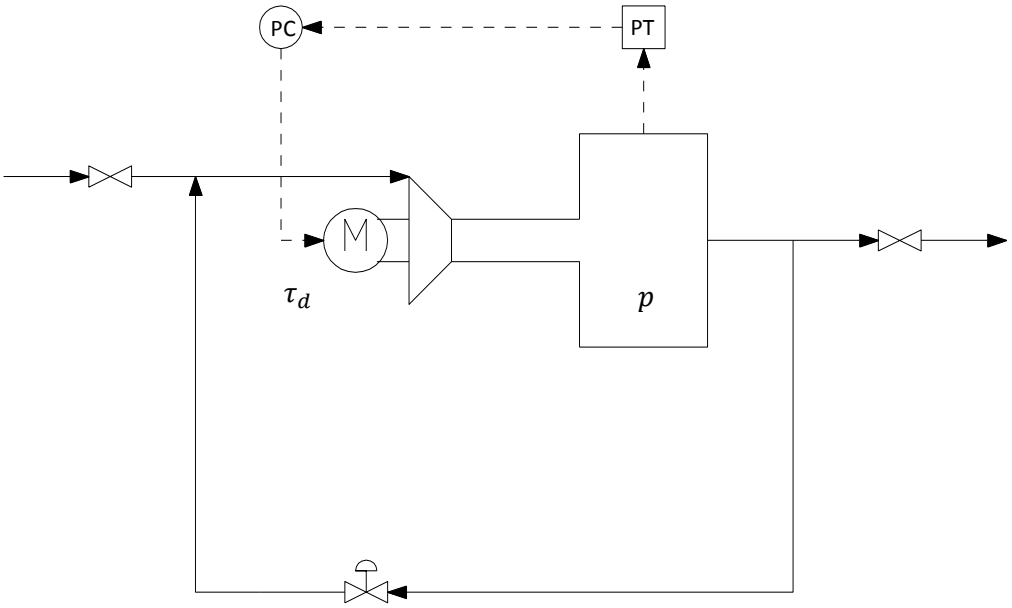


Figure 3-9. Capacity control system showing pressure transmitter PT and pressure controller PC

For variable speed compressors the control of the rotational shaft speed is the most efficient control selection as it responds quickly to set point tracking or disturbance rejection and does not imply a pressure drop as throttle control does. The actuator is a variable speed electric motor that can operate between its minimum and its maxim rotational shaft speed. These values are the boundary of operation for the driver and therefore they represent its saturation limit.

Figure 3-10 represents the block diagram of the closed-loop compression system when controlled by a single PI controller. However it is not possible to directly manipulate the rotational shaft speed in order to adjust the compressor outlet pressure. Therefore the PI controller must have a cascade structure, as represented in Figure 3-11. It has been assumed that the local control system is perfect. This means that the output torque is equal to the set point torque all the time.

The inner loop of the cascade control structure is a speed controller, with rotational shaft speed N as controlled variable and driver torque as manipulated variable. The outer loop is a pressure controller, with compressor outlet pressure as controlled variable. Its output is the set point of the speed controller.

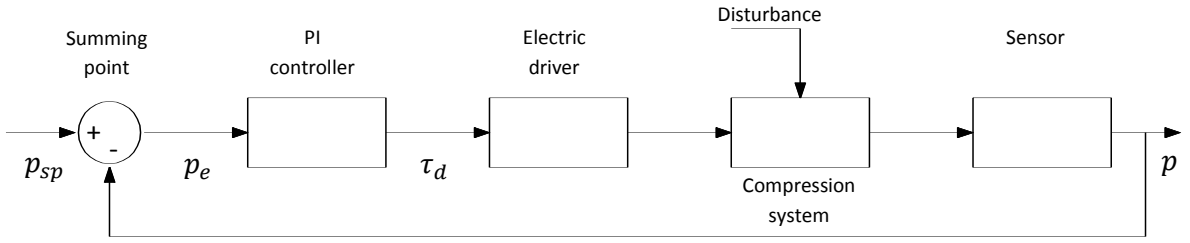


Figure 3-10. Cause-effect block diagram of a single feedback controller

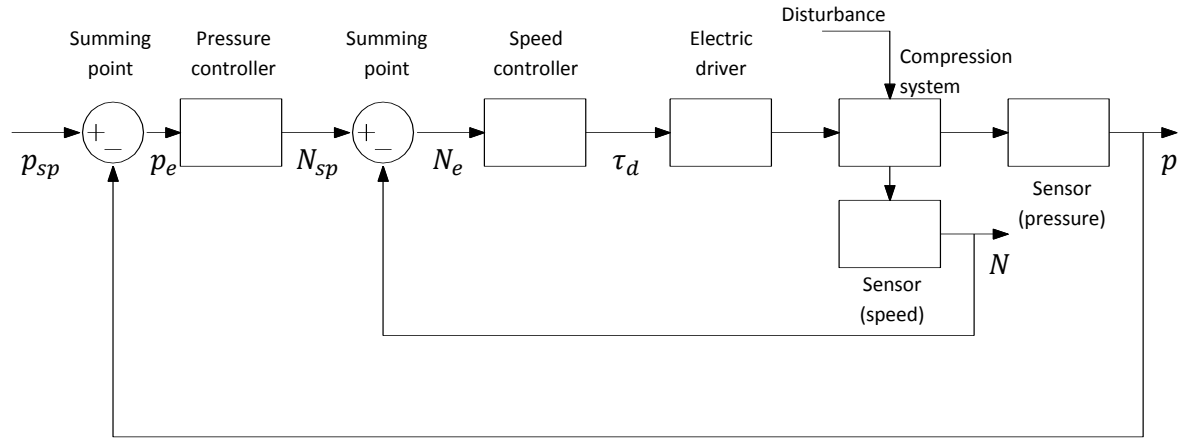


Figure 3-11. Cause-effect block diagram of a cascade feedback controller

3.3.3 Antisurge controller

3.3.3.1 Control structure

The antisurge controller has the control objective to protect the machine from surge. As highlighted in Chapter 2, surge can have very serious consequence on the machine due mainly to the vibrations caused by the flow oscillation and the overheating of the fluid that undergoes continuous cycles of compression. In the literature two main control philosophies have been developed in order to protect compressor from surge:

- Surge avoidance, based on gas recycle
- Dynamic control of surge, aiming at either absorbing the flow disturbances or feeding them back to the compression system.

As presented in the literature review in Chapter 2, the scientific community has been much more active toward development of dynamic control strategies, either passive or active. However these control strategies have not yet found application in the gas compression industry due to safety and reliability issues.

Surge avoidance is based on feedback control and gas recycle. The antisurge controller has the inlet flow rate and differential pressure as measured variables and the inlet flow rate m as controlled variable. If m falls below a predefined control margin m_{ctrl}, defined as:

$$m_{ctrl} = m_{surge} + margin \quad \textbf{(3-34)}$$

then the antisurge controller opens the recycle valve (also called antisurge valve) in order to recycle part of the compressed gas to the inlet of the compressor. This increases the total inlet mass flow rate and brings the operating point of the machine away from the surge region. The schematic representation of the control system is presented in Figure 3-12, where MT is the mass flow transmitter and MC the mass flow controller.

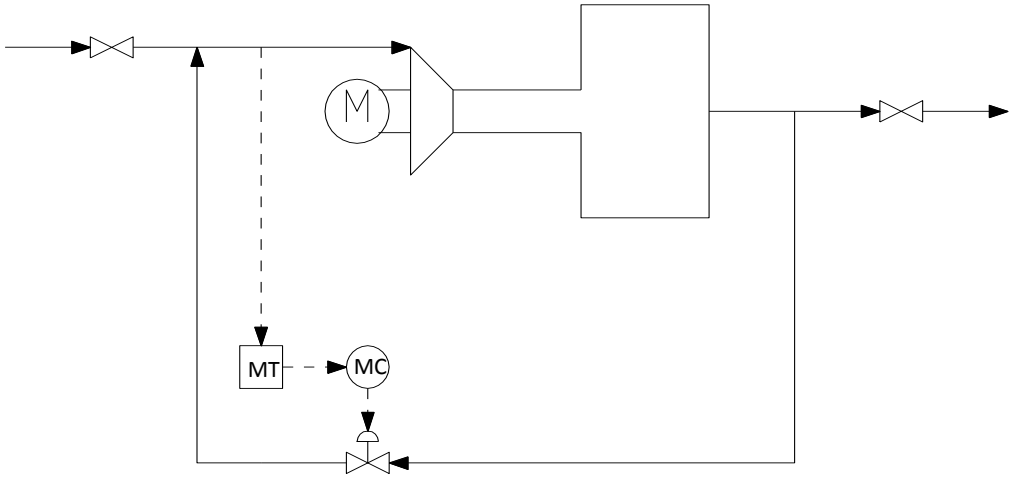


Figure 3-12. Antisurge control system showing mass flow transmitter MT and mass flow controller MC

Figure 3-13 represents the block diagram for the antisurge controller. The antisurge controller acts on the antisurge valve and therefore its opening is the manipulated variable.

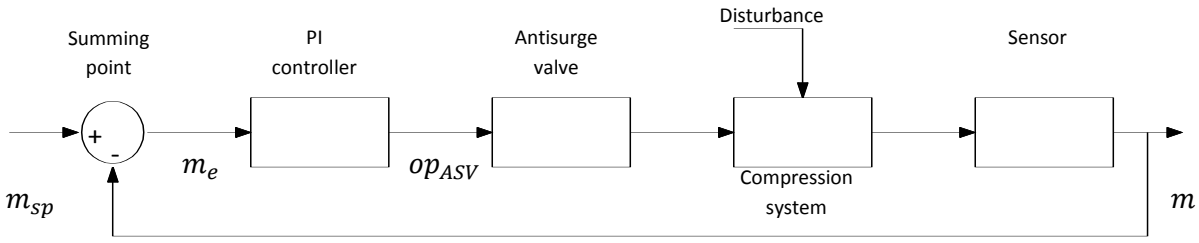


Figure 3-13. Cause-effect block diagram of the antisurge feedback controller

The amount of gas that can flow through this valve depends on the opening of the valve, on the thermodynamic conditions of the gas and also on the valve sizing. The saturation limits for this actuator are its fully closed (i.e. opening 0%) and fully open (i.e. opening 100%) position.

3.3.3.2 Definition of surge region

For a single speed machine the surge point is the point on the performance map with minimum flow. Forward operation takes place if the operating point of the compressor is on the right of the surge point. On the left of the surge point rotating stall and surge take place, until the compressor goes into deep surge and the flow reverses inside the compressor.

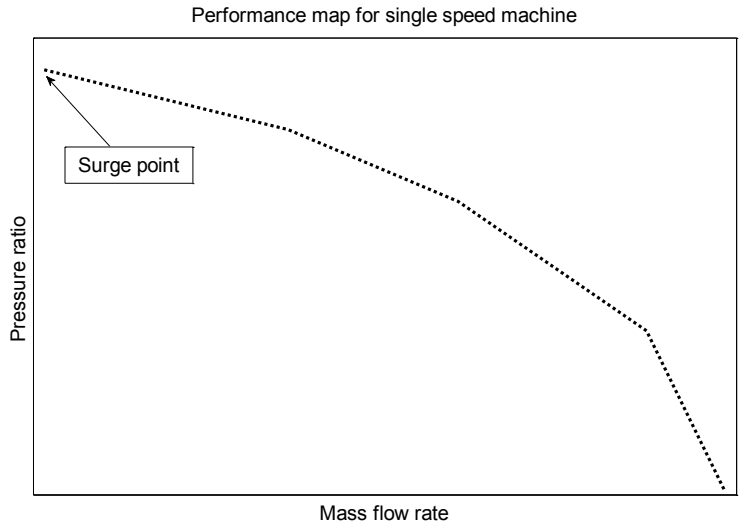


Figure 3-14. Performance map for a single speed compressor

For a multiple speed machine the surge line is defined by the connections between the surge points for the different speed lines.

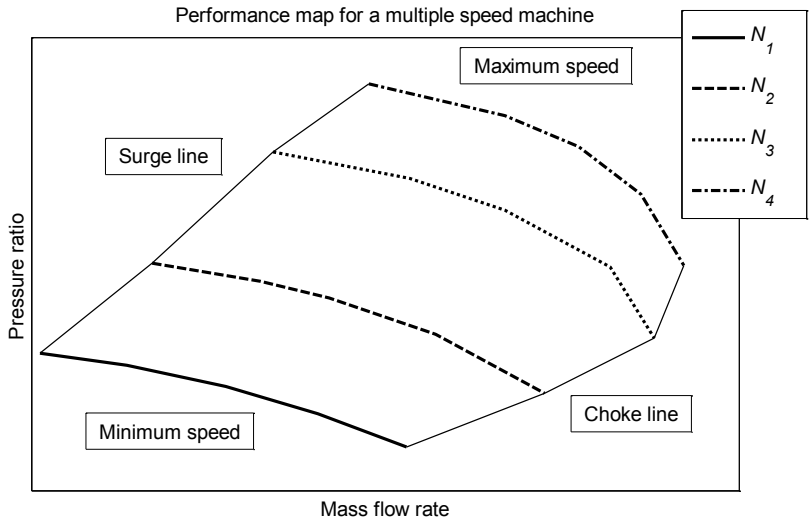


Figure 3-15. Performance map for a multiple speed compressor

Surge points are defined by the compressor supplier by running the machine at constant speed and either:

- Decreasing the compressor inlet flow rate
- Increasing the compressor outlet pressure
- Decreasing the compressor inlet pressure

until surge can be detected by a decrease of the machine performance, noise or vibration. Usually similar tests are performed by the client in order to validate the compressor map in situ.

These compressor maps representing the operation of the compressor at different speeds and the location of the surge region are called steady state performance maps. This is because the inlet conditions of the systems are not changing during testing.

The surge flow rate is a function of radial speed of the shaft and inlet mass flow rate of the compressor:

$$m_{surge} = m_{surge}(\omega, m) \tag{3-35}$$

The distance between the surge line and the control line is defined by a control margin, according to Equation (3-34). Usually both surge and control lines are plotted on the compressor map and therefore their distance from the operating point is easily identifiable. However this type of visualisation, even if very common in both academia and industry, can be misleading. The reason is that the surge line depends on both inlet pressure and temperature and therefore is affected by process disturbances and also by the opening of the recycle valve.

3.3.3.3 Corrected compressor maps

When a compressor operates inside a plant, the boundary conditions of the gas affect its operation. This means that the gas entering the machine is not at the same temperature, pressure and composition that were recorded during the definition of the steady state maps. For this reason corrected compressor maps have been defined, according to Equations (3-11) and (3-12). Steady state compressor maps evaluated at different inlet conditions of the gas become the same map when corrected according to a specific couple of reference temperature and pressure.

3.3.3.4 Dynamic margin representation

The corrected compressor maps can be useful when the inlet conditions are different from the reference conditions, but not when they continuously change over time as happens during a process disturbance. Therefore a different way to visualise the proximity to surge is suggested in this thesis.

The proximity of the machine to surge is represented as the distance between the inlet mass flow rate of the compressor m and the surge control mass flow rate m_{ctrl}. This representation will be employed in the following Chapters in order to represent the distance between the operating point and the surge line over time. This distance is not constant and therefore this type of representation is a valuable qualitative and quantitative instrument for the control engineer. It allows a quick estimation of the distance between the operating point of the machine and the surge region over time. It also helps understanding the influence of inlet boundary disturbances on the surge line.

Figure 3-16 is an illustrative example of this method of representation. The left vertical axis represents the opening of the inlet valve op_{in}, which is decreasing over time according to a negative ramp change from 100% opening to 70% opening. The right vertical axis represents the mass flow rates of the compressor. They include the inlet mass flow rate of the compressor m, the control mass flow rate m_{ctrl} and the surge mass flow rate m_{surge}. The safety margin between m_{ctrl} and

m_{surge} is 20%. The compressor is running at constant rotational shaft speed when the opening of the inlet valve decreases. The graph is representing the effect of this disturbance on the system.

When the inlet valve of the system closes the mass flow rate through the compressor decreases. However the disturbance is also affecting the location of the surge region, represented by m_{surge}, and therefore the distance between the operating point of the compressor m and the surge line. When op_{in} decreases there are two consequences on the system that are affecting m_{surge}. The first consequence is that p_{01} decreases and this is affecting m_{surge} according to equation (3-11). However also the compressor outlet pressure p decreases. Overall p decreases less than p_{01} and this means that the pressure ratio increases. The final result is the increase of m_{surge}, which moves towards m.

The distance between m and m_{surge} has been highlighted on the graph for the steady states preceding and following the disturbance. This distance has clearly decreased and this means that in the steady state after the disturbance the compressor is closer to surge than in the steady state before the disturbance. It would have not been possible to capture these effects with a traditional representation of the operating point over a compressor map.

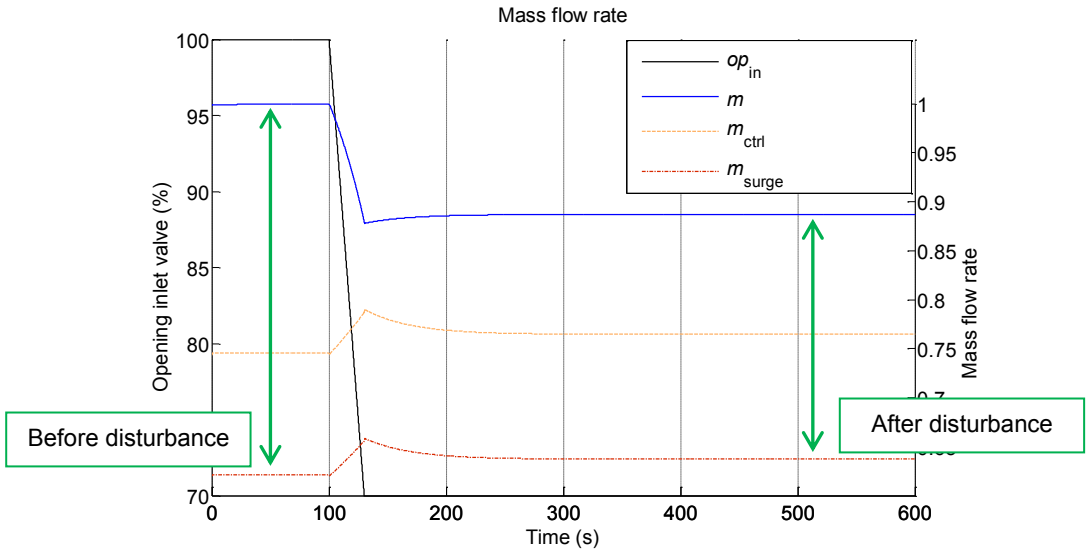


Figure 3-16. Representation of the surge margin over time

3.3.4 Overall control system

The overall control system includes the two control loops presented above. The capacity control loop controls the compressor outlet pressure by manipulating the torque of the driver. The antisurge control loop avoids surge by opening the antisurge recycle valve when the compressor flow rate falls below its minim value. The overall control system is represented in Figure 3-17.

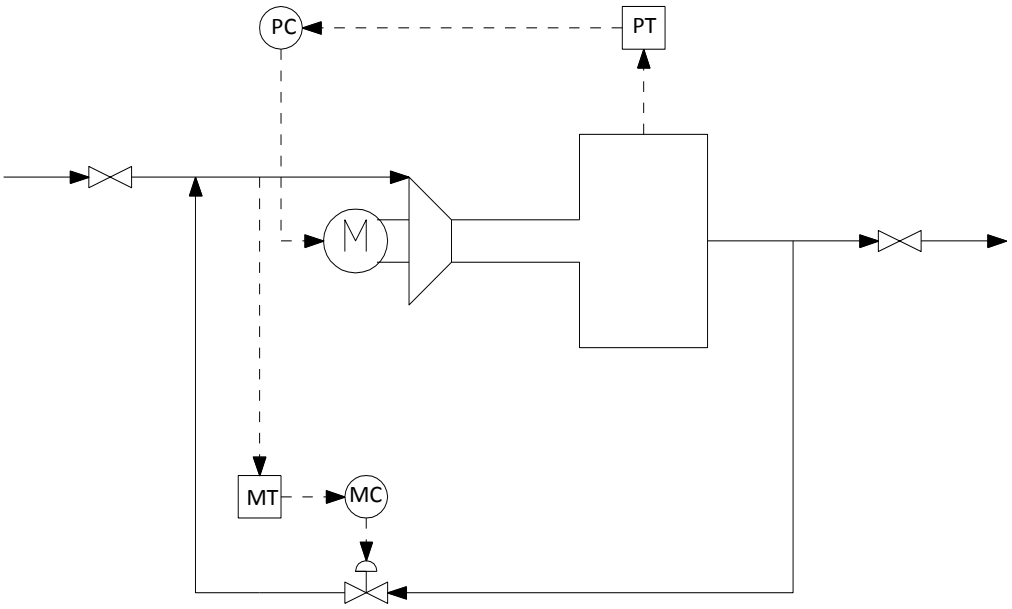


Figure 3-17. Overall control system for a hot gas recycle compressor station

These two control loops are acting on the same process system and therefore they can influence each other. The manipulation of the driver torque affects both inlet and outlet pressures, being the flow rate the same. At the same time a change in the upstream or downstream pressure can reduce the margin between the surge line and the operating point.

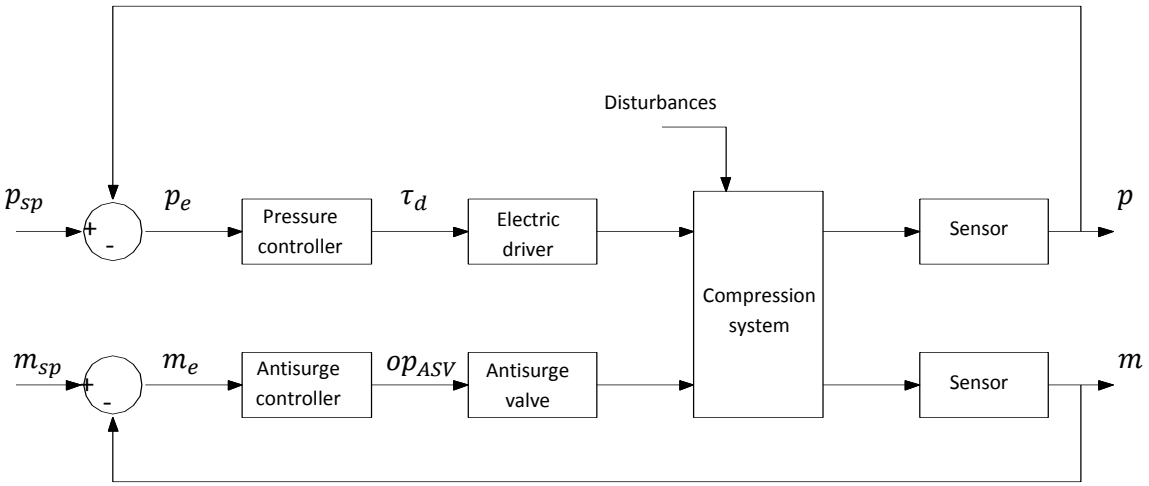


Figure 3-18. Cause-effect block diagram of multiple-input multiple-output control system for compression application

The interaction between the control loops can be advantageous. This happens for example when the action of the capacity controller brings the operating point further from the surge line. However this interaction can also be negative and cause a strong oscillation of the system. In order to reduce this oscillation usual techniques are the detuning or the decoupling of the control loops (Horowitz et al., 2006). However these techniques have some disadvantages:

- Detuning usually reduces the responsiveness of one of the controllers to a disturbance. As surge can happen within milliseconds, the pressure controller is usually slowed down and this decreased the performance in terms of pressure control
- Decoupling is not always possible as it depends on the complexity of the system.

Some examples regarding disadvantageous interactions between control loops will be presented in the following chapters. These issues represent a strong motivation for the improvement of the control system for centrifugal compressors. Therefore the aim is to achieve an overall integrated control system that can properly handle this multiple-input multiple-output system.

3.3.5 Summary

The literature review and industrial survey in Chapter 2 highlighted the use of feedback control algorithms for both capacity and antisurge control. The main reasons are the simplicity of the algorithm structure and the reliability of the control architecture due to the utilisation of standard measurements and actuators.

In this section the overall control system has been modelled by dividing the control system into single control loops for capacity and antisurge control. This system represents the state of the art control system for centrifugal gas compressors in industrial full size applications.

The two separate control loops act on the same process system and therefore influence each other. The interaction can be advantageous but also disadvantageous and therefore this represents an issue in the current state of the art. The limitation of the current state of the art has been presented via analysis of the current practice and literature and will be further investigated in the following chapters.

In conclusion the interaction between the control loops should be reduced in order to guarantee smooth and stable operation and protection of the compressor from surge. The basic structure of the state of the art control systems gives margin for improvement if more advanced control strategies are applied. At the same time other solutions already developed by researchers were not employed. Therefore it is also important to take into account practitioners' feedback.

The next section covers the implementation of both process and control system models into the selected numerical tool.

3.4 Model implementation

The previous part of this chapter has presented the model of the compression system and the model of the feedback control system. These two models have been implemented in a numerical tool and this implementation is presented in this sub-section of the Chapter.

The implementation of the model is the third task of this chapter. This task included the selection of modelling and simulation tool, the method for the resolution of the algebraic and differential equations, the selection of input and output variables. The model of the compression system and of its control system has been implemented in MATLAB Simulink. The implementation of a mathematical model into modelling software is crucial for the correct resolution of the model equations. Decisions were made according to the purpose of research.

This section first presents the modelling and simulation tool and the resolution method. Then it includes the implementation of the open loop model, followed by the implementation of the closed loop model.

3.4.1 Selection of the numerical tool

3.4.1.1 Modelling tool

The models developed in the previous part of the Chapter have been implemented in MATLAB Simulink® environment (version number 8.1 R2013a). Simulink is a block diagram environment for multi-domain simulation and model-based design. It has been selected because it supports modelling, simulation and automatic code generation. It also provides a graphical editor, customizable block libraries, and solvers for modelling and simulating dynamic systems. Simulink is integrated with MATLAB therefore it enables to incorporate MATLAB algorithms into models and to export simulation results to MATLAB for further analysis.

Another important feature of Simulink is the possibility to connect the model to hardware for real-time testing and embedded system deployment. This could allow future testing of the proposed control system on a real compressor. Moreover it is also possible to generate C and C++, HDL, or PLC code directly from the model (MathWorks, 2015g). Therefore the proposed control system can be implemented in any system supporting Simulink itself but also in other programming languages as those cited above. These possibilities are discussed further in Chapter 7.

3.4.1.2 Resolution method

Solvers are numerical integration algorithms that compute the system dynamics over time using information contained in the model. Simulink provides solvers to support the simulation of continuous-time (analog), discrete-time (digital), hybrid (mixed-signal), and multirate systems of any size.

Simulink solvers determine the time of the next simulation step and apply a numerical method to solve the set of ordinary differential equations that represent the model. Solver properties include:

- Fixed step versus variable step
- Discrete versus continuous
- Explicit versus implicit
- One step versus multistep
- Variable order solver.

Explicit continuous variable-step solvers are designed for nonstiff problems. ode45 is the default solver for models with continuous states and it has been selected for the resolution of the model equations. This Runge-Kutta solver is a fifth-order method that performs a fourth-order estimate of the error. This solver is considered more accurate and faster than other solvers, which have been developed mainly for stiff problems (MathWorks, 2015a).

3.4.2 Implementation of the open loop model

The open loop model of the compressor includes the model of the inlet and outlet valves, the model of the compressor, the model of the plenum and the model of the antisurge recycle valve. For the sake of clarity and simplicity the implementation of the hot gas recycle configuration without hold-up volume is presented in this section.

The implementation of the model is presented following the block diagram structure adopted in the modelling tool. The outer block diagram represented the full open loop model, while the inner blocks included:

- Compressor
- Inlet, outlet and recycle valves
- Estimation of outlet temperature and power consumption
- Estimation of the surge limit.

3.4.2.1 Degrees of freedom analysis

A degrees of freedom analysis has been performed in order to guarantee that the system was uniquely specified. The result of the degrees of freedom analysis is summarised in Table 3-1.

Table 3-1. Degrees of freedom analysis for the open loop model of the compression system

Entity	Equations	Variables	Input variables	Output variables
Value	25	32	7	25

Input and output variables have been specified for each block diagram in the following part of the section. Input variables are either manipulated variables or variables defining the boundary of the system. Output variables are the unknown variables that need to be estimated via simulation. They

include the two main controlled variables i.e. compressor outlet pressure and inlet mass flow rate. Model parameters include geometrical parameters and gas properties.

3.4.2.2 Open loop compression system

The open loop system is represented in Figure 3-19.

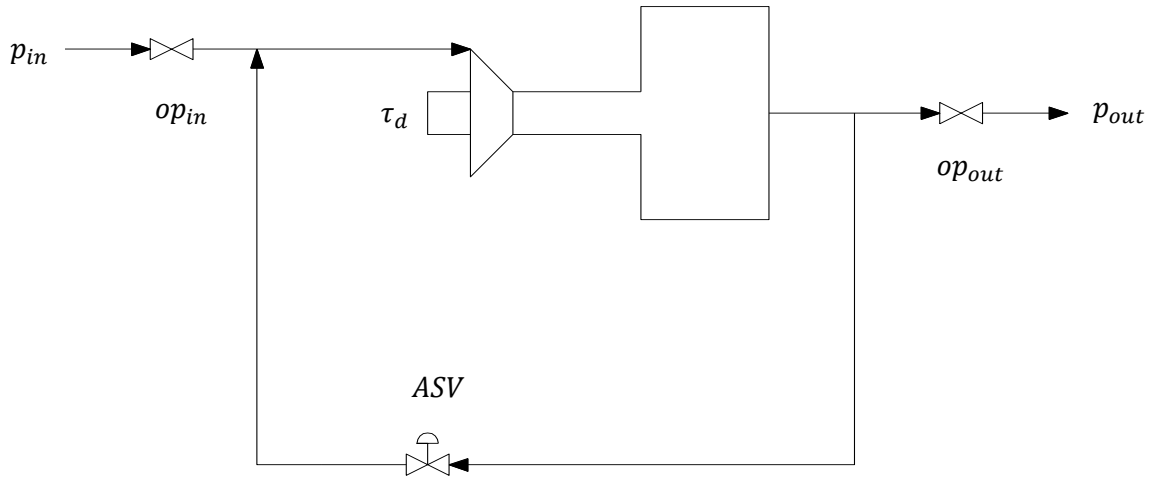


Figure 3-19. Open loop compression system

All the variables of the open loop model have been included and they have been divided between input variables and output variables. Input variables are the known variables while the output variables are the variables estimated during the simulation, as represented in Figure 3-20. The input variables are either manipulated variable or variables representing the boundary of the system and are summarised in Table 3-2 and also represented in Figure 3-20.

Table 3-2. Input and output variables for the open loop compression system

Input variables	Output variables
System inlet pressure p_{in}	Compressor outlet pressure p
System outlet pressure p_{out}	Compressor mass flow rate m
Opening of the inlet valve op_{in}	Rotational shaft speed N
Opening of the outlet valve op_{out}	Compressor inlet temperature T_{01}
Opening of the antisurge valve op_{ASV}	Compressor outlet temperature T_{02}
Torque of the driver τ_d	Surge flow rate m_{surge}

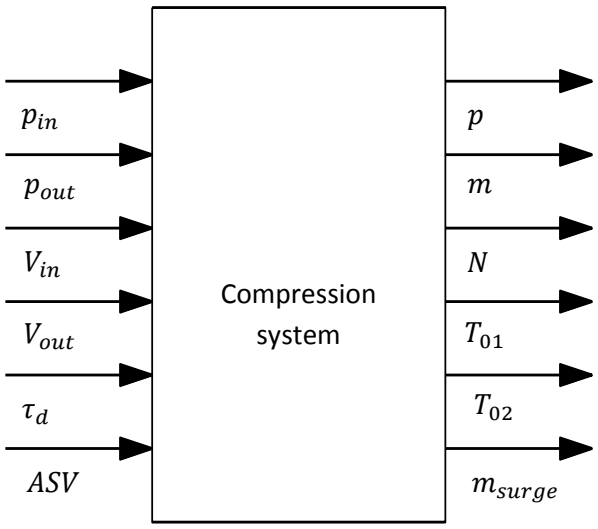


Figure 3-20. Simulink block for the open loop compression system

Inside the main block representing the open loop system, there are sub-blocks employed to represent different parts of the compression systems such as:

- Compressor and plenum
- Inlet section
- Outlet section
- Recycle section.

Additional blocks have also been employed to estimate the outlet temperature and power consumption of the compressor and the location of the surge line. More details on the structure of the Simulink model will be given in the Appendix.

Some equations have been employed multiple times for example in order to estimate the corrected mass flow rate and rotational shaft speed (equations (3-11) and (3-12)) or the specific heat ratio (equations (3-15), (3-16) and (3-17)) of the gas.

3.4.2.3 Compressor and plenum

Input and output variables of the sub-block representing the compressor and the plenum are summarised in Table 3-3.

Table 3-3. Input and output variables for the compressor block

Input variables	Output variables
Inlet pressure of the compressor p_{01} Inlet temperature of the compressor T_{01} Torque of the driver τ_d Outlet flow rate of the plenum m_{out}	Outlet pressure of the compressor p Inlet mass flow rate of the compressor m Radial speed of the shaft ω Rotational shaft speed of the shaft N Pressure ratio of the compressor ψ_c Outlet temperature of the compressor T_{02} Outlet pressure of the compressor p_{02} Polytropic efficiency of the compressor η_p

The equations solved in this sub-block are the following:

- Equation (3-1): mass balance of the compressor in order to estimate p
- Equation (3-2): momentum balance of the compressor in order to estimate m
- Equations (3-3) and (3-4): momentum of momentum balance of the rotating shaft in order to estimate the radial velocity ω and therefore the rotational shaft speed N
- Equation (3-5): estimation of the torque required by the compressor
- Equations (3-6), (3-7), (3-8) and (3-18): the functions describing compressor characteristic Ψ_c (expressed also as ratio between compressor outlet and inlet pressure), compressor polytropic efficiency η_p and compressor outlet temperature T_{02}.

A rate limiter has been implemented in this sub-block in order to limit the rate of change of the rotational shaft speed of the compressor.

3.4.2.4 Inlet section

Input and output variables of the sub-block representing the inlet valve are collected in the following table.

Table 3-4. Input and output variables for the inlet section

Input variables	Output variables
Inlet pressure of the system p_{in} Inlet temperature of the system T_{in} Opening of the inlet valve op_{in} Inlet mass flow rate of the compressor m Recycle mass flow rate m_r	Inlet mass flow rate of the system m_{in} Inlet pressure of the compressor p_{01}

The equations solved are the following:

- Equation (3-21): mass balance for the first node where the freshly fed gas mixes with the recycled gas when the antisurge valve is open. It allows the estimation of m_{in}
- Equation (3-19): the flow through the inlet valve, that allows the estimation of p_{01}
- Equation (3-20): the density of the gas upstream the inlet valve, employed in the previous equation.

3.4.2.5 Outlet section

The outlet section block deals with the variables presented in Table 3-5.

Table 3-5. Input and output variables for the outlet section

Input variables	Output variables
Plenum pressure p Outlet temperature of the compressor T_{02} Outlet pressure of the system p_{out} Opening of the outlet valve op_{out}	Outlet flow rate of the system m_{out}

The equations solved here are:

- Equation (3-22): mass balance for the second node where the compressed gas splits between delivered gas and recycle gas
- Equation (3-9): the estimation of the outlet mass flow rate m_{out}
- Equation (3-10): estimation of the density of the gas upstream the outlet valve ρ, that has been employed in the previous equation.

3.4.2.6 Recycle section

Table 3-6 presents the variables referring to the recycle section.

Table 3-6. Input and output variables for the recycle section

Input variables	Output variables
Inlet pressure of the compressor p_{01} Plenum pressure p Outlet temperature of the compressor T_{02} Opening of the antisurge valve op_{ASV}	Recycle mass flow rate m_r

The equations solved in this sub-block are the following:

- Equation (3-24): mass flow rate through the recycle valve m_r
- Equation (3-10): estimation of the density of the gas upstream the recycle valve, employed in the previous equation.

3.4.2.7 Temperature and power consumption

A further sub-block has been added in order to estimate the temperature of the gas at the inlet of the compressor and the power consumption of the machine employed for compression. The variables employed are summarised in Table 3-7.

Table 3-7. Input and output variables for outlet temperature and power estimation

Input variables	Output variables
Inlet temperature of the system T_{in} Outlet temperature of the compressor T_{02} Inlet mass flow rate of the system m_{in} Inlet mass flow rate of the compressor m Recycle mass flow rate m_r	Inlet temperature of the compressor T_{01} Power consumption of the compressor P_m

The equations solved in this lock are the following:

- Equation (3-25): energy balance for the first node, in order to estimate the compressor inlet temperature T_{01}
- Equation (3-13) and (3-14): estimation of the power consumption of the compressor.

3.4.2.8 Surge limit

A further block has been implemented in order to estimate the surge limit as a function of inlet mass flow rate and rotational shaft speed. Corrected values m_c and N_c have been also estimated in order to take into account the effect of the inlet conditions on the location of the surge region. Therefore the variables employed in this sub-block are listed in Table 3-8.

Table 3-8. Input and output variables for the surge estimation block

Input variables	Output variables
Pressure ratio ψ_c Rotational shaft speed N Inlet pressure of the compressor p_{01} Inlet temperature of the compressor T_{01}	Surge flow rate m_{surge}

The following equation has been employed and solved in order to estimate m_{surge}:

- Equation (3-35): function representing the surge region.

3.4.3 Implementation of the closed loop model

The implementation of the closed loop model required the addition of the control system to the open loop model. The closed loop system has already been represented in a schematic sketch in Figure 3-17. It includes two control loops, the capacity control loop and the antisurge control loop.

3.4.3.1 Generic PID controller

The PID controller block in its parallel form is represented in Figure 3-21.

In this nomenclature the input of the controller u is the error while y is the output of the controller. The error u is the difference between the measured variable and its set point. This block is employed in Simulink in order to solve the equation (3-32). Simulink allows the setting and tuning of the controller gains and the limitation of the block output (MathWorks, 2015f). This latter option can be employed in order to represent in the closed loop model the saturation of the actuators.

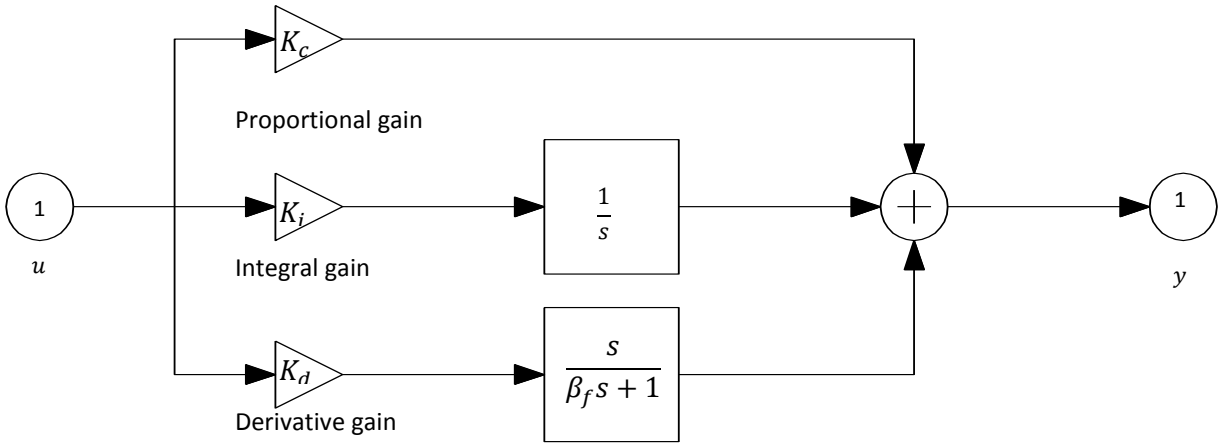


Figure 3-21. Parallel form of a generic PID controller (MathWorks, 2015f)

3.4.3.2 Implementation of the overall control system

The implementation of the overall control system, including capacity control loop and antisurge control loop, has been previously represented in Figure 3-18.

The two sensors for the pressure and flow rate measurement have been considered ideal and therefore there is no difference between controlled variable cv and process variable pv.

The possible disturbances that have been selected as affecting the system include inlet pressure and outlet pressure of the system and the opening of the two boundary valves.

Lower and upper limits and rate limits have been implemented for the outputs of the controllers, according to the following inequalities:

$$N_{min} \leq N \leq N_{max} \quad \textbf{(3-36)}$$

$$\frac{d\,N}{dt} \leq \left(\frac{d\,N}{dt}\right)_{max} \quad \textbf{(3-37)}$$

$$0 \leq \tau_d \leq \tau_{d,max} \quad \textbf{(3-38)}$$

$$0\% \leq op_{ASV} \leq 100\% \quad \textbf{(3-39)}$$

$$\frac{d\,op_{ASV}}{dt} \leq \left(\frac{d\,op_{ASV}}{dt}\right)_{max} \quad \textbf{(3-40)}$$

3.4.4 Summary

The section has included the selection of the numerical tool and the implementation of both open loop and closed loop models. MATLAB Simulink has been selected as numerical tool for modelling and simulation. It allows multi-domain simulation and model-based design. It has been selected

because it supports simulation, automatic code generation, and continuous test and verification of embedded systems. It also gives the possibility to connect the model to hardware for real-time testing and embedded system deployment. This option could be very useful in the future for the implementation of the proposed control systems, presented in the following chapters, in a real system.

The solver ode45 has been selected for the resolution of the model equations. It is a Runge-Kutta solver that is considered accurate and fast in the resolution of nonstiff problems.

Input and output variables have been selected for each block diagram according to the control purpose of this model. Therefore the main output variables are the compressor outlet pressure and the mass flow rate.

The following section presents the validation of the model, the parameters estimated, the estimation method employed and the results.

3.5 Case study

The case study has been provided by the research partner ESD Simulation Training. It is a full industrial system and it is represented in Figure 3-22 and Figure 3-23.

ESD Simulation Training developed a state of the art industrial training simulator based on this case study. The simulator has been validated against operational data coming from a real CO_2 compression system. The simulator provides steady state and dynamic simulation and it is currently employed in the training course 'Carbon Dioxide Compression' (ESD Simulation Training, 2014).

A significant part of the PhD project was spent working in collaboration with ESD in order to support the activity of verification and validation of the simulator against the industrial data. This activity is anticipated in this section of the chapter and described with more details in Appendix.

Therefore this section of the chapter describes the case study, the parameters of the model, the main steps of the methodology of validation of the ESD simulator and the process of data collection. In the next section the Simulink model will be validated against the data collected from the case study here described.

3.5.1 Description of the case study

3.5.1.1 Case study

The case study is based on a multistage centrifugal compressor arranged in a single shaft configuration and driven by an asynchronous electric motor. The multistage compressor consists of four single stages compressors in series. Figure 3-22 is the schematic representation of the multistage compressor. For each single stage of compression there is a heat exchanger HE, a separation vessel V and a compressor C. An additional heat exchange is placed before the exit of the system.

There is a gear box between the second and the third stage of compression. Therefore the first two single stage compressors run at the same speed while the second two single stage compressors run at another speed. The ratio between these two speeds is constant. The single stages have been approached separately in the thesis however they belong to the same machine. In particular the first stage will be employed in Chapter 4 while the third and fourth stages will be employed in Chapters 5 and 6.

The process fluid is a mixture of carbon dioxide and water with small percentages of light hydrocarbons. This composition is typical of a flue gas coming from amine absorption of CO_2 from natural gas (Rufford et al., 2012).

After the calculations were completed all the variables reported in the thesis have been scaled according to their design value at the inlet of the compressor. This is due to non-disclosure agreement with the partner of the project that has provided the industrial case study.

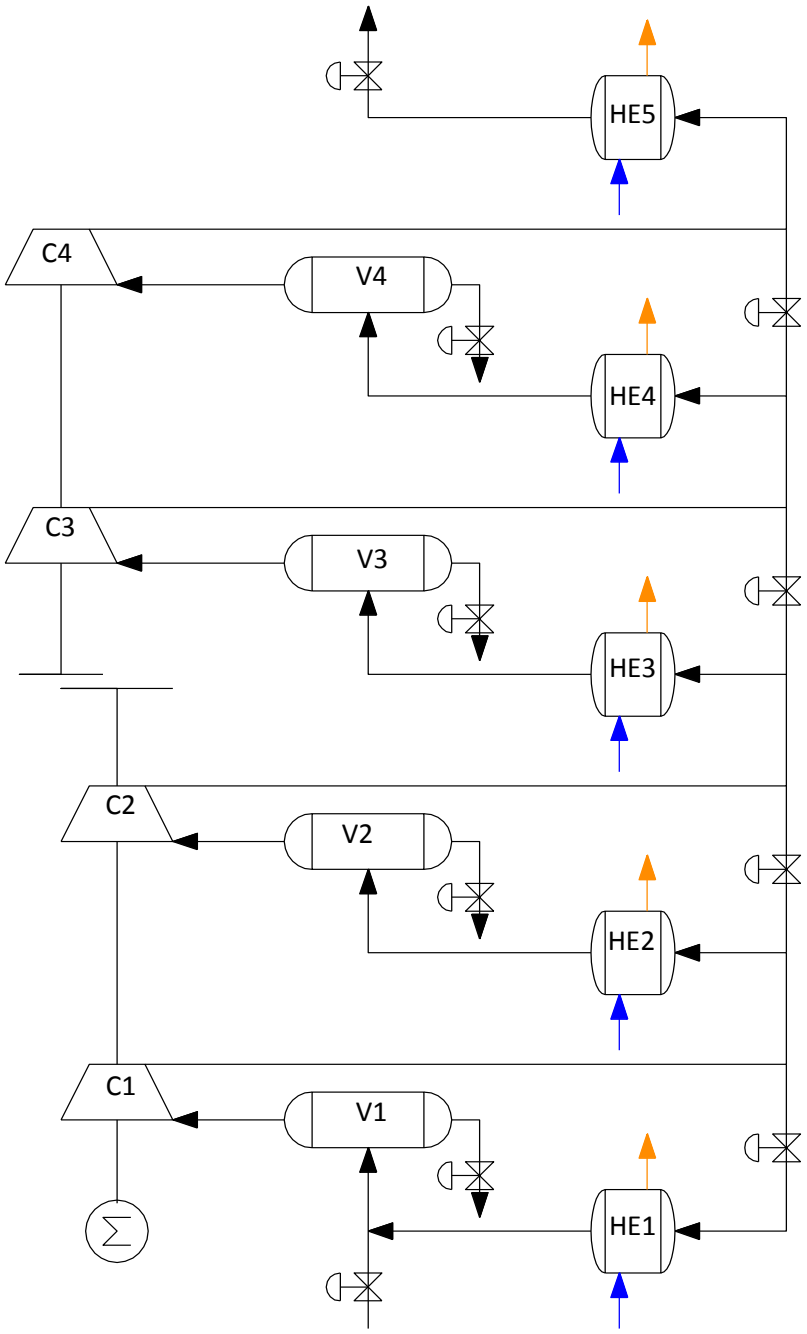


Figure 3-22. Schematic representation of the multistage compressor system (open loop)

Figure 3-23 includes the control system of the process. The pressure controller measures the inlet pressure of the both first compression stage and fourth compressor stage and acts on the motor. The controlled variable is the inlet pressure of the first stage however the inlet pressure of the fourth stage is measured too in order to avoid overpressure towards the exit of the multistage compressor.

Each compression stage has an antisurge controller measuring the inlet flow rate of the stage and acting on the corresponding antisurge recycle valve.

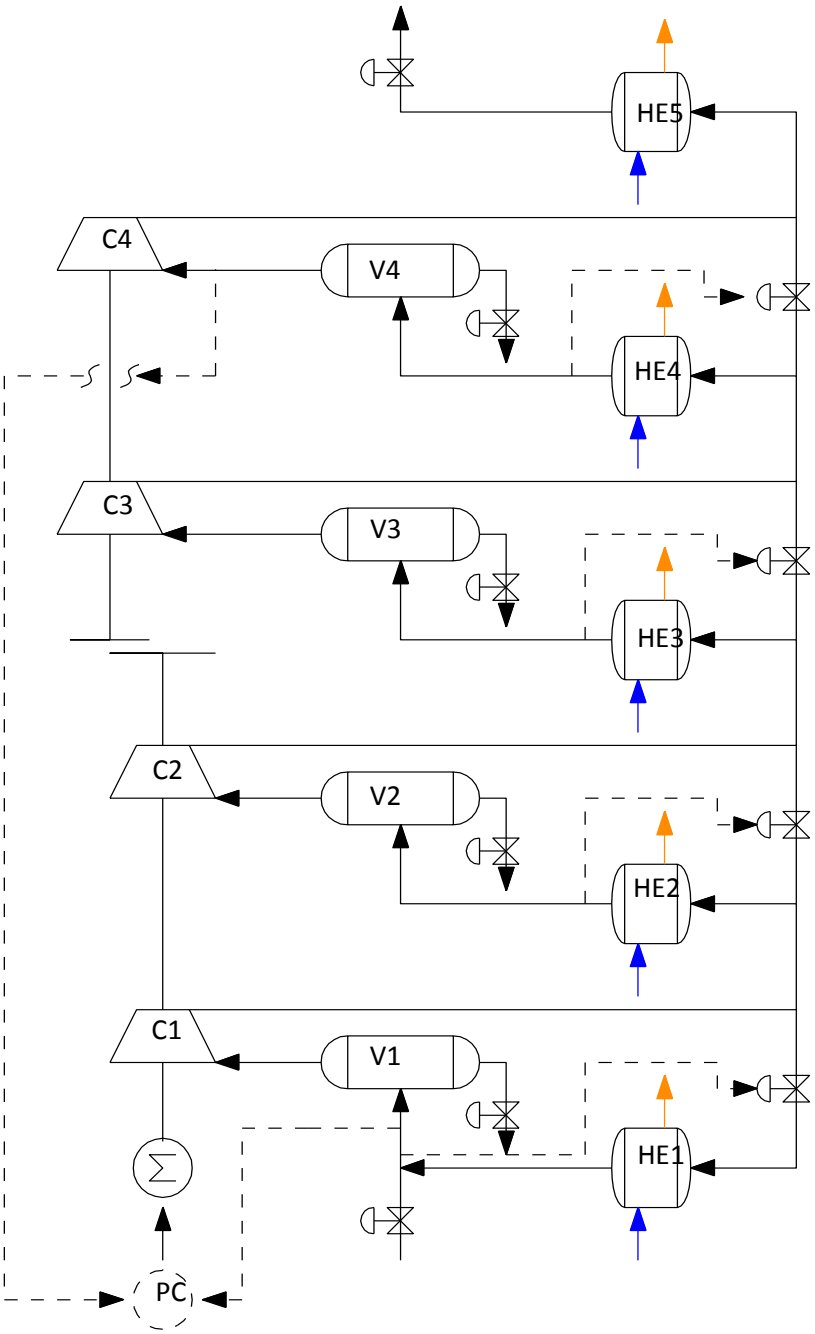


Figure 3-23. Schematic representation of the multistage compressor system (closed loop)

3.5.1.2 Parameters of the model

According to the equations presented in section 3.2, the parameters that were included in the model are the following:

- Sonic velocity at ambient conditions a_{01}
- Plenum volume V

- Duct throughflow area A_1
- Duct length L
- Total moment of inertia of the system J
- Slip factor μ
- Impeller radius r_2
- Inlet, outlet and antisurge valves constants, respectively k_{in}, k_{out}, k_{ASV}
- Reference pressure p_{ref} and temperature T_{ref}
- Gas mass fractions for the two main components, carbon dioxide and water, respectively x_1 and x_2
- Average specific heat ratio γ_{avg}.

The variables refer to a single stage of compression. The first four parameters appear coupled in the model as $\frac{{a^2}_{01}}{V}$ and $\frac{A_1}{L}$ and can be substituted by them. a_{01} is estimated via the following equation:

$$a_{01} = \sqrt{\frac{\gamma R T_{02}}{MW}} \quad \textbf{(3-41)}$$

where γ is the specific heat ratio, R is the universal gas constant, T_{02} is the temperature of the gas at the exit of the compressor and MW is the molecular weight of the process fluid.

The geometrical parameters μ and r_2 have been estimated by the geometry of the compressor. In particular μ has been estimated according to:

$$\mu = 1 - \frac{1}{number\ of\ blades} \quad \textbf{(3-42)}$$

The valve constants have been estimated by mean of steady state data. Reference pressure and temperature have been arbitrary selected.

The composition of the gas and its average specific heat ratio were known parameters.

Optimisation technique has been employed for the estimation of parameters present in the ordinary differential equations. The methodology applied and the results of the estimation of the parameters and the validation of the models has been summarised in section 3.6.

3.5.2 Methodology of validation of ESD simulator

As previously mentioned, part of the PhD was spent working in collaboration with ESD in order to support the activity of validation of their CO_2 simulator. This collaboration provided useful input to ESD, and also provided in-depth training in compressor modelling and control to support the research activity of the PhD.

The methodology for the validation of the simulator included the following steps:

- Validation of the design point of the multistage compressor at steady state
- Validation of the performance maps of the four stages of compression
- Analysis of the off-peak operation
- Analysis of controllers and alarms
- Analysis of cause-effect for trips of single units
- Analysis of shut-down and start-up procedures.

More details on the methodology will be given in Appendix 2. The outcome of the validation process has been the availability of a high fidelity tool correctly representing the operation of the CO_2 compression system in both steady state and dynamic operation.

3.5.3 Data collection

The model of the compressor presented in the thesis was validated against data coming from the industrial case study. Compressor performance maps and data sheets of the multistage machine were used to validate the model during steady state simulations. The industrial simulator was used to validate the dynamic behaviour during transients between steady states.

The ESD simulator was run in open loop (i.e. with the speed controller in manual mode and constant output) and tested via inlet step disturbances. The only variable that was possible to manipulate manually was the inlet pressure of the system. This variable was changed performing step changes experiments and the data from these experiments were recorded. For each stage of compression, the data recorded were the compressor inlet pressure, inlet mass flow rate and outlet pressure.

In the Simulink environment an experiment specifies measured input and output data. During the estimation of the parameters of the model, the experiment input data is used to simulate the model and the model output is compared with the measured experiment output data (Mathworks, 2015c). This optimisation procedure is described in the following section of the chapter.

3.5.4 Summary

This section of the chapter has described the case study and the collaboration with ESD for the validation of their simulator.

The outcome of the collaboration includes the availability of a fully validated simulator tool. This simulator tool has been employed in order to validate the Simulink model presented in the thesis during dynamic operation. In fact the Simulink model is being validated against the ESD simulator, and the ESD simulator is itself a state of the art industrial training simulator that is itself validated against operational data from a real CO_2 compression system.

3.6 Estimation of parameters and model validation

The fourth task of this Chapter is the validation of the model presented in the thesis and implemented in Simulink. This task is fundamental in order to guarantee the accuracy and reliability of the model. The model must be able to predict the performance of the machine in both steady state and dynamic operation and at the design point as well as during off-load operation. The completion of this task guarantees the availability of a model that represents a good reference for the solutions that will be proposed later on in the thesis. Moreover this task guarantees the understanding of the main issues regarding the reference feedback control system.

Section 3.5 has described the case study and the procedure adopted to collect the data necessary in order to validate the model. Two data sets have been collected:

- Data set 1: estimation data
- Data set 2: validation data.

The methodology adopted in this section consists of two mains steps:

- Estimation of the parameters of the model
- Validation of the model.

The estimation of the parameters of the model is necessary in order to estimate the parameters that were not available such as ${a_{01}}^2/V$ and A_1/L. In order to perform this task the first set of data, the estimation data, has been employed.

The validation of the model has been performed after all the parameters have been estimated. The second set of data, the validation data, has been employed in order to guarantee that the estimation of the parameters was accurate.

Therefore the following part of the chapter will cover estimation of model parameters and validation of the model. Finally the section will also include the tuning of the feedback control system.

In the following sections, the term *ESD model* refers to the model in the ESD industrial simulator, which has been validated against industrial data from a real installation. The term *Simulink model* refers to the model used throughout the thesis which was proposed in Section 3.2.

3.6.1 Estimation of model parameters

The estimation of the parameters of the Simulink model has been performed in order to estimate the following parameters, which are inside equations (3-1) and (3-2):

- ${a_{01}}^2/V$
- A_1/L.

In order to estimate these parameters an optimisation technique has been adopted.

3.6.1.1 Optimisation technique

When performing parameter estimation in Simulink, the software formulates an optimization problem. The optimization problem solution is the estimated parameter values set.

This optimization problem consists of:

- The design variables x, which are the model parameters
- The objective function (also called cost function or estimation error) $F(x)$, that calculates a measure of the difference between the simulated and measured responses
- The bounds $\bar{\bar{x}} \leq x \leq \bar{x}$, that represent the limits on the estimated parameter values
- The constraint function $C(x)$, which specifies restrictions on the design variables.

The optimization solver tunes the model parameters in order to satisfy the specified objectives and constraints. The purpose is to obtain a simulated response (y_{sim}) that tracks the measured response or reference signal (y_{ref}).

The cost function, $F(x)$, is the objective function of the optimization problem. The cost function is a function of the raw estimation error, $e(t)$ (also referred to as the error residuals or residuals), defined as:

$$e(t) = y_{ref}(t) - y_{sim}(t) \quad \textbf{(3-43)}$$

The Sum Squared Error (SSE) has been selected as objective function as it is defined according to the following equation:

$$F(x) = \sum_{t=0}^{n} e(t) \times e(t) \quad \textbf{(3-44)}$$

where n is the number of samples in common between measured response and reference signal.

The optimization problem can be:

- A minimization problem, that minimizes the objective function
- A mixed minimization and feasibility problem, that minimizes the objective function subject to specified bounds and constraints
- A feasibility problem, which finds a solution that satisfies the specified constraints.

A minimisation problem has been selected for the estimation of the model parameters. Among the possible optimization methods, including:

- Nonlinear least squares
- Gradient descent
- Simplex search
- Pattern search.

The nonlinear least square method has been selected for this analysis. It minimises the squares of the residuals, according to:

$$\min_x \|F(x)\|_2^2 = \min_x (f_1(x)^2 + f_2(x)^2 + \cdots + f_n(x)^2) \quad \textbf{(3-45)}$$

$$s.t. \bar{\bar{x}} \leq x \leq \bar{x} \quad \textbf{(3-46)}$$

where $f_1(x)$, $f_2(x)$, $f_n(x)$ represent the residuals and n is the number of samples (Mathworks, 2015c).

3.6.1.2 Evaluation of the optimisation

The result of the optimisation technique is the identification of the values of the parameters. The responses from respectively ESD model and Simulink model have been compared by graphical representation.

In order to numerically quantify the deviation between the two responses, both of them have been fitted with a first order transfer function and the transfer function parameters have been compared.

A generic first order plus delay transfer function is represented by the following equation:

$$g(s) = \frac{Ke^{-sB_d}}{s\beta + 1} \quad \textbf{(3-47)}$$

where K is the process gain, B_d is the time delay and β is the time constant.

If the delay is negligible, the outlet pressure and mass flow rate of the compressor can be represented by the following first order transfer functions:

$$g_p(s) = \frac{K_p}{s\beta_p + 1} \quad \textbf{(3-48)}$$

$$g_m(s) = \frac{K_m}{s\beta_m + 1} \quad \textbf{(3-49)}$$

Therefore the parameters that have been employed to compare the response of the reference system with the response of the optimised system are the following:

- Process gains K_p and K_m
- Process time constants β_p and β_m.

Figure 3-24 represent the cause-effect block diagram relating the variation of the inlet pressure of the compressor $\overline{\Delta p_{01}(s)}$ to the variation of respectively the inlet mass flow rate $\overline{\Delta m(s)}$ and the outlet pressure of the compressor $\overline{\Delta p(s)}$ in the s-domain. In fact the data set collected for the estimation of the parameters consisted in the time series of the following variables over a certain period of time:

- Compressor inlet pressure p_{01}

- Compressor outlet pressure p
- Compressor inlet mass flow rate m.

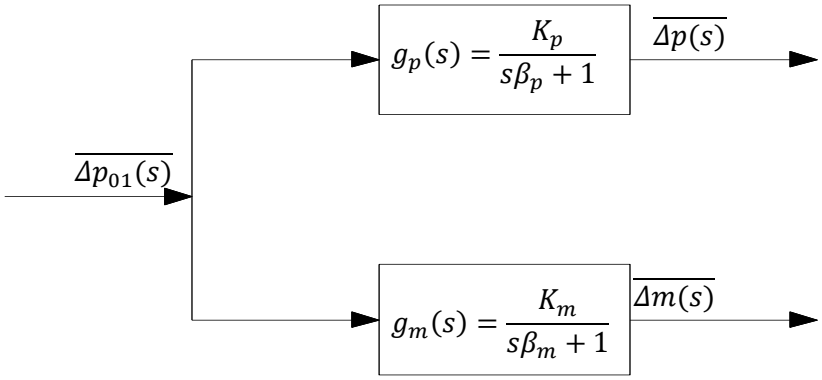


Figure 3-24. Cause-effect block diagram

The transfer functions represented in Figure 3-24 can be expressed as the following linear differential equations:

$$\beta_p \frac{dp}{dt} + p(t) = K_p p_{01}(t) \quad \textbf{(3-50)}$$

$$\beta_m \frac{dm}{dt} + m(t) = K_m p_{01}(t) \quad \textbf{(3-51)}$$

These equations are useful to define the units of process gains and time constants. They are summarised in Table 3-9.

Table 3-9. Units of the process gains and time constants employed for evaluating the model optimisation

Parameter	Unit
K_p	barbar^{-1} → dimensionless
K_m	kgs^{-2}m^{-1}
β_p	s
β_m	s

3.6.1.3 Estimation of parameters for the first stage

The results of the validation of the first stage of compression have been summarised in Table 3-10. This stage has also been employed for the evaluation of the inertia of the system.

Figure 3-25 represents the pressure response of the first stage to an inlet pressure step change. The inlet pressure of the compressor, p_{01}, is represented on the left y-axis while the outlet pressure of the compressor is represented on the right y-axis. p_{ref} is the response of the ESD system while p_{model} is the optimised simulated response of the Simulink model. The figure shows that the model

has a very close match to the response of the industrial simulator. This indicates that the dynamic model is of the correct form and also that the model parameters match closely.

Figure 3-26 represents the flow rate response of the first stage to an inlet pressure step change. The inlet pressure of the compressor p_{01} is represented on the left y-axis while the mass flow rate of the compressor is represented on the right y-axis. m_{ref} is the response of the reference system while m_{model} is the optimised simulated response of the model.

As it is possible to see from the graphs and also from Table 3-11 and Table 3-12 the matching between the reference data and the optimised model is good. The maximum absolute relative error is 4.3% for the time constant while is 0.1% for the process gain.

Table 3-10. Estimated parameters for the first stage of compression

Parameter	Value
$\frac{a^2{}_{01}}{V}$	0.0013 $s^{-2}m^{-1}$
$\frac{A_1}{L}$	10.0 m
J	2.0 kgm^2

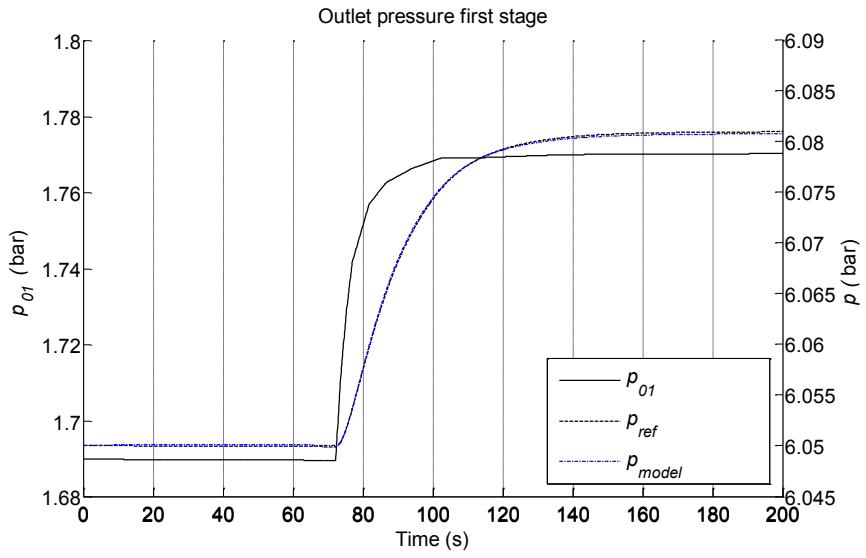


Figure 3-25. Compressor outlet pressure response to inlet pressure disturbance (stage 1)

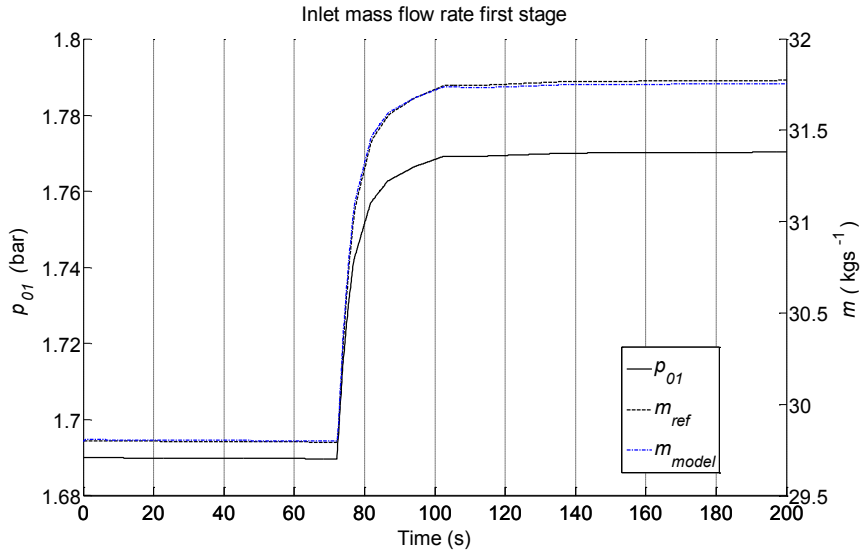


Figure 3-26. Mass flow rate response to inlet pressure disturbance (stage 1)

Table 3-11. Comparison of time constants between reference data and optimised model (stage 1)

Parameter	Reference	Model	Relative error
β_p	19.0 s	18.7 s	1.6%
β_m	4.7 s	4.5 s	4.3%

Table 3-12. Comparison of process gains between reference data and optimised model (stage 1)

Parameter	Reference	Model	Relative error
K_p	0.39	0.39	-0.11%
K_m	24.54 $kgs^{-2}m^{-1}$	24.54 $kgs^{-2}m^{-1}$	0%

The estimation of the inertia of the system presented some difficulties as a rate limiter was installed on the ESD system and it did not allow the precise evaluation of this parameter. However trial and error testing has estimated that its value is around 2 kgm^2, as represented in Figure 3-27. Simulation performed with J equal respectively to 2.5, 5 and 10 show a rate of change of the rotational shaft speed lower than the imposed rate limit and therefore the inertia must have a value lower than 2.5. The simulation corresponding to $J = 2$ kgm^2 is a good matching for the rate required.

For a rotating compressor the moment of inertia can be estimated using the following equation:

$$J = \frac{1}{2} M r^2 \tag{3-52}$$

where M is the mass of the rotor and r is the radius of the rotor. The estimated value of J is considered reasonable for a compressor having the following characteristic:

- Rotor tip diameter: 0.38-1.0 m
- Rotor hub diameter: 0.10-0.25 m

- Rotor length: 0.04-2.0 m
- Material: stainless steel (density 7650 kgm^{-3} (Yaws, 2014)).

Table 3-13 summarises the values of the parameters employed for the estimation.

Table 3-13. Estimation of moment of inertia for two compressor geometries

Parameter	Geometry 1	Geometry 2
Density (kgm^{-3})	7650.00	7650.00
Tip radius (m)	0.19	0.50
Hub radius (m)	0.05	0.13
Length (m)	2.00	0.04
Volume (m^3)	0.01	0.00
Mass (kg)	109.62	16.00
J (kgm^2)	2.00	2.00

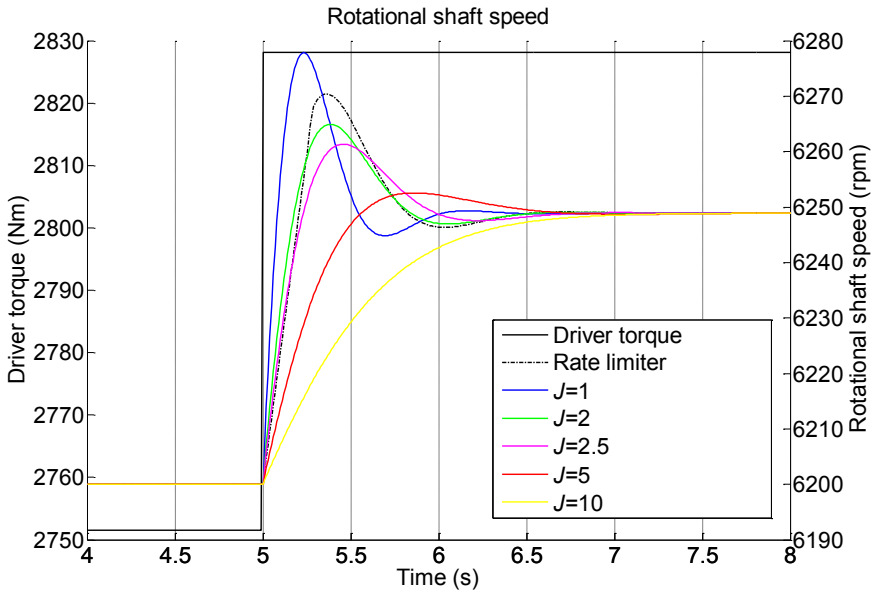


Figure 3-27. Evaluation of the total inertia of the system

3.6.1.4 Estimation of parameters for the second stage

The results of the validation have been summarised in Table 3-14.

Table 3-14. Estimated parameters for the second stage of compression

Parameter	Value
$\frac{a^2{}_{01}}{V}$	0.466 $s^{-2}m^{-1}$
$\frac{A_1}{L}$	0.025 m

Figure 3-28 represents the pressure response of the first stage to an inlet pressure step change while Figure 3-29 represents the flow rate response of the first stage to an inlet pressure step change.

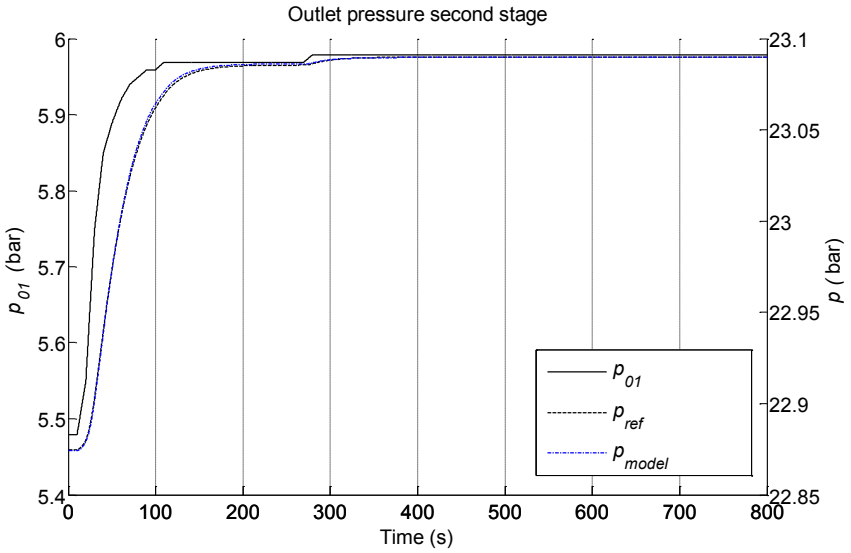


Figure 3-28. Compressor outlet pressure response to inlet pressure disturbance (stage 2)

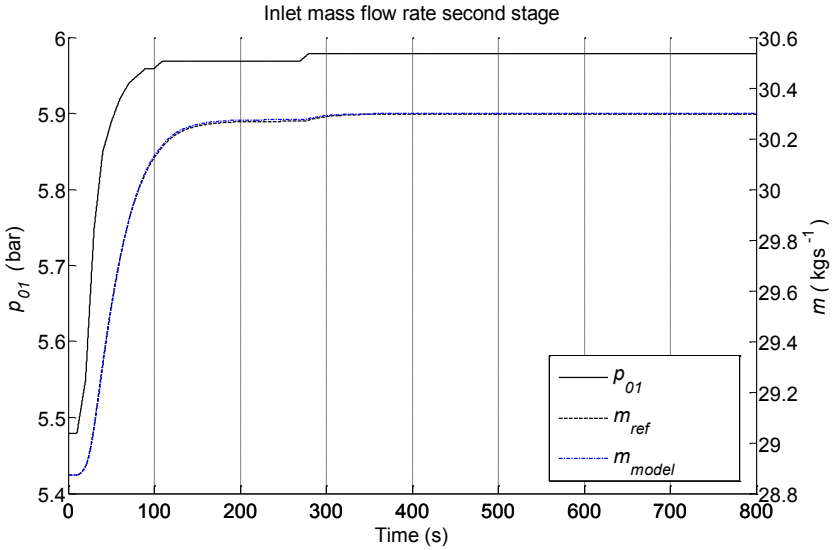


Figure 3-29. Mass flow rate response to inlet pressure disturbance (stage 2)

Also in this case the matching between the reference data and the optimised model is very good. The maximum absolute relative error is 0.94% for the time constant while is 0.18% for the process gain.

Table 3-15. Comparison of time constants between reference data and optimised model (stage 2)

Parameter	Reference	Model	Relative error
β_p	53.0 s	52.5 s	-0.94%
β_m	52.0 s	52.2 s	0.38%

Table 3-16. Comparison of process gains between reference data and optimised model (stage 2)

Parameter	Reference	Model	Relative error
K_p	0.43	0.43	-0.18%
K_m	2.85 $kgs^{-2}m^{-1}$	2.85 $kgs^{-2}m^{-1}$	-0.13%

3.6.1.5 Estimation of parameters for the third stage

The results of the validation have been summarised in Table 3-17.

Table 3-17. Estimated parameters for the third stage of compression

Parameter	Value
$\frac{a^2{}_{01}}{V}$	0.0056 $s^{-2}m^{-1}$
$\frac{A_1}{L}$	0.0111 m

Figure 3-30 represents the pressure response of the first stage to an inlet pressure step change while Figure 3-31 represents the flow rate response of the first stage to an inlet pressure step change.

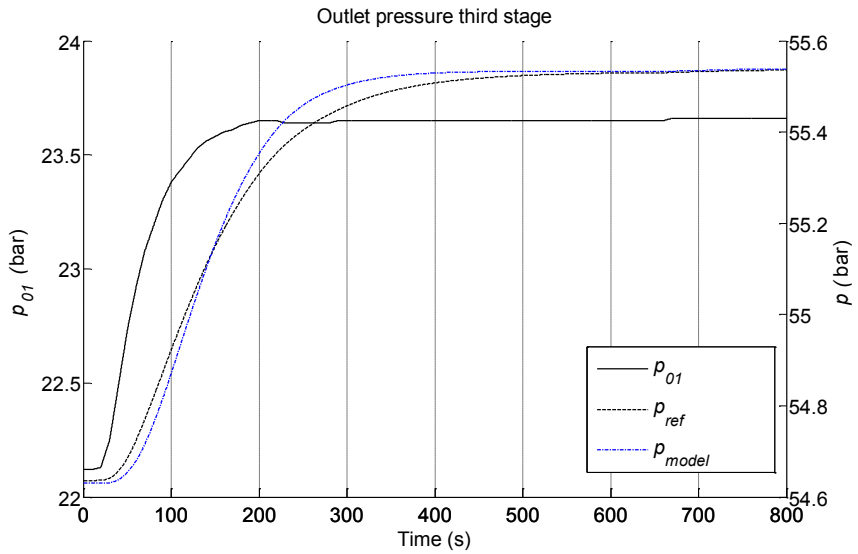


Figure 3-30. Compressor outlet pressure response to inlet pressure disturbance (stage 3)

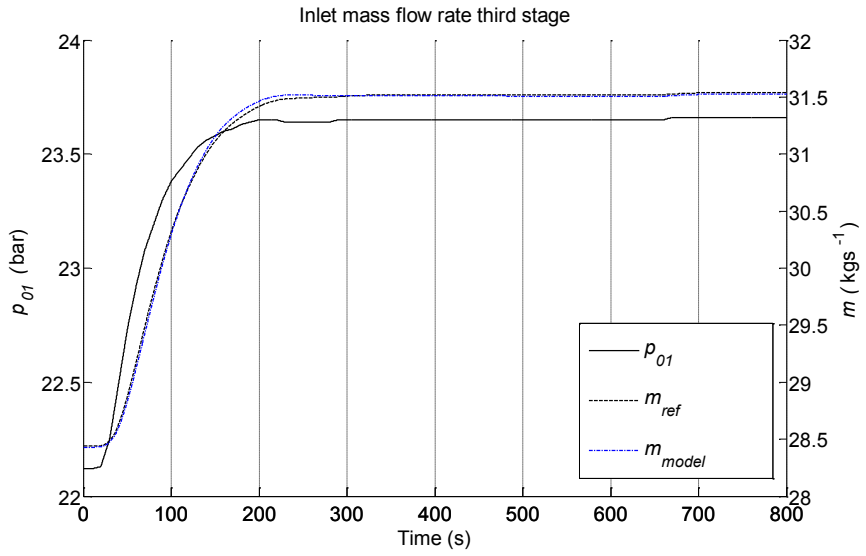


Figure 3-31. Mass flow rate response to inlet pressure disturbance (stage 3)

Again the model of this stage presents a good match with the reference data. The maximum absolute relative error is 2.8% for the time constant while it is 1.02% for the process gain. Figure 3-30 shows a deviation with respect to the reference data. The model presents a faster response than the reference process and this is reflected in the parameter β_p, summarised in Table 3-18. This may indicate that the parameter V employed in the model of the third stage is slightly smaller than what it should be. However the overall deviation is still small and therefore it has been assumed it can be neglected.

Table 3-18. Comparison of time constants between reference data and optimised model (stage 3)

Parameter	Reference	Model	Relative error
β_p	133.7 s	130.0 s	-2.8%
β_m	73.4 s	73.6 s	0.3%

Table 3-19. Comparison of process gains between reference data and optimised model (stage 3)

Parameter	Reference	Model	Relative error
K_p	0.58	0.59	-1.02%
K_m	2.01 $kgs^{-2}m^{-1}$	2.01 $kgs^{-2}m^{-1}$	0.11%

3.6.1.6 Estimation of parameters for the fourth stage

The results of the validation have been summarised in Table 3-20.

Table 3-20. Estimated parameters for the fourth stage of compression

Parameter	Value
$\frac{a^2{}_{01}}{V}$	0.0006 $s^{-2}m^{-1}$
$\frac{A_1}{L}$	0.0025 m

Figure 3-32 represents the pressure response of the first stage to an inlet pressure step change while Figure 3-33 represents the flow rate response of the first stage to an inlet pressure step change.

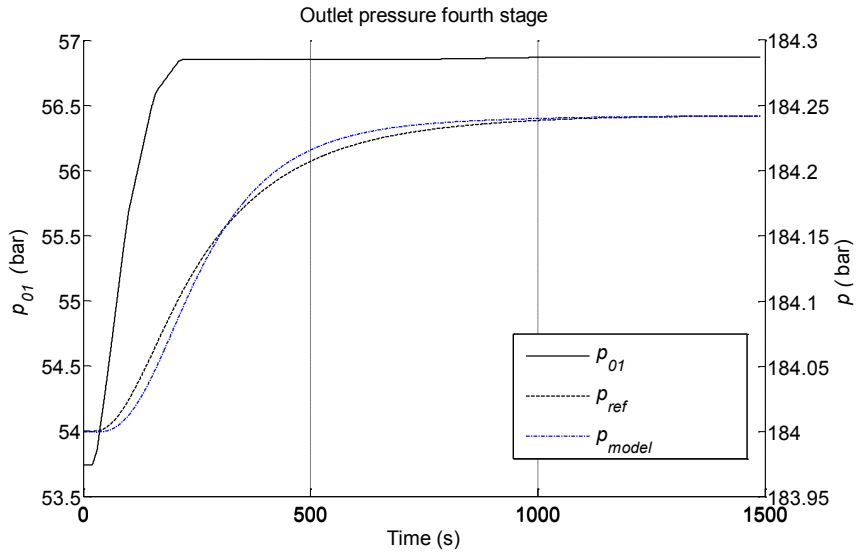


Figure 3-32. Compressor outlet pressure response to inlet pressure disturbance (stage 4)

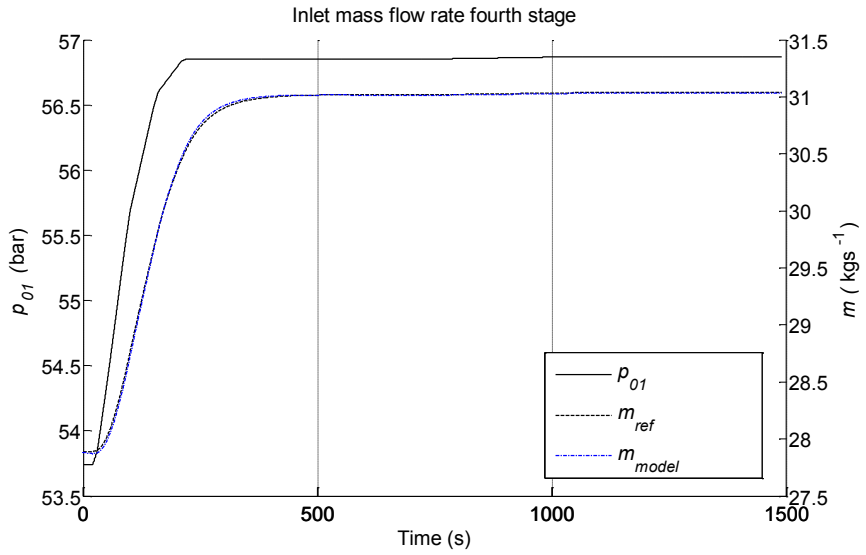


Figure 3-33. Mass flow rate response to inlet pressure disturbance (stage 4)

As it is possible to see from the graphs, the matching between the reference data and the optimised model is good. The maximum absolute relative error is 0.4% for the time constant while is 0.06% for the process gain. Figure 3-32 shows a small deviation between the model curve and the reference curve. Also in this case this may be due to a small underestimation of the parameter V for the fourth compressor. At the same time it is important to highlight that the estimation of the parameters becomes more challenging towards the exit of the series of compressors. This is because the inlet change, represented by the variation over time of p_{01}, has an n-order response, where n depends on the number of units between the location of the step change at the inlet of the series of compressors and the inlet of the single compressor stage under analysis.

Table 3-21. Comparison of time constants between reference data and optimised model (stage 4)

Parameter	Reference	Model	Relative error
β_p	273.0 s	274.2 s	0.4%
β_m	134.0 s	133.6 s	-0.3%

Table 3-22. Comparison of process gains between reference data and optimised model (stage 4)

Parameter	Reference	Model	Relative error
K_p	0.08	0.08	-0.05%
K_m	1.01 $kgs^{-2}m^{-1}$	1.01 $kgs^{-2}m^{-1}$	0.06%

3.6.1.7 Estimation of geometrical dimensions of the compression station

These calculations have been performed for two hypothetical compressor geometries and the results have been reported in Table 3-23. These results demonstrate that the estimated parameters are reasonable and physically meaningful for a compressor application.

Table 3-23 summarises minimum and maximum values of the parameters estimated in the previous part of the thesis. Starting from these values the minimum and maximum values of the volume V, the duct length L and the duct cross sectional area A_1 have been estimated. These ranges have been considered reasonable for this type of application.

The adopted methodology is here explained via an hypothetical example having the specific heat ratio γ equal to 1.2, the compressor outlet temperature T_{02} equal to 450 K, the molecular weight of the gas equal to 42 kmolkg^{-1} and the parameters of the model ${a^2}_{01}/V$ and A_1/L equal to respectively 0.0013 s^{2}m^{-1} and 10 m. The volume V is assumed to be equal to $A_1 \times L$ and R is the universal gas constant. Therefore:

$$ {a^2}_{01} = \frac{\gamma R T_{02}}{10^6 MW} = 0.001\ m^2 s^{-2} $$

$$ V = \frac{{a^2}_{01}}{\frac{{a^2}_{01}}{V}} = 0.82\ m^3 $$

$$ L = \sqrt{\frac{V}{\frac{A_1}{L}}} = 0.29\ m $$

$$ A_1 = \frac{A_1}{L} \times L = 2.87\ m^2 $$

These calculations have been performed for two hypothetical compressor geometries and the results have been reported in Table 3-23. These results demonstrate that the estimated parameters are reasonable and physically meaningful for a compressor application.

Table 3-23. Preliminary estimation of the geometrical dimensions of the compressor station

Parameter	Minimum value	Maximum value
$\frac{A_1}{L}$	0.002 m	10 m
$\frac{{a^2}_{01}}{V}$	0.0006 s^{-2}m^{-1}	0.46 s^{-2}m^{-1}
V	0.002 m^3	2.28 m^3
L	0.3 m	30 m
A_1	0.01 m^2	2.9 m^2

3.6.1.8 Summary

This part of Chapter 3 has presented the methodology and the results of the evaluation of the Simulink model parameters. The evaluation of the parameters has allowed the optimisation of the response of the Simulink model with respect to the data set available from the ESD model. The

optimised model has shown a very good match with the reference data, with the maximum absolute relative error 4.3%.

A second data set has been employed in order to validate the model and this part is presented in the next section.

3.6.2 Model validation

After the evaluation of the parameters of the model, the model itself has to be validated with a different set of data, in order to verify its reliability and robustness. Therefore in the following part the model has been tested comparing its response to the response of the reference system to a different inlet pressure change.

3.6.2.1 Model validation of the first stage

Figure 3-34 represents the pressure response of the first stage to an inlet pressure step change. The inlet pressure of the compressor is represented on the left vertical axis while the outlet pressure of the compressor is represented on the right vertical axis. p_{ref} is the response of the reference system while p_{model} is the optimised response of the model. Figure 3-35 represents the mass flow rate response of the first stage to an inlet pressure step change. The inlet pressure of the compressor is represented on the left vertical axis while the mass flow rate of the compressor is represented on the right vertical axis. m_{ref} is the response of the reference system while m_{model} is the optimised response of the model.

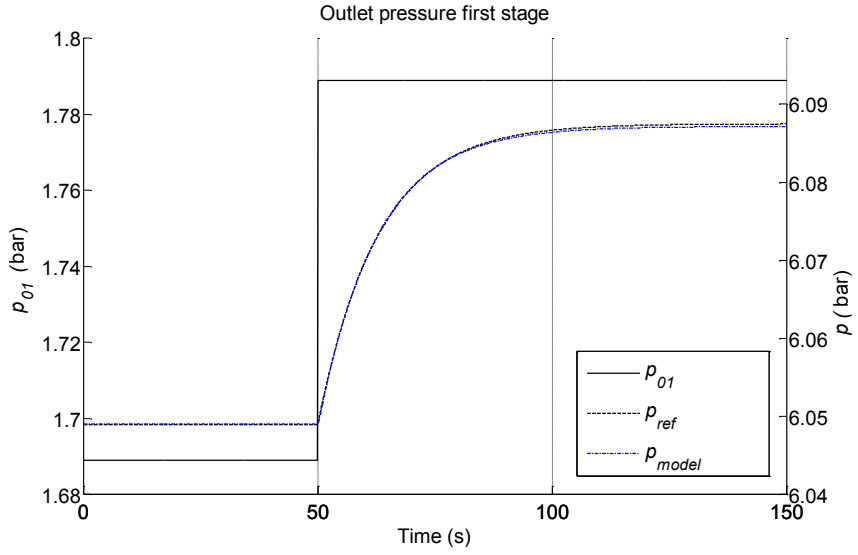


Figure 3-34. Outlet pressure response to inlet pressure step change (stage 1)

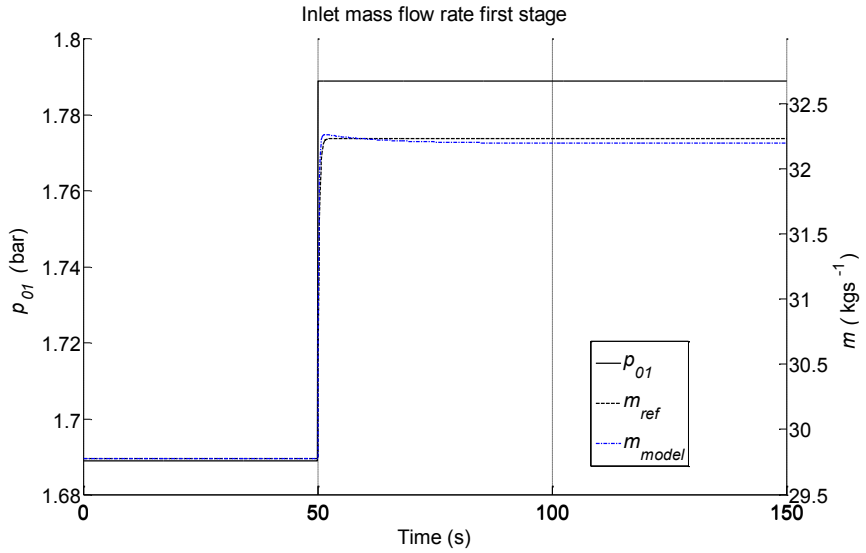


Figure 3-35. Mass flow rate response to inlet pressure step change (stage 1)

As it is possible to see from the graphs, the matching between the reference data and the optimised model is good. The maximum absolute relative error is 5.88% for the time constant while is 1.42% for the process gain.

Table 3-24. Comparison of time constants between reference data and optimised model (stage 1, set data 2)

Parameter	Reference	Model	Relative error
β_p	12.70 s	12.60 s	-0.79%
β_m	0.34 s	0.36 s	5.88%

Table 3-25. Comparison of process gains between reference data and optimised model (stage 1, set data 2)

Parameter	Reference	Model	Relative error
K_p	0.38	0.38	-1.06%
K_m	24.54 $kgs^{-2}m^{-1}$	24.19 $kgs^{-2}m^{-1}$	-1.42%

3.6.2.2 Model validation of the second stage

Figure 3-36 represents the pressure response of the second stage to an inlet pressure step change while Figure 3-37 represents the flow rate response of the second stage to an inlet pressure step change.

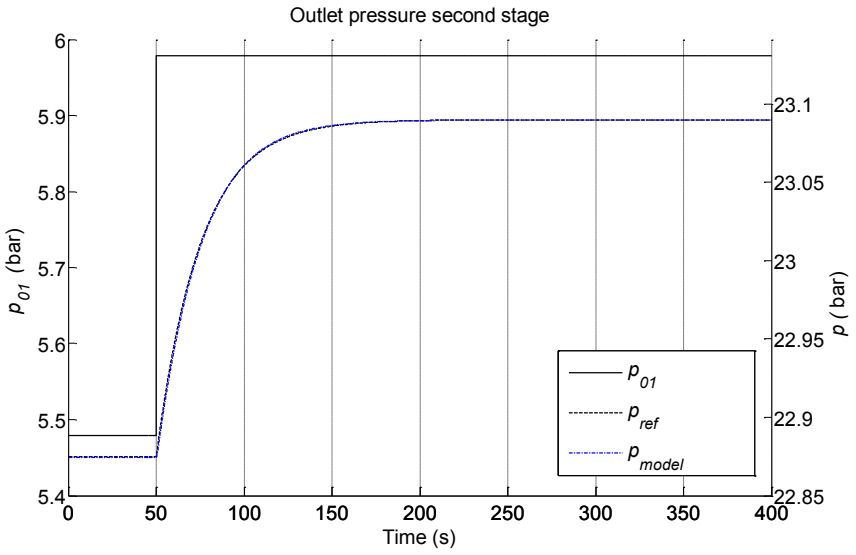


Figure 3-36. Outlet pressure response to inlet pressure step change (stage 2)

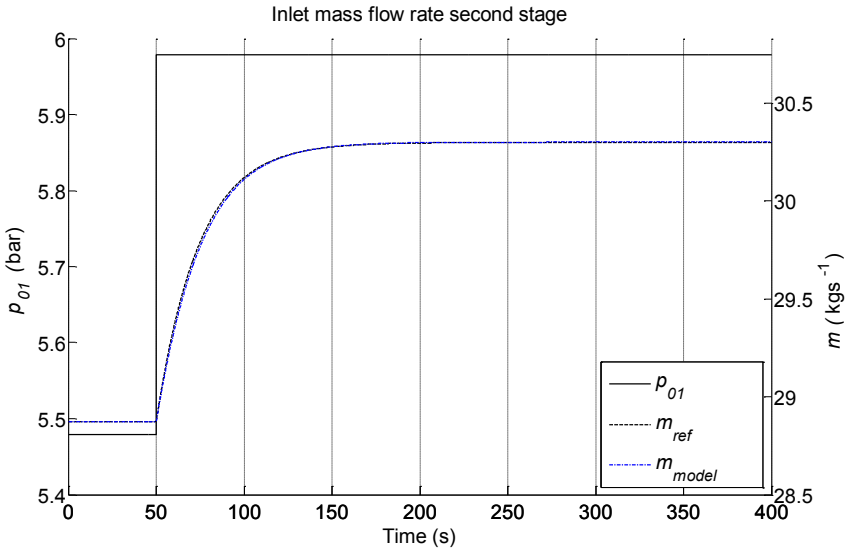


Figure 3-37. Mass flow rate response to inlet pressure step change (stage 2)

As it is possible to see from the graphs, the matching between the reference data and the optimised model is good. The maximum absolute relative error is 4.56% for the time constant while is 0.18% for the process gain.

Table 3-26. Comparison of time constants between reference data and optimised model (stage 2, set data 2)

Parameter	Reference	Model	Relative error
β_p	25.00 s	25.60 s	2.40%
β_m	24.10 s	25.20 s	4.56%

Table 3-27. Comparison of process gains between reference data and optimised model (stage 2, set data 2)

Parameter	Reference	Model	Relative error
K_p	0.43	0.43	0.18%
K_m	2.85 $kgs^{-2}m^{-1}$	2.85 $kgs^{-2}m^{-1}$	0.13%

3.6.2.3 Model validation of the third stage

Figure 3-38 represents the pressure response of the third stage to an inlet pressure step change while Figure 3-39 represents the flow rate response of the third stage to an inlet pressure step change.

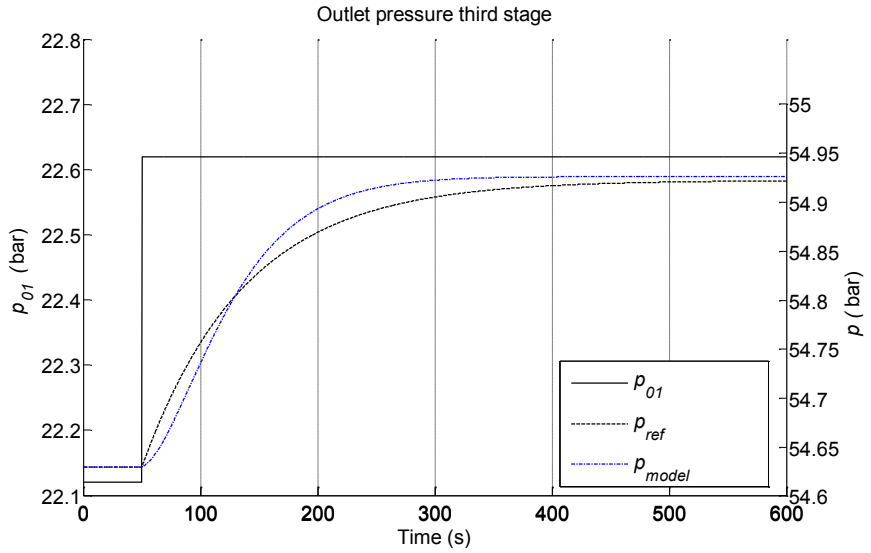


Figure 3-38. Outlet pressure response to inlet pressure step change (stage 3)

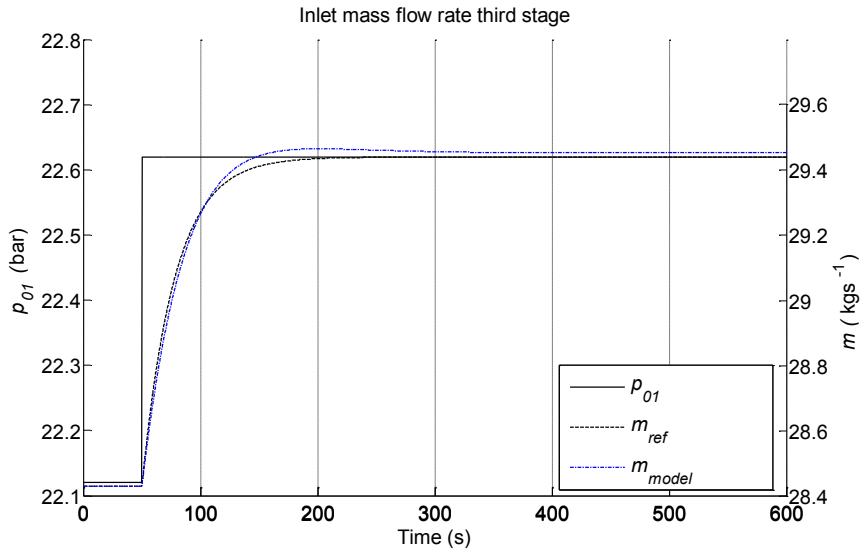


Figure 3-39. Mass flow rate response to inlet pressure step change (stage 3)

As it is possible to see from the graphs, the matching between the reference data and the optimised model is good. The maximum absolute relative error is 4.61% for the time constant while is 1.46% for the process gain. The small deviation of the pressure response has already been highlighted in the previous part of this section. The deviation of the flow rate response shows that the model of the compressor and the reference compressor have different gains. However the relative error is still small, as summarised in Table 3-29.

Table 3-28. Comparison of time constants between reference data and optimised model (stage 3, set data 2)

Parameter	Reference	Model	Relative error
β_p	87.40 s	86.20 s	-1.37%
β_m	28.20 s	29.50 s	4.61%

Table 3-29. Comparison of process gains between reference data and optimised model (stage 3, set data 2)

Parameter	Reference	Model	Relative error
K_p	0.58	0.59	1.46%
K_m	2.01 $kgs^{-2}m^{-1}$	2.04 $kgs^{-2}m^{-1}$	1.27%

3.6.2.4 Model validation of the fourth stage

Figure 3-40 represents the pressure response of the fourth stage to an inlet pressure step change while Figure 3-41 represents the flow rate response of the fourth stage to an inlet pressure step change.

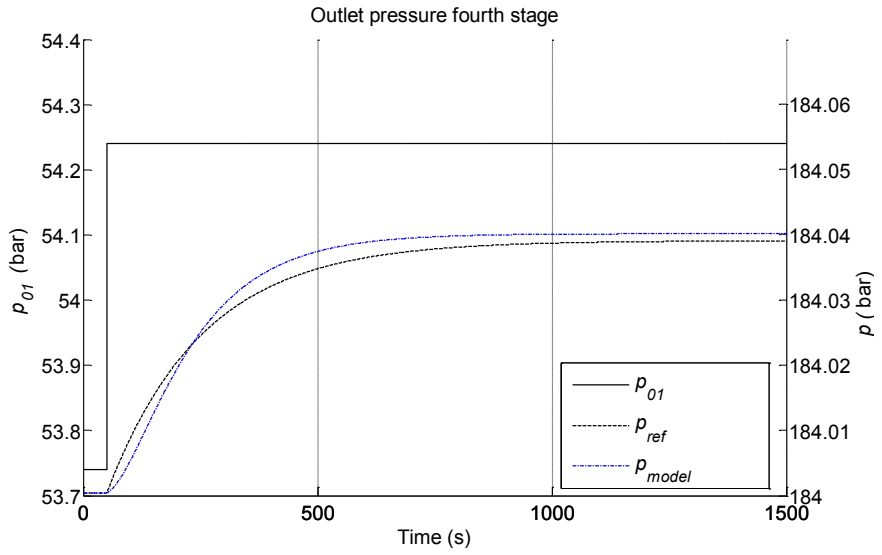


Figure 3-40. Outlet pressure response to inlet pressure step change (stage 4)

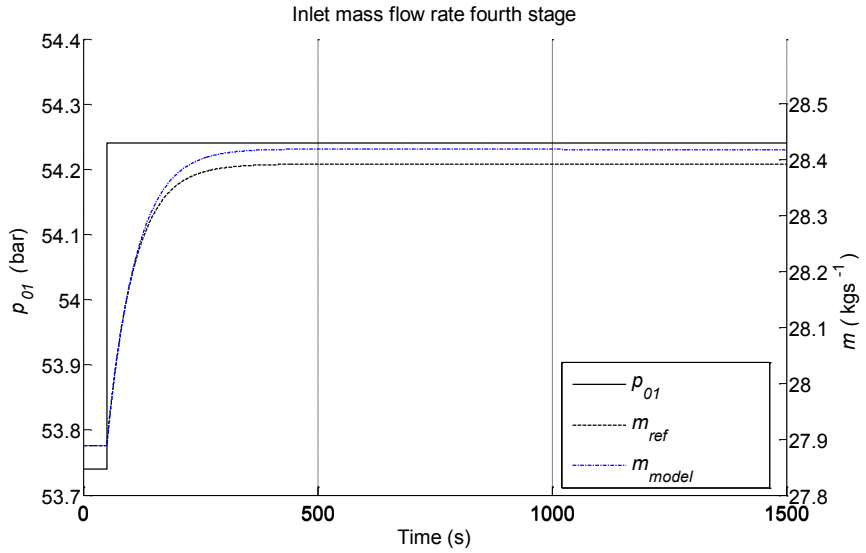


Figure 3-41. Mass flow rate response to inlet pressure step change (stage 4)

As it is possible to see from the graphs, the matching between the reference data and the optimised model is good. The maximum absolute relative error is 4.27% for the time constant while is 5.09% for the process gain. The deviation between the reference data and the model data have already been previously commented and depends on the difficulty in estimating the parameters of the last stage of compression. This is reflected in the values reported in Table 3-30 and Table 3-31.

Table 3-30. Comparison of time constants between reference data and optimised model (stage 4, set data 2)

Parameter	Reference	Model	Relative error
β_p	207.0 s	199.4 s	-3.67%
β_m	58.5 s	61.0 s	4.27%

Table 3-31. Comparison of process gains between reference data and optimised model (stage 4, set data 2)

Parameter	Reference	Model	Relative error
K_p	0.08	0.08	2.85%
K_m	1.01 $kgs^{-2}m^{-1}$	1.06 $kgs^{-2}m^{-1}$	5.09%

3.6.2.5 Summary

The validation of the model has demonstrated its accuracy in predicting the behaviour of the compression system. The maximum absolute relative error is around 5.88% for both pressure and mass flow rate transfer functions.

3.6.3 Control system tuning

The reference control system described in Section 3.3 is used in the ESD model. It has been tuned and the adopted methodology and results are presented in this section. The tuning of the capacity controller has been realised following two different tuning techniques, while the antisurge controller has been tuned in order to guarantee a certain opening time of the recycle valve. For each of the proposed control parameters the stability of the closed loop system has always been verified.

3.6.3.1 Capacity controller

For the initial tuning of the cascade controller the lambda tuning technique has been adopted. The lambda tuning technique has been introduced by Dahlin (1968). The lambda tuning is a design method that gives an overdamped closed loop response with a closed loop pole on the real axis.

A value λ for the target closed loop time constant must be selected. The controller parameters can be estimated using the following equations:

$$K_c = \frac{\tau}{K_p(\lambda + B_d)} \quad \textbf{(3-53)}$$

$$\beta_i = \beta \quad \textbf{(3-54)}$$

where usually $2B_d \leq \lambda \leq 3B_d$ (Thornhill, 2014).

Therefore the parameters presented in Table 3-32 have been estimated for each stage of compression, assuming τ= 1 s and

$$P = K_c \quad \textbf{(3-55)}$$

$$I = \frac{K_c}{\beta_i} \quad \textbf{(3-56)}$$

Table 3-32. Initial tuning of the capacity controller (assuming single loop controller)

Parameters	Stage 1	Stage 2	Stage 3	Stage 4
Process gain K	0.4	0.4	0.6	0.1
Process time constant β	18.7	52.2	130.0	274.2
Process time delay B_d	1.0	1.0	1.0	1.0
Tuning parameter λ	3.0	3.0	3.0	3.0
Controller gain K_c	11.99	30.35	55.08	856.88
Controller time constant β_i	18.70	52.20	130.00	274.20
Matlab parameter P	11.99	30.35	55.08	856.88
Matlab parameter I	0.64	0.58	0.42	3.13
Rise time (10^2 s)	76.6	50.8	161.1	5.2
Settling time (10^2 s)	137.0	89.9	8310.0	6.0

Because rise and settling time values were very slow for such a system, the values summarised in Table 3-33 and Table 3-34 have been adopted for the master and slave loop, taking into account reference settling time for pressure application (Thornhill, 2014).

Table 3-33. Tuning of the master loop of the cascade capacity controller

Master loop	Stage 1	Stage 2	Stage 3	Stage 4
Matlab parameter P	603.82	328.16	31.78	2488.76
Matlab parameter I	46.25	14.78	13.22	22.64
Settling time (s)	226	255	283	472

Table 3-34. Tuning of the slave loop of the cascade capacity controller

Slave loop	Stage 1	Stage 2	Stage 3	Stage 4
Matlab parameter P	0	0.25	0.1	0.05
Matlab parameter I	0.28	0.51	0.084	0.06
Settling time (s)	18.1	35.5	54	77.8

3.6.3.2 Antisurge controller

The antisurge controller was designed in order to be always awake but to act only when the inlet flow rate was below the control flow rate. For this reason the control flow rate is not a proper set point for this controller, but it is rather a lower bound of the operating region of the compressor.

Fast-acting valves are usually selected for antisurge operation. For this reason the antisurge controller has been tuned for each stage of compression in order to guarantee the full opening and closing of the valve within few seconds. In order to avoid wear and tear of the valve a rate limiter has been imposed to the output of the controller. It guarantees the opening time to be 2 seconds and the closing time to be 3 seconds, following the recommendation by Wilson and Sheldon (2006). Larger closing time values have been specified in the literature. However the intention was to leave the antisurge valve open for a short period as possible.

In the following table the tuning parameters of the antisurge controller of the first stage have been summarised.

Table 3-35. Tuning of the antisurge controller of the first stage of compression

Antisurge controller	Stage 1
Matlab parameter P	0
Matlab parameter I	100

The lower and upper limits of the output of the antisurge controller are the fully closed (0% opening) and fully open (100% opening) position of the antisurge valve.

3.6.4 Summary

The validation of the model of the compressor has been presented in this section. Validation allowed estimates of some unknown physical parameters, and the chapter has also shows the estimated values are physically realistic. The case study has been presented together with the parameters to estimate. The estimation of the parameters has been followed by the validation of the model. The validation has given good results and guaranteed the accuracy of the model and its matching with

the case study. Some discrepancies have been discussed and explained. Finally the tuning of the control system has allowed the achievement of the wanted performance in terms of settling time of the compressor and opening time of the antisurge valve.

3.7 Summary of the chapter

This chapter has covered the following tasks:

- Task 1: modelling of the compression system
- Task 2: modelling of the reference control system
- Task 3: implementation of the model
- Task 4: description of the reference case study
- Task 5: validation of the model.

The model of the compression system includes a main forward process line and a secondary recycle line. Various configurations have been considered and they mainly differ because of the thermodynamic condition of the gas and the hold-up volume along the recycle line. There are numerous configurations for the recycle, however they can be mainly characterised by the temperature and the volume of the recycle. Therefore these two parameters will be taken into special account in the following analyses.

The modelling of the ESD control system presented in Section 3.3 represents the state of the art control system for gas compressors. This control system represents the benchmark and reference for comparison of control performance and is also called 'feedback control system'. This reference system has been selected and modelled taking into accounts its widespread use in industrial applications and also the motivations behind its popularity. The two control loops implemented in the system are the capacity control loop and antisurge control loop and they have been presented in detail. The two separate control loops act on the same process system and therefore influence each other. The interaction between the control loops should be reduced in order to guarantee smooth and stable operation and protection of the compressor from surge. The limitation of the current state of the art has been presented via analysis of the current practice and literature and will be further investigated in the following chapters.

The implementation of the closed loop model included the selection of modelling and simulation tool, of the method for the resolution of the algebraic and differential equations, of the input and output variables. The model of the compression system and of its control system has been implemented in MATLAB Simulink. This tool allows multi-domain simulation and model-based design. It has been selected because it supports modelling and simulation of process systems. It also gives the possibility to connect the model to hardware for real-time testing and embedded system deployment. This option could be very useful in the future for the implementation of the proposed control systems, presented in the following chapters, in a real system.

The collaboration with the research partner ESD Simulation Training provided access to real data for the case study described in the chapter. In particular their simulator tool has been validated and then employed to collect the estimation and validation data. In fact the Simulink model is being validated against the ESD simulator, and the ESD simulator is itself a state of the art industrial training simulator that is validated against operational data from a real CO_2 compression system.

The validation of the closed loop model was fundamental in order to guarantee the accuracy and reliability of the model. The estimation of the model parameters has been followed by the validation of the model. The validation has given good results and guaranteed the accuracy of the model and its matching with the case study. The validation of the model also included the tuning of the feedback control system according to the desired performance.

4 Analysis of capacity control solutions

The previous chapter has presented the model of the compression system and the model of the ESD control system. The reference control system consists of two separate control loops including capacity control and antisurge control. The interaction between these two controllers is a known issue and has been approached in the past only via decoupling or detuning. One of the general aims of this thesis is the reduction of the interaction between these two control loops.

The literature review presented in Chapter 2 has highlighted that most of the research regarding compressor control has focused on the antisurge controller, neglecting the capacity controller.

In this chapter a control system focusing on the improvement of the capacity controller is proposed. This controller is a Model-Based Feedforward Controller (MBFC) that employs the performance map of the compressor in order to predict the effect of external disturbances on the operation of the compressor.

The structure of the chapter is the following. Section 4.1 describes the tasks of this chapter. Section 4.2 summarises possible disturbances that can affect a compression system and focuses on the operation of the case study compressor. In Section 4.3 two examples of respectively beneficial and problematic interaction between control loops are presented. Section 4.4 describes the proposed model-based feedforward controller, its implementation and tuning. In Section 4.5 the operation of the proposed control system is compared with the operation of the reference control system during various boundary disturbances including both inlet and outlet variables of the system. Finally Section 4.6 summaries briefly the content of the chapter and draws some conclusions.

4.1 Task description

This chapter of the thesis has three main tasks to fulfil:

- Task 1: demonstration of interactions between control loops
- Task 2: improvement of the response of the capacity controller
- Task 3: reduction of the interaction between control loops.

The second and third chapters have already highlighted the interaction between control loops as a negative issue affecting the overall operation of the compressor. The first task requires giving a demonstration and practical examples of disturbance scenarios that could cause the interaction between control loops. Examples have been selected in order to explain what causes the interaction and what it involves. The first example shows the beneficial effect of the action of the pressure controller on the control of surge while the second example shows the strong problematic interaction between pressure controller and antisurge controller.

The second task aims at improving the performance of the capacity controller. This controller has been mainly neglected by the research and industrial community over the years. However good pressure control can impact on surge occurrence and therefore it must be taken into account. A model-based feedforward controller has been proposed in order to improve the performance of the pressure control loop.

Finally the third task focuses on the reduction of the interaction between control loops. This last task has been fulfilled by means of better pressure control. The chapter will demonstrate that improved pressure control can reduce the risk of surge and therefore avoid the opening of the recycle valve under the same disturbance. Avoiding gas recycle also contributes to the reduction of energy consumption by the compressor. In fact gas that is compressed and recycled rather than delivered represents a cost with no benefit other than the protection of the compressor. Therefore this operation should be limited to cases in which gas recycle is unavoidable for safety purposes.

4.2 Analysis of disturbance scenarios

4.2.1 Disturbance scenarios for compression stations

Dynamic simulations were run in order to compare the time response of the proposed MBFC with respect to the traditional PI controller. The simulation scenarios tested in this thesis come from the literature and also from industrial practice (Dukle and Narayanan, 2003, Patel et al., 2007, Wu et al., 2007). They have been proposed in the past for the validation of compressor and antisurge controllers.

The simulation scenarios usually employed for validation of compressor control include three different categories:

- Process disturbances that can affect the operation of the plant: These come from outside the compressor, either from the upstream or downstream section of the process plant in which the compressor is operating. Inlet and outlet pressures of the system were selected as disturbance variables
- Closure of the inlet and outlet valves of the system: These are manipulated by controllers that are outside the compression plant
- Load pattern: This involves the modification of the control set point in order to meet a specific request called load. The load can be expressed in terms of mass flow rate or pressure. In this specific case the pressure set point of the compressor was changed and the response of the system was recorded.

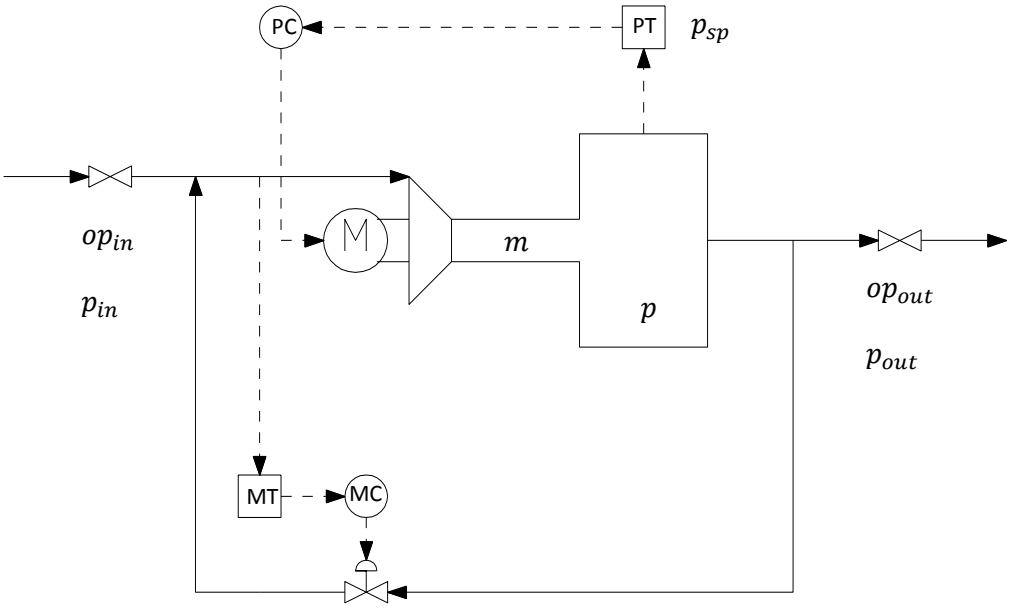


Figure 4-1. Overall control system for a hot gas recycle compression system

Figure 4-1 (duplicated from Figure 3-17 for convenience) highlights the disturbance variables that have been selected. They include:

- The inlet pressure of the system p_{in}

- The opening position of the inlet valve op_{in}
- The outlet pressure of the system p_{out}
- The opening position of the outlet valve op_{out}
- The pressure set point p_{SP}.

The controlled variables are also represented in the figure and they include:

- The compressor outlet pressure p
- The compressor inlet mass flow rate m.

For each of the disturbance variables, two different control configurations have been tested using a range of disturbance types and magnitudes. The disturbances used for testing are considered realistic for a CO_2 post-combustion separation plant (Harun et al., 2012, Karimi et al., 2012, Panahi and Skogestad, 2012).

Specific values for the magnitude and the rate of change of these disturbances are available in the literature. They mainly come from the research field studying the separation of CO_2 from main gas streams. The following disturbances have been suggested as realistic:

- Ramp changes with sign and magnitude ±5% over a period of three hours (Harun et al., 2012)
- Sinusoidal changes with amplitude 15% over a period of one day for a full cycle (Harun et al., 2012)
- Step change with magnitude 5% (Panahi and Skogestad, 2011, Panahi and Skogestad, 2012)
- Ramp changes with sign and magnitude ±10% over a period of ten to thirty minutes (Karimi et al., 2012).

4.2.2 Disturbance scenarios for the specific case study

The disturbances proposed in the literature have been employed as a starting point for the analysis of control performance. During the selection of the magnitudes of the disturbances the purpose was to identify a value able to affect the system without causing the opening of the antisurge valve. The reason is that the focus of this chapter is the improvement of the pressure controller and therefore the opening of the antisurge valve would have affected the operation of the system and made challenging the identification of the contribution due only to the pressure controller.

4.2.2.1 Design point and off-load operation

The starting point of this analysis for the selection of the boundary disturbance has been the datasheet of the case study. In a compressor datasheet it is possible to find the value of the main variables for a reference guaranteed case and for some off-load cases. The off-load cases represent the operation of the compressor at different boundary conditions. Some off-load cases may include:

- Low inlet pressure

- Low inlet temperature
- Low discharge pressure
- High discharge pressure
- Turndown (that means reduced throughput).

Also some more advanced cases may include a combination of the previous cases, for example:

- Low discharge pressure and low inlet pressure
- High discharge pressure and low inlet pressure.

Finally the operation of the compressor is analysed during full recycle operation.

The following table summarises the maximum variation of the boundary variables according to the available datasheet and with respect to the reference guaranteed case.

Table 4-1. Maximum variation for the boundary variables during off-load operation

Boundary variable	Maximum variation
p_{01}	5.6%
T_{01}	4.5%
p_{02}	5.6%
T_{02}	4.1%

The subscript 01 indicates the inlet of the compressor while the subscript 02 indicates the outlet of the compressor.

The maximum variation of inlet and outlet pressure is around 5.6%. However it is important to notice that during off-load operation there are more variables changing at the same time and for this reason the operating point of the machine always lies within compressor map. In fact none of the off-load cases includes gas recycle, excluding the full recycle case itself.

4.2.2.2 Disturbance analysis and selection

The model of the compression system has been tested by changing the value of the single boundary disturbances in order to maintain the operating point within the boundaries of the compressor map. The results of the analysis are summarised in Table 4-2. For each disturbance variable, the maximum variation with respect to its design point has been estimated. This variation affects the system without however causing gas recycle.

Table 4-2. Maximum variation for the boundary disturbances during boundary disturbances

Boundary variable	Maximum variation
p_{in}	±12%
op_{in}	40%
p_{out}	3%
op_{out}	10%
p_{sp}	2%

4.2.2.3 Evaluation of performance for a controller

The purpose of this chapter is the improvement of the pressure controller and also the reduction of the interaction between control loops. In order to analyse the operation of the MBFC and compare it with the traditional PI controller the integral of the square error of the pressure with respect to its set point has been selected. It has been defined as:

$$ISE_p = \int_{t=0}^{t_{final}} (p(t) - p_{SP}(t))^2 dt \quad \textbf{(4-1)}$$

where t_{final} is the duration of the period under analysis, p is the compressor outlet pressure and p_{sp} is the set point of p.

Graphical representations have also been employed in order to compare the response of the two control systems over time.

4.2.3 Summary

In this section of the chapter possible disturbance scenarios for a generic compression system have been presented. Then, following the analysis of the off-load operation of the machine, specific values have been identified for the magnitude of the boundary disturbances. These values apply to the specific case study employed. These disturbance magnitudes will be employed in the analysis presented in the following sections.

4.3 Analysis of the interaction between controllers

In the previous section various disturbance scenarios have been presented. A couple of these cases will be employed in this section in order to show how a boundary disturbance can affect the operation of the control system and especially how the action of the pressure controller can influence the stability of the system.

In this section two disturbance scenarios will be presented and their consequence on the system will be analysed. These consequences can be categorised as *beneficial* or *problematical* interaction. A beneficial interaction happens when the action of the pressure controller on the system increases the distance of the operating point of the machine from the surge region. The purpose of the pressure controller is not to protect the compressor from surge however this can happen as a side effect. A problematical interaction is a real interaction between the two control loops and takes place when the pressure controller pushes the compressor towards the surge region. When the operating point crosses the antisurge control line because of the action of the pressure controller, the antisurge controller detects an event and opens the recycle valve. This action affects the values of both pressure and flowrate and therefore affects the operation of the pressure controller. This interaction might happen only once, or might be cyclic, as will be presented below.

4.3.1 Case study

The ESD case study has been introduced in Chapter 3. It is based on a multistage centrifugal compressor arranged in a single shaft configuration and driven by an asynchronous electric motor. The multistage compressor consists of four single stages compressors in series and the first compression stage has been employed for the analyses presented in this chapter. The configuration employed is the hot gas recycle configuration presented in Chapter 3.2.2. As the proposed model-based feedforward controller will be tested for disturbances that will not cause the opening of the antisurge valve, the configuration of the recycle line does not influence the overall configuration of the system. The results in this section are generated from the Simulink model of a single compressor. It represents the first stage of compression of the four-stage ESD model.

This first stage of compression is at the inlet of the multistage compressor. Therefore it is preceded by a process plant for the treatment of the process fluid. In the case of high-concentration carbon dioxide stream, this plant is usually constituted by separation and dehydration units. This stage of compression is then followed by another stage of compression, placed downstream in series. In between these compressors there is usually a gas cooler and a separation vessel and there may be a control or isolation valve. The process flow sheet has been schematically represented in Figure 3-22 and Figure 3-23.

4.3.2 Beneficial interaction

The following example represents a case of beneficial interaction of the control loops of the compression system. In fact the action of the pressure controller only has a beneficial effect on the distance of the system from surge.

The following two graphs (Figure 4-2 and Figure 4-3) represent the controlled variables p and m and the manipulated variables τ_d and op_{asv} after a negative step change of the system outlet pressure p_{out} starting at time t =10s. The quantity m_{ctrl} is the control flow rate of the antisurge controller. Therefore it represents the minimum allowable flow rate before the antisurge valve opens in order to avoid surge.

When the outlet pressure of the system p_{out} decreases at t=10s, p decreases. The reaction of the pressure controller is to increase the torque of the driver τ_d in order to increase the rotational shaft speed N and bring back the pressure to its set point. Therefore the pressure ratio of the system tends to remain constant as the inlet conditions of the system have not changed and the pressure p is going back to its set point value. If the pressure ratio of a compression system is constant but the rotational shaft speed increases then the compressor inlet mass flow rate increases as well. For this reason it is possible to see that m increases over time. At the same time the control flow rate m_{ctrl} decreases. This is due to the reduction of p_{01} and its effect on the surge mass flow rate, according to the definition of corrected mass flow provided in Chapter 3.

Therefore it is possible to see that the action of the pressure controller has caused:

- The control of the outlet pressure of the compressor p
- The increase of the distance between the mass flow rate of the system m and the control flow rate m_{ctrl}. In fact in Figure 4-2 it is possible to see that the distance between these two variables is higher during the steady state that follows the disturbance than during the steady state that precedes the disturbance.

For this reason this type of interaction, even if it does not involve the antisurge controller, can be seen as beneficial.

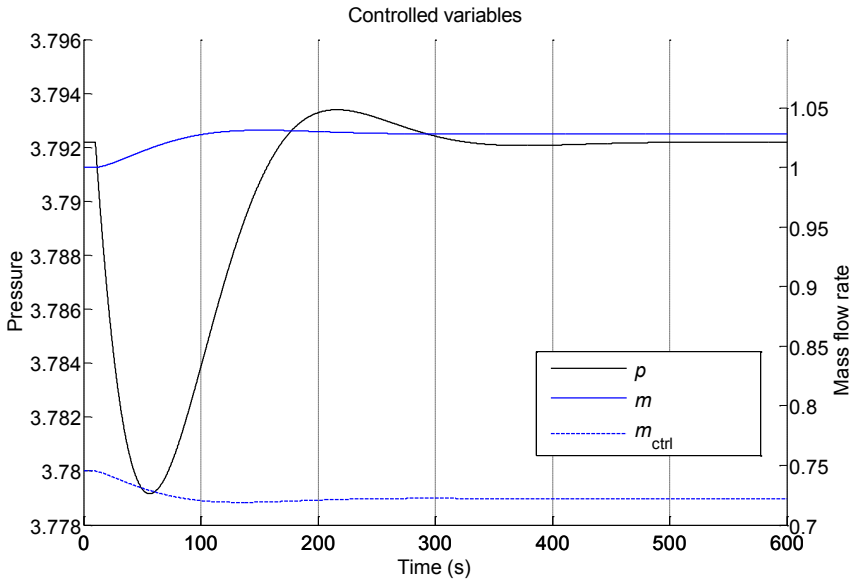


Figure 4-2. Controlled variables during a negative step change of the system outlet pressure starting at *t*=10s

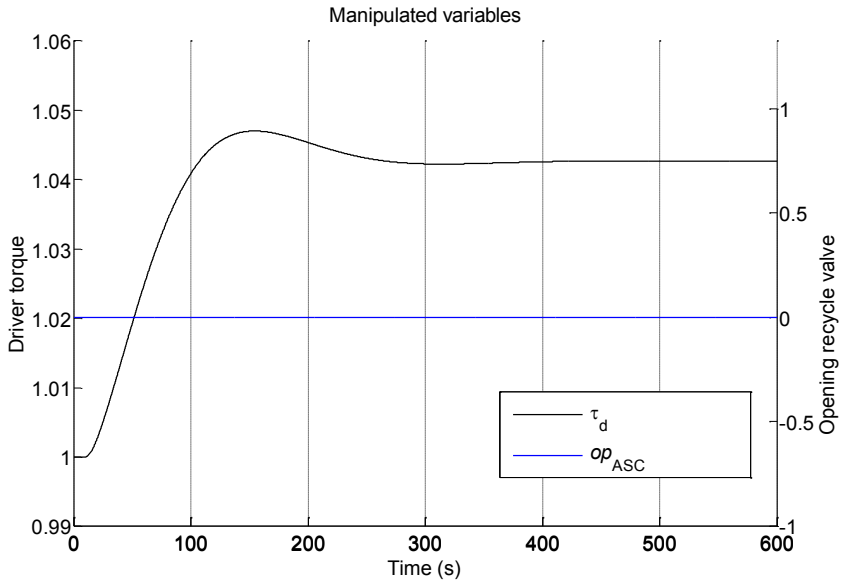


Figure 4-3. Manipulated variables during a negative step change of the system outlet pressure starting at *t*=10s

4.3.3 Problematical interaction

The following example represents a case of problematical interaction of the control loops of the compression system. In fact the action of the pressure controller pushes the compression towards surge and causes the opening of the antisurge valve. When the antisurge valve opens this affects both flow rate and pressure of the system and therefore influence the operation of the pressure controller.

Figure 4-4, Figure 4-5, Figure 4-6 and Figure 4-7 represent the controlled variables p and m and the manipulated variables τ_d and op_{asv} after a negative step change of the opening position of the system outlet valve starting at time t =10s.

Figure 4-4 represents compressor outlet pressure, mass flow rate and control flow rate over time and a zoomed view is represented in Figure 4-5. Figure 4-6 represents the manipulated variables over time and a zoomed view is represented in Figure 4-7.

When the position of the valve changes from 100% to 85% at time t=10s the pressure controller reduces τ_d in order to reduce p. This action reduces the flow rate through the machine m as well. At the same time m_{surge} increases because p_{01} increases. When m approaches the surge control value m_{ctrl} the antisurge controller opens the antisurge valve. However this action causes the reduction of the pressure p. Therefore the pressure controller increases τ_d and m increases. When m becomes bigger than m_{ctrl} the antisurge controller closes the antisurge valve. The consequence is the increase of p above its set point that brings the pressure controller to reduce τ_d and therefore reproduces the same behaviour. The result is the oscillation of the system.

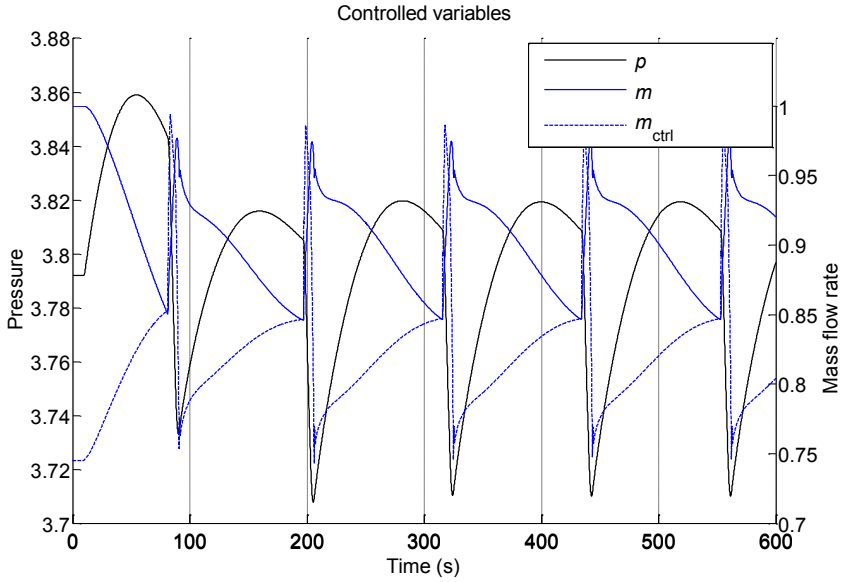


Figure 4-4. Controlled variables during a negative step change of the system outlet pressure starting at t=10s

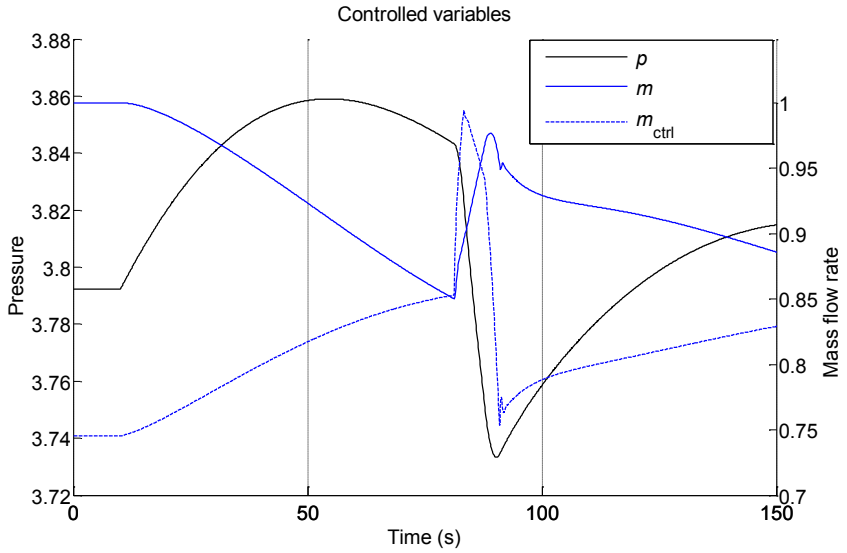


Figure 4-5. Controlled variables during a negative step change of the system outlet pressure starting at *t*=10s (zoomed view)

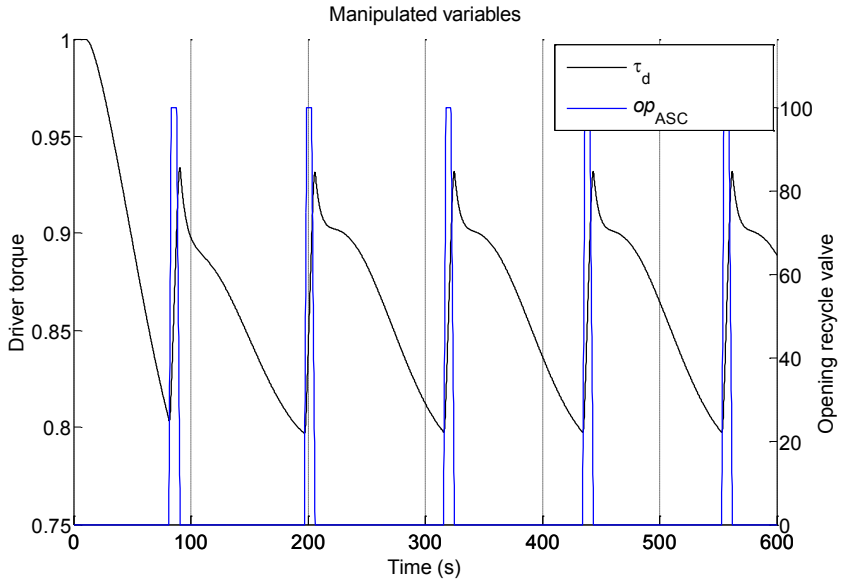


Figure 4-6. Manipulated variables during a negative step change of the system outlet pressure starting at *t*=10s

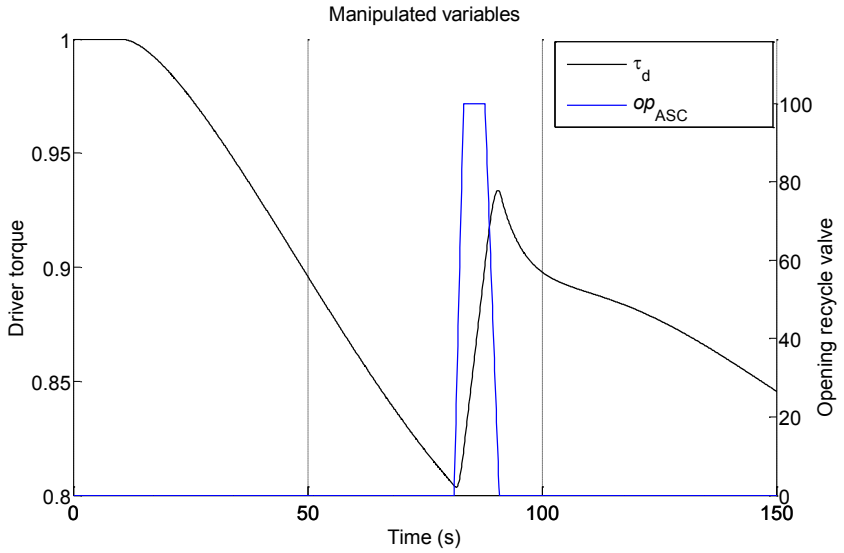


Figure 4-7. Manipulated variables during a negative step change of the system outlet pressure starting at *t*=10s (zoomed view)

4.3.4 Summary

This section of the chapter has shown two examples of interactions between control loops within the compressor control system. In the first case the disturbance scenario has caused a beneficial interaction between control loops. The action of the pressure controller only has guaranteed the control of the compressor outlet pressure and has increased the distance between the compressor operating point and the surge region.

In the second case the reduction of the opening position of the system outlet valve has caused a problematical interaction between the two controllers. The consequence of this interaction has been the oscillation and instability of the system. In this case pressure and antisurge controller have been pushing the compressor into opposite directions. This is a clear example of a disturbance scenario that can cause the oscillation of the system. It also demonstrates the importance of reducing the interaction between control loops.

4.4 Proposed modification to the control system

The previous part of this chapter has given evidence on the type of interactions that can involve pressure and antisurge controllers. Problematical interactions are an issue for the control system as they:

- Push the compressor towards surge
- Do not guarantee good control performance
- Cause oscillations and instabilities.

Therefore there is a need for control performance improvement. A model-based feedforward controller is here proposed with the purpose of:

- Improving the performance of the pressure controller
- Reduce the risk of surge during pressure control.

As has been seen, the pressure controller can push the compressor towards surge. Therefore it needs improvement in order to get a faster response of the system, overall control stability and finally also energy saving. Advanced control concepts such as a model-based feedforward control can reduce the energy consumption (Willems and de Jager, 1999) and this is one of the goals of this work.

4.4.1 Definition of model-based feedforward controller

The proposed controller represents an effort in the direction of control integration for industrial multistage compressors. The model-based feedforward controller presented in this chapter is able to improve the overall control performance because it can:

- Control the outlet pressure of the compressor
- Reduce the risk of surge by reducing the proximity to it during inlet disturbances.

Therefore this control configuration goes in the direction of control integration.

The control approach proposed is based on the characteristic of the compressor. This characteristic is commonly used to define the operating envelope of the machine (especially in regards to surge location) and also for performance estimation but it is not usually adopted for control design. In this thesis it has been used for control purposes as well and this is one of the contributions of the work. It has been implemented in the performance controller in order to estimate the correct rotational speed depending on the inlet conditions of the process fluid.

The model-based controller predicts the rotational shaft speed rather than calculating it via feedback loop only. In its cascade control structure, the master controller is composed of two blocks: the feedback control block and the feedforward control block. At any time the feedforward control block determines the rotational shaft speed according to the instant value of inlet pressure,

temperature and flow rate. The inputs to this block are the inlet disturbances and the set point of the outlet pressure. Inside this controller the inverse characteristic of the compressor is modelled. Therefore the controller can estimate the set point of the speed controller according to the ideal pressure ratio of the machine $\Psi_{c,id}$, defined as:

$$\Psi_{c,id} = \frac{p_{sp}}{p_{01}^*} = f(m^*, N^*) \quad \textbf{(4-2)}$$

At any time t^* the ideal pressure ratio $\Psi_{c,id}$ depends on the instant value of mass flow rate m^*, rotational shaft speed N^*, compressor inlet pressure p_{01}^* and pressure set point.

The compressor characteristic is a non-linear function of mass flow rate and rotational shaft speed and it was fitted using a second degree polynomial function, according to the methodology described in the following section 4.4.2. The discrepancy between the model of the compressor characteristic and the model of the inverse characteristic causes a small deviation between the optimal N and N^*. This is due to the fitting process itself. In fact in the compressor model the pressure ratio is the dependent variable while in the controller model the rotational shaft speed is the dependent variable and also the remote set point of the speed controller. Therefore the presence of the feedback control block can compensate this discrepancy and close the control loop. The remote set point of the speed controller is the sum of the outputs of the two controller blocks, OP_1 and OP_2 , as represented in Figure 4-8.

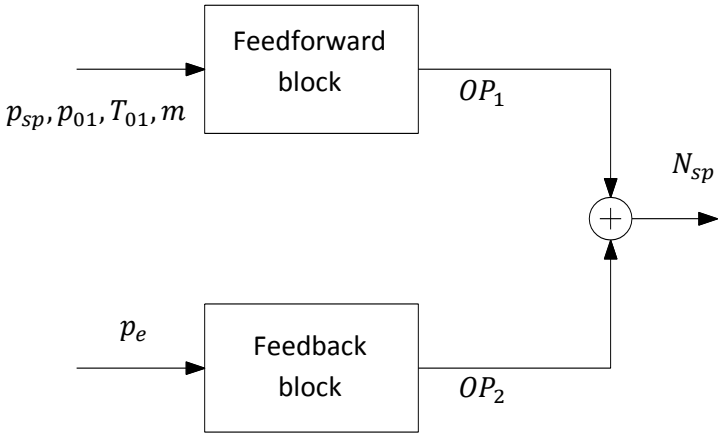


Figure 4-8. Cause-effect block diagram of the model-based feedforward controller (MBFC)

4.4.2 Generation of an empirical compressor map

4.4.2.1 Generation of the map

The performance map of a compressor is generated by the supplier of the compressor by means of laboratory experiments. The compressor is run at various constant rotational shaft speeds. For each speed the flow rate through the compressor is changed by means of a throttling valve and the corresponding performance variable is recorded. For example in a performance map representing the pressure ratio of the compressor as a function of the rotational shaft speed and the compressor

inlet mass flow rate, the pressure ratio is recorded while the machine runs at constant rotational speed and the inlet flow rate changes.

The number of collected points per single rotational speed curve is at discretion of the supplier of the compressor. However it is common to fit a second degree polynomial function with the collected points, which therefore must be at least three.

As previously mentioned, these performance maps are generated at specific inlet conditions, which are the inlet conditions recorded during the lab experiments. Therefore these parameters must be reported in the datasheet of the compressor together with the maps, in order to be able to correct them for different inlet conditions.

Figure 4-9 is an example of a generic compressor map. The horizontal axis represents the inlet flow rate while the vertical axis represents the pressure ratio. Four constant speed curves are represented and named A, B, C and D, where A corresponds to the maximum rotational speed and D corresponds to the minimum rotational speed. The design point of the compressor is on the constant speed curve B and the corresponding flow rate and pressure ratio are indicated in the figure by the green arrows.

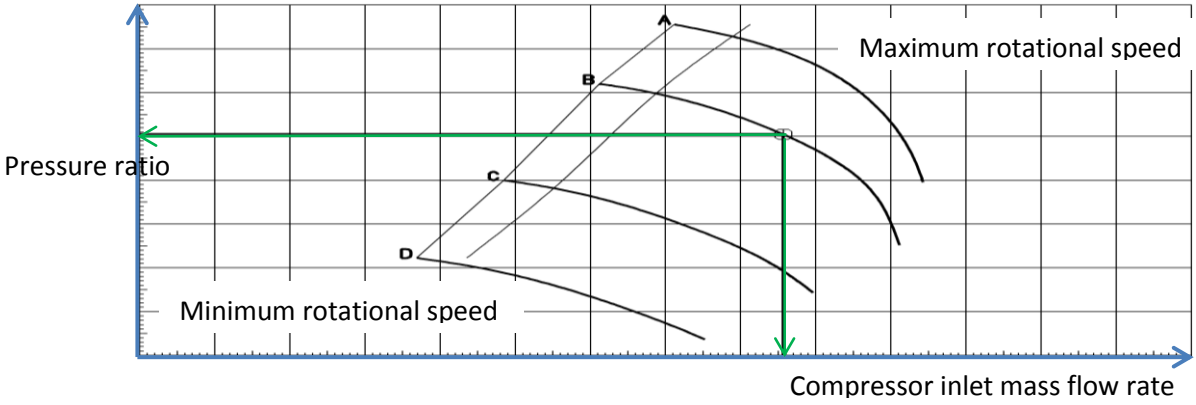


Figure 4-9. Generic representation of a performance map

4.4.2.2 Implementation in the MBFC

The performance maps of the compressor have been implemented in the open loop model by means of the following functions, where Ψ_c is the pressure ratio of the compressor and η_p its polytropic efficiency:

$$\Psi_c = \Psi_c(\omega, m) \tag{3-6}$$

$$\eta_p = \eta_p(\omega, m) \tag{3-8}$$

However in this case they have also been employed in the model-based feedforward controller. The methodology of implementation of the map of the pressure ratio of the compressor into the feed-forward controller has included the following steps:

- For each constant speed curve of the performance maps, some points have been recorded in a form of a table
- These set of points included the following variables: rotational shaft speed N, compressor inlet mass flow rate m, pressure ratio Ψ_c
- These sets of points have been fitted according to a second order polynomial function having the following generic form:

$$z = ax^2 + by^2 + cxy + dx + ey \quad \textbf{(4-3)}$$

  where a, b, c, d and e are the parameters of the polynomial function
- For this specific case z corresponds to N, x corresponds to Ψ_c and y corresponds to m.

In this way the inverse characteristic of the compressor map has been represented in order to estimate the rotational shaft speed N as a function of the actual inlet mass flow rate m and the desired pressure ratio Ψ_c.

The robustness of this methodology to difference between the model of the compressor map and the map of the real compressor and its effect on the performance of the MBFC controller will be discussed in Chapter 7.

4.4.3 Implementation of model-based feedforward controller

The cause-effect block diagram of the closed-loop model-based feedforward controller is represented in Figure 3-11. The master controller is the feedback block in the MBFC controller.

The variables p_e and N_e represent the error of respectively pressure controller and speed controller. The input variables to the MBFC block are the pressure set point, the compressor inlet mass flow rate, the temperature and pressure of the gas at the inlet of the compressor and the error between the pressure and its set point. The output variable of the block is the speed set point for the speed controller representing the slave controller.

The overall control system including MBFC and antisurge controller is represented in Figure 4-11. The antisurge controller has been included in the overall control system. However the disturbances that will be tested in the following part of the chapter have been selected in order to avoid the opening of the antisurge valve. In this way it is possible to analyse the operation of the pressure controller alone, without interference due to the gas recycle activation.

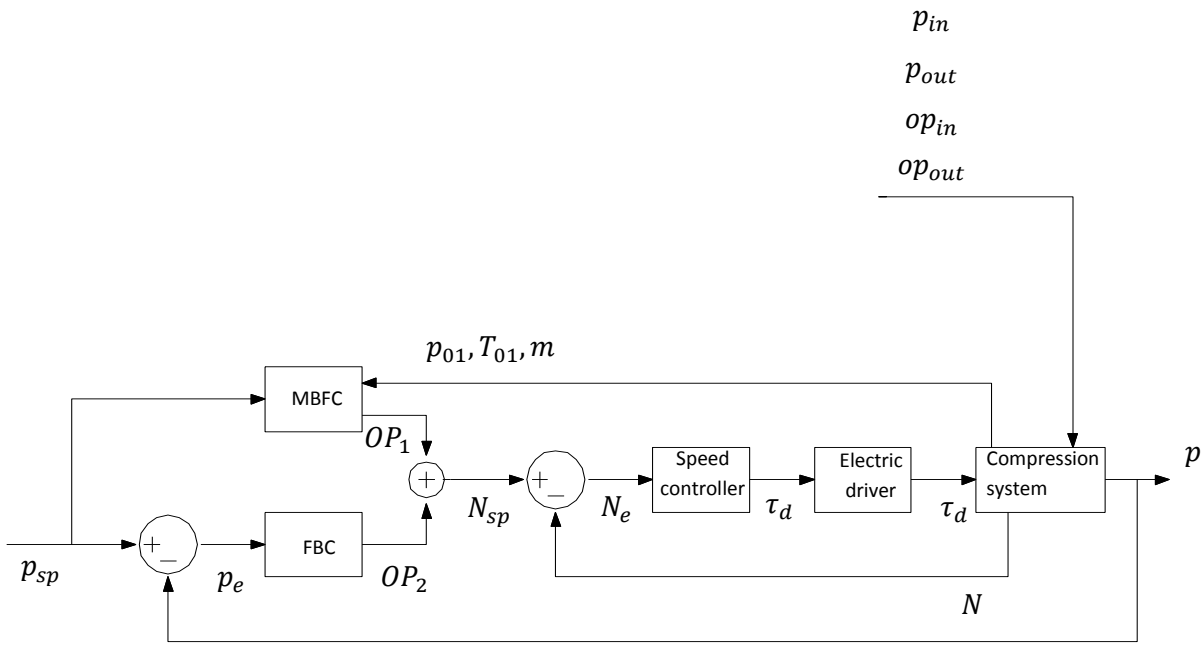


Figure 4-10. Cause-effect block diagram of the closed loop model-based feedforward controller (MBFC)

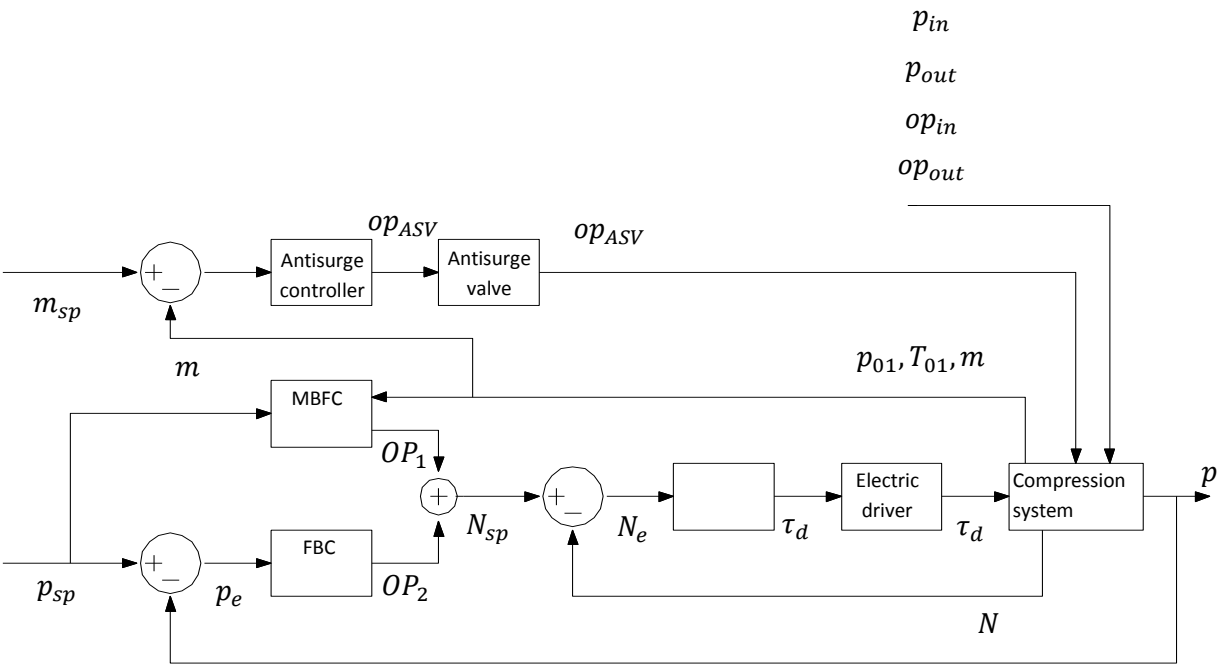


Figure 4-11. Cause-effect block diagram of the overall control system for compression application including model-based feedforward controller and antisurge controller

4.4.4 Tuning of model-based feedforward controller

Both PI and MBFC pressure controllers have a cascade structure. Table 4-3 summarises the tuning parameters while Figure 4-13 represents the time responses of the master (above) and slave (below) control loops for the PI (left) and MBFC (right) pressure controllers. The tuning of the PI controller has been already presented in Chapter 3. The tuning of the MBFC has been performed in order to have a similar dynamic response as the PI master loop. The dynamic response has been measured in terms of rise and settling time of the two master controllers.

Table 4-3. Tuning parameters for slave and master controllers

	Slave Controller	Master Controller PI	Feedback controller within MBFC
P	0.00	603.82	177.43
I	0.28	46.25	7.31
Rise time (s)	10.70	69.40	66.60
Settling time (s)	18.10	226.00	278.00
Overshoot (%)	0.00	0.10	9.04
Peak (-)	1.00	1.10	1.09

In the following figure for each control loops SP represents the set point, PV the controlled variable and OP the output of the single control loop.

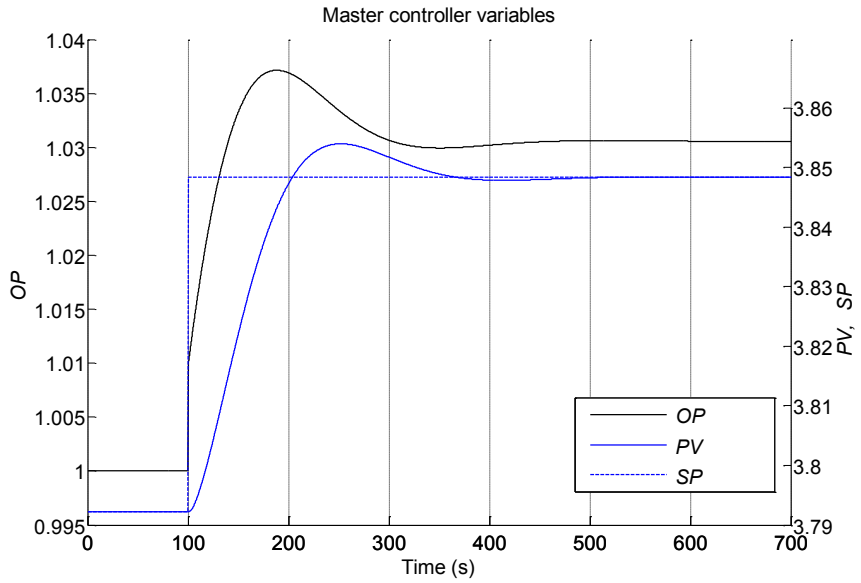


Figure 4-12. Response of the pressure control system to a set point change for PI controller (master loop)

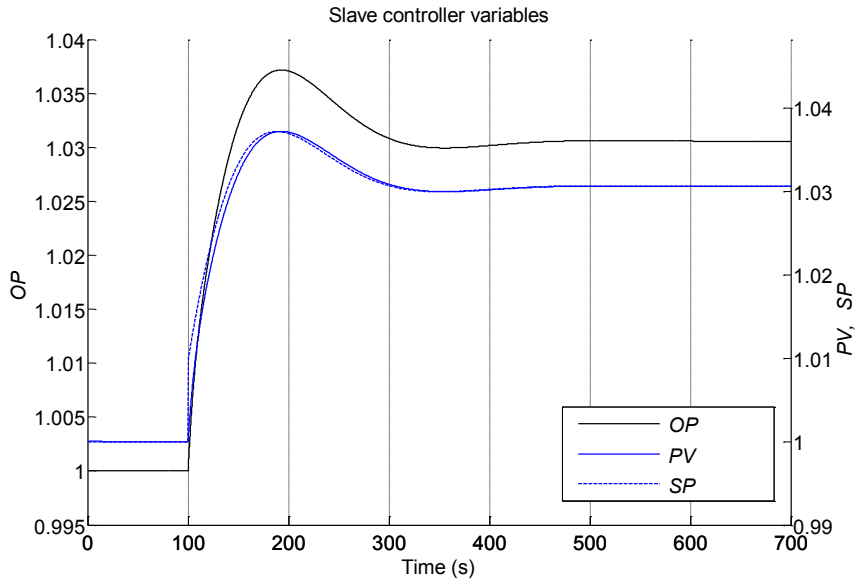


Figure 4-13. Response of the pressure control system to a set point change for PI controller (slave loop)

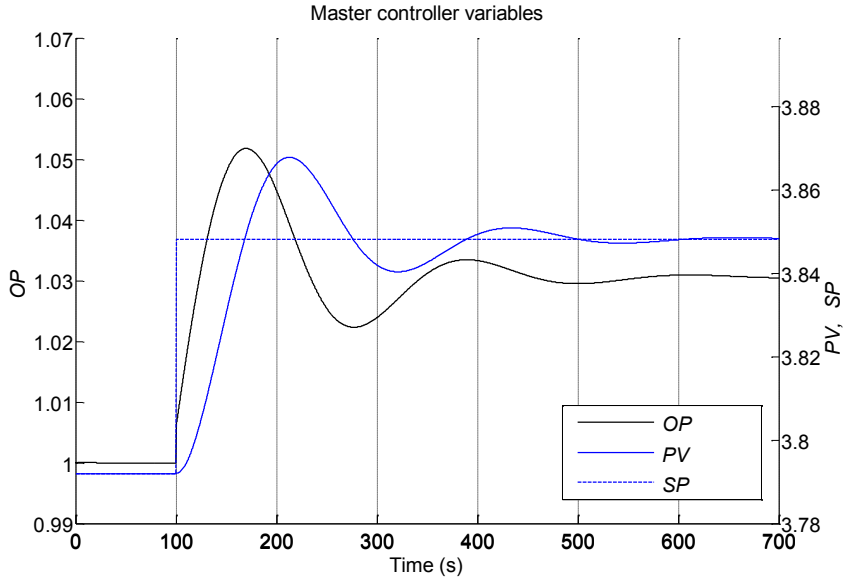


Figure 4-14. Response of the pressure control system to a set point change for MBF controller (master loop)

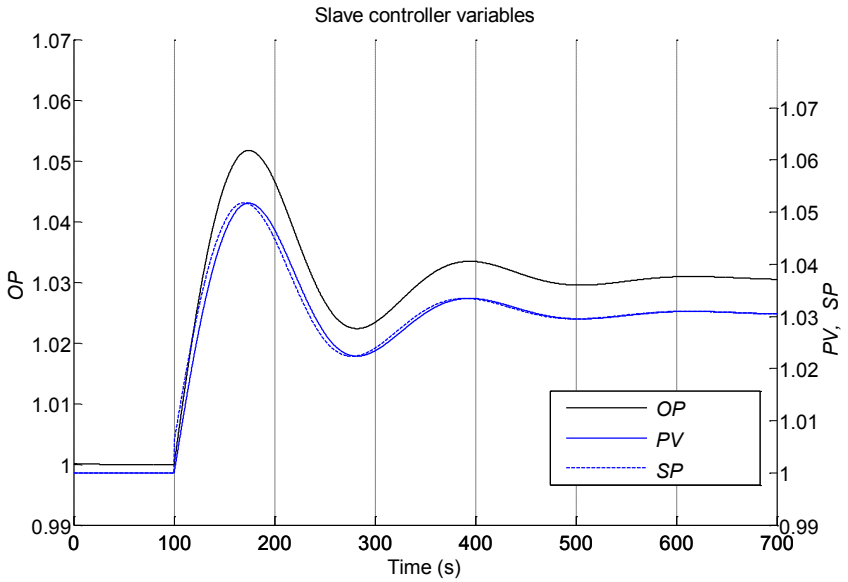


Figure 4-15. Response of the pressure control system to a set point change for MBF controller (slave loop)

4.4.5 Summary

In this part of the chapter the model-based feedforward controller has been defined, implemented and tuned. This model-based controller employs the compressor map in order to estimate the set point for the rotational shaft speed. This controller includes a feedback controller within its master control loop. This feedback controller has been tuned in order to give a similar dynamic response as the ESD master loop controller.

In the next section the traditional PI controller and the proposed MBFC will be compared during a variety of boundary disturbances. Their performance will be analysed by means of graphical representation and performance indicator.

4.5 Simulation results and performance evaluation

The model-based feedforward controller proposed in the previous section has been tested during process disturbances. Its response has been compared with the response of the ESD controller during the same disturbances. The comparison has been performed by means of graphical representation over time and using as performance parameter the integral of the square error ISE_p defined in section 4.2.2.

Initially both inlet and outlet disturbances have been tested. Then the influence of the rate of change of the disturbance on the performance of the MBFC has been analysed. Finally the positive effect of the operation of the MBFC controller on surge occurrence has been demonstrated.

4.5.1 Simulation of boundary disturbances

Initially both inlet and outlet variables have been employed as disturbance variables. As a recall from section 4.2.2, the employed disturbance variables are:

- System inlet pressure (maximum disturbance sign and magnitude ±12%)
- System inlet valve (maximum disturbance sign and magnitude -40%)
- System outlet pressure (maximum disturbance sign and magnitude ±3%)
- System outlet valve (maximum disturbance sign and magnitude -10%)
- Pressure set point (maximum disturbance sign and magnitude ±2%).

Various changes have been employed and they include:

- Step change
- Ramp change, with various rates of change
- Sinusoidal changes with various amplitudes and frequencies.

All simulations have been performed for a duration of thirty minutes and all the disturbances took place at time t=10 s (excluding the sinusoidal disturbances that started at time t=0 s).

4.5.1.1 Inlet pressure of the system

Table 4-4 summarises the results regarding the disturbances involving the inlet pressure of the system p_{in}. Each disturbance scenario is characterised by the magnitude of the disturbance. For ramps, the slope is specified. For each scenario ISE_p has been estimated for PI control ($ISE_{p,PID}$) and for MBFC control ($ISE_{p,MBFC}$) configuration. The relative difference is defined as:

$$Relative\ difference = \frac{ISE_{p,MBFC} - ISE_{p,PID}}{ISE_{p,PID}} \times 100 \quad \textbf{(4-4)}$$

Therefore a negative relative difference defines a better performance of MBFC with respect to PI controller.

For each disturbance scenario the MBFC controller shows a better control performance than the PI controller. Disturbance scenarios with negative sign present a higher value of the relative difference. This is due to the saturation of the speed controller. In fact a change of the inlet pressure of -12% requires the pressure controller to increase the rotational shaft speed to its maximum allowable value. When the speed controller saturates, the pressure is not yet at its set point. This can happen during boundary disturbances and can be handled in different way depending on the magnitude of the disturbance. However it is not affecting the current analysis as both controllers undergo the same situation and therefore their operation can still be compared.

Two graphical examples (Figure 4-16 and Figure 4-17) have also been reported. The system inlet pressure has been represented on the left vertical-axis while the outlet pressure of the compressor has been reported on the right-hand vertical axis. The pressure set point has also been reported as a reference. All the reported variables have been scaled due to a non-disclosure agreement with the project partners. For both disturbance scenarios the response of the PI controller has a larger deviation while the MBFC controller shows a tighter control on pressure. The response of the two controllers is comparable in terms of settling time.

Table 4-4. Disturbance scenarios for the inlet pressure of the system

Disturbance scenario	**1**	**2**	**3**	**4**	**5**	**6**
Type of disturbance	step	step	ramp	ramp	sine	sine
Sign and magnitude (%)	-12	12	-12	12	6	12
Slope	-	-	-0.00033	0.00033	-	-
$ISE_{p,PID}$	172.7	9.7	105.6	1.0	164.3	3688.9
$ISE_{p,MBFC}$	163.9	1.3	104.9	0.1	154.5	3648.6
Relative difference (%)	-5.1	-86.6	-0.7	-89.2	-6.0	-1.1

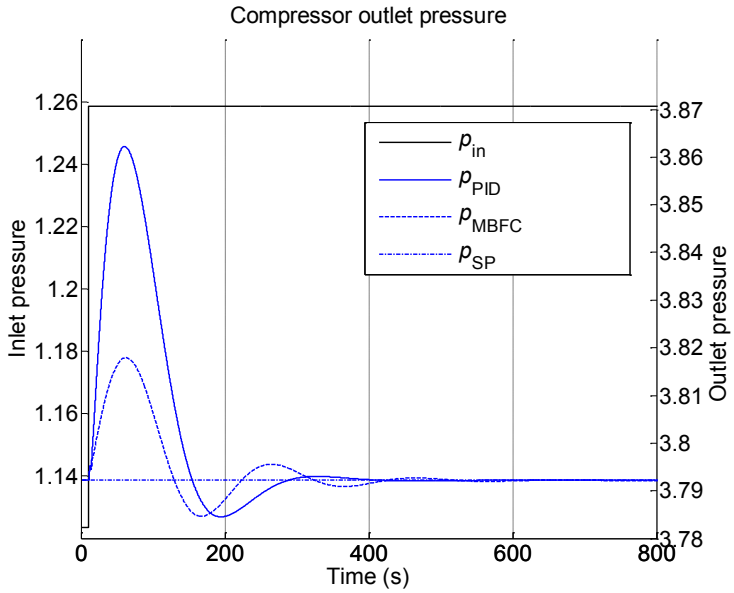


Figure 4-16. Compressor outlet pressure following a positive step change of the system inlet pressure (scenario 2)

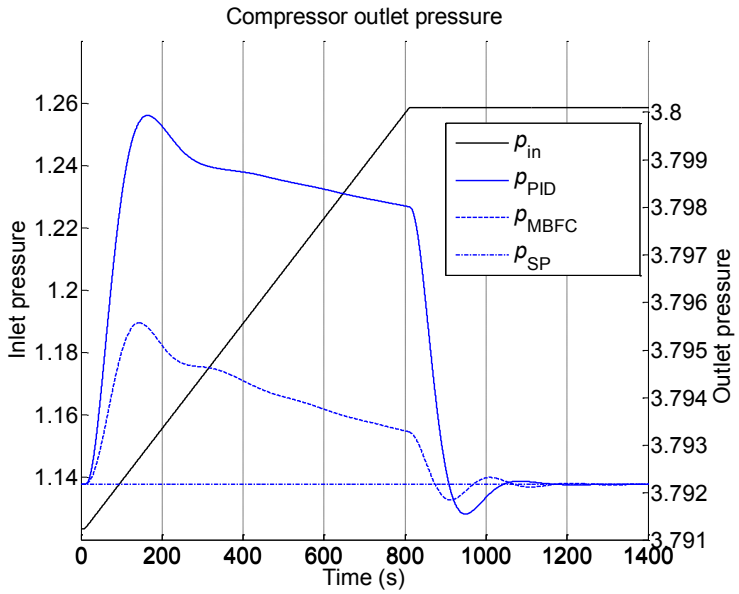


Figure 4-17. Compressor outlet pressure following a positive ramp change of the system inlet pressure (scenario 4)

4.5.1.2 Opening position of the inlet valve

The following table summarises the results regarding the disturbances involving the opening position of the inlet valve of the system op_{in}. Both disturbance scenarios are characterised by a negative step change of the valve opening position. In the first case (scenario 7) op_{in} moves from 100% to 80% while in the second scenario (scenario 8) it closes from 100% to 60%. In both cases the MBFC performs better than the PI controller in terms of pressure control. However it is possible to notice that for a more aggressive disturbance the relative difference between the two controllers is much smaller.

The reason for this difference can be understood by analysing the graphs represented in Figure 4-18 and Figure 4-19. For the first disturbance scenario both controllers are able to bring the pressure back to its set point. This happens in a similar settling time, which is around 400 seconds. However in the second disturbance scenario the pressure steady state value following the disturbance is lower than the pressure set point value. This is because the driver has reached its maximum speed limit, as represented in Figure 4-20.

Table 4-5. Disturbance scenarios for the inlet valve of the system

Disturbance scenario	**7**	**8**
Type of disturbance	step	step
Sign and magnitude (%)	-20	-40
$ISE_{p,PID}$	2.2	373.6
$ISE_{p,MBFC}$	0.7	365.7
Relative difference (%)	-69.7	-2.1

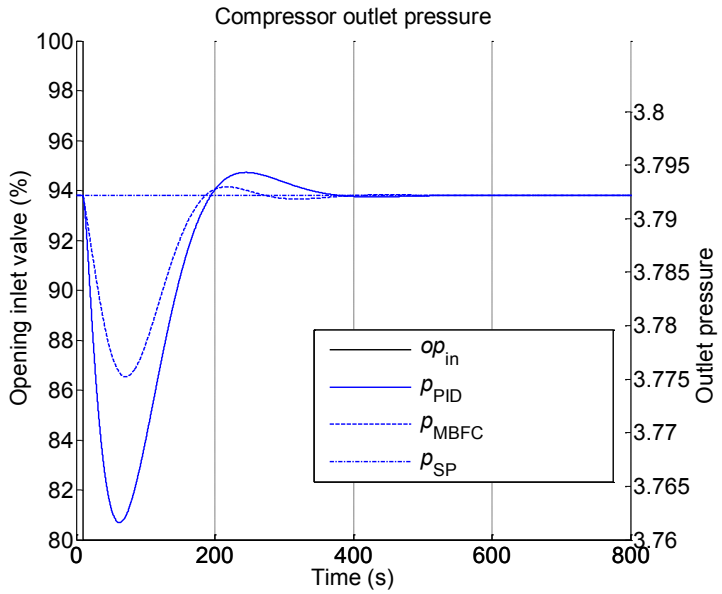


Figure 4-18. Compressor outlet pressure following a negative step change (-20%) of the opening position of the inlet valve (scenario 7)

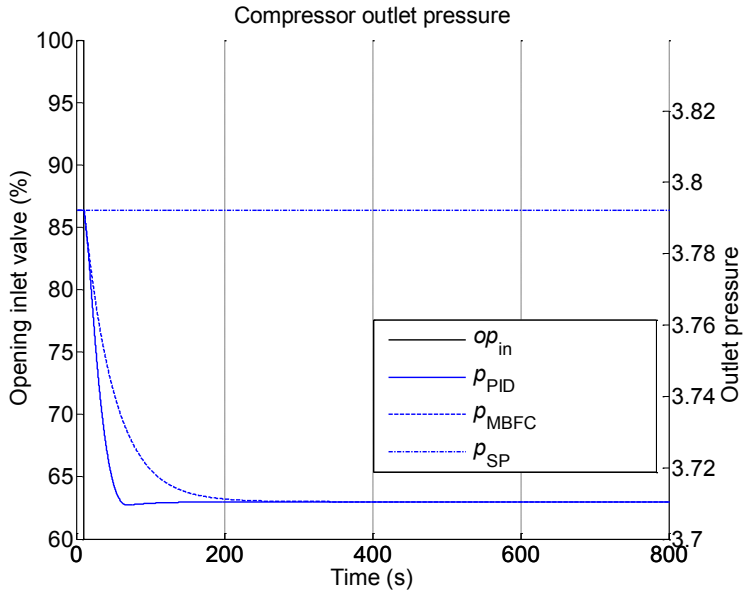


Figure 4-19. Compressor outlet pressure following a negative step change (-40%) of the opening position of the inlet valve (scenario 8)

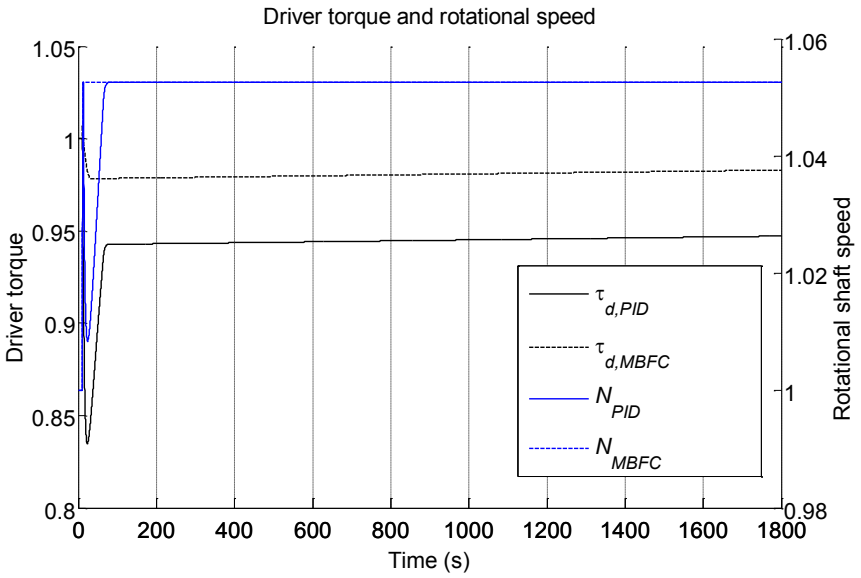


Figure 4-20. Driver torque and rotational shaft speed (scenario 8)

4.5.1.3 Outlet pressure of the system

The following table summarises the results regarding the disturbances involving the outlet pressure of the system p_{out}. Each disturbance scenario is characterised by the type of disturbance and the disturbance sign and magnitude. For ramps, also the slope is specified.

In all the tested disturbance scenarios the MBFC performs better than the PI controller. Two graphical examples have also been represented in Figure 4-21 (scenario 11) and Figure 4-22 (scenario 14). The left vertical axis represent the outlet pressure of the system while the right vertical axis represents the outlet pressure of the compressor. For both disturbance scenarios the response of the PI controller has a larger deviation while the MBFC controller shows a tighter control on pressure over time. Therefore these results show that the integral of the square error of the MBFC controller is lower than the integral of the square error of the PI controller and this means that the MBFC performs better than the PI controller over time.

Table 4-6. Disturbance scenarios for the outlet pressure of the system

Disturbance scenario	**9**	**10**	**11**	**12**	**13**	**14**
Type of disturbance	step	step	ramp	ramp	sine	sine
Sign and magnitude (%)	-3	3	-3	3	1.50	3
Slope	-	-	-0.00097	0.00097	-	-
$ISE_{p,PID}$	3.3	3.1	1.7	1.5	0.8	3.1353
$ISE_{p,MBFC}$	2.8	2.6	0.8	0.8	0.4	1.3417
Relative difference (%)	-15.2	-16.1	-52.9	-46.7	-50.0	-57.2

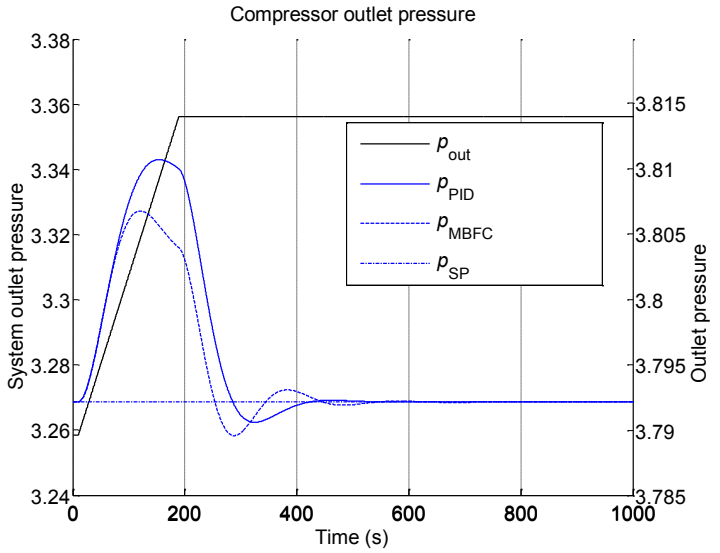


Figure 4-21. Compressor outlet pressure following a positive ramp change of the system outlet pressure (scenario 12)

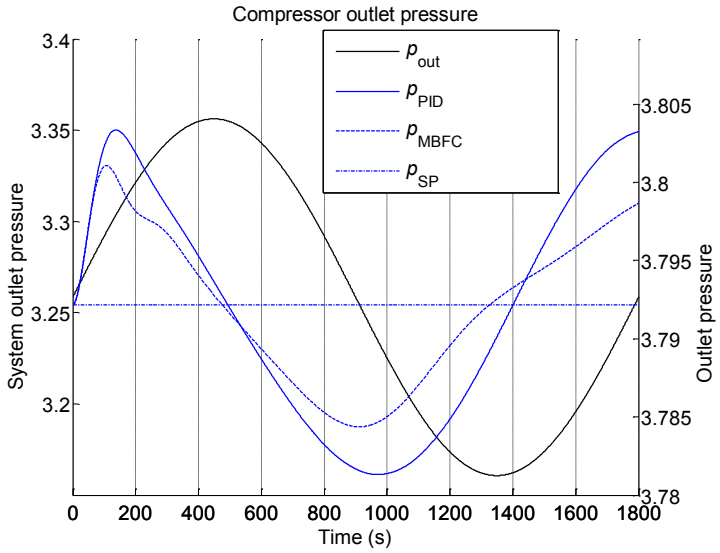


Figure 4-22. Compressor outlet pressure following a sinusoidal change of the system outlet pressure (scenario 14)

4.5.1.4 Opening position of the outlet valve

The following table summarises the results regarding the disturbances involving the opening position of the outlet valve of the system op_{out}. Both disturbance scenarios are characterised by a negative step change of the valve opening position. In the first case (scenario 15) op_{in} moves from 100% to 95% while in the second scenario (scenario 16) it closes from 100% to 90%. In both cases the MBFC performs better than the PI controller in terms of pressure control. These two cases have also been represented in Figure 4-23 and Figure 4-24.

Table 4-7. Disturbance scenarios for the outlet valve of the system

Disturbance scenario	15	16
Type of disturbance	step	step
Sign and magnitude (%)	-5	-10
$ISE_{p,PID}$	1.0	3.7
$ISE_{p,MBFC}$	0.8	3.4
Relative difference (%)	-16.4	-9.2

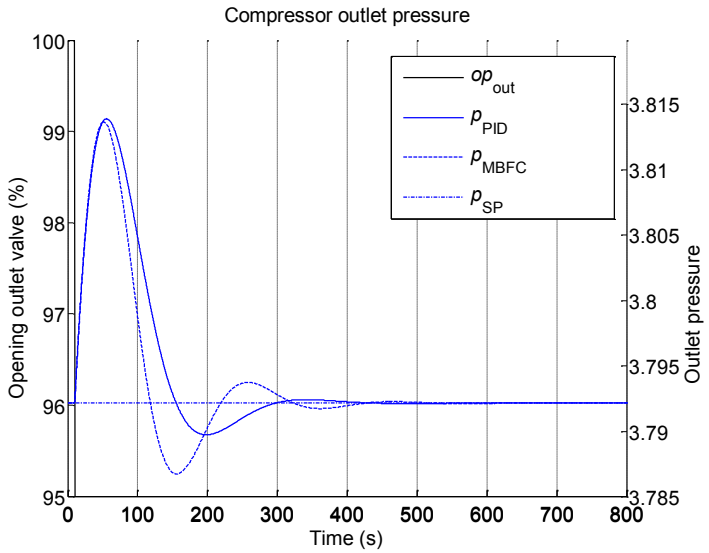


Figure 4-23. Compressor outlet pressure following a negative step change (-5%) of the opening position of the outlet valve (scenario 15)

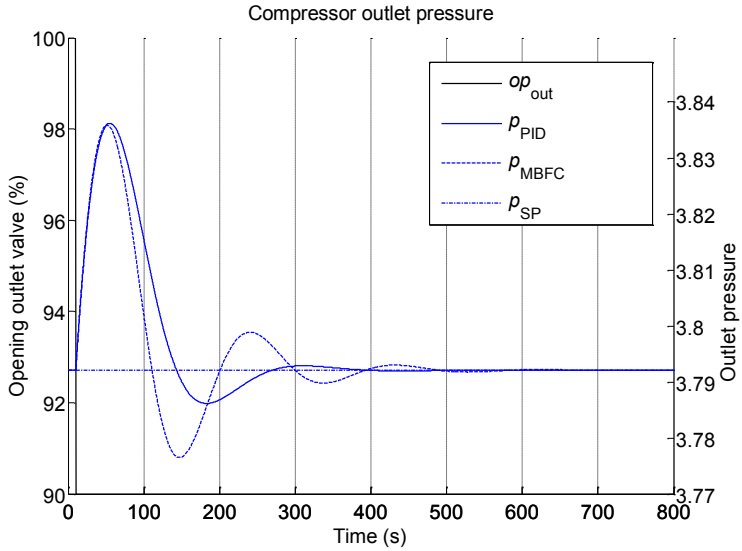


Figure 4-24. Compressor outlet pressure following a negative step change (-10%) of the opening position of the outlet valve (scenario 16)

4.5.1.5 Pressure set point

The following table summarises the results regarding the disturbances involving the pressure set point p_{SP}. In this case the performance of the two control system can be considered equivalent. The same conclusion can be derived from Figure 4-25.

Table 4-8. Disturbance scenarios for the pressure set point of the system

Disturbance scenario	17	18
Type of disturbance	step	step
Sign and magnitude (%)	-2	2
$ISE_{p,PID}$	6.0	6.4
$ISE_{p,MBFC}$	6.0	6.4
Relative difference (%)	0.0	-1.3

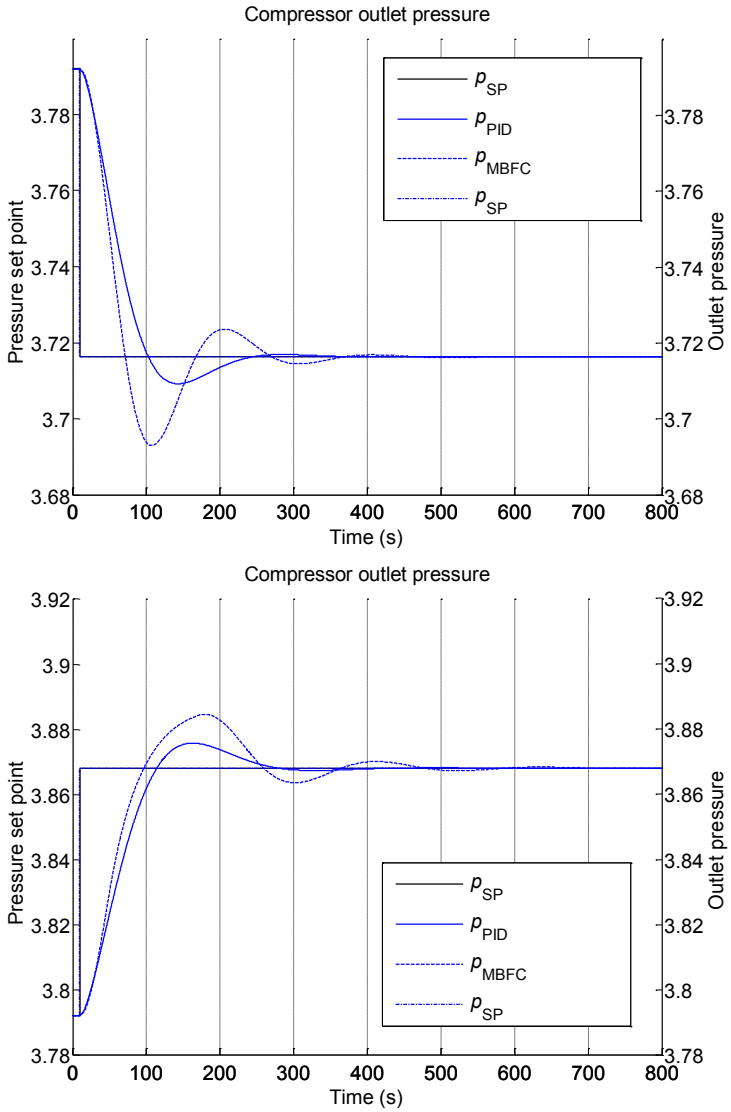


Figure 4-25. Compressor outlet pressure following a negative (-2%, above) and positive (2%, below) of the pressure set point (scenarios 17 above, scenario 18 below)

4.5.1.6 Summary

In all the tested disturbances the MBFC controller has shown a better control performance in comparison to the PI controller. The feedforward block of the MBFC has helped to counteract the effect of the disturbance on the system. The performance of the controllers has been estimated by means of the performance parameter ISE_p and also by means of graphical representation of the controlled variable.

When high value of ISE_p were recorded it was always due to the saturation of the speed controller. However also in these cases the MBFC demonstrated tighter pressure control over time. In case of set point change MBFC controller performed slightly better than the PI controller however in this case their performance can be considered equivalent.

4.5.2 Analysis of responses to the inlet pressure disturbance

The purpose of the analysis presented in this section has been to verify the influence of the rate of change of the disturbance on the performance of the MBFC. For this reason various disturbance scenarios have been performed and analysed. The inlet pressure has been selected as disturbance variables as the MBFC has been designed focussing mainly on this variable. The reason is that the first stage of compression has been selected as case study and therefore this stage is mostly affected by inlet disturbances, as explained in section 4.2.

Ramp and sinusoidal functions have been selected as disturbances as they offer a variety of rate of changes expressed in terms of slope (for the ramps) or frequency (for the sinusoidal disturbances).

4.5.2.1 Ramp scenarios

Various disturbance scenarios having a ramp change have been tested. The change has been maintained constant (±12%) while the slope has been decreased from ±1 to ±0.001. The results of the analysis are summarised in Table 4-9.

Also in this case the value of the relative difference for the disturbances having positive sign is much bigger than the value of the disturbances having negative sign. The reason is again the saturation of the speed controller, as represented in Figure 4-26 and Figure 4-27, where the two scenarios having slope ±0.01 have been represented as an example.

For different ramp change slopes, there is no influence of the rate of change of the disturbance on the performance of the MBFC with respect to the PI controller. The relative difference is always around 5% for negative disturbances and around 86.5% for positive disturbances. Only the last two scenarios (number 25 and number 26) present a small difference in comparison to the other scenarios. However this difference cannot be considered representative, as shown in Figure 4-28, Figure 4-29, Figure 4-30 and Figure 4-31, which show a normal behaviour of both PI and MBFC for these disturbance scenarios.

Table 4-9. Ramp disturbance scenarios for the inlet pressure of the system

Disturbance scenario	**19**	**20**	**21**	**22**	**23**	**24**	**25**	**26**
Sign and magnitude (%)	-12	12	-12	12	-12	12	-12	12
Slope	-1	1	-0.1	0.1	-0.01	0.01	-0.001	0.001
$ISE_{p,PID}$	172.6	9.7	172.5	9.6	171.0	9.4	148.3	3.4
$ISE_{p,MBFC}$	163.9	1.3	163.9	1.3	162.6	1.3	145.7	0.4
Relative difference (%)	-5.1	-86.5	-5.0	-86.5	-4.9	-86.2	-1.8	-89.2

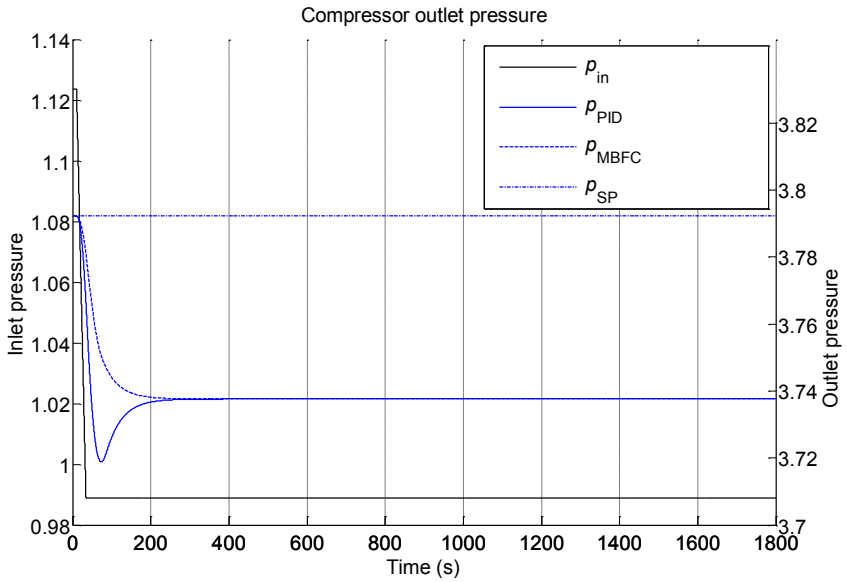


Figure 4-26. Compressor outlet pressure following negative ramp changes (slope -0.01, scenario 23) of the system inlet pressure

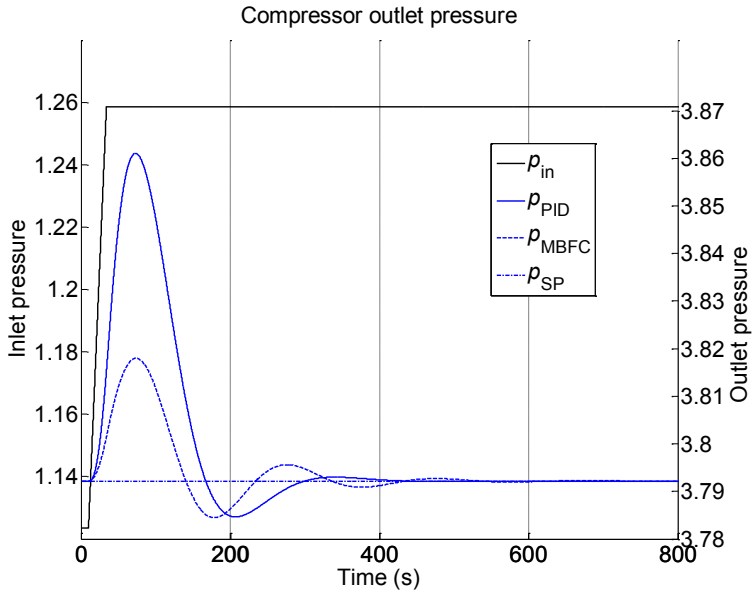


Figure 4-27. Compressor outlet pressure following positive ramp changes (slope 0.01, scenario 24) of the system inlet pressure

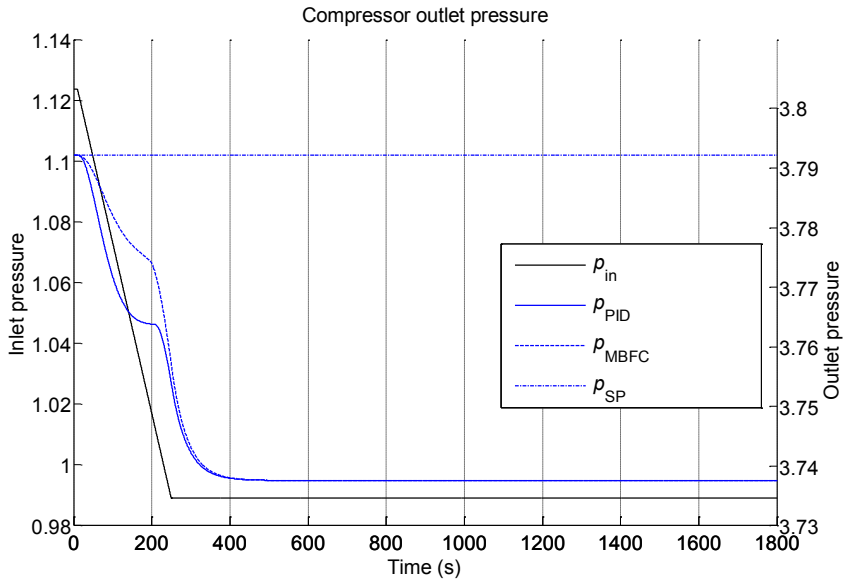


Figure 4-28. Compressor outlet pressure following negative ramp changes (slope -0.001, scenario 25) of the system inlet pressure

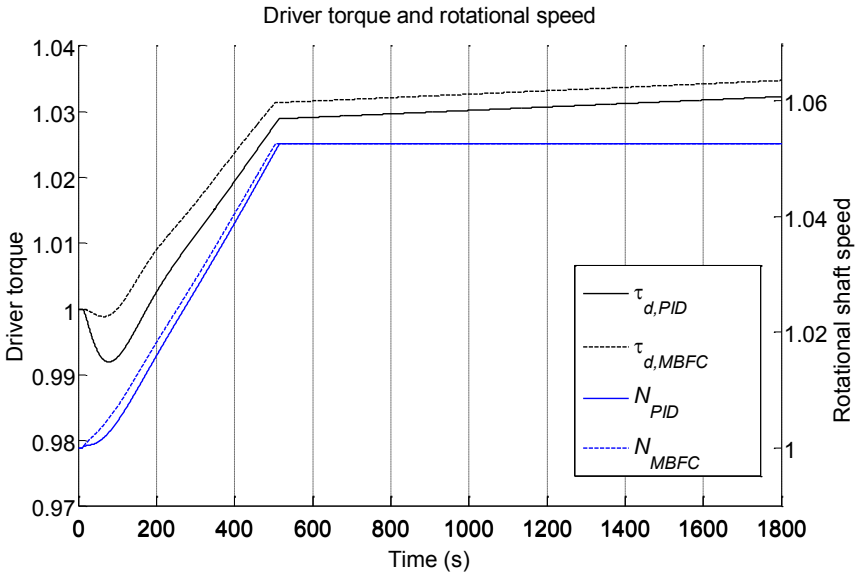


Figure 4-29. Driver torque and rotational shaft speed following negative ramp changes (slope -0.001, scenario 25) of the system inlet pressure

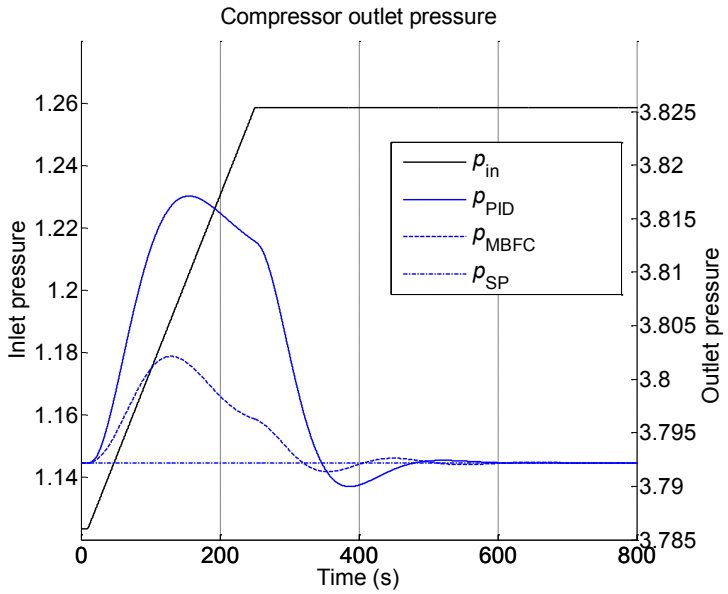


Figure 4-30. Compressor outlet pressure following positive ramp changes (slope 0.001, scenario 26) of the system inlet pressure

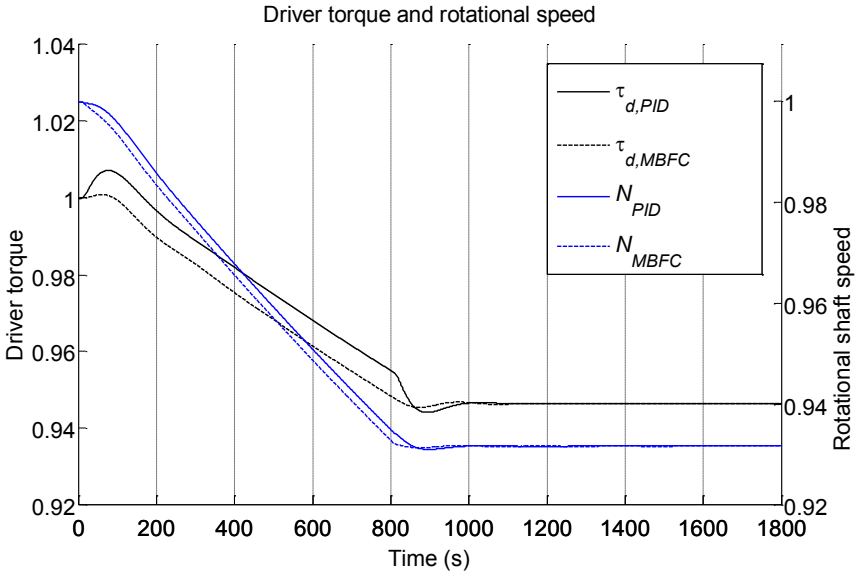


Figure 4-31. Driver torque and rotational shaft speed following positive ramp changes (slope 0.001, scenario 26) of the system inlet pressure

4.5.2.2 Sinusoidal scenarios

Various disturbance scenarios having a sinusoidal nature have been tested. The amplitude of the disturbances has been maintained constant (5%) while the radial frequency of the oscillation has been decreased from $2\pi/10$ to $2\pi/3600$ rads^{-1}. The results of the analysis are summarised in Table 4-10.

In all the analysed scenarios the MBFC controller performs better than the PI controller. The relative difference is in the range 76.5-90.4 excluding the first scenario (scenario 27). However in this case the ISE_p for both controller is very low.

In the following figures the outlet pressure of the compressor (Figure 4-32) and the driver torque and rotational shaft speed (Figure 4-33) have been represented for the scenario 31. The response of the PI controller shows a larger deviation while the MBFC controller shows a tighter control.

Table 4-10. Sinusoidal disturbance scenarios for the inlet pressure of the system

Disturbance scenario	**27**	**28**	**29**	**30**	**31**	**32**	**33**	**34**
Amplitude	5%	5%	5%	5%	5%	5%	5%	5%
Radial frequency (rads^{-1})	$\frac{2\pi}{10}$	$\frac{2\pi}{30}$	$\frac{2\pi}{60}$	$\frac{2\pi}{100}$	$\frac{2\pi}{600}$	$\frac{2\pi}{1200}$	$\frac{2\pi}{1800}$	$\frac{2\pi}{3600}$
$ISE_{p,PID}$	0.0	0.7	5.0	16.9	17.7	4.2	1.9	0.4
$ISE_{p,MBFC}$	0.0	0.1	0.5	2.2	3.7	0.9	0.4	0.1
Relative difference (%)	-31.7	-87.3	-90.4	-86.7	-79.2	-79.0	-76.5	-84.0

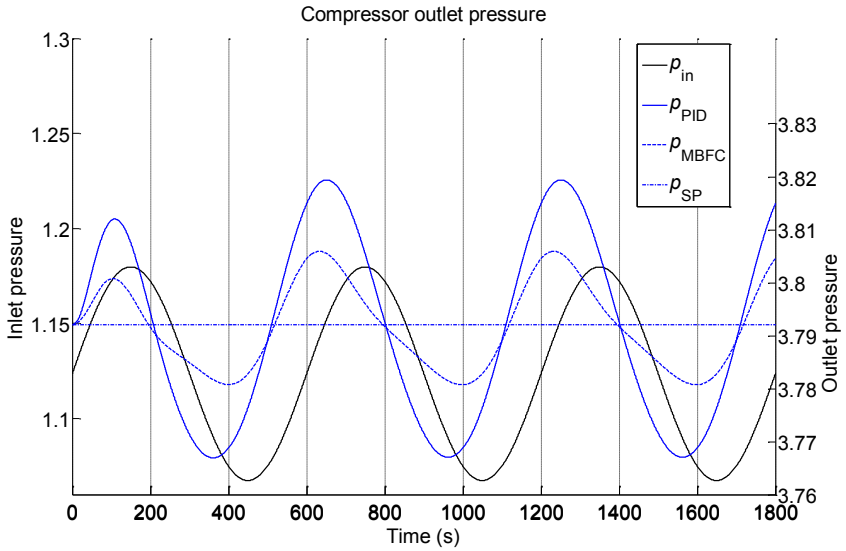


Figure 4-32. Compressor outlet pressure following sinusoidal changes (radial frequency 0.01 rads^{-1}, scenario 31) of the system inlet pressure

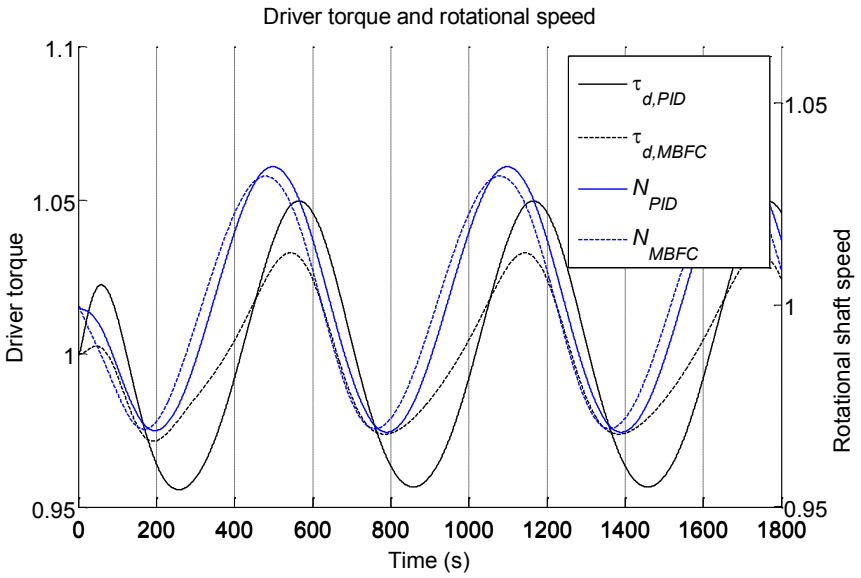


Figure 4-33. Driver torque and rotational shaft speed following sinusoidal changes (radial frequency 0.01 rads^{-1}, scenario 31) of the system inlet pressure

4.5.2.3 Summary

In all the tested disturbances the MBFC controller has shown a better control performance in comparison to the PI controller. The rate of change of the disturbance has not influenced the performance of the model-based feedforward controller. When high value of ISE_p were recorded it was always due to the saturation of the speed controller. However also in these cases the MBFC demonstrated tighter pressure control over time.

4.5.3 Reduction of interaction between control loops

The previous part of the chapter has demonstrated that the MBFC performs better than the PI controller under various inlet and outlet disturbance. The nature of the disturbance does not influence its control performance. Therefore the MBFC shows a tighter control on the compressor outlet pressure over time.

The consequences of this tighter control can also be represented in terms of compressor mass flow rate. In the following two images inlet and control mass flow rates have been represented during a faster (scenario 29) or slower (scenario 31) sinusoidal disturbance of the system inlet pressure. In both cases it is possible to notice that the MBFC has a smaller oscillation of the mass flow rate and of the control flow rate. For this reason the margin between them is wider over time. Therefore it is possible to see that a better pressure control allows a smaller oscillation of the mass flow rate over time, especially for high frequency disturbances.

The same disturbance scenarios have been represented on steady-state corrected compressor maps in Figure 4-36 and Figure 4-37. The wide oscillation of the flow rate when the compression system is controlled by the PI system is clearly visible on the compressor map for the scenario 29. During the

transients the MBFC controller is able to keep the operating point further from the surge line. For scenario 31 the behaviour of the mass flow rate is similar and therefore less noticeable on the compressor map.

In conclusion the action of the MBFC on the compression system in order to control the compressor outlet pressure has also demonstrated to reduce the distance between the operating point of the machine and the surge region during an oscillatory disturbance of the system inlet pressure.

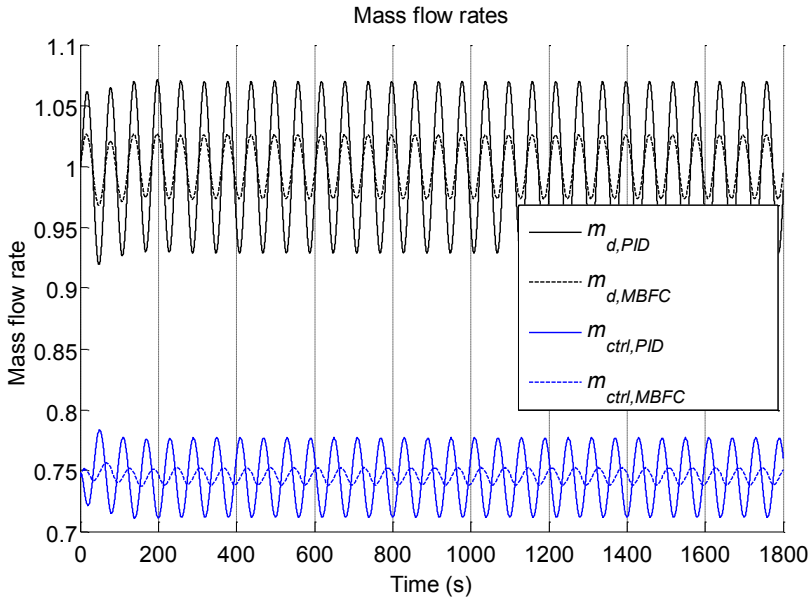


Figure 4-34. Compressor mass flow rates following sinusoidal changes (radial frequency 0.105 rads^{-1}, scenario 29) of the system inlet pressure

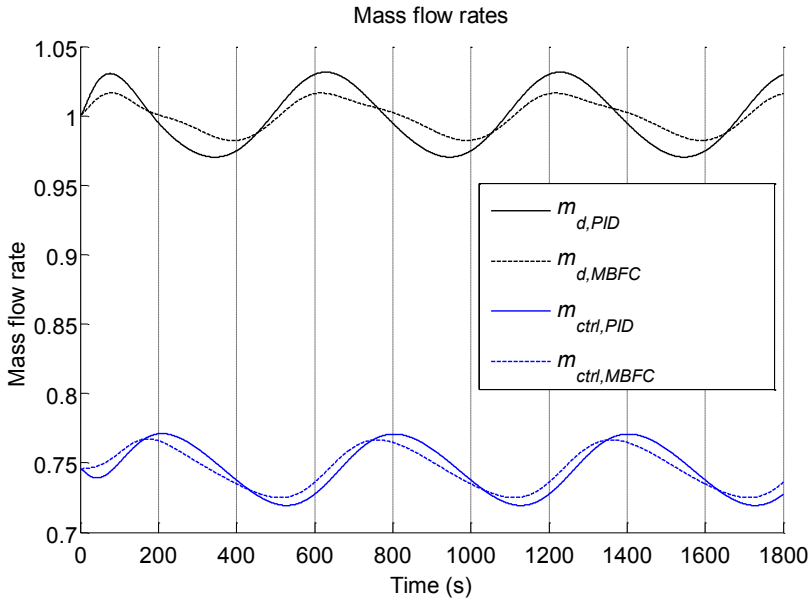


Figure 4-35. Compressor mass flow rates following sinusoidal changes (radial frequency 0.01 rads^{-1}, scenario 31) of the system inlet pressure

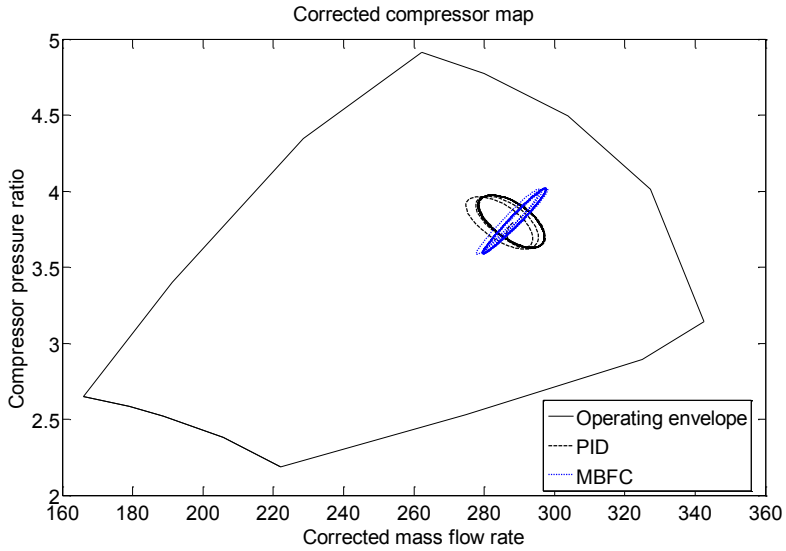


Figure 4-36. Oscillation of the operating point of the compressor following a sinusoidal disturbance (radial frequency 0.105 rads^{-1}, scenario 29) of the system inlet pressure

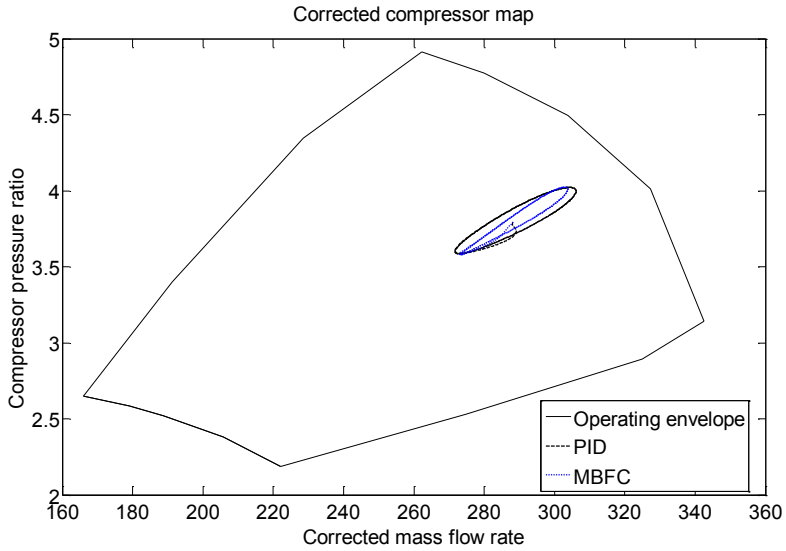


Figure 4-37. Oscillation of the operating point of the compressor following a sinusoidal disturbance (radial frequency 0.01 rads^{-1}, scenario 31) of the system inlet pressure

4.5.4 Summary

In this part of the chapter the model-based feedforward controller has been compared with the traditional cascade PI controller during a variety of boundary disturbances. In all the tested cases the MBFC has demonstrated to perform better than the traditional PI. The performance has been demonstrated using a performance parameter and also via graphical representation.

The rate of change of the disturbance does not affect the operation of the MBFC in terms of pressure control. However for disturbances having faster rate of change the action of the MBFC reduces the oscillation of the mass flow rate and therefore reduces the distance between the operating point of the compressor and the surge line.

4.6 Summary of the chapter

This chapter of the thesis had three main tasks to fulfil:

- Task 1: demonstration of control loops interactions
- Task 2: improvement of the response of the capacity controller
- Task 3: reduction of the interaction between control loops.

In order to accomplish the first task two examples of interactions between control loops within the compressor control system have been reported. In the first example the disturbance scenario has caused a beneficial interaction between control loops. The action of the pressure controller only has guaranteed the control of the compressor outlet pressure and the increasing of the distance between the compressor operating point and the surge region. In the second case the reduction of the opening position of the system outlet valve leads to a problematical interaction between the two controllers. This is a clear example of a disturbance scenario that can cause the oscillation of the system. It also demonstrates the importance of reducing the interaction between control loops.

The improvement of the performance of the capacity controller has been achieved by proposing a model-based feedforward controller. It has been defined, implemented, tuned and tested. This model-based controller employs the compressor map in order to estimate the set point for the rotational shaft speed. The controller has been compared with the traditional cascade PI controller during a variety of boundary disturbances. In all the tested cases the MBFC has demonstrated to perform better than the traditional PI. The performance has been demonstrated using a performance parameter and also via graphical representation. Simulation results have also demonstrated that the rate of change of the disturbance does not affect the operation of the MBFC in terms of pressure control.

Finally the simulation results have demonstrated that better pressure control reduced the oscillation of compressor mass flow rate and surge flow rate over time and therefore reduces the risk of gas recycle and potentially surge.

5 Analysis of antisurge control solutions

The previous chapter has proposed a control method for improving the response of the pressure controller. Results have also demonstrated that tighter pressure control reduces the risk of surge over time, especially during cyclical disturbances. Therefore the model-based feedforward controller proposed in Chapter 4 represents a step forward in the integration of pressure and surge control.

This chapter proposes a model predictive control system for integrated pressure and surge control of centrifugal compressors. When the recycle antisurge valve opens, a compressor becomes a Multiple-Input Multiple-Output (MIMO) system. Model Predictive Control (MPC) is considered the most appropriate control for this type of system (Seborg et al., 2004b). In the literature it has already been demonstrated that model predictive control was applicable for the control of complex compression systems (Øvervåg, 2013, Smeulers et al., 1999) and for surge prevention via close coupled valve (Johansen, 2002) and drive torque actuation (Cortinovis et al., 2012). However the minimization of the recycle flow rate and the temperature effects have not been previously taken into account. Therefore various tuning sets have been tested in order to analyse the response of the control system, which has been reported in the thesis. Moreover, temperature effects have been taken into account in the model of the process and in the constraint formulation of the MPC optimization problem.

The proposed control system is based on linear model predictive control. Different disturbance and control tuning scenarios were tested and the response of the model predictive controller was analysed, evaluated and also compared with a traditional control system.

The structure of the chapter is the following. Section 1 summaries the tasks of the chapter. Section 2 presents the disturbance scenarios, including a description of the case study, its full load and off-load operation, the selection of the disturbance scenarios and the evaluation of the controller performance. In Section 3 the control variables are presented. They include controlled, manipulated and disturbance variables. Section 4 describes the model predictive controller and also presents the optimization problem and its constraints, the cost function and the estimation of the states. Controller implementation and tuning are included at the end of the section. Section 5 summarises the results of the simulations, analysing the performance of the controller during various disturbance scenarios and employing various tuning sets. Finally Section 5 summaries the content of the chapter.

5.1 Task description

This chapter of the thesis has three main tasks to fulfil:

- Task 1: analysis of the open loop response of the compression system
- Task 2: integration of pressure and surge control action
- Task 3: reduction of the recycle flow rate by means of advance control design.

The first task requires a qualitative analysis of the response of the open loop system to process disturbances. The system is kept at constant rotational shaft speed and the effect of various disturbances is demonstrated. This analysis allows a better understanding of the behaviour of the open loop system and therefore provides a basis for understanding the MPC closed loop response.

The second task of the chapter involves the design and implementation of a model predictive controller able to deal at the same time with pressure and surge control. The need for integrated pressure and surge control has already been demonstrated in Chapter 4. Here further examples show the interaction between control loops and how an MPC controller can deal with it. Temperature effects have been taken into account in the formulation of the controller constraints. The MPC is tested during various disturbance scenarios and its response is analysed and explained by means of performance indicators and graphical representations. The response of the control system is also analysed when one of the actuators saturates and therefore becomes unavailable for control purposes.

The third task includes the analysis of various controller tunings. The purpose of the analysis is to verify the response of the system and give priority to different control objectives. The initial tuning reflects the desire to minimise the recycle flow rate while controlling the outlet pressure of the system and avoiding surge at the same time. Other tuning sets will be tested later on and the results will show the effect of the tuning on the response of the MPC controller.

5.2 Analysis of disturbance scenarios

In this section of the chapter the case study is presented, together with its operation at full and partial load. Dynamic simulations were run in order to analyse the response of the open loop and close loop system.

The types of disturbance have been selected according to the scenario proposed in the literate and employed for compressor and surge control validation. The references have already been presented in Chapter 4.2.1. Disturbance variables include:

- Closing of the inlet valve op_{in}
- Closing of the outlet valve op_{out}
- Inlet pressure of the system p_{in}
- Outlet pressure of the system p_{out}
- Pressure set point p_{SP}.

The types of disturbances include negative (for the boundary valves) and positive and negative step changes (for all the other disturbance variables). The magnitudes of the disturbances have been selected taking into account:

- The variation of inlet and outlet pressure and temperature during off-load operation
- The effect of the disturbance on the system, for example if it caused the saturation of an actuator.

5.2.1 Case study

The case study has already been introduced before (Chapters 3.5.1 and 4.3.1) and is based on a multistage centrifugal compressor arranged in a single shaft configuration and driven by an asynchronous electric motor. The fourth compression stage has been employed for the analyses presented in this chapter.

This stage has been selected because it is the last stage of compression and it is the stage compressing the process fluid from subcritical condition to supercritical condition. The process fluid is composed of carbon dioxide and a small percentage (0.1% w/w) of water vapour. The same stage will be employed for the analysis presented in the next chapter. In fact the focus of Chapter 6 is the effect of recycling supercritical fluid for surge prevention on the response of the control system.

This compression stage is characterised by its own compressor maps, design point and operational ranges. The compressor maps employed include pressure ratio map, polytropic efficiency map and also outlet temperature map. For this stage the map of the compressor outlet temperature had to be employed because the process fluid is non-ideal and therefore the function proposed by Camporeale et al. (2006) (equation 3-18) is not valid anymore. The map of the compressor outlet temperature represents the temperature of the gas at the outlet of the compressor as a function of

inlet mass flow rate and rotational shaft speed. Moreover the Span and Wagner equation of state (Span and Wagner, 1996) has been employed in order to estimate the density of the process fluid at high temperature and pressure.

The configuration employed is the hot gas recycle configuration presented in Chapter 3.2.2.1. The reason for employing this configuration is that the temperature effects are analysed in the chapter. A constraint on the maximum value of the outlet temperature of the compressor has been imposed on the MPC controller. Therefore the hot gas recycle configuration requires a wider range of operating temperature than the cold gas recycle configuration.

After the analyses have been completed, the results have been scaled according to the inlet conditions of the compression stage. This is because of the non-disclosure agreement with the partners of the project.

5.2.2 Design point and off-load operation

Following the same procedure employed in Chapter 4.2.2, the process datasheet referring to this specific case study has been employed in order to analyse its design point and off-load operation. The maximum variation of the boundary conditions has been summarised in Table 4-1. The subscript 01 indicates the inlet of the compressor while the subscript 02 indicates the outlet of the compressor.

Table 5-1. Maximum variation for the boundary variables during off load operation

Boundary variable	Maximum variation
p_{01}	12.5%
T_{01}	2.5%
p_{02}	18%
T_{02}	2.9%

The maximum variation of inlet and outlet pressure is around 18%. However it is important to notice that during off-load operation there are more variables changing at the same time and for this reason the operating point of the machine always lies within compressor map. In fact none of the off-load cases includes gas recycle, excluding the full recycle case itself.

5.2.3 Disturbance analysis and selection

The model of the compression system has been tested by changing the value of the single boundary disturbances. The results of the analysis are summarised in Table 4-2. For each disturbance variable, the maximum variation with respect to its design point has been estimated. Step changes have been employed for all the disturbance variables. The biggest magnitudes have been employed for the inlet

and outlet valve in order to cause respectively the saturation of the driver and a very wide opening of the antisurge valve. All the simulations have been performed for 3600s and all disturbances started at time t=10s.

Table 5-2. Maximum variation for the boundary disturbances during boundary disturbances

Boundary variable	Maximum variation
p_{in}	-2.81% to 32.94%
op_{in}	-80%
p_{out}	-0.5% to +1%
op_{out}	-95%
p_{sp}	-1.1 to 0.5%

5.2.4 Evaluation of performance for a controller

The performance of the proposed model predictive controller will be evaluated by means of graphical representation of controlled and manipulated variables over time and also by means of performance indicators. These performance indicators include the integral of the square error for pressure control ISE_p, the scaled recycle mass flow M and the scaled power consumption of the compressor E.

5.2.4.1 Pressure control performance

ISE_p has already been introduced in Chapter 4.2.2.3 and it is here repeated:

$$ISE_p = \int_{t=0}^{t_{final}} (p(t) - p_{SP}(t))^2 dt \quad \textbf{(5-1)}$$

This performance indicator is the integral of the square error. The error is the difference between the outlet pressure of the compressor p and its set point p_{SP} over time. t_{final} represents the time length of the analysed simulation (in this case it is always equal to 3600 seconds). Therefore ISE_p gives an idea of the performance of the controller in terms of pressure control. In an ideal situation ISE_p would be equal to 0. The units of ISE_p are bar^{2}s as the pressure is measured in bar while the time in seconds.

5.2.4.2 Recycle performance indicator

The scaled mass flow M calculates the amount of gas that has been recycled over the time interval $t = 0$ to $t = t_{final}$. This value is divided by the amount of gas that is compressed during one hour of forward operation at steady state and at the design point. Variable m_r is the recycle mass flow rate while m is the inlet compressor mass flow rate.

$$M = \frac{\int_{t=0}^{t_{final}} m_r dt}{\int_{t=0}^{t=1h} m dt} \quad \textbf{(5-2)}$$

Because in this case the analysed time interval is one hour, M would be 0 if there was no recycle and would be 1 in full recycle operation. The parameter is dimensionless.

5.2.4.3 Energy consumption indicator

E is the scaled power consumption of the compressor. This parameter calculates the energy consumption of the compressor during the time interval $t = 0$ to $t = t_{final}$ with respect to the power consumption of the machine during one hour of operation at steady state and design point. The parameter is dimensionless.

$$E = \frac{\int_{t=0}^{t_{final}} P_m dt}{\int_{t=0}^{t=1h} P_m dt} \quad \textbf{(5-3)}$$

P_m is the power consumption of the compressor and it has been estimated according to equation (3-13). Therefore if E is equal to 1 it means that the compressor has either been running at steady state and design point or that it is consuming as much as it would in that condition. Therefore this parameter is useful especially when used in conjunction with M. In fact if for example E increases but M does not this means the higher power consumption is not due to the gas recycle.

5.2.5 Summary

In this section of the chapter the disturbance scenarios have been presented. First of all the case study has been summarised together with its full load and off-load operation. Then the disturbance variables, type and magnitudes have been selected and summarised. Finally performance parameters have been proposed in order to analyse the performance of the controller in terms of pressure control, amount of gas recycled and power consumed. These parameters will be employed later on in order to analyse the behaviour of the model predictive controller and also to compare different control tuning sets.

5.3 Control variables

In this section of the chapter the control variables employed in the model predictive controller are presented. They include controlled variables, manipulated variables and disturbance variables.

5.3.1 Controlled variables

The main purpose of the MPC controller is to control the outlet pressure of the compressor p while avoiding surge. This means that the pressure p has to be at its set point while the flow rate m has to be above the surge control limit. The surge control limit is defined as the surge limit plus a safety margin that has been set to 20%. Therefore:

$$m_{ctrl} = 1.2 m_{surge} \tag{5-4}$$

This means that the MPC controller has to control p and m at the same time. Moreover the rotational shaft speed of the compressor has to be measured in order to guarantee that it stays within its minimum and maximum boundary limits. Also the outlet temperature of the compressor has to be measured in order to guarantee it does not exceed its maximum boundary. Therefore the measured variables are:

- The compressor outlet pressure p
- The compressor inlet mass flow rate m
- The rotational shaft speed N
- The compressor outlet temperature T_{02}.

These variables are the controlled variables however the tuning of the controller will determine which variables have to be tightly controlled and which variables have to be within their boundaries. This is the reason why the controller set points are usually called references in the MPC terminology.

5.3.2 Manipulated variables

The manipulated variables MV of the MPC controller are:

- The driver torque τ_d
- The opening of the antisurge valve op_{ASV}.

The torque of the driver has been selected as one of the manipulated variables (Gravdahl et al., 2002). The opening of the antisurge valve has been selected because passive surge control via gas recycle is the most popular control approach in industrial applications, as explained in Chapter 2.

5.3.3 Disturbance variables

Disturbance variables have already been presented in the previous section however they will be here recalled:

- Opening position of the inlet valve op_{in}
- Opening position of the outlet valve op_{out}
- Inlet pressure of the system p_{in}
- Outlet pressure of the system p_{out}
- Pressure set point p_{SP}.

These variables are not measured by the MPC controller with the exception of the pressure set point.

5.3.4 Summary

In this section of the chapter all the control variables have been listed and justified. They include controlled, manipulated and disturbance variables.

5.4 Model predictive controller

In this section of the chapter the proposed model predictive controller is presented. It is a linear model predictive controller as it is based on the linearized model of the compression system. Constraints on controlled and measured variables have been imposed in the MPC formulation. Model predictive control has already been proposed in the past for the control of single and multiple compressors and also for surge control. The main contributions of the controller here presented are:

- The minimisation of the gas recycle flow rate
- The analysis of the temperature effects due to gas recycle.

Moreover various controller tunings have been proposed, tested and compared. Each control tuning set has been designed according to specific control purposes.

5.4.1 Linearized model of the process

The plant model in the MPC formulation is a linear-time-invariant state-space model. The MPC controller performs all the estimation and optimization calculations using a discrete-time, delay-free, state-space system, with dimensionless input and output variables (MathWorks, 2015d). Therefore the following model-conversion steps are carried out:

- Conversion to state-space: the model of the open loop plant is converted to a linear-time-invariant state-space model
- Discretization and resampling: discretisation is necessary because the plant model is continuous-time; resampling is necessary as the sample time of the model differs from the sample time of the MPC controller
- Delay removal (if present)
- Conversion to dimensionless input and output variables.

The open-loop plant model has already been specified in Chapter 3. According to its formulation, the states of the state-space model are the compressor outlet pressure p, the compressor inlet mass flow rate m and the shaft radial velocity ω.

5.4.2 Overview of the optimization problem

The model predictive controller solves an optimization problem at each control interval. The optimization problem is a Quadratic Program (QP) problem. The solution of this problem determines the values of the manipulated variables to be used in the plant until the next control interval.

The quadratic program problem QP includes the following features (MathWorks, 2015e):

- The *cost* or *objective function*, that is a scalar, nonnegative measure of controller performance to be minimized

- The *constraints*, which are conditions the solution must satisfy, such as physical bounds on the manipulated variables and plant output variables
- The *decision*, which is the adjustments of the manipulated variables that minimize the cost function while satisfying the constraints.

The QP solver of the model predictive controller converts the optimization problem to the general form:

$$\min_{\Delta z_k} J(z_k) \tag{5-5}$$

where z_k is the quadratic program decision. The MATLAB toolbox employs the KWIK algorithm in order to solve the QP problem (MathWorks, 2015e).

5.4.3 Cost function

The *cost or objective function* is the sum of four terms, each focusing on a particular aspect of controller performance, according to MathWorks (2015e):

$$J(z_k) = J_y(z_k) + J_u(z_k) + J_{\Delta u}(z_k) + J_\varepsilon(z_k) \tag{5-6}$$

Each term of the cost function includes tuning weights that help balancing competing objectives.

5.4.3.1 Output reference tracking function

$J_y(z_k)$ is the *output reference tracking* function. This function aims at keeping the selected plant outputs at or near specified reference values, according to the following equation:

$$J_y(z_k) = \sum_{j=1}^{n_y} \sum_{i=1}^{p} \left\{ \frac{w_{i,j}^y}{s_j^y} \left[r_j(k+i|k) - y_j(k+i|k) \right] \right\}^2 \tag{5-7}$$

where:

- k is the current control interval
- p is the prediction horizon, that is equivalent to the number of intervals
- n_y is the number of plant output variables
- z_k is the QP decision, given by the following equation:

$$z_k^T = [u(k|k)^T \; u(k+1|k)^T \; \dots \; u(k+p-1|k)^T \varepsilon_k \;] \tag{5-8}$$

- $y_j(k+i|k)$ is the predicted value of j-th plant output at i-th prediction horizon step (in engineering units)
- $r_j(k+i|k)$ is the reference value of j-th plant output at i-th prediction horizon step (in engineering units)
- s_j^y is the scale factor for j-th plant output (in engineering units)

- $w_{i,j}^{y}$ is the tuning weight for the j-th plant output at i-th prediction horizon time step (dimensionless). If the tuning weight does not change over time, as in the case proposed, then $w_{i,j}^{y}$=w_{j}^{y}.

The controller receives $r_j(k+i|k)$ values for the entire prediction horizon and uses the state observer to predict the plant output. At interval k the state estimates of the controller and the values of the manipulated variables are available.

5.4.3.2 Manipulated variable tracking function

$J_u(z_k)$ is the *manipulated variable tracking* function. This function aims at keeping selected manipulated variables at or near specified target values. This function is particularly useful in applications where there are more manipulated variables than plant outputs. Therefore this function does not have a critical role in the application presented in this thesis.

The manipulated variable tracking function is defined according to the following equation:

$$J_u(z_k) = \sum_{j=1}^{n_u} \sum_{i=0}^{p-1} \left\{ \frac{w_{i,j}^{u}}{s_j^{u}} \left[u_j(k+i|k) - u_{j,target}(k+i|k) \right] \right\}^2 \quad \textbf{(5-9)}$$

where:

- n_u is the number of manipulated variables
- $u_{j,target}(k+1|k)$ is the target value for the j-th manipulated variable at the i-th prediction horizon step (in engineering units)
- s_j^{u} is the scale factor for the j-th manipulated variable (in engineering units)
- $w_{i,j}^{u}$ is the tuning weight for the j-th manipulated variable at i-th prediction horizon step (dimensionless).

The controller receives $u_{j,target}(k+i|k)$ values for the entire horizon and uses the state observer in order to predict the plant output.

5.4.3.3 Manipulated variable move suppression

$J_{\Delta u}(z_k)$ is the *manipulated variable move suppression* function. This function aims at reducing the adjustments of the manipulated variables, according to:

$$J_{\Delta u}(z_k) = \sum_{j=1}^{n_u} \sum_{i=0}^{p-1} \left\{ \frac{w_{i,j}^{\Delta u}}{s_j^{u}} \left[u_j(k+i|k) - u_j(k+i|k) \right] \right\}^2 \quad \textbf{(5-10)}$$

where $w_{i,j}^{\Delta u}$ is the tuning weight for the movement of the j-th manipulated variable at i-th prediction horizon step (dimensionless).

5.4.3.4 Constraints violations function

$J_\varepsilon(z_k)$ is the *constraints violations* function. This function aims at avoiding input and output constraint violations. When constraints violation is unavoidable, soft constraints allow a feasible quadratic program solution under such conditions. The MPC controller employs a dimensionless, nonnegative slack variable, ε_k, which quantifies the worst-case constraint violation. The corresponding performance measure is given by:

$$J_\varepsilon(z_k) = \rho_\varepsilon \varepsilon_k^2 \quad \textbf{(5-11)}$$

where:

- ε_k is the slack variable at control interval k (dimensionless)
- ρ_ε is the constraint violation penalty weight (dimensionless).

5.4.4 Controller state estimation

The state vector x_c^T is defined by the following equation:

$$x_c^T(k) = [x_p^T(k)\ x_{id}^T(k)\ x_{od}^T(k)\ x_n^T(k)] \quad \textbf{(5-12)}$$

where:

- x_c is the controller state, comprising $n_{xp} + n_{xid} + n_{xod} + n_{xn}$ state variables
- x_p is the plant model state vector, of length n_{xp}
- x_{id} is the input disturbance model state vector, of length n_{xid}
- x_{od} is the output disturbance model state vector, of length n_{xod}
- x_n is the measurement noise model state vector, of length n_{xn}.

All the previous variables have been represented in Figure 5-1. The MPC controller makes use of the state observer in order to:

- Estimate values of unmeasurable states needed for predictions
- Predict the effect of the proposed manipulated variable adjustment on the output values of the plant.

The controller updates its state automatically using the latest plants measurements.

The observer input signals are:

- The dimensionless plant manipulated inputs
- The dimensionless plant measured disturbance inputs

while the outputs of the observer are the n_y dimensionless plant putputs.

The controller states are estimated by means of a steady state Kalman filter (Kalman, 1960).

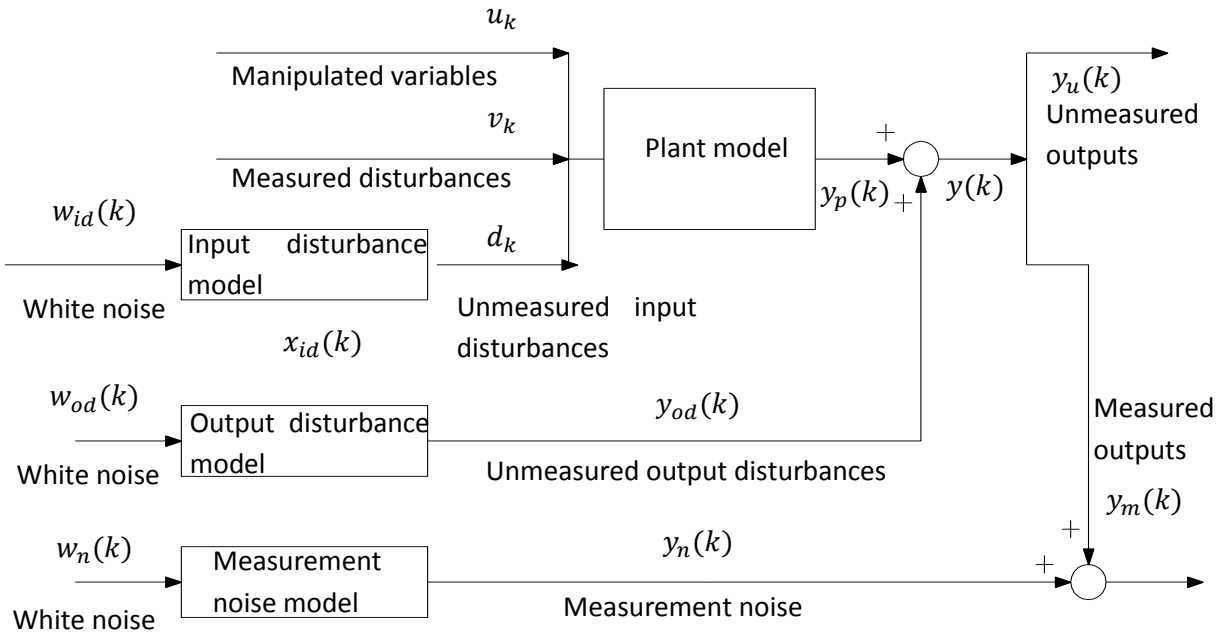


Figure 5-1. Controller state variables, modified from MathWorks (2015b)

5.4.5 Optimization constraints

The MPC controller solves a constrained optimisation problem in order to decide the control action of the compression system. The constraints of the optimization problem are the lower and upper boundaries for both measured variables and manipulated variables.

For steady state operation at the design point, the value of measured and manipulated variable has been summarised in Table 5-3. These values have been scaled according to the conditions of the gas at the inlet of the compressor stage.

For each measured and manipulated variable, constraints have been specified in the MPC formulation. The values of the constraints are summarised in Table 5-4. The constraints for the measured variables are soft constraints. This means that they can be violated for short periods of time if necessary for the resolution of the optimisation problem. The constraints of the manipulated variable are hard constraints. This means they cannot be violated for any reason.

Table 5-3. Scaled measured and manipulated variables at the design point

Variable	Value at design point (dimensionless)
p	3.19
m	1
N	1
T_{02}	1.38
τ_d	1
op_{ASV}	0

Table 5-4. Constraints for measured and manipulated variables

Variables constraints (dimensionless)
$3.14 \leq p \leq 3.28$
$m_{surge} + margin = m_{ctrl} \leq m$
$0.80 \leq N \leq 1.05$
$0.86 \leq T_{02} \leq 1.65$
$0 \leq \tau_d \leq 57.94$
$0 \leq op_{ASV} \leq 1$

Pressure constraints represent a variation of ±2%. Mass flow rate constraint represents the surge control limit. Rotational shaft speed constraints depend on the minimum and maximum rotational shaft speeds of the driver. The maximum temperature constraint has been imposed to 20% and guarantees the integrity of the machine during hot gas recycling.

Regarding the manipulated variable, torque constraints depend again on the driver while the antisurge valve constraint represent its fully open and fully closed position.

Also the rate of change of the manipulated variables has been limited according to the following values:

$$rc_{\tau_d} \leq 0.1 \quad \textbf{(5-13)}$$

$$rc_{op_{ASV}} \leq 0.1 \quad \textbf{(5-14)}$$

where rc_{τ_d} represents the rate of change of the torque express in rpms^{-1} while $rc_{op_{ASV}}$ represents the rate of change of the antisurge valve express in %s^{-1}.

5.4.6 Controller implementation

The MPC controller has been implemented in MATLAB Simulink® environment (version number 8.1 R2013a). The full closed loop model includes the open loop model presented in Chapter 3 and the model predictive controller. The solver ode45 has been selected for the integration of the closed-loop model equations. The implementation in MATLAB Simulink® required to provide the following information to the software:

- Model of the open loop plant
- Sampling time
- Prediction and control horizons
- Measured and manipulated variables, together with their names, units and values at initial steady state

- Optimisation constraints related to measured and manipulated variables
- Surge margin
- Controller tuning set, constituted by tuning weights.

5.4.7 Controller tuning

The tuning of the MPC controller contains two groups of tuning parameters. The first group contains sampling period and control horizons. The second group contains the tuning weights that are included in the objective function.

5.4.7.1 Control horizons

According to Seborg et al. (2004b) the following rules of thumb should be employed in order to determine the model horizon MH, the control horizon CH and the prediction horizon PH depending on the sampling period Δt and the settling time for the open loop response of the system t_s:

$$MH\Delta t = t_s \quad \textbf{(5-15)}$$

$$30 \leq MH \leq 120 \quad \textbf{(5-16)}$$

$$MH/_3 \leq CH \leq MH/_2 \quad \textbf{(5-17)}$$

$$PH = MH + CH \quad \textbf{(5-18)}$$

Various horizons have been tested in order to obtain an accurate response of the controller in a reasonable amount of time. Table 5-5 summarises sampling period and control horizons that have been selected for the MPC controller. The sampling period was enough to capture fast dynamics but not too small as to slow down the calculations, while MH, CH and PH were selected accordingly.

Table 5-5. Sampling period and control horizons

Name	Value
Sampling period (s)	4
MH (s)	68.55
CH (s)	40
PH (s)	160

5.4.7.2 Tuning weights

The objective function of the optimization problem contains weights for both manipulated variables and process output variables. These weights constitute the controller tuning set. The MPC controller has been tuned in order to guarantee good pressure control while avoiding as much as possible the

opening of the antisurge valve. The reason for doing that is that gas recycle increases the operating cost of the system as more gas must be compressed by the machine without being delivered.

Three different sets of control tuning parameters have been defined. The second and third tuning sets will be presented later in the chapter. The first tuning set is summarised in Table 5-7. The control tuning parameters are called weights in the MPC formulation. The weights on the control variables are represented with the symbol w while the weights on the rate of change of the manipulated variables are represented with the symbol wr. The variable associated with the weight is indicated in the subscript. All the weights are dimensionless, as previously stated.

The process of tuning included the following steps:

- Step 1: initial tuning. The initial tuning weights are summarised in Table 5-6. The initial tuning weight were equal to 0 for the manipulated variables and equal to 1 for the controlled variables
- Step 2: tuning of the weights of the controlled variables. The tuning weights associated with the controlled variable were changed in order to prioritize the control of respectively the compressor outlet pressure p, the compressor inlet flow rate m, the rotational shaft speed N and the compressor outlet temperature T_{02}
- Step 3: tuning of the weights of the manipulated variables. The values of the weights of the manipulated variables were increased in order to prioritise the use of the driver torque and avoid when possible the opening of the antisurge valve. The purpose of this tuning was to avoid gas recycle by taking advantage of the flexibility of the electric driver, which can speed up and slow down quickly
- Step 4: first tuning iteration. During this step, steps 2 and 3 were repeated until the response of the closed loop system to a disturbance was satisfactory
- Step 5: rate limitation. The tuning weights associated with the rate of change of the manipulated variables were increased in order to avoid continuous oscillations over time
- Step 6: second tuning iteration. During this step, steps 2 and 3 were repeated until the response of the closed loop system to a disturbance was satisfactory. The tuning weights were finalised and summarised in Table 5-7.

Table 5-6. Initial tuning parameters for model predictive controller (tuning set 1)

Name	Value
w_{τ_d}	0
wr_{τ_d}	0
w_{ASV}	0
wr_{ASV}	0
w_p	1
w_m	1
w_N	1
$w_{T_{02}}$	1

Table 5-7. Final tuning parameters for model predictive controller (tuning set 1)

Name	Value
w_{τ_d}	0
wr_{τ_d}	0.1
w_{ASV}	10
wr_{ASV}	0.1
w_p	1
w_m	0.08
w_N	0.0001
$w_{T_{02}}$	0.0001

5.4.8 Summary

In this section of the chapter the architecture of the model predictive controller has been presented. The chapter presents the linearization of the open loop plant and gives an overview of the optimization problem. The selected cost function is explained together with the estimation of the controller states and the optimization constraints. Finally this section covers the implementation of the controller and its tuning.

5.5 Simulation results and performance evaluation

This section of the chapter reports the results of the dynamic simulations. First of all the response of the open loop system has been analysed during boundary disturbances. This analysis helps understanding the response of the system when it runs at constant rotational shaft speed. Therefore it gives insight on the effect of process disturbances on the open loop system.

Then the MPC controller has been tested during various disturbance scenarios. Its response has been analysed and compared with the response of a traditional PI controller, which has been well-tuned using lambda tuning. Saturation of the actuators has also been analysed. Temperature effects have been reported and analysed. Various tuning sets have been proposed and compared in order to achieve different control objectives. The results of the simulations have been analysed by means of graphical representation and performance indicators.

5.5.1 Analysis of the response of the open loop system

The open loop system has been tested during boundary disturbances. Disturbance variables have been changed and the response of the open loop system has been recorded. These simulations have been performed at constant rotational shaft speed N.

The purpose of this analysis is to give insights on the way the boundary disturbances affect the compression system. This analysis is qualitative rather than quantitative and wants to provide a better understanding of the operation of the compressor. The final purpose is to understand the response of the open loop system in order to intuitively understand the response of the closed loop system later on. The action of the MPC controller involves the solution of a quadratic program problem, as previously explained, and therefore its understanding is not always straightforward. Therefore this analysis helps in achieving this purpose.

The magnitudes and directions of the disturbances that have been employed during the open loop simulations are summarised in Table 5-8. Some of these disturbances are smaller than the magnitudes of the disturbances employed during the closed loop simulations, summarised in Table 4-2. This is because the open loop system is not able to remain stable during a strong disturbance if the control system is not in place. Therefore a small disturbance moves the operating point from its initial steady state condition to a new steady state condition. This new steady state condition is not the design point of the plant however it is still within the operating region of the compression system and therefore it is possible to represent it.

Table 5-8. Maximum variation for the boundary disturbances during boundary disturbances

Boundary variable	Maximum variation
p_{in}	±2%
op_{in}	-30%
p_{out}	±2%
op_{out}	-30%

5.5.1.1 Inlet valve of the system

The inlet valve of the system and its location within the process layout are represented in Figure 3-4, Chapter 3.

The first simulation lasted 1200 seconds and involved the closing of the inlet valve of the system. At time t=10s the inlet valve closed by a negative step change of -30% and the response of the open-loop system has been recorded. This response is represented in terms of compressor outlet pressure p and inlet flow rate m and it is represented in Figure 5-2. These two variables have been selected as they are the main measured variables of the system. The compressor outlet pressure is represented on the left vertical axis while the compressor inlet mass flow rate has been represented in the right vertical axis.

When the inlet valve closes, both pressure and flow rate decrease. The rate of change of the pressure is lower than the rate of change of the flow rate. This phenomenon comes from the values of the time constants presented in Chapter 3, as the pressure time constant is bigger than the mass flow rate time constant. This is because, according to the geometrical dimension of the duct-plenum system, the ratio between the square of the sonic velocity ${a_{01}}^2$ and the volume of the plenum V is smaller than the ratio between the cross sectional area of the duct A_1 and the length of the duct L.

After the closing of the inlet valve, m decreases because the passage area of the valve is reduced. When the flow rate of a compressor decreases at constant rotational shaft speed, the pressure ratio of the machine increases. This happens because the compressor inlet pressure p_{01} decreases and therefore p decreases as a consequence of it.

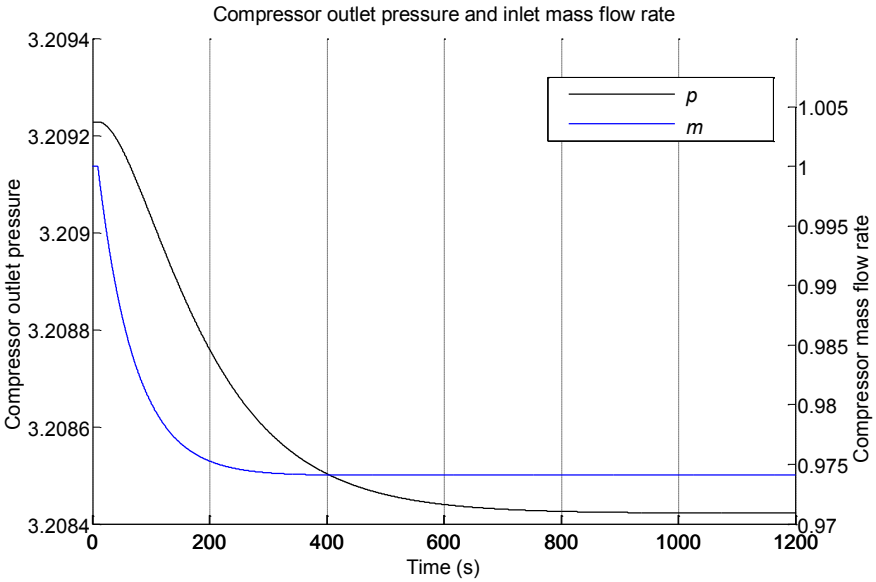


Figure 5-2. Open loop system response following inlet valve opening

5.5.1.2 Outlet valve of the system

This simulation involved the closing of the outlet valve of the system. The sign and magnitude of the step change is -30%. The response of the open loop system is represented in Figure 5-3.

After the closing of the valve, m decreases because the passage area of the valve is reduced. This means that the pressure ratio increases and this is because the pressure drop through the outlet valve increases (Towler and Sinnott, 2013). Therefore p increase as well, as represented in figure.

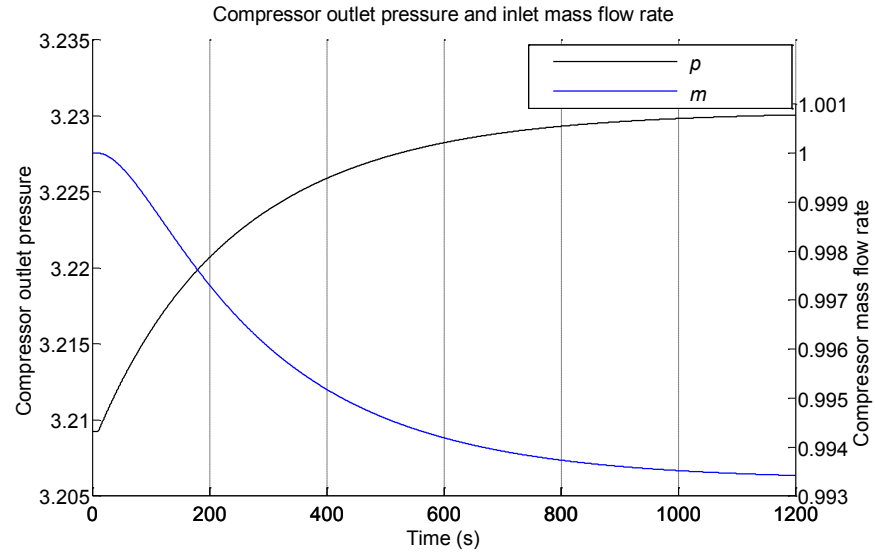


Figure 5-3. Open loop system response following outlet valve opening

5.5.1.3 Inlet pressure of the system

This simulation involved the changing of the inlet pressure of the system.

When the inlet pressure of the compression system decreases by a negative step change of sign and magnitude -2% and the rotational shaft speed is constant, the compressor outlet pressure p decreases as a consequence. This causes the reduction of the mass flow rate through the machine, as represented in Figure 5-4.

When the inlet pressure of the compression system increases by a positive step change of magnitude 2% and the rotational shaft speed is constant, the compressor outlet pressure p increases as a consequence. This causes the increase of the mass flow rate through the machine, as represented in Figure 5-5.

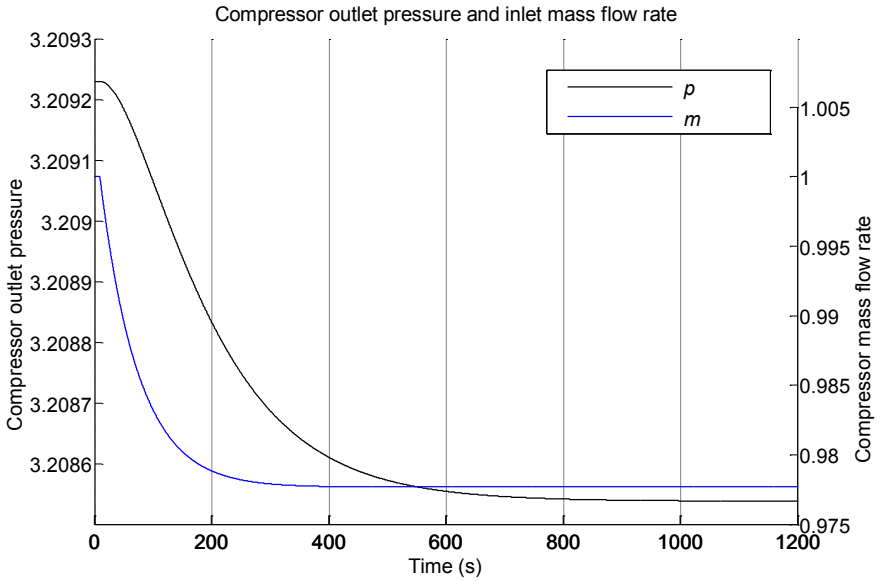


Figure 5-4. Open loop system response following system inlet pressure decreasing

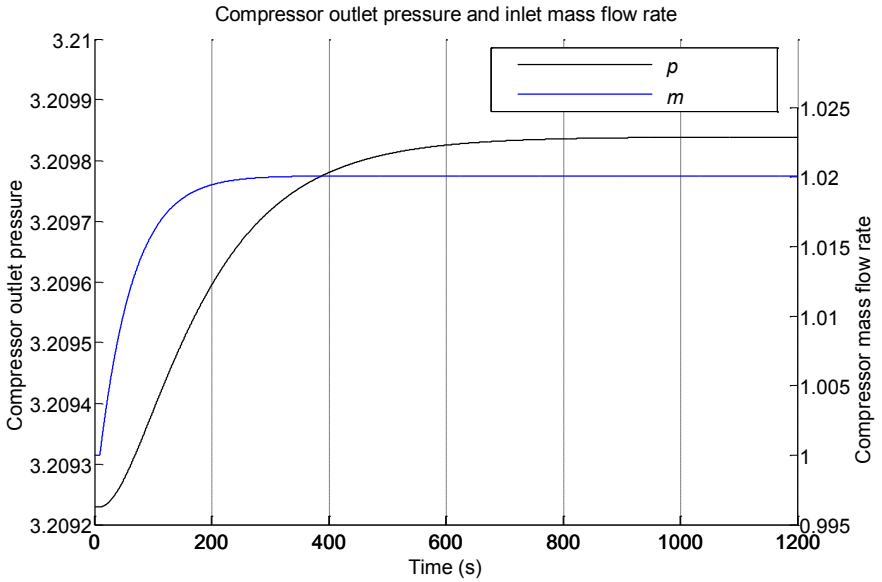


Figure 5-5. Open loop system response following system inlet pressure increasing

5.5.1.4 Outlet pressure of the system

This simulation involved the changing of the outlet pressure of the system.

When the outlet pressure of the compression system decreases by a negative step change of sign and magnitude -2% and the rotational shaft speed is constant, the compressor outlet pressure p decreases as a consequence. This causes the increase of the mass flow rate through the machine, as represented in Figure 5-6.

When the outlet pressure of the compression system increases by a positive step change of magnitude 2% and the rotational shaft speed is constant, the compressor outlet pressure p increases as a consequence. This causes the decrease of the mass flow rate through the machine, as represented in Figure 5-7.

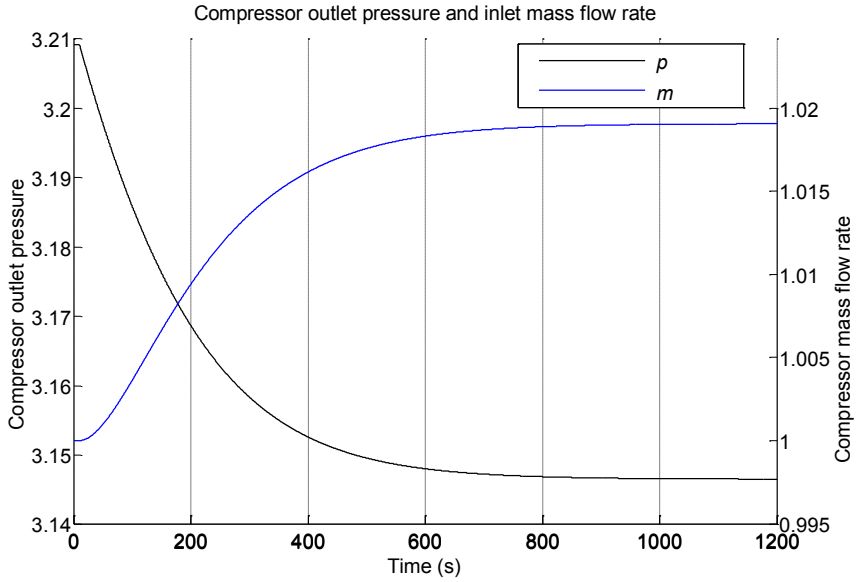


Figure 5-6. Open loop system response following system outlet pressure decreasing

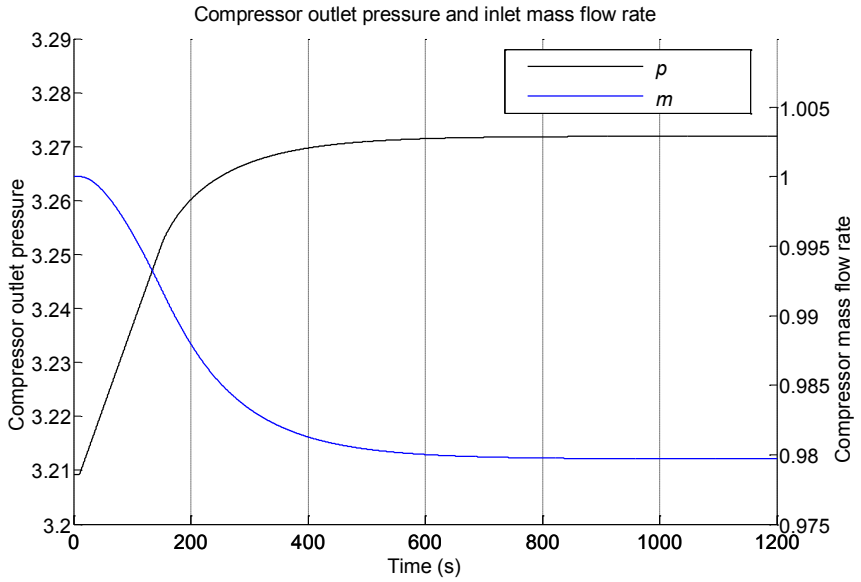


Figure 5-7. Open loop system response following system outlet pressure increasing

5.5.2 Analysis of the model predictive controller response

Various disturbance scenarios have been employed to test the response of the model predictive controller. For each disturbance variable, the disturbance scenarios differ because of the magnitude and sign of the disturbance itself. The results have been reported employing the three performance parameters presented in section 5.2.4: ISE_p, M and E. Moreover some graphical representations have also been employed to report the values of manipulated and controlled variables over time.

5.5.2.1 Steady state operation

Table 5-9 reports the values of the performance indicators during steady state operation at the design point. ISE_p is equal to 0.32 bar^{2}s while M is equal to 0.02 and therefore this means that the compressor outlet pressure is almost equal to its set point while the antisurge valve is closed. E is equal to 1 as expected for this type of operation.

Table 5-9. Steady state operation at the design point

Scenario	0 – steady state at design point
ISE_p(bar^{2}s)	0.32
M (-)	0.02
E (-)	1.00

5.5.2.2 Closing of the inlet valve

Table 5-10 reports the values of the performance indicators when the position of the inlet valve changes from fully opened position to partially opened position. For example for scenario 2 the sign and magnitude of the disturbance is -10%. This means that the valve closes by 10% from its fully opened position. Therefore the new opening position of the valve is 90%.

The disturbance scenario 1 is equal to the scenario 0 reported above. However it has been repeated in the table for direct comparison. In scenarios 2, 3 and 4 ISE_p increases with the increasing of the magnitude of the disturbance. M is always 0 as there is no need for recycle. At the same time E increases because of the increase of m due to the action on the driver torque.

Scenario 3 has been selected for illustrating the action of the controller. Figure 5-8 shows the manipulated variables during the analysed time period of duration one hour. The antisurge valve stays closed while the driver torque increases in order to increases the rotational shaft speed and therefore bring back the pressure to its set point. However the action of the MPC controller overshoots the driver torque. This is because of the tuning of the model predictive controller. In fact the MPC controller does not have any restriction in the manipulation of the driver torque as the corresponding weight is equal to zero. On the other hand it must give priority to the control of the outlet pressure as the corresponding weight is equal to 1 and therefore bigger than the weight associated with the mass flow rate m, equal to 0.08. The consequence is that the action on the driver torque is too aggressive and the pressure at the outlet of the compressor is not yet at its set point after almost one hour of operation. This is represented in Figure 5-9 where the opening of the

inlet valve is represented on the left vertical axis while the outlet pressure of the compressor and its set point are represented on the right vertical axis. Figure 5-10 shows the mass flow rates of the compressor. m is the inlet flow rate of the compressor, m_{ctrl} is the control flow rate while m_{surge} is the surge flow rate. The action of the MPC controller on the driver torque causes the increase of the inlet flow rate. Moreover it causes the increase of the pressure at the inlet of the compressor p_{01} and this is the reason why the surge flow rate increases over time, according to equation (3-11).

Table 5-10. Disturbance scenarios for the inlet valve of the system

Disturbance scenario	**1**	**2**	**3**	**4**
Sign and magnitude (%)	0.00	-10.00	-20.00	-29.00
ISE_p (bar^{2}s)	0.32	68.28	460.28	1732.96
M (-)	0.02	0.00	0.00	0.00
E (-)	1.00	1.02	1.06	1.11

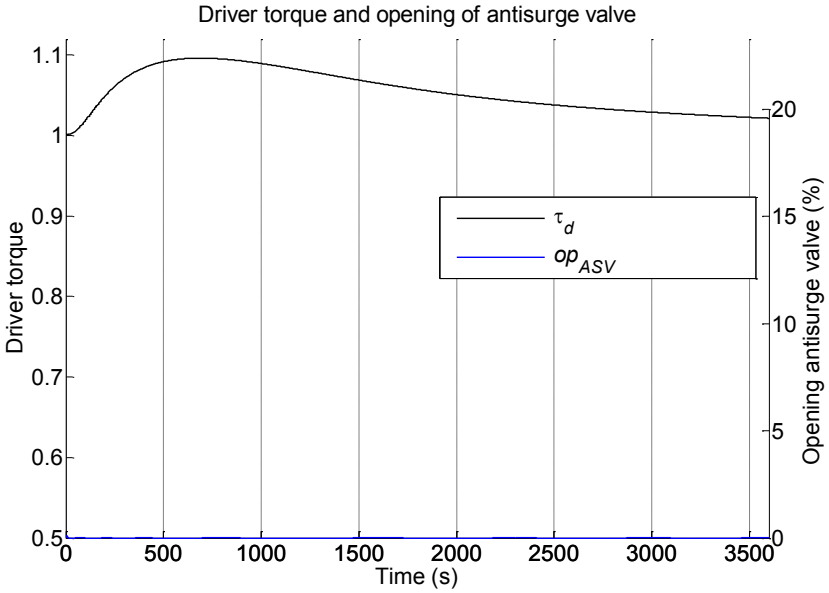


Figure 5-8. Manipulated variables during disturbance scenario 3

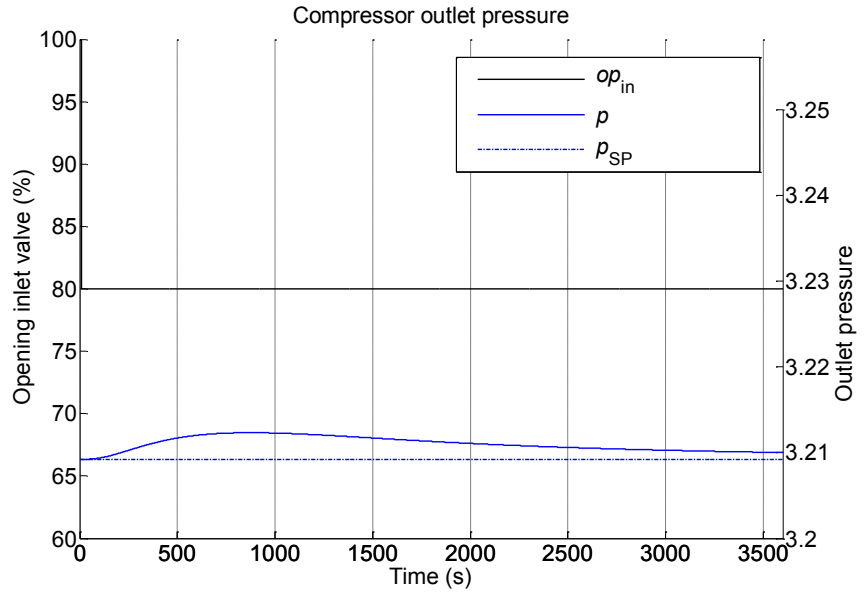


Figure 5-9. Compressor outlet pressure during disturbance scenario 3

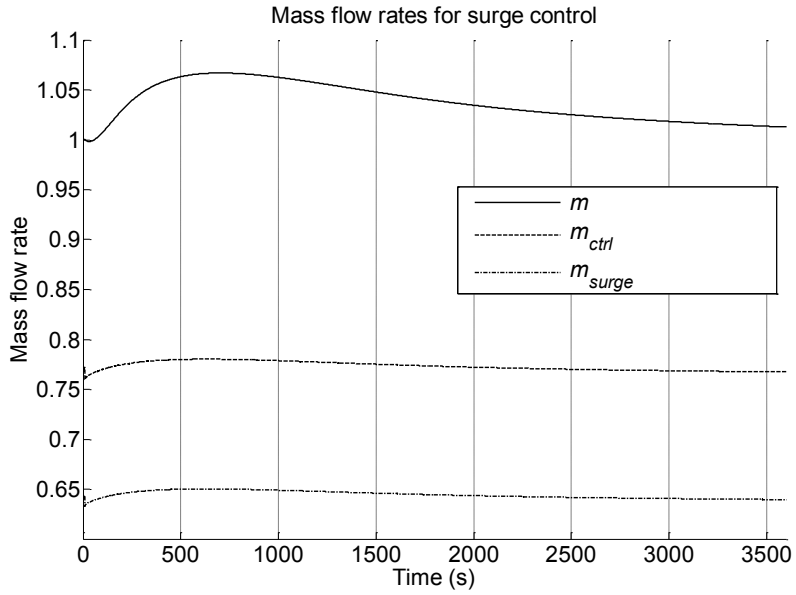


Figure 5-10. Compressor mass flow rates during disturbance scenario 3

5.5.2.3 Closing of the outlet valve

Table 5-11 reports the values of the performance indicators when the position of the outlet valve changes from fully opened position to partial opened position.

Also in this case the disturbance scenario 1 has been repeated in the table for direct comparison. In scenarios 5, 6 and 7 ISE_p increases with the increasing of the magnitude of the disturbance. As explained in section 5.5.1, the closing of the outlet valve causes the increase of the pressure p when the system is in open loop. For this reason in closed loop the MPC controller decreases the driver torque in order to reduce the rotational shaft speed N and bring the pressure back to its set point.

However this action reduces the flow rate m. In order to compensate for this, the MPC controller opens the antisurge valve and M increases. However it is possible to see that E decreases. This is because the flow rate through the compressor is still lower than the flow rate at the design point. At this point it is important to notice that the opening of the antisurge valve decreases the compressor outlet pressure and therefore it contributes to the control of this variable.

Scenario 6 has been selected to illustrate the action of the controller. Figure 5-11 shows the manipulated variables over time. The driver torque decreases for the reasons explained above while the antisurge valve opens. However the action of the MPC controller is very slow and the pressure is still above its set point after almost one hour of operation, as represented in Figure 5-12. Figure 5-13 shows the mass flow rates of the compressor. The action of the MPC controller causes the decrease of the pressure at the inlet of the compressor p_{01} and this is the reason why the surge flow rate decreases over time.

Table 5-11. Disturbance scenarios for the outlet valve of the system

Disturbance scenario	1	5	6	7
Sign and magnitude (%)	0.00	-40.00	-70.00	-95.00
ISE_p (bar^{2}s)	0.32	797.74	3308.27	7948.91
M (-)	0.02	3.25	5.97	8.50
E (-)	1.00	0.95	0.92	0.89

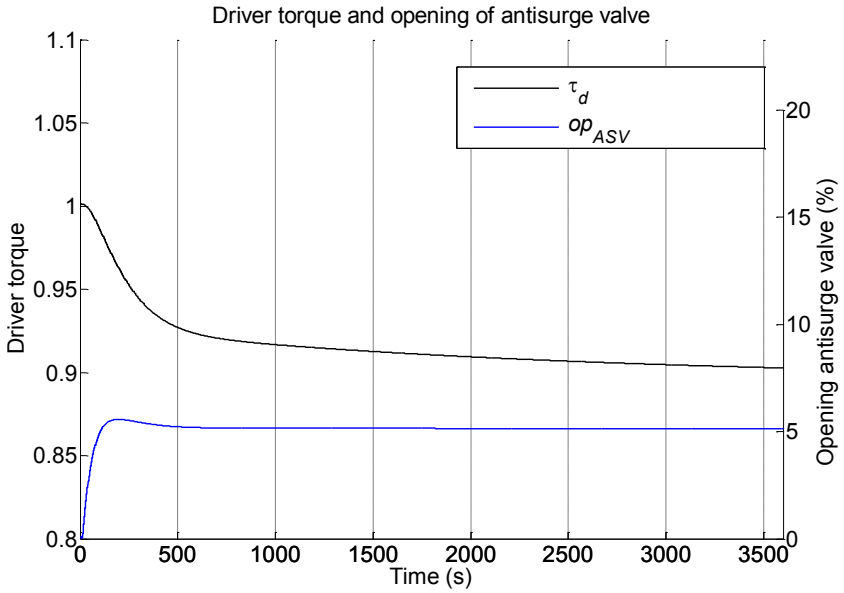


Figure 5-11. Manipulated variables during disturbance scenario 6

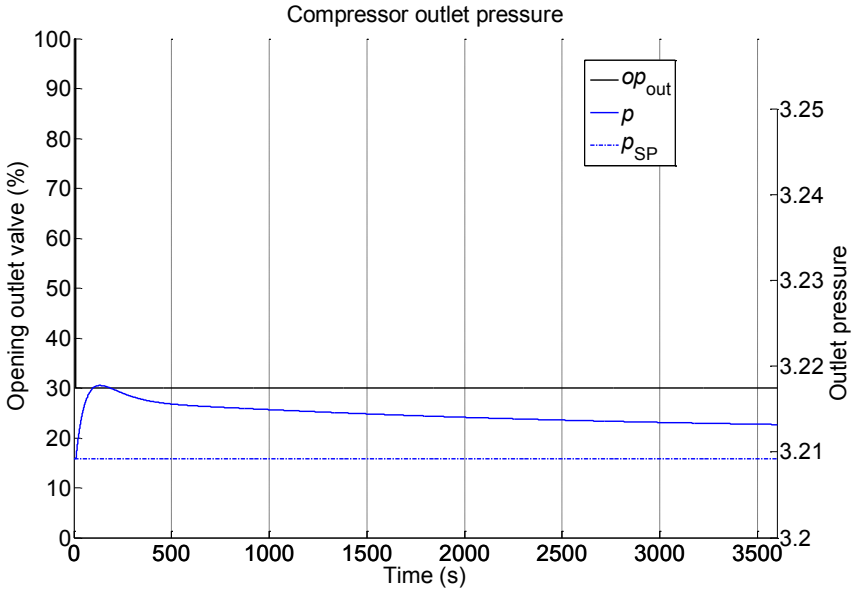


Figure 5-12. Compressor outlet pressure during disturbance scenario 6

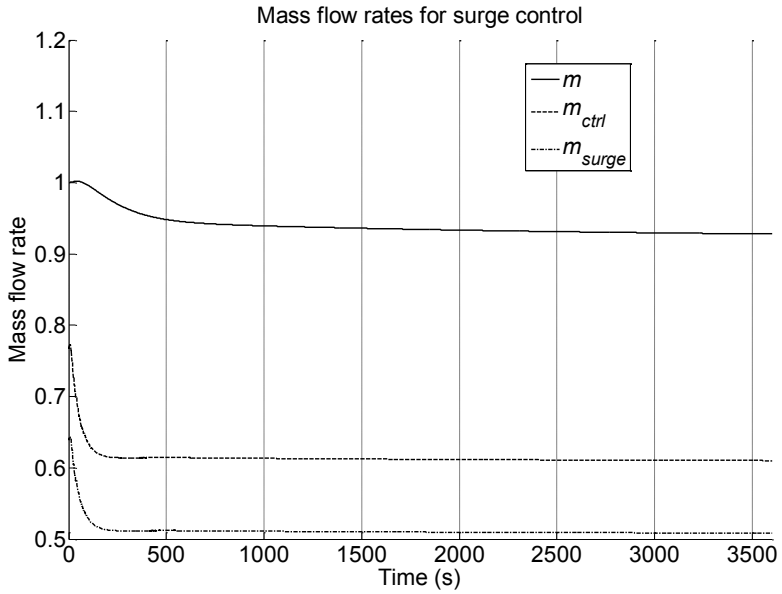


Figure 5-13. Compressor mass flow rates during disturbance scenario 6

5.5.2.4 Inlet pressure of the system

Table 5-12 reports the values of the performance indicators when the inlet pressure of the system changes over time. The scenarios can be grouped under two categories. During scenarios 8 and 9 p_{in} decreases while during scenarios 10 and 11 p_{in} increases.

In scenarios 8 and 9 ISE_p increases with the increasing of the magnitude of the disturbance. M is equal to 0 and E increases. This means that the compressor inlet flow rate is increasing. This is

because the decrease of the inlet pressure would cause a decrease of the compressor outlet pressure during open loop operation. Therefore the MPC controller increases the torque of the driver in order to increase the rotational shaft speed and bring back p to its set point.

Also in scenarios 10 and 11 ISE_p increases with the increasing of the magnitude of the disturbance. However in these cases M increases and E decreases. This is because when p_{in} increases p increases too and the MPC controller reduces the driver torque. However this action reduces the mass flow rate as well and therefore the MPC controller opens the antisurge valve. The flow rate through the machine is still below the design point value and therefore the power consumption decreases.

Scenario 9 has been selected for illustrating the action of the controller. Figure 5-14 shows the manipulated variables over time. The driver torque increases however also in this case it overshoots while the antisurge valve is closed. Therefore the compressor outlet pressure is still above its set point after one hour of operation, as represented in Figure 5-15. Figure 5-16 represents the mass flow rates of the compressor. The action of the MPC controller increases p_{01} and therefore m_{surge} increases over time.

Table 5-12. Disturbance scenarios for the inlet pressure of the system

Disturbance scenario	8	9	10	11
Sign and magnitude (%)	-2.81	-1.28	15.74	32.94
ISE_p(bar^{2}s)	1882.83	366.44	17677.30	65384.30
M (-)	0.00	0.00	2.24	5.24
E (-)	1.12	1.05	0.75	0.56

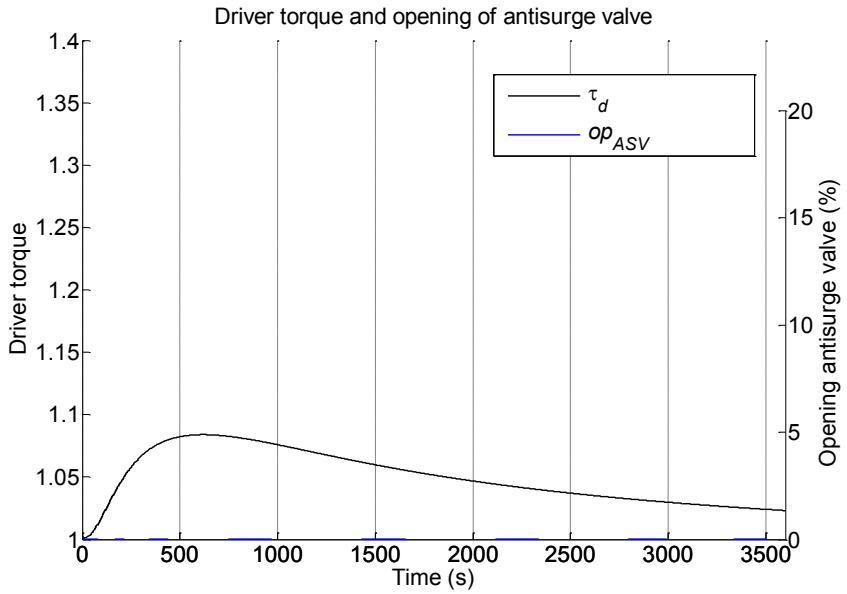


Figure 5-14. Manipulated variables during disturbance scenario 9

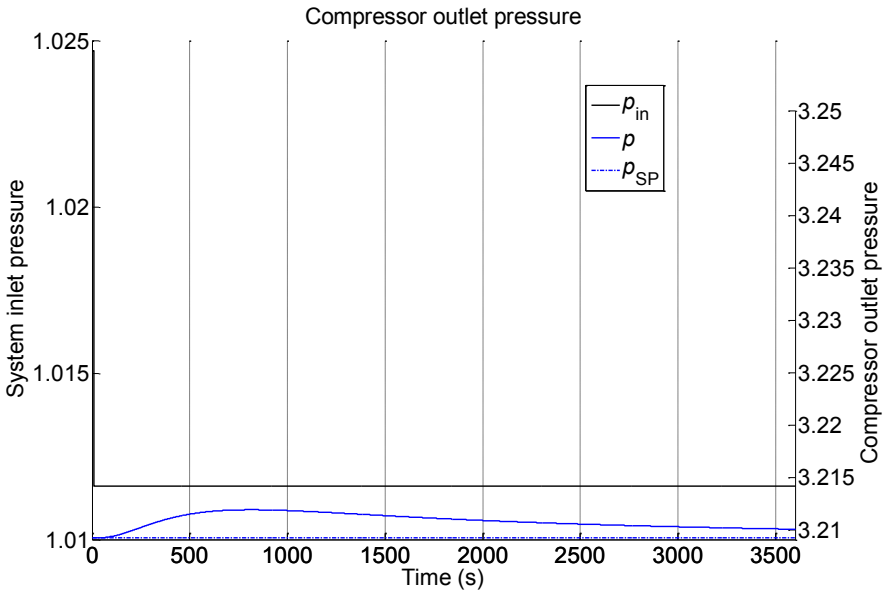


Figure 5-15. Compressor outlet pressure during disturbance scenario 9

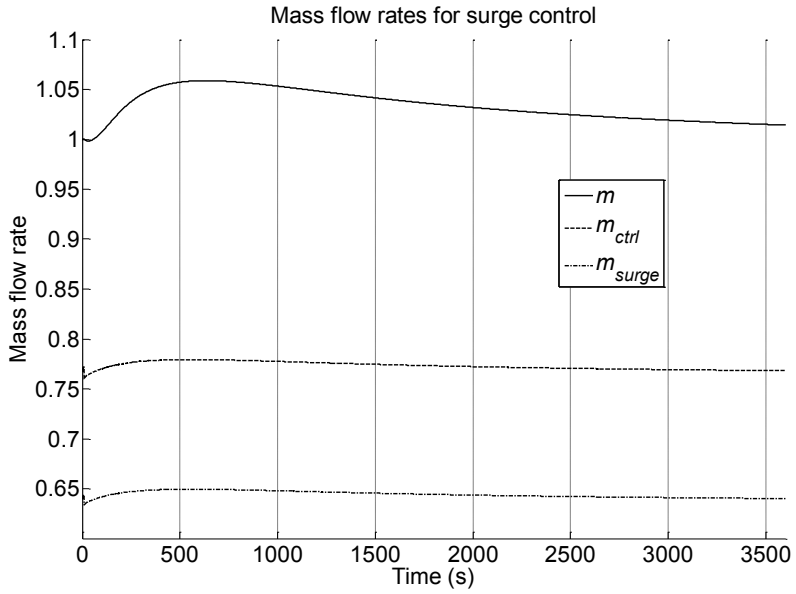


Figure 5-16. Compressor mass flow rates during disturbance scenario 9

5.5.2.5 Outlet pressure of the system

Table 5-13 reports the values of the performance indicators when the outlet pressure of the system changes over time. The scenarios can be grouped under two categories. During scenarios 12 and 13 p_{out} decreases while during scenarios 14 and 15 p_{out} increases.

In scenarios 12 and 13 ISE_p increases with the increasing of the magnitude of the disturbance. M is equal to 0 and E increases. This means that the compressor inlet flow rate is increasing. This is

because the decrease of the system outlet pressure p_{out} would cause a decrease of the compressor outlet pressure p during open loop operation. Therefore the MPC controller increases the torque of the driver in order to increase the rotational shaft speed and bring p back to its set point.

Also in scenarios 14 and 15 ISE_p increases with the increasing of the magnitude of the disturbance. However in these cases M increases and E decreases. This is because the action of the controller on the driver torque causes the reduction of the mass flow rate and therefore the opening of the antisurge valve. The flow rate through the machine is still below the design point value and therefore the power consumption decreases.

Scenario 13 has been selected for illustrating the action of the controller. Figure 5-17 shows the manipulated variables over time. The driver torque increases while the antisurge valve is closed. The reason why the torque does not increase anymore is because the rotational shaft speed is at its maximum value and therefore p cannot achieve its set point, as represented in Figure 5-18. Figure 5-19 represents the mass flow rates for surge control. Also in this scenario m increases because the torque increases.

Table 5-13. Disturbance scenarios for the outlet pressure of the system

Disturbance scenario	12	13	14	15
Sign and magnitude (%)	-0.44	-0.11	0.11	0.93
ISE_p (bar^{2}s)	6070.88	428.45	23.02	8191.95
M (-)	0.00	0.00	0.68	8.60
E (-)	1.16	1.04	0.99	0.89

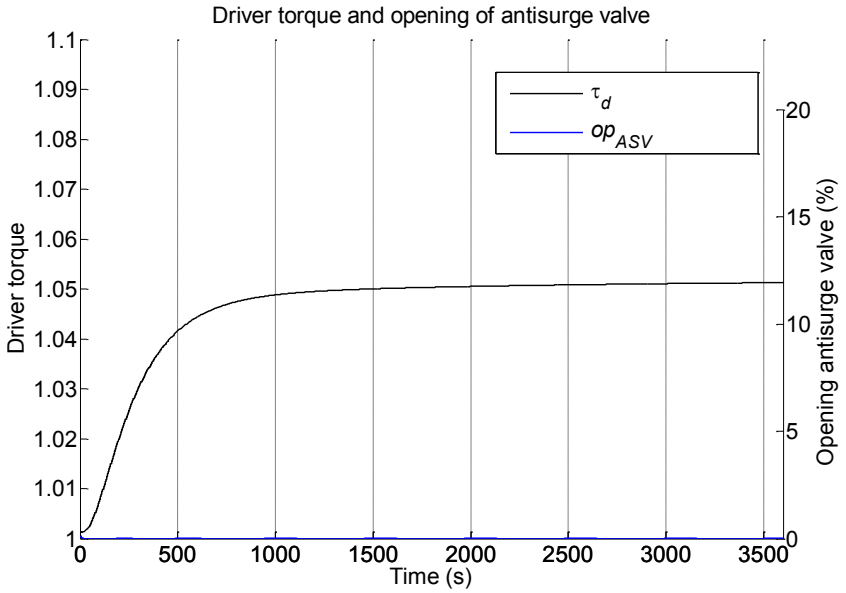


Figure 5-17. Manipulated variables during disturbance scenario 13

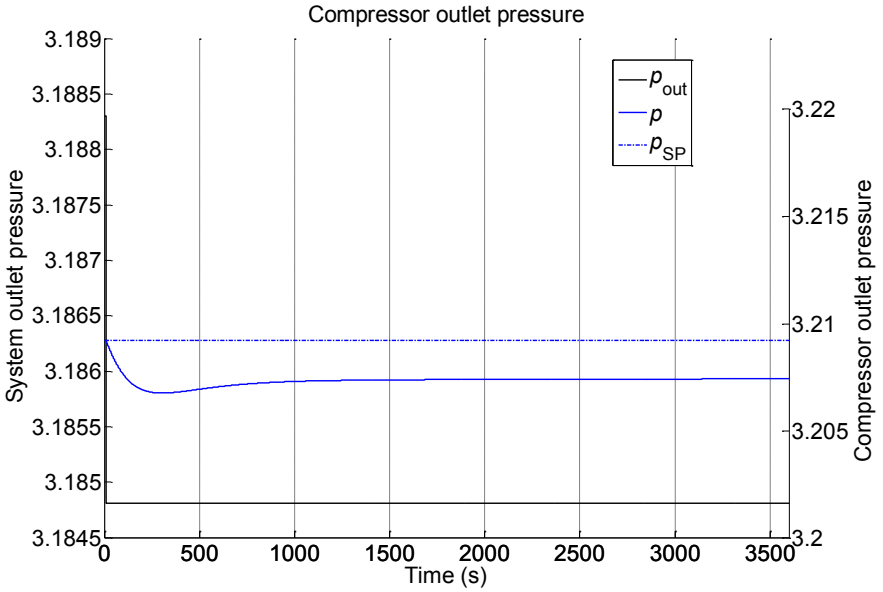


Figure 5-18. Compressor outlet pressure during disturbance scenario 13

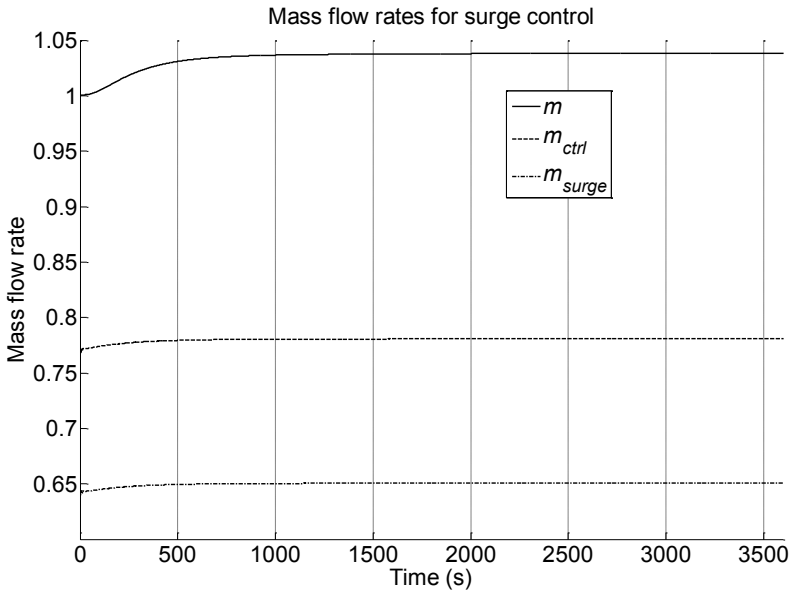


Figure 5-19. Compressor mass flow rates during disturbance scenario 13

5.5.2.6 Pressure set point

Table 5-14 reports the values of the performance indicators when the pressure set point changes over time. Also in this case the scenarios can be grouped under two categories. During scenarios 16 and 17 p_{SP} decreases while during scenarios 18 and 19 p_{SP} increases.

In scenarios 16 and 17 ISE_p increases with the increasing of the magnitude of the disturbance. At the same time M increases while E increases. This is because the action of the controller on the

driver torque in order to reduce p causes the reduction of the mass flow rate and therefore the opening of the antisurge valve. The flow rate through the machine is still below the design point value and therefore the power consumption decreases.

Also in scenarios 18 and 19 ISE_p increases with the increasing of the magnitude of the disturbance. In these two cases M is equal to 0 while E increases. The reason is that the MPC controller is increasing the driver torque in order to increase the compressor outlet pressure. This causes the increase of the compressor mass flow rate. The antisurge valve does not open for two reasons:

- There is no need to increase the inlet flow rate as it is already above its design point
- The opening of the antisurge valve would decrease the value of p and therefore would not be beneficial in terms of pressure control.

Scenario 17 has been selected for illustrating the action of the controller. Figure 5-20 shows the manipulated variables over time. The driver torque decreases while the antisurge valve opens. The compressor outlet pressure p is still above its set point, as represented in Figure 5-21. The reason is that the new set point is very close to the outlet pressure of the compression system. The compressor inlet mass flow rate decreases because N decreases and m_{surge} increases because p_{01} increases, due to the opening of the antisurge valve.

Table 5-14. Disturbance scenarios for the pressure set point of the system

Disturbance scenario	16	17	18	19
Sign and magnitude (%)	-1.09	-0.54	0.11	0.38
ISE_p (bar^{2}s)	8237.43	1178.81	415.16	4339.81
M (-)	9.18	4.14	0.00	0.00
E (-)	0.87	0.93	1.04	1.16

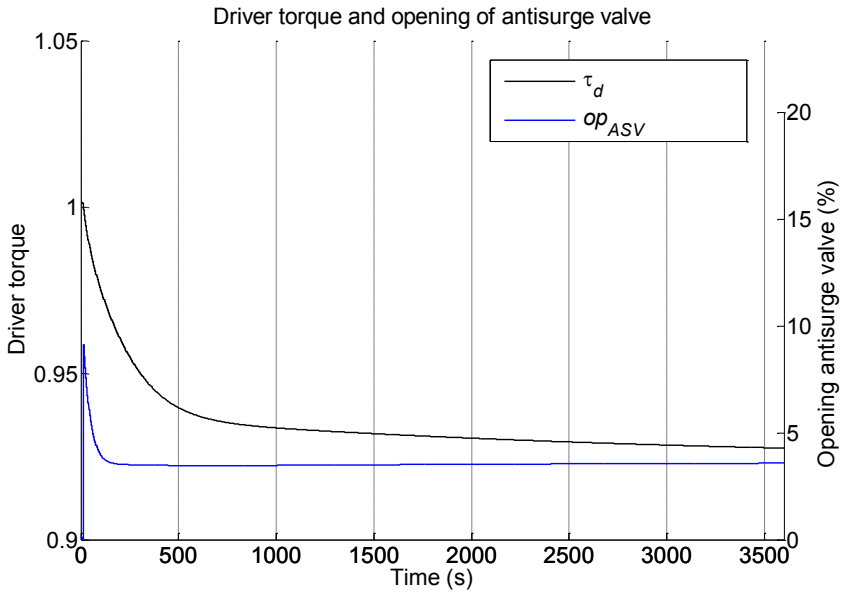


Figure 5-20. Manipulated variables during disturbance scenario 17

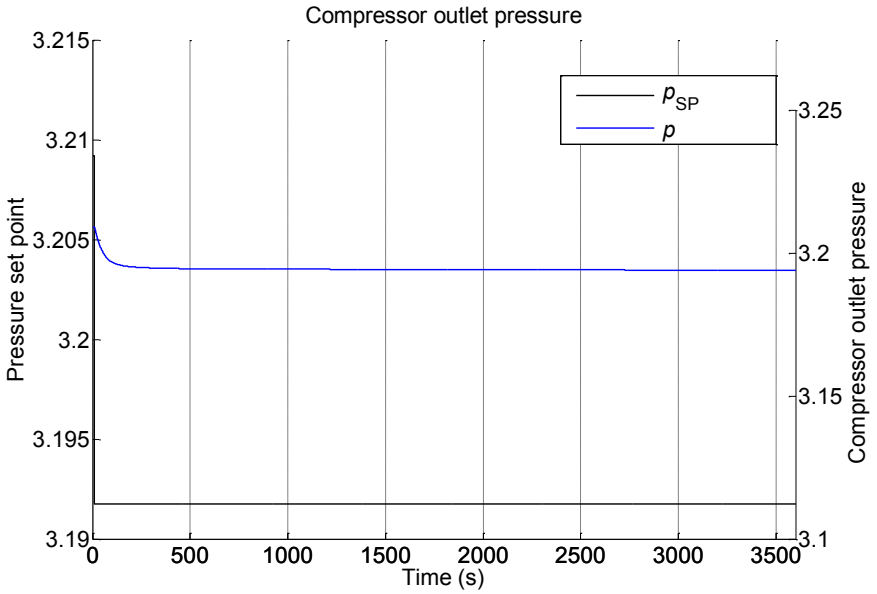


Figure 5-21. Compressor outlet pressure during disturbance scenario 17

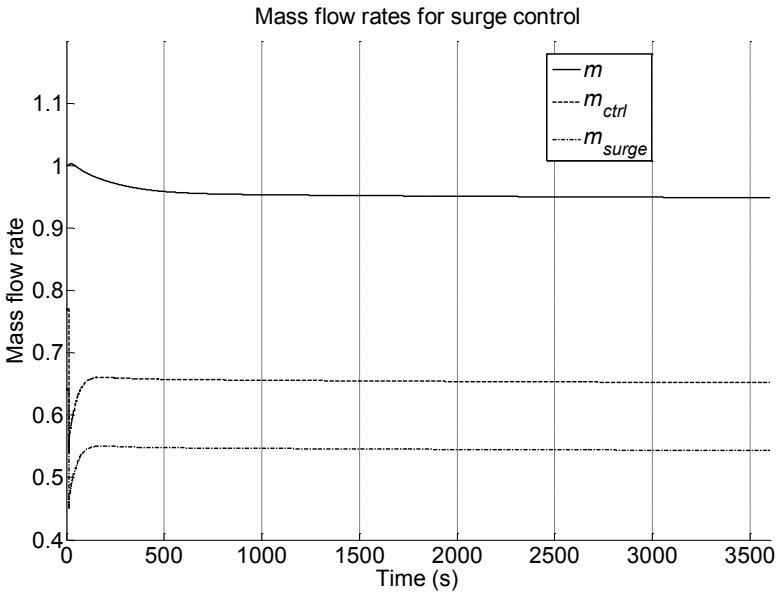


Figure 5-22. Compressor mass flow rates during disturbance scenario 17

5.5.2.7 Saturation of the manipulated variables

A further disturbance scenario has been simulated in order to analyse the response of the system when the rotational shaft speed saturates. The results of the scenario have been summarised in Table 5-15. The opening of the inlet valve has been changed from fully opened position 100% to 20% opening. It is interesting to notice that the value of ISE_p is quite high while the antisurge valve opens and E decreases. More insight on this case can be taken from the following graphs. Figure

5-23 represents the manipulated variables over time. The driver torque increases until a maximum value while the antisurge valve oscillates over time. Figure 5-25 shows also the rotational shaft speed, which is equal to its maximum limit value. The saturation of the driver does not allow to control the compressor outlet pressure, which remains below its set point, as represented in Figure 5-26.

The reason for the oscillation of the antisurge valve can be understood by looking at Figure 5-27. In this disturbance scenario m and m_{ctrl} cross each other over time and therefore cause the abrupt opening and closing of the antisurge valve. The closing of the inlet valve pushes the MPC controller to increase the driver torque until the maximum allowable rotational shaft speed. However this increase is not sufficient to achieve the pressure set point and therefore both p and m are below their design point values. When m and m_{ctrl} crosses each other the antisurge valve opens. However this action causes the further reduction of p and therefore the antisurge valve closes again. This oscillatory behaviour is due to the fact that when the driver saturates, the MPC is unable to control two variables using only a single manipulated variable.

It is interesting to notice this is the only case in which the MPC controller has allowed m to approach m_{ctrl}. In fact in all the other cases it has preferred to reduce the pressure controller performance while keeping the flow rate away from the surge region. This is due to the tuning of the MPC controller. The controller is still giving priority to the control of pressure over the control of flow rate. Following this specific disturbance, the controller can manipulate only one variable, the antisurge valve, while the other one, the driver torque, is saturated. Therefore the MPC is programmed to prioritise the control of pressure even if this variable is always below its set point.

Table 5-15. Disturbance scenario 20: saturation of the rotational shaft speed

Disturbance scenario	**20**
Disturbance variable	op_{in}
Sign and magnitude (%)	-80
ISE_p (bar^{2}s)	17375.39
M (-)	0.51
E (-)	0.83

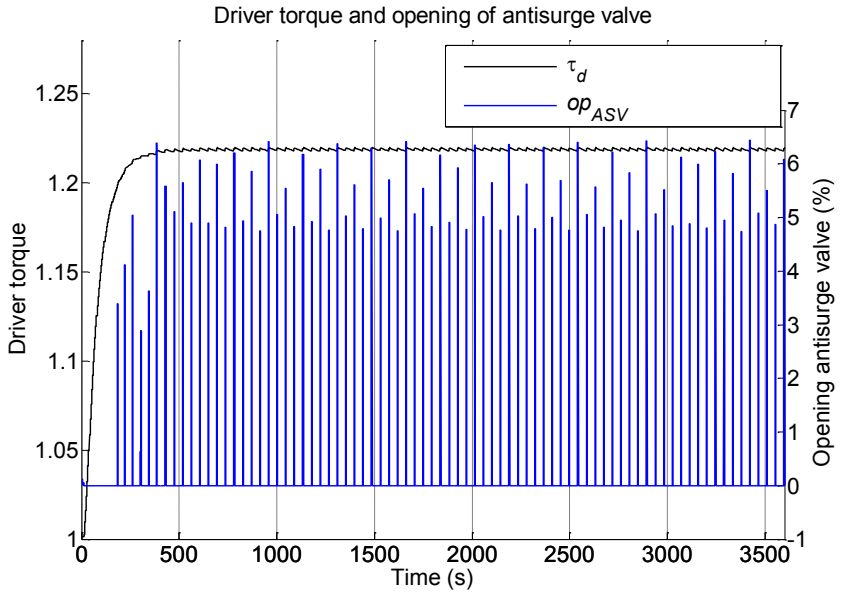


Figure 5-23. Manipulated variables during disturbance scenario 20

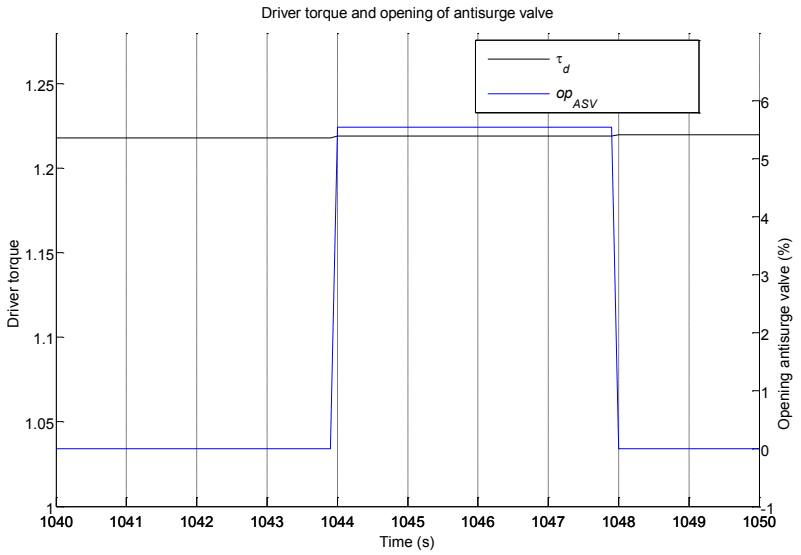


Figure 5-24. Manipulated variables during disturbance scenario 20 (zoomed view)

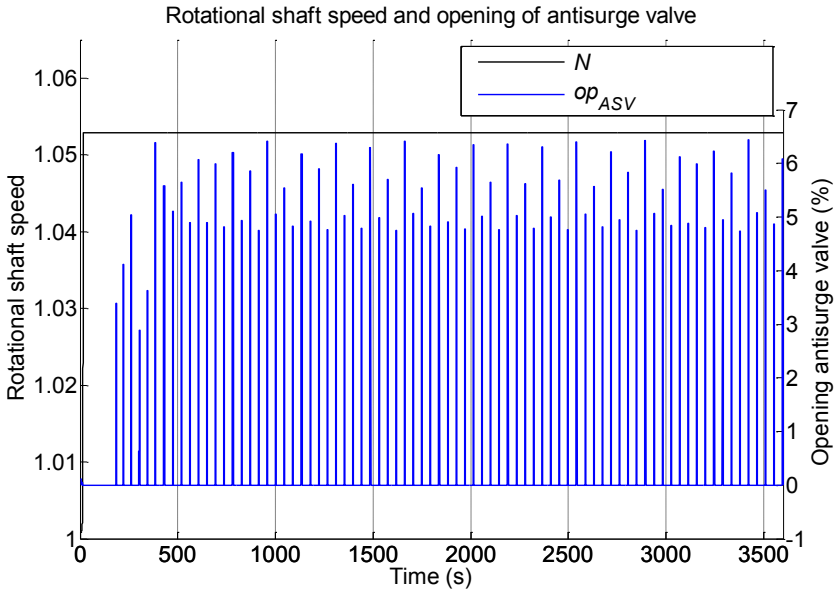


Figure 5-25. Rotational shaft speed and opening of antisurge valve during disturbance scenario 20

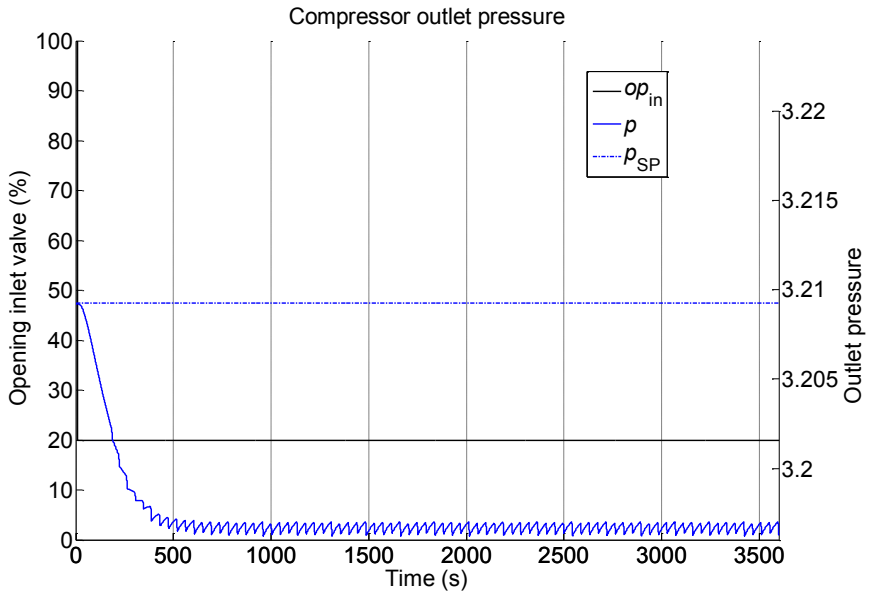


Figure 5-26. Compressor outlet pressure during disturbance scenario 20

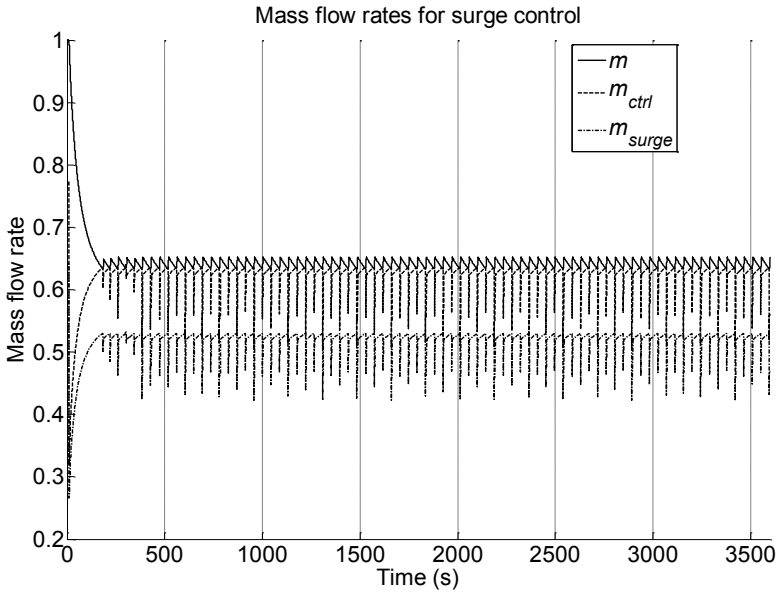


Figure 5-27. Compressor mass flow rates during disturbance scenario 20

5.5.2.8 Constraint on compressor outlet temperature

In the MPC formulation a constraint has been imposed on the value of the compressor outlet temperature T_{02}. This temperature point is located at the exit of the compressor and it is the hottest point due to the process of compression. Therefore this variable has been identified as critical when hot gas is recycled from the outlet of the compressor to the inlet of the compressor. An upper limit has been imposed in order to protect the compressor and to guarantee its integrity. A margin of 20% has been selected, therefore:

$$T_{02,max} = 1.2T_{02,ss} \tag{5-19}$$

where $T_{02,ss}$ is the value of the compressor outlet temperature during steady state operation at the design point.

In order to analyse the effect of the gas recycle on this variable, among the previously presented disturbance scenarios four scenarios have been selected and analysed. These scenarios have the highest amount of gas recycled in the time interval analysed and they have been summarised in Table 5-16.

Table 5-16. Disturbance scenarios with highest recycle flow rate

Disturbance scenario	**7**	**11**	**15**	**16**
Disturbance variable	op_{out}	p_{in}	p_{out}	p_{sp}
M (-)	8.50	5.24	8.60	9.18

For each of these cases, in the following figures the power consumption of the compressor P_m, the compressor outlet temperature T_{02} and the maximum outlet temperature $T_{02,max}$ have been reported. The figures report the power consumption on the left vertical axis and the gas

temperature on the right vertical axis. As it is possible to see from the figures, even if the recycle flow rate was high, the outlet temperature is always:

- Lower than its maximum limit value
- Decreasing over time.

This is because when gas is recycled back from the outlet of the compressor to the inlet of the compressor, the power consumption of the machine decreases. The value of the power consumption mainly depends on the compressor mass flow rate and on the inlet and outlet compressor temperatures. T_{01} increases because the fresh gas having temperature T_{in} mixes with the recycled gas having temperature T_{02}. However at the same time the MPC controller is providing to the system a lower value of the driver torque in order to reduce p. Therefore the provided power is decreasing and T_{02} decreases as well. Nevertheless it is important to guarantee that the gas temperature does not exceed its upper limit and therefore this constraint has been maintained in the MPC formulation.

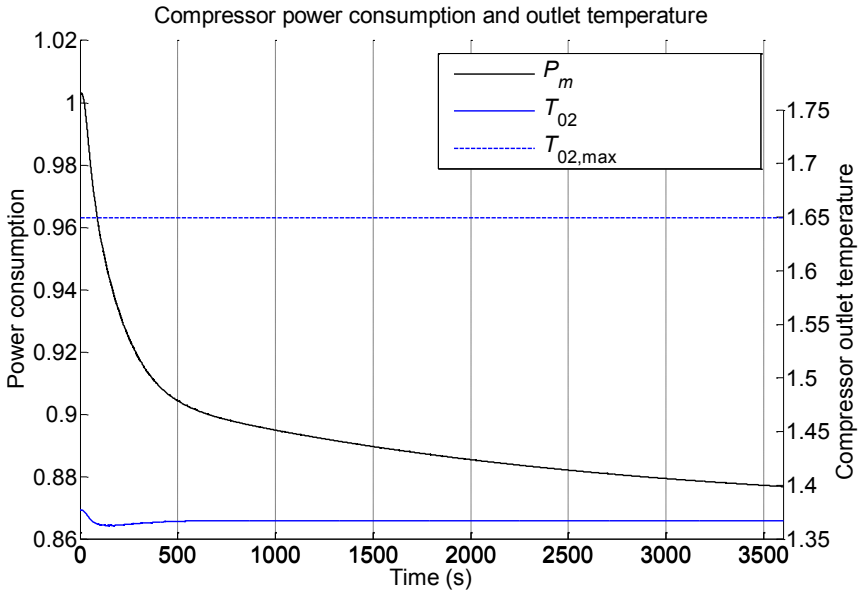


Figure 5-28. Compressor power consumption and outlet temperature during disturbance scenario 7

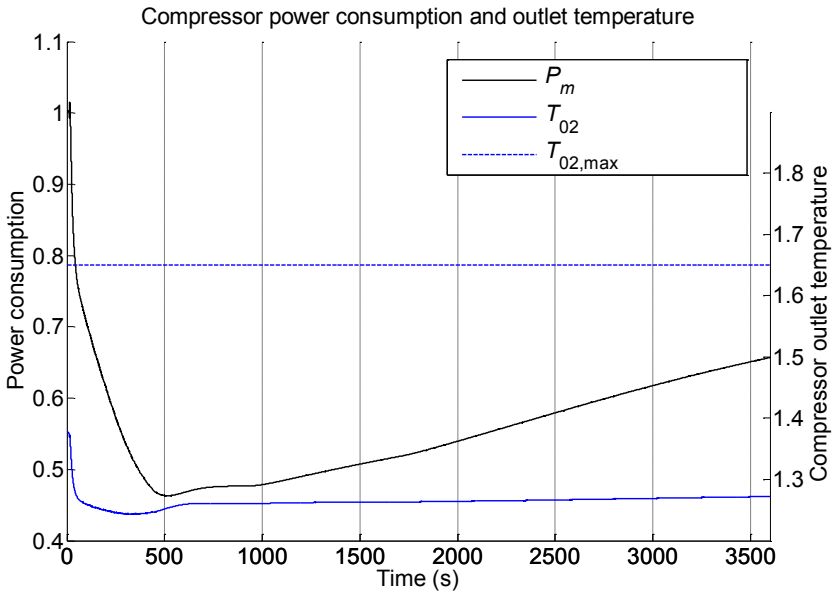


Figure 5-29. Compressor power consumption and outlet temperature during disturbance scenario 11

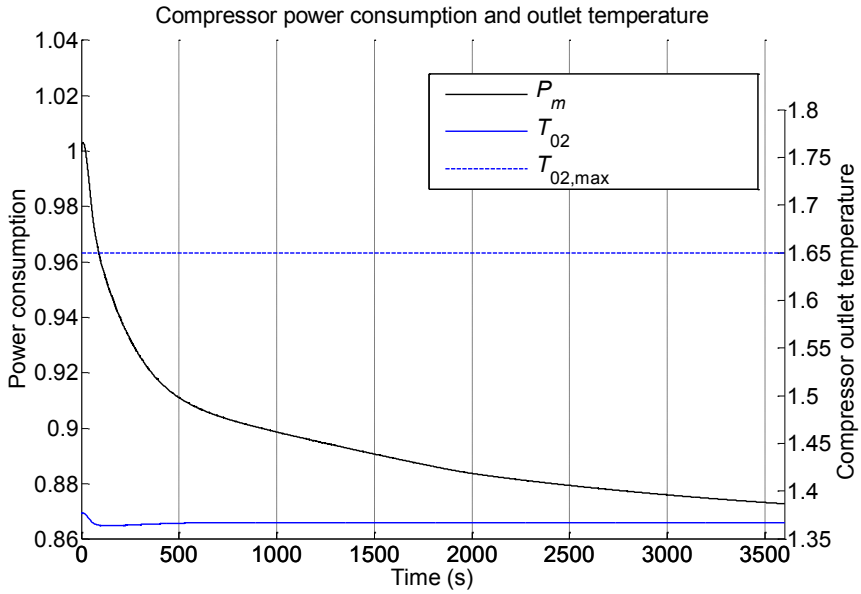


Figure 5-30. Compressor power consumption and outlet temperature during disturbance scenario 15

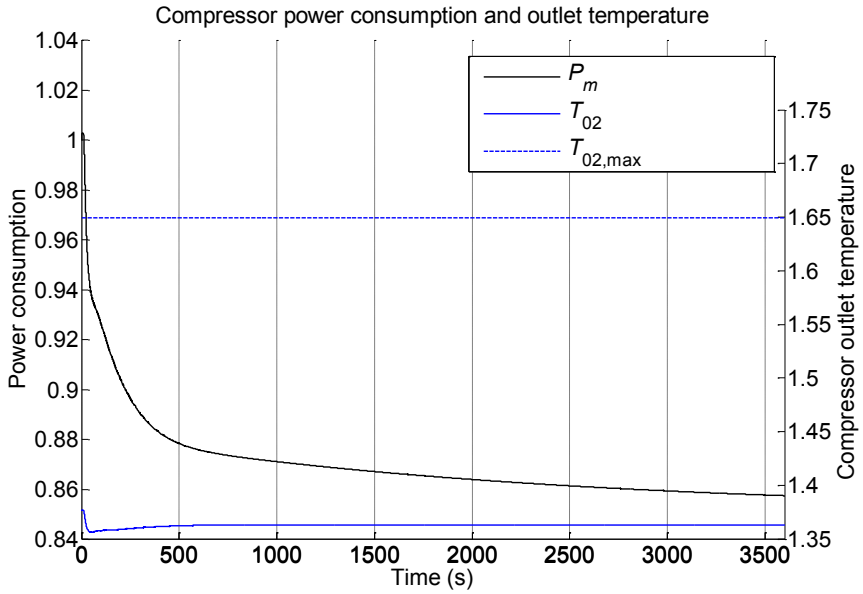


Figure 5-31. Compressor power consumption and outlet temperature during disturbance scenario 16

5.5.2.9 Summary

In this section of the chapter the response of the MPC controller has been analysed during various disturbance scenarios. The open loop response of the system has been initially analysed in order to understand the effect of boundary disturbances on the compression system. Then the response of the closed loop system has been analysed by means of performance parameters and graphical representation of manipulated and controlled variables.

In all the presented cases, the MPC controller is programmed to control both pressure p and flow rate m at the same time. Therefore it acts on the driver torque in order to maintain the pressure set point. Moreover it opens the antisurge valve when the compressor inlet mass flow rate decreases. This action helps the control of pressure as the opening of the antisurge valve reduces the compressor outlet pressure p. Moreover when the controller recirculate gas the power consumption, expressed by the parameter E, is always lower than the design point power consumption.

The action of the controller on the driver torque causes overshoot and therefore the system is slow to achieve its pressure set point. At the same time the control constraints have never been violated.

5.5.3 Comparison between PI and MPC responses

In this section of the chapter the response of the MPC controller is compared with the response of a traditional PI controller during the same disturbance scenario. The interaction between control loops in a PI controller has already been demonstrated in Chapter 4. Here other examples are reported and then compared with the MPC response.

5.5.3.1 PI tuning

The tuning parameters of the PI controller have been reported in Table 4-3. Also in this case the slave controller has been tuned in order to have a faster response than the master controller in the cascade control configuration. The response of the two control loops to a positive step change of the pressure set point has been represented in Figure 5-32. The output of the controller (OP) is represented on the left vertical axis while the controlled variable (PV) and its set point (SP) are represented on the right vertical axis. For the master controller OP is the set point of the slave controller while PV is the compressor outlet pressure p. For the slave controller OP is the value of the driver torque while PV is the rotational shaft speed of the compressor. The transfer function of the controller including tuning parameters P and I was presented in Chapter 3 and here repeated for convenience:

$$g_c(s) = K_c\left(1 + \frac{1}{\tau_i s} + \frac{T_d s}{\frac{\tau_d}{N_f}s + 1}\right) \quad \textbf{(3-33)}$$

$$P = K_c \quad \textbf{(3-55)}$$

$$I = \frac{K_c}{\tau_i} \quad \textbf{(3-56)}$$

Table 5-17. Tuning parameters for slave and master controllers

	Slave Controller	Master Controller PI
P	0.05	2488.76
I	0.06	22.64
Rise time (s)	3.08	142.00
Settling time (s)	77.80	472.00
Overshoot (%)	0.08	0.11
Peak (-)	1.08	1.11

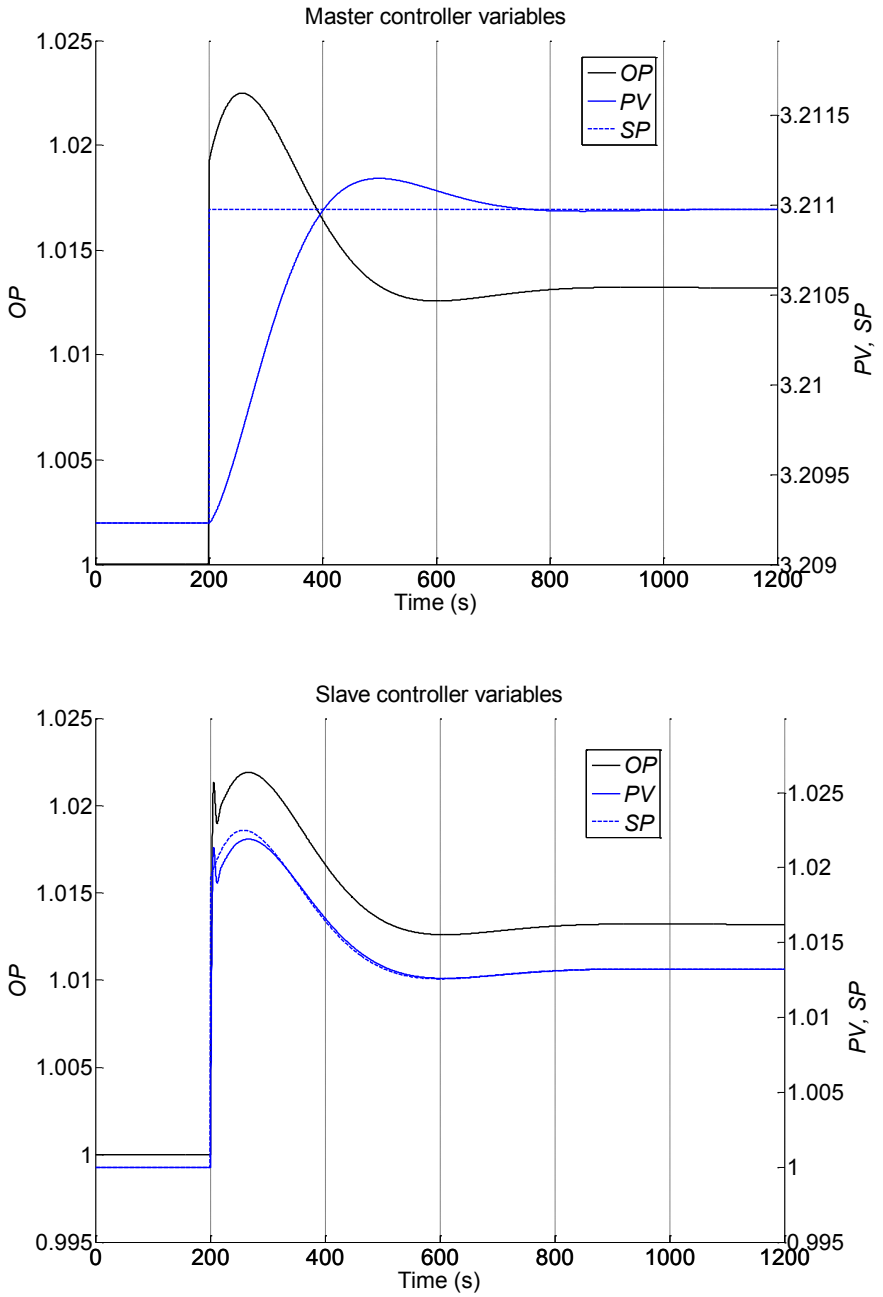


Figure 5-32. Response of the pressure control system to a set point change for PI control

5.5.3.2 Inlet valve disturbance scenarios

Various disturbance scenarios have been tested in order to compare PI response and MPC response. Table 5-18 summarises the results of the simulations. For all the disturbance scenarios, ISE_p increases with the increasing of the disturbance magnitudes. M is equal to 0 for the first three cases and then starts increasing as the antisurge valve opens. E decreases because m decreases over time due to the increase of the driver torque.

The most interesting scenarios involve gas recycling and therefore are scenario 24 and scenario 25. Scenario 24 has also been reported in the following figures. In both cases, the rotational shaft speed reaches its upper limit and therefore the compressor outlet pressure cannot achieve its set point.

Figure 5-33 represents the opening of the inlet valve on the left vertical axis and the gas pressure on the right vertical axis. For both controllers the driver has reached its maximum limit and therefore the pressure cannot achieve its set point. The mass flow rates are represented in Figure 5-34. When the inlet mass flow rate m and the control flow rate m_{ctrl} cross each other, the response of the PI controller starts oscillating. This is because when the antisurge valve opens, the inlet temperature of the compressor T_{01} increases. Therefore m_{surge} decreases and m_{ctrl} become smaller than m. Therefore the antisurge valve closes. However at this point p_{01} decreases again, m_{surge} increases and therefore m becomes smaller than m_{ctrl}. This cyclic behaviour is represented in Figure 5-26 and Figure 5-27.

Table 5-18. Comparison between PI and MPC response during inlet valve disturbance scenarios

Disturbance scenario	21	22	23	24	25
Sign and magnitude (%)	0.00	-40.00	-78.00	-79.00	-82.00
$ISE_{p,PID}$ (bar^{2}s)	0.00	1.14	10291	13938	90492
$ISE_{p,MPC}$ (bar^{2}s)	0.32	3302.07	10201	13057	41575
M_{PID} (-)	0.00	0.00	0.00	0.11	10.91
M_{MPC} (-)	0.02	0.00	0.00	0.03	3.58
E_{PID} (-)	1.00	1.03	0.88	0.84	0.78
E_{MPC} (-)	1.00	1.18	0.89	0.84	0.79

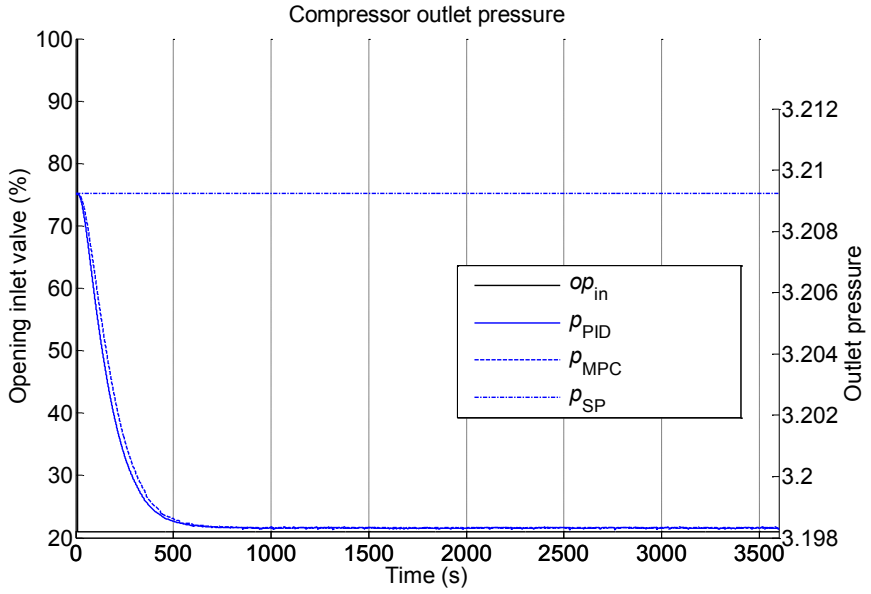


Figure 5-33. Compressor outlet pressure during disturbance scenario 24

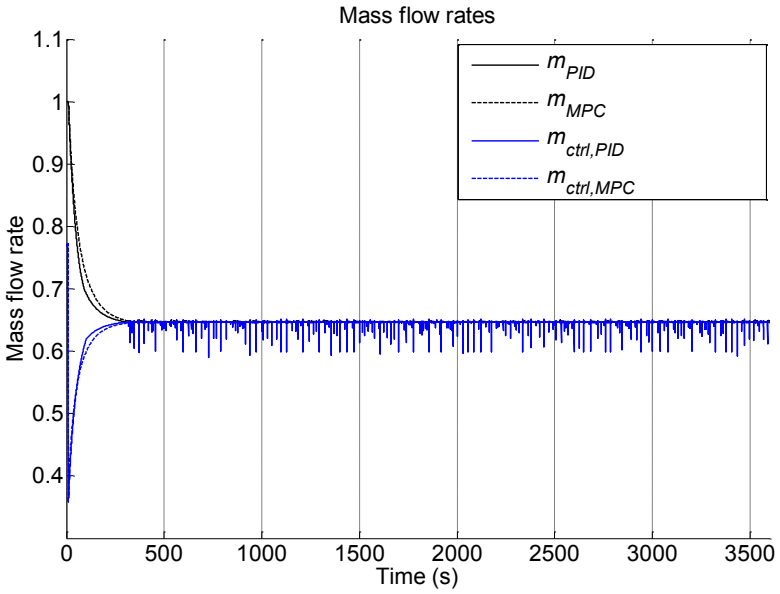


Figure 5-34. Compressor mass flow rates during disturbance scenario 24

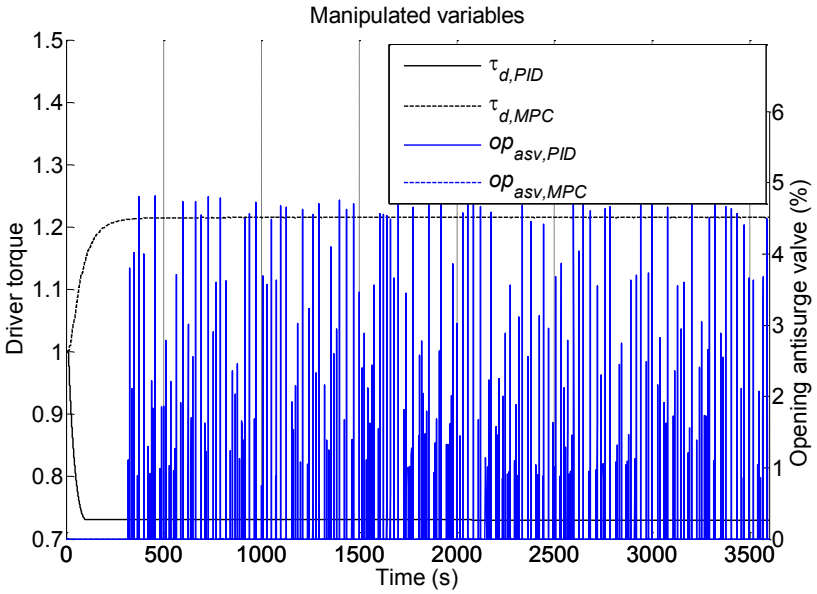


Figure 5-35. Manipulated variables during disturbance scenario 24

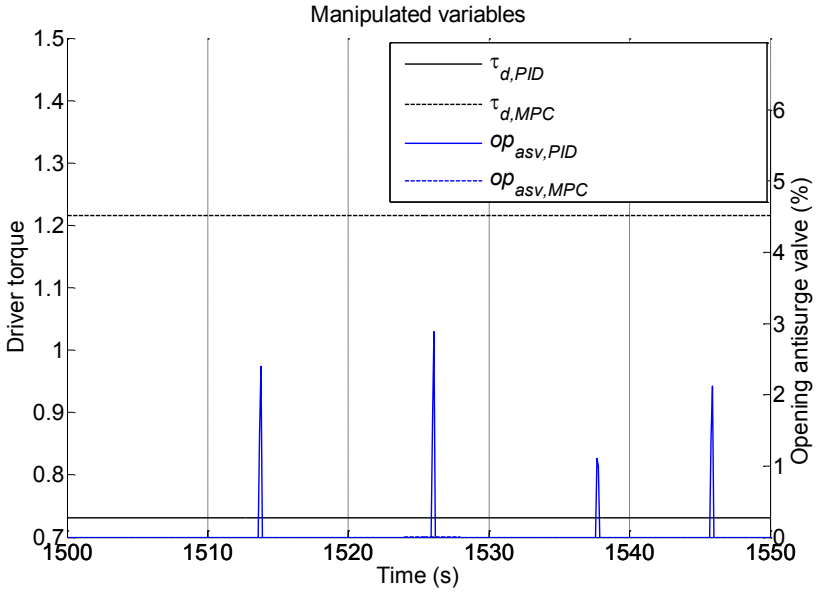


Figure 5-36. Manipulated variables during disturbance scenario 24 (zoomed view)

5.5.3.3 Outlet valve disturbance scenarios

Table 5-19 summarises the results of the simulations for disturbance scenarios involving the outlet valve of the system. For all the disturbance scenarios, ISE_p increases with the increasing of the disturbance magnitude. M is initially equal to 0 and then starts increasing as the antisurge valve opens. E decreases because m decreases over time due to the decrease of the driver torque. For scenarios 27 and 28 the MPC controller presents bigger ISE_p, higher M and also higher E. However during scenarios 29 and 30 the ISE_p of the MPC controller is lower than the ISE_p of the PI controller. At the same time for the last scenario the PI controller recycles more gas however it consumes the same energy as it does in scenario 29. This is because the oscillation of the response of the PI controller decreases its pressure control performance. This oscillation can be identified by looking at the pressure response in Figure 5-37 and flow rate response in Figure 5-38. Figure 5-39 represents the manipulated variables of the system, with the driver torque on the left vertical axis and the opening of the antisurge valve on the right vertical axis. When the antisurge valve opens the torque increases until m becomes bigger than m_{ctrl}. At that point the antisurge valve closes, the compressor outlet pressure increases and the torque starts decreasing again. Therefore this causes the reduction on the flow rate until it becomes smaller than the control flow rate and the antisurge valve opens again. Also during this disturbance, the antisurge valve is oscillating because of the effect of the compressor inlet temperature T_{01} on the value of m_{surge}.

Table 5-19. Comparison between PI and MPC response during out valve disturbances

Disturbance scenario	26	27	28	29	30
Sign and magnitude (%)	0.00	-10.00	-20.00	-25.00	-29.00
$ISE_{p,PID}$ (bar^{2}s)	0.00	13.16	62.13	376.07	2739.42
$ISE_{p,MPC}$ (bar^{2}s)	0.32	33.24	159.59	265.33	373.56
M_{PID} (-)	0.00	0.00	0.00	0.97	7.85
M_{MPC} (-)	0.02	0.80	1.59	2.00	2.32
E_{PID} (-)	1.00	0.90	0.80	0.75	0.75
E_{MPC} (-)	1.00	0.99	0.98	0.97	0.96

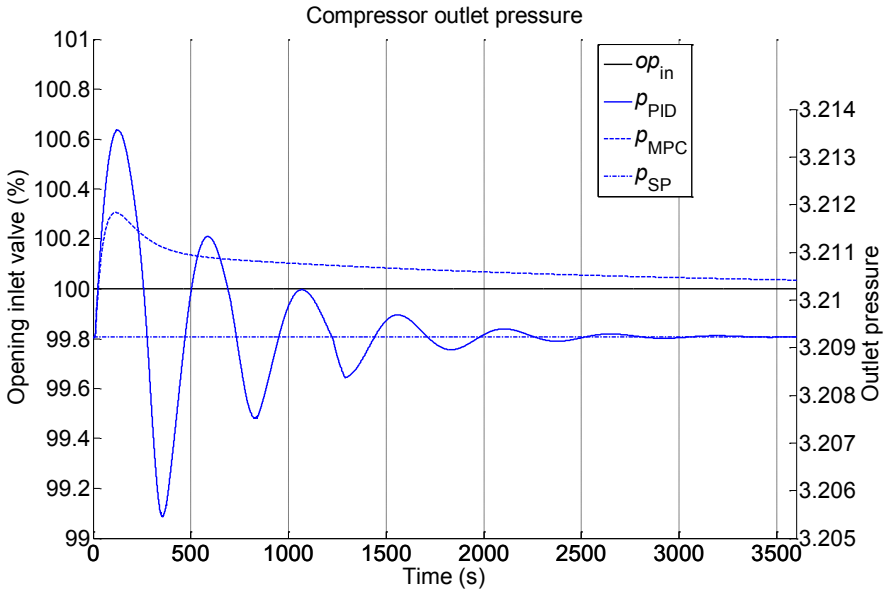


Figure 5-37. Compressor outlet pressure during disturbance scenario 29

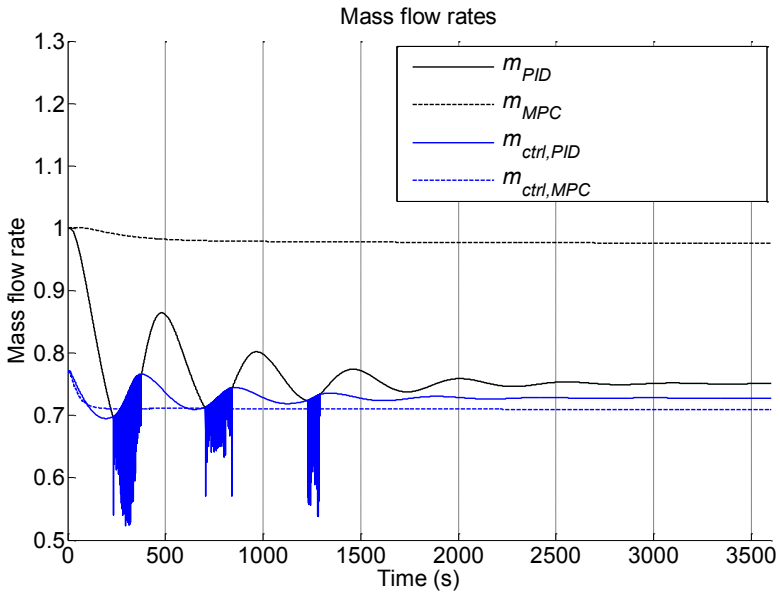


Figure 5-38. Compressor mass flow rates during disturbance scenario 29

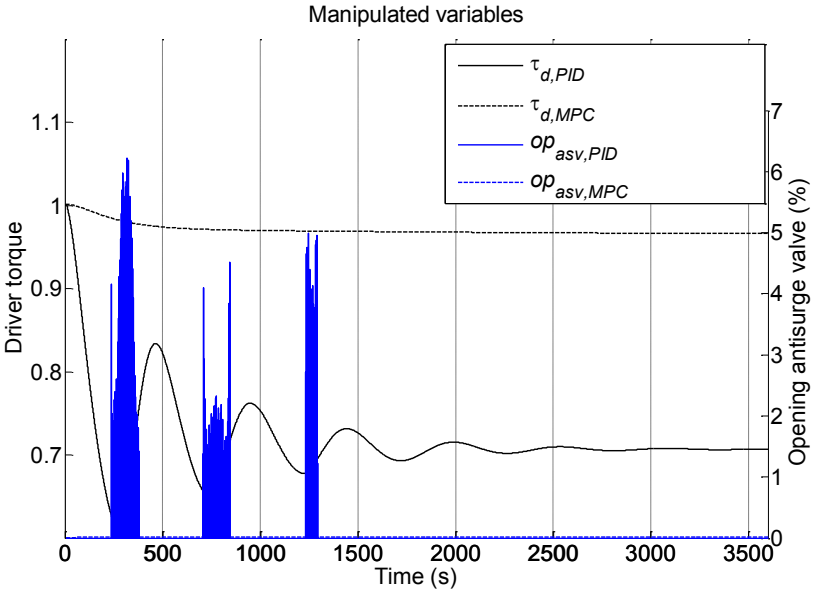


Figure 5-39. Manipulated variables during disturbance scenario 29

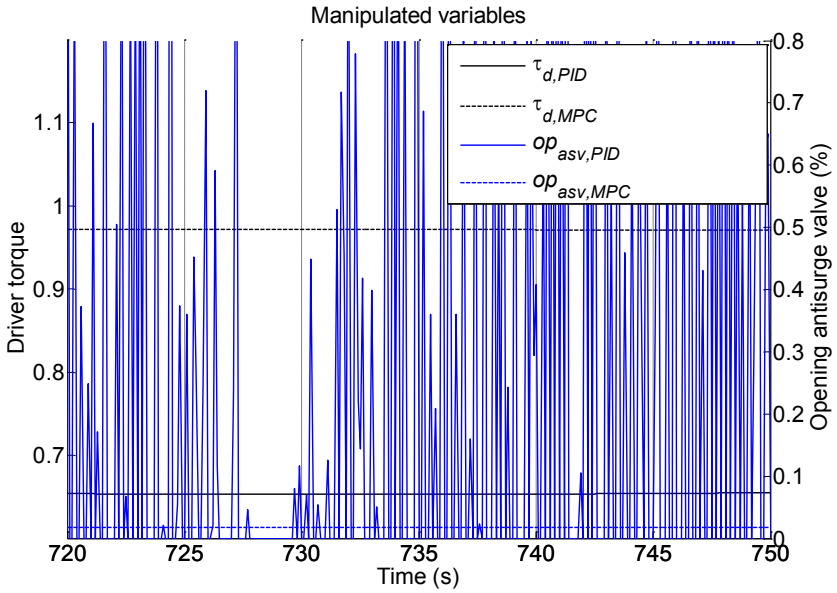


Figure 5-40. Manipulated variables during disturbance scenario 29 (zoomed view)

5.5.3.4 Summary

In this section of the chapter a further disturbance scenario has been simulated in order to compare the response of the PI controller with the response of the MPC controller. The results have demonstrated that the MPC controller can deal with a strong boundary disturbance while the PI controller response oscillates instead. When the system is controlled by the PI controller, the two control loops interact with each other pushing the compressor in opposite direction. When the MPC

is controlling the system, it finds a compromise between pressure and flow rate control and therefore avoid the oscillation of the compression system.

Moreover the MPC controller is able to deal with the control of the outlet temperature of the compressor. In fact the MPC takes this constraint into account during the solution of the optimization problem. On the other hand, the PI controller is not able to deal with this type of problem in the current configuration. The PI configuration may be modified in order to include a safety interlock system monitoring the outlet temperature of the compressor. However this configuration would not help to deal with the control of pressure and surge as it would trip the compressor when the outlet temperature is above its upper limit. Therefore the MPC controller performs better than the PI controller when controlling a compression system and protecting it from surge and overheating.

5.5.4 Second set of tuning parameters

The analysis of the response of the MPC controller presented in section 5.5.2 has highlighted some important findings. In all the presented cases, the MPC controller tried to control both pressure p and flow rate m at the same time, by manipulating driver torque and antisurge valve. However the action of the controller on the driver torque caused overshoot and therefore the system generally was slow to settle to its pressure set point.

In this section of the chapter another set of tuning parameters is proposed. The set is summarised in Table 5-20. The tuning weights are dimensionless. The weight of the mass flow rate w_m has been changed from 0.08 to 0.72. Increasing the tuning weight of a measured variable means to increase its weight in the objective function. Therefore the controller will try to control this variable better than when its weight was lower. This modification has been proposed in order to see its effect on both pressure and flow rate control.

The same disturbance scenarios proposed before have been employed in order to test the response of the controller under this new tuning set. Then the responses of the controller under tuning set 1 and tuning set 2 have been compared in order to evaluate the effect of the tuning on the response of the closed loop system.

Table 5-20. Tuning parameters for model predictive controller (tuning set 2)

Name	Value
w_{τ_d}	0
wr_{τ_d}	0.1
w_{ASV}	10
wr_{ASV}	0.1
w_p	1
w_m	0.72
w_N	0.0001
$w_{T\tau_{02}}$	0.0001

5.5.4.1 Steady state

Table 5-21 reports the values of the performance indicators during steady state operation at the design point. ISE_p and M are equal to 0 and therefore this means that the compressor outlet pressure is equal to its set point while the antisurge valve is closed. E is equal to 1 as expected for this type of operation.

Table 5-21. Steady state operation at the design point

Scenario	0 – steady state at design point
ISE_p (bar^{2}s)	0.39
M (-)	0.01
E (-)	1.00

5.5.4.2 Closing of the inlet valve

Table 5-22 reports the values of the performance indicators when the position of the inlet valve changes from fully opened position to partially opened position.

In scenarios 2, 3 and 4 ISE_p increases with the increasing of the magnitude of the disturbance. M is always 0 as there is no need for recycle. At the same time E is equal to 1 or slightly above 1 for all the scenarios. The reason is that the controller tries to maintain the compressor inlet flow rate close to its design point by manipulating cautiously the driver torque.

When comparing the response of the MPC under tuning set 1 with its response under tuning set 2, there are some differences. The most important difference is the value of ISE_p, which is smaller under tuning set 2 than under tuning set 1. The reason is that under tuning set 2 the MPC controller maintains m closer to its design point, as explained above. The consequence is that the driver torque response does not overshoot and the pressure stays closer to its set point over time. E is smaller under tuning set 2 than under tuning set 1 and this is because in the former case m is lower over time.

Scenario 3 has been selected for comparing the response of the tuning set 1 ($ts1$) with the response of the tuning set 2 ($ts2$). Figure 5-41 represents the manipulated variables of the system. The left vertical axis represents the driver torque while the right vertical axis represents the opening of the antisurge valve. The response of the second tuning does not overshoot and therefore the compressor outlet pressure stays closer to its set point over time, as represented in Figure 5-42. The mass flow rate changes little over time under $ts2$ (Figure 5-43).

Table 5-22. Disturbance scenarios for the inlet valve of the system

Disturbance scenario	**1**	**2**	**3**	**4**
Sign and magnitude (%)	0.00	-10.00	-20.00	-29.00
ISE_p (bar^{2}s)	0.39	0.34	2.29	7.04
M (-)	0.01	0.00	0.00	0.00
E (-)	1.00	1.00	1.01	1.02

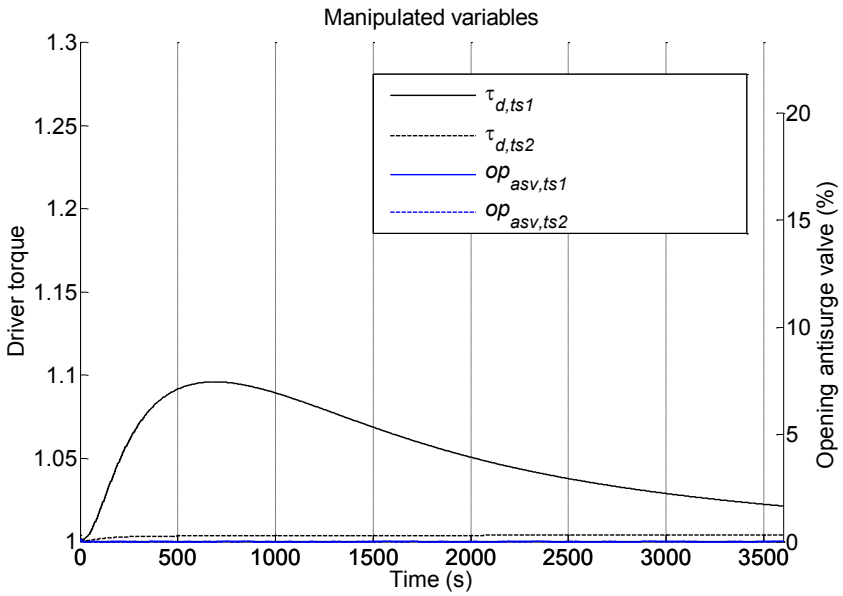


Figure 5-41. Manipulated variables during disturbance scenario 3

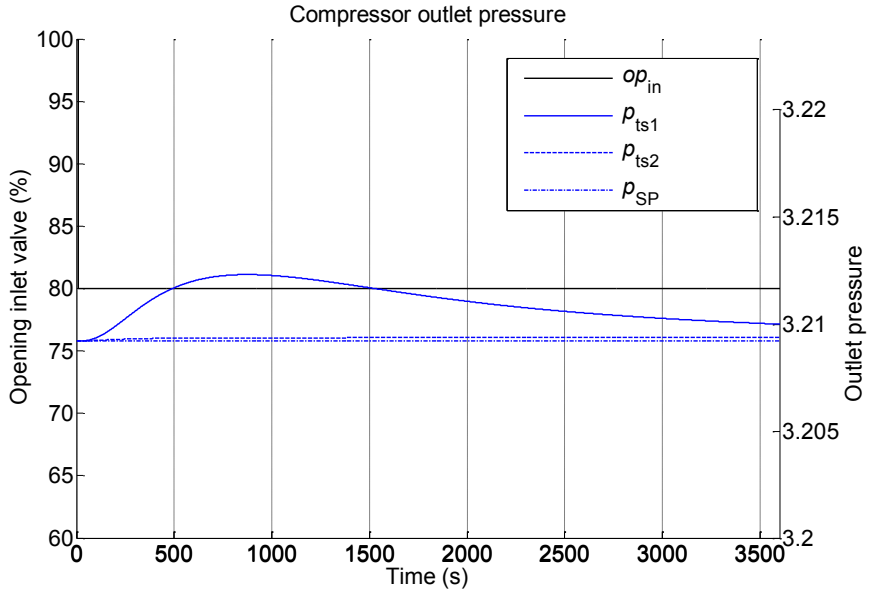


Figure 5-42. Compressor outlet pressure during disturbance scenario 3

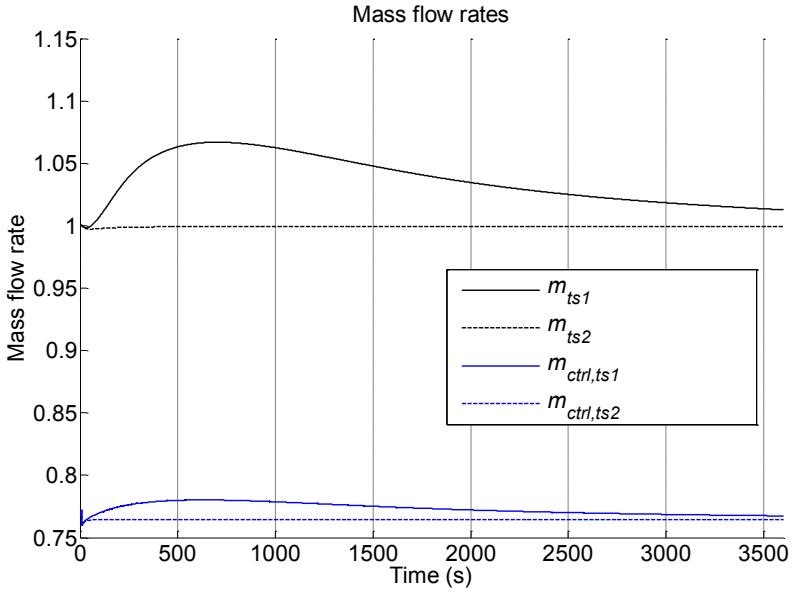


Figure 5-43. Compressor mass flow rates during disturbance scenario 3

5.5.4.3 Closing of the outlet valve

Table 5-23 reports the values of the performance indicators when the position of the outlet valve changes from fully opened position to partially opened position.

Also with this control tuning, in scenarios 5, 6 and 7 ISE_p increases with the increasing of the magnitude of the disturbance. At the same time E decreases and M increases because the mass flow rate of the compressor m is lower than its design point over the time of the simulation.

When comparing the response of the MPC controller under the first tuning with its response under this second tuning, ISE_p, M and E are bigger when the MPC controller is under tuning set 2. The recycle is higher because the MPC controller wants to bring m closer to its reference value. In turn, this action causes the increase of the power consumption and therefore the increase of E with respect to the previous tuning.

Figure 5-44 represents the manipulated variables of scenario 6 over time for the two tuning cases. Under the second tuning set the MPC controller opens more the antisurge valve and has a higher value of the driver torque. The reason is that it wants to keep the controller mass flow rate closer to its design point, as represented in Figure 5-46.

Table 5-23. Disturbance scenarios for the outlet valve of the system

Disturbance scenario	1	5	6	7
Sign and magnitude (%)	0.00	-40.00	-70.00	-95.00
ISE_p (bar^{2}s)	0.39	877.05	3543.64	8248.53
M (-)	0.01	3.56	6.53	9.29
E (-)	1.00	0.98	0.98	0.97

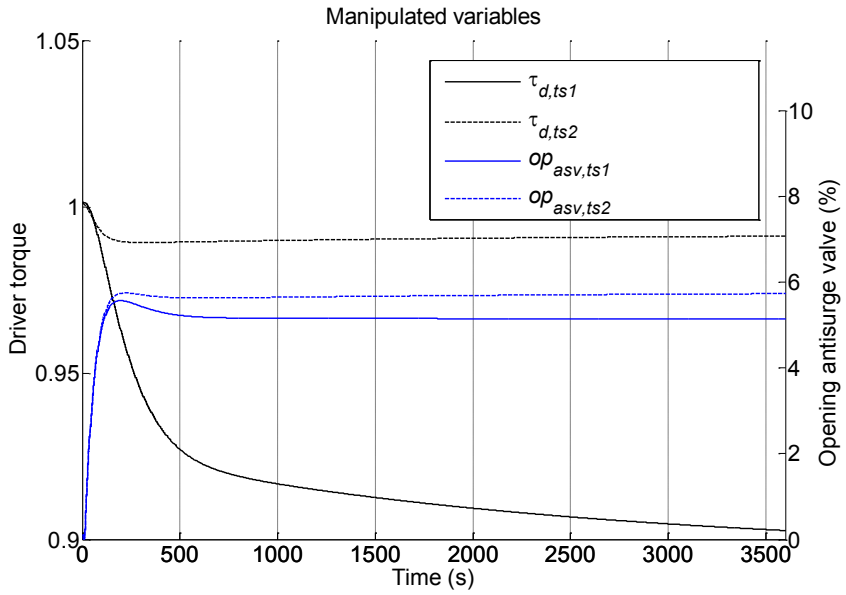


Figure 5-44. Manipulated variables during disturbance scenario 6

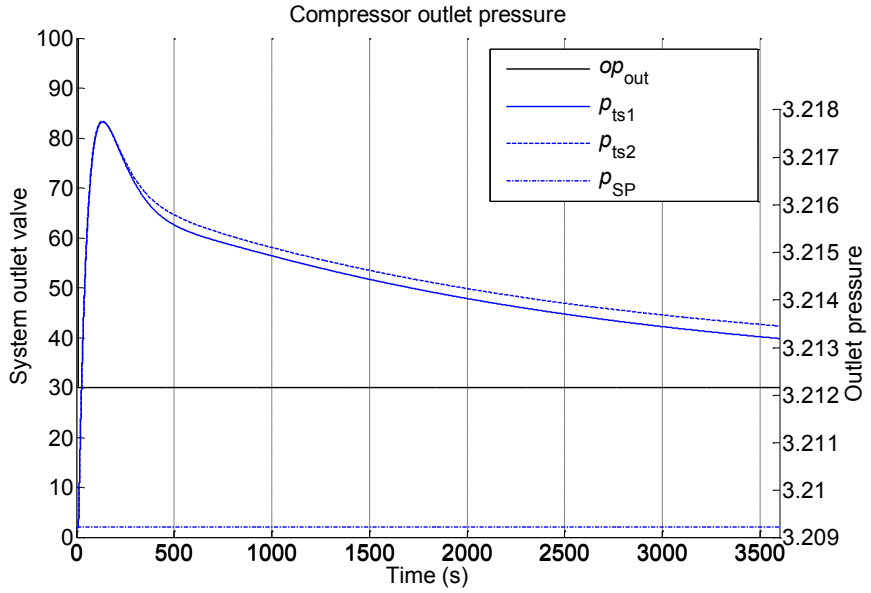


Figure 5-45. Compressor outlet pressure during disturbance scenario 6

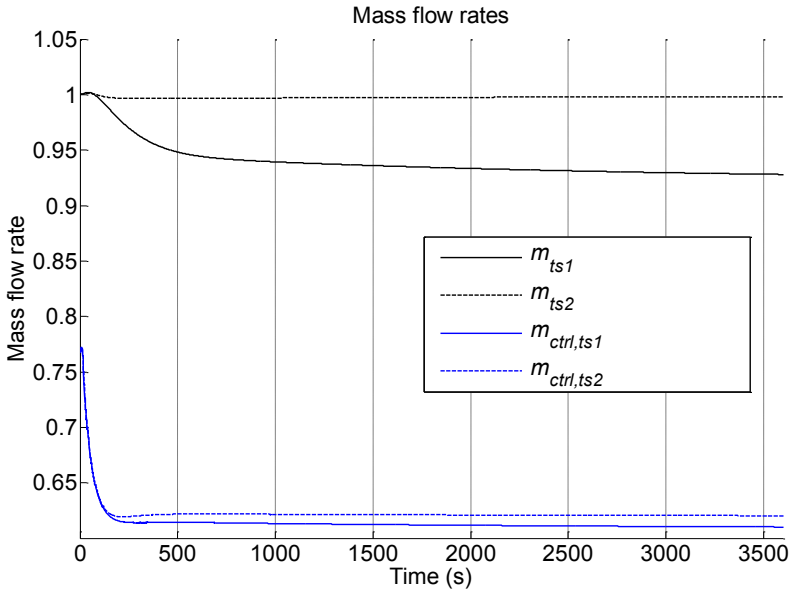


Figure 5-46. Compressor inlet mas flow rate during disturbance scenario 6

5.5.4.4 Inlet pressure of the system

Table 5-24 reports the values of the performance indicators when the inlet pressure of the system changes over time. Also under this tuning, the scenarios can be grouped under two categories. During scenarios 8 and 9 p_{in}decreases while during scenarios 10 and 11 p_{in} increases.

In scenarios 8 and 9 ISE_p increases with the increasing of the magnitude of the disturbance. M is equal to 0 and E increases. This is because the MPC controller is increasing the driver torque in

order to bring back p to its set point. Also in scenarios 10 and 11 ISE_p increases with the increasing of the magnitude of the disturbance. However in these cases M increases and E decreases. The reason is that the MPC controller is decreasing the driver torque while opening the antisurge valve.

When comparing the response of the controller under the first tuning set with the response under this second tuning set, it is possible to notice that under the second tuning ISE_p is lower, M is higher and E is higher. The reason is that with $ts2$ the driver torque response does not overshoot. The recycle is higher in order to control m and keep it closer to its design point. Therefore when recycle is involved, M is higher, m is higher and consequently also E is higher than with the tuning set 1.

Scenario 9 has been selected for comparing the action of the two controllers. The second tuning set does not overshoot therefore p stays closer to its set point over time. The manipulated variables are represented in Figure 5-47 while the controlled variables p and m are represented respectively in Figure 5-48 and Figure 5-49.

Table 5-24. Disturbance scenarios for the inlet pressure of the system

Disturbance scenario	8	9	10	11
Sign and magnitude (%)	-2.81	-1.28	15.74	32.94
ISE_p (bar^{2}s)	10.69	2.18	12752.26	34202.94
M (-)	0.00	0.00	2.60	5.88
E (-)	1.03	1.01	0.85	0.73

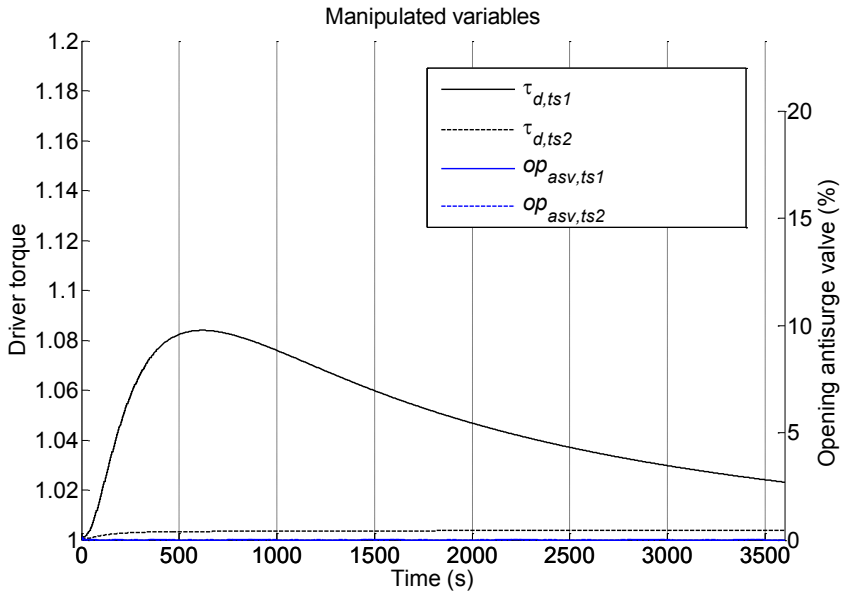


Figure 5-47. Manipulated variables during disturbance scenario 9

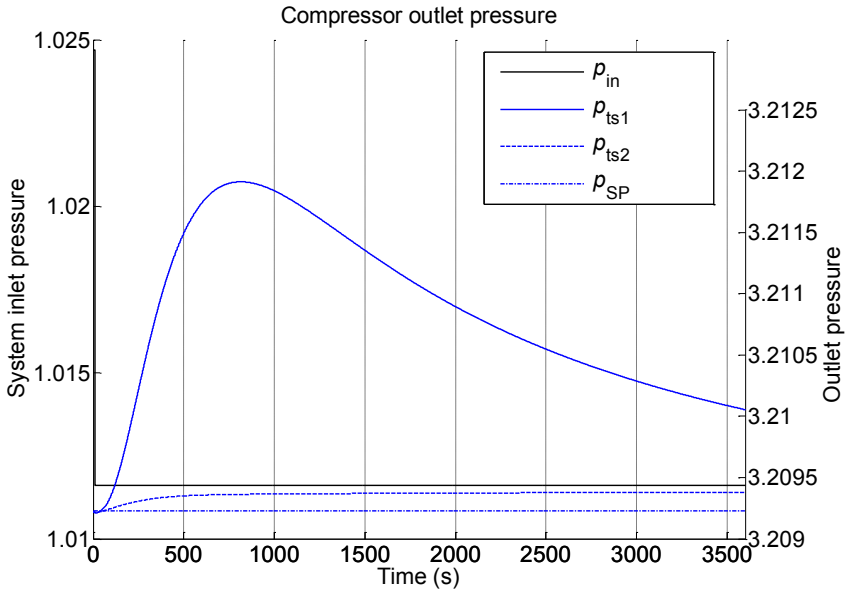


Figure 5-48. Compressor outlet pressure during disturbance scenario 9

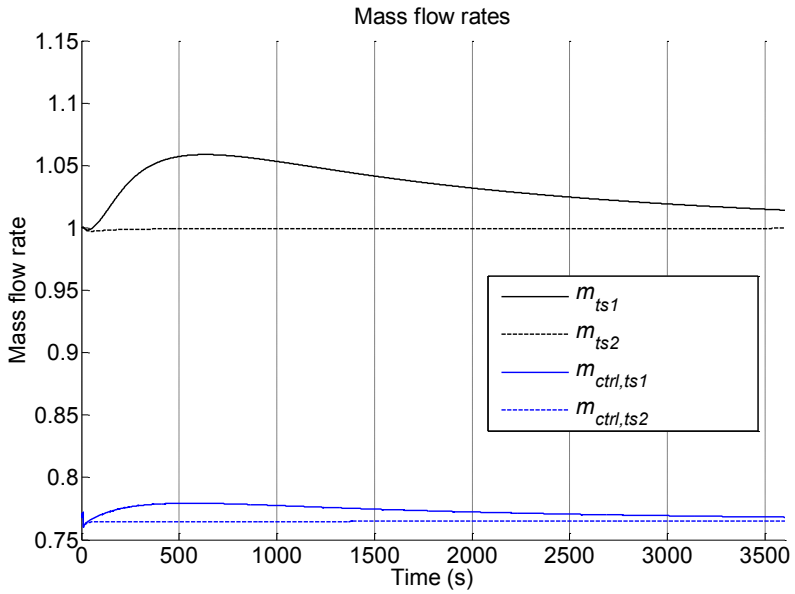


Figure 5-49. Compressor mass flow rates during disturbance scenario 9

5.5.4.5 Outlet pressure of the system

Table 5-25 reports the values of the performance indicators when the outlet pressure of the system changes over time. Also in this case the scenarios can be grouped under two categories. During scenarios 12 and 13 p_{out} decreases while during scenarios 14 and 15 p_{out} increases.

In scenarios 12 and 13 ISE_p increases with the increasing of the magnitude of the disturbance. M is equal to 0 and E is constant and equal to 1. Also in scenarios 14 and 15 ISE_p increases with the

increasing of the magnitude of the disturbance. However in these cases M increases and E decreases. This is because when the system outlet pressure decreases the controller does not open the antisurge valve as this would decrease p even further. Instead when the system inlet pressure increases the action of the antisurge valve helps to control both p and m.

When comparing the response of the controller under tuning set 1 and under tuning set 2, all the performance metrics have higher values under the second set of tuning parameters. This is because when the outlet pressure of the system decreases, the MPC controller increases the driver torque in order to increase the compressor outlet pressure p. However this action increases also m and therefore it is limited in order to keep the flow rate close to its design value. When the outlet pressure of the system increases, the MPC controller decreases the driver torque to control the compressor outlet pressure however it also need to recycle more flow rate in order to control m. Therefore M increases and consequently E.

Scenario 13 has been selected for comparing the action of the two controllers. The second tuning set does not overshoot and therefore N does not saturate. However p is further from its set point over time. This is because m is more stable thanks to the higher recycle and that in turn contributes to decreasing p.

Table 5-25. Disturbance scenarios for the outlet pressure of the system

Disturbance scenario	12	13	14	15
Sign and magnitude (%)	-0.44	-0.11	0.11	0.93
ISE_p (bar^{2}s)	20865.50	1312.07	25.51	8392.60
M (-)	0.00	0.00	0.73	9.35
E (-)	1.00	1.00	1.00	0.97

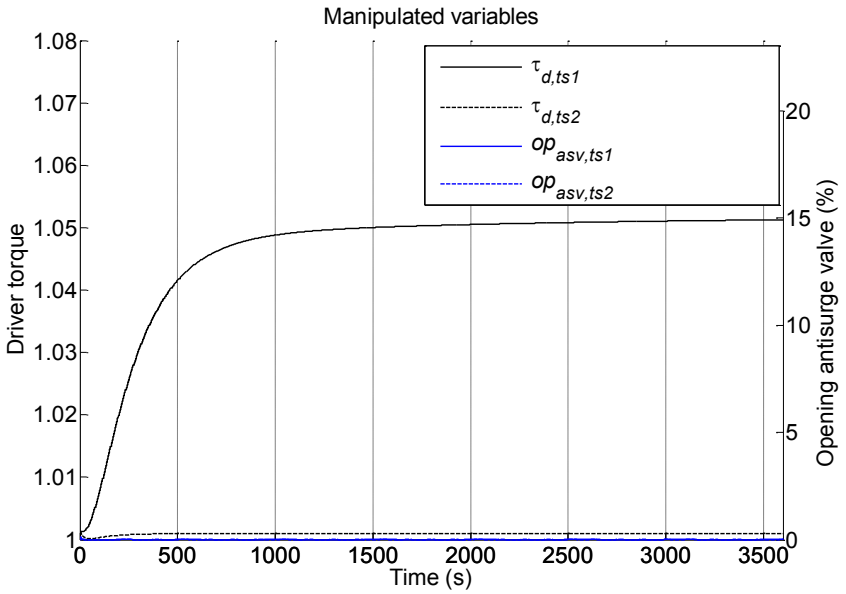


Figure 5-50. Manipulated variables during disturbance scenario 13

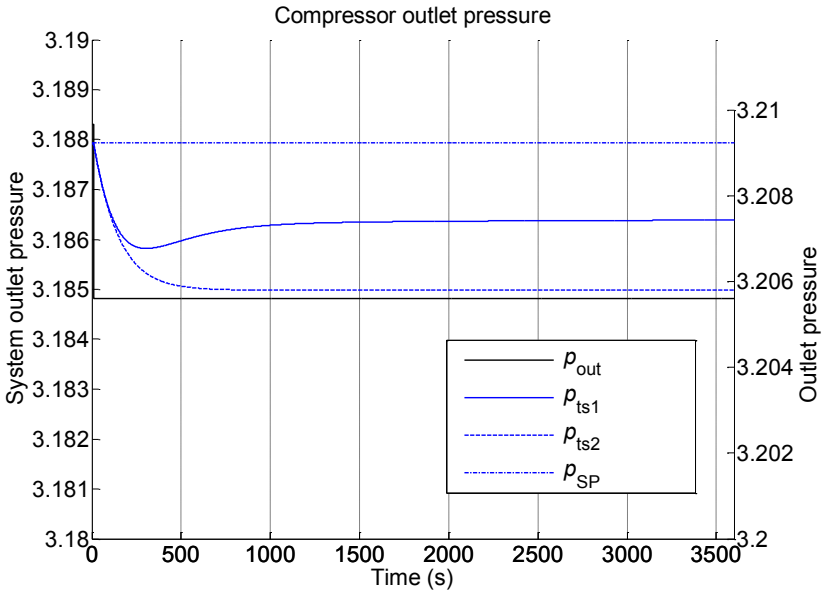


Figure 5-51. Compressor outlet pressure during disturbance scenario 13

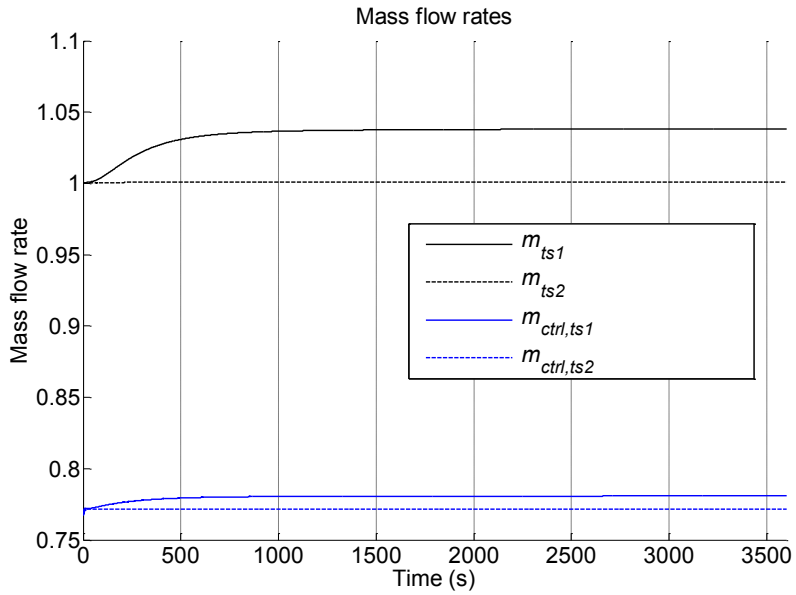


Figure 5-52. Compressor mass flow rates during disturbance scenario 13

5.5.4.6 Pressure set point

Table 5-26 reports the values of the performance indicators when the pressure set point changes over time. Also in this case the scenarios can be grouped under two categories. During scenarios 16 and 17 p_{SP} decreases while during scenarios 18 and 19 p_{SP} increases.

In scenarios 16 and 17 ISE_p increases with the increasing of the magnitude of the disturbance. At the same time M increases while E increases. This is because the MPC controller reduces the driver

torque while increasing the recycle by opening the antisurge valve. Also in scenarios 18 and 19 ISE_p increases with the increasing of the magnitude of the disturbance. In these two cases M is equal to 0 while E increases. The reason is that the controller increases the delivered torque and gas recycle is not necessary.

When comparing the response of the closed loop system under tuning set 1 with the response under tuning set 2, all the performance parameters have higher values under the second tuning set. This is generally due to the smaller action on the driver torque. When the set point of the compressor outlet pressure decreases, m decreases and therefore the controller increase the recycle flow rate in order to control it. At the same time the opening of the antisurge valve contributes to the reduction of the compressor outlet pressure. When the pressure set point increases, the MPC controller increase the driver torque but tries to avoid increasing m too much and therefore the control performance of p decreases and ISE_p increases.

Scenario 17 has been selected for comparing the action of the two controllers. Figure 5-53 represents the manipulated variables while Figure 5-54 and Figure 5-55 represent respectively the compressor outlet pressure and mass flow rates. From the figures it is possible to see that under the second tuning set the action of the torque is smaller while the compressor inlet flow rate is more stable.

Table 5-26. Disturbance scenarios for the pressure set point of the system

Disturbance scenario	16	17	18	19
Sign and magnitude (%)	-1.09	-0.54	0.11	0.38
ISE_p (bar^{2}s)	8787.23	1291.28	1404.73	17161.93
M (-)	10.09	4.51	0.00	0.00
E (-)	0.96	0.98	1.00	1.00

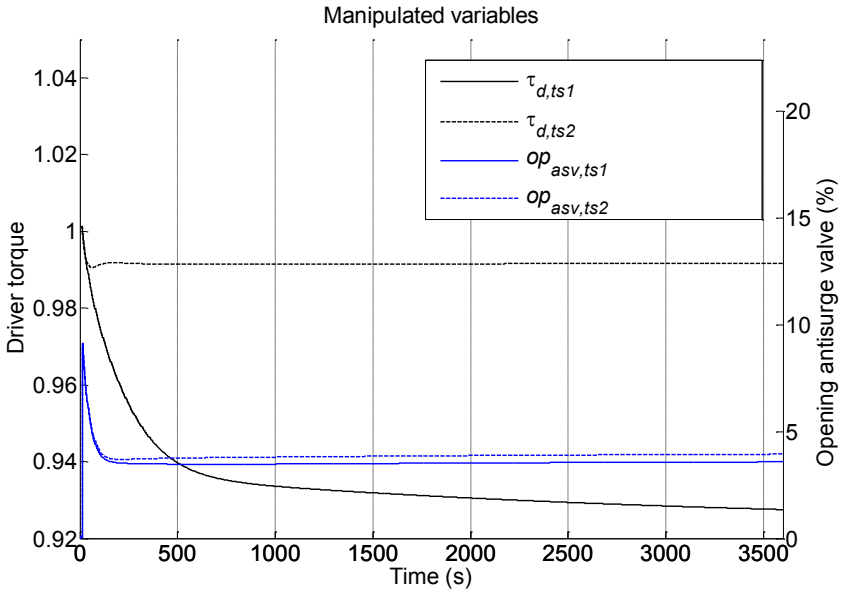


Figure 5-53. Manipulated variables during disturbance scenario 17

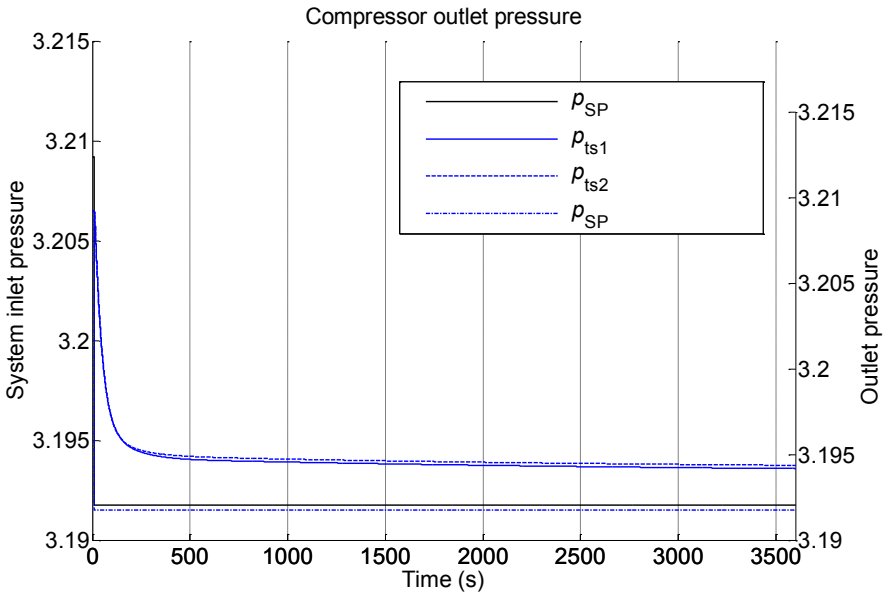


Figure 5-54. Compressor outlet pressure during disturbance scenario 17

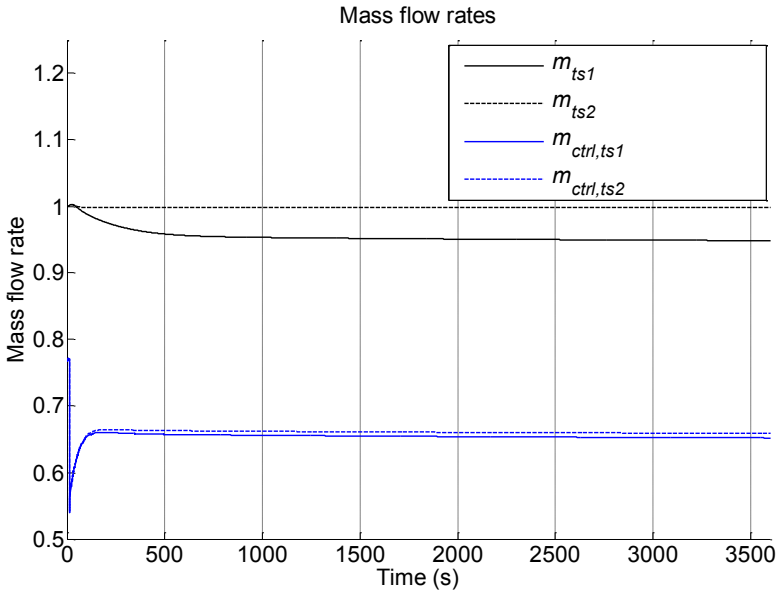


Figure 5-55. Compressor mass flow rates during disturbance scenario 17

5.5.4.7 Saturation of the manipulated variables

A further disturbance scenario has been simulated in order to analyse the response of the system when a manipulated variable saturates. The results of the scenario have been summarised in Table 5-27. The opening of the inlet valve has been changed from fully opened position to 20% opened position. Figure 5-56 represents the manipulated variables over time. The driver torque increases until a maximum value while the antisurge valve stays open. Figure 5-57 shows also the rotational shaft speed, which is equal to its maximum limit value. The saturation of the driver does not allow

control of the compressor outlet pressure, which remains below its set point, as represented in Figure 5-58.

When comparing the response of the controller under different tuning sets, the response of the MPC controller under tuning set 2 is stable and does not oscillate. This is because the controller is placing the pressure control at a lower priority in order to keep the flow rate well above its control value m_{ctrl}. The consequence is that ISE_p, M and E are higher than under tuning set 1 however the system does not oscillate.

Table 5-27. Disturbance scenario 20: saturation of the rotational shaft speed

Disturbance scenario	**20**
Disturbance variable	Vin
Sign and magnitude (%)	-80
ISE_p (bar^{2}s)	19104.30
M (-)	3.46
E (-)	1.13

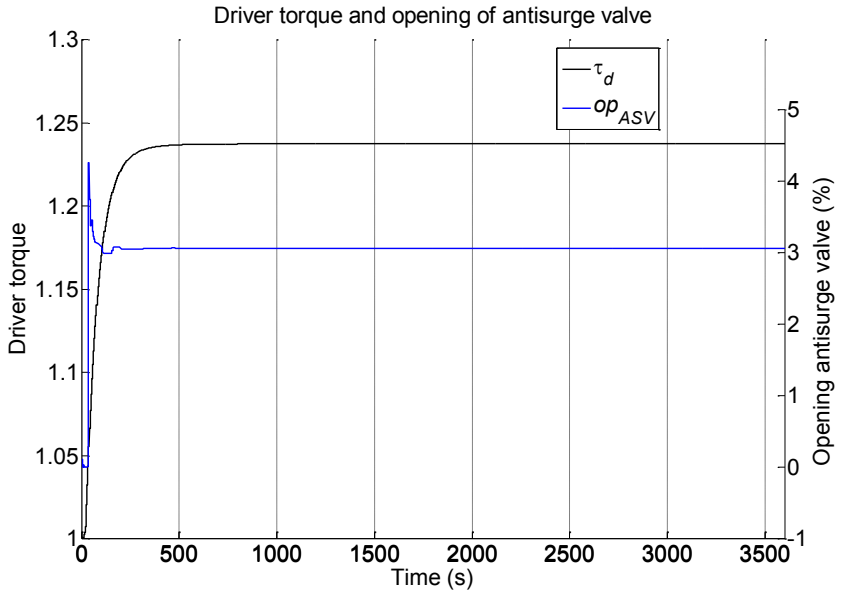


Figure 5-56. Manipulated variables during disturbance scenario 20

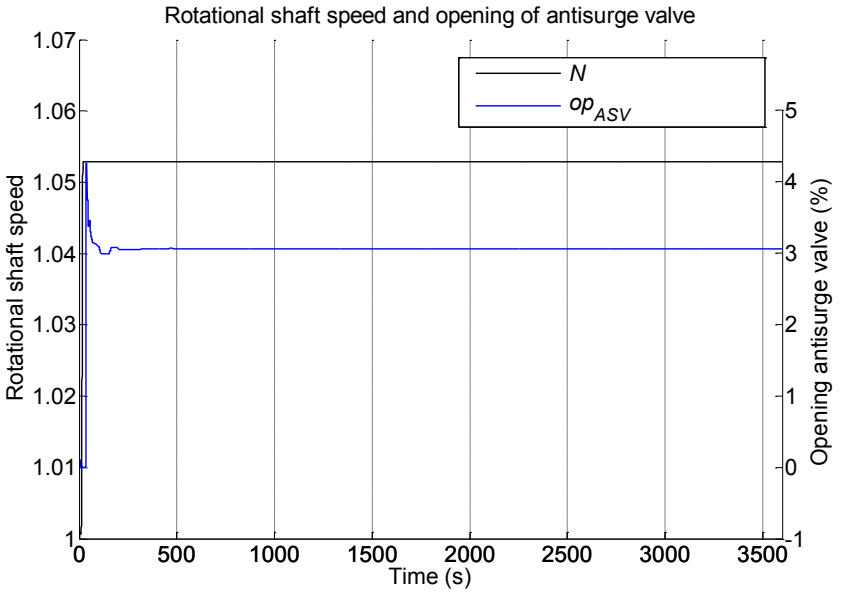


Figure 5-57. Rotational shaft speed and opening of antisurge valve during disturbance scenario 20

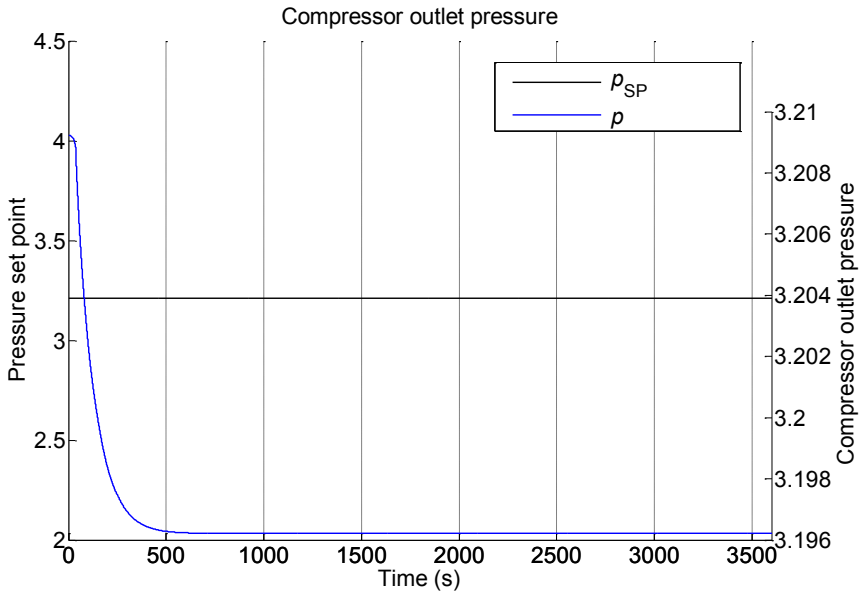


Figure 5-58. Compressor outlet pressure during disturbance scenario 20

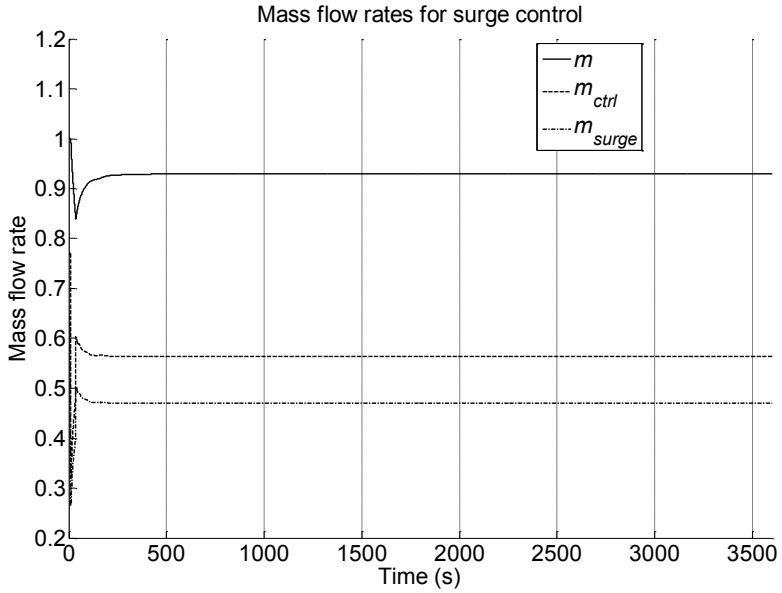


Figure 5-59. Compressor mass flow rates during disturbance scenario 20

5.5.4.8 Summary

In the section of the chapter the disturbance scenarios have been tested a second time by employing a different tuning set for the MPC controller. The weight of the compressor inlet mass flow rate has been increase from 0.08 to 0.72.

The effect on the response of the controller can be summarised in the following way. Under this new tuning set, the MPC controller is still trying to control p and m at the same time. The constraint on the outlet temperature of the compressor is still present in the MPC configuration and therefore it avoids the overheating of the machine during recycling. Because the weight of m has been increased, the controller recycles more when recycle is beneficial for both pressure and flow control. This cause the increase of the power consumption however it guarantees better control performance with respect to p. When gas recycling is not necessary as the action on the driver torque causes the increase of m, the control performance in terms of pressure decreases. When the driver saturates as it arrives to its upper limit of speed, the response of the controller does not oscillate. This is because the controller allows a lower performance in terms of pressure control in order to keep the inlet mass flow rate away from its control limit m_{ctrl}.

5.5.5 Third set of tuning parameters

In this section of the chapter a third set of tuning parameters is proposed. The set is summarised in Table 5-28. The weight of the antisurge valve w_{ASV} has been changed from 10 to 0.1. Decreasing the tuning weight of a manipulated variable means to decrease its weight in the objective function. Therefore the controller will try to manipulate this variable more than when its weight was higher. This modification has been proposed in order to see its effect on both pressure and flow rate control.

The same disturbance scenarios proposed before have been employed in order to test the response of the controller under this new tuning set. Then the responses of the controller under tuning set 1 and tuning set 3 have been compared in order to evaluate the effect of the tuning on the response of the closed loop system.

Table 5-28. Tuning parameters for model predictive controller (tuning set 3)

Name	Value
w_{τ_d}	0
wr_{τ_d}	0.1
w_{ASV}	0.1
wr_{ASV}	0.1
w_p	1
w_m	0.08
w_N	0.0001
$w_{T\tau_{02}}$	0.0001

5.5.5.1 Steady state

Table 5-29 reports the values of the performance indicators during steady state operation at the design point. ISE_p and M are equal to 0 and therefore this means that the compressor outlet pressure is equal to its set point while the antisurge valve is closed. E is equal to 1 as expected for this type of operation.

Table 5-29. Steady state operation at the design point

Scenario	0 – steady state at design point
ISE_p (bar^{2}s)	0.00
M (-)	0.00
E (-)	1.00

5.5.5.2 Closing of the inlet valve

Table 5-30 reports the values of the performance indicators when the position of the inlet valve changes from fully opened position to partially opened position.

In scenarios 2, 3 and 4 ISE_p increases with the increasing of the magnitude of the disturbance. M is always 0 as there is no need for recycle. At the same time E is equal to 1 or slightly above 1 for all the scenarios. The reason is that the controller tries to maintain the compressor inlet flow rate close to its design point by manipulating cautiously the driver torque.

When comparing the response of the MPC under tuning set 1 with its response under tuning set 3, only minor differences can be appreciated. Therefore it is possible to say that the response of the controller under the two different tuning set is the same for this disturbance scenario.

Table 5-30. Disturbance scenarios for the inlet valve of the system

Disturbance scenario	1	2	3	4
Sign and magnitude (%)	0.00	-10.00	-20.00	-29.00
ISE_p (bar^{2}s)	0.00	68.50	460.31	1736.20
M (-)	0.00	0.00	0.00	0.00
E (-)	1.00	1.02	1.06	1.11

5.5.5.3 Closing of the outlet valve

Table 5-31 reports the values of the performance indicators when the position of the outlet valve changes from fully opened position to partially opened position.

Also with this control tuning, in scenarios 5, 6 and 7 ISE_p increases with the increasing of the magnitude of the disturbance. At the same time E decreases and M increases because the mass flow rate of the compressor m is lower than its design point over the time of the simulation.

When comparing the response of the MPC controller under the first tuning with its response under this third tuning, ISE_p has a much lower value during all cases under $ts3$, while M is slightly higher together with E. The reason is that under tuning set 3 the MPC controller is employing both driver torque and antisurge valve in order to reduce the compressor outlet pressure.

Figure 5-60 represents the manipulated variables of scenario 6 over time for the two tuning cases. Figure 5-61 and Figure 5-62 represent respectively the compressor outlet pressure and inlet mass flow rate during the disturbance scenario. The compressor outlet pressure p is close to its set point under $st3$ compared with its value under $st1$.

Table 5-31. Disturbance scenarios for the outlet valve of the system

Disturbance scenario	1	5	6	7
Sign and magnitude (%)	0.00	-40.00	-70.00	-95.00
ISE_p (bar^{2}s)	0.00	2.02	9.06	22.01
M (-)	0.00	3.95	6.95	9.47
E (-)	1.00	0.98	0.98	0.98

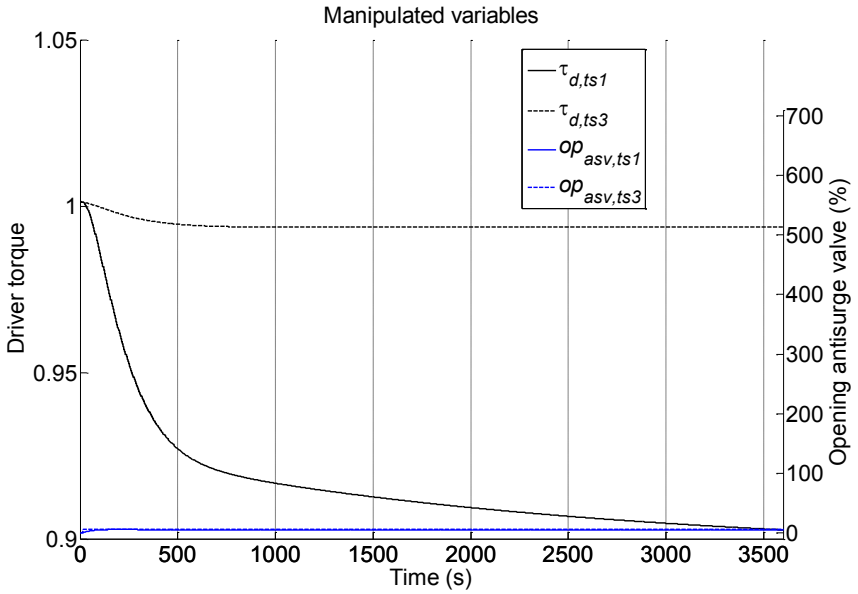


Figure 5-60. Manipulated variables during disturbance scenario 6

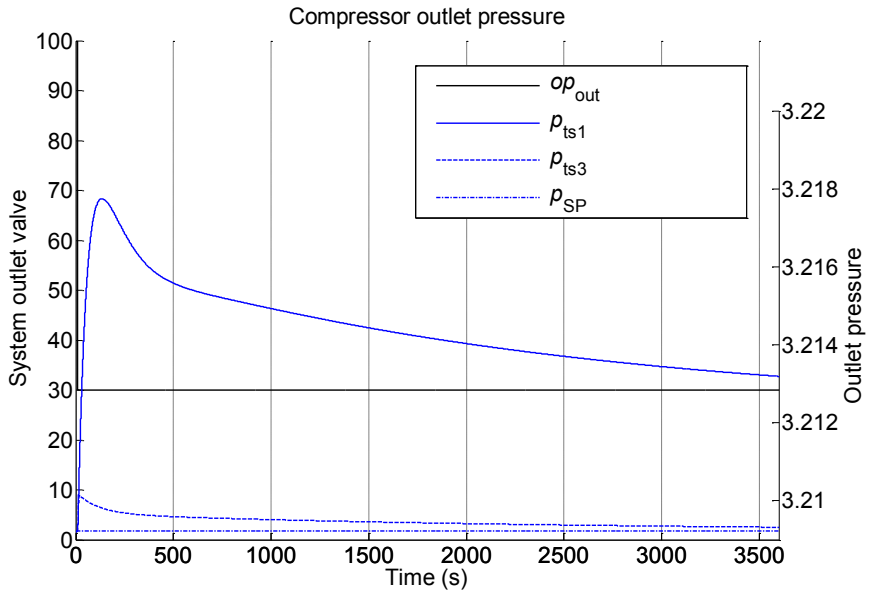


Figure 5-61. Compressor outlet pressure during disturbance scenario 6

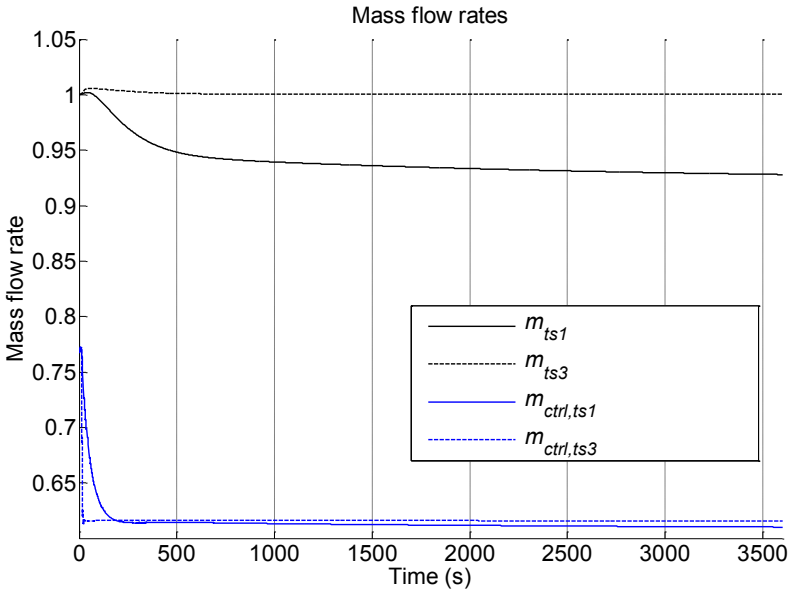


Figure 5-62. Compressor mass flow rates during disturbance scenario 6

5.5.5.4 Inlet pressure of the system

Table 5-32 reports the values of the performance indicators when the inlet pressure of the system changes over time. Also under this tuning, the scenarios can be grouped under two categories. During scenarios 8 and 9 p_{in} decreases while during scenarios 10 and 11 p_{in} increases.

In scenarios 8 and 9 ISE_p increases with the increasing of the magnitude of the disturbance. M is equal to 0 and E increases. This is because the MPC controller is increasing the driver torque in order to bring back p to its set point. Also in scenarios 10 and 11 ISE_p increases with the increasing of the magnitude of the disturbance. However in these cases M increases and E decreases. The reason is that the MPC controller is decreasing the driver torque while opening the antisurge valve.

When comparing the response of the controller under the first tuning set with the response under this third tuning set, it is possible to notice that under the third tuning ISE_p is lower, M is lower and E is higher when the inlet pressure of the system increases (scenarios 10 and 11). The reason is that under this new control tuning, the antisurge valve is employed together with the driver torque in order to control p. Moreover the driver torque does not overshoot and therefore the controller goes quickly to its new steady state. When the inlet pressure of the system decreases (scenarios 8 and 9) and the gas recycle cannot be employed for pressure control, the response of the controller under the two tunings can be considered equivalent.

Scenario 10 has been selected for comparing the action of the two controllers. Figure 5-63 represents the manipulated variables while Figure 5-64 represents the compressor outlet pressure and Figure 5-65 the compressor mass flow rates. From the figures it is possible to see that, under tuning set 3, the driver torque does not overshoot and therefore the antisurge valve does not need to open too much. Moreover the pressure stays closer to its set point over time and m slightly increases.

Table 5-32. Disturbance scenarios for the inlet pressure of the system

Disturbance scenario	8	9	10	11
Sign and magnitude (%)	-2.81	-1.28	15.74	32.94
ISE_p (bar^{2}s)	1883.18	366.47	356.66	1397.32
M (-)	0.00	0.00	0.07	0.16
E (-)	1.12	1.05	0.86	0.74

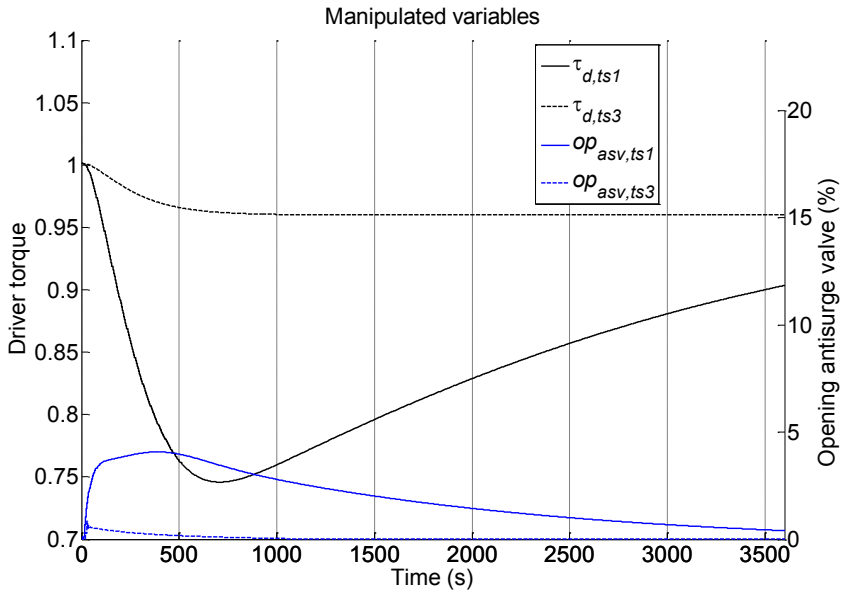


Figure 5-63. Manipulated variables during disturbance scenario 10

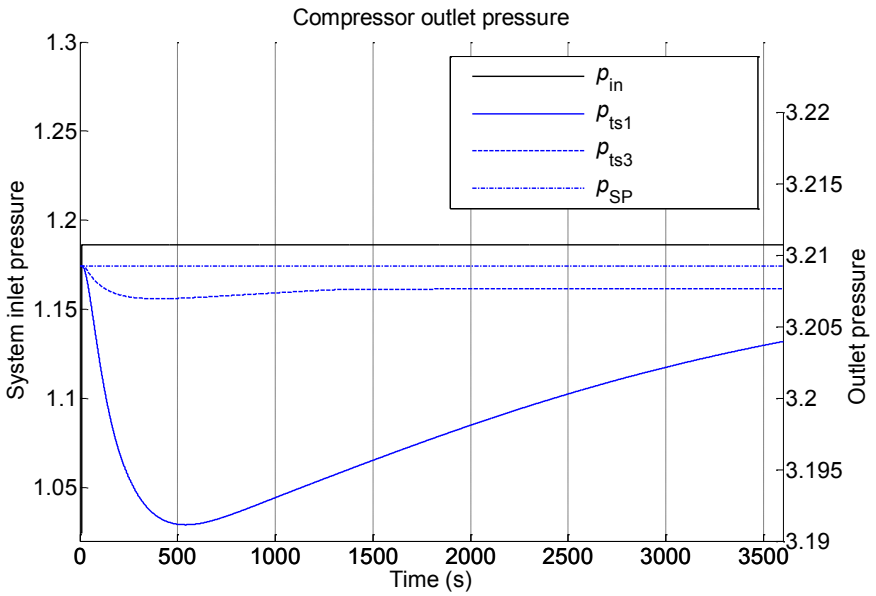


Figure 5-64. Compressor outlet pressure during disturbance scenario 10

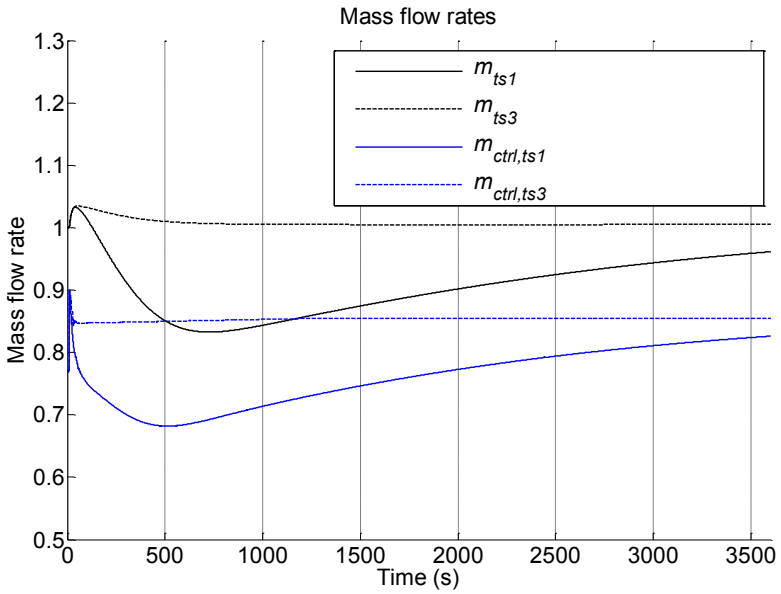


Figure 5-65. Compressor mass flow rates during disturbance scenario 10

5.5.5.5 Outlet pressure of the system

Table 5-33 reports the values of the performance indicators when the outlet pressure of the system changes over time. Also in this case the scenarios can be grouped under two categories. During scenarios 12 and 13 p_{out} decreases while during scenarios 14 and 15 p_{out} increases.

In scenarios 12 and 13 ISE_p increases with the increasing of the magnitude of the disturbance. M is equal to 0 and E increases. Also in scenarios 14 and 15 ISE_p increases with the increasing of the magnitude of the disturbance. However in these cases M increases and E decreases. This is because when the system outlet pressure decreases the controller does not open the antisurge valve as this would decrease p even further. Instead when the system inlet pressure increases the action of the antisurge valve helps to control both p and m.

When comparing the response of the controller under tuning set 1 and under tuning set 3, the response of the controller is the same when recycle is not needed, that means for scenario 12 and scenario 13. However when recycle is needed (scenarios 14 and 15), under this new tuning the MPC controller shows a lower ISE_P and higher M. Both driver torque and antisurge valve are employed for pressure control. The action of the controller on τ_d is smaller and a higher recycle is employed.

Scenario 14 has been selected for comparing the action of the two controllers. Figure 5-66 represents the manipulated variables while Figure 5-67 and Figure 5-68 represent respectively the compressor outlet pressure and mass flow rates.

Table 5-33. Disturbance scenarios for the outlet pressure of the system

Disturbance scenario	12	13	14	15
Sign and magnitude (%)	-0.44	-0.11	0.11	0.93
ISE_p (bar^{2}s)	6070.49	428.31	0.06	25.68
M (-)	0.00	0.00	0.85	9.98
E (-)	1.16	1.04	1.00	0.98

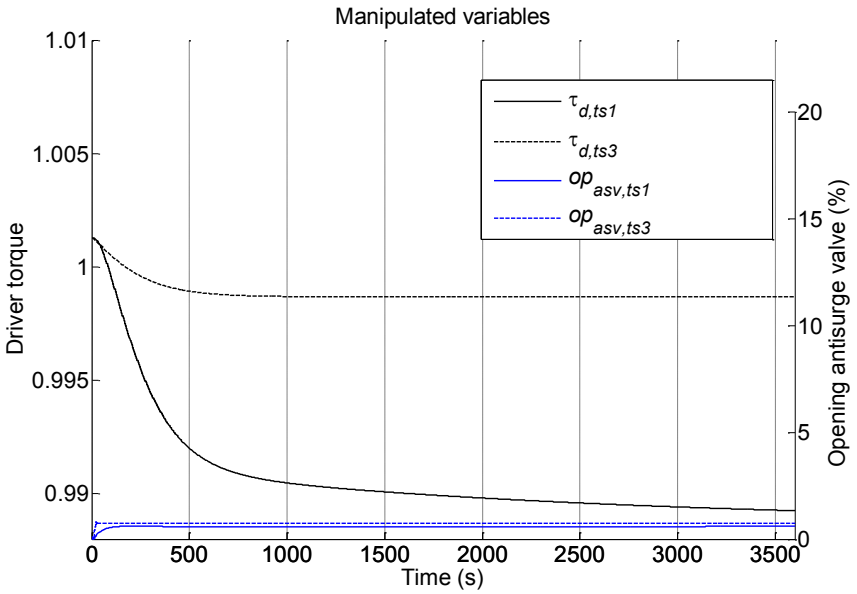


Figure 5-66. Manipulated variables during disturbance scenario 14

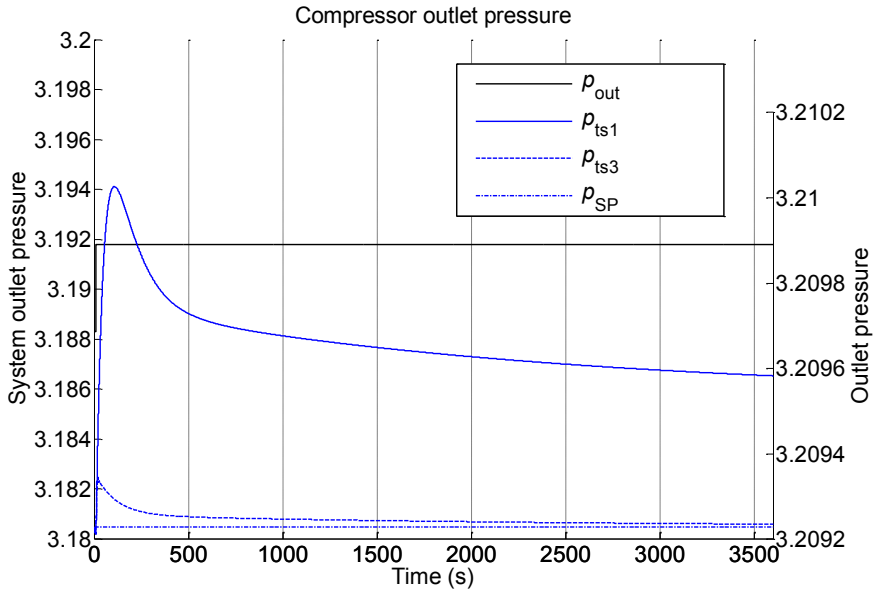


Figure 5-67. Compressor outlet pressure during disturbance scenario 14

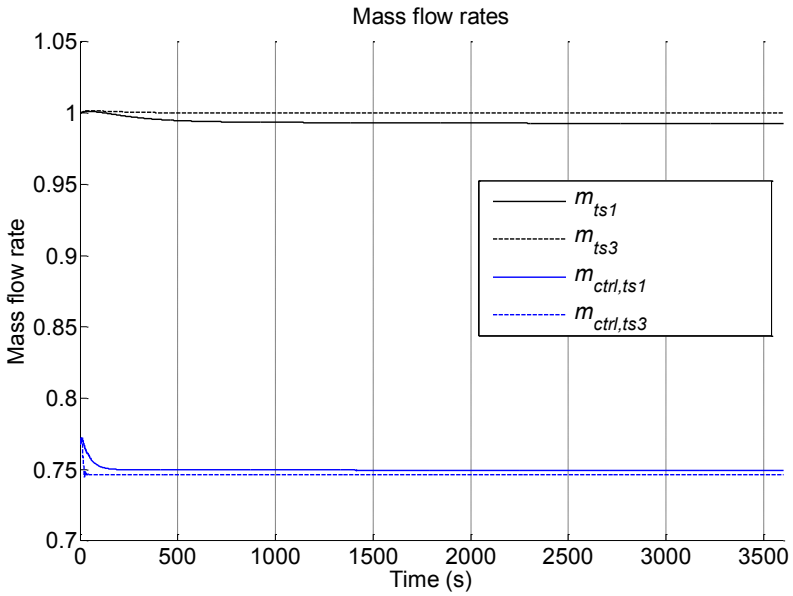


Figure 5-68. Compressor mass flow rates during disturbance scenario 14

5.5.5.6 Pressure set point

Table 5-34 reports the values of the performance indicators when the pressure set point changes over time. Also in this case the scenarios can be grouped under two categories. During scenarios 16 and 17 p_{SP} decreases while during scenarios 18 and 19 p_{SP} increases.

In scenarios 16 and 17 ISE_p increases with the increasing of the magnitude of the disturbance. At the same time M increases while E decreases. This is because the MPC controller reduces the driver torque while increasing the recycle by opening the antisurge valve. Also in scenarios 18 and 19 ISE_p increases with the increasing of the magnitude of the disturbance. In these two cases M is equal to 0 while E increases. The reason is that the controller increases the delivered torque and gas recycle is not necessary.

When comparing the response of the closed loop system under tuning set 1 with the response under tuning set 3, the controller responds in the same way to a positive change of the pressure set point. However when the pressure set point decreases, the response under tuning set 3 shows a much smaller ISE_p and higher M and E. Also in this case both driver torque and antisurge valve have been employed for pressure control.

Scenario 17 has been selected for comparing the action of the two controllers. Under tuning set 3, both torque and opening of the antisurge valve are higher and this is the reason why the controller is able to achieve its new set point, as represented in Figure 5-70.

Table 5-34. Disturbance scenarios for the pressure set point of the system

Disturbance scenario	16	17	18	19
Sign and magnitude (%)	-1.09	-0.54	0.11	0.38
ISE_p (bar^{2}s)	237.95	41.22	414.84	4338.67
M (-)	10.30	5.98	0.00	0.00
E (-)	0.97	0.98	1.04	1.16

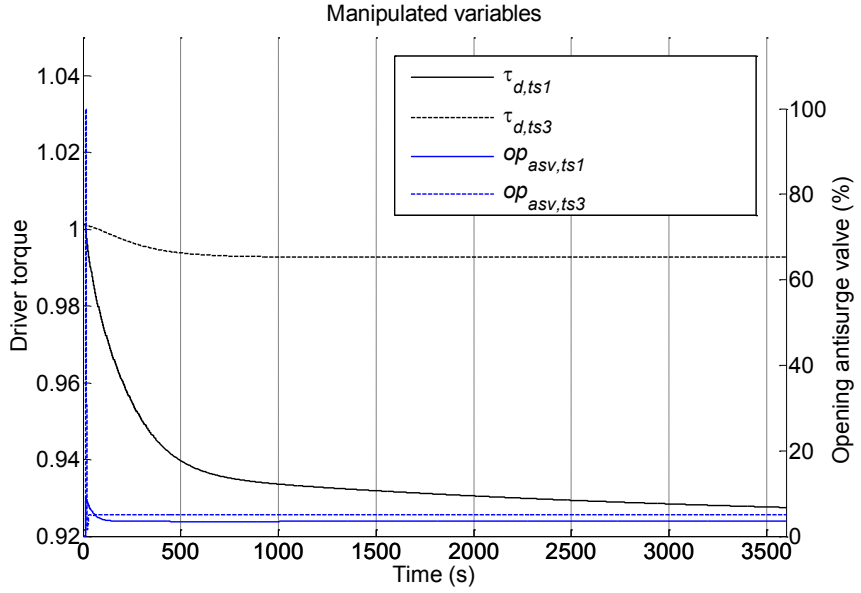


Figure 5-69. Manipulated variables during disturbance scenario 17

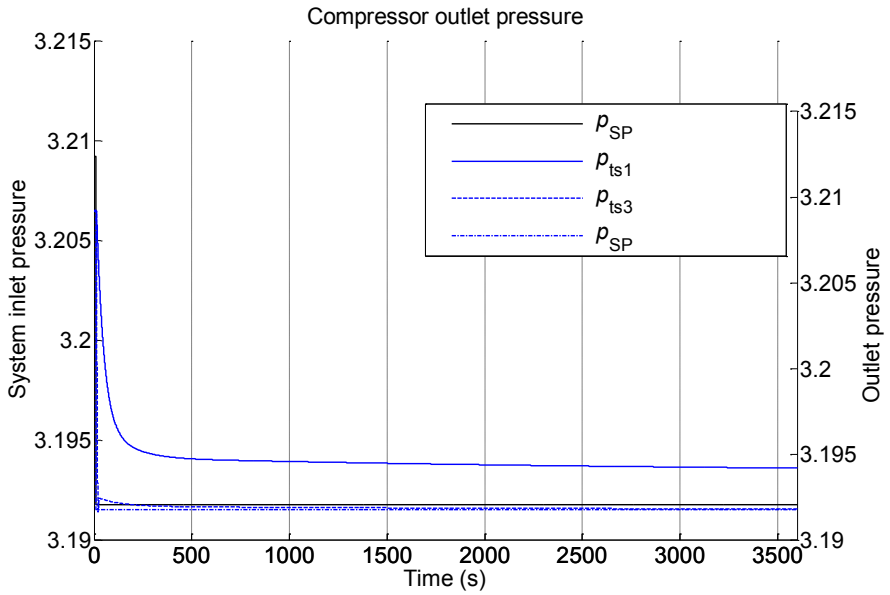


Figure 5-70. Compressor outlet pressure during disturbance scenario 17

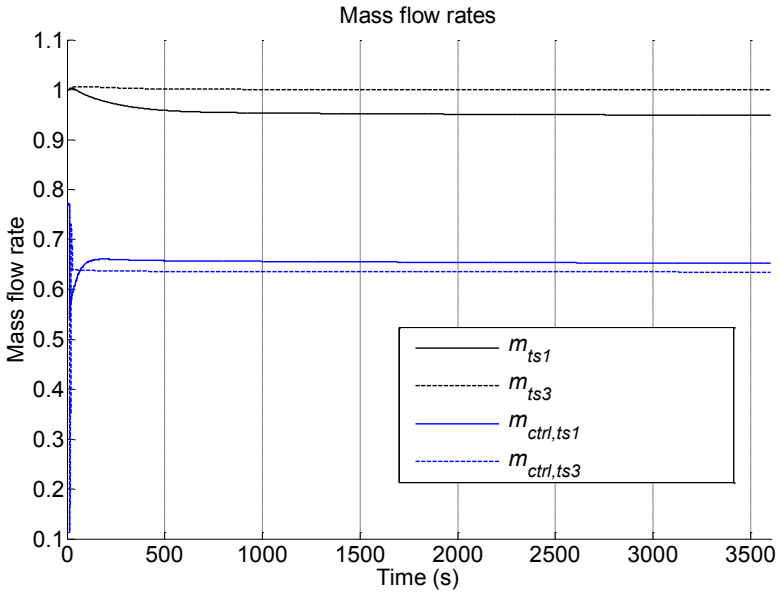


Figure 5-71. Compressor mass flow rates during disturbance scenario 17

5.5.5.7 Saturation of the manipulated variables

A further disturbance scenario has been simulated in order to analyse the response of the system when a manipulated variable saturates. The results of the scenario have been summarised in Table 5-35. The opening of the inlet valve has been changed from fully opened position to 20% opened position. Figure 5-72 represents the manipulated variables over time. The driver torque increases until a maximum value while the antisurge valve stays open. Figure 5-73 shows also the rotational shaft speed, which is equal to its maximum limit value. The saturation of the driver prevents control of the compressor outlet pressure, which remains below its set point, as represented in Figure 5-74.

During the saturation of the driver to its maximum speed, the response of the MPC controller is the same under set tuning 1 and set tuning 3. The reason is that also under this new tuning the controller is trying to increase p. Opening the antisurge valve would not help the pressure control performance. However it is necessary in order to avoid surge and therefore the antisurge valve oscillates, as it happened under tuning set 1.

Table 5-35. Disturbance scenario 20: saturation of the rotational shaft speed

Disturbance scenario	**20**
Disturbance variable	Vin
Sign and magnitude (%)	-80
ISE_p (bar^{2}s)	17324.24
M (-)	0.50
E (-)	0.83

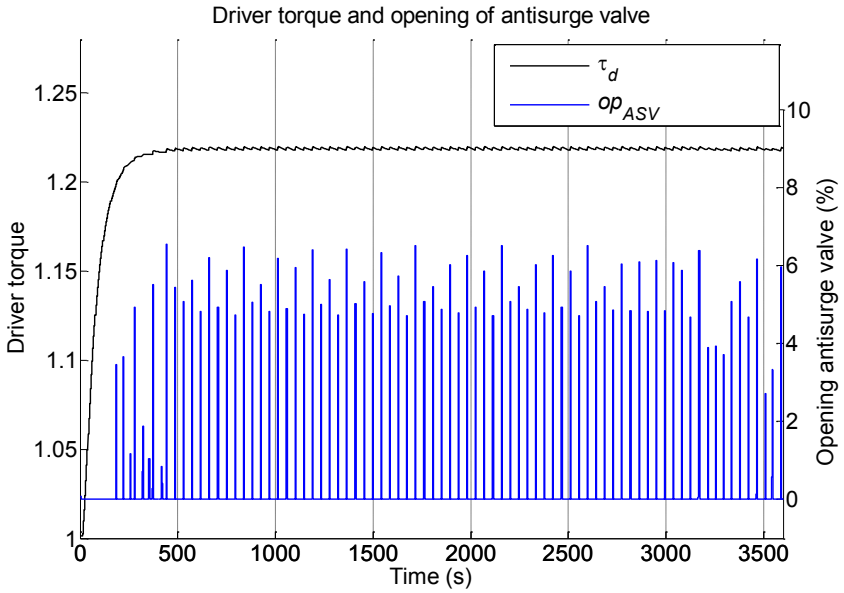


Figure 5-72. Manipulated variables during disturbance scenario 20

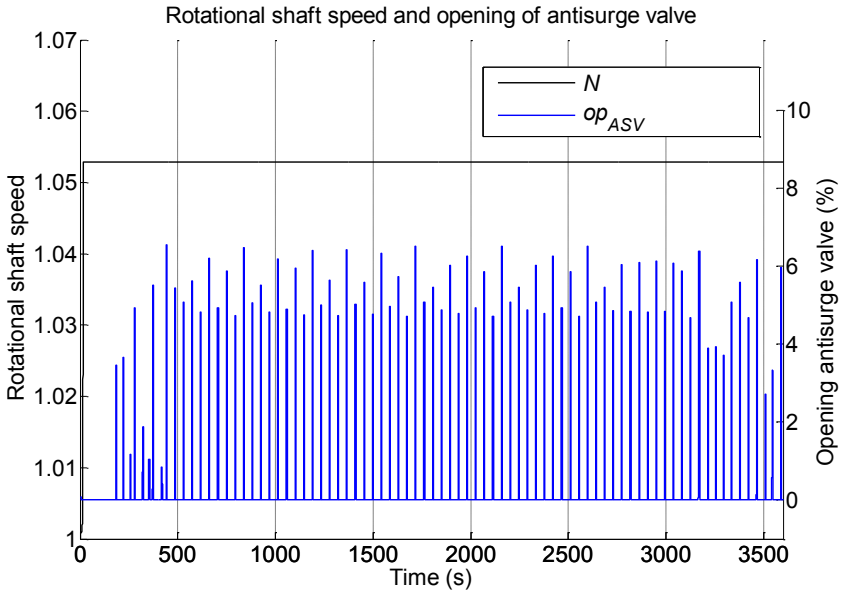


Figure 5-73. Rotational shaft speed and opening of antisurge valve during disturbance scenario 20

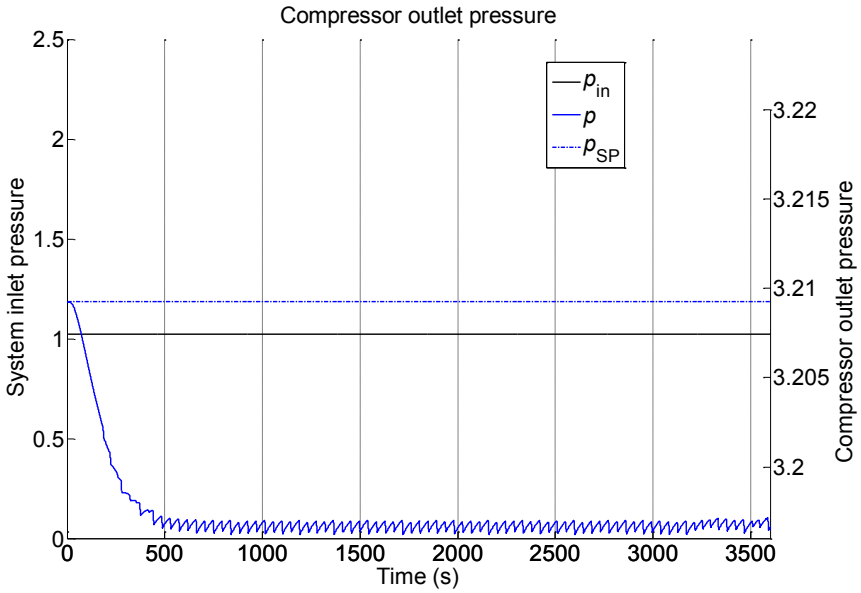


Figure 5-74. Compressor outlet pressure during disturbance scenario 20

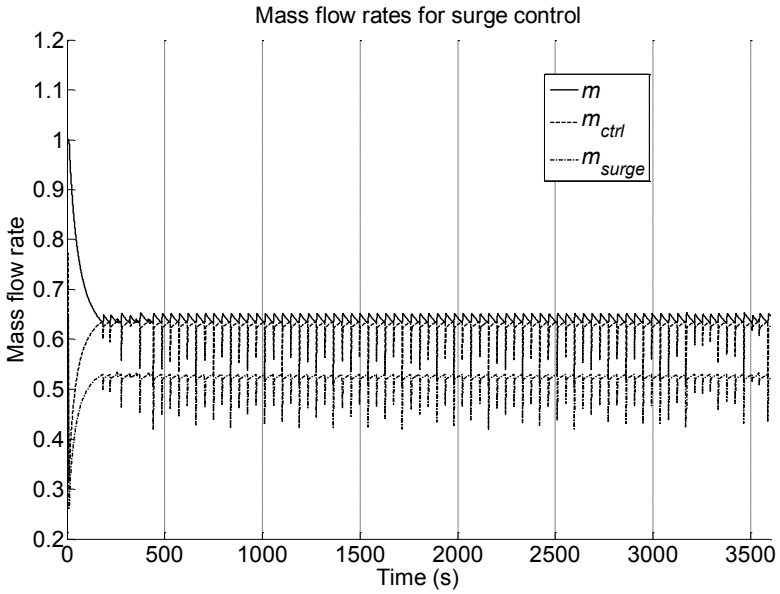


Figure 5-75. Compressor mass flow rates during disturbance scenario 20

5.5.5.8 Summary

In the section of the chapter the disturbance scenarios have been tested a third time by employing a different tuning set for the MPC controller. The weight of the antisurge valve has been decreased from 10 to 0.1.

The effect on the response of the controller can be summarised in the following way. Under this new tuning set, the MPC controller gives priority to the control of pressure over the control of the mass

flow rate. When gas recycling is beneficial for pressure control, it is employed by the controller together with the driver torque. This high gas recycle causes the increase of E with respect to the original first tuning. However when gas recycling is not beneficial for pressure control, the performance of the controller under tuning set 3 is the same as it was under tuning set 1. Finally when the driver saturates to its maximum speed, the controller oscillates as under tuning set 1, for similar reasons.

5.5.6 Discussion

In this chapter a linear model predictive controller has been proposed in order to control the compressor outlet pressure while avoiding the surge of the machine. The controller has been tuned using three different tuning set:

- The first tuning set ($ts1$) gave priority to the control of pressure over the control of flow rate. Moreover it limited the use of the antisurge valve with respect to the use of the driver torque
- The second tuning set ($ts2$) gave priority to the control of pressure over the control of flow however employed a higher weight for the controller of m in comparison with $ts1$
- The third tuning set ($ts3$) gave priority to the control of pressure over the control of flow rate however increased the utilisation of the antisurge valve as a manipulated variable for both pressure and surge control, with respect to $ts1$.

The simulation results have demonstrated that the MPC controller behaves differently according to its tuning. In fact under the first set of tuning parameters the MPC controller was able to control both pressure and flow rate at the same time. Gas recycling was employed in order to increase the compressor inlet flow rate when necessary. During these cases the power consumption did not increase in comparison to the power consumption during steady state operation at design point. When gas recycling was not employed, only the driver torque was manipulated in order to control the compressor outlet pressure. However the high difference between the pressure weight w_p and the flow weight w_m caused the overshoot of the controller response. Therefore the controller was slow to bring the pressure to its set point. The only time in which the MPC started oscillating was due to the saturation of the driver. In that occasion the controller could not solve the optimisation problem as it is not possible to control two variables by manipulating only one actuator. Moreover that was the only occasion in which the MPC controller let the compressor inlet mass flow rate go closer to the surge region. In all the other simulations the controller compromised on pressure control in order to keep m well above m_{ctrl}.

Under the second set of tuning parameters the MPC controller recycled more when recycle was beneficial for both pressure and flow control. This caused the increase of the power consumption however it guaranteed better control performance with respect to p. When gas recycling was not necessary as the action on the driver torque caused the increase of the compressor inlet mass flow rate, the control performance in terms of pressure decreased. During the saturation of the driver, the response of the controller did not oscillate. This is because the controller allowed a lower performance in terms of pressure control in order to keep the inlet mass flow rate away from its control limit.

Finally when the MPC was under the third set of tuning parameters, the control performance in terms of pressure increased when recycle was beneficial. However this also caused the increase of the power consumption of the machine. When gas recycling was not necessary, the controller showed the same control response as under tuning set 1. It is for this reason that the controller oscillated when the driver saturated.

In conclusion the response of the controller under these three different tuning sets can be summarised in the following way:

- The first set of tuning parameters is appropriate when the control of pressure does not have to be tight. If it is acceptable to maintain the compressor outlet pressure within its lower and higher constraints but not closely to its set point, this tuning set allows lower recycle and also lower power consumption
- The second set of tuning parameters is appropriate when surge occurrence is a main issue for the system and therefore a higher performance in terms of flow rate control is desired
- Finally the third set of tuning parameters is appropriate when a better performance in terms of pressure control is desired. However this operation will involve higher recycle and therefore higher power consumption.

It is possible to say that there are some disturbance scenarios in which is not possible to tightly control the compressor outlet pressure while avoiding the surge of the machine without recycling gas. Therefore the tuning of the controller can be performed in order to reflect the desire of the control engineer. Priority can be given respectively to energy saving (tuning set 1), surge avoidance (tuning set 2) or pressure control performance (tuning set 3). This decision depends on many factors and therefore cannot be generalised. However this chapter provides useful insights in order to understand the issues related to control and operation of centrifugal compressors. Moreover it provides a tool that can perform the integrated control of pressure and surge.

5.6 Summary of the chapter

This chapter of the thesis had three main tasks to fulfil:

- Task 1: analysis of the open loop response of the compression system
- Task 2: integration of pressure and surge control action
- Task 3: reduction of the recycle flow rate by means of advance control design.

The analysis of the open loop response of the compression system was performed in order to give insight on the effect of boundary disturbances on the operation of the compressor.

Moreover a linear model predictive controller has been proposed in order to control the compressor outlet pressure while avoiding surge. Different disturbance scenarios have been tested and three tuning sets have been proposed. The results demonstrate that the MPC controller is able to control the outlet pressure of the compressor while avoiding surge. Therefore pressure and surge control actions have been integrated in a single controller. The results also demonstrate that the MPC controller is more suitable than a PI controller for a multiple-input multiple-output process system such as a centrifugal compressor.

The parameters ISE_p, M and E have been employed for the analysis of the performance of the controllers and for the comparison between PI and MPC control for compressor applications. They are useful for the analysis presented in the thesis however they do not capture everything that a control engineer would be interested in. In fact they do not take into account practical aspects such as:

- The cost of the control system and its additional devices, including capital and operating cost
- The additional effort required to monitor and maintain an advanced control system
- The wearing of the valve during frequent oscillations
- The human factor represented by the action of the operator.

Therefore the MPC controller performs better than the PI controller in terms of system stability and protection of the machine against overheating due to hot gas recycle. However other factors such as those presented above have to be taken into account when a selection between the two control types must be performed.

Under certain disturbances it is not possible to keep the pressure at its set point while avoiding surge without recycling. Therefore the tuning of the MPC controller was performed in order to give priority to respectively energy saving (tuning set 1), surge avoidance (tuning set 2) or pressure control performance (tuning set 3). The first tuning set has fulfilled the third task of the chapter. In all the tested cases the MPC controller performed as requested. The other tuning sets have demonstrated that the MPC controller can be tuned accordingly to the desired control purpose. The decision regarding the type of tuning to adopt depends on many factors and cannot be generalised. However this chapter has provided useful insights on the operation and control of compressors and also a simulation tool able to integrate the control of pressure and surge in a single controller.

6 Investigation of supercritical fluid recycle for surge control

The previous chapter has proposed a model predictive controller able to control the compression system according to the desired control purposes. Various tunings have been employed in order to give priority respectively to the energy saving, the control of surge or the control of pressure.

It has already been mentioned that the compression stage employed was compressing the process fluid from subcritical to supercritical conditions. Compressing carbon dioxide to supercritical pressure and temperature requires the implementation of some additional features into the model of the compressor. These features will be further explained in this chapter. Moreover the effect of the temperature of the recycle will be analysed.

Common recycle configurations include hot gas recycle and cold gas recycle, as explained in Chapter 3. The motivations for the selection of the type of recycle configuration usually include the temperature profile of the gas along the machine and the response delay for surge protection. However in this chapter a further issue will be investigated. It will be demonstrated that the temperature of the gas along the recycle line influences the operation of the compressor, its control and also the occurrence of surge.

The chapter is structured in the following way. Section 1 presents the main tasks that the chapter will fulfil. Section 2 presents the case study and the features of the model of the compressor. It also includes the analysis of the disturbance scenarios, the evaluation of the performance of the controller and the control system adopted. In section 3 the two recycle configurations will be tested and compared during various disturbance scenarios. Section 4 will focus on the operation in recycle mode, in order to emphasise the effect of the temperature of the recycle on the operation of the compressor. Section 5 will analyse operation in full recycle, comparing subcritical and supercritical operation. Finally section 6 will summarise the content of the chapter and its main highlights.

6.1 Task description

The purpose of this chapter is to understand the effect of the recycle temperature on the operation of the closed-loop compression system. In order to achieve this goal, two process configurations will be compared:

- The hot gas recycle configuration
- The cold gas recycle configuration.

These configurations will be tested during various disturbance scenarios and under the control of the same control system. The temperature of the recycled gas affects both the recycle flow rate and the location of the surge line. Therefore the chapter will give insights on this phenomenon by analysing the operation of the compressor during boundary disturbances.

The initial general purpose has been divided in the following tasks:

- Task 1: analysis of disturbance scenarios causing gas recycling
- Task 2: verification of surge avoidance during disturbance scenarios
- Task 3: estimation of control performance in terms of pressure control and stability of the closed-loop system
- Task 4: estimation of the energy consumption of the system
- Task 5: analysis of full recycle operation in subcritical and supercritical gas compression.

The first task helps to identify which disturbance scenarios cause the opening of the recycle valve and therefore the operation of the compressor in partial or full recycle mode. These disturbance scenarios can either:

- Cause the reduction of the compressor inlet mass flow rate on their own
- Cause a reaction of the pressure controller that pushes the compression system towards the surge line and therefore causes the opening of the antisurge valve by the antisurge controller.

The second task verifies if a process configuration is able to avoid surge within a certain safety margin between surge and control line. This ability depends on many factors and the temperature of the recycle is one of them.

The third tasks evaluates if the recycle configuration influences the performance of the overall system in terms of pressure control but also in terms of overall stability of the system.

Task 4 aims at estimating the energy consumption of the process during partial recycle operation.

Finally the fifth task requires the understanding of the implication of supercritical compression on compressor operation and control. The comparison between subcritical and supercritical compression is challenging because of the operational range of the compressor. Chapter 5 has already introduced a case study where the carbon dioxide is compressed from subcritical pressure and temperature to supercritical pressure and temperature. This chapter will give more insights on the issues related with supercritical compression.

6.2 Analysis of disturbance scenarios

In this section of the chapter the ESD case study is presented, together with some features of supercritical compression. These features have been implemented in the Simulink model of the compressor in order to take into account the compression of the process fluid to supercritical pressure and temperature. The disturbance scenarios are proposed and justified and the performance indicators are summarised and explained. Finally the control system implemented in the closed loop configuration is presented.

6.2.1 Case study

The case study employed in this chapter has already been introduced. It is based on a multistage centrifugal compressor arranged in a single shaft configuration and driven by an asynchronous electric motor. The fourth compression stage has been employed for the analyses presented in this chapter. This stage is the last stage of compression and it is the stage compressing the process fluid from subcritical condition to supercritical condition. It has been employed for analysing the effect of the recycle configuration on the compressor operation when dealing with supercritical state. In order to do so, two recycle configurations have been employed:

- The hot gas recycle configuration, presented in Chapter 3.2.2.1 and also employed in Chapter 5
- The cold gas recycle configuration, presented in Chapter 3.2.2.2.

Even at the lowest rotational shaft speed and minimum allowable flow rate, the fourth compressor compresses the process fluid to supercritical conditions. This means that the CO_2-rich fluid leaving the compression stage is always above its critical pressure and temperature. The only occasion in which the outlet fluid is not in supercritical state is during the start-up and shut-down of the machine. However these transient operations cannot be considered representative of the normal operation of the compressor. Therefore the third stage of compression has been employed in order to compare subcritical compression and supercritical compression during full-recycle operation. The third stage has the same model and runs at the same rotational shaft speed as the fourth stage of compression. Therefore in summary:

- The third stage of compression has been employed as representative of subcritical compression
- The fourth stage of compression has been employed as representative of supercritical compression.

After the analyses have been completed, the results have been scaled according to the inlet conditions of each compression stage. This is because of the non-disclosure agreement with the partners of the project.

6.2.1.1 Enthalpy of vaporisation

When a fluid is above its critical pressure and temperature, its behaviour deviates significantly from that of an ideal gas. This phenomenon is reflected in some specific features of the model of the compressor. In particular a supercritical fluid is characterised by high density and low viscosity. Therefore it has some properties in common with the gas phase and some properties in common with the liquid phase.

At this point it is important to notice that the state change from subcritical gas to supercritical fluid does not involve any enthalpy of vaporisation. In fact the critical point is characterised by enthalpy of vaporisation equal to zero, as represented in Figure 6-1.

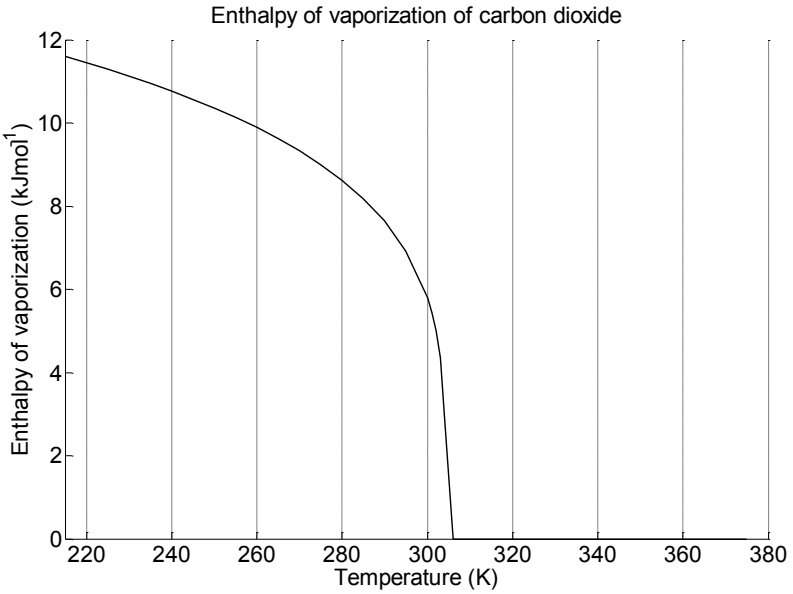


Figure 6-1. Enthalpy of vaporization of carbon dioxide as a function of the temperature of the gas (modified from Knovel (2015))

6.2.1.2 Gas compressibility and equation of state

For an ideal gas, at low pressure and temperature, the equation of state is the ideal gas law:

$$pV = ZnRT \tag{6-1}$$

where p is the pressure of the gas, V is the volume, n is the number of moles, R is the ideal gas constant and T is the temperature. The compressibility factor Z is a function of both pressure and temperature of the gas and it is equal to 1 for ideal gas condition.

When the gas is not ideal, such as at high temperature and pressure, equation (6-1) must be modified in order to take into account the variation of the compressibility of the gas. The influence of the pressure of the gas on Z is stronger than the influence of the temperature. In fact at atmospheric pressure and for temperature greater than the critical temperature the variation of Z is lower than 1% (Coulson et al., 1999).

Many other equations of state have been proposed and employed in order to estimate the properties of a non-ideal gas. The most commonly employed equations of state for carbon dioxide in supercritical state have been presented in Chapter 2 and include:

- Peng-Robinson equation of state (Peng and Robinson, 1976)
- Soave-Redlich-Kwong equation of state (Soave, 1972)
- Span and Wagner equation of state (Span and Wagner, 1996).

The Span and Wagner equation of state gives good prediction for pure or almost pure carbon dioxide (Aursand et al., 2013). For this reason it has been employed in the past for the three-dimensional computational fluid dynamic analysis of a high speed centrifugal compressor operating with supercritical carbon dioxide (Pecnik et al., 2012) and it has been selected also for the current study. This equation has been employed in order to define the density of the gas depending on its pressure and temperature. The density has been implemented in the simulation tool by means of a look-up table with linear interpolation method. As the dimension of the table has a size limit due to computational issues, the look-up table employed for the fourth stage of compression covered the temperature range 330.15-523.15 K and the pressure range 40-260 bar (Anwar and Carroll, 2010).

6.2.1.3 Compressor outlet temperature

For low temperature and pressure, the temperature of the fluid at the exit of the compressor can be estimated using the equation from Camporeale et al. (2006) presented in Chapter 3:

$$T_{02} = T_{01}\left[1 + \frac{1}{\eta_p}\left(\Psi_c^{\,(k-1)/k} - 1\right)\right] \quad \textbf{(3-18)}$$

where T_{01} and T_{02} are the temperature of the gas respectively at the inlet and at outlet of the compressor, η_p is the polytropic efficiency, Ψ_c is the pressure ratio, $k = {c_p}/{c_v}$ is the heat ratio and $T_m = {(T_{01} + T_{02})}/{2}$. However, for the supercritical compression the map of the compressor outlet temperature had to be employed because the condition of the process fluid is far from ideal and therefore the function proposed by Camporeale et al. (2006) (equation (3-18)) is no longer valid.

6.2.2 Disturbances analysis and selection

The types of disturbance have been selected according to the scenarios proposed in the literature and employed for compressor and surge control validation. Disturbance variables include:

- Opening position of the inlet valve op_{in}
- Opening position of the outlet valve op_{out}
- Inlet pressure of the system p_{in}
- Outlet pressure of the system p_{out}.

The types of the disturbances include negative (for the boundary valves) and positive and negative (for the boundary pressures) step changes. The magnitudes of the disturbances have been selected taking into account:

- The variation of inlet and outlet pressure and temperature during off-load operation
- The effect of the disturbance on the system, such as gas recycling and surge occurrence.

The model of the compression system has been tested by changing the value of the single boundary disturbances. The results of the analysis are summarised in Table 4-2. The magnitudes of the disturbances are different from the magnitudes of the disturbances presented in Table 5-2. The reason is that Chapter 5 presented a single type of compressor configuration, having a hot gas recycle. In this chapter, the operations of two different configurations, having respectively hot or cold gas recycle, are compared. Therefore it has been necessary to determine a range of disturbance magnitudes that was suitable for both configurations. In fact the operating range of the two process configurations is not the same.

Step changes have been employed for all the disturbance variables. All the simulations have been performed for 1800 s and all disturbances started at time t=10s.

Table 6-1. Maximum variation for the disturbance variables during boundary disturbances

Boundary variable	Maximum variation
p_{in}	-15 to 53%
op_{in}	-88%
p_{out}	-0.44 to 0.38%
op_{out}	-30%

6.2.3 Evaluation of performance for a controller

In order to estimate the performance of the controller and also the effect of the recycle configuration of the operation of the compressor, some performance indicators have been employed.

The performance of the controller in terms of pressure control has been estimated by employing the parameter ISE_p previously introduced.

The performance of the controller in terms of surge control has been estimated by graphical representation of the compressor inlet flow rate m and the surge flow rate m_{surge}. Surge took place when the lines representing these two variables crossed each other.

The power consumption of the machine has been estimated by employing the parameter M and E. The parameter E_{tot} is here introduced and it is defined according to the following equation:

$$E_{tot} = \frac{\int_{t=0}^{t_{final}} (P_m - Q)dt}{\int_{t=0}^{t=1h} P_m dt} \quad \textbf{(6-2)}$$

where P_m is the power consumption of the compression due to the compression process itself and Q is the flow rate of heat removed from the recycled gas in the cold gas recycle configuration. Therefore in the hot gas recycle configuration E_{tot} depends only on P_m while in the cold gas recycle configuration it depends on both P_m and Q. Q is always equal to 0 or negative as the heat flow is leaving the system and not provided to the system.

6.2.4 Control system implementation

The control system that has been adopted for the comparisons of hot and cold recycles, as explained in the next section, is the PI control system introduced in Chapter 3. It is composed of two controllers. The capacity controller has a cascade structure with a speed controller in the slave loop and a pressure controller in the master loop. The manipulated variable of the capacity controller is the torque provided by the driver. The antisurge control is a PI feedback controller and it acts on the antisurge valve when the compressor inlet flow rate m is lower than the control flow rate m_{ctrl}. The tuning of the control system has already been presented in Chapter 5.

The reason for employing a traditional multiple-loop control system is that this is the most popular control system adopted in industrial application, as has been explained in Chapter 2.

6.2.5 Summary

This section of the chapter has presented the case study and the features implemented in the model of the compressor in order to account for the supercritical compression. The fourth stage of compression has been employed in the simulation of supercritical compression operation. The third stage of compression has been employed later on in the chapter in the simulation of subcritical compression operation. The disturbance scenarios have been proposed and they will be employed for the comparison between hot gas recycle configuration and cold gas recycle configuration. Finally the performance indicators have been summarised and the implemented control system explained.

6.3 Preliminary analysis

In this part of the chapter the hot gas recycle configuration and the cold gas recycle configuration for the fourth stage of compression have been tested and compared. Boundary disturbances have been employed in order to analyse the response of the overall control system and the influence of the temperature of the recycled gas on the stability of the system. The main purposes of the analysis are:

- The study of the response of the cold gas recycle configuration to boundary disturbances
- The comparison between the two process configurations during gas recycling.

The hot gas recycle configuration has already been employed in Chapter 5 while the cold gas recycle configuration is here tested for the first time.

6.3.1 Steady-state operation

Table 6-2 reports the value of the performance indicators for steady state operation at the design point of the closed-loop system. As the recycle line is not involved and the antisurge valve is closed, this table reflects both hot and cold recycle configurations. In fact they differ only when the recycle valve is open.

As expected for this type of operation, ISE_p is equal to 0. This means that the compressor outlet pressure is at its set point during the full simulation. M is equal to 0 as the recycle valve is closed. E is equal to 0.5 as the power consumption of the system over half an hour of operation is scaled using the power consumption of one hour of operation at steady state. Finally Q is equal to 0 as M is equal to 0. Therefore E_{tot} is equal to E.

Table 6-2. Steady state operation at the design point

Scenario	0 – steady state at design point
ISE_p (bar^{2}s)	0.00
M (-)	0.00
E (-)	0.50
Q (-)	0.00
E_{tot} (-)	0.50

6.3.2 Inlet valve of the system

6.3.2.1 Hot gas recycle configuration

Table 6-3 reports the results of the hot gas recycle configuration when the inlet valve of the system closes from the fully open position to partially open position. The sign and magnitude of the disturbance are indicated in the table. For example for the first disturbance scenario the valve closes by -20%: this means that it moves from fully open position (100% opening) to 80% opening position.

The table also summarises ISE_p, M, E, Q and E_{tot} for each disturbance scenario. Q is always equal to 0 as the hot gas recycle configuration is adiabatic and there is no heat removal during its operation. Red numbers for disturbance scenarios indicate that during that scenario the compressor experienced surge. Surge takes place when the compressor inlet flow rate m and the surge mass flow rate m_{surge} cross each other.

The results collected in the table reflect what has already been reported in Chapter 5 for similar disturbance scenarios and same process configuration. The results can be summarised in the following way:

- ISE_p increases with the increase of the magnitude of the disturbance
- M is equal to 0 for the first two scenarios and then become positive when the recycle valve opens. It also increases with the increase of the magnitude of the disturbance as more recycled gas is necessary
- E increases for the first two scenarios while it decreases during the second two scenarios. This is because in scenarios 1 and 2 the inlet temperature of the compressor remains constant while the inlet mass flow rate decreases slightly and the compressor outlet temperature increases, therefore the power consumption increases. However during scenarios 3 and 4 the mass flow rate through the compressor is much smaller than its design value and this affects P_m and therefore E
- Q is always equal to 0 and therefore E_{tot} is equivalent to E.

However a stronger disturbance scenario has been tested this time (scenario 4) and it has caused the surge of the compressor. The values of the performance parameters have been reported in the table. However it has been assumed that the compressor did not fall into deep surge, which would have involved negative flow rate. Therefore the value of the performance parameters for this scenario should be employed more for a qualitative rather than quantitative analysis.

6.3.2.2 Cold gas recycle configuration

Table 6-4 reports the results of the same disturbance scenarios when the compressor configuration includes a cold gas recycle. For disturbance scenarios 1 and 2 there is no difference between the response of the cold gas configuration and the hot gas configuration as the recycle valve does not open. However when the action of the antisurge controller opens the recycle valve the response of the two configurations differs. In fact the cold gas recycle configuration surges during both scenario 3 and scenario 4. The reason for that can be explained by analysing scenario 3, which has been selected for graphical representation.

Figure 6-2 represents the mass flow rate of the compressor with the hot gas recycle configuration. The quantity m is the compressor inlet mass flow rate, m_{ctrl} is the control mass flow rate and m_{surge} is the surge mass flow rate. The margin between m_{surge} and m_{ctrl} is 20%. When m and m_{ctrl} cross each other the antisurge controller opens the recycle valve. Figure 6-3 represents the same variables for the cold gas recycle configuration.

6.3.2.3 Comparison of recycle configurations

When comparing Figure 6-2 and Figure 6-3, it is possible to see the effect of the recycle temperature on the operation of the controller. In fact in the hot gas recycle configuration when m and m_{ctrl} cross each other the antisurge valve opens. When it opens, both the compressor inlet pressure p_{01} and the inlet temperature T_{01} increase. However the temperature changes significantly, while the pressure change is small and therefore this affects the surge flow rate. In particular m_{surge} decreases and therefore m_{ctrl} decreases as well. The reason can be understood by looking at equation (3-11):

$$m_{surge,c} = \frac{m_{surge}\sqrt{T_{01}/T_{ref}}}{p_{01}/p_{ref}} \tag{3-11}$$

When the antisurge valve opens, both T_{01} and p_{01} increase, while $m_{surge,c}$ remains constant due to the definition of corrected compressor map and therefore m_{surge} decreases. The consequence is that m_{ctrl} becomes smaller than m and the antisurge controller closes the recycle valve. However this action decreases p_{01} and T_{01} and when m_{ctrl} becomes bigger than m the cycle repeats.

In the cold gas recycle configuration when m and m_{ctrl} cross each other and the antisurge valve opens, p_{01} increases while T_{01} does not. This is because the recycled gas is cooled down from the outlet temperature of the compressor T_{02} to the same temperature as the freshly fed gas T_{in}. Therefore the compressor inlet temperature T_{01} is constant and equal to T_{in}. For this reason m_{ctrl} increases even further and therefore the recycle valve remains open. This causes the decrease of the compressor outlet pressure p and therefore the pressure controller increases the driver torque. This action increases m until it becomes bigger than m_{ctrl}. At this point the recycle valve closes, the compressor outlet pressure increases and the pressure controller decreases the drive torque. The consequence is that the compressor inlet mass flow rate m decreases until it crosses m_{ctrl}, the recycle valve opens again and the cycle repeats. The reason why m_{surge} increases when the antisurge valve is closed is that m is decreasing while p is increasing. Therefore the pressure ratio is increasing and m_{surge} too. This is what happens during scenario 3 where the driver is running at its maximum speed.

Therefore both recycle configurations oscillate because of the boundary disturbance and in particular the antisurge valve opens and closes over time. However the frequency of oscillation of the cold recycle configuration is lower than the frequency of oscillation of the hot recycle configuration. At this point it is clear why the cold gas recycle configuration surges at a smaller disturbance magnitude compared with the hot gas recycle configuration. This is due to the effect of the recycle temperature on the surge value. When the recycle valve opens the change in the surge flow rate is rapid and can push m_{surge} above m, as represented in Figure 6-3.

Figure 6-4 compares the compressor outlet pressure of the hot gas recycle configuration (p_{HGR}) and of the cold gas recycle configuration (p_{CGR}) during disturbance scenario 3. For the same disturbance scenario, Figure 6-5 shows the manipulated variables of the system. As a reminder, τ is the driver trorque while op_{asv} is the opening of the antisurge valve.

Table 6-3. Disturbance scenarios for the inlet valve of the system for hot gas recycle configuration

Disturbance scenario	1	2	3	4
Sign and magnitude (%)	-20.00	-65.00	-79.00	-88.00
ISE_p (bar^{2}s)	0.11	23.37	6220.31	46866.21
M (-)	0.00	0.00	0.02	4.84
E (-)	0.50	0.56	0.42	0.34
Q (-)	0.00	0.00	0.00	0.00
E_{tot} (-)	0.50	0.56	0.42	0.34

Table 6-4. Disturbance scenarios for the inlet valve of the system for cold gas recycle configuration

Disturbance scenario	1	2	3	4
Sign and magnitude (%)	-20.00	-65.00	-79.00	-88.00
ISE_p (bar^{2}s)	0.11	23.39	9252.67	334701.69
M (-)	0.00	0.00	0.63	4.17
E (-)	0.50	0.56	0.45	0.41
Q (-)	0.00	0.00	-0.08	-0.51
E_{tot} (-)	0.50	0.56	0.52	0.93

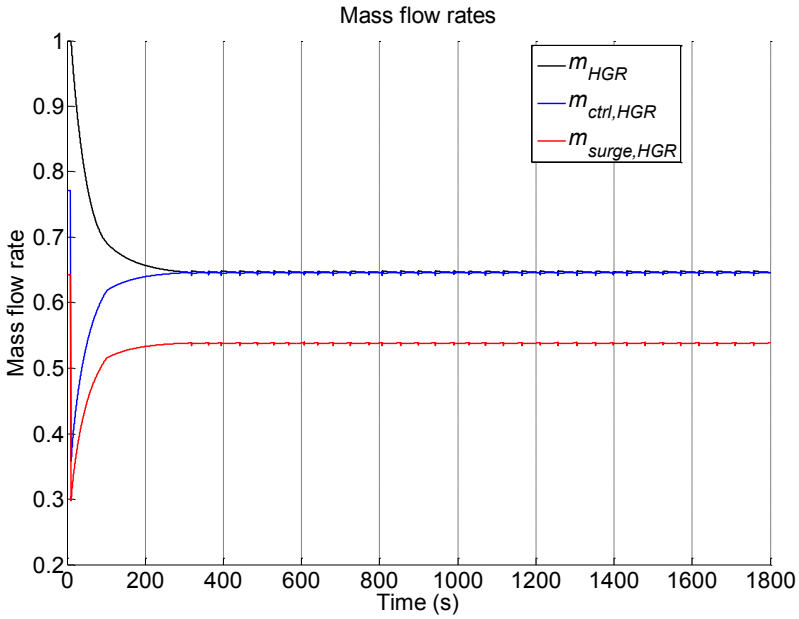


Figure 6-2. Mass flow rates for hot gas recycle configuration (disturbance scenario 3)

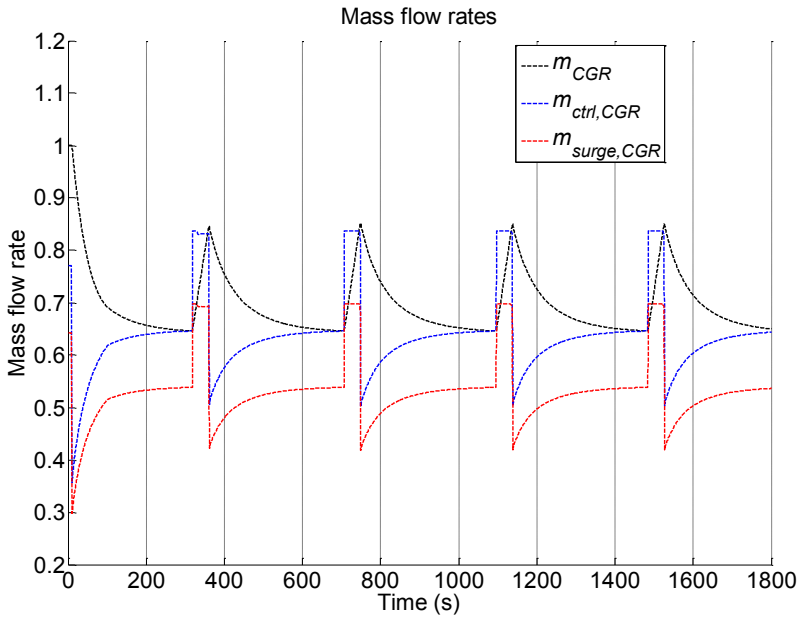


Figure 6-3. Mass flow rates for cold gas recycle configuration (disturbance scenario 3)

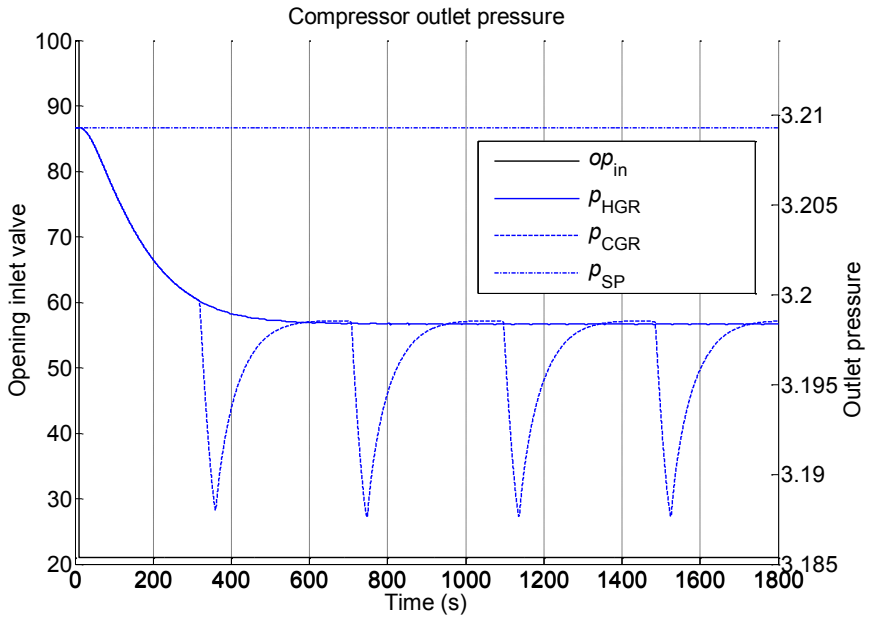


Figure 6-4. Compressor outlet pressure (disturbance scenario 3)

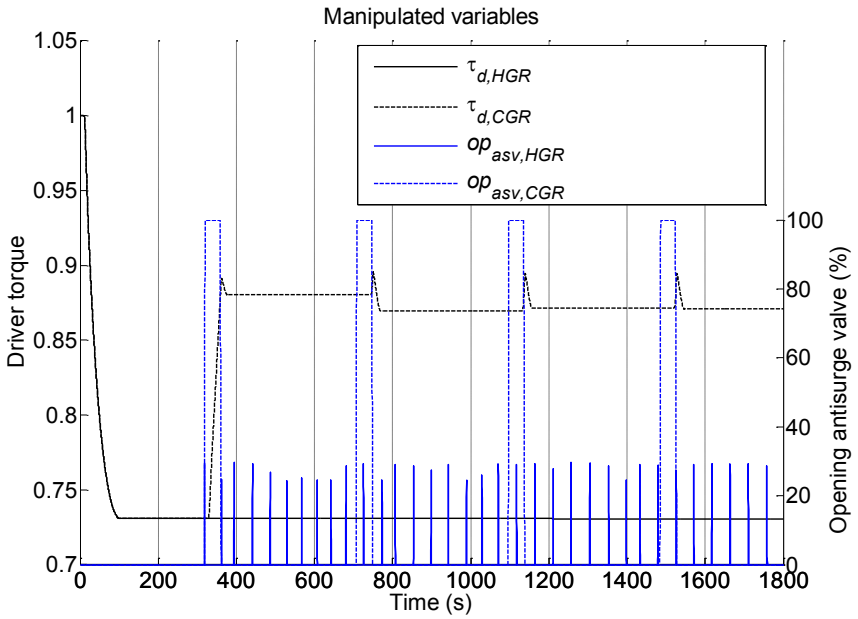


Figure 6-5. Manipulated variables (disturbance scenario 3)

6.3.3 Outlet valve of the system

Table 6-5 reports the results of the hot gas recycle configuration when the outlet valve of the system closes from the fully open position to a partially open position. The sign and magnitude of the disturbance is indicated in the table. For example for disturbance scenario 5 the valve closes by -15%: this means that the outlet valve moves from fully open position (100% opening) to 85% opening position. Scenario 0 has been repeated for direct comparison.

The results collected in this table can be summarised in the following way:

- ISE_p increases with the increase of the magnitude of the disturbance
- M is equal to 0 for the first two scenarios and then become positive when the recycle valve opens. It also increases with the increase of the magnitude of the disturbance as more recycled gas is necessary
- E decreases and this is mainly because m decreases over time due to the decrease of the rotational shaft speed N
- Q is always equal to 0 and therefore E_{tot} is equivalent to E.

Table 6-6 reports the results of the same disturbance scenarios when the compressor configuration includes a cold gas recycle. For disturbance scenarios 0 and 5 there is no difference between the response of the cold gas configuration and the hot gas configuration as the recycle valve does not open. However when the action of the antisurge controller opens the recycle valve the response of the two configurations differs. In fact in the cold gas recycle configuration:

- ISE_p increases with the increase of the magnitude of the disturbance

- M is equal to 0 for the first two scenarios and then become positive when the recycle valve opens. It also increases with the increase of the magnitude of the disturbance as higher recycled gas is necessary
- E decreases with the increasing of the disturbance magnitude. It is higher in scenarios 6 and 7 than in scenario 5 because the interaction between pressure and surge controller causes the oscillation of the system and increases m with respect to scenario 5
- Q increases with the increase of the amount of gas recycled and this cause the increase of E_{tot} when the recycle valve opens.

However when comparing the hot configuration with the cold configuration:

- The hot recycle configuration has a better pressure control performance. In fact it has a lower ISE_p than the cold gas recycle configuration. This is due to the oscillation of the cold recycle system due to the interaction between the control loops
- The hot recycle configuration shows also smaller overall power consumption. This is due to both E and Q. The reason is that the mass flow rate through the compressor m is lower in the hot gas recycle configuration. Moreover this configuration does not require the cooling of the recycled gas
- None of the tested disturbance scenarios caused the surge of the compressor, in any of the recycle configurations.

Scenario 6 has been employed to represent and compare the response of the two configurations. The mass flow rates of the hot recycle configuration are represented in Figure 6-6 while the flow rates of the cold recycle configuration are represented in Figure 6-7.

In the hot recycle configuration m and m_{ctrl} cross each other when the action of the pressure controller decreases the torque of the driver in order to decrease the rotational shaft speed of the machine and consequently the compressor outlet pressure. The recycle valve oscillates at high frequency and this is because of the effect of the hot recycled gas on the location of surge. This effect has already been presented above and also in Chapter 5.

In the cold gas configuration the opening of the recycle valve increases m_{surge} and therefore m_{ctrl}. The consequence is that the recycle valve stays open until the compressor outlet pressure p decreases. When this happens the pressure controller increases the driver torque and the consequence is the increase of m that become bigger than m_{ctrl}. Therefore the antisurge valve closes.

Figure 6-8 compares the compressor outlet pressure of the two process configuration during disturbance scenario 6. During the same disturbance scenario, Figure 6-9 shows the manipulated variables of the two configurations. They include the torque of the driver and the opening of the antisurge valve.

As a summary it is possible to say that the disturbance scenario 6 has caused the oscillation of both hot and cold recycle configurations. This oscillation was mainly caused by the effect of the recycle on the location of the surge region. However in the cold recycle configuration it was also caused by the interaction between pressure controller and surge controller. Therefore the result is that the hot gas

recycle oscillates at high frequency for a short period of time and then stabilises at a new set point. The cold recycle configuration instead continues to oscillate, however at a lower frequency.

Table 6-5. Disturbance scenarios for the outlet valve of the system for hot gas recycle configuration

Disturbance scenario	0	5	6	7
Sign and magnitude (%)	0	-15	-21	-29
ISE_p (bar^{2}s)	0.00	31.39	76.61	759.65
M (-)	0.00	0.00	0.02	0.49
E (-)	0.50	0.42	0.39	0.38
Q (-)	0.00	0.00	0.00	0.00
E_{tot} (-)	0.50	0.42	0.39	0.38

Table 6-6. Disturbance scenarios for the outlet valve of the system for cold gas recycle configuration

Disturbance scenario	0	5	6	7
Sign and magnitude (%)	0	-15	-21	-29
ISE_p (bar^{2}s)	0.00	31.39	1553.64	3180.76
M (-)	0.00	0.00	0.61	1.13
E (-)	0.50	0.42	0.44	0.43
Q (-)	0.00	0.00	-0.07	-0.12
E_{tot} (-)	0.50	0.42	0.50	0.56

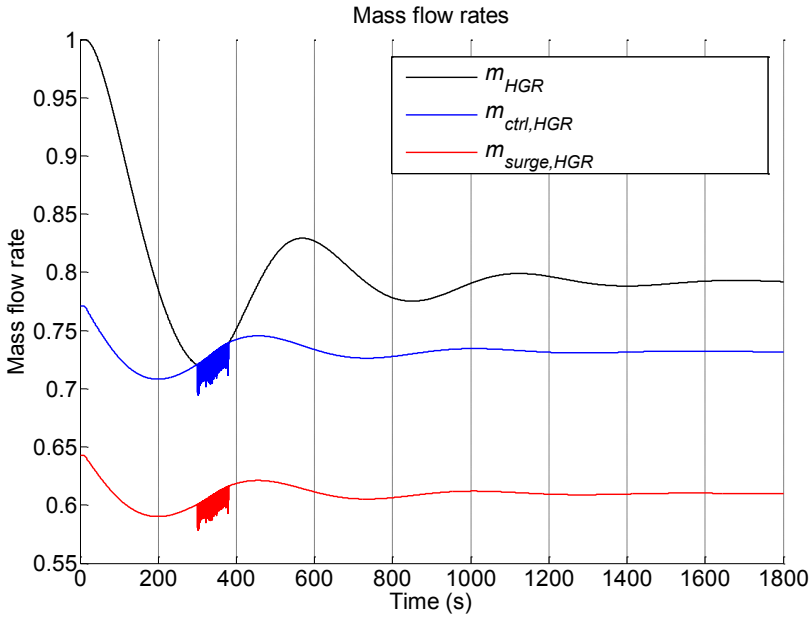


Figure 6-6. Mass flow rates for hot gas recycle configuration (disturbance scenario 6)

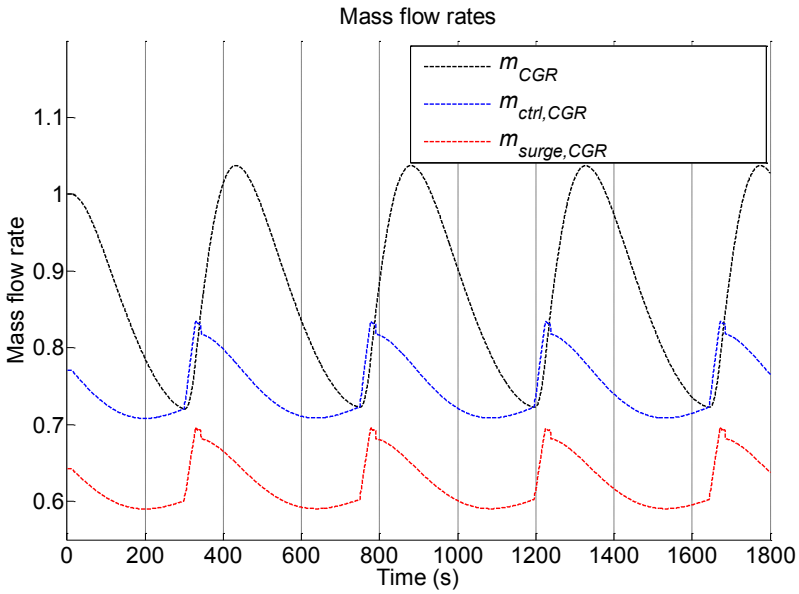


Figure 6-7. Mass flow rates for cold gas recycle configuration (disturbance scenario 6)

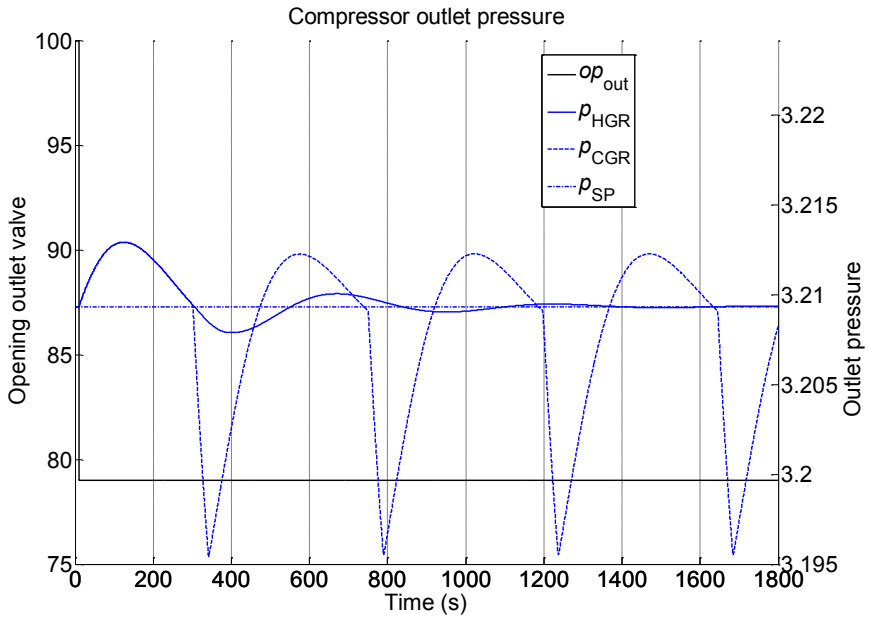


Figure 6-8. Compressor outlet pressure (disturbance scenario 6)

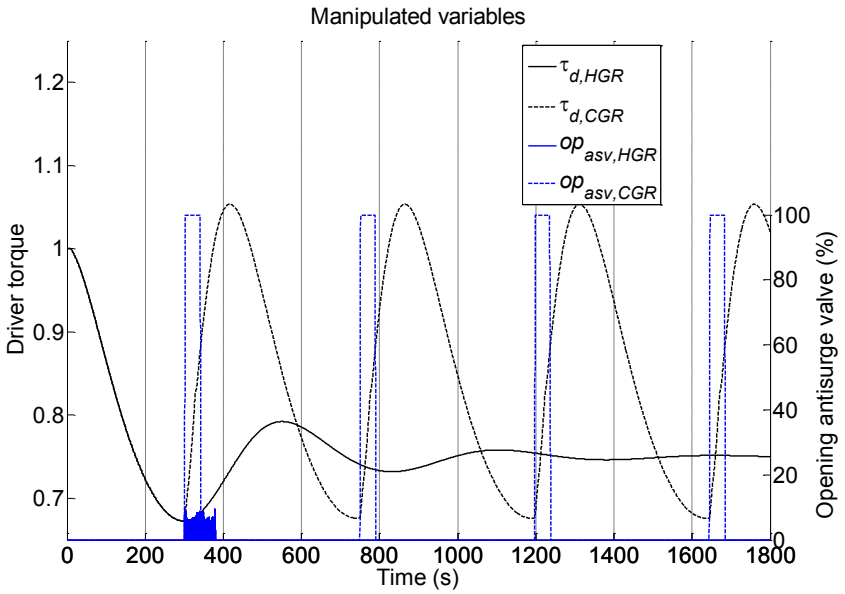


Figure 6-9. Manipulated variables (disturbance scenario 6)

6.3.4 Inlet pressure of the system

Table 6-7 reports the results of the hot gas recycle configuration when the inlet pressure of the system p_{in} changes following a negative (scenarios 8 and 9) or positive (scenarios 10 and 11) step change. The results collected in the table can be summarised in the following way:

- For the first two scenarios where the inlet pressure of the system decreases, ISE_p increases with the increase of the magnitude of the disturbance. M is equal to 0 as m is always above m_{ctrl} and E increases because the mass flow rate through the compressor increases
- For the second two scenarios where the inlet pressure of the system increases ISE_p increases with the increase of the magnitude of the disturbance. M is equal to 0 for scenario 10 and the positive for scenario 11 where gas recycling is necessary for surge prevention. E decreases because of the decreases of the mass flow rate m through the compressor.

Table 6-8 reports the results of the same disturbance scenarios when the compressor configuration includes a cold gas recycle. For disturbance scenarios 8, 9 and 10 there is no difference between the response of the cold gas configuration and the hot gas configuration as the recycle valve does not open.

However for scenario 11 the cold recycle configuration presents higher ISE_p, M and E_{tot} than the hot recycle configuration. The motivation for this behaviour can be understood by analysing controlled and manipulated variables over time. Figure 6-10 represents the mass flow rates for the hot recycle configuration while Figure 6-12 represents the mass flow rates for the cold recycle configuration. These two figures clearly represent how the recycled gas has a different impact on the system depending on its temperature. The initial impact of the disturbance on the two systems is the same and this is due to the increase of p_{01} due to the increase of p_{in}. When the inlet pressure of the compressor increases it causes the increase of m_{surge} and therefore m_{ctrl}, which become larger than m and causes the opening of the antisurge valve, as represented in Figure 6-11 and Figure 6-12.

However when the recycle valve opens the response of the two systems differs and the impact of the recycle temperature on the system is also due to the supercritical state of the fluid. In the hot recycle configuration when the antisurge valve opens both T_{01} and p_{01} increase and this causes the reduction of m_{ctrl}. Therefore it becomes smaller than m and the antisurge valve closes. This causes the oscillation of the valve until the action of the pressure controller causes the increase of m.

In the cold gas recycle configuration when the antisurge valve opens this causes the increase of p_{01} however T_{01} remains constant. The consequence is that m_{ctrl} increases even more and therefore the valve remains open for longer and does not oscillate. For this reason this configuration recycles more gas and therefore consumes more energy over time.

Figure 6-13 compares the outlet pressures of the compressor for the two configurations during disturbance scenario 11. For the same scenario Figure 6-14 compares the manipulated variables of the system under the two configurations. The image is zoomed even more in Figure 6-15, where it is possible to recognise the action of the rate limiter on the opening and closing of the antisurge valve in the hot gas recycle configuration.

Table 6-7. Disturbance scenarios for the inlet pressure of the system for hot gas recycle configuration

Disturbance scenario	**8**	**9**	**10**	**11**
Sign and magnitude (%)	-14.89	-1.28	15.74	49.79
ISE_p (bar^{2}s)	31.60	0.10	7.98	33.04
M (-)	0.00	0.00	0.00	0.03
E (-)	0.56	0.50	0.45	0.38
Q (-)	0.00	0.00	0.00	0.00
E_{tot} (-)	0.56	0.50	0.45	0.38

Table 6-8. Disturbance scenarios for the inlet pressure of the system for cold gas recycle configuration

Disturbance scenario	**8**	**9**	**10**	**11**
Sign and magnitude (%)	-14.89	-1.28	15.74	49.79
ISE_p (bar^{2}s)	31.60	0.10	7.98	132.18
M (-)	0.00	0.00	0.00	0.13
E (-)	0.56	0.50	0.45	0.38
Q (-)	0.00	0.00	0.00	-0.01
E_{tot} (-)	0.56	0.50	0.45	0.39

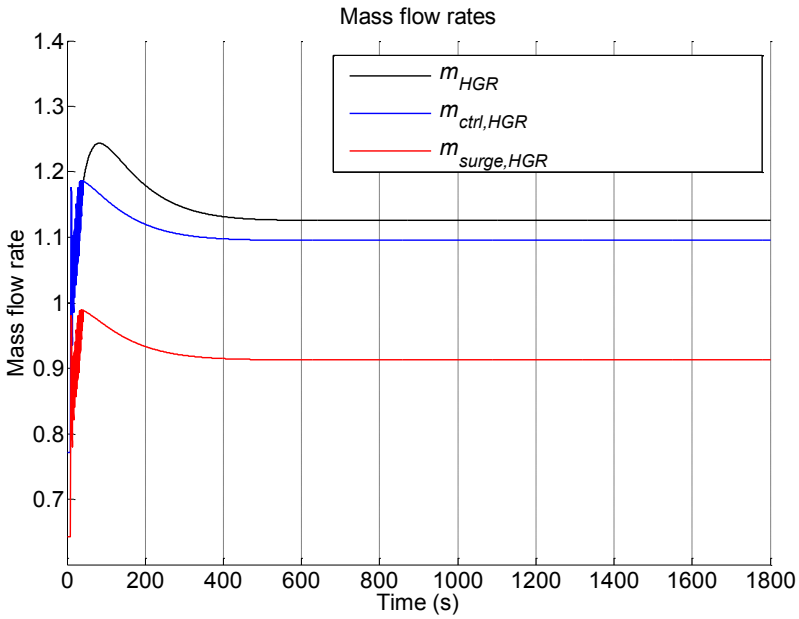


Figure 6-10. Mass flow rates for hot gas recycle configuration (disturbance scenario 11)

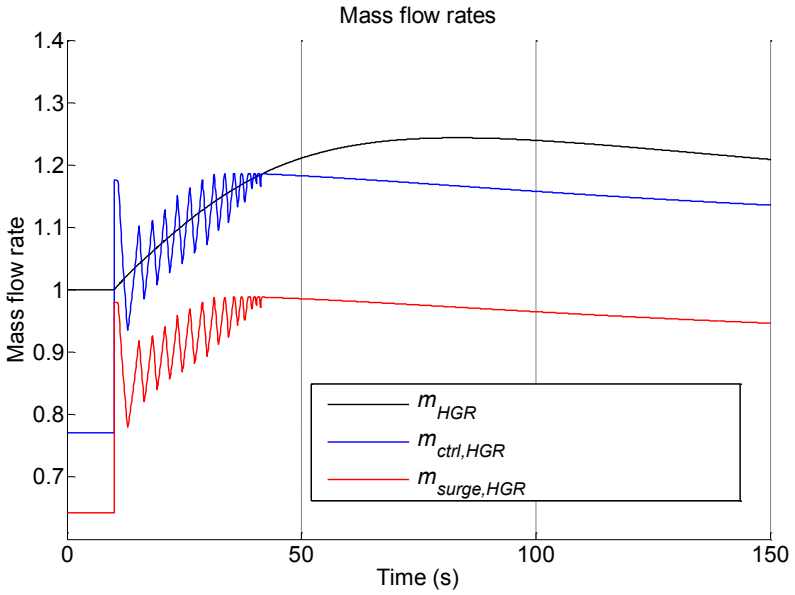


Figure 6-11. Mass flow rates for hot gas recycle configuration (disturbance scenario 11, zoomed view)

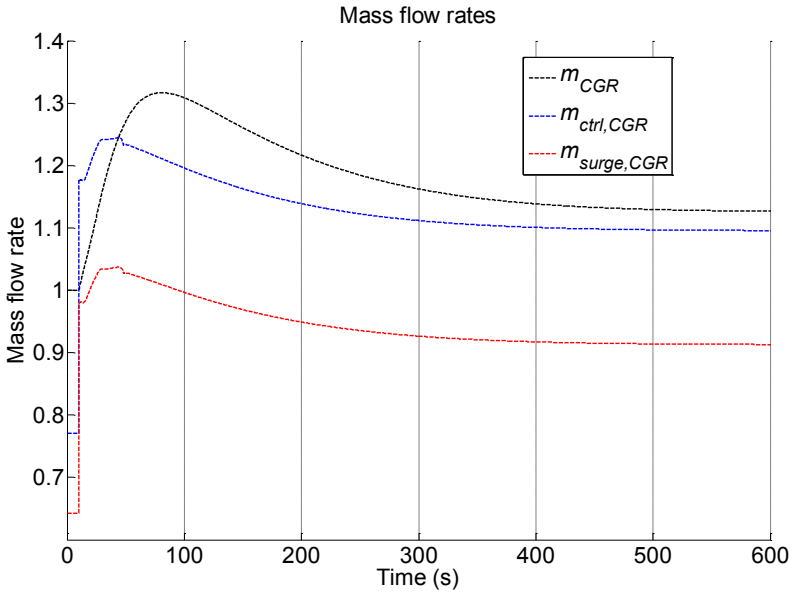


Figure 6-12. Mass flow rates for cold gas recycle configuration (disturbance scenario 11, zoomed view)

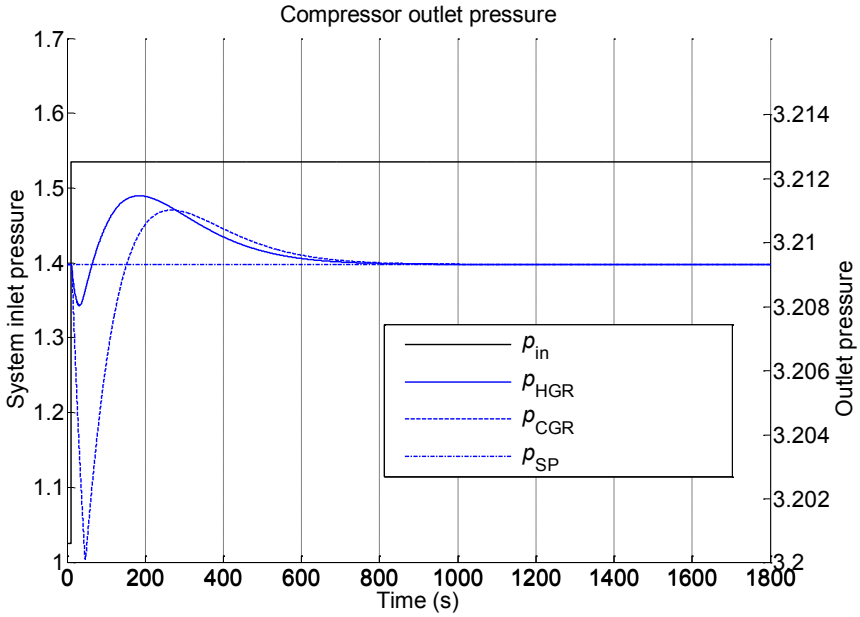


Figure 6-13. Compressor outlet pressure (disturbance scenario 11)

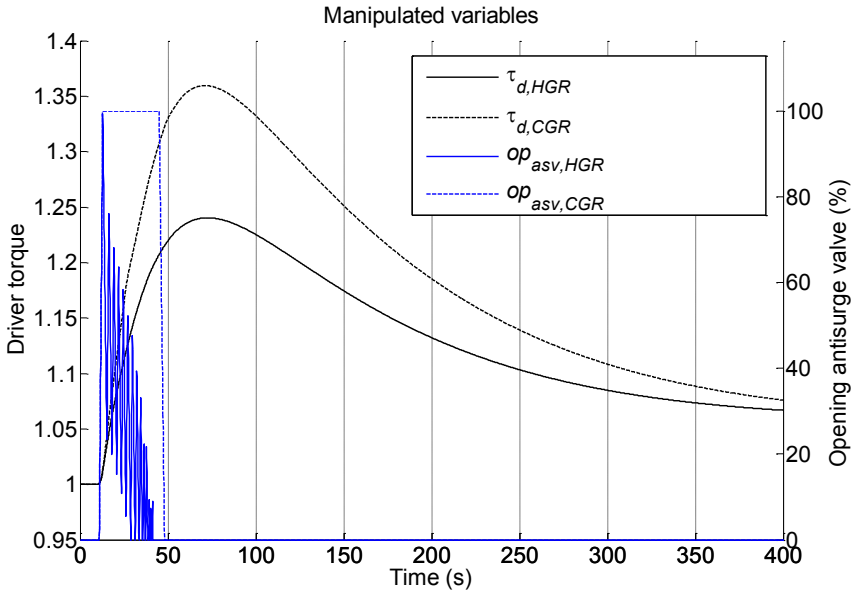


Figure 6-14. Manipulated variables (disturbance scenario 11, zoomed view)

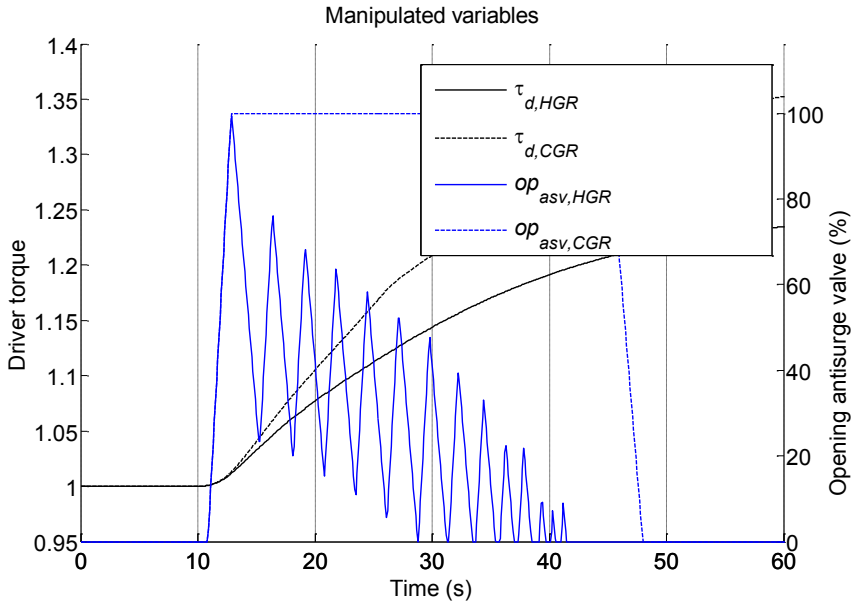


Figure 6-15. Manipulated variables (disturbance scenario 11, zoomed view)

6.3.5 Outlet pressure of the system

Table 6-9 reports the results of the hot gas recycle configuration when the outlet pressure of the system changes because of negative (scenarios 12 and 13) and positive (scenarios 14 and 15) step disturbances. The results collected in the table can be summarised in the following way:

- For the first two scenarios where the outlet pressure of the system decreases, ISE_p increases with the increase of the magnitude of the disturbance. M is equal to 0 as m is always above m_{ctrl} and E increases because of the increase of the inlet mass flow rate
- For the second two scenarios where the outlet pressure of the system increases, ISE_p increases with the increase of the magnitude of the disturbance. M is equal to 0 for scenario 14 and the positive for scenario 15 where gas recycling is necessary for surge prevention. E decreases because of the decrease of the compressor inlet mass flow rate.

Table 6-10 reports the results of the same disturbance scenarios when the compressor configuration includes a cold gas recycle. For disturbance scenarios 12, 13 and 14 there is no difference between the response of the cold gas configuration and the hot gas configuration as the recycle valve does not open.

However for scenario 15 the cold recycle configuration presents higher ISE_p, M and E_{tot}. This is because of the high oscillation of the control system in the cold gas recycle configuration. This scenario has also been represented in the following figures. Figure 6-16 represents the mass flow rates for the hot gas recycle configuration while Figure 6-18 represents the mass flow rates for the cold gas recycle configuration. Both systems oscillate because of the pressure disturbance. However, as happened during scenario 6, the frequency of oscillation of the antisurge valve is higher in the hot configuration than in the cold configuration. This is due to the effect of the recycled gas on the location of the surge region. The compressor outlet pressure for both configurations is represented in Figure 6-19 while the manipulated variables are represented in Figure 6-20. In the hot gas recycle configuration the amplitude of oscillation of the driver torque is smaller than in the cold gas recycle configuration. At the same time however the frequency of oscillation of the antisurge valve is higher in the hot recycle configuration than in the cold recycle configuration.

Table 6-9. Disturbance scenarios for the outlet pressure of the system for hot gas recycle configuration

Disturbance scenario	12	13	14	15
Sign and magnitude (%)	-0.44	-0.11	0.11	0.33
ISE_p (bar^{2}s)	2509.72	8.30	8.84	152.19
M (-)	0.00	0.00	0.00	0.29
E (-)	0.58	0.54	0.46	0.37
Q (-)	0.00	0.00	0.00	0.00
E_{tot} (-)	0.58	0.54	0.46	0.37

Table 6-10. Disturbance scenarios for the outlet pressure of the system for cold gas recycle configuration

Disturbance scenario	12	13	14	15
Sign and magnitude (%)	-0.44	-0.11	0.11	0.33
ISE_p (bar^{2}s)	2509.66	8.30	8.84	1371.86
M (-)	0.00	0.00	0.00	1.00
E (-)	0.58	0.54	0.46	0.41
Q (-)	0.00	0.00	0.00	-0.11
E_{tot} (-)	0.58	0.54	0.46	0.52

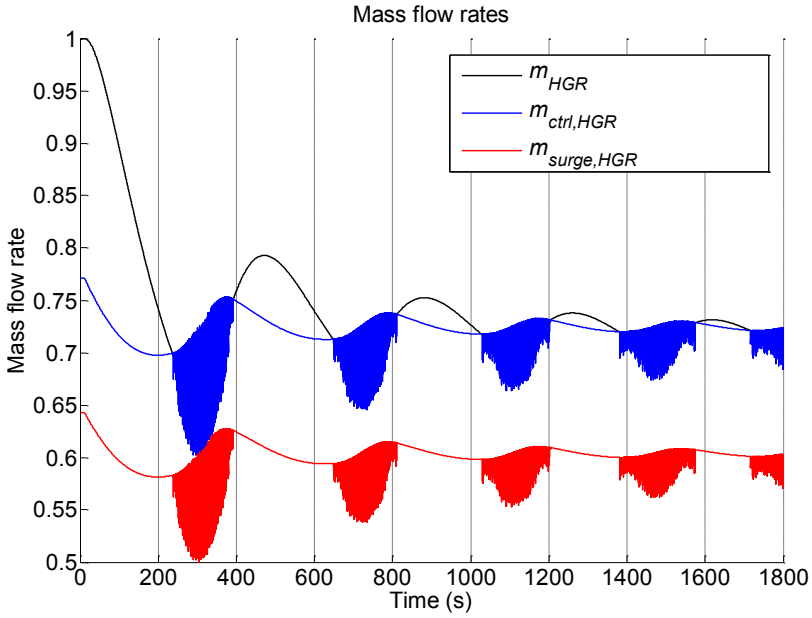


Figure 6-16. Mass flow rates for hot gas recycle configuration (disturbance scenario 15)

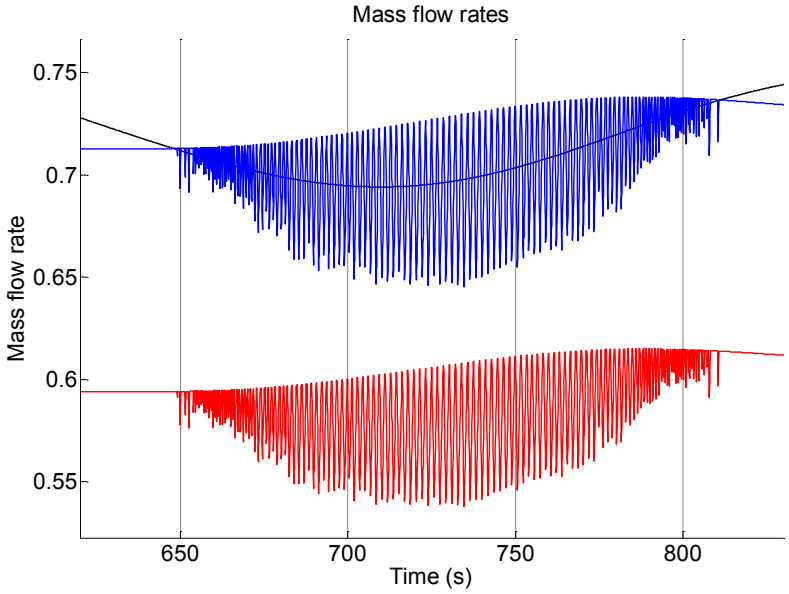


Figure 6-17. Mass flow rates for hot gas recycle configuration (disturbance scenario 15, zoomed view)

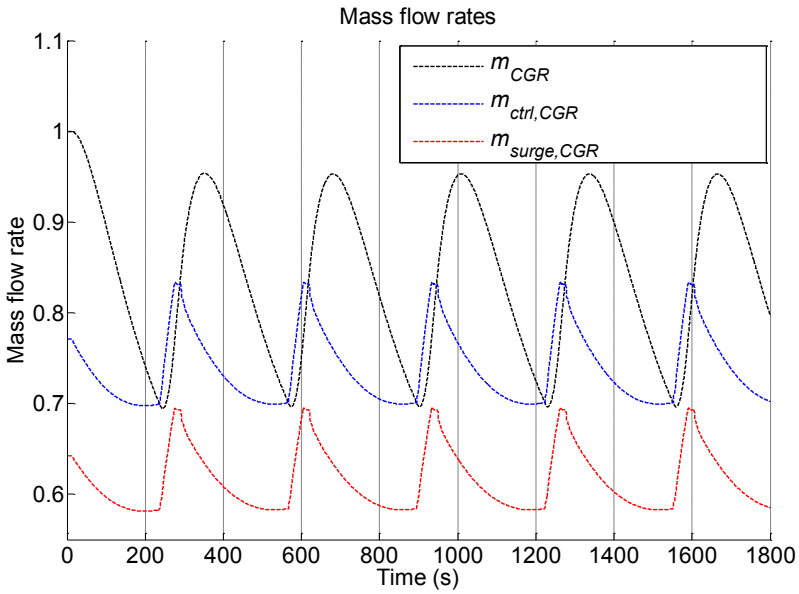


Figure 6-18. Mass flow rates for cold gas recycle configuration (disturbance scenario 15)

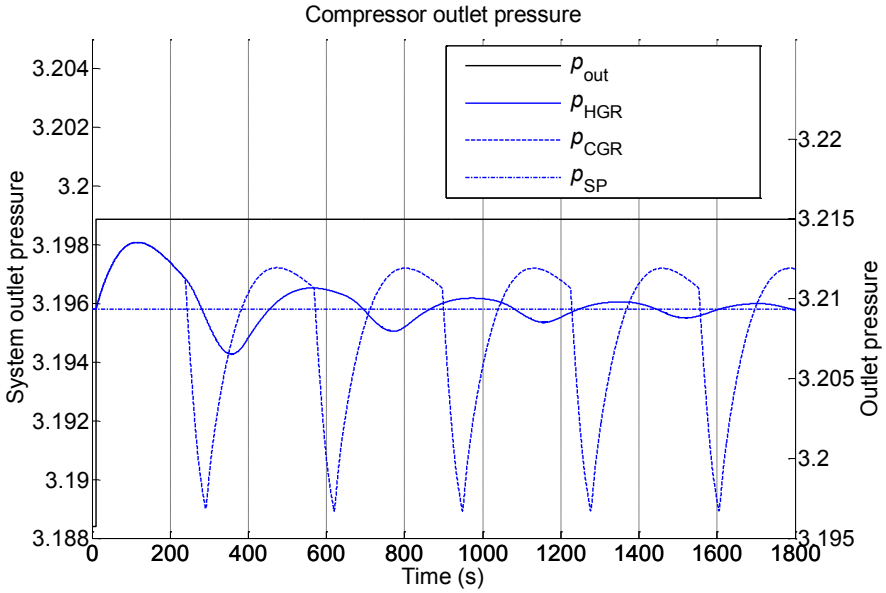


Figure 6-19. Compressor outlet pressure (disturbance scenario 15)

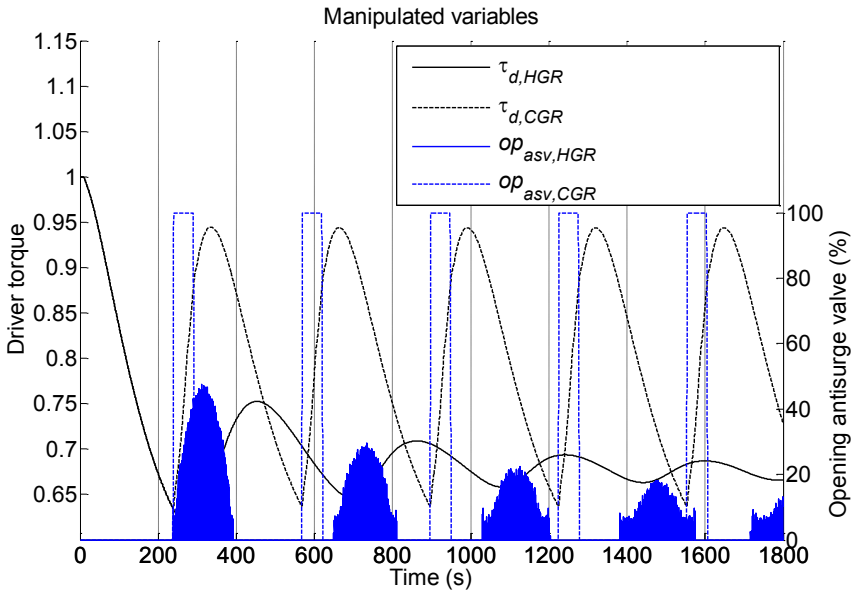


Figure 6-20. Manipulated variables (disturbance scenario 15)

6.3.6 Summary

In this section of the chapter boundary disturbances have been tested on both hot and cold gas recycle configurations. The responses of the configurations have been analysed on their own and in comparison with each other.

When the disturbance does not cause the reduction of the compressor inlet mass flow rate and the opening of the recycle valve, the response of the two configurations is the same. However when the recycle valve opens, the response of the two configurations can be summarised in the following way:

- In the hot gas recycle configuration both p_{01} and T_{01} increase however T_{01} increases more and therefore m_{surge} decreases. This cause the closure of the antisurge valve
- In the cold gas recycle configuration T_{01} is constant while p_{01} increases. Therefore m_{surge} increases even further and this keeps the recycle valve open. This affect the pressure at the outlet of the compressor and therefore it causes a reaction from the pressure controller. The driver torque increases and therefore m increases until it becomes larger than m_{ctrl} and the valve closes.

Therefore both systems can oscillate however at different frequency. The following section of the chapter will investigate which disturbances cause the reduction of the inlet flow rate until recycling is needed.

6.4 Further analysis

Further disturbance scenarios have been tested in order to analyse the behaviour of the compression system during partial recycling operation. The reason is that the scenarios tested in the previous section of the chapter have either increased or decreased the mass flow rate through the compressor depending on the sign of the disturbance. In this section of the chapter only disturbance scenarios causing the reduction of the mass flow rate m have been tested. In this way it is possible to compare the different recycle configurations during various recycling operations. The compressor is still compressing the carbon dioxide from subcritical condition to supercritical condition.

The disturbance scenarios include the following types of disturbances:

- The closure of the boundary valves of the system op_{in} and op_{out}
- The increase of the inlet pressure of the system p_{in}
- The increase of the outlet pressure of the system p_{out}.

In each sub-section the reason why these types of disturbance cause the recycle of flow rate will be explained in detail. Also for these disturbance scenarios, the disturbance took place at time t=10s and the response of the system has been analysed for thirty minutes.

6.4.1 Further analysis on boundary valve disturbances

6.4.1.1 Inlet valve of the system

In this section of the chapter the disturbance scenarios involving the closing of the inlet valve of the system are investigated.

When the inlet valve of the system partially closes, the open loop response involves the reduction of both mass flow rate m and compressor outlet pressure p. Therefore the reaction of the control system is to increase the driver torque, in order to increase the rotational shaft speed and therefore increase the compressor outlet pressure and bring it back to its set point.

Generally speaking the increase of the rotational shaft speed of the compressor causes the increase of m. However at a certain opening position of the inlet valve the compressor must run at its maximum speed in order to control the outlet pressure.

If the inlet valve closes even further, the rotational shaft speed stays at its maximum value while the compressor flow rate decreases until it becomes lower than the control flow rate. At this point the antisurge controller opens the recycle valve in order to increase the total inlet flow rate. This action reduces even further the compressor outlet pressure and therefore the pressure controller keeps the rotational shaft speed at its maximum value.

As a summary it is possible to say that the reduction of the opening position of the inlet valve causes gas recycling only when the driver saturates at its maximum allowable rotational shaft speed.

Table 6-11 reports the results of the hot gas recycle configuration when the disturbance is between -78% and -85%. The same disturbance scenarios have been tested for the cold recycle configuration and the results have been reported in Table 6-12. The disturbance scenario 16 presents the same response from both configuration systems as the recycle valve did not open.

When comparing the hot configuration with the cold configuration, the difference between the responses of the two systems can be summarised in the following way:

- The cold configuration surged for all the tested scenarios (3, 17, and 18)
- This is due to the effect of the cold recycled gas on the location of the surge region
- When p_{01} increases and T_{01} remains constant, as it happens in the cold gas recycle configuration, m_{surge} increases and can cross m and therefore cause surge.

In the cold configuration, surge happens even if more gas is recycled (M is always bigger than in the hot configuration). The consequence is that the power consumption of this configuration is higher and this is due to both the power consumption due to compression (E) and the heat removal required along the recycle line (Q).

Finally, the cold gas recycle configuration has a lower performance in terms of pressure control and this is represented by the parameter ISE_p, which is always higher than in the hot recycle configuration.

Table 6-11. Disturbance scenarios for the inlet valve of the system for hot gas recycle configuration

Disturbance scenario	16	3	17	18
Sign and magnitude (%)	-78.00	-79.00	-80.00	-85.00
ISE_p (bar^{2}s)	4795.89	6220.31	8229.63	30854.59
M (-)	0.00	0.02	0.23	3.16
E (-)	0.44	0.42	0.41	0.37
Q (-)	0.00	0.00	0.00	0.00
E_{tot} (-)	0.44	0.42	0.41	0.37

Table 6-12. Disturbance scenarios for the inlet valve of the system for cold gas recycle configuration

Disturbance scenario	16	3	17	18
Sign and magnitude (%)	-78.00	-79.00	-80.00	-85.00
ISE_p (bar^{2}s)	4795.88	9252.67	14328.08	37663.16
M (-)	0.00	0.63	1.49	3.46
E (-)	0.44	0.45	0.45	0.44
Q (-)	0.00	-0.08	-0.18	-0.42
E_{tot} (-)	0.44	0.52	0.63	0.86

6.4.1.2 Outlet valve of the system

In this section of the chapter the disturbance scenarios involving the closing of the outlet valve of the system are investigated. When the outlet valve of the system partially closes, the open loop

response involves the increase of the compressor outlet pressure p and the decreases of the compressor inlet mass flow rate m. Therefore the reaction of the control system is to decrease the driver torque in order to reduce the rotational shaft speed and therefore the compressor outlet pressure. However this causes a further reduction of the compressor inlet mass flow rate, until the point when m becomes smaller than m_{ctrl} and the antisurge controller opens the recycle valve.

Table 6-13 reports the results of the hot gas recycle configuration when the disturbance is between -20% and -30%. The same disturbance scenarios have been tested for the cold recycle configuration and the results have been reported in Table 6-14. The disturbance scenario 19 presents the same response from both configuration systems as the recycle valve did not open.

Comparing the hot configuration with the cold configuration once again, it is possible to notice the following aspects:

- The cold configuration recycles more gas that in turn has to be cooled down from T_{02} to T_{in}. Therefore its overall power consumption, expressed by means of the parameter E_{tot}, is higher than the power consumption of the hot recycle configuration
- Moreover the control performance in terms of pressure control, expressed by the parameter ISE_p, is lower than the performance of the hot recycle configuration
- During the disturbance scenario 22 the cold recycle configuration surged while the hot recycle configuration did not. This is due to the effect of the cold recycled gas on the value of the surge flow rate.

Table 6-13. Disturbance scenarios for the outlet valve of the system for hot gas recycle configuration

Disturbance scenario	19	20	21	22
Sign and magnitude (%)	-20.00	-24.00	-28.00	-30.00
ISE_p (bar^{2}s)	62.11	164.83	574.47	985.71
M (-)	0.00	0.10	0.42	0.57
E (-)	0.40	0.38	0.38	0.38
Q (-)	0.00	0.00	0.00	0.00
E_{tot} (-)	0.40	0.38	0.38	0.38

Table 6-14. Disturbance scenarios for the outlet valve of the system for cold gas recycle configuration

Disturbance scenario	19	20	21	22
Sign and magnitude (%)	-20.00	-24.00	-28.00	-30.00
ISE_p (bar^{2}s)	62.12	2026.46	3049.72	3324.52
M (-)	0.00	0.74	1.09	1.16
E (-)	0.40	0.43	0.43	0.43
Q (-)	0.00	-0.08	-0.12	-0.13
E_{tot} (-)	0.40	0.51	0.55	0.56

6.4.1.3 Summary

This section of the chapter has focused on disturbance scenarios involving the closure of the boundary valves of the system. In particular it has focused on disturbances causing gas recycling. In

all the tested scenarios the cold gas recycle configuration presented lower pressure control performance and higher energy consumption than the hot gas recycle configuration.

Moreover the cold gas recycle configuration surged at a lower magnitude of disturbance with respect to the hot gas recycle configuration. This is due to the effect of the cold gas recycling on the inlet pressure and temperature of the compressor. These effects are enhanced by the properties of supercritical CO_2 because of the large density change with temperature.

6.4.2 Further analysis on boundary pressure disturbances

6.4.2.1 Inlet pressure of the system

In this section of the chapter the disturbance scenarios involving the increase of the inlet pressure of the system are investigated. When the inlet pressure of the system increases, the open loop response involves the increase of both compressor outlet pressure and inlet mass flow rate. Therefore in the closed loop configuration the pressure controller reduces the driver torque in order to reduce the compressor outlet pressure. However this action affects the inlet pressure of the compressor and therefore the surge limit m_{surge}, until m_{ctrl} becomes bigger than m. At that point the recycle valve opens in order to increase m.

Table 6-15 reports the results of the hot gas recycle configuration when the magnitude of the disturbance is between 27.7% and 53.2%. The same disturbance scenarios have been tested for the cold recycle configuration and the results have been reported in Table 6-16. The disturbance scenario 23 presents the same response from both configuration systems as the recycle valve did not open.

When comparing the hot configuration with the cold configuration, it is possible to notice the following aspects:

- The cold recycle configuration recycles more gas and therefore M is higher
- Its power consumption is higher and therefore E_{tot} is higher
- Both configurations surge during disturbance scenario 26.

Disturbance scenario 26 has been represented in the following figures in order to explain the cause of the surge of the system under both recycle configurations. This scenario has similar dynamics than the disturbance scenario 11 reported in section 6.3.4. Also during scenario 26 when the inlet pressure increases it causes the increase of the compressor inlet pressure p_{01}. Therefore this affects the value of m_{surge} that suddenly increases following the same step dynamic as the inlet disturbance. This happens before the antisurge valve can open and this is the reason why it affects both configuration systems in the same way.

However when the recycle valve opens the two configurations react in different ways. In fact in the hot recycle configuration the opening of the antisurge valve reduces immediately the value of m_{ctrl} that become smaller than m and therefore the recycle valve closes again. However when this happens m becomes smaller than m_{ctrl} and therefore the recycle valve reopens. Therefore the

antisurge valve oscillates until the pressure controller acting on the driver torque increases the rotational shaft speed and therefore also the compressor inlet mass flow rate.

In the cold recycle configuration the opening of the recycle valve causes the increase of the flow control limit and therefore the recycle valve stays open until m increases due to the action of the pressure controller on the driver torque.

Table 6-15. Disturbance scenarios for the inlet pressure of the system for hot gas recycle configuration

Disturbance scenario	23	24	25	26
Sign and magnitude (%)	27.66	36.17	44.68	53.19
ISE_p (bar^{2}s)	16.14	21.35	27.73	37.62
M (-)	0.00	0.00	0.02	0.04
E (-)	0.42	0.40	0.39	0.37
Q (-)	0.00	0.00	0.00	0.00
E_{tot} (-)	0.42	0.40	0.39	0.37

Table 6-16. Disturbance scenarios for the inlet pressure of the system for cold gas recycle configuration

Disturbance scenario	23	24	25	26
Sign and magnitude (%)	27.66	36.17	44.68	53.19
ISE_p (bar^{2}s)	16.14	72.45	104.30	156.40
M (-)	0.00	0.08	0.11	0.14
E (-)	0.42	0.41	0.39	0.38
Q (-)	0.00	-0.01	-0.01	-0.01
E_{tot} (-)	0.42	0.41	0.40	0.39

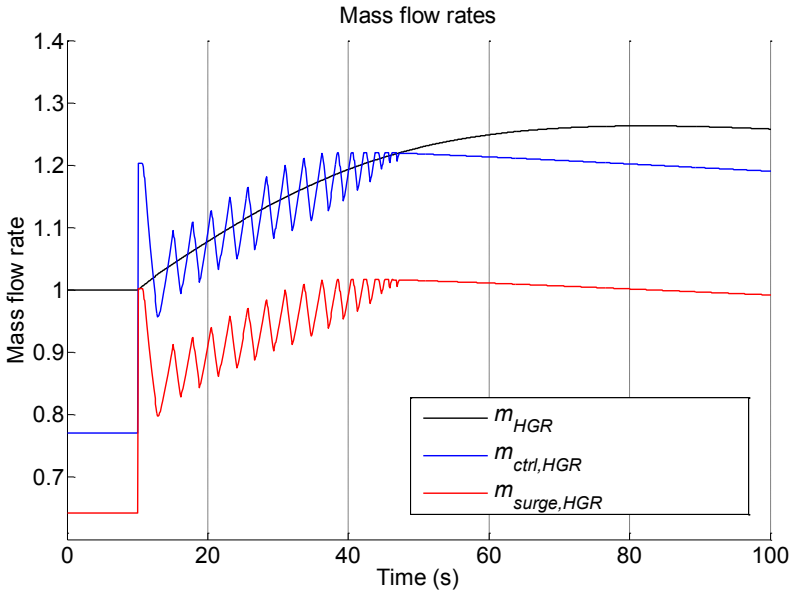


Figure 6-21. Mass flow rates for hot gas recycle configuration (disturbance scenario 26, zoomed view)

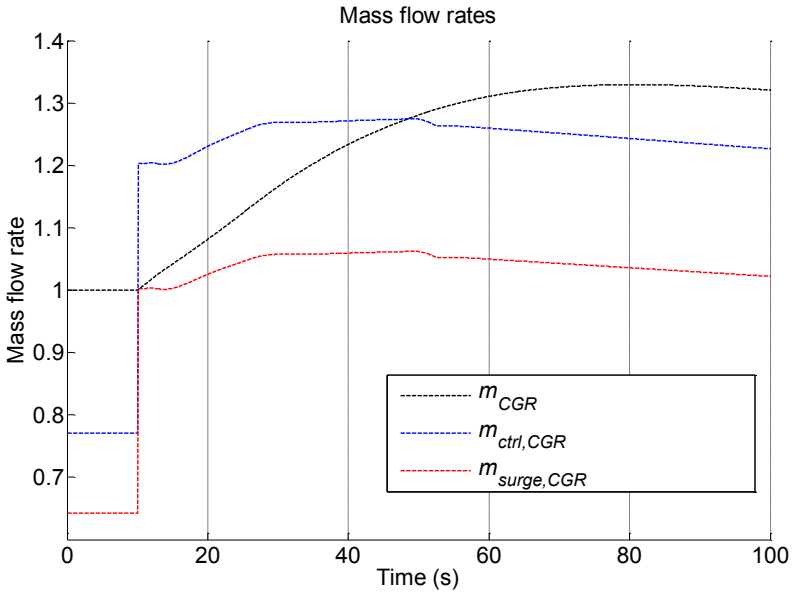


Figure 6-22. Mass flow rates for cold gas recycle configuration (disturbance scenario 26, zoomed view)

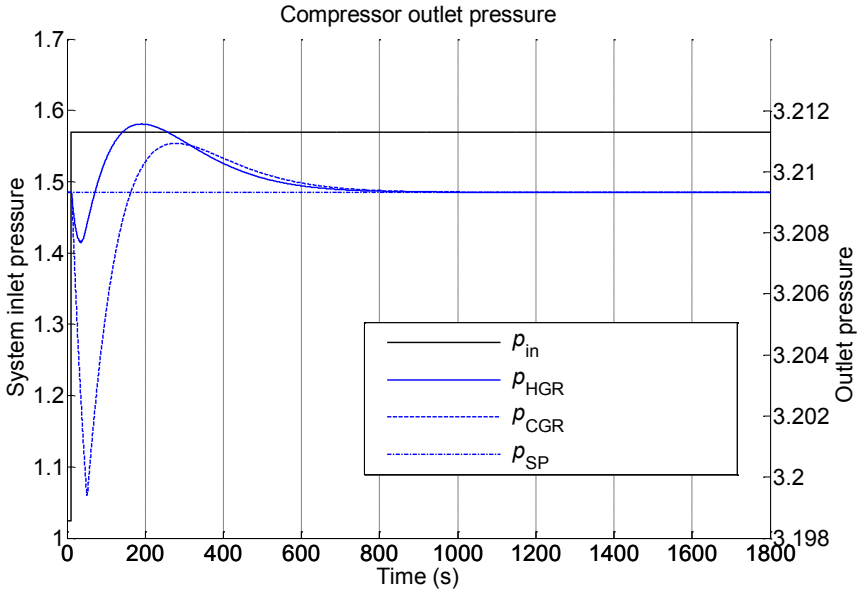


Figure 6-23. Compressor outlet pressure (disturbance scenario 26)

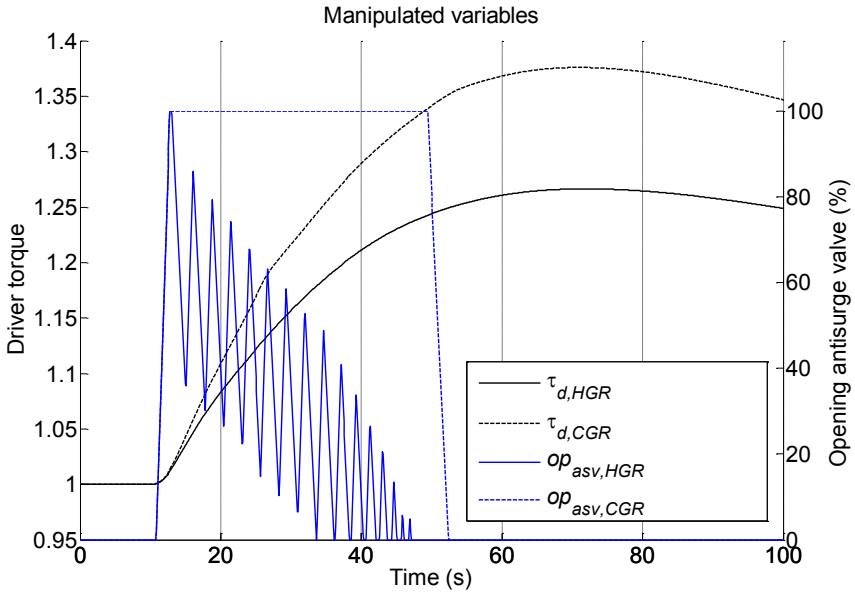


Figure 6-24. Manipulated variables (disturbance scenario 26, zoomed view)

6.4.2.2 Outlet pressure of the system

In this section of the chapter the disturbance scenarios involving the increase of the outlet pressure of the system are investigated. When the outlet pressure of the system increases, the open loop response involves the increase of the compressor outlet pressure and the decrease of the inlet mass flow rate. Therefore in the closed loop configuration the pressure controller reduces the driver torque in order to reduce the compressor outlet pressure. However this action reduces even further the compressor inlet mass flow rate, until it becomes smaller than m_{ctrl} and the antisurge valve opens.

Table 6-17 reports the results of the hot gas recycle configuration when the magnitude of the disturbance is between 0.2% and 0.4%. The same disturbance scenarios have been tested for the cold recycle configuration and the results have been reported in Table 6-18. The disturbance scenario 27 presents the same response from both configuration systems as the recycle valve did not open.

When comparing the hot configuration with the cold configuration, it is possible to notice that:

- In the cold gas recycle configuration, more gas is recycled back for surge protection
- This increases the power consumption of the system represented by the parameters E and Q and therefore E_{tot}
- Moreover the control performance in terms of pressure of the cold recycle configuration is worse than the performance of the hot recycle configuration.

Table 6-17. Disturbance scenarios for the outlet pressure of the system for hot gas recycle configuration

Disturbance scenario	27	28	15	29
Sign and magnitude (%)	0.22	0.27	0.33	0.38
ISE_p (bar^{2}s)	37.05	63.45	152.19	341.18
M (-)	0.00	0.02	0.29	0.65
E (-)	0.41	0.38	0.37	0.36
Q (-)	0.00	0.00	0.00	0.00
E_{tot} (-)	0.41	0.38	0.37	0.36

Table 6-18. Disturbance scenarios for the outlet pressure of the system for cold gas recycle configuration

Disturbance scenario	27	28	15	29
Sign and magnitude (%)	0.22	0.27	0.33	0.38
ISE_p (bar^{2}s)	37.05	984.48	1371.86	1806.97
M (-)	0.00	0.62	1.00	1.42
E (-)	0.41	0.42	0.41	0.41
Q (-)	0.00	-0.07	-0.11	-0.15
E_{tot} (-)	0.41	0.49	0.52	0.56

6.4.2.3 Summary

This section of the chapter has focused on disturbance scenarios involving the boundary pressures of the system. In particular it has focused on disturbances causing gas recycling. In all the tested scenarios the cold gas recycle configuration presented lower pressure control performance and higher energy consumption than the hot gas recycle configuration.

When the inlet pressure of the system increases, this type of disturbance can cause the surge of the compressor because it affects the value of the surge limit even before the recycle valve opens. Therefore it affects both configurations in the same way.

6.5 Analysis of full recycle operation

Additional analyses have been performed in order to compare supercritical gas recycle with subcritical gas recycle for surge prevention.

The fourth stage of compression has been employed in the previous analyses and it represents the last stage of compression in the multistage configuration. The multistage configuration was presented in Chapter 3 and it is here repeated in its open loop configuration in Figure 3-22. The fourth compressor represents the stage compressing the process fluid from subcritical state to supercritical state.

The third compressor is the stage before the fourth compressor in the multistage configuration. It has the same model as the fourth stage and it runs at the same speed, as both machines are on the same shaft. However the operating region is different as the third stage of compression operates in subcritical condition while the fourth stage operates in supercritical condition. For these reasons the third compressor has been employed as representative of subcritical compression while the fourth compressor has been employed as representative of supercritical compression.

In the selection between cold and hot gas recycle the process parameters that are usually considered include time delay in the process response and machine integrity (Botros, 2011). However when dealing with supercritical compression operation it is also important to take into account the amount of gas recycled. The performed analysis included the following steps:

- The third compressor was simulated while running in full recycle mode in the hot gas recycle configuration. The results of the simulation where recorded and scaled
- The third compressor was simulated while running in full recycle mode in the cold gas recycle configuration. The results of the simulation where recorded and scaled
- The amount of gas recycled during full recycle operation in the hot configuration and in the cold configuration were compared
- The fourth compressor was simulated while running in full recycle mode in the hot gas recycle configuration. The results of the simulation where recorded and scaled
- The fourth compressor was simulated while running in full recycle mode in the cold gas recycle configuration. The results of the simulation where recorded and scaled
- The amount of gas recycled during full recycle operation in the hot configuration and in the cold configuration were compared
- Results have been summarised in Table 6-19 and Table 6-20.

Results show that the subcritical compressor operating in full recycle mode is able to recycle 22.64 % more gas by means of a cold gas recycle rather than a hot gas recycle. However in the supercritical compressor this amount rises to 81.50 %.

Table 6-19 summarises the recycle pressure, temperature and flow rate during full recycle operation for the third stage in both hot and cold gas recycle configuration. Table 6-20 summarises the recycle pressure, temperature and flow rate during full recycle operation for the fourth stage in both hot and cold gas recycle configuration. The full recycle flow rate reported in the table depends on the

recycle pressure and temperature upstream of the recycle valve. Therefore it is affected by the recycle configuration. All the reported parameters have been scaled according to the inlet design value of each variable at the entrance of the corresponding stage.

During subcritical compression, represented by the third stage in Table 6-19, the cold gas recycle configuration allows the recycle of 22.6% more gas than the hot gas recycle configuration. However during supercritical compression, represented by the fourth stage in Table 6-20, the cold gas recycle configuration recycles 81.50% more gas than the hot gas recycle configuration. This is due to the dramatic change of density of a supercritical gas especially when it is cooled down toward its critical point. This result is decisive when full recycle is needed and a hot gas recycle configuration may not provide a sufficient amount of gas for surge protection.

Table 6-19. Recycle variables for subcritical compression (third stage of compression)

Variable (dimensionless)	Hot recycle configuration	Cold recycle configuration
Recycle pressure	2.20	2.20
Recycle temperature	1.25	1.00
Full recycle flow rate	0.89	1.09

Table 6-20. Recycle variables for supercritical compression (fourth stage of compression)

Variable (dimensionless)	Hot recycle configuration	Cold recycle configuration
Recycle pressure	2.63	2.63
Recycle temperature	1.37	1.00
Full recycle flow rate	0.65	1.17

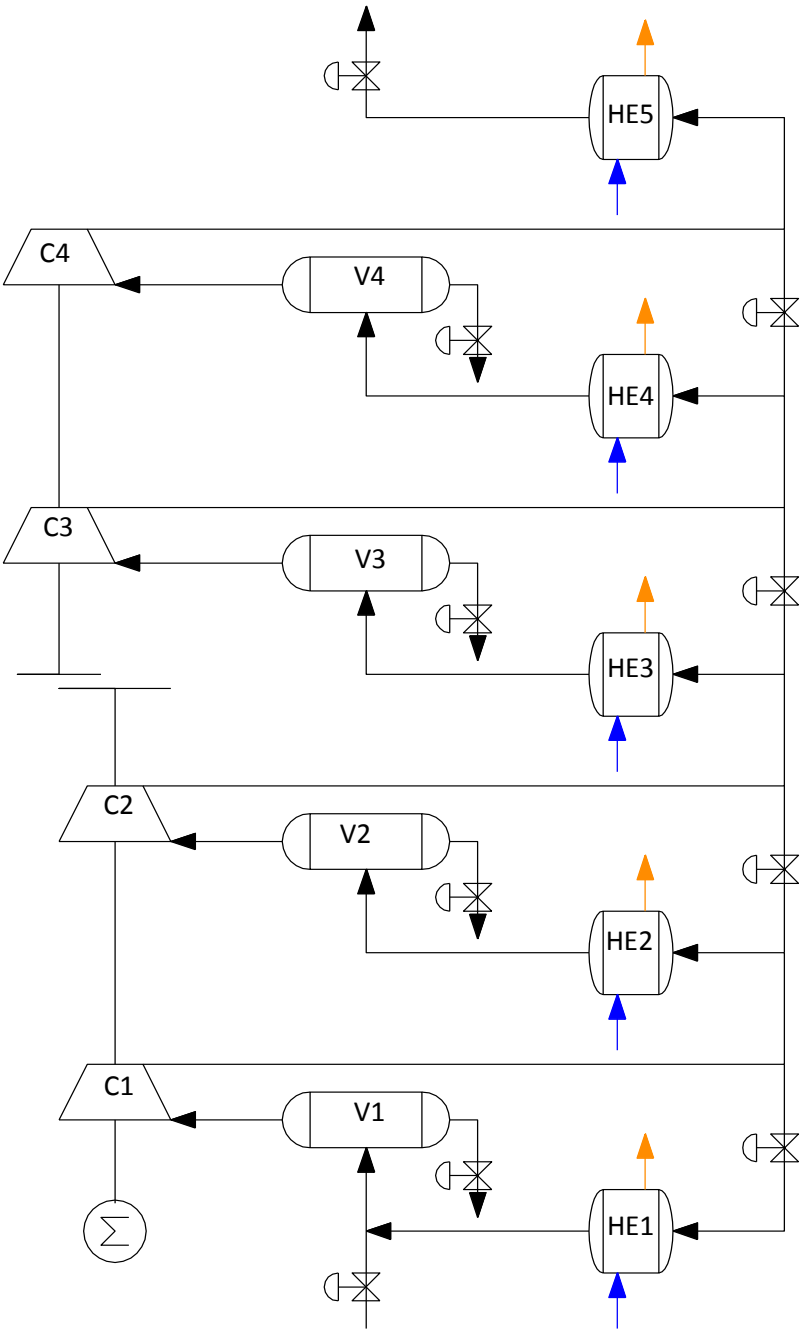


Figure 6-25. Schematic representation of the multistage compressor system (open loop)

6.6 Discussion

6.6.1 Selection of gas recycle configuration

In the selection between hot and cold gas recycle the process parameters that are usually considered include time delay in the process response and machine integrity. In particular recycling of hot gas should be limited over time in order to guarantee the integrity of the machine. This chapter however has demonstrated that other aspects should be taken into account as well, such as:

- Surge occurrence
- Energy consumption
- Maximum recycle flow rate during full recycle operation.

The advantages of employing a hot gas recycle configuration include:

- The process layout is simple and the configuration of the recycle line includes only two main items: the recycle pipeline and the antisurge valve
- The time constant of the recycle line is small. This is due to the small hold-up volume along the recycle line. Therefore the system is able to respond quickly when surge may occur and gas must be recycled back in order to increase the inlet flow rate of the machine
- Surge takes place when strong disturbances occur. This is due to the effect of the inlet temperature of the compressor on the location of the surge line
- The amount of gas recycled is small and this is due to oscillation of the recycle valve
- As a consequence of the previous point, the energy consumption of the system is low as less gas is recycled. Moreover the recycled gas is not cooled down before being mixed with the freshly fed gas.

On the other hand, the hot gas recycle configuration has some disadvantages such as:

- The oscillation of the antisurge valve during operation in partial recycle mode. This is due to the effect of the inlet temperature of the compressor on the location of surge. In fact when the antisurge valve opens, the inlet temperature of the compressor increases and this reduces the value of the surge flow rate. As a consequence, the antisurge control system closes the antisurge valve
- The machine can overheat due to the high temperature of the recycled gas. The expansion of the gas that takes place along the recycle line causes a partial cooling that depends on the operating condition. However the temperature of the recycled gas is still higher than the temperature of the freshly fed gas and therefore the recycle of hot gas should be limited over time
- During full recycle operation, the maximum amount of gas recycled is lower than if the gas was at lower temperature. This happens because the flow through a valve depends on the density of the gas, as explained in Chapter 3, and the density of the gas depends on its temperature and pressure.

The cold gas recycle configuration is the alternative to the hot gas recycle configuration and its advantages are the following:

- The gas is cooled down during the recycle and therefore there are no issues related with overheating of the machine and loss of integrity for prolonged operation in recycle mode
- Therefore there is no limit to this operation. In theory the system could continuously run in partial or full recycle mode if needed
- The oscillations of the antisurge valve are limited if compared with the oscillation of the hot gas recycle configuration. This is because when the cooled gas is recycled back, the inlet pressure of the system increases while the inlet temperature does not, and this increases the surge flow rate, as previously explained in section 6.3.2.3.

However the cold gas recycle configuration has some down sides such as the following:

- The system is more complicated as it includes a heat exchanger along the recycle line
- The presence of the heat exchanger represents both a capital and an operating cost, both of them depending on the type of exchanger. In the thesis cooling has been assumed as a cost, however it could be recovered, depending on the overall process configuration. On the other hand the operation of the heat exchanger would depend on the disturbances affecting the compression system and therefore should be limited
- The heat exchanger increases the hold-up volume along the recycle line and therefore the time constant of the system. This could be a problem when quick action is needed for incipient surge
- The increase of the surge flow rate due to the increase of the inlet pressure while recycling also means that this configuration may undergoes surge under small disturbances
- Moreover the reduced oscillation of the antisurge valve means that the system recycles more gas if it has a cold recycle line.

Therefore the selection between the two configurations is not straightforward and all the previously mentioned aspects should be taken into account.

For an existing compression station, cold gas recycle would be more suitable as it would guarantee the possibility of running the system always in partial recycle if needed. Moreover the smaller frequency of oscillation would stress less the system. On the other hand there could be issue such as the cost of the cooling system and the space availability. If the compression station always runs in recycle mode but the refurbishment of the compressor would be too expensive, than heat integration could be taken into account as an option to recover some of the costs related with the cold recycle configuration.

For a new compression station, where the desire is to limit capital cost and stable operation is expected, a hot gas recycle configuration could guarantee smaller capital and operating cost and also surge protection when occasionally needed. On the other hand if the economics of the project allows that, than the ideal solution would be to install both cold and hot recycle systems. The hot recycle should be employed for urgent limited operation while the cold recycle should be employed for more long-run recycle operation.

The same idea would apply to a multistage compressor. Each stage should have a hot gas recycle connecting the output of the stage to the input of the stage. Then a cold gas recycle could cover each stage, each couple of stages or even the full multistage compressor. Each of the previous configurations would require in-depth steady state and dynamic analyses and real time optimization in order to guarantee its safety, reliability and optimal operation.

6.6.2 Subcritical and supercritical compression

The comparison between subcritical and supercritical compression is challenging because of the operational range of the compressor. In fact, even at the lowest pressure ratio and compressor inlet flow rate, carbon dioxide always exits the last stage of compression in supercritical state. Therefore it is not possible to simulate the operation of the same stage in supercritical condition and in subcritical condition. For this reason it has been decided to limit the comparison to the full recycle steady state operation. The reasons for this decision include the following considerations.

In order to compare the compression operation under two different conditions such as subcritical compression and supercritical compression, there are two options. The first option would be to run the same machine under the two conditions while the second option would be to run two machines under the two conditions. In the second case the two machines should have the same model.

However the same compressor cannot be working at either subcritical or supercritical condition. In fact the gas enters the machine always subcritical and exits it always supercritical, even at the lowest possible load. An example could clarify this point. The critical point of carbon dioxide is 304.21 K temperature and 73.83 bar pressure, while a typical centrifugal compressor has a pressure ratio usually between 5 and 22. This value applies to a multistage compressor, which is usually composed of four stages. Therefore each stage would have a pressure ratio between 1.25 and 5.5. In the most conservative case the pressure ratio would be equal to 1.25. If the inlet pressure is equal to 60 bar, then the outlet pressure would be equal to 75 bar. This value is already above the critical pressure of carbon dioxide. Therefore it is not possible to operate the same compressor in subcritical and supercritical condition.

The second case included two different machines having the same model. That was the case of the third and fourth compressor stages. However the operating ranges of these two stages are different, as it is their design point and therefore the position of the operating point within the compressor map. Therefore this means their distance from surge is different.

For the reasons mentioned above, the analysis of the gas recycle has been selected as the most representative analysis for the operation of the compressor in supercritical condition. This is because:

- The process fluid expands from supercritical condition to subcritical condition along the recycle line
- The amount of flow through the recycle valve depends on the density of the gas, according to the equation (3-24), here repeated

$$m_{r,HR} = op_{ASV} k_r \sqrt{\rho(p - p_{01})} \quad \textbf{(3-24)}$$

- The density of the gas is one of the properties that is mostly affected by the change of phase.

6.7 Summary of the chapter

This chapter had five tasks to fulfil. The first task involved the analysis of the disturbance scenarios able to cause the recycle of the gas from the outlet of the compressor to the inlet of the compressor. These disturbances have been identified as follow:

- Closure of the inlet valve of the system
- Closure of the outlet valve of the system
- Increase of the inlet pressure of the system
- Increase of the outlet pressure of the system.

The second task required the analysis of the recycle configurations in order to identify their tendency towards surge. The results demonstrate that the cold gas recycle configuration surges at a lower magnitude of disturbance. This is because of the effect of the cold recycled gas on the location of the surge region.

The third task was the estimation of pressure control and stability of the compression system. The reported results have demonstrated that the cold gas recycle has a lower performance in terms of pressure control. This is due to the higher amount of gas recycled over time. However this configuration oscillates less than the hot recycle configuration. The oscillation is due to the continuous opening and closing of the antisurge valve, which has to react quickly in case the mass flow rate at the inlet of the compressor becomes smaller than the control flow rate.

The high amount of gas recycled in the cold gas configuration increases its power consumption with respect to the hot recycle configuration. The fourth task was the identification of the energy consumption of the two systems and the results indicate that the cold recycle configuration has an higher energy consumption due to both gas compression and recycle gas cooling.

Finally subcritical and supercritical full recycle operation has been analysed in order to fulfil the fifth task of this chapter. The comparison between subcritical and supercritical compression is challenging because of the operational range of the compressor. The results of the analysis demonstrated that a subcritical compressor operating in full recycle mode is able to recycle 22.64 % more gas by means of a cold gas recycle rather than a hot gas recycle. However in the supercritical compressor this amount rises to 81.50 %. This result is decisive when full recycle is needed for surge protection.

7 Critical discussion and future work

This chapter contains the critical discussion on the analyses and results presented before in the thesis. It also suggests future directions of the research work here developed.

The chapter is organised in subsections covering the following topics:

- The general problem of compressor operation and control and how it has been approached
- The critical evaluation of the adopted methodology
- The critical evaluation of the reported findings
- The future research development.

7.1 Summary of the methodology

The PhD project has identified research challenges and needs to be addressed in the compression industry dealing with carbon dioxide:

- The cost of gas conditioning and especially the cost of compression
- The control and stability of the compression station
- The identification of the key issues in the compression and recycling of supercritical carbon dioxide.

Therefore the general aims of this thesis have been the following:

- The reduction of the cost of gas compression
- The reduction of the interactions between controllers in order to achieve process controllability and stability
- The identification of the key issues in the compression and recycling of supercritical carbon dioxide.

The main findings from background and literature review can be summarised as follows.

Regarding centrifugal compressor modelling, the model proposed by Greitzer (1976b) is a strong reference that has been employed and further developed by other researchers. The main contributions include Hansen et al. (1981) who demonstrated that the model from Greitzer, originally developed for axial compressors, was also applicable to centrifugal compressors and Fink et al. (1992) who included the conservation of angular momentum in the turbocharger spool.

Dynamic control was firstly proposed in 1989 as a method to stabilise the compression system by feeding back additional disturbances. However it has not been successful in industrial application, mainly because of safety and reliability of such a system. Model predictive control was also proposed to control compression system. However, temperature effects and minimisation of the recycle have not been included.

Finally regarding the compression of carbon dioxide, some studies have reported on compression and transportation of supercritical CO_2. However the focus of research has mainly been the optimisation of the thermal cycle rather than the effect on compressor operation. Therefore there is a gap in the literature on the effect of supercritical fluid on compressor operation and control.

The outcome of the literature review led to more specific research objectives for the PhD, which included:

- Modelling and simulation of a compression station
- Reduction of control loop interaction by integrated control approach
- Investigation of supercritical CO_2 compression, operation and control.

7.1.1 Research tasks

These research objectives have been divided in the following tasks:

- Modelling of the open loop compression system
- Modelling of the reference control system
- Implementation of the closed loop model
- Description of the reference case study
- Validation of the closed loop model
- Demonstration of interactions between control loops in the reference pressure controller
- Improvement of the response of the capacity controller and reduction of the interaction between control loops
- Analysis of the open loop response of the compression system
- Integration of pressure and surge control action
- Reduction of the recycle flow rate
- Analysis of the effect of the recycle configurations on surge occurrence, pressure control and stability of the compression system and energy consumption.

7.1.2 Contribution of the project

The results presented in the thesis will be explored in the following sections however they include these main contributions:

- Analysis of the effect of boundary disturbances on open and closed loop system
- Improvement of the response of the capacity controller
- Integration of pressure and surge control
- Definition of performance parameters for performance monitoring tools
- Representation of the operating point from surge over time
- Analysis of the effect of the recycle configuration on the response of the control system during supercritical compression of carbon dioxide.

7.2 Critical evaluation of the adopted methodology

7.2.1 Mathematical modelling of compressors

In this thesis the adopted approach includes dynamic modelling and simulation. There are various categories of mathematical models, including (Seborg et al., 2004c):

- Theoretical models, developed using first principles
- Empirical models, obtained by fitting experimental data
- Semi-empirical models, which are the combination of the previous two types of models.

Theoretical models provide physical insight into the process behaviour and are also valid over a wide range of operating conditions. At the same time they are expensive and time-consuming to develop. Theoretical dynamic models can be solved by means of a variety of numerical integration techniques and the computational effort is generally proportional to the complexity of the model itself.

Experimentation is another type of approach which includes direct testing of the process or unit under analysis, usual in scaled-down size. The main advantage of experimentation is the possibility to directly test the unit, during both steady state and dynamic operation, at the design point but also in off-load conditions. In theory, experimentation may require only limited theoretical knowledge on the unit under analysis. Most commonly, it is employed together with modelling and simulation in order to better understand the behaviour of the machine. Experimentation is common when:

- A theoretical model of the unit or process is not available
- Some of the parameters of the model are not available and must be estimated through testing.

This thesis reports the results of dynamic simulations of compressor stations and the model employed has been validated against industrial data. These data were available through a fully validated industrial simulator, based on real plant data. The methodology of validation of the industrial simulator is presented in the Appendix of the thesis. Therefore the model was validated against experimental data in an indirect way.

This type of approach based on indirect validation has the following advantages:

- The fully-validated industrial simulator represents an accurate, reliable and robust source of data
- It allows testing of a wide variety of operating conditions, at steady state and during transient operation
- The effect of a specific disturbance variable on both open and closed loop can be simulated and the response of the system can be recorded.

On the other hand, some disadvantages include the following issues:

- Only specific input variables can be manipulated, according to the architecture of the industrial simulator

- Step change disturbances can be simulated only at specific physical point of the plant layout, where input variables can be manipulated
- The safety interlock system is in place and cannot be deactivated. Therefore it was not possible to test severe off-load conditions for the single stages as each stage was affecting the other stages, causing the shutdown of the multistage compressor.

As step change disturbances could be simulated only at specific points, this increased the complexity of the parameter estimation process. An example is here presented by means of Figure 7-1. Points A, B and C represents three points were it was possible to read the value of the pressure of the process fluid in the Graphical User Interface (GUI) of the industrial simulator. Point A was the only point at the inlet of the process where the pressure could be manipulated. The manipulation was possible via step changes only. This figure shows that between point A and B there is a vessel while between point B and point C there is the first stage of compression.

Figure 7-2 shows the response of the system when the pressure of the flow changes by a positive step change in point A. The unit between point A and point B is a separation vessel, which is characterised by a first order response. Therefore the pressure of the flow in point B shows a first order response to the pressure step change taking place in point A.

The unit between point B and point C is the first stage of compression. A compressor shows a first order response to a pressure step change. However the change of pressure in point B is already following a first order dynamic and therefore the change of pressure in C shows a second order dynamic.

The example represented in Figure 7-2 is only a qualitative example and related to the first stage of the multistage configuration. However, it serves the purpose to demonstrate:

- How the stages are affecting each other
- Why the architecture of the industrial simulator increased the difficulty of the parameter estimation.

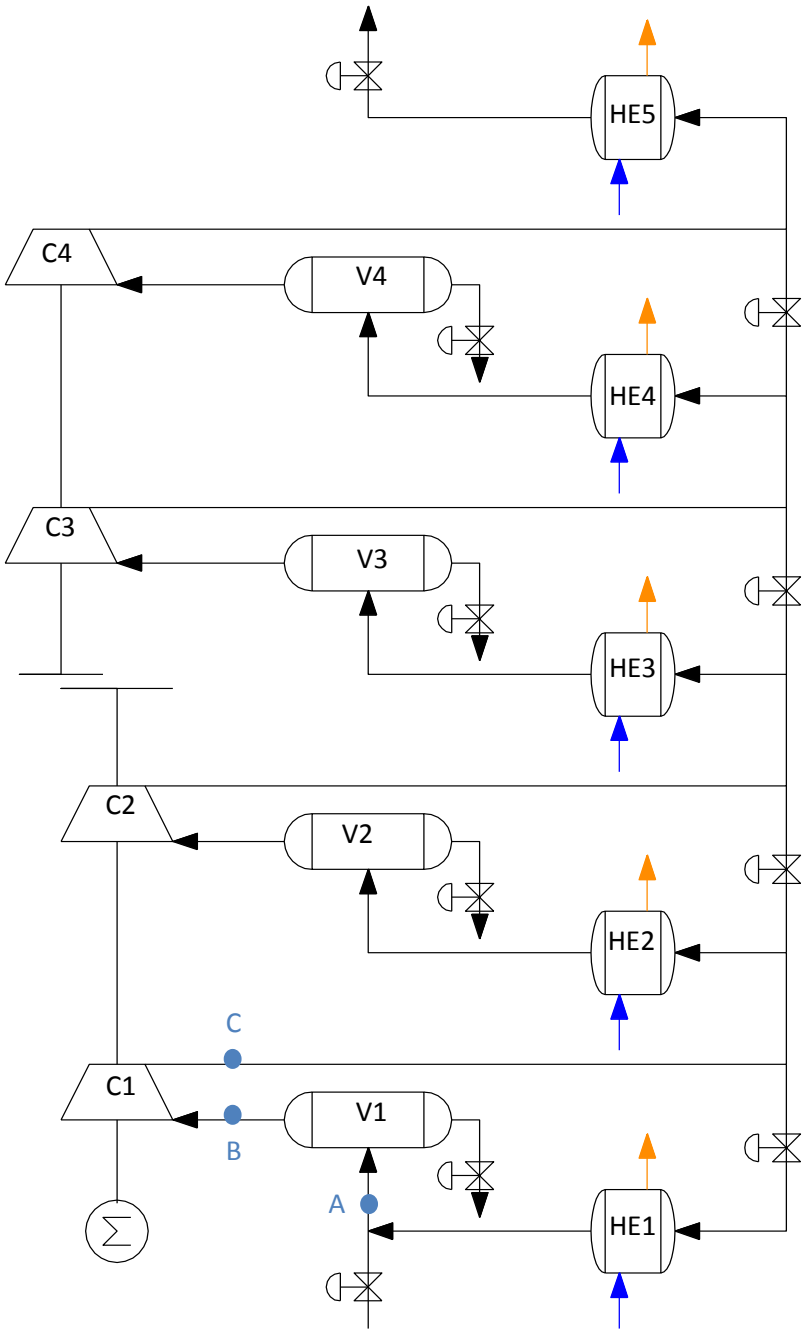


Figure 7-1. Schematic representation of the multistage compressor system (open loop) – modified from Figure 3-24

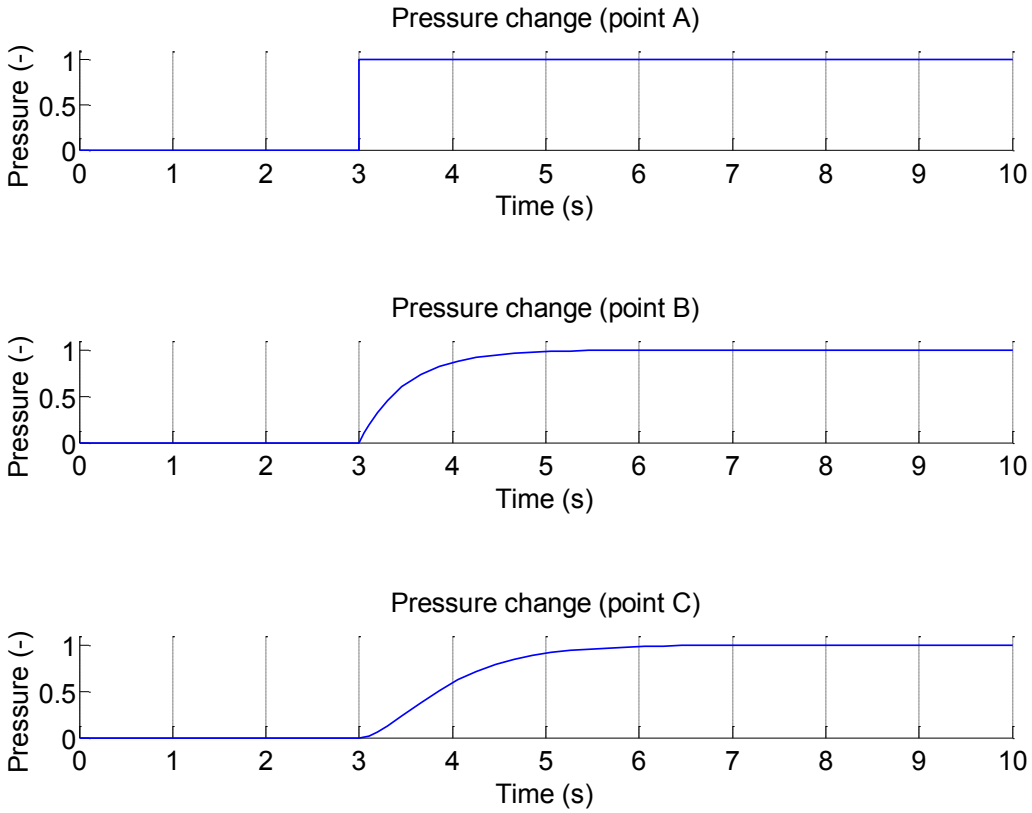


Figure 7-2. Qualitative representation of pressure change along the points A, B and C

7.2.2 Parameter estimation and model validation

In this thesis both parameter estimation and model validation have been employed in order to guarantee the accuracy and reliability of the dynamic model of the compressor.

According to the literature, *parameter estimation* or *identification* consists in estimating the mathematical parameters by fitting the response of the model against a data set and adjusting the parameters until the response of the model and the response of the plant correspond. The procedure of parameter estimation has been presented in Chapter 3.6.1.

Model validation follows parameter estimation. During model validation, the simulated response is compared with a set of data obtained from experimental testing. However a different set of data must be employed in order to guarantee the quality of the validation result. Model validation has been presented in Chapter 3.6.2.

In this thesis, the estimation of the parameters and the validation of the model have been performed according to the following steps:

- Some parameters of the model (such as the sonic velocity at ambient conditions a_{01}, the total moment of inertia of the system J, the slip factor μ, the impeller radius r_2, the valves

constants k_{in}, k_{out}, k_{ASV}) have been estimated by means of algebraic calculations based on the available geometrical data of the plant
- Some of the parameters could not be identified by means of algebraic calculation. These parameters include the plenum volume V, the duct throughflow area A_1 and the duct length L. For these parameters, mathematical optimisation has been employed and reported in Chapter 3.6.1.1.
- The overall response of the system has been validated against a second set of data in order to guarantee the accuracy of the model.

Finally additional calculations, reported in Chapter 3.6.1.7, have been performed in order to demonstrate that the estimated parameters are physically meaningful for the case study under analysis. Specifically, two different and hypothetical compressor geometries have been proposed and used in order to estimate the corresponding values of a_{01}, V, L and A_1. These calculations demonstrate that the proposed values are reasonable. Moreover they also show that the adopted methodology avoids problems of ill-conditioning issue. This has been achieved by estimation of specific parameters while coupled as they were in the mathematical formulation of the process model. Estimating the single parameters could have brought to the identification of parameters values without a physical meaning in the context of compressor modelling.

7.2.3 Model-based control

Process control strategies can be classified according to Seborg et al. (2004c) as:

- *Feedback control strategy*, where the controlled variable is measured and employed to adjust the manipulated variable, while the disturbance variable is not measured
- *Feedforward control strategy*, where the controlled variable is not measured but the disturbance variable is measured
- *Feedforward-feedback control strategy*, where both controlled variables and disturbance variable are measured
- *Multi-loop control strategy*, consisting of multiple single loop controllers
- *Multivariable control strategy*, where each manipulated variable is adjusted based on the measurements of all the controlled variables.

In this thesis, two model-based control approaches have been proposed:

- Chapter 4 proposed a *model-based feedforward controller* in order to improve the performance of the closed loop system in terms of pressure control
- In Chapter 5 a *model predictive controller* was proposed in order to control both pressure and surge.

In predictive control, the adjustments of the manipulated variables are based on the dynamic model of the process, which indicates the effect of the manipulated variables on the controlled variables. Therefore, the performance of a predictive controller heavily depends on the dynamic model of the process.

7.2.3.1 Model-based feedforward control

The model based feedforward controller presented in Chapter 4 is based on a non-linear compressor map. This map is not a first principles model, however it represents the mathematical relationship between pressure ratio, rotational shaft speed and inlet flow rate. An accurate compressor map is a precise representation of the compressor behaviour. However it could also be a source of mismatching. The compressor map is particularly sensitive to:

- The pressure and the temperature of the process fluid at the inlet of the compressor
- The molecular weight of the process fluid.

In the thesis the composition of the gas (and therefore its molecular weight) has been assumed constant. Corrected compressor maps have been employed in order to take into account the influence of the inlet conditions of the fluid on the operation of the compressor and especially on its surge line.

Generally only few curves (four or five) are represented in a compressor map. For each point located between two lines, the value of pressure ratio, mass flow rate and rotational shaft speed must be interpolated.

Finally another phenomenon that can affect the accuracy of the compressor map against the real operation of the compressor is fouling. Fouling is a physical phenomenon consisting in the deposition of small solid particles inside the compressor. These particles change the internal geometry of the compressor and therefore its performance maps. Changes in the compressor map are a potential source of plant-model mismatch, which can affect the performance of a model-based feed-forward controller. Therefore a solution is needed to make the controller robust to errors and changes in the compressor map. A potential way to address the problem is to update the maps online. One example of this type of methodology is presented in Cortinovis et al. (2014), who propose the adoption of an algorithm able to compare historical process data with newly collected data and decide if the actual map is enough accurate or needs to be updated.

7.2.3.2 Model predictive control

The compressor map can be a source of model mismatch also in model predictive control applications. The advantages of model predictive control include (Seborg et al., 2004b):

- The formulation of a mathematical relationship between input variables, disturbance variables and output variables
- The constraint of input and output variables
- The resolution of the control problem via mathematical optimization.

The success of MPC depends on the accuracy of the process model. The process model that is employed in the prediction of the future values of the controlled variables is either:

- An empirical dynamic model
- A transfer function model
- A state-space model.

When employing linear model predictive control, the dynamic model of the process plant is linearized in the vicinity of a specific point, usually the design point. Therefore the model employed by the MPC controller is already a simplified version of the process model, and not exactly the same model as the process plant model.

At the same time, the controller updates its state automatically using the latest plant measurements. Therefore this process of updating the linearized model by means of continuous measurements and adjustments helps preventing mismatching, even when:

- The model of the plant is already simplified
- The model has a low degree of accuracy
- The process is changing over time, for example for the reason listed in the section above.

In conclusion, the MPC formulation is going to deliver robustness by updating the model.

7.2.4 Hierarchy and timescales of process control

The general hierarchy of process control include the following elements (Seborg et al., 2004a):

- Measurement and actuation (timescale: less than 1 second)
- Safety and equipment protection (timescale: less than 1 second)
- Regulatory control (timescale: seconds to minutes)
- Multivariable and constraint control (timescale: minutes to hours)
- Real-time optimization (timescale: hours to days)
- Planning and scheduling (timescale: days to months).

The above list shows how different the timescales are depending on their position in the process control hierarchy.

Looking specifically at compression applications, the phenomenon of surge and its control falls under the category “safety and equipment protection” while the control of the compressor outlet pressure falls under the category “regulatory control”. Finally model predictive control falls under the category “Multivariable and constraint control”. These three categories have timescales varying from less than a second to hours. The following table recalls Table 5-5 that summarises sampling time and model horizon MH, control horizon CH and prediction horizon PH proposed for the model predictive control application.

It is important to recall that surge happens in 20 to 50 ms (CCC, 2013). However this time interval is valid when the operating point of the machine is already on the surge line, and a minimal disturbance can surge the compressor. For surge control systems aiming at reducing the safety margin between surge and control line, and therefore aiming at pushing the operating point of the machine as close to surge as possible, this variability of timescale, from 20 ms to several hours, could be a serious issue. A possible solution valid for fast responding model predictive control application is multi-parametric control (Pistikopoulos et al., 2006). Multi-parametric control stores in a look-up

table the optimal solution and therefore does not need the time to solve the optimization problem but it is rather reading it in the map.

Moreover when modelling around the surge line it would be advisable to model also the part of the compressor map including positive performance and negative flow rate, in order to be able to model flow reversal inside the compressor. In this thesis, the aim was not to reduce the safety margin of the compressor. Therefore the adopted timescales are reasonable for the purpose of the reported research.

Future developments of the work presented in the thesis may therefore include multi-parametric control that would enable to build a fast responding MPC. Such MPC would be able to deal with surge occurrence and therefore with both positive and negative flow through the compressor.

Table 5-5. Sampling period and control horizons

Name	Value
Sampling period (s)	4
MH (s)	68.55
CH (s)	40
PH (s)	160

7.3 Critical evaluation of reported findings

7.3.1 Analysis of boundary disturbances

7.3.1.1 Open loop operation

In the thesis the boundary disturbances have been tested on both open loop system and closed loop system.

When the compression system operates in open loop, this means that the manipulated variables are not changing over time. Their value is usually their design point value. Therefore the torque supplied by the driver τ_d does not change and the antisurge valve stays closed. However when the compressor is operating in open loop at steady state, if the inlet flow rate m changes the radial speed ω and therefore the rotational shaft speed N changes too. This is because of the following equation:

$$\tau_d = \tau_c = \mu r_2^2 \omega m \tag{7-1}$$

where μ is the slip factor and r_2 the radius of the impeller.

Therefore it is more common to have the compressor rotating at constant speed N. This is not a strictly open loop operation as it involves the adjustment of the driver torque however it uses just the speed controller while the pressure controller is not used.

7.3.1.2 Effect of disturbances on open loop system

The operation of the compression system running at constant rotational shaft speed has been analysed during boundary disturbances. The results of the analysis are summarised in the following table where the arrows indicate the increase or the decrease of the controlled variable depending on the sign of the change of the disturbance variable.

Table 7-1. Summary of the effect of the disturbance on controlled variables

Disturbance variable	Change	Effect on p	Effect on m
System inlet valve	↓	↓	↓
System outlet valve	↓	↑	↓
System inlet pressure	↑	↑	↑
System inlet pressure	↓	↓	↓
System outlet pressure	↑	↑	↓
System outlet pressure	↓	↓	↑

This qualitative analysis can be used as a reference in order to understand which effect the disturbance will have on the compression system. If the compression system is running at constant rotational shaft speed, the results of the analysis will indicate if the controlled variables will increase or decrease depending on the origin and sign of the disturbance. However if the compressor is running in closed loop these results are still valuable as they help understanding the response of the control system. A reduction of the compressor outlet pressure causes the increase of the torque driver while a reduction of the compressor mass flow rate can cause the opening of the surge valve.

In particular it is interesting to notice that:

- The closure of a boundary valve will always cause the decrease of the inlet flow rate. However, it could cause the increase or decrease of the compressor outlet pressure, depending on the origin of the disturbance
- If the disturbance variable is the inlet pressure of the system, the change of p and m will have the same sign of the disturbance itself
- If the disturbance variable is the outlet pressure of the system, the change of p will have the same sign as the disturbance while the change of m will have the opposite sign.

7.3.1.3 Effect of disturbances on closed loop system

Finally it is interesting to notice that any disturbance causing the increase of the compressor outlet pressure will also cause the reduction of the mass flow rate. It may also cause the opening of the recycle valve. This is because when the compressor outlet pressure increases, the pressure controller will decrease the torque of the driver in order to decrease the rotational shaft speed and bring back the pressure p to its set point. However this action will affect m as well. Therefore the higher risk of surge is related with disturbance having in open loop:

- An increase of p and
- A decrease of m.

These disturbances are:

- The closure of the outlet valve of the system
- The increase of the outlet pressure of the system.

Therefore some of the disturbances coming from the outlet boundary of the compressor are dangerous for surge occurrence. In particular disturbances characterised by higher backpressure can surge the compressor. The backpressure is defined as “the resistance to a moving fluid to its direction of flow caused by an obstruction, bend, or friction in a pipe or vessel” (Schaschke, 2014). Therefore both the previously mentioned disturbances represent an increase of the resistance the compressed fluid is facing. It is already known from the literature that in a series of compressors, the high pressure compressor will tend to surge earlier than the low pressure compressor (Boyce, 2003). This phenomenon has been explained by Boyce by analysing the matching of the compressors and the intercasing pressure drop between them. However the analysis of the open loop response highlights another reason why surge can happen at the exit of a compressor rather than at its entrance.

7.3.1.4 Influence of inlet conditions on surge location

In the thesis corrected compressor maps have been employed in order to take into account the influence of the inlet conditions of the gas on the location of the surge line. In particular the corrected mass flow rate m_c has been expressed as a function of actual mass flow rate m, inlet temperature T_{01} and pressure p_{01} of the gas, according to the following equation:

$$m_c = \frac{m\sqrt{T_{01}/T_{ref}}}{p_{01}/p_{ref}} \quad \textbf{(3 -11)}$$

When dealing with surge control it is interesting to notice that certain disturbances can push the compressor toward surge while other disturbances can move surge towards the operating point. This is because disturbances coming from the inlet side of the compressor influence the location of the surge region. The same happens when the recycle valve opens and the recycled gas affects the compressor inlet pressure and temperature and therefore the location of surge.

Also the action of the pressure controller can push the system towards surge. This is because the operating point that would guarantee the wanted value of the pressure under certain boundary condition is outside the operating region of the compressor.

7.3.2 Industrial approaches to compressor control

7.3.2.1 The perspective from Compressor Control Corporation

Compressor Control Corporation (CCC) is a leader company specialised in turbomachinery and compressor control. CCC controllers are widely used in industrial applications involving centrifugal compressors.

The training programme of the PhD project included a two weeks course on control of turbomachinery. The course took place in May 2013 in the offices of CCC in Milan (Italy). ESD Simulation Training helped to secure the training placement. The exposure to CCC technology and approach helped in shaping the content and the direction of the research activity, as it highlighted the main challenges of compressor control from an industrial and practical perspective rather than academic and theoretical point of view.

As highlighted in various part of the thesis (mainly in Chapters 1, 2, 4 and 5), one of the main issues of compressor control is the interaction between the pressure control loop and the surge control loop. CCC suggests three options to deal with this problem (CCC, 2013):

- Detuning the control loops in order to minimize the interaction. However the company highlighted how this decision can result into poor pressure control, large surge control margins and poor surge protection
- Manual intervention by the operator. However CCC emphasised that this option reduces the overall performance as surge protection is limited and the antisurge valve is usually left partially open by the operator
- Decoupling the interactions. CCC suggested this is the preferred option among the three possible options as it gives good performance control accuracy and good surge protection while reducing energy wasting on gas recycle or blow off.

CCC privileges the decoupling of the control loops in order to deal with their interactions. This approach is based on feedback and feedforward control and does not take advantage of the compressor map. A different approach has been suggested in this thesis for reducing the interaction between control loops. Model-based control has been proposed precisely because it is able to deal with a multivariable MIMO system.

7.3.2.2 Evaluation of industrial relevance of the work of the thesis

There are many accounts of dynamic control of compressors in the academic literature. As reported in the literature review presented in Chapter 2, dynamic control consists in enlarging the operating range of the compressor by either actively suppressing surge (active dynamic control) or by absorbing and dissipating surge oscillations (passive dynamic control). Promising results of dynamic surge control applications have been reported by numerous authors including Epstein et al. (1989), Gravdahl and Egeland (1999), Gysling et al. (1991), Uddin and Gravdahl (2011), Willems and de Jager (1998). However, according to Uddin and Gravdahl (2012), none of these control approaches has found an application in the industrial environment. Uddin and Gravdahl (2012) attributed the reason for this lack of success to the cost, safety and reliability of the devices required in order to guarantee

the operation of dynamic controllers. Therefore they proposed a back-up solution in case of failure of the dynamic controller.

The approach adopted in this thesis has been different from the approach of the authors mentioned above. The presence of industrial partners in the Energy SmartOps consortium and their high interaction with the academic members of the project has highlighted the importance of:

- Answering real questions, in order to work on real problem
- Taking a research direction toward outcomes that could be implemented in real plants.

The same feedback came from previous professional experiences and from new collaborations with industrial partners such as ESD Simulation Training, Xodus Group and Compressor Control Corporation. The high capital cost of a centrifugal compressor and other costs related with maintenance and lack of production have pushed industry away from dynamic control solutions coming from academia. The reason for this has already been mentioned by Uddin and Gravdahl (2012): if the dynamic control system fails, the compressor goes immediately into surge. Therefore what has been proposed in the thesis in terms of compressor control had the aim to address the real industrial problems. It addresses the concerns of Uddin and Gravdahl concerning safety and reliability by maintaining the operating point of the compressor always on the right side of the surge line.

This thesis has not directly addressed the cost issue, however. To do this would require consultation with end users, suppliers such as CCC, and also with industrial insurance underwriters to determine capital, operating and liability costs. It was outside the scope of the PhD to do this.

7.3.3 Gas recycle configuration

The practice of hot and cold gas recycle is widely used in design of compression systems. Both configurations are employed in the industrial practice for start-up, shut-down, partial load operation and surge prevention. However few academic contributions report on recycle dynamics for surge control (Botros, 2011, Botros et al., 1996a, Botros et al., 1996b) and none of them has analysed the effect of the temperature on the operation of the compression station.

More specifically, when compressing carbon dioxide from subcritical state to supercritical state, the effects of the compressor configuration on its operation are emphasised by the large variation of thermodynamic properties of the gas around the critical point. The density of the fluid is particularly important as it affects the amount of gas that flows through the antisurge valve especially during full recycle operation.

The results of the analysis on the gas recycle have demonstrated which configuration is more suitable for different type of plants. This discussion has been reported at the end of Chapter 6.

7.4 Future research development

7.4.1 Compressor modelling

7.4.1.1 Real time testing

MATLAB Simulink gives the possibility to connect the model to hardware for real-time testing and embedded system deployment. This feature may be employed in the future development of the research presented in this thesis. It could allow the testing of the proposed control system on a real compressor.

Moreover it is also possible to generate C and C++, HDL, or PLC code directly from the model (MathWorks, 2015g). Therefore the proposed control system may be implemented in any system supporting Simulink itself but also other programming languages as those cited above.

7.4.1.2 Process parameters

The literature review has highlighted the importance of some process parameters on the surge of the single stage compressor. These parameters include:

- Hold up volume in the recycle line
- Prestroke time of the antisurge valve
- Inertia of the overall compressor-driver system.

Process variables and parameters not strictly related with the compressor itself but rather linked with the recycle line are affecting surge. A further development of the research work presented in the thesis may include a quantitative evaluation of the effect of the hold-up volume on the surge of the compressor. In particular, various recycle configurations can be tested in order to verify the influence of the recycle volume on:

- Surge occurrence
- Stability of the system
- Delay in the closed loop response.

Figure 7-3 shows two different process layouts studied during the CCC training. Both of them include a gas turbine driving three compressors in series on a single shaft configuration. However in the first layout the heat exchangers have been placed before each separation vessel. In the second layout the heat exchangers have been placed downstream of the compressor. The downstream volume along the recycle line has been highlighted using blue and black clouds. For each compression stage it would be interesting to understand quantitatively the relation between the upstream and downstream volume and the occurrence of surge.

The reason for recommending this as future work is that the critical review of the academic literature presented in Chapter 2 suggested the dynamic behaviour of the outlet pressure has an influence on surge. To do the work, the model presented in Section 3.2.3 can be employed for analysing the effect of the hold up volume along the recycle line on surge occurrence. The compressor thesis model would be duplicated and configured as shown in Figure 7-3 with

appropriate choices of recycle and inter-compressor volumes. The findings could be very useful for both single and multistage configurations and would represent a guideline for the design of new compression systems and respective layouts.

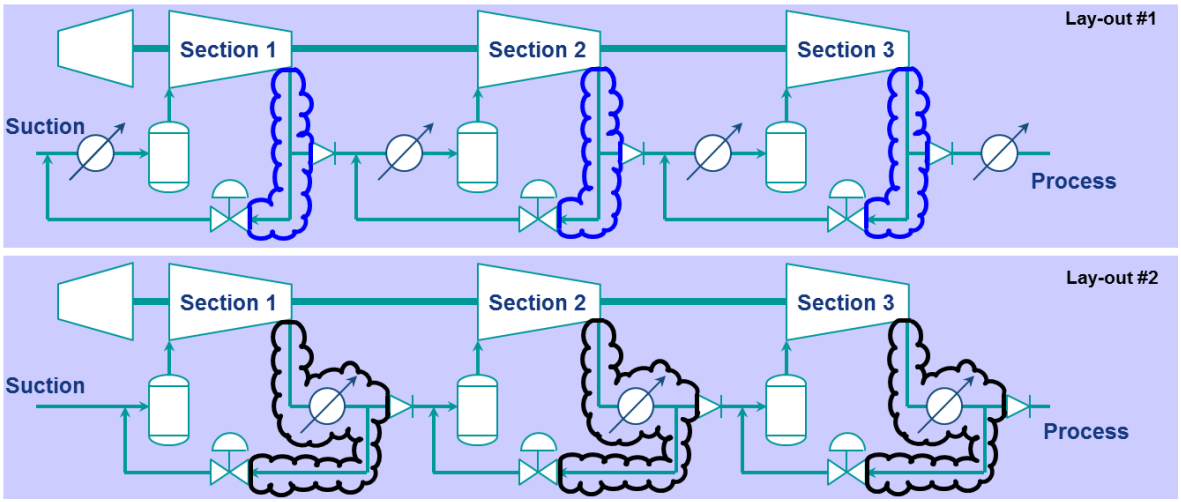


Figure 7-3. Antisurge piping configurations – modified from CCC (2013)

7.4.1.3 Multistage configurations

A model of a multistage compressor would be beneficial for the analysis of compressor operation and control. A multistage compressor includes multiple single stage compressors, which can be in series or in parallel or both. When the single stage compressors are placed in series, the purpose is to increase the outlet pressure because each stage of compression increases the overall pressure ratio of the machine. A multistage compressor is constituted by single stage compressors but also by interstage units, such as heat exchangers, separation vessels and non-return valves. Therefore all these units have to be modelled together with the single stage compressors.

When the single or multiple stage compressors are placed in parallel, the purpose is to increase the overall flow rate. This configuration can also be helpful when one of the trains must be shut down and the other train can continue to work.

In the open loop configuration these models would allow investigation of the influence of a compression stages on each other. Some progress has already been made towards this research goal. The basic structure of the open loop and closed loop model of the multistage compressor has been developed in Aspen HYSYS.

7.4.2 Compressor control

7.4.2.1 Capacity control of multistage compressors

The fully validated model of a multistage compression configuration would allow investigation of the control configuration of such a system.

For a series of compressors in a train configuration the selection of controlled variables can be optimised in order to select the most appropriate variable representing the capacity of the system. Possible controlled variables include input pressure, output pressure, delivered mass flow rate. The matching of the single stages would also be critical in order to minimise the overall energy consumption.

For parallel trains, load sharing must be taken into account. Various control philosophies can be tested and the load sharing can be optimised in order to reduce the power consumption of the overall system. For example the configuration may be tested by applying different load sharing techniques and analysis of the advantages and disadvantages. In particular, load sharing techniques for parallel compressors include:

- Equal load
- Equal distance from surge
- Real time optimization of overall power consumption.

7.4.2.2 Antisurge control of multistage compressors

In the thesis various recycle configurations have been tested and compared. A further development of this part may include the analysis of both hot and cold recycle installed on the same compressor stage or group of compressors. This analysis would be particularly interesting in a multistage configuration where various recycle configurations could be tested. For example in the surge control configuration a logic could be implemented in order to decide which recycle configuration employs depending on the origin, the type and the rate of change of the process disturbance.

In the past years the main research focus of the academic community has been on surge control rather than on joint capacity and surge control. Capacity control was almost neglected however it interacts with surge control and therefore an overall control approach is appropriate. It is important to remember that both controllers act on the same system and therefore, once more, the integration of the two control objective must be taken into account while dealing with compressor control.

Traditional control based on surge avoidance does not represent a robust control solution as it incurs an interaction between control loops. Dynamic control has not yet found a widespread industrial implementation mainly due to safety reasons. In this thesis model predictive control has been successfully tested in compressor application. Linear model predictive control has been employed in order to control pressure and surge for compressor operation. The employed objective function aimed at reducing the distance between measured variables and their set points according to the tuning weights. Other objective functions could be tested in order to reduce the power

consumption of the compressor while avoiding surge. In that case other constraints should be relaxed in order to have a feasible solution.

Non-linear model predictive control has already been employed in the literature for surge control however not for pressure and surge control together. Therefore a further development in this research area would be the definition and testing of a non-linear model predictive controller.

7.4.2.3 Adaptation of the compressor model

Following the previous discussion on model-based control and model mismatch, the compressor model may be adapted to variation of the boundary conditions of the system. This would be particularly interesting in the case of:

- Fouling
- Variation of the process fluid composition.

These two phenomena usually take place for longer periods of time and therefore should not be considered as disturbance variables of the system. The model of the compressor may be adapted by recording the operating conditions of the machine over time and redrawing an updated version of the compressor maps, with a focus on pressure ratio and efficiency.

7.4.3 Supercritical compression

The analysis of the literature review has highlighted a huge gap in the research field of compression of supercritical carbon dioxide. Some works were aimed at analysing the fluid dynamic of carbon dioxide inside a compressor around and above the critical point. Even the most recent publications (Kim et al., 2014, Moore et al., 2012, Utamura et al., 2012) have highlighted discrepancies between numerical and experimental results. Accurate models describing the effects of real gases in the supercritical state, fluid turbulence and density fluctuation are lacking and therefore further investigations in this field are needed.

Few compressor configurations were specifically designed for the compression of carbon dioxide. In most cases natural gas facilities are employed. Control systems for carbon dioxide compression systems usually neglect the control of the compressor itself. The reason is that technology based on supercritical CO_2 is still in its early stage and therefore still aims at optimising the process operation. Therefore this research field would benefit from process and control configuration specifically developed for carbon dioxide applications such as advanced controllers for compressor applications integrated with the controller of the overall system.

The results reported in the thesis are based on the assumption that the correction of the compressor maps is still based on the equations (3-11) and (3-12) even when the machine is operating in supercritical state. However this assumption should be verified and validated by experimental

results. In the literature the performances of a centrifugal compressor in supercritical state have been investigated only in steady state or quasi steady state conditions.

The methodologies and results reported in the thesis can be adopted by the research community and developed in order to be suitable for real time testing, various process layouts, multistage configurations and integration with process performance controllers.

8 Conclusions

This is the conclusive chapter of the thesis. It provides the conclusion of the PhD project as part of the Energy SmartOps Project, the conclusion of the thesis as a detailed report on the research activity and finally the conclusion of the technical outcomes achieved during the PhD.

8.1 Conclusion of the project

The PhD project is part of the Energy SmartOps ("Energy savings from smart operation of electrical, process and mechanical equipment") Project, funded by the Marie Curie Initial Training Networks (ITN). The principal aim of Energy SmartOps is to realise energy saving from integrated operation and it has been divided in various research objectives and work packages.

The PhD project is part of:

- Research objective 2: to devise new algorithms for overall performance monitoring and control
- Work package 2: turbomachinery
- Sub-task4: control systems for centrifugal CO_2 compressors.

The main outcomes of the PhD project include publications and presentations at international conferences, collaboration with the partners of the Energy SmartOps consortium and outreach activities. The list of publications includes the following papers:

- Budinis, S. & Thornhill, N. F. (2014). An integrated control technique for compressor operation. *10th International Conference on Control*, 9th-11th July 2014 Loughborough University (Budinis and Thornhill, 2014)
- Budinis, S. & Thornhill, N. F. (2015). Control of centrifugal compressors via model predictive control for enhanced oil recovery applications. *2nd IFAC Workshop on Automatic Control in Offshore Oil and Gas Production*, May 2015a Florianópolis, Brazil (Budinis and Thornhill, 2015a)
- Budinis, S. & Thornhill, N. F. (2015). Supercritical gas recycle analysis for surge control of centrifugal compressors. *PSE2015/ESCAPE25*, May 2015b Copenhagen, Denmark (Budinis and Thornhill, 2015b)
- Budinis, S. & Thornhill, N. F. (2015). Supercritical gas recycle analysis for surge control of centrifugal compressors. *Computer Aided Chemical Engineering: Special Issue* (invited paper) (Budinis and Thornhill, 2015c).

8.2 Conclusion of the thesis

The thesis has been structured in order to present in a logical sequence the following initial aspects:

- The general aims of the Energy SmartOps project
- The general aims of the PhD project
- The analysis of the industrial background and of the literature review
- The specific aims of the PhD project.

Then the specific aims of the PhD project have been divided in tasks and subtasks and the fulfilment of these tasks have constituted the methodology of the thesis. This has consisted in:

- Modelling, implementation, validation and testing of the open loop system
- Modelling, tuning and testing of the closed loop system.

In the closed loop system a traditional state-of-the-art control system has been initially employed. Its limitations such as control loops interactions have been demonstrated via dynamic simulations.

In Chapter 4 a model-based feedforward controller has been proposed and tested in order to improve the response of the pressure controller. In Chapter 5 a linear model predictive controller has also been proposed in order to integrate pressure and surge controller, avoiding control loops interactions and constraining manipulated and measured variables within predefined boundaries.

Chapter 6 has explored the effect of the recycle configuration on the operation of the compressor during partial and full recycle. Operating the compressor in partial and full recycle is common for surge prevention. However it is particularly interesting when dealing with carbon dioxide in supercritical state. The reason is that, if the compression from subcritical to supercritical condition takes place when CO_2 flows through the compressor, the opposite transition takes place along the recycle line. The thermodynamic conditions of the gas affect the amount of gas that can be recycled, especially during full recycle operation.

The last part of the thesis covers the discussion of the results and the conclusion.

8.3 Conclusion of the research

8.3.1 Aims of the research activity

The topic of the research activity has been control and operation of centrifugal gas compressors, with an emphasis on compression of carbon dioxide. In particular, the three main topics of research are:

- Analysis and improvement of the capacity controller
- Analysis and improvement of antisurge controller and its integration with the performance controller
- Investigation of supercritical transition in the compression of carbon dioxide.

These challenges have been employed in order to define the general aims of the thesis:

- The reduction of the cost of gas compression
- The reduction of the interactions between controllers in order to achieve process controllability and stability
- The identification of the key issues in the compression and recycling of supercritical carbon dioxide.

Following the literature review, more specific research objectives have been defined and they include modelling and simulation of a compression station, reduction of control loop interaction by integrated control approach and investigation of supercritical CO_2 compression, operation and control.

Strengths and weaknesses of the adopted methodologies and of the reported finding have been covered in Chapter 7, which reports on topics such as:

- Mathematical modelling of compressors
- Parameter estimation and model validation
- Model-based control
- Hierarchy and timescale of process control.

Chapter 7 also reports the suggested direction for future research activities.

8.3.2 Tasks and contributions

The research objectives of the thesis have been divided in the following tasks:

- Modelling of the open loop compression system
- Modelling of the reference control system
- Implementation of the closed loop model
- Description of the reference case study

- Validation of the closed loop model
- Demonstration of interactions between control loops in the reference pressure controller
- Improvement of the response of the capacity controller and reduction of the interaction between control loops
- Analysis of the open loop response of the compression system
- Integration of pressure and surge control action
- Reduction of the recycle flow rate
- Analysis of the effect of the recycle configurations on surge occurrence, pressure control and stability of the compression system and energy consumption.

The novel contributions of the thesis can be summarised as follow:

- Identification of research needs for compressor control
- Analysis of the effect of boundary disturbances on open and closed loop system
- Improvement of the response of the capacity controller
- Integration of pressure and surge control
- Definition of performance parameters for performance monitoring tools
- Representation of the distance of the operating point from surge over time
- Analysis of the effect of the recycle configuration on the response of the control system during supercritical compression of carbon dioxide.

These contributions have been achieved by means of design, dynamic modelling and simulation of compression systems.

8.3.3 Modelling of compression systems

The aim of the study to build a compressor dynamic model and validate it against real data has been achieved. The model of the compression system includes a main forward process line and a secondary recycle line. The types of recycle configurations are numerous however they can be mainly characterised by the temperature and the volume of the recycle.

The implementation of the model included the selection of modelling and simulation tool, of the method for the resolution of the algebraic and differential equations, of the input and output variables. The models of the compression system and of its control system have been implemented in MATLAB Simulink. This tool allows multi-domain simulation and model-based design and also gives the possibility to connect the model to hardware for real-time testing and embedded system deployment. This option could be very useful in the future for the implementation of the proposed control systems in a real system.

The validation of the model was fundamental in order to guarantee the accuracy and reliability of the model. The estimation of the model parameters has been followed by the validation of the model. The validation has given good results and guaranteed the accuracy of the model and its matching with the case study.

The analysis of the open loop response of the compression system was performed in order to give insight on the effect of boundary disturbances on the operation of the compressor. The analysis was mainly focus on understanding the effect of the disturbance on the controlled variables i.e. compressor outlet pressure p and inlet mass flow rate m.

Therefore the main outcomes of the thesis on modelling of compression systems include:

- A fully validated non-linear dynamic model for compressor applications
- The evaluation of the effects of boundary disturbance on both open and closed loop compression systems.

A key finding consisted in the effect of the variation of the pressure of the system on the mass flow rate through the compressor, depending on the origin of the pressure disturbance. This has helped to understand the response of the compressor when in open or closed loop.

8.3.4 Interaction between control loops

The aim of reducing the interaction between pressure control loop and antisurge control loop has been achieved.

A standard control system for centrifugal compressor consists of two control loops: the pressure control loop and the antisurge control loop. This standard control system represents the state of the art control system for gas compressors and this concept has already been reported and demonstrated against literature in Chapters 1 and 2. This control system has been selected and modelled taking into accounts its diffusion in industrial applications and also the motivations behind its popularity. The two control loops implemented in the system are the capacity control loop and antisurge control loop and they have been presented in detail.

The two separate control loops act on the same process system and therefore influence each other. The interaction between the control loops should be reduced in order to guarantee smooth and stable operation and protection of the compressor from surge. Two examples of interactions between control loops within the compressor control system have been reported and they demonstrate the importance of taking into account this issue when dealing with control of compressors.

Among the tested process disturbances, those causing gas recycling have been identified. These disturbances cause a problematic interaction between the control loops and cause the opening of the recycle valve. They include:

- Closure of the boundary valves of the system
- Increase of the boundary pressures of the system.

Therefore the main outcomes of the research study include:

- The demonstration of beneficial and problematic interactions between control loops

- The identification of specific boundary disturbances causing reduction of flow rate and therefore pushing the compressor toward surge
- The reduction of the interaction between control loops by means of model predictive control.

The results have demonstrated how the pressure and surge controllers interact when they have separate control loops and how the implementation of a model predictive controller can avoid this issue.

8.3.5 Performance parameters and surge margin representation

The aims of the study were to evaluate the control performance of various control systems and to represent the surge margin in a clear and understandable way. Both these aims have been achieved.

Performance parameters have been proposed in order to estimate the performance of the control system. These parameters take into account various aspects of the operation of the control system. They estimate the following parameters:

- The distance between the compressor outlet pressure and its set point over time
- The amount of gas recycled for surge protection
- The energy consumption due to gas compression and recycle cooling when present.

Graphical representations of the compressor inlet flow rate and the surge flow rate over time have been employed for verifying surge occurrence. The margin between the operating point of the compressor and the surge region is usually represented over a compressor map. However this representation does not take into account the effect of the inlet condition of the compressor on the location of the surge line. Moreover it is not appropriate for representing dynamic operation during transients of the machine. Therefore a different representation has been proposed and employed specifically with the purpose of estimating the distance of the compressor from surge over time. This representation allowed to:

- Quickly identify the distance between operating point and surge point over time
- Identify the influence of the inlet disturbances on the surge flow rate.

Therefore the main outcomes of the thesis include:

- Performance parameters specifically designed for compressor applications
- The representation of the distance between operating point of the compressor and surge margin in a simple and understandable way that also shows the effect on inlet disturbances on surge line location.

The work was presented at the 2nd IFAC Workshop on Automatic Control in Offshore Oil and Gas Production in May 2015 (Budinis and Thornhill, 2015a).

8.3.6 Control of pressure

The aim of the study to improve the performance of the pressure controller during boundary disturbances has been achieved.

The improvement of the performance of the capacity controller has been achieved by proposing a model-based feedforward controller. It has been defined, implemented, tuned and tested. This model-based controller employs the compressor map in order to estimate the set point for the rotational shaft speed. The controller has been compared with the traditional cascade PI controller during a variety of boundary disturbances. In all the tested cases the MBFC has demonstrated to perform better than the traditional PI. The performance has been demonstrated using a performance parameter and also via graphical representation. Simulation results have also demonstrated that the rate of change of the disturbance does not affect the operation of the MBFC in terms of pressure control. The results have also demonstrated that better pressure control reduces the oscillation of compressor mass flow rate and surge flow rate over time and therefore reduces the risk of gas recycle and potentially surge.

The results have also demonstrated that better pressure control reduces the oscillation of compressor mass flow rate and surge flow rate over time and therefore reduces the risk of gas recycle and potentially surge. One of the aims of the thesis was to achieve this goal, and these improvements illustrate it is feasible and realistic to do that.

Therefore the outcomes of the thesis also include a model-based feedforward controller able to improve the performance in terms of pressure control. The initial outcome of the work was presented at the AIChE Annual Meeting in November 2013 (Budinis et al., 2013). Further results were presented at the 10th International Conference on Control in July 2014 (Budinis and Thornhill, 2014).

8.3.7 Control of surge

The aim of the study to integrate pressure and surge control has been achieved.

In order to further improve the response of the overall system and to integrate pressure and surge control, a linear model predictive controller has been proposed in order to control the compressor outlet pressure while avoiding surge. Different disturbance scenarios have been tested and three tuning sets have been proposed. The results demonstrate that the MPC controller is able to control the outlet pressure of the compressor while avoiding surge. Therefore pressure and surge control action have been integrated in a single controller. The results also demonstrate that the MPC controller is more suitable than a PI controller for a multiple-input multiple-output process system such as a centrifugal compressor.

The proposed model predictive controller has demonstrated to be:

- Suitable for compressor applications

- Able to control both compressor outlet pressure and surge
- Adaptable via tuning to various control purposes such as energy saving, surge avoidance and pressure control performance.

The work was presented at the 2nd IFAC Workshop on Automatic Control in Offshore Oil and Gas Production in May 2015 (Budinis and Thornhill, 2015a).

8.3.8 Reduction of recycle flow rate

The aim of the study to reduce the amount of gas recycled during boundary disturbances has been achieved. In fact one of the general aims of the thesis was to reduce the recycle flow rate. The reason was that the energy to compress the gas is wasted when it is recycled.

The results have demonstrated that under certain disturbances it is not possible to keep the pressure at its set point while avoiding surge without recycling. The tuning of the controller must be performed accordingly to the wanted outcome. Three control tuning sets were proposed in order to give priority to respectively energy saving, surge avoidance or pressure control performance. In all the tested cases the MPC controller performed as requested. The other tuning sets have demonstrated that the MPC controller can be tuned accordingly to the desired control purpose. The decision regarding the type of tuning to adopt depends on many factors and cannot be generalised. However this chapter has provided useful insights on the operation and control of compressors and also a simulation tool able to integrate the control of pressure and surge in a single controller.

The work was presented at the 2nd IFAC Workshop on Automatic Control in Offshore Oil and Gas Production in May 2015 (Budinis and Thornhill, 2015a).

8.3.9 Effect of recycle configuration on control stability

The aim of the study to analyse the effect of the recycle configuration on the operation of the compressor has been achieved.

The effect of the recycle configuration on the operation of the control system was analysed. Hot and cold gas recycle configurations were compared employing various parameters such as their tendency towards surge, control performance and system stability, the power consumption and the operation in full recycle mode. The results demonstrate that the cold gas recycle configuration surges at a lower magnitude of disturbance. This is because of the effect of the cold recycled gas on the location of the surge region.

The reported results have also demonstrated that the cold gas recycle has a lower performance in terms of pressure control. This is due to the higher amount of gas recycled over time. However this configuration oscillates less than the hot recycle configuration. The oscillation is due to the continuous opening and closing of the antisurge valve, which has to react quickly in case the mass

flow rate at the inlet of the compressor becomes smaller than the control flow rate. This part of the work was presented at the PSE2015-ESCAPE25 Conference in May 2015 (Budinis and Thornhill, 2015b).

The high amount of gas recycled in the cold gas configuration increase its power consumption with respect to the hot recycle configuration. This is due to both gas compression and recycled gas cooling.

Subcritical and supercritical compressions have been compared during full recycle operation. The conclusion is that a subcritical compressor operating in full recycle mode is able to recycle 22.64 % more gas by means of a cold gas recycle rather than a hot gas recycle. However in the supercritical compressor this amount rises to 81.50 %. This result is decisive when full recycle is needed for surge protection.

In the selection between hot and cold gas recycle the process parameters that are usually considered include time delay in the process response and machine integrity. In particular recycling of hot gas should be limited over time in order to guarantee the integrity of the machine. The reported results however have demonstrated that other aspects should be taken into account as well, such as:

- Surge occurrence
- Energy consumption
- Maximum recycle flow rate during full recycle operation.

These aspects have been taken into account during the research work and have been reported in the thesis.

8.3.10 Final comment

Operation and control of centrifugal compressors has a prominent role in both academic and industrial research. Existing challenges are continuous and safe operation, system stability and reduction of operating and capital costs. Therefore this thesis has successfully contributed to extending the field of safe and stable compressor operation and control.

9 Appendix

9.1 Appendix 1: Implementation of the open loop model of the compression system

Appendix 1 shows the structure of the Simulink model of a generic open loop compression system. The model includes a main block with input and output variables. The main block includes various sub-blocks that will be presented. The equations relating input and output variables have been presented in Chapter 3.

9.1.1 Main block

The main block of the Simulink model represents the open loop compression system having a hot gas recycle configuration. Inlet and outlet variables have been represented in Figure 3-20. The inlet variables are disturbances variables and manipulated variables including:

- System inlet pressure p_{in}
- System outlet pressure p_{out}
- Opening position of system inlet valve op_{in}
- Opening position of system outlet valve op_{out}
- Driver torque τ_d
- Opening position of antisurge valve op_{ASV}.

Outlet variables include controlled variables and other output variables that are important for estimating the performance of the compressor:

- Compressor outlet pressure p
- Compressor inlet flow rate m
- Rotational shaft speed N
- Compressor inlet temperature T_{01}
- Compressor outlet temperature T_{02}
- Surge flow rate m_{surge}.

Inside this main block there are other six blocks as represented in Figure 2-5. These blocks are:

- The inlet block
- The outlet block
- The recycle block
- The compressor block
- The inlet temperature and power consumption block
- The surge limit block.

Each of these blocks will be explained in more detail in the following part of Appendix 1. An additional block has been added in order to estimate m_{pout} according to equation (3-22). A saturation block has been added in order to guarantee the positive sign of the surge flow rate m_{surge}. The structure of the main Simulink block is represented in Figure 9-3.

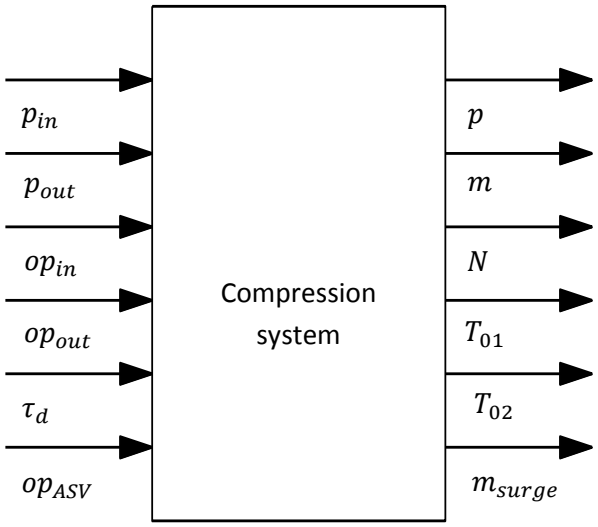


Figure 9-1. Inlet and outlet variables of the Simulink main block

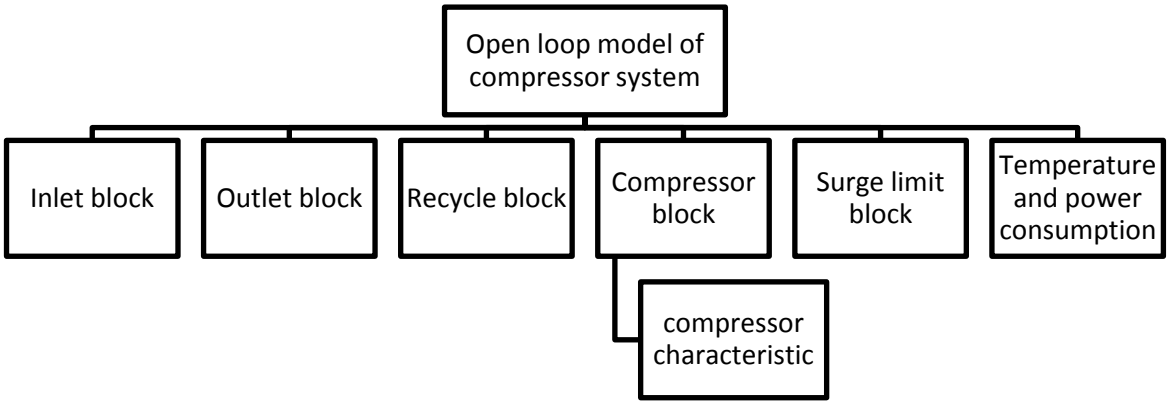


Figure 9-2. Structure of the Simulink main block (tree diagram)

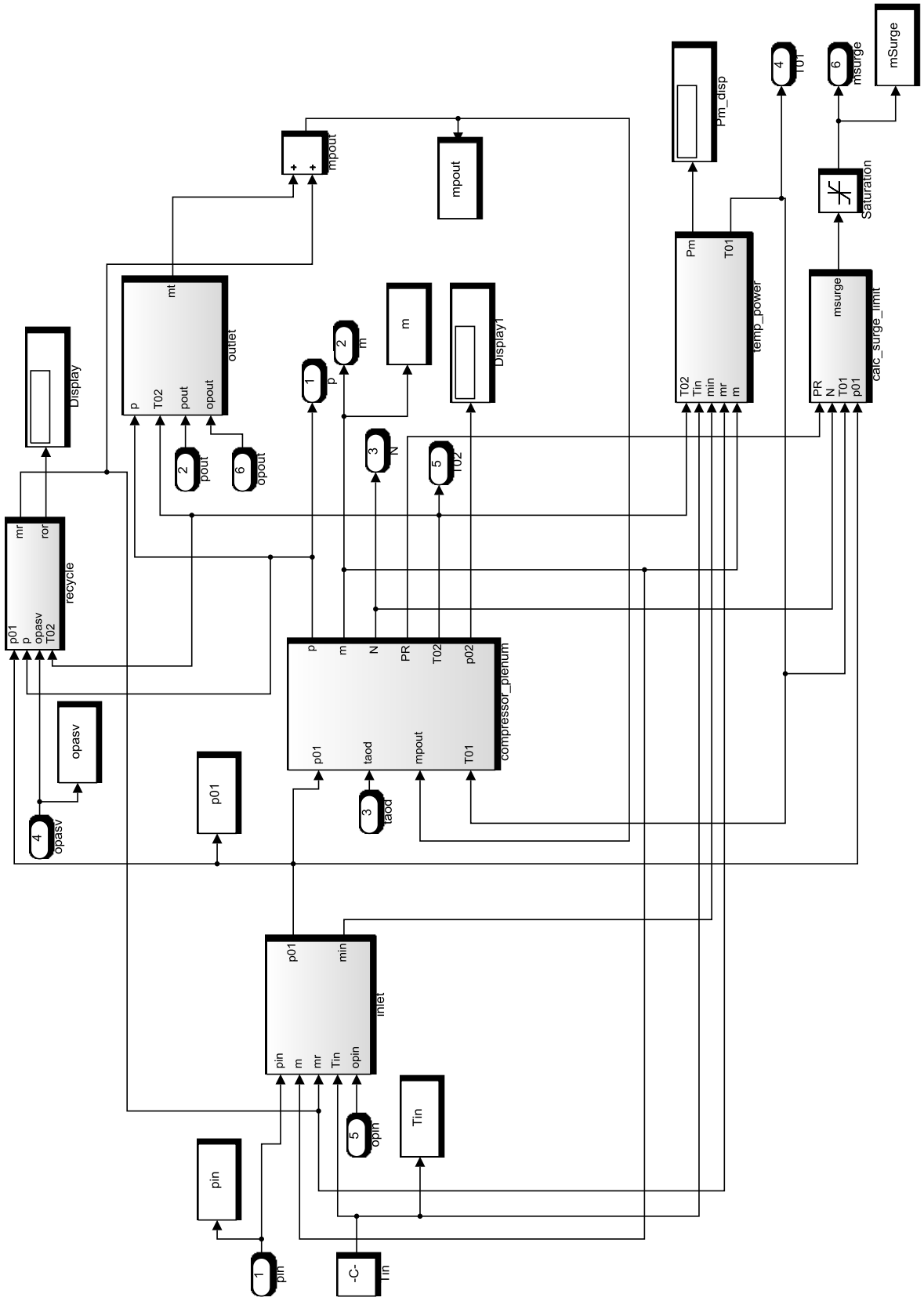


Figure 9-3. Structure of the Simulink main block

9.1.2 Inlet block

The inlet block has been employed in order to estimate variables corresponding to the inlet section of the compressor, such as the system inlet flow rate m_{in} and the compressor inlet pressure p_{01}. Input and output variables are summarised in Figure 9-4. The structure of the block is represented in Figure 9-5.

A saturation block has been employed in order to guarantee the positive sign of m_{in}. From a physical point of view this means that the recycle flow rate m_r cannot be higher than the flow rate through the compressor m. If the recycle flow rate is higher than the compressor flow rate during a transient operation, this means that the inlet flow rate is equal to zero and the compressor is operating in full recycle mode.

A memory block has been employed in order to define the value of the compressor inlet pressure p_{01} at time t=0 s. The memory block holds and delays its input by one integration time step.

The block *density_mix_stage1* estimates the density of the fluid at the inlet of the system as a function of the system inlet pressure p_{in} and temperature T_{in}. Two dimensional look-up tables have been employed for this purpose.

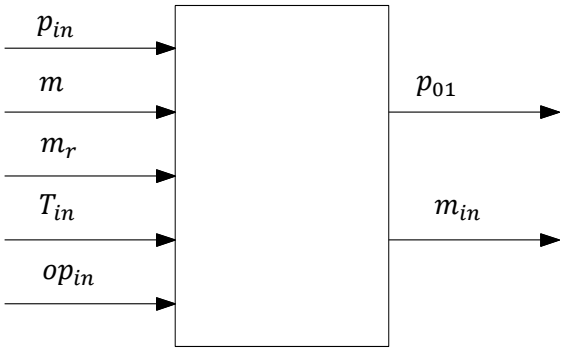


Figure 9-4. Inlet and outlet variables of the Simulink inlet block

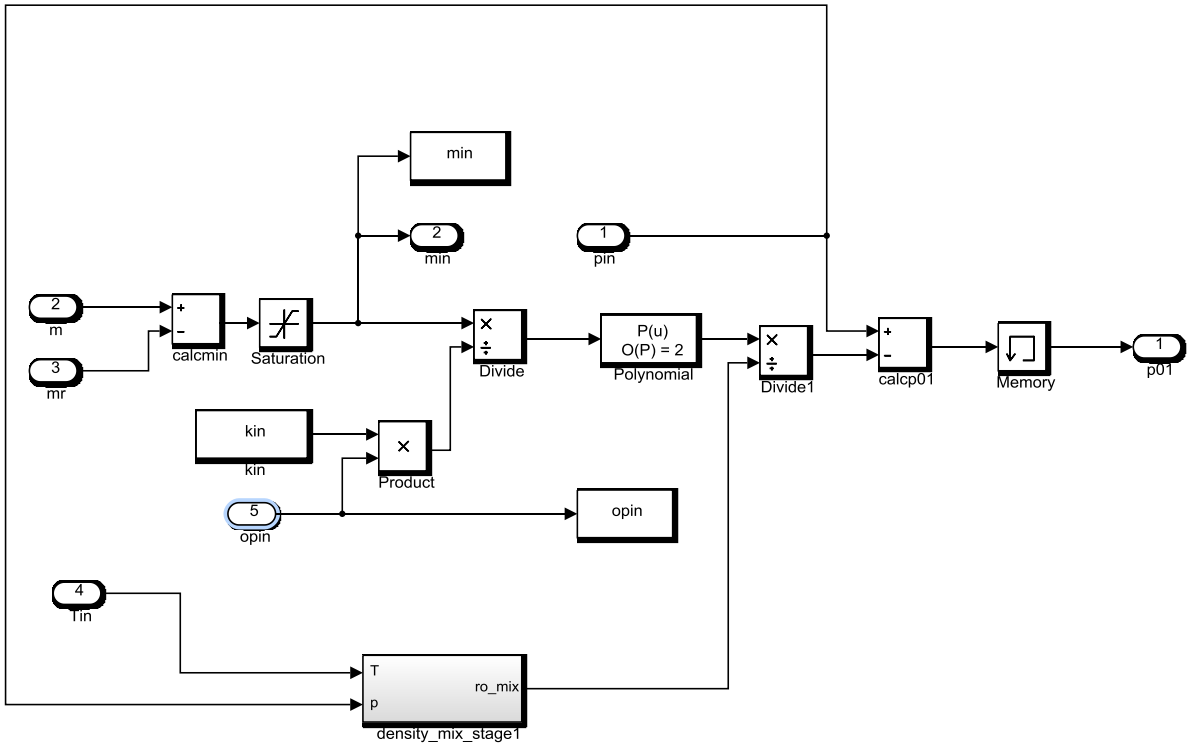


Figure 9-5. Structure of the Simulink inlet block

9.1.3 Outlet block

The outlet block has been employed in order to estimate variables corresponding to the outlet section of the compressor, such as the system outlet flow rate m_t. Input and output variables are summarised in Figure 9-6. The structure of the block is represented in Figure 9-7.

A saturation block has been employed in order to guarantee the positive sign of the argument of the square root block. From a physical point of view this means that the outlet valve is a non-return valve. If the compressor outlet pressure p becomes lower than the system outlet pressure p_{out} during a transient operation, this means that the outlet flow rate m_t is equal to zero and the compressor is operating in full recycle mode. This phenomenon can actually take place during transient operation. This is because the system outlet pressure has a constant value and this value can be above the minimum pressure delivered by the compressor, depending on the compressor inlet pressure, mass flow rate and rotational shaft speed. The saturation block has therefore two functions. The first function is numerical, in fact it avoids having a negative number as argument of the square root represented in Figure 9-7. The second function is to actually represent the presence of a non-return valve, by filtering all the inlet values below zero.

The block *density_mix_stage1* estimates the density of the fluid at the outlet of the system as a function of the compressor outlet pressure p and temperature T_{02}. Two dimensional look-up tables have been employed for this purpose.

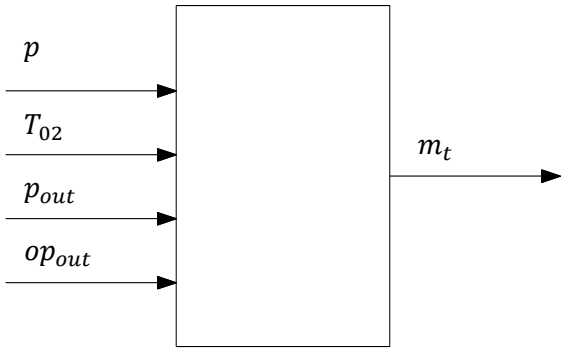


Figure 9-6. Inlet and outlet variables of the Simulink outlet block

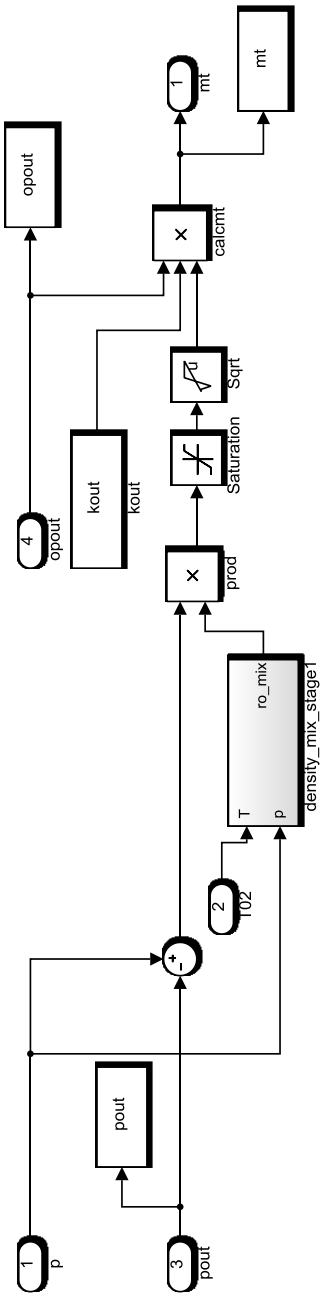


Figure 9-7. Structure of the Simulink outlet block

9.1.4 Recycle block

The recycle block has been employed in order to estimate variables corresponding to the recycle section of the compressor, such as the recycle flow rate m_r and the recycle density ρ_r. Input and output variables are summarised in Figure 9-8. The structure of the block is represented in Figure 9-9.

A saturation block has been employed in order to guarantee the positive sign of the argument of the square root block. From a physical point of view this means that the compressor inlet pressure p_{01}

must be always above or equal to the compressor outlet pressure p, as expected. If this does not happen then the recycle flow rate m_r must be equal to zero.

The block *density_mix_stage1* estimates the density of the fluid in the recycle section as a function of the compressor outlet pressure p and temperature T_{02}. Two dimensional look-up tables have been employed for this purpose.

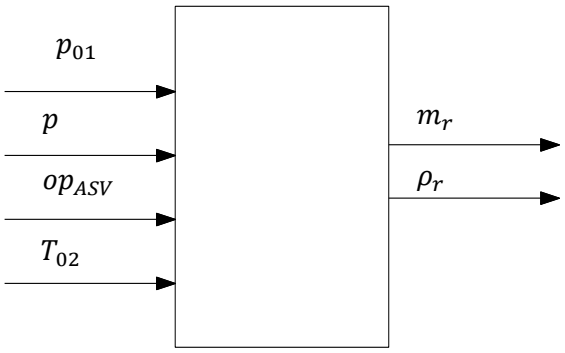


Figure 9-8. Inlet and outlet variables of the Simulink recycle block

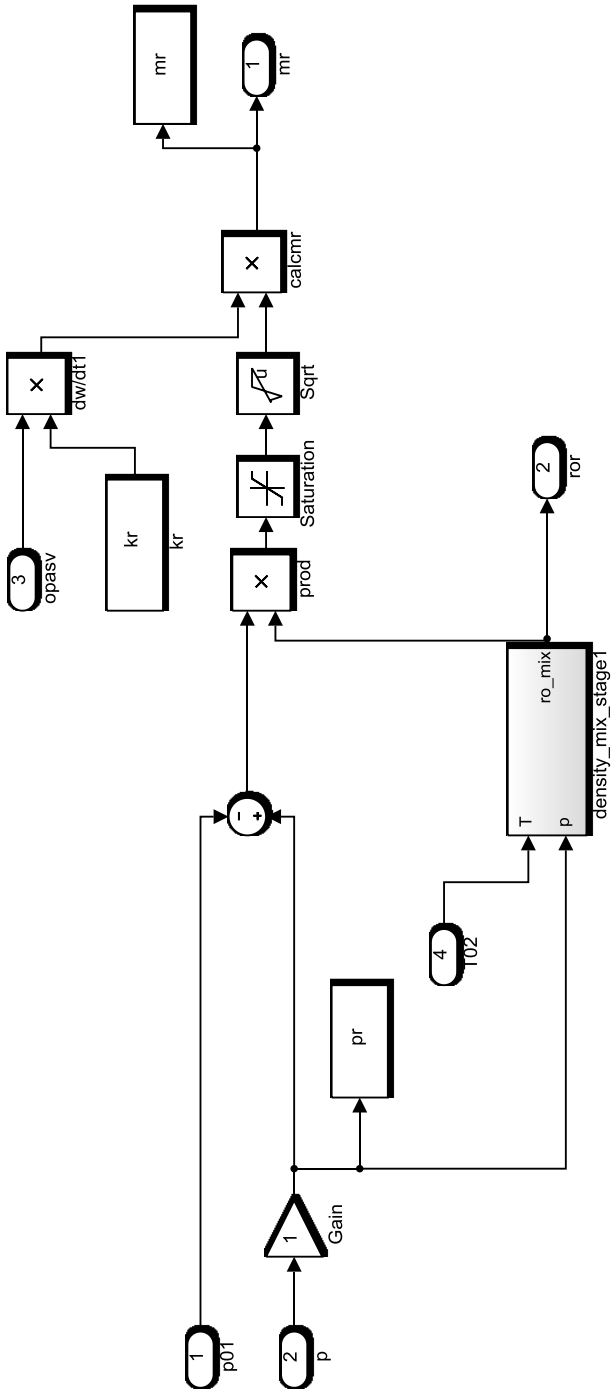


Figure 9-9. Structure of the Simulink recycle block

9.1.5 Compressor block

The compressor block, called *compressor_plenum* block, has been employed in order to solve the differential equations of the compressor and estimate the variables p, m and ω. A gain block has been employed to convert ω to N according to equation (3-4). The output variables of this block include also the pressure ratio of the compressor Ψ_c and the compressor outlet temperature and

pressure T_{02} and p_{02}, as represented in Figure 9-10. Figure 9-11 represents the structure of the block.

A rate limiter block has been employed in order to represent the rate limiter present in the real system. Its effect on the operation of the compressor and on the estimation of the moment of inertia of the system has been discussed in Chapter 3.

The sub-block called *compressor characteristic* has been employed in order to estimate the pressure ratio Ψ_c, the polytropic efficiency η_p and the compressor outlet temperature T_{02}. Its structure is represented in Figure 9-12. The estimation of the outlet temperature of the compressor has been performed by means of equation (3-18) for subcritical compression and by means of compressor map for supercritical compression, as explained in Chapter 6.

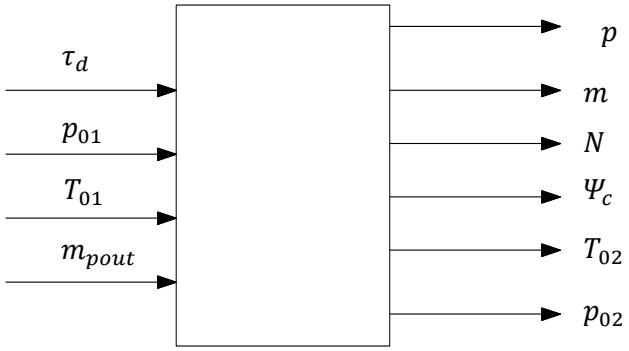


Figure 9-10. Inlet and outlet variables of the Simulink compressor block

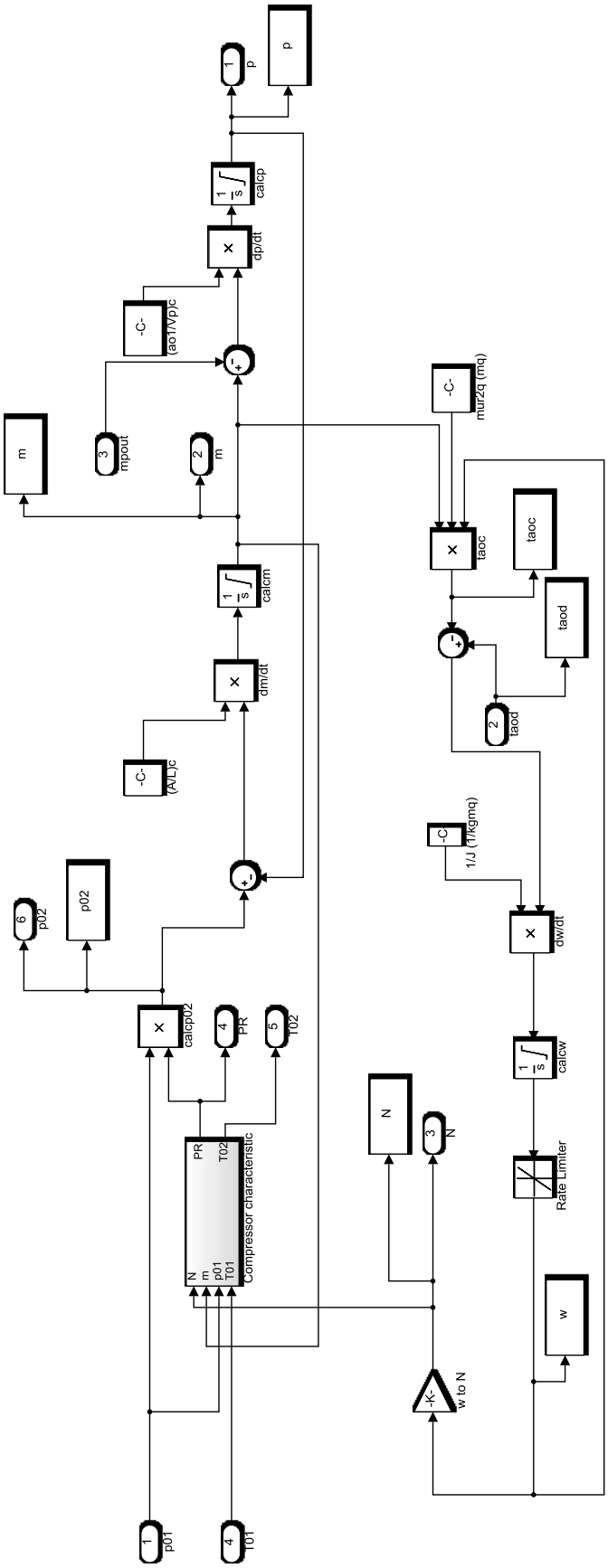


Figure 9-11. Structure of the Simulink compressor block

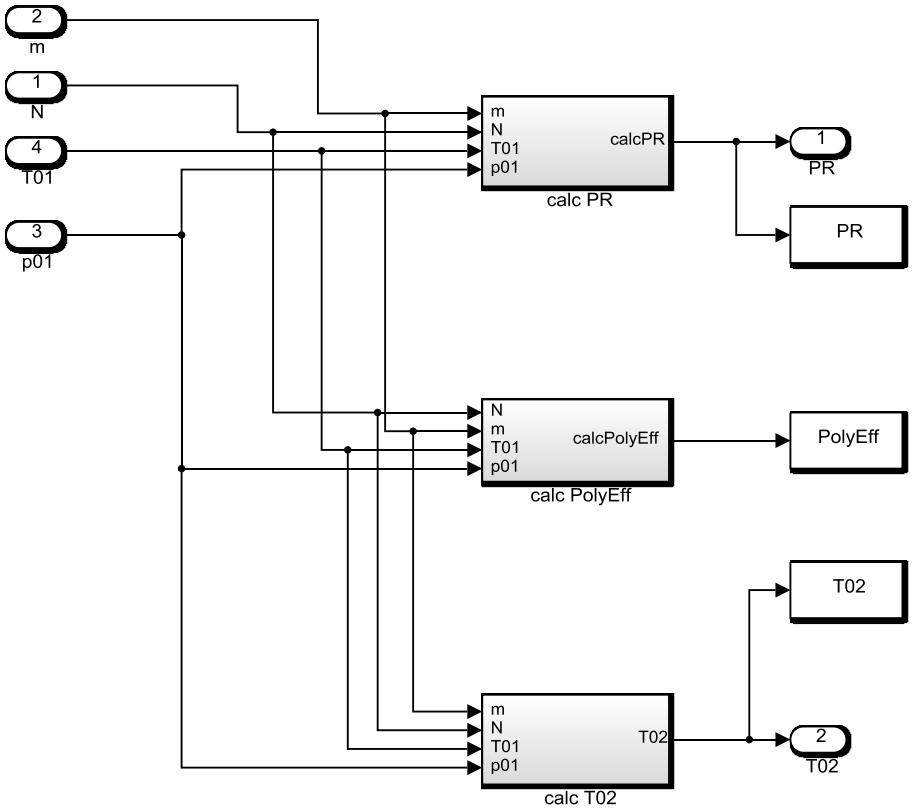


Figure 9-12. Structure of the Simulink compressor characteristic block

9.1.6 Inlet temperature and power block

A block called *temp_power* block has been employed in order to estimate the inlet temperature of the compressor T_{01} and the power consumption P_m. Inlet and outlet variables have been summarised in Figure 9-13 while the block structure has been represented in Figure 9-14. If the recycle valve is closed the compressor inlet temperature T_{01} is equal to the system inlet temperature T_{in}. Otherwise T_{01} is estimated by means of equation (3-25). The power consumption of the compressor depends on the compressor inlet and outlet temperature, respectively T_{01} and T_{02}, and on the mass flow rate through the compressor m, according to equation (3-13).

A memory block has been employed in order to initialise the variable T_{01} to its steady state value.

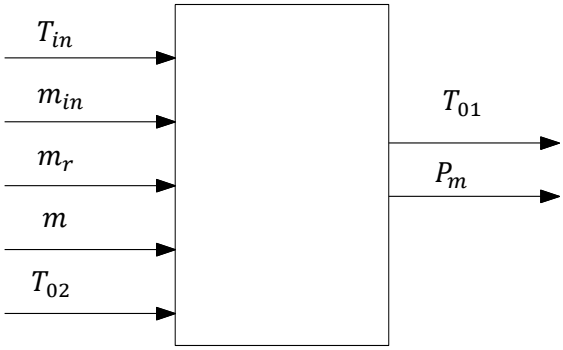


Figure 9-13. Inlet and outlet variables of the Simulink temperature-power block

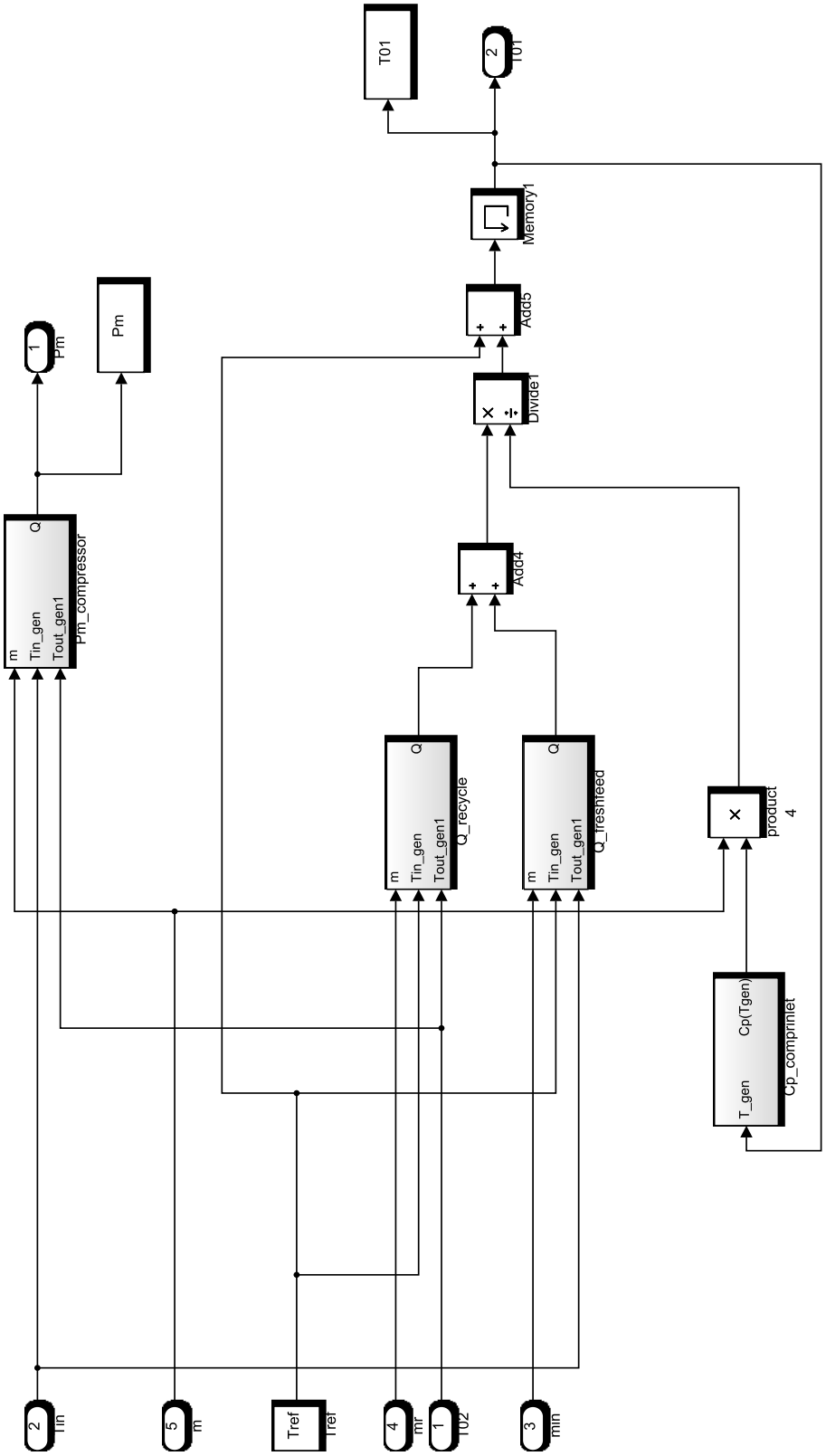


Figure 9-14. Structure of the Simulink block for estimating compressor inlet temperature and power consumption

9.1.7 Surge margin block

The sure margin block, called *calc_surge_limit*, has been employed in order to estimate the surge flow rate m_{surge} by means of equation (3-35). Input and output variables are summarised in Figure 9-15 while the structure of the block is represented in Figure 9-16. Both corrected and non-corrected surge flow rate have been estimated and a manual switch has been employed in order to select the desired value.

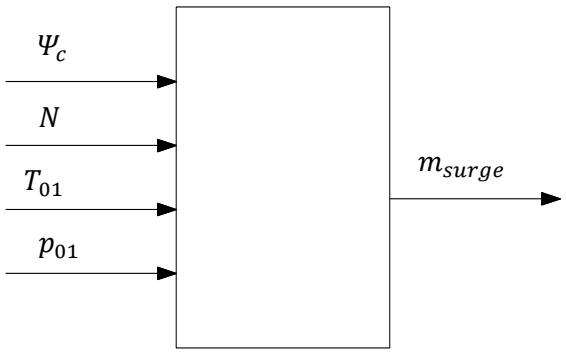


Figure 9-15. Inlet and outlet variables of the Simulink surge margin block

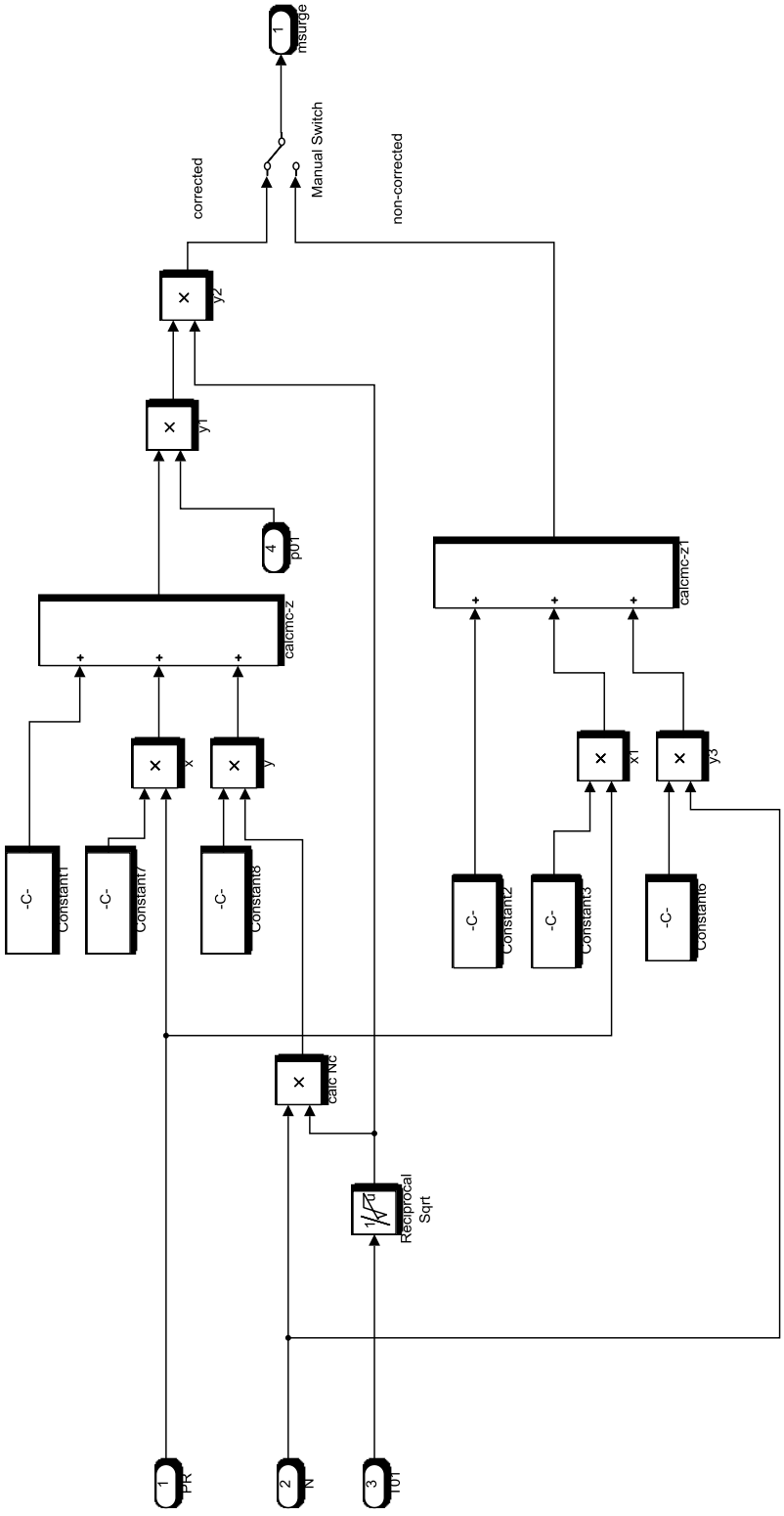


Figure 9-16. Structure of the Simulink surge limit block

9.2 Appendix 2: methodology of validation of ESD Simulation Tool

This Appendix gives more details on the procedure of validation of the simulation tool developed and employed by the research partner ESD Simulation Training. This procedure has already been introduced in Chapter 3. Here more details are given on the software interface and on the steps of the validation methodology. The numerical results of the validation analysis have not been reported because of the non-disclosure agreement with the research partner. Therefore the focus on this Appendix is on the methodology of validation.

9.2.1 Software interface

The main window of the simulation software contains buttons that permit the user to display the corresponding subsections of the simulator. Moreover it is possible to pause and resume the simulator and to visualise the Emergency Shut Down (ESD) page, the Alarms Page and the Trends Page. The simulation usually runs as fast as real time.

The main window is represented in Figure 9-17 and gives a general overview of the process layout. The process is divided into single subsections corresponding to the single stage of compression. Therefore there are four main subsections. In every single subsection there are buttons to show the previous or the following subsection, following the stream of the process fluid, as highlighted in Figure 9-18. The values of the process variables have been hidden by means of blue rectangles.

In the Trends Window it is possible to visualise the trends of various process variables. For each process variable it is possible to see its description, the present value, the unit and the date of the simulation. It is also possible to move its position into the graph area by changing its range of representation. The set of variables can be customised, as each variable can be removed and substituted by another variable.

The water content of the compressor inlet stream is an important variable. In fact carbon dioxide can dissolve in water and form carbonic acid, which is corrosive for compressors and pipelines. Therefore for each subsection it is possible to display the water content curve of the inlet stream. Moreover from each compressor window it is possible to plot the pressure-head curve representing the pressure head of the compressor.

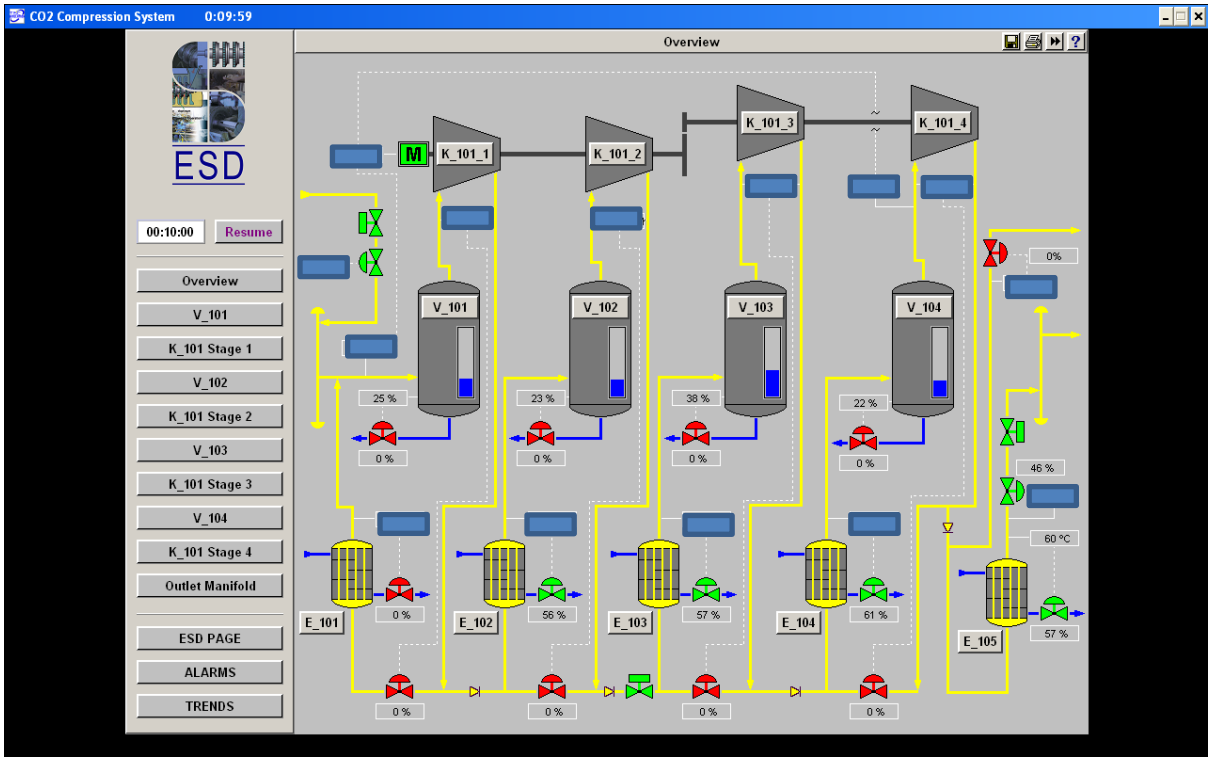


Figure 9-17. Main window of the ESD simulation tool

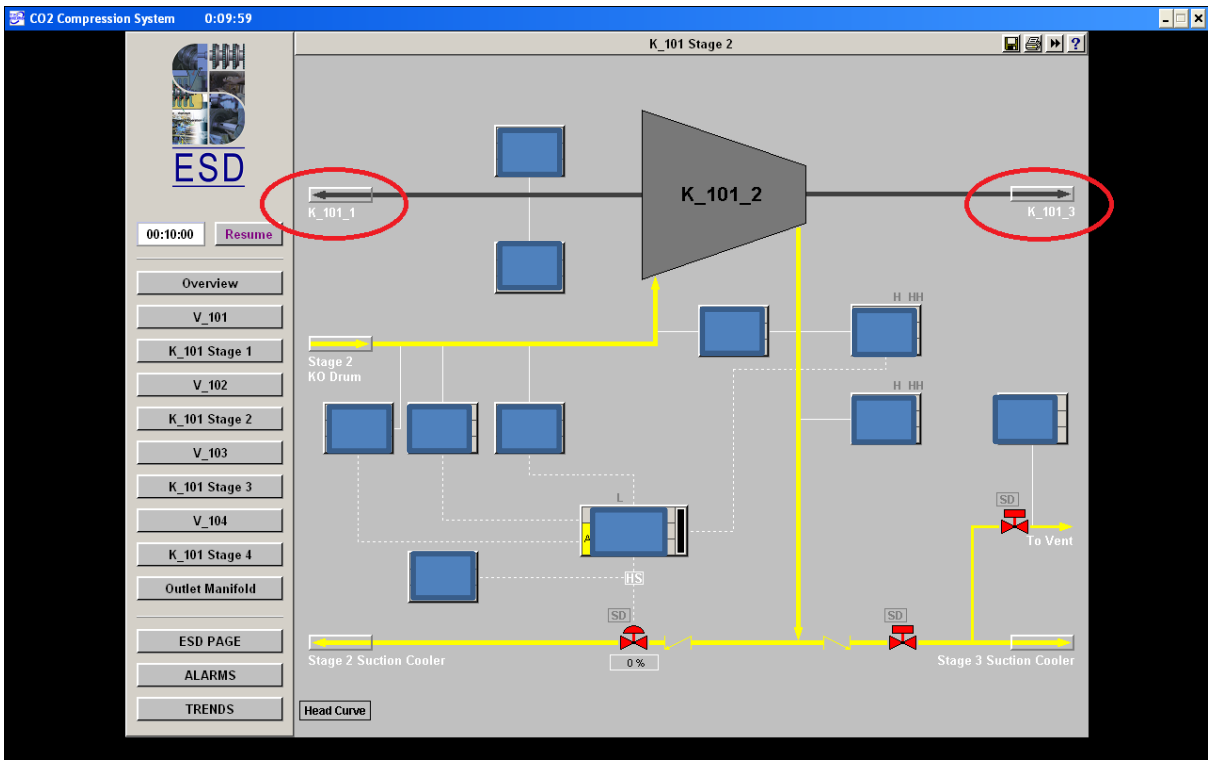


Figure 9-18. Second compressor of the multistage configuration

9.2.2 Steady state validation

The first step of the validation methodology included the comparison between the technical specification and the warm start-up condition of the software. The warm start up condition is equivalent to the design condition.

The speed controller, highlighted in Figure 9-19, was changed to automatic mode in order to manually change the set point of the controller. Then the simulation was left running until stabilisation and the values of the specified variables were checked again. A maximum limit error of ±2% has been imposed in order to guarantee the accuracy of the simulation tool. In this analysis the error was defined as:

$$error = \frac{Simulation\ value - Specification\ value}{Specification\ value}\%$$

Therefore the error was defined as the percentage error of the value of the warm start-up variable compared with the given specification.

Three test cases were validated during steady state operation:

- Case 0: warm start up case
- Case 1: high discharge pressure case
- Case 2: low discharge pressure case.

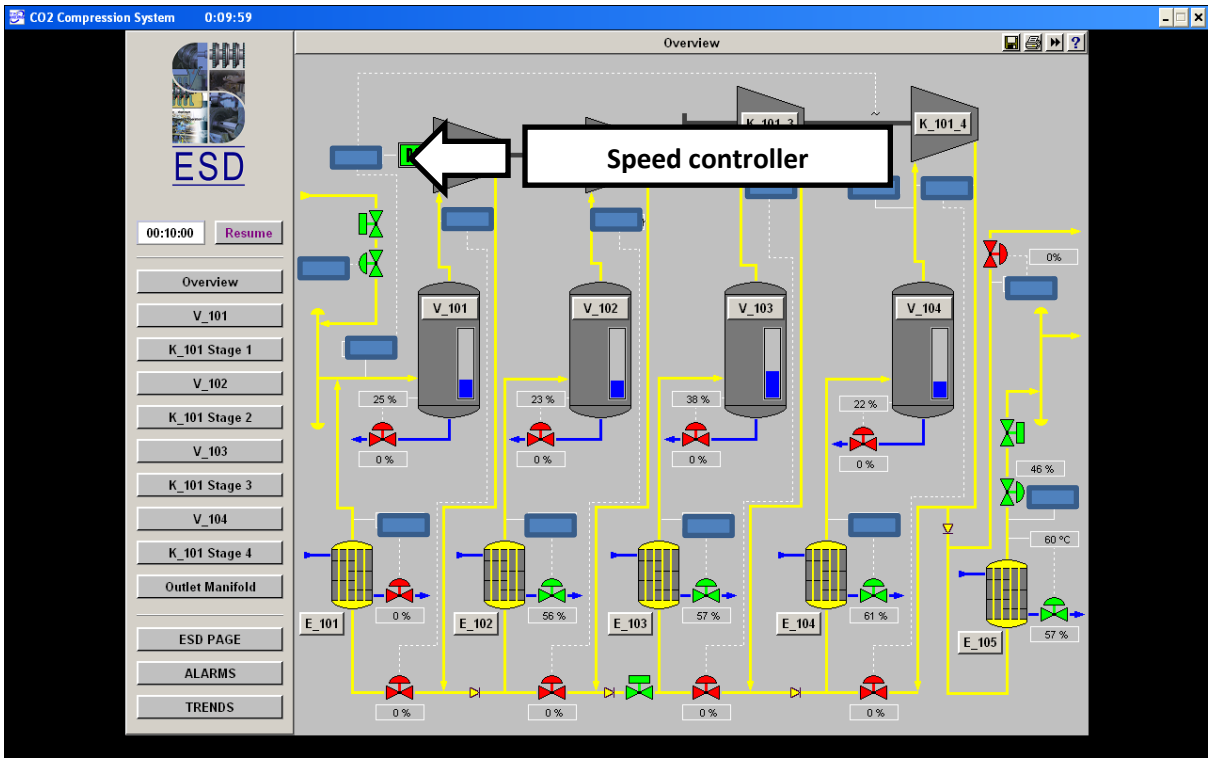


Figure 9-19. Speed controller

9.2.3 Analysis of performance maps

The purpose of the analysis of the performance maps of the multistage compressor was to verify that the compressor performance maps implemented in the simulation tool matched the vendor maps within a range of ±2%. Two types of analysis were performed:

- Visual analysis, consisting of over imposing the maps provided by the compressor vendor on the maps implemented into the simulator
- Operative analysis, consisting of moving the operating point of the machine to different areas of the compressor map and verifying the new steady state point against the given specification.

Both analyses gave good results. The performance maps in the simulation tool matched the performance maps provided by the vendor of the compressor within the range ±2%.

9.2.4 Off-peak point analysis

The purpose of the analysis of the off-peak operation of the machine was to verify that the simulation tool worked correctly even when away from the design point of the system. Three representative off-peak points were analysed and they included:

- Low suction pressure
- High discharge pressure
- Low suction flow.

A conservative approach was adopted. In fact each off-peak point was taken from the vendor datasheet in its lowest or highest value, depending on the process variable itself.

The manipulated variables employed in order to move the operating point of the system toward off-peak points were:

- Suction pressure of the system
- Discharge pressure of the system
- Suction flow of the system.

The outcome of the off-peak test was the validation of the operation of the compressor when its operating point is away from the design point.

9.2.5 Controller and alarm analysis

The purpose of the analysis of controllers and alarms was to:

- Analyse the saturation point of the controllers
- Analyse the behaviour of alarms.

Controllers and alarms were analysed in the warm start up case and in three major deviations including the following off peak cases:

- Low suction pressure
- High discharge pressure
- Low suction flow rate.

Various disturbances were employed in order to test the saturation of the controller and to activate the alarms of the system. The disturbances included both inlet and outlet disturbances.

The results of the analysis demonstrated that inlet disturbances caused the recycle trip of the fourth stage of compression. The other three stages followed it afterward. Outlet disturbances could not be used to test the action of the antisurge controller because unit trips caused the emergency shutdown of the system before the antisurge control system was activated.

9.2.6 Cause-effect analysis on trips

The purpose of the cause-effect analysis for the trips of single units was verifying the sequences following trips. Eleven controllers were tested for trip and they included:

- Four level controllers
- Two pressure controllers
- Five temperature controllers.

During steady state operation all the level control valves were fully closed. Therefore HH (High-High) trip was unlikely to happen. Step procedure in order to analyse the LL (Low-Low) trip included:

- Level controller in manual mode
- Level control valve fully open.

Various pressure controllers were installed in the system. For the pressure controllers, there were two possible options in order to test the trip. The step procedure for the first option included the following steps:

- Inlet pressure at minimum value but still above the LL pressure level
- Pressure controller in manual mode
- Corresponding valve fully open.

The step procedure for the second option included the following steps:

- Inlet pressure controller in manual mode
- Corresponding valve fully open
- Inlet isolation valve fully closed.

Finally the step procedure for analysing the trip of the temperature controller included the following steps:

- Temperature controller in manual mode
- Cooling water valve fully closed.

9.2.7 Shut down procedure

Normal shutdown was performed on the warm start case. In the warm start case the compressor is running at the design condition with all controllers in automatic mode and the compressor speed cascaded to suction pressure control.

The compressor was shut down in manual mode with operator intervention at all stages. The sequential events needed to be performed in order to logically unload, shut down and depressurise the multistage centrifugal compressor.

On modern process plants the shutdown of a large compressor is usually performed by a logic program associated with the process control system of the plant or the control system of the equipment itself. In either case the shutdown is automatic with minimal operator intervention. The only interaction between the operator and the logic system may be to initiate various sub-sequences (for example: “unload compressor”, “stop drive”, “depressurise casing”).

The shutdown procedure consisted of the following steps:

- Loading of the warm start scenario
- The opening of the inlet valve, highlighted in Figure 9-20, was reduced to a setting of 50%. This action had the effect of forcing the antisurge valves to partially open forcing the compressor into recycle on all stages
- The inlet valve was closed until the discharge flow from the compressor had reduced substantially. The discharge pressure controller closed the discharge valve as the flowrate decayed. When the valve was closed to 10-15% the compressor driver was stopped
- When driver was stopped the antisurge valves failed 100% open
- The inlet and outlet isolation valves did shut to box-in the compressor
- The casing was depressurised. This was done by opening the blowdown valves at the first stage discharge and the third and fourth stage suction. The fourth stage was depressurised through the discharge vent header. The inter-stage isolation valve closed on a motor stop. This was followed by full depressurisation of the system
- Finally the plant was set up for the next start-up. This included setting the controllers to the appropriate mode with the correct set points.

The shut-down procedure was successfully completed. The simulator was able to properly represent the behaviour of the compressor through all the steps of the shutdown process.

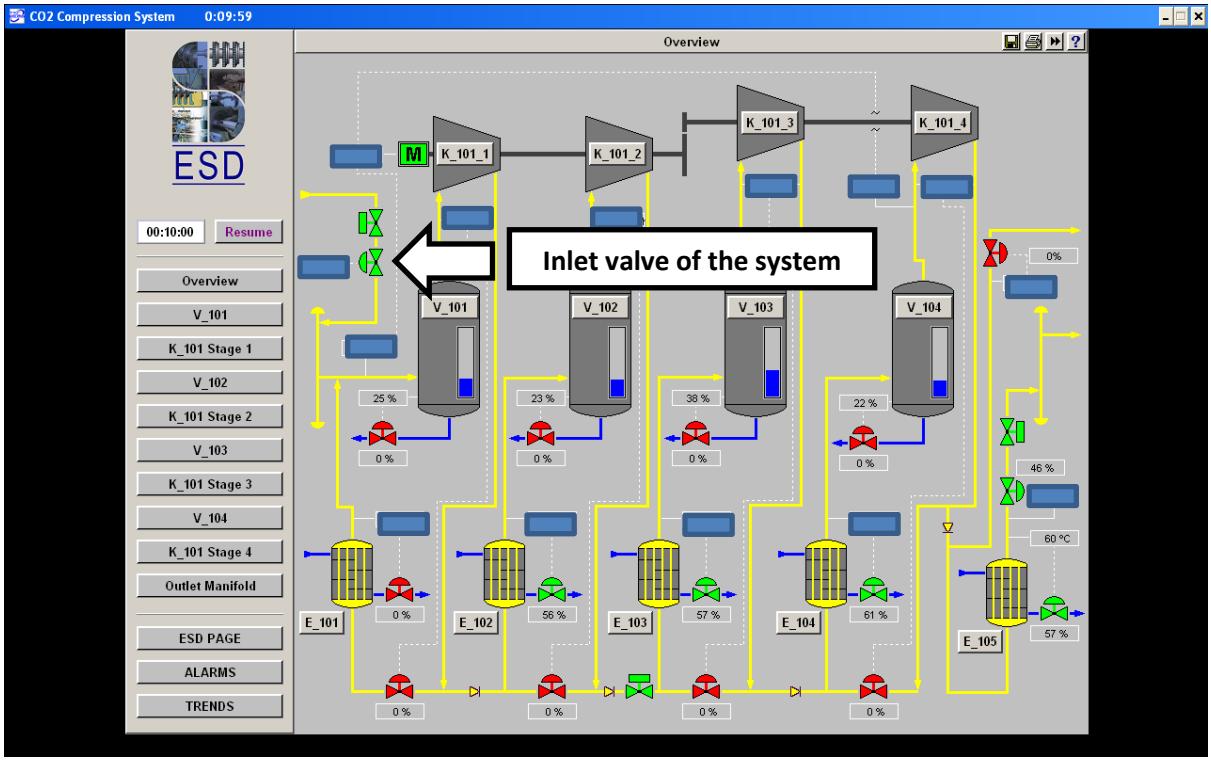


Figure 9-20. Inlet valve of the system

9.2.8 Start-up procedure

In the depressurised case the compressor is shut down with the four stages at a reduced pressure close to atmospheric. This is also called cold start case.

The preparation for the cold start up procedure included the following steps:

- The inter-stage isolation valve, highlighted in Figure 9-21, was closed between the second and third stages and the casing blowdown valves were open
- All the antisurge valves were fully open with the antisurge controllers in automatic mode and the output of the hand controllers set to 100% in order to hold the antisurge valves open
- The discharge header pressure controller was set on manual mode with an output of 10%
- The drive speed controller was set to automatic mode with a predefined set point
- The suction pressure controller was set to manual mode
- The fourth stage suction pressure controller was set to manual mode.

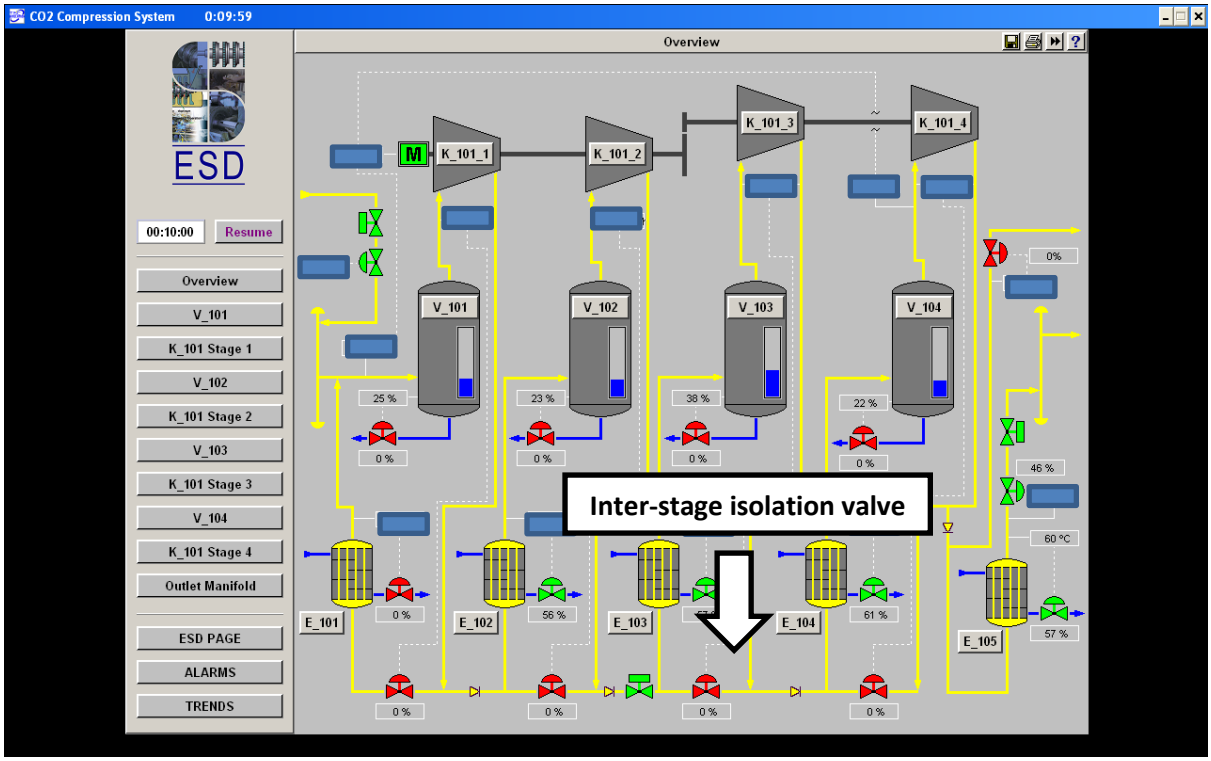


Figure 9-21. Inter-stage isolation valve

The compressor was started in a manual mode with operator intervention at all stages. Also in this case the sequential events needed to be performed in order to start-up the multistage centrifugal compressor.

On modern process plants the start-up of a large compressor is usually performed by a logic program associated with the process control system of the plant or the control system of the equipment itself. In either case the start-up is automatic with operator intervention minimal. The only interaction between the operator and the logic system may be to initiate various sub-sequences (for example: “start driver”, “drain casing”, “load compressor”).

The procedure of start-up of the compressor included the following steps:

- Loading of the cold start scenario
- The inlet shut down valve was open and the inlet valve was set to an 30% opening
- The inter-stage isolation valve was opened when the pressure differential across it was sufficiently low
- The motor was started
- When the motor was at the speed controller set point the start-up proceeded
- The start-up progressed by sequentially raising the speed of the rotating shaft and partially closing the antisurge control valves. Speed increment was limited in order to develop head slowly
- As the head developed the flow into the compressor raised
- When the speed of the compressor was above the 70% of the design speed and the antisurge valves were open at 50% the antisurge controllers were moved into automatic mode, starting from the first stage

- The inlet valve was set to 50% opening in order to increase the flow through, and rotational speed was increased too
- The discharge header pressure controller was set to automatic mode and the set point was set to a predefined value
- The remaining antisurge controllers were switched to automatic mode. The order of switching was backwards with the last being the fourth stage
- The suction pressure controller was switched to automatic mode
- The signal selector of the speed controller was set to suction pressure
- The speed controller was switched to cascade mode
- Once the compressor was stable the discharge vent header pressure controller was raised to its design value
- The discharge pressure controller was set to manual mode with a predefined output
- The discharge valve was opened when its differential was lower than 2.0 bar
- The discharge vent header set point was raised to its design value
- The system was stabilised and the alarm and ESD panels were checked in order to cancel any cleared alarms.

The start-up procedure was successfully completed. The simulator was able to properly represent the behaviour of the compressor through all the steps of the start-up process.

9.2.9 Summary

This Appendix is reporting on the methodology of validation of the ESD Simulation Tool. The methodology of validation included various steps such as:

- Steady state validation
- Analysis of the performance maps
- Analysis of the off-peak operation points
- Analysis of controllers and alarms
- Cause-effect analysis on trips
- Verification of shutdown and start-up procedures.

The validation was positive and successful. Adopted methodology and outcome were reported to ESD Simulation Training over four internal reports.

The validation guarantees the accuracy and reliability of the ESD Simulation Tool when simulating the operation of the multistage compressor at full and partial load, during normal and abnormal situations and also during start-up and shut-down.

This specific activity of validation and more generally the collaboration with ESD Simulation training was pivotal in the shaping of the content of this thesis.

References

D. Aaron & C. Tsouris (2005). Separation of CO_2 from flue gas: A review. *Separation Science and Technology,* 40**,** 321-348.

ALSTOM (2014). CO_2 solutions, *Alstom Brochure TPWR/PRSHT/CO2SOL/EN/5.2014/CHE/2015* [Online]. Alstom Power, Baden, Switzerland. Available: www.alstom.com/Global/Power/Resources/Documents/Brochures/co2-capture-storage-ccs-solutions.pdf [Accessed 4/ 11/ 2014].

S. Anwar & J. J. Carroll (2010). Density (kg/m^3) of carbon dioxide as a function of temperature and pressure. *Carbon Dioxide Thermodynamic Properties Handbook.* John Wiley & Sons, Inc.

G. L. Arnulfi, F. Blanchini, P. Giannattasio, D. Micheli & P. Pinamonti (2006). Extensive study on the control of centrifugal compressor surge. *Proceedings of the Institution of Mechanical Engineers Part A - Journal of Power and Energy,* 220**,** 289-304.

G. L. Arnulfi, P. Giannattasio, C. Giusto, A. F. Massardo, D. Micheli & P. Pinamonti (1999a). Multistage centrifugal compressor surge analysis: Part I—experimental investigation. *Journal of Turbomachinery,* 121**,** 305-311.

G. L. Arnulfi, P. Giannattasio, C. Giusto, A. F. Massardo, D. Micheli & P. Pinamonti (1999b). Multistage centrifugal compressor surge analysis: Part II—numerical simulation and dynamic control parameters evaluation. *Journal of Turbomachinery,* 121**,** 312-320.

P. Aursand, M. Hammer, S. T. Munkejord & O. Wilhelmsen (2013). Pipeline transport of CO_2 mixtures: Models for transient simulation. *International Journal of Greenhouse Gas Control,* 15**,** 174-185.

B. W. Batson (1996). Invariant coordinate systems for compressor control. *International Gas Turbine and Aeroengine Congress & Exhibition*, 10-13 June 1996 Birmingham (UK).

F. Blanchini & P. Giannattasio (2002). Adaptive control of compressor surge instability. *Automatica,* 38**,** 1373-1380.

B. Bohagen & J. T. Gravdahl (2008). Active surge control of compression system using drive torque. *Automatica,* 44**,** 1135-1140.

K. O. Boinov, E. A. Lomonova, A. J. A. Vandenput & A. Tyagunov (2006). Surge control of the electrically driven centrifugal compressor. *IEEE Transactions on Industry Applications,* 42**,** 1523-1531.

K. K. Botros (1994). Transient phenomena in compressor stations during surge. *Journal of Engineering for Gas Turbines and Power-Transactions of the ASME,* 116**,** 133-142.

K. K. Botros (2011). Single versus dual recycle system dynamics of high pressure ratio, low inertia centrifugal compressor stations. *Journal of Engineering for Gas Turbines and Power-Transactions of the ASME,* 133**,** 122402: 1-12.

K. K. Botros, P. J. Campbell & D. B. Mah (1991). Dynamic simulation of compressor station operation including centrifugal-compressor and gas-turbine. *Journal of Engineering for Gas Turbines and Power, Transactions of the ASME,* 113**,** 300-311.

K. K. Botros & J. F. Henderson (1994). Developments in centrifugal-compressor surge control - a technology-assessment. *Journal of Turbomachinery-Transactions of the ASME,* 116**,** 240-249.

K. K. Botros, B. J. Jones & D. J. Richards (1996). Recycle dynamics during centrifugal compressor ESD, start-up and surge control. *International Pipeline Conference*, 1996a Calgary, Canada. Medium: X; Size: pp. 957-966.

K. K. Botros, W. M. Jungowski & D. J. Richards (1996b). Compressor station recycle system dynamics during emergency shutdown. *Journal of Engineering for Gas Turbines and Power-Transactions of the ASME,* 118**,** 641-653.

M. P. Boyce (2003). *Centrifugal Compressors - A Basic Guide*, PennWell. Available: http://app.knovel.com/hotlink/toc/id:kpCCABG001/centrifugal-compressors

M. P. Boyce (2012). *Gas Turbine Engineering Handbook (4th Edition)*, Elsevier. Available: http://app.knovel.com/hotlink/toc/id:kpGTEHE017/gas-turbine-engineering-2/gas-turbine-engineering-2

R. N. Brown (2005). *Compressors - Selection and Sizing (3rd Edition)*, Elsevier.

S. Budinis & N. F. Thornhill (2014). An integrated control technique for compressor operation. *10th International Conference on Control*, 9th-11th July 2014 Loughborough University.

S. Budinis & N. F. Thornhill (2015). Control of centrifugal compressors via model predictive control for enhanced oil recovery applications. *2nd IFAC Workshop on Automatic Control in Offshore Oil and Gas Production*, May 2015a Florianópolis, Brazil.

S. Budinis & N. F. Thornhill (2015). Supercritical gas recycle analysis for surge control of centrifugal compressors. *PSE2015/ESCAPE25*, May 2015b Copenhagen, Denmark.

S. Budinis & N. F. Thornhill (2015c). Supercritical gas recycle analysis for surge control of centrifugal compressors. *Computer Aided Chemical Engineering: Special Issue*.

S. Budinis, N. F. Thornhill & D. Fabozzi (2013). A control technique based on compressor characteristics with applications to carbon capture and storage systems. *2013 AIChE Annual Meeting*, 7th November 2013 San Francisco CA.

E. F. Camacho & C. B. Alba (2013). Constrained model predictive control. *Model Predictive Control.* London: Springer.

S. M. Camporeale, B. Fortunato & M. Mastrovito (2006). A modular code for real time dynamic simulation of gas turbines in Simulink. *Journal of Engineering for Gas Turbines and Power, Transactions of the ASME,* 128**,** 506-517.

CCC (2013). Challenges and Opportunities in Turbomachinery Control. *Internal course material.*

G. Centi & S. Perathoner (2009). Opportunities and prospects in the chemical recycling of carbon dioxide to fuels. *Catalysis Today,* 148**,** 191-205.

R. Chacartegui, D. Sanchez, A. Munoz & T. Sanchez (2011). Real time simulation of medium size gas turbines. *Energy Conversion and Management,* 52**,** 713-724.

M. Chaczykowski & A. J. Osiadacz (2012). Dynamic simulation of pipelines containing dense phase/supercritical CO_2-rich mixtures for carbon capture and storage. *International Journal of Greenhouse Gas Control,* 9**,** 446-456.

T. Conboy, J. Pasch & D. Fleming (2013). Control of a supercritical CO_2 recompression Brayton cycle demonstration loop. *Journal of Engineering for Gas Turbines and Power-Transactions of the ASME,* 135**,** 12.

A. Cortinovis, D. Pareschi, M. Mercangoez & T. Besselmann (2012). Model predictive anti-surge control of centrifugal compressors with variable-speed drives. *IFAC Workshop on Automatic Control in Offshore Oil and Gas Production*, 31 May - 1 June 2012 Norwegian University of Science and Technology, Trondheim, Norway.

A. Cortinovis, M. Zovadelli, M. Mercangoz, D. Pareschi, A. De Marco, S. Bittanti & Ieee (2014). Online Adaptation of Performance Maps for Centrifugal Gas Compressors. *2014 European Control Conference (Ecc)***,** 1036-1041.

J. M. Coulson, J. F. Richardson, J. R. Backhurst & J. H. Harker (1999). *Coulson and Richardson's Chemical Engineering Volume 1 - Fluid Flow, Heat Transfer and Mass Transfer (6th Edition)*, Elsevier. Available: http://app.knovel.com/hotlink/toc/id:kpCRCEVFF2/coulson-richardsons-chemical-3/coulson-richardsons-chemical-3

E. B. Dahlin (1968). Designing and tuning digital controllers. *Instrumentation and Control Systems,* June 1968**,** 77.

J. Daintith (2008). *Dictionary of Chemistry (6th Edition)*, Oxford University Press.

DIPPR (2012). *DIPPR Project 801 - Full Version*, Design Institute for Physical Property Research/AIChE. Available: http://app.knovel.com/hotlink/toc/id:kpDIPPRPF7/dippr-project-801-full/dippr-project-801-full

N. Dukle & K. Narayanan (2003). Validating anti-surge control systems. Available: http://www.eptq.com/view_edition.aspx?strYID=2003.

H. W. Emmons, C. E. Pearson & H. P. Grant (1955). Compressor surge and stall propagation. *Transaction of the American Society of Mechanical Engineers*, 1955. New York: American Society of Mechanical Engineers.

A. H. Epstein, J. E. F. Williams & E. M. Greitzer (1989). Active suppression of aerodynamic instabilities in turbomachines. *Journal of Propulsion and Power,* 5**,** 204-211.

ESD Simulation Training (2014). Carbon dioxide compression, [Online]. Available: https://www.esd-simulation.com/course/carbon-dioxide-compression [Accessed 12/01/2014 2014].

M. R. Feulner, G. J. Hendricks & J. D. Paduano (1996). Modeling for control of rotating stall in high-speed multistage axial compressors. *Journal of Turbomachinery-Transactions of the ASME,* 118**,** 1-10.

D. A. Fink, N. A. Cumpsty & E. M. Greitzer (1992). Surge dynamics in a free-spool centrifugal-compressor system. *Journal of Turbomachinery-Transactions of the ASME,* 114**,** 321-332.

J. K. Fink (2012). *Petroleum Engineer's Guide to Oil Field Chemicals and Fluids*, Elsevier. Available: http://app.knovel.com/hotlink/toc/id:kpPEGOFCF1/petroleum-engineer-s/petroleum-engineer-s

GE (2011). Carbon capture & sequestration - CO_2 management systems for higher plant performance and lower emissions, *GE Brochure GE_CCS_Brochure_012611-2.indd* [Online]. GE Oil & Gas, Florence, Italy. Available: www.ge-energy.com/content/multimedia/_files/downloads/CCS.pdf [Accessed 4/ 11/ 2014].

J. Gibbins & H. Chalmers (2008). Carbon capture and storage. *Energy Policy,* 36**,** 4317-4322.

A. Grancharova, T. A. Johansen & P. Tondel (2007). Computational aspects of approximate explicit nonlinear model predictive control. *In:* Findeisen, R., Allgower, F. & Biegler, L. T. (eds.) *Assessment and Future Directions of Nonlinear Model Predictive Control.* Berlin: Springer.

A. S. Grandison & M. J. Lewis (1996). *Separation Processes in the Food and Biotechnology Industries - Principles and Applications*, Woodhead Publishing. Available: http://app.knovel.com/hotlink/toc/id:kpSPFBIPA6/separation-processes/separation-processes

J. T. Gravdahl & O. Egeland (1999). Centrifugal compressor surge and speed control. *IEEE Transactions on Control Systems Technology,* 7**,** 567-579.

J. T. Gravdahl, O. Egeland & S. O. Vatland (2002). Drive torque actuation in active surge control of centrifugal compressors. *Automatica,* 38**,** 1881-1893.

J. T. Gravdahl, F. Willems, B. de Jager & O. Egeland (2004). Modeling of surge in free-spool centrifugal compressors: Experimental validation. *Journal of Propulsion and Power,* 20**,** 849-857.

E. M. Greitzer (1976a). Surge and rotating stall in axial-flow compressors .2. Experimental results and comparison with theory. *Journal of Engineering for Power-Transactions of the ASME,* 98**,** 199-217.

E. M. Greitzer (1976b). Surge and rotating stall in axial-flow compressors. 1. Theoretical compression system model. *Journal of Engineering for Power-Transactions of the ASME,* 98**,** 190-198.

E. M. Greitzer & F. K. Moore (1986). A theory of post-stall transients in axial-compression systems. 2. Application. *Journal of Engineering for Gas Turbines and Power-Transactions of the ASME,* 108**,** 231-239.

G. X. Gu, A. Sparks & S. S. Banda (1999). An overview of rotating stall and surge control for axial flow compressors. *IEEE Transactions on Control Systems Technology,* 7**,** 639-647.

D. L. Gysling, J. Dugundji, E. M. Greitzer & A. H. Epstein (1991). Dynamic control of centrifugal-compressor surge using tailored structures. *Journal of Turbomachinery-Transactions of the ASME,* 113**,** 710-722.

K. E. Hansen, P. Jorgensen & P. S. Larsen (1981). Experimental and theoretical-study of surge in a small centrifugal-compressor. *Journal of Fluids Engineering-Transactions of the ASME,* 103**,** 391-395.

N. Harun, T. Nittaya, P. L. Douglas, E. Croiset & L. A. Ricardez-Sandoval (2012). Dynamic simulation of MEA absorption process for CO_2 capture from power plants. *International Journal of Greenhouse Gas Control,* 10**,** 295-309.

F. B. Horowitz, B. P. Gupta & B. G. Liptak (2006). Compressor control and optimization. *In:* Liptak, B. G. (ed.) *Instrument Engineers' Handbook.* 4th ed. Boca Raton, FL: Taylor & Francis Group.

A. J. Hunt, E. H. K. Sin, R. Marriott & J. H. Clark (2010). Generation, capture, and utilization of industrial carbon dioxide. *Chemsuschem,* 3**,** 306-322.

IPCC (2007). Climate Change 2007: Synthesis Report. Geneva, Switzerland.

Z. Jiang, T. Xiao, V. L. Kuznetsov & P. P. Edwards (2010). Turning carbon dioxide into fuel. *Philosophical Transactions of the Royal Society a-Mathematical Physical and Engineering Sciences,* 368**,** 3343-3364.

T. A. Johansen (2002). On multi-parametric nonlinear programming and explicit nonlinear model predictive control. *Proceedings of the 41st IEEE Conference on Decision and Control*, 2002 New York. IEEE, 2768-2773.

R. E. Kalman (1960). A New Approach to Linear Filtering and Prediction Problems. *Journal of Basic Engineering,* 82**,** 35-45.

M. Karimi, M. Hillestad & H. F. Svendsen (2012). Investigation of the dynamic behavior of different stripper configurations for post-combustion CO_2 capture. *International Journal of Greenhouse Gas Control,* 7**,** 230-239.

M. O. Khan (1984). Basic Practices in Compressor Selection, [Online]. Available: http://docs.lib.purdue.edu/cgi/viewcontent.cgi?article=1508&context=icec [Accessed 07/ 01/ 2015].

H. A. Kidd & H. F. Miller (2010). Compression solutions for CO_2 applications (traditional centrifugal and supersonic technology), *insight Magazine Winter 2010* [Online]. Dresser-Rand, New York, USA. Available: www.dresser-rand.com/insights/Winter10/insights_Winter10_ENote.pdf [Accessed 4/ 11/ 2014].

M. H. Kim, J. Pettersen & C. W. Bullard (2004). Fundamental process and system design issues in CO_2 vapor compression systems. *Progress in Energy and Combustion Science,* 30**,** 119-174.

S. G. Kim, J. Lee, Y. Ahn, J. I. Lee, Y. Addad & B. Ko (2014). CFD investigation of a centrifugal compressor derived from pump technology for supercritical carbon dioxide as a working fluid. *Journal of Supercritical Fluids,* 86**,** 160-171.

M. King (2010). Compressor control. *Process Control: A Practical Approach.* Singapore: Wiley.

Knovel (2015). *Knovel Critical Tables (2nd Edition)*, Knovel. Available: http://app.knovel.com/hotlink/toc/id:kpKCTE000X/knovel-critical-tables/knovel-critical-tables

C. Lettieri, N. Baltadjiev, M. Casey & Z. Spakovszky (2014). Low-flow-coefficient centrifugal compressor design for supercritical CO_2. *Journal of Turbomachinery-Transactions of the ASME,* 136**,** 9.

Y. J. Lin, T. H. Pan, D. S. H. Wong, S. S. Jang, Y. W. Chi & C. H. Yeh (2011). Plantwide control of CO_2 capture by absorption and stripping using monoethanolamine solution. *Industrial & Engineering Chemistry Research,* 50**,** 1338-1345.

M. M. Maroto-Valer (2010). *Developments and Innovation in Carbon Dioxide (CO_2) Capture and Storage Technology, Volume 1 - Carbon Dioxide (CO_2) Capture, Transport and Industrial Applications*, Woodhead Publishing. Available: http://app.knovel.com/hotlink/toc/id:kpDICDCOC2/developments-innovation-2/developments-innovation-2

MathWorks (2015a). Choose a Solver, *Matlab Online Documentation* [Online]. Available: http://uk.mathworks.com/help/simulink/ug/choosing-a-solver.html [Accessed 07/ 01/ 2015].

MathWorks (2015b). Controller State Estimation, *Matlab Online Documentation* [Online]. Available: http://uk.mathworks.com/help/mpc/ug/controller-state-

estimation.html?searchHighlight=controller%20state%20estimation [Accessed 07/ 01/ 2015].
Mathworks (2015c). How the software formulates parameter estimation as an optimization problem, *Matlab Online Documentation* [Online].
MathWorks (2015d). MPC Modeling, *Matlab Online Documentation* [Online]. Available: http://uk.mathworks.com/help/mpc/gs/mpc-modeling.html?searchHighlight=MPC%20linear%20model#bujvuw0 [Accessed 07/ 01/ 2015].
MathWorks (2015e). Optimization Problem, *Matlab Online Documentation* [Online]. Available: http://uk.mathworks.com/help/mpc/ug/optimization-problem.html?refresh=true [Accessed 07/ 01/ 2015].
MathWorks (2015f). PID Controller, *Matlab Online Documentation* [Online]. Available: http://uk.mathworks.com/help/simulink/slref/pidcontroller.html [Accessed 07/ 01/ 2015].
MathWorks (2015g). Simulink Features, [Online]. Available: http://uk.mathworks.com/products/simulink/features.html [Accessed 07/ 01/ 2015].
S. T. McCoy & E. S. Rubin (2008). An engineering-economic model of pipeline transport of CO_2 with application to carbon capture and storage. *International Journal of Greenhouse Gas Control,* 2**,** 219-229.
S. Mirsky, W. Jacobson, D. Tiscornia, J. McWhirter & M. Zaghloul (2012). Development and design of antisurge and performance control systems for centrifugal compressors. *Proceedings of the Forty-Second Turbomachinery Symposium*, October 1-3 2012 Houston, Texas.
P. J. H. Z. Molenaar (2007). *Model Predictive Compressor Surge Control.*
F. K. Moore & E. M. Greitzer (1986). A theory of post-stall transients in axial-compression systems 1. Development of equations. *Journal of Engineering for Gas Turbines and Power-Transactions of the ASME,* 108**,** 68-76.
J. J. Moore, A. Lerche, T. Allison, B. Moreland & J. Pacheco (2012). Development of an internally cooled centrifugal compressor for carbon capture and storage applications. *Proceedings of the ASME Turbo Expo 2012, Vol 5*, 2012 New York. Amer Soc Mechanical Engineers, 997-1006.
M. Morini, M. Pinelli & M. Venturini (2007). Development of a one-dimensional modular dynamic model for the simulation of surge in compression systems. *Journal of Turbomachinery-Transactions of the ASME,* 129**,** 437-447.
M. Morini, M. Pinelli & M. Venturini (2009). Analysis of biogas compression system dynamics. *Applied Energy,* 86**,** 2466-2475.
I. Omae (2006). Aspects of carbon dioxide utilization. *Catalysis Today,* 115**,** 33-52.
T. F. Øvervåg (2013). *Centrifugal Compressor Load Sharing with the use of MPC.* Master of Science in Engineering Cybernetics, Norwegian University of Science and Technology.
J. D. Paduano, A. H. Epstein, L. Valavani, J. P. Longley, E. M. Greitzer & G. R. Guenette (1993). Active control of rotating stall in a low-speed axial compressor. *Journal of Turbomachinery-Transactions of the ASME,* 115**,** 48-56.
S. C. Page, A. G. Williamson & I. G. Mason (2009). Carbon capture and storage: Fundamental thermodynamics and current technology. *Energy Policy,* 37**,** 3314-3324.
M. Panahi & S. Skogestad (2011). Economically efficient operation of CO_2 capturing process part I: Self-optimizing procedure for selecting the best controlled variables. *Chemical Engineering and Processing,* 50**,** 247-253.
M. Panahi & S. Skogestad (2012). Economically efficient operation of CO_2 capturing process. Part II. Design of control layer. *Chemical Engineering and Processing,* 52**,** 112-124.
V. Patel, J. Feng, S. Dasgupta, P. Ramdoss & J. Wu (2007). Application of dynamic simulation in the design, operation, and troubleshooting of compressor systems. *Thirty-sixth Turbomachinery Symposium*, 2007 Turbomachinery Laboratory, Texas A&M University.

R. Pecnik, E. Rinaldi & P. Colonna (2012). Computational fluid dynamics of a radial compressor operating with supercritical CO_2. *Journal of Engineering for Gas Turbines and Power-Transactions of the ASME,* 134**,** 8.

I. Penarrocha, R. Llopis, L. Tarrega, D. Sanchez & R. Cabello (2014). A new approach to optimize the energy efficiency of CO_2 transcritical refrigeration plants. *Applied Thermal Engineering,* 67**,** 137-146.

D. Peng & D. B. Robinson (1976). New two-constant equation of state. *Industrial & Engineering Chemistry Fundamentals,* 15**,** 59-64.

E. N. Pistikopoulos, M. C. Georgiadis & V. Dua (2006). *Multi-Parametric Model-Based Control. Volume.2, Theory and Applications,* Weinheim, Wiley-VCH, John Wiley, distributor.

S. I. Plasynski, J. T. Litynski, H. G. McIlvried & R. D. Srivastava (2009). Progress and new developments in carbon capture and storage. *Critical Reviews in Plant Sciences,* 28**,** 123-138.

R. P. Pohanish (2012). *Sittig's Handbook of Toxic and Hazardous Chemicals and Carcinogens (6th Edition)*, Elsevier.

S. J. Qin & T. A. Badgwell (2003). A survey of industrial model predictive control technology. *Control Engineering Practice,* 11**,** 733-764.

G. Quartarone, N. Anglani & S. Riverso (2013). Model Predictive Control: first application of a novel control strategy for adjustable speed drive compressors. *39th Annual Conference of the IEEE Industrial Electronics Society (Iecon 2013)*, 2013 2013. 7892-7897.

T. E. Rufford, S. Smart, G. C. Y. Watson, B. F. Graham, J. Boxall, J. C. Diniz da Costa & E. F. May (2012). The removal of CO_2 and N_2 from natural gas: A review of conventional and emerging process technologies. *Journal of Petroleum Science and Engineering,* 94–95**,** 123-154.

M. Salazar & F. Mendez (2014). PID control for a single-stage transcritical CO_2 refrigeration cycle. *Applied Thermal Engineering,* 67**,** 429-438.

C. Schaschke (2014). *Dictionary of Chemical Engineering*, Oxford University Press. Available: http://app.knovel.com/hotlink/toc/id:kpDCE00021/dictionary-chemical-engineering/dictionary-chemical-engineering

D. E. Seborg, T. F. Edgar & D. A. Mellichamp (2004a). Introduction to process control. *Process Dynamics And Control.* 2nd ed. Hoboken, NJ: Wiley.

D. E. Seborg, T. F. Edgar & D. A. Mellichamp (2004b). Model predictive control. *Process Dynamics And Control.* 2nd ed. Hoboken, NJ: Wiley.

D. E. Seborg, T. F. Edgar & D. A. Mellichamp (2004c). *Process Dynamics and Control,* Hoboken, NJ, Wiley.

Siemens (2007). Compressor, *CAD image of an STC-SH single-shaft centrifugal compressor with horizontally split casing* [Online]. Available: http://www.siemens.com/press/en/presspicture/?press=/en/presspicture/2009/fossil_power_generation/efpg20070701-04.htm [Accessed 9th May 2013].

Siemens (2014). Integrally Geared Turbocompressors, *Brochure E50001-G420-A114-X-4A00 STC_GV_LowRes* [Online]. Available: http://www.energy.siemens.com/us/pool/hq/compression/integrally-geared-compressors/STC-GV/E50001-G420-A114-X-4A00%20STC_GV_LowRes.pdf [Accessed 4/ 11/ 2014].

J. P. M. Smeulers, W. J. Bouman & H. A. Van Essen (1999). Model predictive control of compressor installations. *International Conference on Compressors and Their Systems*, September 13-15 1999. City University London, London, England, 555-565.

G. Soave (1972). Equilibrium constants from a modified Redlich-Kwong equation of state. *Chemical Engineering Science,* 27**,** 1197-&.

C. S. Song (2006). Global challenges and strategies for control, conversion and utilization of CO_2 for sustainable development involving energy, catalysis, adsorption and chemical processing. *Catalysis Today,* 115**,** 2-32.

R. Span & W. Wagner (1996). A new equation of state for carbon dioxide covering the fluid region from the triple-point temperature to 1100 K at pressures up to 800 MPa. *Journal of Physical and Chemical Reference Data,* 25**,** 1509-1596.

A. Stodola (1924). *Dampf und Gasturbinen,* Berlin, Sechste au9age: Julius Springer.

SULZER (2010). Your partner for a cleaner future: Sulzer pumps for carbon capture and storage, *Brochure E10050* [Online]. Available: www.sulzer.com/en/-/media/Documents/ProductsAndServices/Pumps_and_Systems/General/Brochures/YourPartnerForCleanerFuture_E10050.pdf [Accessed 4/ 11/ 2014].

R. Svensson, M. Odenberger, F. Johnsson & L. Stromberg (2004). Transportation systems for CO_2 - application to carbon capture and storage. *Energy Conversion and Management,* 45**,** 2343-2353.

T. W. Swaddle (1990). *Inorganic Chemistry - An Industrial and Environmental Perspective*, Elsevier. Available: http://app.knovel.com/hotlink/toc/id:kpICAIEP01/inorganic-chemistry-an/inorganic-chemistry-an

N. F. Thornhill (2014). Process dynamics and control. *Course material.* Chemical Engineering Department: Imperial College London.

G. E. Totten, S. R. Westbrook & R. J. Shah (2003). *Fuels and Lubricants Handbook - Technology, Properties, Performance, and Testing: (MNL 37WCD),* West Conshohocken, PA, USA., ASTM International.

G. Towler & R. K. Sinnott (2013). *Chemical Engineering Design - Principles, Practice and Economics of Plant and Process Design (2nd Edition)*, Elsevier. Available: http://app.knovel.com/hotlink/toc/id:kpCEDPPEP4/chemical-engineering/chemical-engineering

N. Uddin & J. T. Gravdahl (2011). Active compressor surge control using piston actuation. *Proceedings of the ASME Dynamic Systems and Control Conference and Bath/ASME Symposium on Fluid Power and Motion Control*, 2011. 69-76.

N. Uddin & J. T. Gravdahl (2012). Introducing back-up to active compressor surge control system. *IFAC Workshop on Automatic Control in Offshore Oil and Gas Production*, May 31 - June 1 2012 University of Science and Technology, Trondheim, Norway.

M. Utamura, T. Fukuda & M. Aritomi (2012). Aerodynamic characteristics of a centrifugal compressor working in supercritical carbon dioxide. *Energy Procedia,* 14**,** 1149-1155.

M. Venturini (2005). Development and experimental validation of a compressor dynamic model. *Journal of Turbomachinery, Transactions of the ASME,* 127**,** 599-608.

L. Wang (2009). *Model Predictive Control System Design And Implementation Using Matlab*, New York ; London : Springer.

M. H. White (1972). Surge control for centrifugal compressors. *Chemical Engineering,* 79**,** 54-62.

S. F. Whittle (1953). *Jet. The Story of a Pioneer,* London, Frederick Muller Ltd.

F. Willems & B. de Jager (1998). Modeling and control of rotating stall and surge: An overview. *Proceedings of the 1998 IEEE International Conference on Control Applications, Vols 1 and 2*, 1998 New York. IEEE, 331-335.

F. Willems & B. de Jager (1999). Modeling and control of compressor flow instabilities. *IEEE Control Systems Magazine,* 19**,** 8-18.

J. Wilson & A. Sheldon (2006). Matching antisurge control valve performance with integrated rated turbomachinery control, systems. *Hydrocarbon Processing,* 85**,** 55-58.

J. Wu, J. Feng, S. Dasgupta & I. Keith (2007). A realistic dynamic modeling approach to support LNG plant compressor operations. *LNG journal* [Online]. Available: http://www.lngjournal.com/lng/index.php/.

G. Wypych (2014). *Knovel Solvents - A Properties Database*, ChemTec Publishing. Available: http://app.knovel.com/hotlink/toc/id:kpKSAPD005/knovel-solvents-properties/knovel-solvents-properties

C. L. Yaws (2014). *Yaws' Critical Property Data for Chemical Engineers and Chemists*, Knovel. Available: http://app.knovel.com/hotlink/toc/id:kpYCPDCECD/yaws-critical-property/yaws-critical-property

Z. X. Zhang, G. X. Wang, P. Massarotto & V. Rudolph (2006). Optimization of pipeline transport for CO_2 sequestration. *Energy Conversion and Management,* 47**,** 702-715.